Lecture Notes on Nonlinear Dynamics
(A Work in Progress)

Daniel Arovas
Department of Physics
University of California, San Diego

October 22, 2009

Contents

0.1 Preface

This is a proto-preface. A more complete preface will be written after these notes are completed.

These lecture notes are intended to supplement a graduate level course in nonlinear dynamics.

Chapter 0

Reference Materials

No one book contains all the relevant material. Here I list several resources, arranged by topic. My personal favorites are marked with a diamond (◇).

0.1 Dynamical Systems

◇ S. Strogatz, *Nonlinear Dynamics and Chaos* (Addison-Wesley, 1994)

◇ S. Neil Rasband, *Chaotic Dynamics of Nonlinear Systems* (Wiley, 1990)

◇ J. Guckenheimer and P. Holmes, *Nonlinear Oscillations, Dynamical Systems, and Bifurcations of Vector Fields* (Springer, 1983)

- E. A. Jackson, *Perspectives of Nonlinear Dynamics*, 2 vols. (Cambridge, 1991)

- A. J. Lichtenberg and M. A. Lieberman, *Regular and Stochastic Motion* (Springer, 1983)

- R. Z. Sagdeev, D. A. Usikov, and G. M. Zaslavsky, *Nonlinear Physics from the Pendulum to Turbulence and Chaos* (Harwood Academic, 1988)

- M. Lakshmanan and S. Rajasekar, *Nonlinear Dynamics : Integrability, Chaos, and Patterns* (Springer, 2003)

- H. G. Schuster and W. Just, *Deterministic Chaos*, 4th ed. (Wiley-VCH, 2005)

- M. Tabor, *Chaos and Integrability in Nonlinear Dynamics* (Wiley, 1989)

- E. Ott, *Chaos in Dynamical Systems*, 2nd ed. (Cambridge, 2002)

0.2 Hamiltonian Mechanics

◇ G. M. Zaslavsky, *Hamiltonian Chaos and Fractional Dynamics* (Oxford, 2005)

◇ J. V. José and E. J. Saletan, *Classical Dynamics : A Contemporary Approach* (Cambridge, 1998)

- V. I. Arnold, V. V. Kozlov, and A. I. Neishtadt, *Mathematical Aspects of Classical and Celestial Mechanics* (Springer, 2006)

- A. L. Fetter and J. D. Walecka, *Nonlinear Mechanics* (Dover, 2006)

- I. Percival and D. Richards, *Introduction to Dynamics* (Cambridge, 1982)

0.3 Differential Equations

◇ D. Zwillinger, *Handbook of Differential Equations*, 3rd ed. (Academic Press, 1998)

◇ A. H. Nayfeh, *Introduction to Perturbation Techniques* (Wiley, 1981)

◇ C. M. Bender and S. A. Orszag, *Advanced Mathematical Methods for Scientists and Engineers* (Springer, 1999)

◇ V. I. Arnold, *Ordinary Differential Equations* (MIT Press, 1973)

- V. I. Arnold, *Geometrical Methods in the Theory of Ordinary Differential Equations* (Springer, 1988)

- L. Perko, *Differential Equations and Dynamical Systems*, 3rd ed. (Springer, 2001)

- J. A. Sanders and F. Verhulst, *Averaging Methods in Nonlinear Dynamical Systems* (Springer, 1985).

0.4 Synchronization

◇ Y. Kuramoto, *Chemical Oscillations, Waves, and Turbulence* (Dover, 2003)

- A. Pikovsky, M. Rosenblum, and J. Kurths, *Synchronization : A Universal Concept in Nonlinear Sciences* (Cambridge, 2001)

0.5 Nonlinear Wave Equations

◇ G. B. Whitham, *Linear and Nonlinear Waves* (Wiley, 1999)

◇ A. Scott, *Nonlinear Science*, 2nd ed. (Oxford, 2003)

- E. Infeld and G. Rowlands, *Nonlinear Waves, Solitons, and Chaos* (Cambridge, 2000)

- R. Rajaraman, *Solitons and Instantons* (North-Holland, 1987)

- H.-K. Rhee, R. Aris, and N. R. Amundson, *First-Order Partial Differential Equations* (2 vols.) (Dover, 1986)

- L. I. Pismen, *Vortices in Nonlinear Fields* (Oxford, 1999)

0.6 Pattern Formation

◇ P. Manneville, *Instabilities, Chaos, and Turbulence* (Imperial College Press, 2004)

◇ D. Walgraef, *Spatio-Temporal Pattern Formation* (Springer, 1996)

- P. Manneville, *Dissipative Structures and Weak Turbulence* (Academic Press, 1990)

- L. M. Pismen, *Patterns and Interfaces in Dissipative Dynamics* (Springer, 2006)

- M. I. Rabinovich, A. B. Ezersky, and P. D. Weidman, *The Dynamics of Patterns* (World Scientific, 2000)

- R. Hoyle, *Pattern Formation : An Introduction to Methods* (Cambridge, 2006)

0.7 Biological Applications

◇ J. D. Murray, *Mathematical Biology*, (3rd ed., 2 vols.) (Springer, 2002)

- E. M. Izhikevich, *Dynamical Systems in Neuroscience* (MIT Press, 2007)

- L. Edelstein-Keshet, *Mathematical Models in Biology* (SIAM, 2005)

- J. Hofbauer and K. Sigmund, *Evolutionary Games and Population Dynamics* (Cambridge, 1998)

- M. A. Nowak, *Evolutionary Dynamics* (Harvard, 2006)

Chapter 1

Dynamical Systems

1.1 Introduction

1.1.1 Phase space and phase curves

Dynamics is the study of motion through phase space. The phase space of a given dynamical system is described as an N-dimensional manifold, $\mathcal{M}$. A (differentiable) manifold $\mathcal{M}$ is a topological space that is locally diffeomorphic to $\mathbb{R}^N$.[1] Typically in this course $\mathcal{M}$ will $\mathbb{R}^N$ itself, but other common examples include the circle $\mathbb{S}^1$, the torus $\mathbb{T}^2$, the sphere $\mathbb{S}^2$, *etc.*

Let $g_t \colon \mathcal{M} \to \mathcal{M}$ be a one-parameter family of transformations from $\mathcal{M}$ to itself, with $g_{t=0} = 1$, the identity. We call g_t the t-advance mapping. It satisfies the composition rule

$$g_t\, g_s = g_{t+s} \ . \tag{1.1}$$

Let us choose a point $\boldsymbol{\varphi}_0 \in \mathcal{M}$. Then we write $\boldsymbol{\varphi}(t) = g_t\, \boldsymbol{\varphi}_0$, which also is in $\mathcal{M}$. The set $\big\{ g_t\, \boldsymbol{\varphi}_0 \,\big|\, t \in \mathbb{R}\,,\, \boldsymbol{\varphi}_0 \in \mathcal{M} \big\}$ is called a *phase curve*. A graph of the motion $\boldsymbol{\varphi}(t)$ in the product space $\mathbb{R} \times \mathcal{M}$ is called an *integral curve*.

1.1.2 Vector fields

The *velocity* vector $\boldsymbol{V}(\boldsymbol{\varphi})$ is given by the derivative

$$\boldsymbol{V}(\boldsymbol{\varphi}) = \frac{d}{dt}\bigg|_{t=0} g_t\, \boldsymbol{\varphi} \ . \tag{1.2}$$

The velocity $\boldsymbol{V}(\boldsymbol{\varphi})$ is an element of the *tangent space* to $\mathcal{M}$ at $\boldsymbol{\varphi}$, abbreviated $\mathrm{T}\mathcal{M}_{\boldsymbol{\varphi}}$. If $\mathcal{M}$ is N-dimensional, then so is each $\mathrm{T}\mathcal{M}_{\boldsymbol{\varphi}}$ (for all $\boldsymbol{p}$). However, $\mathcal{M}$ and $\mathrm{T}\mathcal{M}_{\boldsymbol{\varphi}}$ may

[1] A *diffeomorphism* $F \colon \mathcal{M} \to \mathcal{N}$ is a differentiable map with a differentiable inverse. This is a special type of *homeomorphism*, which is a continuous map with a continuous inverse.

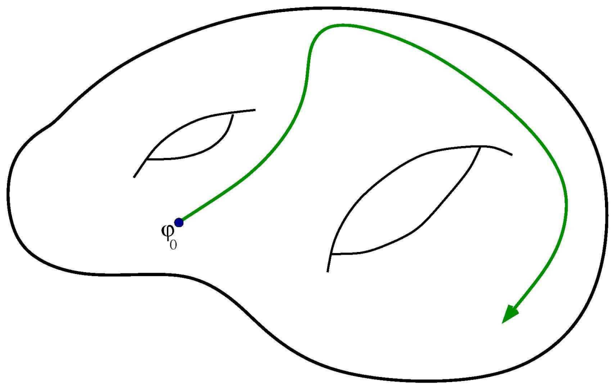

Figure 1.1: An example of a phase curve.

differ topologically. For example, if $\mathcal{M} = \mathbb{S}^1$, the circle, the tangent space at any point is isomorphic to $\mathbb{R}$.

For our purposes, we will take $\boldsymbol{\varphi} = (\varphi_1, \ldots, \varphi_N)$ to be an N-tuple, *i.e.* a point in $\mathbb{R}^N$. The equation of motion is then

$$\frac{d}{dt}\,\boldsymbol{\varphi}(t) = \boldsymbol{V}\big(\boldsymbol{\varphi}(t)\big) \ . \tag{1.3}$$

Note that any N^{th} order ODE, of the general form

$$\frac{d^N x}{dt^N} = F\bigg(x, \frac{dx}{dt}, \ldots, \frac{d^{N-1}x}{dt^{N-1}}\bigg) \ , \tag{1.4}$$

may be represented by the first order system $\dot{\boldsymbol{\varphi}} = \boldsymbol{V}(\boldsymbol{\varphi})$. To see this, define $\varphi_k = d^{k-1}x/dt^{k-1}$, with $k = 1, \ldots, N$. Thus, for $j < N$ we have $\dot\varphi_j = \varphi_{j+1}$, and $\dot\varphi_N = f$. In other words,

$$\overbrace{\frac{d}{dt}\begin{pmatrix} \varphi_1 \\ \vdots \\ \varphi_{N-1} \\ \varphi_N \end{pmatrix}}^{\dot{\boldsymbol{\varphi}}} = \overbrace{\begin{pmatrix} \varphi_2 \\ \vdots \\ \varphi_N \\ F\big(\varphi_1, \ldots, \varphi_N\big) \end{pmatrix}}^{\boldsymbol{V}(\boldsymbol{\varphi})} \ . \tag{1.5}$$

1.1.3 Existence / uniqueness / extension theorems

Theorem : Given $\dot{\boldsymbol{\varphi}} = \boldsymbol{V}(\boldsymbol{\varphi})$ and $\boldsymbol{\varphi}(0)$, if each $\boldsymbol{V}(\boldsymbol{\varphi})$ is a smooth vector field over some open set $\mathcal{D} \in \mathcal{M}$, then for $\boldsymbol{\varphi}(0) \in \mathcal{D}$ the initial value problem has a solution on some finite time interval $(-\tau, +\tau)$ and the solution is unique. Furthermore, the solution has a unique extension forward or backward in time, either indefinitely or until $\boldsymbol{\varphi}(t)$ reaches the boundary of $\mathcal{D}$.

Corollary : *Different trajectories never intersect!*

1.1.4 Linear differential equations

A homogeneous linear N^{th} order ODE,

$$\frac{d^N x}{dt^N} + c_{N-1}\,\frac{d^{N-1}x}{dt^{N-1}} + \ldots + c_1\,\frac{dx}{dt} + c_0\,x = 0 \tag{1.6}$$

may be written in matrix form, as

$$\frac{d}{dt}\begin{pmatrix} \varphi_1 \\ \varphi_2 \\ \vdots \\ \varphi_N \end{pmatrix} = \overbrace{\begin{pmatrix} 0 & 1 & 0 & \cdots & 0 \\ 0 & 0 & 1 & \cdots & 0 \\ \vdots & \vdots & \vdots & & \vdots \\ -c_0 & -c_1 & -c_2 & \cdots & -c_{N-1} \end{pmatrix}}^{M} \begin{pmatrix} \varphi_1 \\ \varphi_2 \\ \vdots \\ \varphi_N \end{pmatrix} . \tag{1.7}$$

Thus,

$$\dot{\boldsymbol{\varphi}} = M\boldsymbol{\varphi} \ , \tag{1.8}$$

and if the coefficients c_k are time-independent, *i.e.* the ODE is *autonomous*, the solution is obtained by exponentiating the constant matrix Q:

$$\boldsymbol{\varphi}(t) = \exp(Mt)\,\boldsymbol{\varphi}(0) \ ; \tag{1.9}$$

the exponential of a matrix may be given meaning by its Taylor series expansion. If the ODE is not autonomous, then $M = M(t)$ is time-dependent, and the solution is given by the path-ordered exponential,

$$\boldsymbol{\varphi}(t) = \mathcal{P}\exp\left\{\int_0^t dt'\,M(t')\right\}\boldsymbol{\varphi}(0) \ , \tag{1.10}$$

As defined, the equation $\dot{\boldsymbol{\varphi}} = \boldsymbol{V}(\boldsymbol{\varphi})$ is autonomous, since g_t depends only on t and on no other time variable. However, by extending the phase space from $\mathcal{M}$ to $\mathbb{R}\times\mathcal{M}$, which is of dimension $(N+1)$, one can describe arbitrary time-dependent ODEs.

1.1.5 Lyapunov functions

For a general dynamical system $\dot{\boldsymbol{\varphi}} = \boldsymbol{V}(\boldsymbol{\varphi})$, a *Lyapunov function* $L(\boldsymbol{\varphi})$ is a function which satisfies

$$\boldsymbol{\nabla} L(\boldsymbol{\varphi})\cdot\boldsymbol{V}(\boldsymbol{\varphi}) \le 0 \ . \tag{1.11}$$

There is no simple way to determine whether a Lyapunov function exists for a given dynamical system, or, if it does exist, what the Lyapunov function is. However, if a Lyapunov function can be found, then this severely limits the possible behavior of the system. This is because $L\big(\boldsymbol{\varphi}(t)\big)$ must be a monotonic function of time:

$$\frac{d}{dt}\,L\big(\boldsymbol{\varphi}(t)\big) = \boldsymbol{\nabla} L\cdot\frac{d\boldsymbol{\varphi}}{dt} = \boldsymbol{\nabla} L(\boldsymbol{\varphi})\cdot\boldsymbol{V}(\boldsymbol{\varphi}) \le 0 \ . \tag{1.12}$$

Thus, the system evolves toward a local minimum of the Lyapunov function. In general this means that oscillations are impossible in systems for which a Lyapunov function exists. For example, the relaxational dynamics of the magnetization M of a system are sometimes modeled by the equation

$$\frac{dM}{dt} = -\Gamma \, \frac{\partial F}{\partial M} \ , \tag{1.13}$$

where $F(M,T)$ is the *free energy* of the system. In this model, assuming constant temperature T, $\dot{F} = F'(M)\,\dot{M} = -\Gamma\,\big[F'(M)\big]^2 \le 0$. So the free energy $F(M)$ itself is a Lyapunov function, and it monotonically decreases during the evolution of the system. We shall meet up with this example again in the next chapter when we discuss imperfect bifurcations.

1.2 $N = 1$ Systems

We now study phase flows in a one-dimensional phase space, governed by the equation

$$\frac{du}{dt} = f(u) \ . \tag{1.14}$$

Again, the equation $\dot{u} = h(u,t)$ is first order, but not autonomous, and it corresponds to the $N = 2$ system,

$$\frac{d}{dt}\begin{pmatrix} u \\ t \end{pmatrix} = \begin{pmatrix} h(u,t) \\ 1 \end{pmatrix} \ . \tag{1.15}$$

The equation 1.14 is easily integrated:

$$\frac{du}{f(u)} = dt \qquad \Longrightarrow \qquad \boxed{t - t_0 = \int\limits_{u_0}^{u} \frac{du'}{f(u')}} \ . \tag{1.16}$$

This gives $t(u)$; we must then invert this relationship to obtain $u(t)$.

Example : Suppose $f(u) = a - bu$, with a and b constant. Then

$$dt = \frac{du}{a - bu} = -b^{-1}\, d\ln(a - bu) \tag{1.17}$$

whence

$$t = \frac{1}{b}\ln\left(\frac{a - b\,u(0)}{a - b\,u(t)}\right) \quad \Longrightarrow \quad u(t) = \frac{a}{b} + \Big(u(0) - \frac{a}{b}\Big)\exp(-bt) \ . \tag{1.18}$$

Even if one cannot analytically obtain $u(t)$, the behavior is very simple, and easily obtained by graphical analysis. Sketch the function $f(u)$. Then note that

$$\dot{u} = f(u) \quad \Longrightarrow \quad \begin{cases} f(u) > 0 & \dot{u} > 0 \quad \Rightarrow \quad \text{move to right} \\ f(u) < 0 & \dot{u} < 0 \quad \Rightarrow \quad \text{move to left} \\ f(u) = 0 & \dot{u} = 0 \quad \Rightarrow \quad \text{fixed point} \end{cases} \tag{1.19}$$

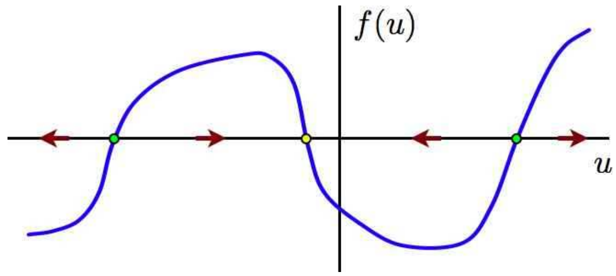

Figure 1.2: Phase flow for an $N = 1$ system.

The behavior of $N = 1$ systems is particularly simple: $u(t)$ flows to the first stable fixed point encountered, where it then (after a logarithmically infinite time) stops. The motion is monotonic – the velocity $\dot{u}$ never changes sign. Thus, *oscillations never occur for $N = 1$ phase flows.*[2]

1.2.1 Classification of fixed points ($N = 1$)

A *fixed point* u^* satisfies $f(u^*) = 0$. Generically, $f'(u^*) \neq 0$ at a fixed point.[3] Suppose $f'(u^*) < 0$. Then to the left of the fixed point, the function $f(u < u^*)$ is positive, and the flow is to the right, *i.e.* toward u^*. To the right of the fixed point, the function $f(u > u^*)$ is negative, and the flow is to the left, *i.e.* again toward u^*. Thus, when $f'(u^*) < 0$ the fixed point is said to be *stable*, since the flow in the vicinity of u^* is to u^*. Conversely, when $f'(u^*) > 0$, the flow is always away from u^*, and the fixed point is then said to be *unstable*. Indeed, if we linearize about the fixed point, and let $\epsilon \equiv u - u^*$, then

$$\dot{\epsilon} = f'(u^*)\,\epsilon + \tfrac{1}{2}\,f''(u^*)\,\epsilon^2 + \mathcal{O}(\epsilon^3) \ , \tag{1.20}$$

and dropping all terms past the first on the RHS gives

$$\epsilon(t) = \exp\Big[f'(u^*)\,t\Big]\,\epsilon(0) \ . \tag{1.21}$$

The deviation decreases exponentially for $f'(u^*) < 0$ and increases exponentially for $f(u^*) > 0$. Note that

$$t(\epsilon) = \frac{1}{f'(u^*)}\,\ln\left(\frac{\epsilon}{\epsilon(0)}\right) \ , \tag{1.22}$$

so the approach to a stable fixed point takes a logarithmically infinite time. For the unstable case, the deviation grows exponentially, until eventually the linearization itself fails.

[2]When I say 'never' I mean 'sometimes' – see the section 1.3.

[3]The system $f(u^*) = 0$ and $f'(u^*) = 0$ is overdetermined, with two equations for the single variable u^*.

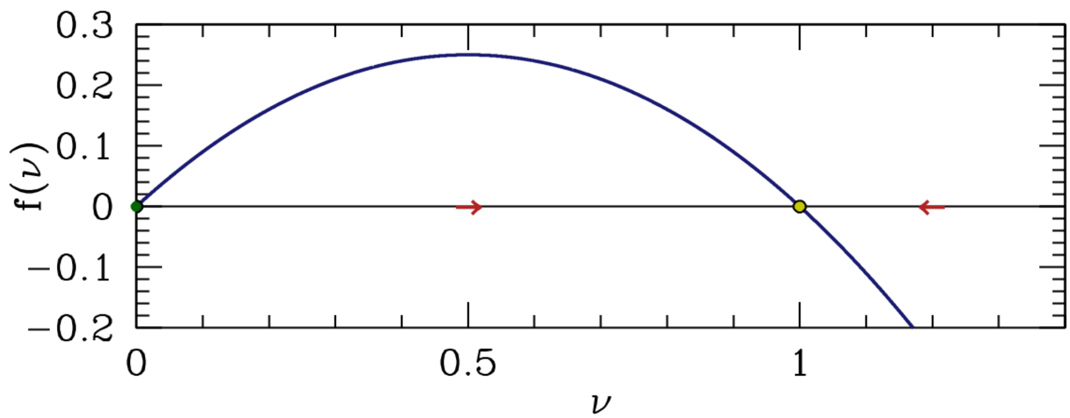

Figure 1.3: Flow diagram for the logistic equation.

1.2.2 Logistic equation

This model for population growth was first proposed by Verhulst in 1838. Let N denote the population in question. The dynamics are modeled by the first order ODE,

$$\frac{dN}{dt} = rN\Big(1 - \frac{N}{K}\Big) \ , \tag{1.23}$$

where N, r, and K are all positive. For $N \ll K$ the growth rate is r, but as N increases a quadratic nonlinearity kicks in and the rate vanishes for $N = K$ and is negative for $N > K$. The nonlinearity models the effects of competition between the organisms for food, shelter, or other resources. Or maybe they crap all over each other and get sick. Whatever.

There are two fixed points, one at $N^* = 0$, which is unstable ($f'(0) = r > 0$). The other, at $N^* = K$, is stable ($f'(K) = -r$). The equation is adimensionalized by defining $\nu = N/K$ and $s = rt$, whence

$$\dot{\nu} = \nu(1-\nu) \ . \tag{1.24}$$

Integrating,

$$\frac{d\nu}{\nu(1-\nu)} = d\ln\Big(\frac{\nu}{1-\nu}\Big) = ds \qquad \Longrightarrow \qquad \boxed{\nu(s) = \frac{\nu_0}{\nu_0 + \big(1-\nu_0\big)\exp(-s)}} \ . \tag{1.25}$$

As $s \to \infty$, $\nu(s) = 1 - \big(\nu_0^{-1} - 1\big)\, e^{-s} + \mathcal{O}(e^{-2s})$, and the relaxation to equilibrium ($\nu^* = 1$) is exponential, as usual.

Another application of this model is to a simple autocatalytic reaction, such as

$$A + X \rightleftharpoons 2X \ , \tag{1.26}$$

i.e. X catalyses the reaction $A \longrightarrow X$. Assuming a fixed concentration of A, we have

$$\dot{x} = \kappa_+ \, a\, x - \kappa_- \, x^2 \ , \tag{1.27}$$

where x is the concentration of X, and $\kappa_\pm$ are the forward and backward reaction rates.

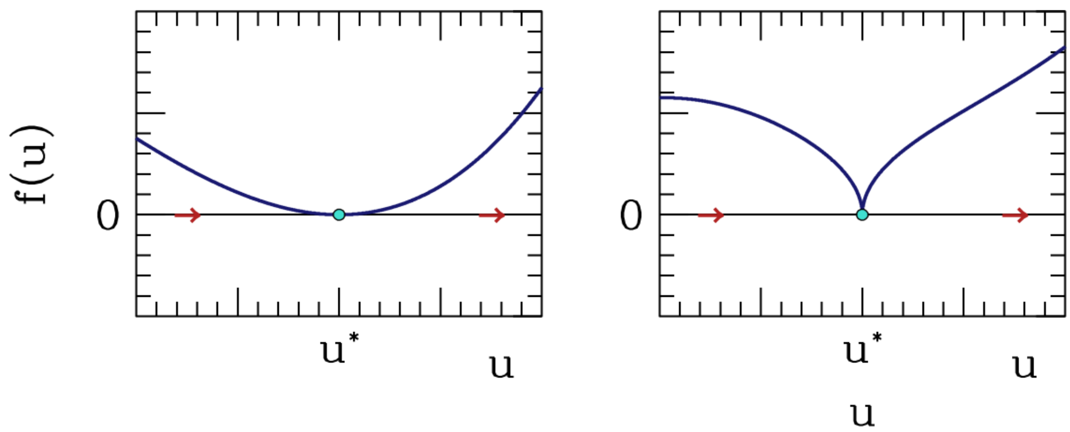

Figure 1.4: $f(u) = A\left|u - u^*\right|^\alpha$, for $\alpha > 1$ and $\alpha < 1$.

1.2.3 Singular $f(u)$

Suppose that in the vicinity of a fixed point we have $f(u) = A\left|u - u^*\right|^\alpha$, with $A > 0$. We now analyze both sides of the fixed point.

$u < u^*$: Let $\epsilon = u^* - u$. Then

$$\dot{\epsilon} = -A\,\epsilon^\alpha \quad \Longrightarrow \quad \frac{\epsilon^{1-\alpha}}{1-\alpha} = \frac{\epsilon_0^{1-\alpha}}{1-\alpha} - At \ , \tag{1.28}$$

hence

$$\epsilon(t) = \Big[\epsilon_0^{1-\alpha} + (\alpha - 1)A\,t\Big]^{\frac{1}{1-\alpha}} \ . \tag{1.29}$$

This, for $\alpha < 1$ the fixed point $\epsilon = 0$ is reached in a finite time: $\epsilon(t_c) = 0$, with

$$t_c = \frac{\epsilon_0^{1-\alpha}}{(1-\alpha)\,A} \ . \tag{1.30}$$

For $\alpha > 1$, we have $\lim_{t\to\infty} \epsilon(t) = 0$, but $\epsilon(t) > 0 \ \forall\ t < \infty$.

The fixed point $u = u^*$ is now *half-stable* – the flow from the left is toward u^* but from the right is away from u^*. Let's analyze the flow on either side of u^*.

$u > u^*$: Let $\epsilon = u - u^*$. Then $\dot{\epsilon} = A\,\epsilon^\alpha$, and

$$\epsilon(t) = \Big[\epsilon_0^{1-\alpha} + (1 - \alpha)A\,t\Big]^{\frac{1}{1-\alpha}} \ . \tag{1.31}$$

For $\alpha < 1$, $\epsilon(t)$ escapes to $\epsilon = \infty$ only after an infinite time. For $\alpha > 1$, the escape to infinity takes a finite time: $\epsilon(t_c) = \infty$, with

$$t_c = \frac{\epsilon_0^{1-\alpha}}{(\alpha-1)\,A} \ . \tag{1.32}$$

In both cases, higher order terms in the (nonanalytic) expansion of $f(u)$ about $u = u^*$ will eventually come into play.

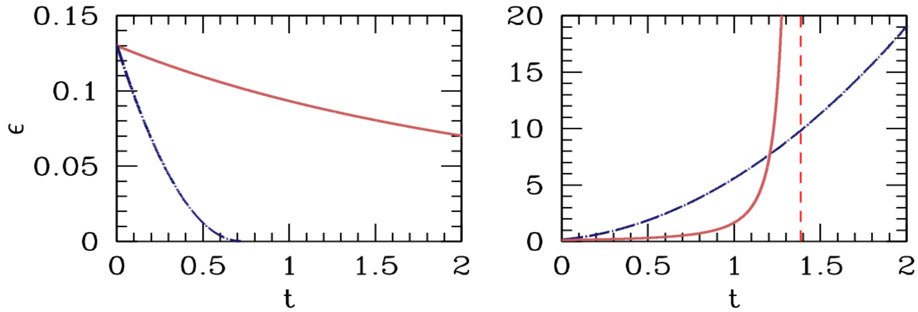

Figure 1.5: Solutions to $\dot{\epsilon} = \mp A\,\epsilon^{\alpha}$. Left panel: $\epsilon = u^* - u$, with $\alpha = 1.5$ (solid red) and $\alpha = 0.5$ (dot-dashed blue); $A = 1$ in both cases. Right panel: $\epsilon = u - u^*$, $\alpha = 1.5$ (solid red) and $\alpha = 0.5$ (dot-dashed blue); $A = 4$ in both cases

1.2.4 Recommended exercises

It is constructive to sketch the phase flows for the following examples:

$$
\begin{aligned}
\dot{v} &= -g & \dot{u} &= A\sin(u) \\
m\dot{v} &= -mg - \gamma v & \dot{u} &= A\,(u-a)(u-b)(u-c) \\
m\dot{v} &= -mg - cv^2\,\mathrm{sgn}(v) & \dot{u} &= au^2 - bu^3 \ .
\end{aligned}
$$

In each case, identify all the fixed points and assess their stability. Assume all constants A, a, b, c, γ, *etc.* are positive.

1.2.5 Non-autonomous ODEs

Non-autonomous ODEs of the form $\dot{u} = h(u,t)$ are in general impossible to solve by quadratures. One can always go to the computer, but it is worth noting that in the *separable* case, $h(u,t) = f(u)\,g(t)$, one can obtain the solution

$$
\frac{du}{f(u)} = g(t)\,dt \quad\Longrightarrow\quad \boxed{\int\limits_{u_0}^{u} \frac{du'}{f(u')} = \int\limits_{0}^{t} dt'\,g(t')} \ , \tag{1.33}
$$

which implicitly gives $u(t)$. Note that $\dot{u}$ may now change sign, and $u(t)$ may even oscillate. For an explicit example, consider the equation

$$
\dot{u} = A\,(u+1)\,\sin(\beta t) \ , \tag{1.34}
$$

the solution of which is

$$
u(t) = -1 + \big(u_0 + 1\big)\,\exp\left\{\frac{A}{\beta}\left[1 - \cos(\beta t)\right]\right\} . \tag{1.35}
$$

In general, the non-autonomous case defies analytic solution. Many have been studied, such as the Riccati equation,

$$\frac{du}{dt} = P(t)u^2 + Q(t)u + R(t) \ . \tag{1.36}$$

Riccati equations have the special and remarkable property that one can generate *all* solutions (*i.e.* with arbitrary boundary condition $u(0) = u_0$) from *any* given solution (*i.e.* with any boundary condition).

1.3 Flows on the Circle

We had remarked that oscillations are impossible for the equation $\dot{u} = f(u)$ because the flow is to the first stable fixed point encountered. If there are no stable fixed points, the flow is unbounded. However, suppose phase space itself is bounded, *e.g.* a circle $\mathbb{S}^1$ rather than the real line $\mathbb{R}$. Thus,

$$\dot{\theta} = f(\theta) \ , \tag{1.37}$$

with $f(\theta + 2\pi) = f(\theta)$. Now if there are no fixed points, $\theta(t)$ endlessly winds around the circle, and in this sense we can have oscillations.

1.3.1 Nonuniform oscillator

A particularly common example is that of the nonuniform oscillator,

$$\dot{\theta} = \omega - \sin\theta \ , \tag{1.38}$$

which has applications to electronics, biology, classical mechanics, and condensed matter physics. Note that the general equation $\dot{\theta} = \omega - A\sin\theta$ may be rescaled to the above form. A simple application is to the dynamics of a driven, overdamped pendulum. The equation of motion is

$$I\ddot{\theta} + b\,\dot{\theta} + I\omega_0^2 \sin\theta = N \ , \tag{1.39}$$

where I is the moment of inertia, b is the damping parameter, N is the external torque (presumed constant), and ω_0 is the frequency of small oscillations when $b = N = 0$. When b is large, the inertial term $I\ddot{\theta}$ may be neglected, and after rescaling we arrive at eqn. 1.38.

The book by Strogatz provides a biological example of the nonuniform oscillator: fireflies. An individual firefly will on its own flash at some frequency f. This can be modeled by the equation $\dot{\phi} = \beta$, where $\beta = 2\pi f$ is the angular frequency. A flash occurs when $\phi = 2\pi n$ for $n \in \mathbb{Z}$. When subjected to a periodic stimulus, fireflies will attempt to synchronize their flash to the flash of the stimulus. Suppose the stimulus is periodic with angular frequency $\varOmega$. The firefly synchronization is then modeled by the equation

$$\dot{\phi} = \beta - A\sin(\phi - \varOmega t) \ . \tag{1.40}$$

Here, A is a measure of the firefly's ability to modify its natural frequency in response to the stimulus. Note that when $0 < \phi - \varOmega t < \pi$, *i.e.* when the firefly is leading the stimulus,

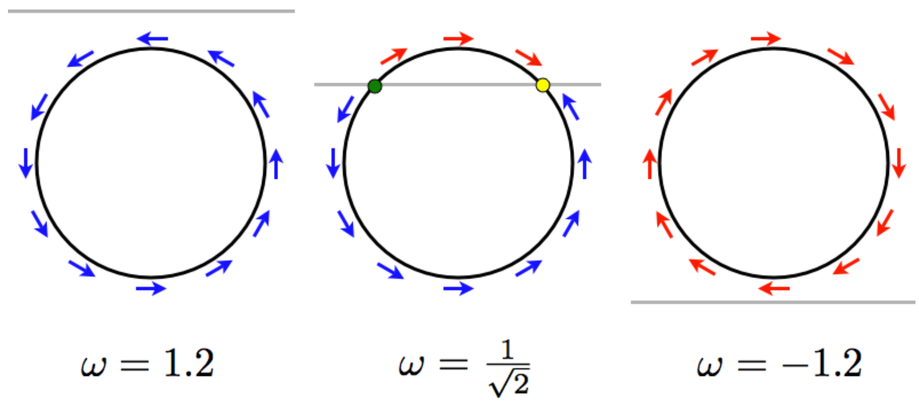

Figure 1.6: Flow for the nonuniform oscillator $\dot{\theta} = \omega - \sin\theta$ for three characteristic values of ω.

the dynamics tell the firefly to slow down. Conversely, when $-\pi < \phi - \Omega t < 0$, the firefly is lagging the stimulus, the the dynamics tell it to speed up. Now focus on the difference $\theta \equiv \phi - \Omega t$. We have

$$\dot{\theta} = \beta - \Omega - A\sin\theta \ , \tag{1.41}$$

which is the nonuniform oscillator. We can adimensionalize by defining

$$s \equiv At \quad , \quad \omega \equiv \frac{\beta - \Omega}{A} \ , \tag{1.42}$$

yielding $\frac{d\theta}{ds} = \omega - \sin\theta$.

Fixed points occur only for $\omega < 1$, for $\sin\theta = \omega$. To integrate, set $z = \exp(i\theta)$, in which case

$$\begin{aligned} \dot{z} &= -\tfrac{1}{2}(z^2 - 2i\omega z - 1) \\ &= -\tfrac{1}{2}(z - z_-)(z - z_+) \ , \end{aligned} \tag{1.43}$$

where $\nu = \sqrt{1-\omega^2}$ and $z_\pm = i\omega \pm \nu$. Note that for $\omega^2 < 1$, ν is real, and $z(t \to \mp\infty) = z_\pm$. This equation can easily be integrated, yielding

$$z(t) = \frac{(z(0) - z_-)\, z_+ - (z(0) - z_+)\, z_- \ \exp(\nu t)}{(z(0) - z_-) - (z(0) - z_+)\ \exp(\nu t)} \ , \tag{1.44}$$

For $\omega^2 > 1$, the motion is periodic, with period

$$T = \int\limits_0^{2\pi} \frac{d\theta}{|\omega| - \sin\theta} = \frac{2\pi}{\sqrt{\omega^2 - 1}} \ . \tag{1.45}$$

The situation is depicted in Fig. 1.6.

1.4 Appendix I : Evolution of Phase Space Volumes

Recall the general form of a dynamical system, $\dot{\boldsymbol{\varphi}} = \boldsymbol{V}(\boldsymbol{\varphi})$. Usually we are interested in finding integral curves $\boldsymbol{\varphi}(t)$. However, consider for the moment a collection of points in phase space comprising a region $\mathcal{R}$. As the dynamical system evolves, this region will also evolve, so that $\mathcal{R} = \mathcal{R}(t)$. We now ask: how does the volume of $\mathcal{R}(t)$,

$$\text{vol}\big[\mathcal{R}(t)\big] = \int\limits_{\mathcal{R}(t)} d\mu \ , \tag{1.46}$$

where $d\mu = d\varphi_1 d\varphi_2 \cdots d\varphi_N$ is the phase space measure, change with time. We have, explicitly,

$$\begin{aligned} \text{vol}\big[\mathcal{R}(t+dt)\big] &= \int\limits_{\mathcal{R}(t+dt)} d\mu \\ &= \int\limits_{\mathcal{R}(t)} d\mu \left\| \frac{\partial\varphi_i(t+dt)}{\partial\varphi_j(t)} \right\| \\ &= \int\limits_{\mathcal{R}(t)} d\mu \left\{ 1 + \boldsymbol{\nabla}\!\cdot\!\boldsymbol{V}\, dt + \mathcal{O}\big((dt)^2\big) \right\} \ , \end{aligned} \tag{1.47}$$

since

$$\frac{\partial\varphi_i(t+dt)}{\partial\varphi_j(t)} = \delta_{ij} + \frac{\partial V_i}{\partial\varphi_j}\bigg|_{\boldsymbol{\varphi}(t)} dt + \mathcal{O}\big((dt)^2\big) \ , \tag{1.48}$$

and, using $\ln\det M = \mathrm{Tr}\ln M$,

$$\det(1+\epsilon A) = 1 + \epsilon\,\mathrm{Tr}A + \mathcal{O}(\epsilon^2) \ . \tag{1.49}$$

Thus,

$$\frac{d}{dt}\,\text{vol}\big[\mathcal{R}(t)\big] = \int\limits_{\mathcal{R}(t)} d\mu\, \boldsymbol{\nabla}\!\cdot\!\boldsymbol{V} \tag{1.50}$$

$$= \int\limits_{\partial\mathcal{R}(t)} d\Sigma\, \hat{\boldsymbol{n}}\cdot\boldsymbol{V} \ , \tag{1.51}$$

where in the last line we have used Stokes' theorem to convert the volume integral over $\mathcal{R}$ to a surface integral over its boundary $\partial\mathcal{R}$.

1.5 Appendix II : Lyapunov Characteristic Exponents

Suppose $\boldsymbol{\varphi}(t)$ is an integral curve – *i.e.* a solution of $\dot{\boldsymbol{\varphi}} = \boldsymbol{V}(\boldsymbol{\varphi})$. We now ask: how do nearby trajectories behave? Do they always remain close to $\boldsymbol{\varphi}(t)$ for all t? To answer this, we write $\widetilde{\boldsymbol{\varphi}}(t) \equiv \boldsymbol{\varphi}(t) + \boldsymbol{\eta}(t)$, in which case

$$\frac{d}{dt}\,\eta_i(t) = M_{ij}(t)\,\eta_j(t) + \mathcal{O}\big(\eta^2\big) \ , \tag{1.52}$$

where

$$M_{ij}(t) = \frac{\partial V_i}{\partial \varphi_j}\bigg|_{\boldsymbol{\varphi}(t)} \ . \tag{1.53}$$

The solution, valid to first order in $\delta\varphi$, is

$$\eta_i(t) = Q_{ij}(t,t_0)\,\eta_j(t_0) \ , \tag{1.54}$$

where the matrix $Q(t,t_0)$ is given by the *path ordered exponential,*

$$Q(t,t_0) = \mathcal{P}\exp\Bigg\{\int\limits_{t_0}^{t} dt'\,M(t')\Bigg\} \tag{1.55}$$

$$\equiv \lim_{N\to\infty}\Big(1+\frac{\Delta t}{N}\,M(t_{N-1})\Big)\cdots\Big(1+\frac{\Delta t}{N}\,M(t_1)\Big)\,\Big(1+\frac{\Delta t}{N}\,M(t_0)\Big) \ , \tag{1.56}$$

with $\Delta t = t - t_0$ and $t_j = t_0 + (j/N)\Delta t$. $\mathcal{P}$ is the *path ordering operator*, which places earlier times to the right:

$$\mathcal{P}\,A(t)\,B(t') = \begin{cases} A(t)\,B(t') & \text{if } t > t' \\ \\ B(t')\,A(t) & \text{if } t < t' \ . \end{cases} \tag{1.57}$$

The distinction is important if $\big[A(t),B(t')\big] \neq 0$. Note that Q satisfies the composition property,

$$Q(t,t_0) = Q(t,t_1)\,Q(t_1,t_0) \tag{1.58}$$

for any $t_1 \in [t_0,t]$. When M is time-independent, as in the case of a *fixed point* where $\boldsymbol{V}(\boldsymbol{\varphi}^*) = 0$, the path ordered exponential reduces to the ordinary exponential, and $Q(t,t_0) = \exp\big(M(t-t_0)\big)$.

Generally it is impossible to analytically compute path-ordered exponentials. However, the following example may be instructive. Suppose

$$M(t) = \begin{cases} M_1 & \text{if } t/T \in \big[2j, 2j+1\big] \\ \\ M_2 & \text{if } t/T \in \big[2j+1, 2j+2\big] \ , \end{cases} \tag{1.59}$$

for all integer j. $M(t)$ is a 'matrix-valued square wave', with period $2T$. Then, integrating over one period, from $t=0$ to $t=2T$, we have

$$A \equiv \ \exp\Bigg\{\int\limits_0^{2T} dt\,M(t)\Bigg\} = e^{(M_1+M_2)\,T} \tag{1.60}$$

$$A_{\mathcal{P}} \equiv \mathcal{P}\exp\Bigg\{\int\limits_0^{2T} dt\,M(t)\Bigg\} = e^{M_2\,T}\,e^{M_1\,T} \ . \tag{1.61}$$

In general, $A \neq A_{\mathcal{P}}$, so the path ordering has a nontrivial effect[4].

The Lyapunov exponents are defined in the following manner. Let $\hat{\boldsymbol{e}}$ be an N-dimensional unit vector. Define

$$\Lambda(\boldsymbol{\varphi}_0, \hat{\boldsymbol{e}}) \equiv \lim_{t\to\infty} \lim_{b\to 0} \frac{1}{t-t_0} \ln \left(\frac{\|\boldsymbol{\eta}(t)\|}{\|\boldsymbol{\eta}(t_0)\|} \right)_{\boldsymbol{\eta}(t_0)=b\,\hat{\boldsymbol{e}}} , \tag{1.62}$$

where $\|\cdot\|$ denotes the Euclidean norm of a vector, and where $\boldsymbol{\varphi}_0 = \boldsymbol{\varphi}\big(t_0\big)$. A theorem due to Oseledec guarantees that there are N such values $\Lambda_i(\boldsymbol{\varphi}_0)$, depending on the choice of $\hat{\boldsymbol{e}}$, for a given $\boldsymbol{\varphi}_0$. Specifically, the theorem guarantees that the matrix

$$\hat{\mathcal{Q}} \equiv \big(Q^{\rm t} Q\big)^{1/(t-t_0)} \tag{1.63}$$

converges in the limit $t \to \infty$ for almost all $\boldsymbol{\varphi}_0$. The eigenvalues Λ_i correspond to the different eigenspaces of R. Oseledec's theorem (also called the 'multiplicative ergodic theorem') guarantees that the eigenspaces of Q either grow ($\Lambda_i > 1$) or shrink ($\Lambda_i < 1$) *exponentially* fast. That is, the norm any vector lying in the $i^{\rm th}$ eigenspace of Q will behave as $\exp\big(\Lambda_i\,(t-t_0)\big)$, for $t \to \infty$.

Note that while $\hat{\mathcal{Q}} = \hat{\mathcal{Q}}^{\rm t}$ is symmetric by construction, Q is simply a general real-valued $N \times N$ matrix. The left and right eigenvectors of a matrix $M \in {\rm GL}(N, \mathbb{R})$ will in general be different. The set of eigenvalues λ_α is, however, common to both sets of eigenvectors. Let $\{\psi_\alpha\}$ be the right eigenvectors and $\{\chi^*_\alpha\}$ the left eigenvectors, such that

$$M_{ij}\,\psi_{\alpha,j} = \lambda_\alpha\,\psi_{\alpha,i} \tag{1.64}$$

$$\chi^*_{\alpha,i}\,M_{ij} = \lambda_\alpha\,\chi^*_{\alpha,j} \ . \tag{1.65}$$

We can always choose the left and right eigenvectors to be orthonormal, *viz.*

$$\big\langle\, \chi_\alpha \,\big|\, \psi_\beta \,\big\rangle = \chi^*_{\alpha,i}\,\psi_{\beta,j} = \delta_{\alpha\beta} \ . \tag{1.66}$$

Indeed, we can define the matrix $S_{i\alpha} = \psi_{\alpha,i}$, in which case $S^{-1}_{\alpha j} = \chi^*_{\alpha,j}$, and

$$S^{-1}\,M\,S = {\rm diag}\big(\lambda_1, \ldots, \lambda_N\big) \ . \tag{1.67}$$

The matrix M can always be decomposed into its eigenvectors, as

$$M_{ij} = \sum_\alpha \lambda_\alpha\,\psi_{\alpha,i}\,\chi^*_{\alpha,j} \ . \tag{1.68}$$

If we expand $\boldsymbol{u}$ in terms of the right eigenvectors,

$$\boldsymbol{\eta}(t) = \sum_\beta C_\beta(t)\,\boldsymbol{\psi}_\beta(t) \ , \tag{1.69}$$

[4] If $\big[M_1, M_2\big] = 0$ then $A = A_{\mathcal{P}}$.

then upon taking the inner product with $\boldsymbol{\chi}_\alpha$, we find that C_α obeys

$$\dot{C}_\alpha + \langle\, \chi_\alpha \,|\, \dot{\psi}_\beta \,\rangle\, C_\beta = \lambda_\alpha\, C_\alpha \ . \tag{1.70}$$

If $\dot{\boldsymbol{\psi}}_\beta = 0$, *e.g.* if M is time-independent, then $C_\alpha(t) = C_\alpha(0)\, e^{\lambda_\alpha t}$, and

$$\eta_i(t) = \sum_\alpha \overbrace{\sum_j \eta_j(0)\, \chi^*_{\alpha,j}}^{C_\alpha(0)}\ e^{\lambda_\alpha t}\, \psi_{\alpha,i} \ . \tag{1.71}$$

Thus, the component of $\boldsymbol{\eta}(t)$ along $\boldsymbol{\psi}_\alpha$ increases exponentially with time if $\mathrm{Re}(\lambda_\alpha) > 0$, and decreases exponentially if $\mathrm{Re}(\lambda_\alpha) < 0$.

Chapter 2

Bifurcations

2.1 Types of Bifurcations

2.1.1 Saddle-node bifurcation

We remarked above how $f'(u)$ is in general nonzero when $f(u)$ itself vanishes, since two equations in a single unknown is an overdetermined set. However, consider the function $F(x,\alpha)$, where α is a control parameter. If we demand $F(x,\alpha)=0$ and $\partial_x F(x,\alpha)=0$, we have two equations in two unknowns, and in general there will be a zero-dimensional solution set consisting of points $(x_{\rm c},\alpha_{\rm c})$. The situation is depicted in Fig. 2.1.

Let's expand $F(x,\alpha)$ in the vicinity of such a point $(x_{\rm c},\alpha_{\rm c})$:

$$\begin{aligned} F(x,\alpha) &= F(x_{\rm c},\alpha_{\rm c}) + \frac{\partial F}{\partial x}\bigg|_{(x_{\rm c},\alpha_{\rm c})}(x-x_{\rm c}) + \frac{\partial F}{\partial \alpha}\bigg|_{(x_{\rm c},\alpha_{\rm c})}(\alpha-\alpha_{\rm c}) + \frac{1}{2}\,\frac{\partial^2 F}{\partial x^2}\bigg|_{(x_{\rm c},\alpha_{\rm c})}(x-x_{\rm c})^2 \\ &\qquad + \frac{\partial^2 F}{\partial x\,\partial\alpha}\bigg|_{(x_{\rm c},\alpha_{\rm c})}(x-x_{\rm c})\,(\alpha-\alpha_{\rm c}) + \frac{1}{2}\,\frac{\partial^2 F}{\partial \alpha^2}\bigg|_{(x_{\rm c},\alpha_{\rm c})}(\alpha-\alpha_{\rm c})^2 + \ldots \qquad (2.1) \\ &= A\,(\alpha-\alpha_{\rm c}) + B\,(x-x_{\rm c})^2 + \ldots\ , \qquad (2.2) \end{aligned}$$

where we keep terms of lowest order in the deviations δx and $\delta\alpha$. If we now rescale $u \equiv \sqrt{B/A}\,(x-x_{\rm c})$, $r \equiv \alpha-\alpha_{\rm c}$, and $\tau = At$, we have, neglecting the higher order terms, we obtain the 'normal form' of the saddle-node bifurcation,

$$\frac{du}{d\tau} = r + u^2\ . \qquad (2.3)$$

The evolution of the flow is depicted in Fig. 2.2. For $r<0$ there are two fixed points – one stable ($u^* = -\sqrt{-r}$) and one unstable ($u = +\sqrt{-r}$). At $r=0$ these two nodes coalesce and annihilate each other. (The point $u^*=0$ is half-stable precisely at $r=0$.) For $r>0$ there are no longer any fixed points in the vicinity of $u=0$. In Fig. **??** we show the flow in the extended (r,u) plane. The unstable and stable nodes annihilate at $r=0$.

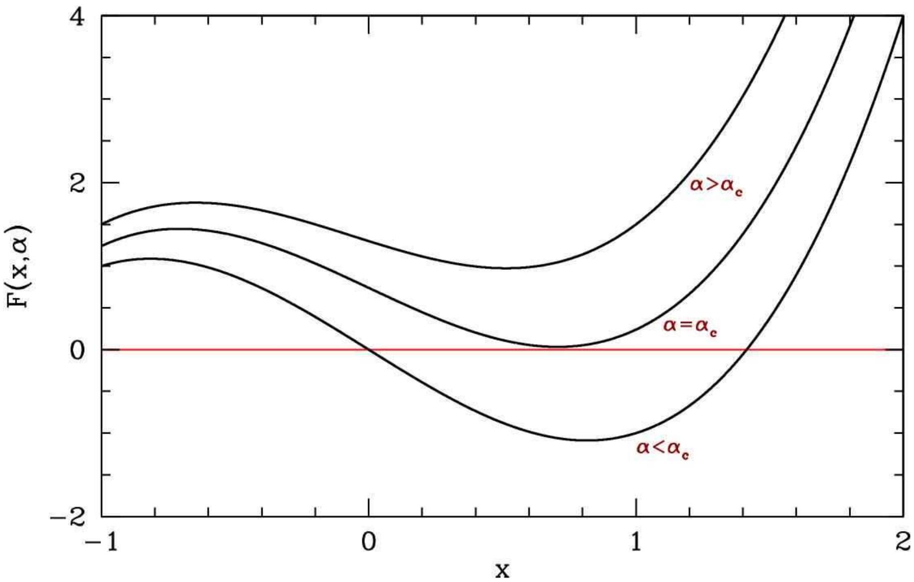

Figure 2.1: Evolution of $F(x,\alpha)$ as a function of the control parameter α.

2.1.2 Transcritical bifurcation

Another situation which arises frequently is the *transcritical bifurcation*. Consider the equation $\dot{x} = f(x)$ in the vicinity of a fixed point x^*.

$$\frac{dx}{dt} = f'(x^*)\,(x - x^*) + \tfrac{1}{2}\, f''(x^*)(x - x^*)^2 + \ldots \ . \tag{2.4}$$

We rescale $u \equiv \beta\,(x - x^*)$ with $\beta = -\frac{1}{2}\, f''(x^*)$ and define $r \equiv f'(x^*)$ as the control parameter, to obtain, to order u^2,

$$\frac{du}{dt} = ru - u^2 \ . \tag{2.5}$$

Note that the sign of the u^2 term can be reversed relative to the others by sending $u \to -u$ and $r \to -r$.

Consider a crude model of a laser threshold. Let n be the number of photons in the laser cavity, and N the number of excited atoms in the cavity. The dynamics of the laser are approximated by the equations

$$\dot{n} = GNn - kn \tag{2.6}$$

$$N = N_0 - \alpha n \ . \tag{2.7}$$

Here G is the gain coefficient and k the photon decay rate. N_0 is the pump strength, and α is a numerical factor. The first equation tells us that the number of photons in the cavity grows with a rate $GN - k$; gain is proportional to the number of excited atoms, and the loss rate is a constant cavity-dependent quantity (typically through the ends, which are semi-transparent). The second equation says that the number of excited atoms is equal to

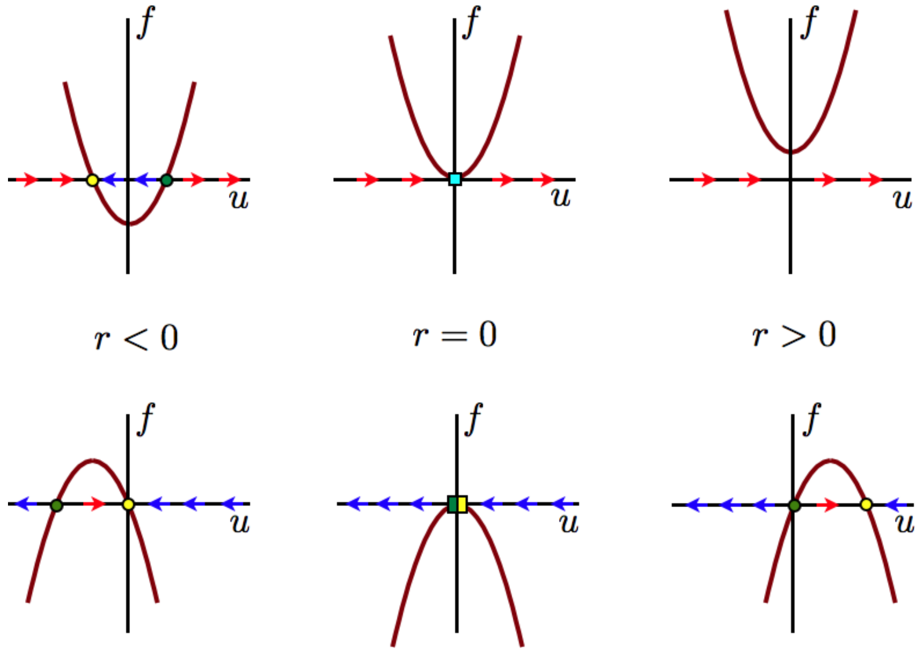

Figure 2.2: Flow diagrams for the saddle-node bifurcation $\dot{u} = r + u^2$ (top) and the transcritical bifurcation $\dot{u} = ru - u^2$ (bottom).

the pump strength minus a term proportional to the number of photons (since the presence of a photon means an excited atom has decayed). Putting them together,

$$\dot{n} = (GN_0 - k)\, n - \alpha G n^2 \ , \tag{2.8}$$

which exhibits a transcritical bifurcation at pump strength $N_0 = k/G$. For $N_0 < k/G$ the system acts as a lamp; for $N_0 > k/G$ the system acts as a laser.

What happens in the transcritical bifurcation is an exchange of stability of the fixed points at $u^* = 0$ and $u^* = r$ as r passes through zero. This is depicted graphically in the bottom panel of Fig. 2.2.

2.1.3 Pitchfork bifurcation

The pitchfork bifurcation is commonly encountered in systems in which there is an overall parity symmetry ($u \to -u$). There are two classes of pitchfork: supercritical and subcritical. The normal form of the supercritical bifurcation is

$$\dot{u} = ru - u^3 \ , \tag{2.9}$$

which has fixed points at $u^* = 0$ and $u^* = \pm\sqrt{r}$. Thus, the situation is as depicted in fig. 2.4 (top panel). For $r < 0$ there is a single stable fixed point at $u^* = 0$. For $r > 0$, $u^* = 0$ is unstable, and flanked by two stable fixed points at $u^* = \pm\sqrt{r}$.

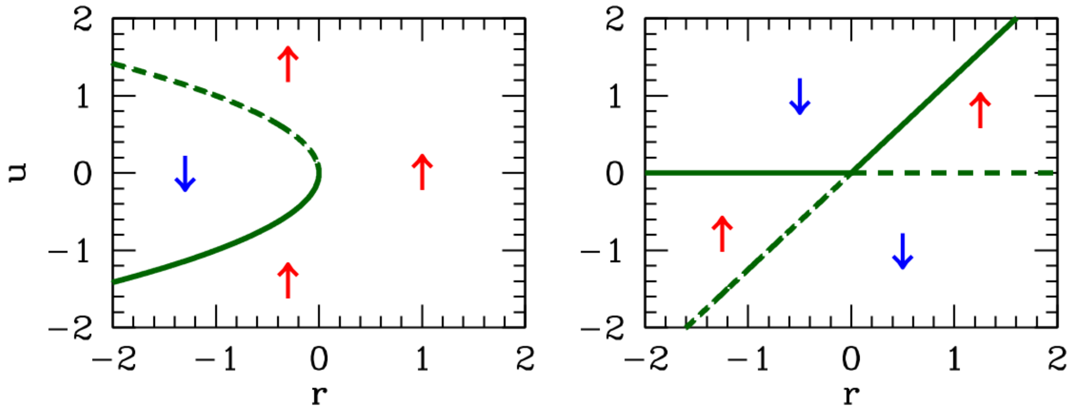

Figure 2.3: Extended phase space (r, u) flow diagrams for the saddle-node bifurcation $\dot{u} = r + u^2$ (left) and the transcritical bifurcation $\dot{u} = ru - u^2$ (right).

If we send $u \to -u$, $r \to -r$, and $t \to -t$, we obtain the *subcritical pitchfork*, depicted in the bottom panel of fig. 2.4. The normal form of the subcritical pitchfork bifurcation is

$$\dot{u} = ru + u^3 \ . \tag{2.10}$$

The fixed point structure in both supercritical and subcritical cases is shown in Fig. 2.5.

2.1.4 Imperfect bifurcation

The imperfect bifurcation occurs when a symmetry-breaking term is added to the pitchfork. The normal form contains two control parameters:

$$\dot{u} = h + ru - u^3 \ . \tag{2.11}$$

Here, the constant h breaks the parity symmetry if $u \to -u$.

This equation arises from a crude model of magnetization dynamics. Let M be the magnetization of a sample, and $F(M)$ the free energy. Assuming M is small, we can expand $F(M)$ as

$$F(M) = -HM + \tfrac{1}{2}aM^2 + \tfrac{1}{4}bM^4 + \ldots \ , \tag{2.12}$$

where H is the external magnetic field, and a and b are temperature-dependent constants. This is called the *Landau expansion* of the free energy. We assume $b > 0$ in order that the minimum of $F(M)$ not lie at infinity. The dynamics of $M(t)$ are modeled by

$$\frac{dM}{dt} = -\Gamma \, \frac{\partial F}{\partial M} \ , \tag{2.13}$$

with $\Gamma > 0$. Thus, the magnetization evolves toward a local minimum in the free energy. Note that the free energy is a decreasing function of time:

$$\frac{dF}{dt} = \frac{\partial F}{\partial M} \, \frac{dM}{dt} = -\Gamma \bigg(\frac{\partial F}{\partial M} \bigg)^{\!2} \ . \tag{2.14}$$

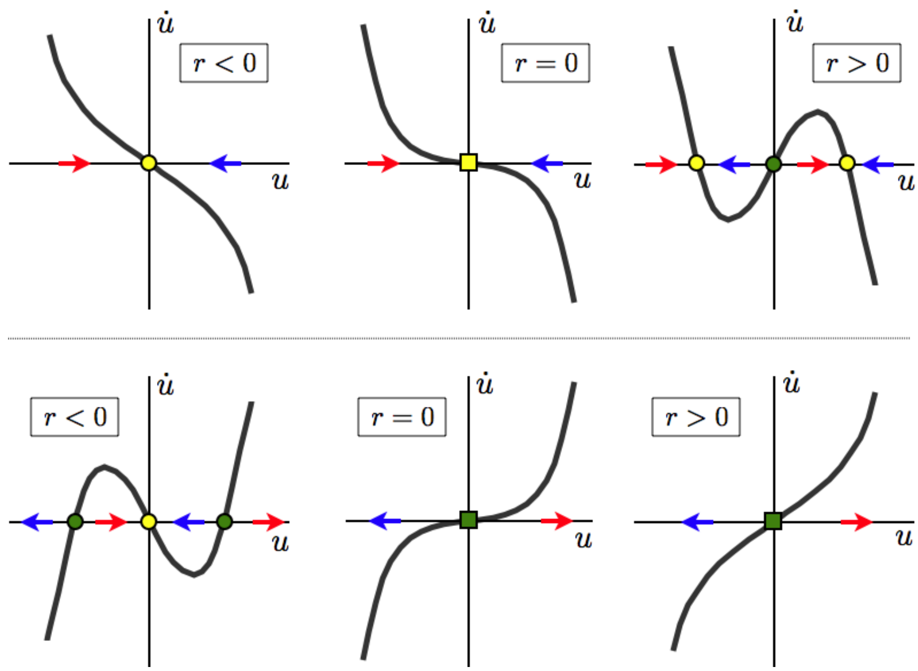

Figure 2.4: Top: supercritical pitchfork bifurcation $\dot{u} = ru - u^3$. Bottom: subcritical pitchfork bifurcation $\dot{u} = ru + u^3$.

By rescaling $M \equiv \alpha u$ with $\alpha = (b\,\Gamma)^{-1/2}$ and defining $r \equiv -(\Gamma/b)^{1/2}$ and $h \equiv (\Gamma^3\,b)^{1/2}\,H$, we obtain the normal form

$$\dot{u} = h + ru - u^3 = -\frac{\partial f}{\partial u} \tag{2.15}$$

$$f(u) = -\tfrac{1}{2}ru^2 + \tfrac{1}{4}u^4 - hu\ . \tag{2.16}$$

Here, $f(u)$ is a scaled version of the free energy.

Fixed points satisfy the equation

$$u^3 - ru - h = 0\ , \tag{2.17}$$

and correspond to extrema in $f(u)$. By the fundamental theorem of algebra, this cubic polynomial may be uniquely factorized over the complex plane. Since the coefficients are real, the complex conjugate $\bar{u}$ satisfies the same equation as u, hence there are two possibilities for the roots: either (i) all three roots are real, or (ii) one root is real and the other two are a complex conjugate pair. Clearly for $r<0$ we are in situation (ii) since $u^3 - ru$ is then monotonically increasing for $u \in \mathbb{R}$, and therefore takes the value h precisely once for u real. For $r>0$, there is a region $h \in \big[-h_c(r), h_c(r)\big]$ over which there are three real roots. To find $h_c(r)$, we demand $f''(u) = 0$ as well as $f'(u) = 0$, which says that two roots have merged, forming an inflection point. One easily finds $h_c(r) = \frac{2}{3\sqrt{3}}\,r^{3/2}$.

Examples of the function $f(u)$ for $r>0$ are shown in the left panel of Fig. 2.6 for three different values of h. For $|h| < h_c(r)$ there are three extrema satisfying $f'(u^*) = 0$: $u_1^* <$

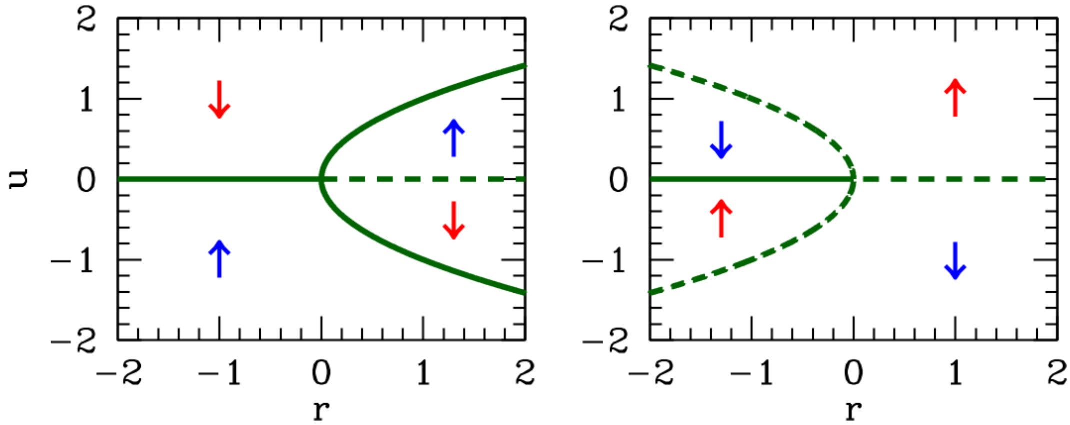

Figure 2.5: Extended phase space (r, u) flow diagrams for the supercritical pitchfork bifurcation $\dot{u} = ru - u^3$ (left), and subcritical pitchfork bifurcation $\dot{u} = ru + u^3$ (right).

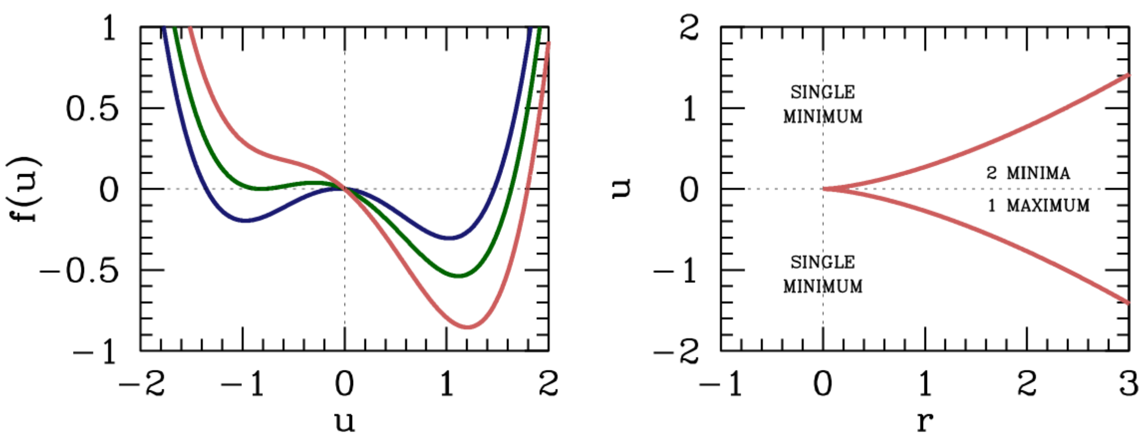

Figure 2.6: Left: scaled free energy $f(u) = -\frac{1}{2}ru^2 + \frac{1}{4}u^4 - hu$, with $h = 0.2\,h_c$ (blue), $h = h_c$ (green), and $h = 2\,h_c$ (red), where $h_c = \frac{2}{3\sqrt{3}}\,r^{3/2}$. Right: phase diagram for the imperfect bifurcation $\dot{u} = -f'(u) = h + ru - u^3$.

$u_2^* < 0 < u_3^*$, assuming (without loss of generality) that $h > 0$. Clearly u_1^* is a local minimum, u_2^* a local maximum, and u_3^* the global minimum of the function $f(u)$. The 'phase diagram' for this system, plotted in the (r, h) control parameter space, is shown in the right panel of Fig. 2.6.

In Fig. **??** we plot the fixed points $u^*(r)$ for fixed h. A saddle-node bifurcation occurs at $r = r_c(h) = \frac{3}{2^{2/3}}\,|h|^{2/3}$. For $h = 0$ this reduces to the supercritical pitchfork; for finite h the pitchfork is deformed and even changed topologically. Finally, in Fig. 2.7 we show the behavior of $u^*(h)$ for fixed r. When $r < 0$ the curve retraces itself as h is ramped up and down, but for $r > 0$ the system exhibits the phenomenon of *hysteresis*, *i.e.* there is an irreversible aspect to the behavior. Fig, 2.7 shows a *hysteresis loop* when $r > 0$.

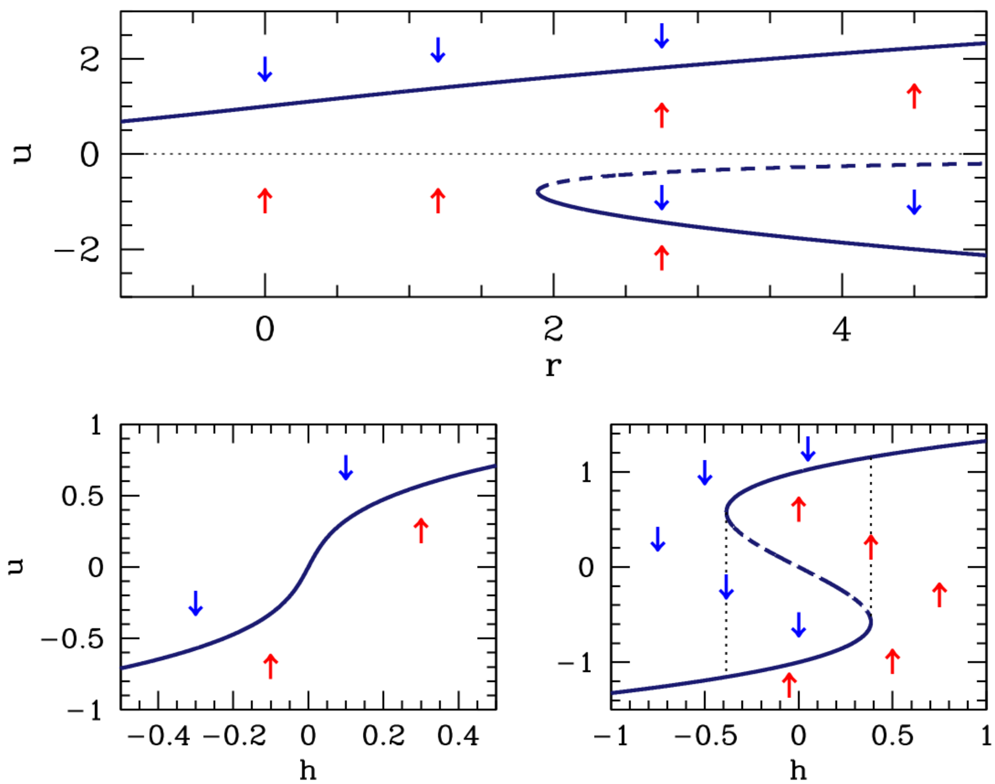

Figure 2.7: Top: extended phase space (r, u) flow diagram for the imperfect pitchfork bifurcation $\dot{u} = h + ru - u^3$ for $h = 1$. This is in a sense a deformed supercritical pitchfork. Bottom: extended phase space (h, u) flow diagram for the imperfect pitchfork bifurcation $r = -0.2$ (left panel) and $r = 1$ (right panel). For $r < 0$ the behavior is completely reversible. For $r > 0$, a regime of irreversibility sets in between $-h_c$ and $+h_c$, where $h_c = 2(r/3)^{3/2}$. The system then exhibits the phenomenon of hysteresis. The dotted vertical lines show the boundaries of the hysteresis loop.

2.2 Examples

2.2.1 Population dynamics

Consider the dynamics of a harvested population,

$$\dot{N} = rN\left(1 - \frac{N}{K}\right) - H(N) \ , \tag{2.18}$$

where $r, K > 0$, and where $H(N)$ is the *harvesting rate*.

`(a)` Suppose $H(N) = H_0$ is a constant. Sketch the phase flow, and identify and classify all fixed points.

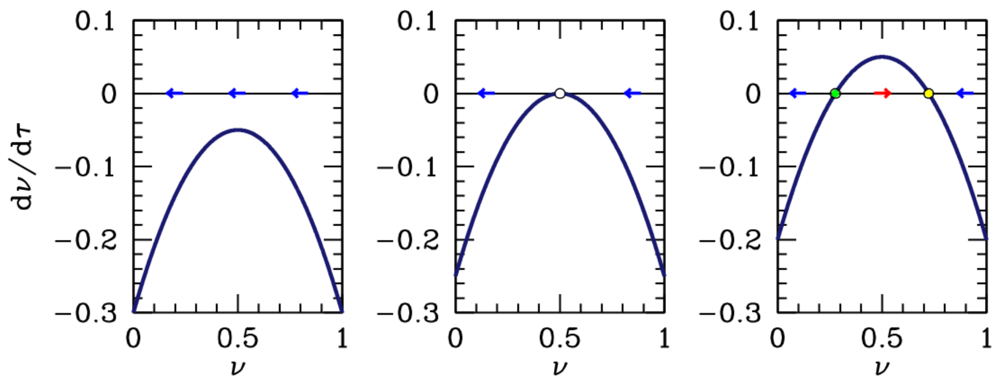

Figure 2.8: Phase flow for the constantly harvested population, $\dot{\nu} = \nu(1-\nu) - h$, for $h = 0.30$ (left), $h = 0.25$ (center), and $h = 0.20$ (right). The critical harvesting rate is $h_c = \frac{1}{4}$.

Solution : We examing $\dot{N} = f(N)$ with

$$f(N) = rN - \frac{r}{K}\,N^2 - H_0 \ . \tag{2.19}$$

Setting $f'(N) = 0$ yields $N = \frac{1}{2}K$. $f(N)$ is a downward-opening parabola whose maximum value is $f\big(\frac{1}{2}K\big) = \frac{1}{4}rK - H_0$. Thus, if $H_0 > \frac{1}{4}rK$, the harvesting rate is too large and the population always shrinks. A saddle-node bifurcation occurs at this value of H_0, and for larger harvesting rates, there are fixed points at

$$N_\pm = \tfrac{1}{2}K \pm \tfrac{1}{2}K\sqrt{1 - \frac{4H_0}{rK}} \ , \tag{2.20}$$

with N_- unstable and N_+ stable. By rescaling the population $\nu = N/K$, time $\tau = rt$ and harvesting rate $h = H_0/rK$, we arrive at the equation

$$\dot{\nu} = \nu(1-\nu) - h \ . \tag{2.21}$$

The critical harvesting rate is then $h_c = \frac{1}{4}$. See fig. 2.8.

(b) One defect of the constant harvesting rate model is that $N = 0$ is not a fixed point. To remedy this, consider the following model for $H(N)$:

$$H(N) = \frac{B\,N^2}{N^2 + A^2} \ , \tag{2.22}$$

where A and B are (positive) constants. Show that one can rescale (N, t) to (n, τ), such that

$$\frac{dn}{d\tau} = \gamma\, n\left(1 - \frac{n}{c}\right) - \frac{n^2}{n^2+1} \ , \tag{2.23}$$

where γ and c are positive constants. Provide expressions for n, τ, γ, and c.

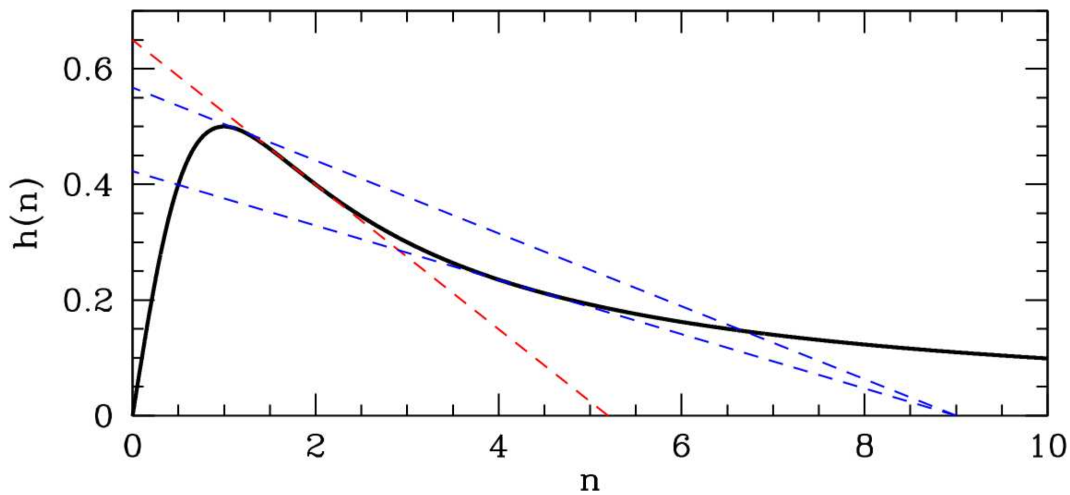

Figure 2.9: Plot of $h(n) = n/(n^2+1)$ (thick black curve). Straight lines show the function $y(n) = \gamma\big(1 - \frac{n}{c}\big)$ for different values of c and γ. The red line is tangent to the inflection point of $h(n)$ and determines the minimum value $c^* = 3\sqrt{3}$ for a bifurcation. The blue lines show the construction for determining the location of the two bifurcations for $c > c^*$ (in this case, $c = 9$). See the analysis in the text.

Solution : Examining the denominator of $H(N)$, we must take $N = An$. Dividing both sides of $\dot{N} = f(N)$ by B, we obtain

$$\frac{A}{B}\frac{dN}{dt} = \frac{rA}{B}\,n\Big(1 - \frac{A}{K}\,n\Big) - \frac{n^2}{n^2+1} \ ,$$

from which we glean $\tau = Bt/A$, $\gamma = rA/B$, and $c = K/A$.

`(c)` Show that for c sufficiently small that there is a unique asymptotic ($\tau \to \infty$) value for the (scaled) population n, for any given value of γ. Thus, there are no bifurcations as a function of the control parameter γ for c fixed and $c < c^*$.

`(d)` Show that for $c > c^*$, there are two bifurcations as a function of γ, and that for $\gamma_1^* < \gamma < \gamma_2^*$ the asymptotic solution is bistable, *i.e.* there are two stable values for $n(\tau \to \infty)$. Sketch the solution set 'phase diagram' in the (c, γ) plane. *Hint: Sketch the functions $\gamma(1 - n/c)$ and $n/(n^2+1)$. The $n \neq 0$ fixed points are given by the intersections of these two curves. Determine the boundary of the bistable region in the (c, γ) plane parametrically in terms of n.* Find c^* and $\gamma_1^*(c) = \gamma_2^*(c)$.

Solution `(c)` *and* `(d)` : We examine

$$\frac{dn}{d\tau} = g(n) = \left\{\gamma\Big(1 - \frac{n}{c}\Big) - \frac{n}{n^2+1}\right\} n \ . \tag{2.24}$$

There is an unstable fixed point at $n = 0$, where $g'(0) = \gamma > 0$. The other fixed points occur when the term in the curvy brackets vanishes. In fig. 2.9 we plot the function $h(n) \equiv n/(n^2+1)$ *versus* n. We seek the intersection of this function with a two-parameter

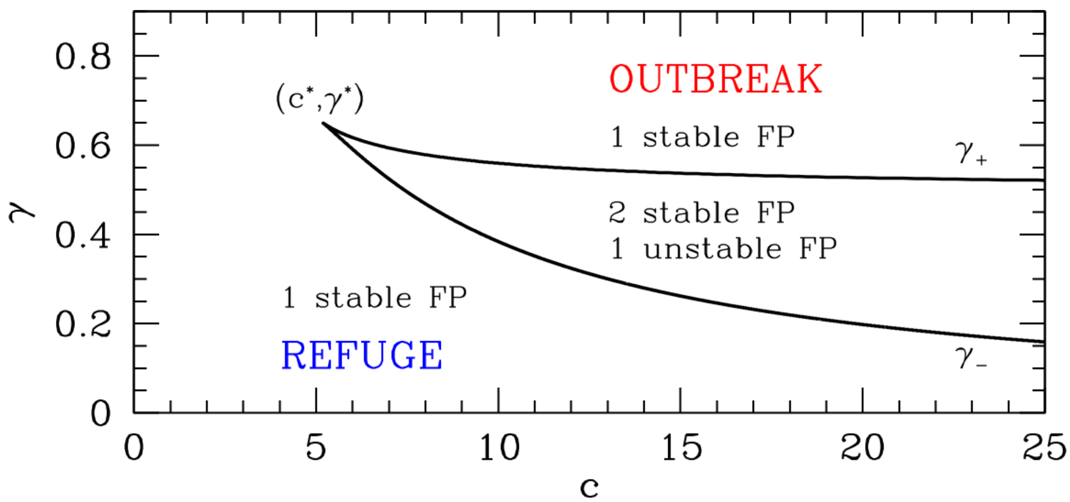

Figure 2.10: Phase diagram for the equation $\dot{n} = \gamma(1-n/c)\,n - n^2/(n^2+1)$, labeling $n \neq 0$ fixed points. (The point $n=0$ is always unstable.)

family of straight lines, given by $y(n) = \gamma\,(1-n/c)$. The n-intercept is c and the y-intercept is γ. Provided $c > c^*$ is large enough, there are two bifurcations as a function of γ, which we call $\gamma_\pm(c)$. These are shown as the dashed blue lines in figure 2.9 for $c=9$.

Both bifurcations are of the saddle-node type. We determine the curves $\gamma_\pm(c)$ by requiring that $h(n)$ is tangent to $y(n)$, which gives two equations:S

$$h(n) = \frac{n}{n^2+1} = \gamma\Big(1-\frac{n}{c}\Big) = y(n) \tag{2.25}$$

$$h'(n) = \frac{1-n^2}{(n^2+1)^2} = -\frac{\gamma}{c} = y'(n)\ . \tag{2.26}$$

Together, these give $\gamma(c)$ parametrically, *i.e.* as $\gamma(n)$ and $c(n)$:

$$\gamma(n) = \frac{2n^3}{(n^2+1)^2} \qquad , \qquad c(n) = \frac{2n^3}{(n^2-1)}\ . \tag{2.27}$$

Since $h(n)$ is maximized for $n=1$, where $h(1)=\frac{1}{2}$, there is no bifurcation occurring at values $n<1$. If we plot $\gamma(n)$ *versus* $c(n)$ over the allowed range of n, we obtain the phase diagram in fig. 2.10. The cusp occurs at (c^*,γ^*), and is determined by the requirement that the two bifurcations coincide. This supplies a third condition, namely that $h'(n)=0$, where

$$h''(n) = \frac{2n\,(n^2-3)}{(n^2+1)^3}\ . \tag{2.28}$$

Hence $n=\sqrt{3}$, which gives $c^* = 3\sqrt{3}$ and $\gamma^* = \frac{3\sqrt{3}}{8}$. For $c<c^*$, there are no bifurcations at any value of γ.

2.3 Appendix I : The Bletch

Problem: The bletch is a disgusting animal native to the Forest of Jkroo on the planet Barney. The bletch population obeys the equation

$$\frac{dN}{dt} = aN^2 - bN^3 \ , \tag{2.29}$$

where N is the number of bletches, and a and b are constants. (Bletches reproduce asexually, but only when another bletch is watching. However, when there are three bletches around, they beat the `@!!*$&*` out of each other.)

(a) Sketch the phase flow for N. (Strange as the bletch is, you can still rule out $N < 0$.) Identify and classify all fixed points.

(b) The bletch population is now *harvested* (they make nice shoes). To model this, we add an extra term to the dynamics:

$$\frac{dN}{dt} = -hN + aN^2 - bN^3 \ , \tag{2.30}$$

where h is the harvesting rate. Show that the phase flow now depends crucially on h, in that there are two qualitatively different flows, depending on whether $h < h_c(a,b)$ or $h > h_c(a,b)$. Find the critical harvesting rate $h_c(a,b)$ and sketch the phase flows for the two different regimes.

(c) In equilibrium, the rate at which bletches are harvested is $R = hN^*$, where N^* is the equilibrium bletch population. Suppose we start with $h = 0$, in which case N^* is given by the value of N at the stable fixed point you found in part (a). Now let h be increased very slowly from zero. As h is increased, the equilibrium population changes. Sketch R *versus* h. What value of h achieves the biggest bletch harvest? What is the corresponding value of R_{max}?

Solution:

(a) Setting the RHS of eqn. 2.29 to zero suggests the rescaling

$$N = \frac{a}{b}\, n \qquad , \qquad t = \frac{b}{a^2}\, \tau \ . \tag{2.31}$$

This results in

$$\frac{dn}{d\tau} = n^2 - n^3 \ . \tag{2.32}$$

The point $n = 0$ is a (nonlinearly) repulsive fixed point, and $n = 1$, corresponding to $N = a/b$, is attractive. The flow is shown in fig. 2.11.

By the way, the dynamics can be integrated, using the method of partial fractions, to yield

$$\frac{1}{n_0} - \frac{1}{n} + \ln\left(\frac{n}{n_0} \cdot \frac{1-n_0}{1-n}\right) = \tau \ . \tag{2.33}$$

Figure 2.11: Phase flow for the scaled bletch population, $\dot{n} = n^2 - n^3$.

(b) Upon rescaling, the harvested bletch dynamics obeys the equation

$$\frac{dn}{d\tau} = -\nu n + n^2 - n^3 \ , \tag{2.34}$$

where $\nu = bh/a^2$ is the dimensionless harvesting rate. Setting the RHS to zero yields $n(n^2 - n + \nu) = 0$, with solutions $n^* = 0$ and

$$n^*_\pm = \tfrac{1}{2} \pm \sqrt{\tfrac{1}{4} - \nu} \ . \tag{2.35}$$

Thus, for $\nu > \frac{1}{4}$ the only fixed point (for real n) is at $n^* = 0$ (stable) – the bletch population is then *overharvested*. For $\nu > \frac{1}{4}$, there are three solutions: a stable fixed point at $n^* = 0$, an unstable fixed point at $n^* = \frac{1}{2} - \sqrt{\frac{1}{4} - \nu}$, and a stable fixed point at $n^* = \frac{1}{2} + \sqrt{\frac{1}{4} - \nu}$. The critical harvesting rate is $\nu_c = \frac{1}{4}$, which means $h_c = a^2/4b$.

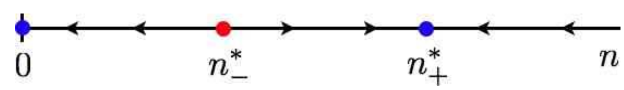

Figure 2.12: Phase flow for the harvested bletch population, $\dot{n} = -\nu n + n^2 - n^3$.

(c) The scaled bletch harvest is given by $r = \nu\, n^*_+(\nu)$. Note $R = h\, N^*_+ = \frac{a^3}{b^2}\, r$. The optimal harvest occurs when $\nu\, n^*$ is a maximum, which means we set

$$\frac{d}{d\nu}\left\{\tfrac{1}{2}\nu + \nu\sqrt{\tfrac{1}{4} - \nu}\right\} = 0 \quad \Longrightarrow \quad \nu_{\text{opt}} = \tfrac{2}{9} \ . \tag{2.36}$$

Thus, $n^*_+(\nu_{\text{opt}}) = \frac{2}{3}$ and $r_{\text{opt}} = \frac{4}{27}$, meaning $R = 4a^3/27\, b^2$. Note that at $\nu = \nu_c = \frac{1}{4}$ that $n^*_+(\nu_c) = \frac{1}{2}$, hence $r(\nu_c) = \frac{1}{8}$, which is smaller than $(\nu_{\text{opt}}) = \frac{2}{3}$. The harvest $r(\nu)$ discontinuously drops to zero at $\nu = \nu_c$, since for $\nu > \nu_c$ the flow is to the only stable fixed point at $n^* = 0$.

2.4 Appendix II : Landau Theory of Phase Transitions

Landau's theory of phase transitions is based on an expansion of the free energy of a thermodynamic system in terms of an *order parameter*, which is nonzero in an ordered phase and zero in a disordered phase. For example, the magnetization M of a ferromagnet in zero external field but at finite temperature typically vanishes for temperatures $T > T_c$, where T_c is the *critical temperature*, also called the *Curie temperature* in a ferromagnet. A

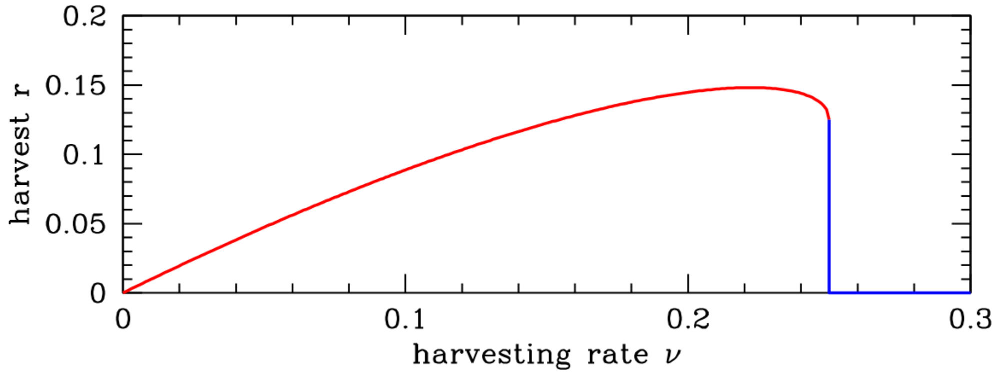

Figure 2.13: Scaled bletch harvest r *versus* scaled harvesting rate ν. Optimal harvesting occurs for $\nu_{\rm opt} = \frac{2}{9}$. The critical harvesting rate is $\nu_{\rm c} = \frac{1}{4}$, at which point the harvest discontinuously drops to zero.

low order expansion in powers of the order parameter is appropriate sufficiently close to $T_{\rm c}$, *i.e.* at temperatures such that the order parameter, if nonzero, is still small.

The simplest example is the quartic free energy,

$$f(m) = f_0 + \tfrac{1}{2}am^2 + \tfrac{1}{4}bm^4 \ , \tag{2.37}$$

where m is a dimensionless measure of the magnetization density, and where f_0, a, and b are all functions of the dimensionless temperature θ, which in a ferromagnet is the ratio $\theta = k_{\rm B}T/\mathcal{J}$, where $\mathcal{J} = \sum_j J_{ij}$ is a sum over the couplings. Let us assume $b > 0$, which is necessary if the free energy is to be bounded from below[1]. The equation of state ,

$$\frac{\partial f}{\partial m} = 0 = am + bm^3 \ , \tag{2.38}$$

has three solutions in the complex m plane: (i) $m = 0$, (ii) $m = \sqrt{-a/b}$, and (iii) $m = -\sqrt{-a/b}$. The latter two solutions lie along the (physical) real axis if $a < 0$. We assume that $a(\theta$ is monotonically increasing, and that there exists a unique temperature $\theta_{\rm c}$ where $a(\theta_{\rm c}) = 0$. Minimizing f, we find

$$\theta < \theta_{\rm c} \quad : \quad f = f_0 - \frac{a^2}{4b} \tag{2.39}$$

$$\theta > \theta_{\rm c} \quad : \quad f = f_0 \ . \tag{2.40}$$

The free energy is continuous at $\theta_{\rm c}$ since $a(\theta_{\rm c}) = 0$. The specific heat, however, is discontinuous across the transition, with

$$c\big(\theta_{\rm c}^+\big) - c\big(\theta_{\rm c}^-\big) = -\theta_{\rm c}\,\frac{\partial^2}{\partial\theta^2}\bigg|_{\theta=\theta_{\rm c}} \left(\frac{a^2}{4b}\right) = -\frac{\theta_{\rm c}\,\big[a'(\theta_{\rm c})\big]^2}{2b(\theta_{\rm c})} \ . \tag{2.41}$$

[1]It is always the case that f is bounded from below, on physical grounds. Were b negative, we'd have to consider higher order terms in the Landau expansion.

The presence of a magnetic field h breaks the $\mathbb{Z}_2$ symmetry of $m \to -m$. The free energy becomes

$$f(m) = f_0 + \tfrac{1}{2}am^2 + \tfrac{1}{4}bm^4 - hm \ , \tag{2.42}$$

and the mean field equation is

$$bm^3 + am - h = 0 \ . \tag{2.43}$$

This is a cubic equation for m with real coefficients, and as such it can either have three real solutions or one real solution and two complex solutions related by complex conjugation. Clearly we must have $a < 0$ in order to have three real roots, since bm^3+am is monotonically increasing otherwise. The boundary between these two classes of solution sets occurs when two roots coincide, which means $f''(m) = 0$ as well as $f'(m) = 0$. Simultaneously solving these two equations, we find

$$h^*(a) = \pm \frac{2}{3^{3/2}} \, \frac{(-a)^{3/2}}{b^{1/2}} \ , \tag{2.44}$$

or, equivalently,

$$a^*(h) = -\frac{3}{2^{2/3}} \, b^{1/3} \, |h|^{2/3}. \tag{2.45}$$

If, for fixed h, we have $a < a^*(h)$, then there will be three real solutions to the mean field equation $f'(m) = 0$, one of which is a global minimum (the one for which $m \cdot h > 0$). For $a > a^*(h)$ there is only a single global minimum, at which m also has the same sign as h. If we solve the mean field equation perturbatively in h/a, we find

$$m(a,h) = \frac{h}{a} - \frac{b\,h^3}{a^4} + \mathcal{O}(h^5) \qquad\qquad (a > 0) \tag{2.46}$$

$$= \frac{h}{2\,|a|} - \frac{3\,b^{1/2}\,h^2}{8\,|a|^{5/2}} + \mathcal{O}(h^3) \qquad (a < 0) \ . \tag{2.47}$$

2.4.1 Landau coefficients from mean field theory

A simple variational density matrix for the Ising ferromagnet yields the dimensionless free energy density

$$f(m,h,\theta) = -\tfrac{1}{2}\, m^2 - hm + \theta \left\{ \left(\frac{1+m}{2}\right) \ln\left(\frac{1+m}{2}\right) + \left(\frac{1-m}{2}\right) \ln\left(\frac{1-m}{2}\right) \right\} . \tag{2.48}$$

When m is small, it is appropriate to expand $f(m,h,\theta)$, obtaining

$$f(m,h,\theta) = -\theta \ln 2 - hm + \tfrac{1}{2}(\theta - 1)\, m^2 + \tfrac{\theta}{12}\, m^4 + \tfrac{\theta}{30}\, m^6 + \tfrac{\theta}{56}\, m^8 + \ldots \ . \tag{2.49}$$

Thus, we identify

$$a(\theta) = \theta - 1 \qquad , \qquad b(\theta) = \tfrac{1}{3}\theta \ . \tag{2.50}$$

We see that $a(\theta) = 0$ at a critical temperature $\theta_{\rm c} = 1$.

The free energy of eqn. 2.48 behaves qualitatively just like it does for the simple Landau expansion, where one stops at order m^4. Consider without loss of generality the case $h > 0$.

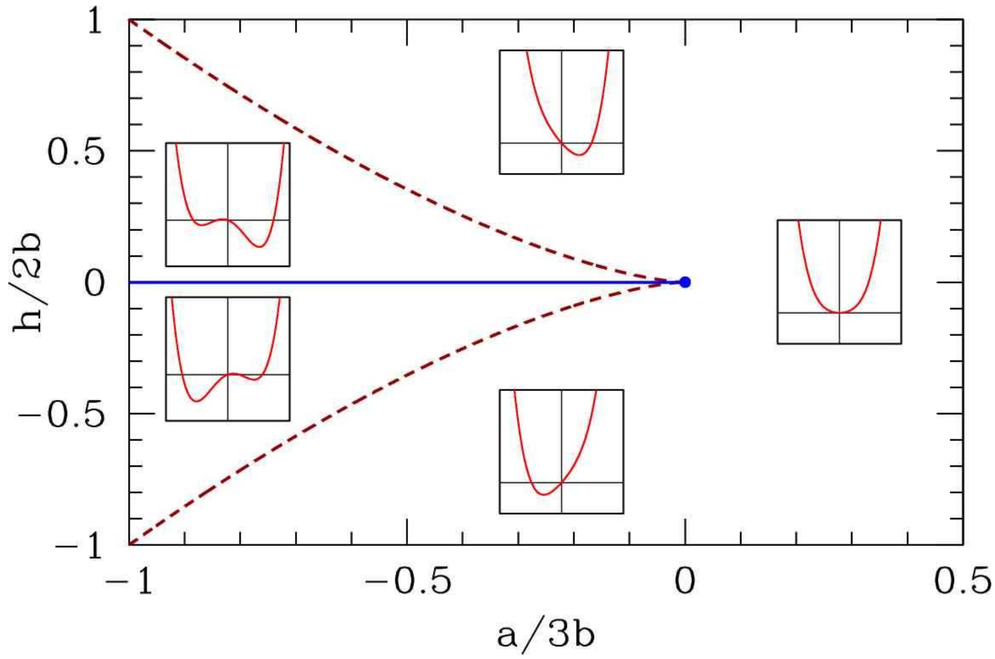

Figure 2.14: Phase diagram for the quartic mean field theory $f = f_0 + \frac{1}{2}am^2 + \frac{1}{4}bm^4 - hm$, with $b > 0$. There is a first order line at $h = 0$ extending from $a = -\infty$ and terminating in a critical point at $a = 0$. For $|h| < h^*(a)$ (dashed red line) there are three solutions to the mean field equation, corresponding to one global minimum, one local minimum, and one local maximum. Insets show behavior of the free energy $f(m)$.

The minimum of the free energy $f(m,h,\theta)$ then lies at $m > 0$ for any θ. At low temperatures, the double well structure we found in the $h = 0$ case is tilted so that the right well lies lower in energy than the left well. This is depicted in fig. 2.15. As the temperature is raised, the local minimum at $m < 0$ vanishes, annihilating with the local maximum in a saddle-node bifurcation. To find where this happens, one sets $\frac{\partial f}{\partial m} = 0$ and $\frac{\partial^2 f}{\partial m^2} = 0$ simultaneously, resulting in

$$h^*(\theta) = \sqrt{1-\theta} - \frac{\theta}{2}\ln\left(\frac{1+\sqrt{1-\theta}}{1-\sqrt{1-\theta}}\right). \tag{2.51}$$

The solutions lie at $h = \pm h^*(\theta)$. For $\theta < \theta_c = 1$ and $h \in \left[-h^*(\theta)\,,\,+h^*(\theta)\right]$, there are three solutions to the mean field equation. Equivalently we could in principle invert the above expression to obtain $\theta^*(h)$. For $\theta > \theta^*(h)$, there is only a single global minimum in the free energy $f(m)$ and there is no local minimum. Note $\theta^*(h = 0) = 1$.

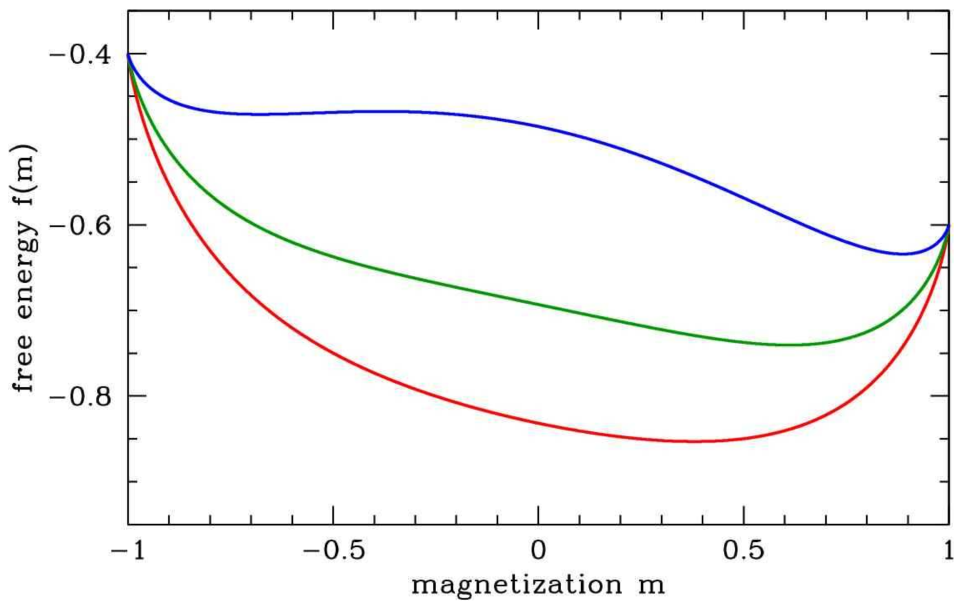

Figure 2.15: Mean field free energy $f(m)$ at $h = 0.1$. Temperatures shown: $\theta = 1.2$ (red), $\theta = 1.0$ (dark green), and $\theta = 0.7$ (blue).

2.4.2 Magnetization dynamics

Dissipative processes drive physical systems to minimum energy states. We can crudely model the dissipative dynamics of a magnet by writing the phenomenological equation

$$\frac{dm}{dt} = -\Gamma \, \frac{\partial f}{\partial m} \ . \tag{2.52}$$

This drives the free energy f to smaller and smaller values:

$$\frac{df}{dt} = \frac{\partial f}{\partial m} \, \frac{dm}{dt} = -\Gamma \bigg(\frac{\partial f}{\partial m}\bigg)^2 \le 0 \ . \tag{2.53}$$

Clearly the *fixed point* of these dynamics, where $\dot{m} = 0$, is a solution to the mean field equation $\frac{\partial f}{\partial m} = 0$. At the solution to the mean field equation, one has

$$\frac{\partial f}{\partial m} = 0 \qquad \Rightarrow \qquad m = \tanh\bigg(\frac{m+h}{\theta}\bigg) \ . \tag{2.54}$$

The phase flow for the equation $\dot{m} = -\Gamma f'(m)$ is shown in fig. 2.16. As we have seen, for any value of h there is a temperature θ^* below which the free energy $f(m)$ has two local minima and one local maximum. When $h = 0$ the minima are degenerate, but at finite h one of the minima is a global minimum. Thus, for $\theta < \theta^*(h)$ there are three solutions to the mean field equations. In the language of dynamical systems, under the dynamics of eqn. 2.52, minima of $f(m)$ correspond to attractive fixed points and maxima to repulsive fixed points. If $h > 0$, the rightmost of these fixed points corresponds to the

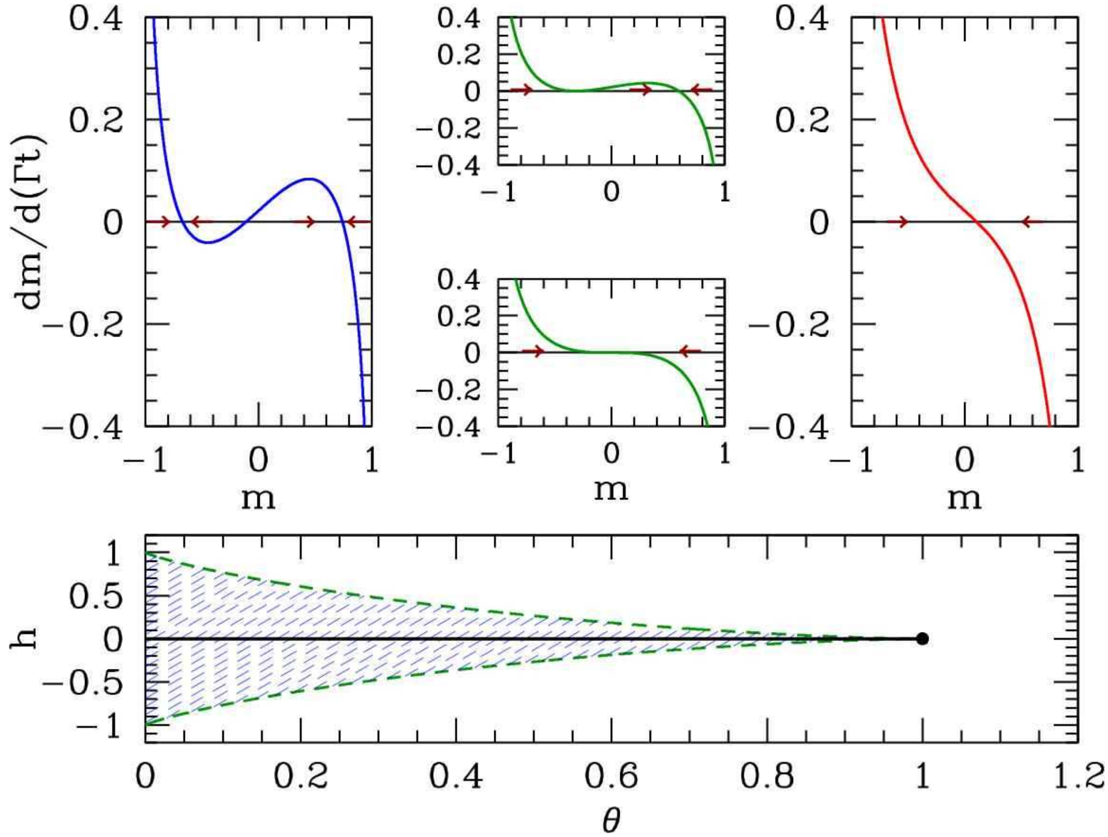

Figure 2.16: Dissipative magnetization dynamics $\dot{m} = -f'(m)$. Bottom panel shows $h^*(\theta)$ from eqn. 2.51. For (θ, h) within the blue shaded region, the free energy $f(m)$ has a global minimum plus a local minimum and a local maximum. Otherwise $f(m)$ has only a single global maximum. Top panels show an imperfect bifurcation in the magnetization dynamics at $h = 0.0215$, for which $\theta^* = 0.90$ Temperatures shown: $\theta = 0.80$ (blue), $\theta = \theta^*(h) = 0.90$ (green), and $\theta = 1.2$. The rightmost stable fixed point corresponds to the global minimum of the free energy. The bottom of the middle two upper panels shows $h = 0$, where both of the attractive fixed points and the repulsive fixed point coalesce into a single attractive fixed point (supercritical pitchfork bifurcation).

global minimum of the free energy. As θ is increased, this fixed point evolves smoothly. At $\theta = \theta^*$, the (metastable) local minimum and the local maximum coalesce and annihilate in a saddle-note bifurcation. However at $h = 0$ all three fixed points coalesce at $\theta = \theta_c$ and the bifurcation is a supercritical pitchfork. As a function of t at finite h, the dynamics are said to exhibit an *imperfect bifurcation*, which is a deformed supercritical pitchfork.

The solution set for the mean field equation is simply expressed by inverting the tanh function to obtain $h(\theta, m)$. One readily finds

$$h(\theta, m) = \frac{\theta}{2} \ln\!\left(\frac{1+m}{1-m}\right) - m \ . \tag{2.55}$$

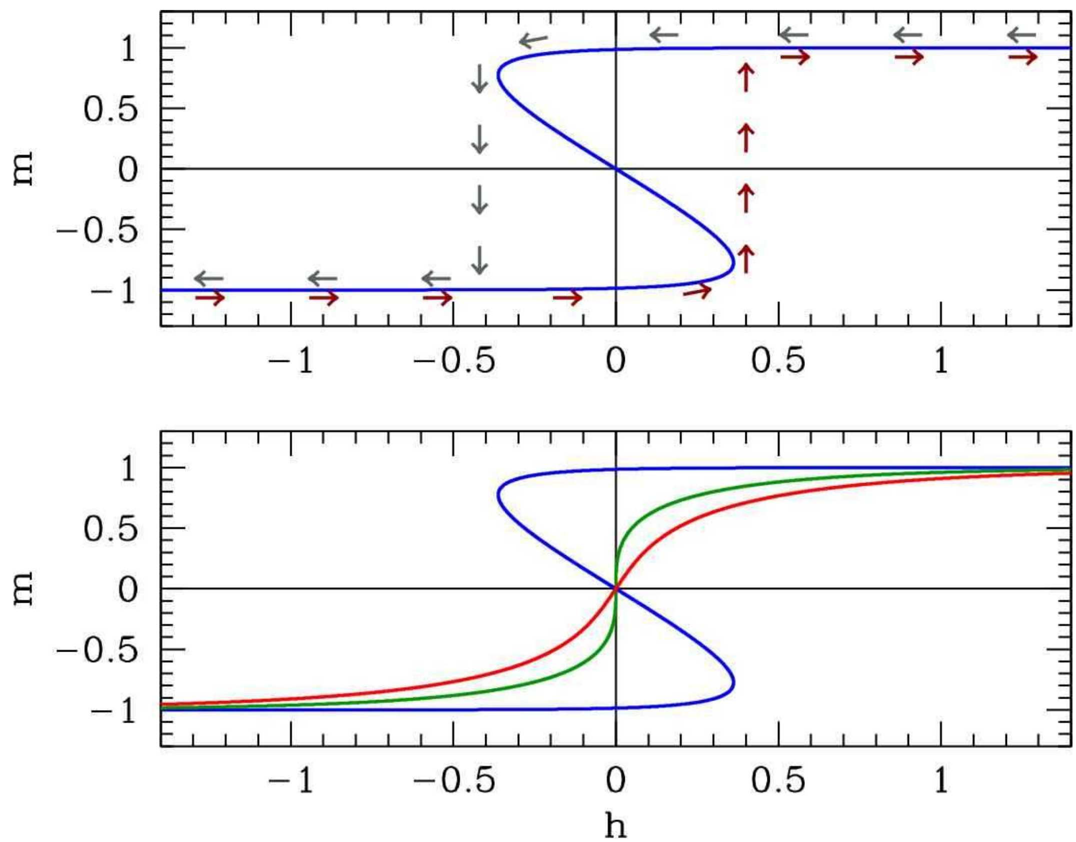

Figure 2.17: Top panel : hysteresis as a function of ramping the dimensionless magnetic field h at $\theta = 0.40$. Dark red arrows below the curve follow evolution of the magnetization on slow increase of h. Dark grey arrows above the curve follow evolution of the magnetization on slow decrease of h. Bottom panel : solution set for $m(\theta, h)$ as a function of h at temperatures $\theta = 0.40$ (blue), $\theta = \theta_c = 1.0$ (dark green), and $t = 1.25$ (red).

As we see in the bottom panel of fig. 2.17, $m(h)$ becomes multivalued for field values $h \in \big[-h^*(\theta)\,,\,+h^*(\theta)\big]$, where $h^*(\theta)$ is given in eqn. 2.51. Now imagine that $\theta < \theta_c$ and we slowly ramp the field h from a large negative value to a large positive value, and then slowly back down to its original value. On the time scale of the magnetization dynamics, we can regard $h(t)$ as a constant. Thus, $m(t)$ will flow to the nearest stable fixed point. Initially the system starts with $m = -1$ and h large and negative, and there is only one fixed point, at $m^* \approx -1$. As h slowly increases, the fixed point value m^* also slowly increases. As h exceeds $-h^*(\theta)$, a saddle-node bifurcation occurs, and two new fixed points are created at positive m, one stable and one unstable. The global minimum of the free energy still lies at the fixed point with $m^* < 0$. However, when h crosses $h = 0$, the global minimum of the free energy lies at the most positive fixed point m^*. The dynamics, however, keep the system stuck in what is a metastable phase. This persists until $h = +h^*(\theta)$, at which point another saddle-note bifurcation occurs, and the attractive fixed point at $m^* < 0$ annihilates with the repulsive fixed point. The dynamics then act quickly to drive m to the only remaining fixed point. This process is depicted in the top panel of fig. 2.17. As one can see from the figure, the the system follows a stable fixed point until the fixed point disappears, even though that fixed point may not always correspond to a global minimum of the free energy. The resulting $m(h)$ curve is then not reversible as a function of time, and it possesses a characteristic shape known as a *hysteresis loop*. Etymologically, the word *hysteresis* derives from the Greek $\upsilon\sigma\tau\varepsilon\rho\eta\sigma\iota\varsigma$, which means 'lagging behind'. Systems which are hysteretic exhibit a *history-dependence* to their status, which is not uniquely determined by external conditions. Hysteresis may be exhibited with respect to changes in applied magnetic field, changes in temperature, or changes in other externally determined parameters.

2.4.3 Cubic terms in Landau theory : first order transitions

Next, consider a free energy with a cubic term,

$$f = f_0 + \tfrac{1}{2}am^2 - \tfrac{1}{3}ym^3 + \tfrac{1}{4}bm^4 \ , \tag{2.56}$$

with $b > 0$ for stability. Without loss of generality, we may assume $y > 0$ (else send $m \to -m$). Note that we no longer have $m \to -m$ (*i.e.* $\mathbb{Z}_2$) symmetry. The cubic term favors positive m. What is the phase diagram in the (a, y) plane?

Extremizing the free energy with respect to m, we obtain

$$\frac{\partial f}{\partial m} = 0 = am - ym^2 + bm^3 \ . \tag{2.57}$$

This cubic equation factorizes into a linear and quadratic piece, and hence may be solved simply. The three solutions are $m = 0$ and

$$m = m_\pm \equiv \frac{y}{2b} \pm \sqrt{\left(\frac{y}{2b}\right)^2 - \frac{a}{b}} \ . \tag{2.58}$$

We now see that for $y^2 < 4ab$ there is only one real solution, at $m = 0$, while for $y^2 > 4ab$ there are three real solutions. Which solution has lowest free energy? To find out, we compare the energy $f(0)$ with $f(m_+)$[2]. Thus, we set

$$f(m) = f(0) \quad \Longrightarrow \quad \tfrac{1}{2}am^2 - \tfrac{1}{3}ym^3 + \tfrac{1}{4}bm^4 = 0 \ , \tag{2.59}$$

and we now have two quadratic equations to solve simultaneously:

$$0 = a - ym + bm^2 \tag{2.60}$$

$$0 = \tfrac{1}{2}a - \tfrac{1}{3}ym + \tfrac{1}{4}bm^2 = 0 \ . \tag{2.61}$$

Eliminating the quadratic term gives $m = 3a/y$. Finally, substituting $m = m_+$ gives us a relation between a, b, and y:

$$y^2 = \tfrac{9}{2}\,ab \ . \tag{2.62}$$

[2]We needn't waste our time considering the $m = m_-$ solution, since the cubic term prefers positive m.

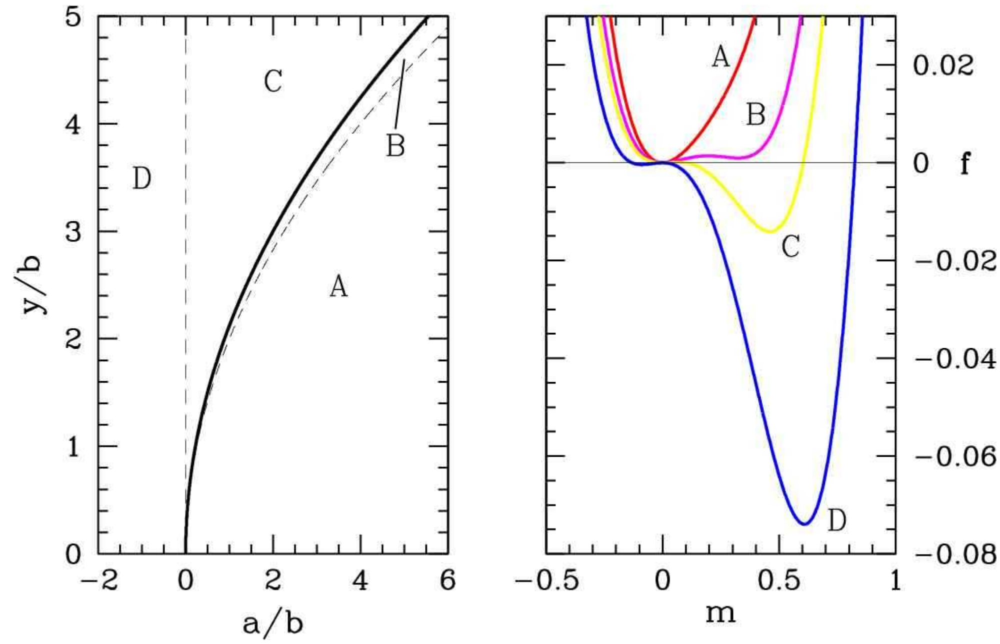

Figure 2.18: Behavior of the quartic free energy $f(m) = \frac{1}{2}am^2 - \frac{1}{3}ym^3 + \frac{1}{4}bm^4$. A: $y^2 < 4ab$; B: $4ab < y^2 < \frac{9}{2}ab$; C and D: $y^2 > \frac{9}{2}ab$. The thick black line denotes a line of first order transitions, where the order parameter is discontinuous across the transition.

Thus, we have the following:

$$\begin{aligned} a > \frac{y^2}{4b} \quad &: \quad \text{1 real root } m = 0 \\ \frac{y^2}{4b} > a > \frac{2y^2}{9b} \quad &: \quad \text{3 real roots; minimum at } m = 0 \\ \frac{2y^2}{9b} > a \quad &: \quad \text{3 real roots; minimum at } m = \frac{y}{2b} + \sqrt{\left(\frac{y}{2b}\right)^2 - \frac{a}{b}} \end{aligned}$$

The solution $m = 0$ lies at a local minimum of the free energy for $a > 0$ and at a local maximum for $a < 0$. Over the range $\frac{y^2}{4b} > a > \frac{2y^2}{9b}$, then, there is a global minimum at $m = 0$, a local minimum at $m = m_+$, and a local maximum at $m = m_-$, with $m_+ > m_- > 0$. For $\frac{2y^2}{9b} > a > 0$, there is a local minimum at $a = 0$, a global minimum at $m = m_+$, and a local maximum at $m = m_-$, again with $m_+ > m_- > 0$. For $a < 0$, there is a local maximum at $m = 0$, a local minimum at $m = m_-$, and a global minimum at $m = m_+$, with $m_+ > 0 > m_-$. See fig. 2.18.

2.4.4 Magnetization dynamics

Suppose we now impose some dynamics on the system, of the simple relaxational type

$$\frac{dm}{dt} = -\Gamma \, \frac{\partial f}{\partial m} \,, \tag{2.63}$$

where Γ is a phenomenological kinetic coefficient. Assuming $y > 0$ and $b > 0$, it is convenient to adimensionalize by writing

$$m \equiv \frac{y}{b} \cdot u \qquad , \qquad a \equiv \frac{y^2}{b} \cdot \bar{r} \qquad , \qquad t \equiv \frac{b}{\Gamma y^2} \cdot s \ . \tag{2.64}$$

Then we obtain

$$\frac{\partial u}{\partial s} = -\frac{\partial \varphi}{\partial u} \ , \tag{2.65}$$

where the dimensionless free energy function is

$$\varphi(u) = \tfrac{1}{2}\bar{r}u^2 - \tfrac{1}{3}u^3 + \tfrac{1}{4}u^4 \ . \tag{2.66}$$

We see that there is a single control parameter, $\bar{r}$. The fixed points of the dynamics are then the stationary points of $\varphi(u)$, where $\varphi'(u) = 0$, with

$$\varphi'(u) = u\,(\bar{r} - u + u^2) \ . \tag{2.67}$$

The solutions to $\varphi'(u) = 0$ are then given by

$$u^* = 0 \qquad , \qquad u^* = \tfrac{1}{2} \pm \sqrt{\tfrac{1}{4} - \bar{r}} \ . \tag{2.68}$$

For $r > \frac{1}{4}$ there is one fixed point at $u = 0$, which is attractive under the dynamics $\dot{u} = -\varphi'(u)$ since $\varphi''(0) = \bar{r}$. At $\bar{r} = \frac{1}{4}$ there occurs a saddle-node bifurcation and a pair of fixed points is generated, one stable and one unstable. As we see from fig. 2.14, the interior fixed point is always unstable and the two exterior fixed points are always stable. At $r = 0$ there is a transcritical bifurcation where two fixed points of opposite stability collide and bounce off one another (metaphorically speaking).

At the saddle-node bifurcation, $\bar{r} = \frac{1}{4}$ and $u = \frac{1}{2}$, and we find $\varphi(u = \frac{1}{2}; \bar{r} = \frac{1}{4}) = \frac{1}{192}$, which is positive. Thus, the thermodynamic state of the system remains at $u = 0$ until the value of $\varphi(u_+)$ crosses zero. This occurs when $\varphi(u) = 0$ and $\varphi'(u) = 0$, the simultaneous solution of which yields $\bar{r} = \frac{2}{9}$ and $u = \frac{2}{3}$.

Suppose we slowly ramp the control parameter $\bar{r}$ up and down as a function of the dimensionless time s. Under the dynamics of eqn. 2.65, $u(s)$ flows to the first stable fixed point encountered – this is always the case for a dynamical system with a one-dimensional phase space. Then as $\bar{r}$ is further varied, u follows the position of whatever locally stable fixed point it initially encountered. Thus, $u\big(\bar{r}(s)\big)$ evolves smoothly until a bifurcation is encountered. The situation is depicted by the arrows in fig. 2.19. The equilibrium thermodynamic value for $u(\bar{r})$ is discontinuous; there is a first order phase transition at $\bar{r} = \frac{2}{9}$, as we've already seen. As r is increased, $u(\bar{r})$ follows a trajectory indicated by the magenta arrows. For an negative initial value of u, the evolution as a function of $\bar{r}$ will be *reversible*. However, if $u(0)$ is initially positive, then the system exhibits *hysteresis*, as shown. Starting with a large positive value of $\bar{r}$, $u(s)$ quickly evolves to $u = 0^+$, which means a positive infinitesimal value. Then as r is decreased, the system remains at $u = 0^+$ even through the first order transition, because $u = 0$ is an attractive fixed point. However, once r begins to go negative, the $u = 0$ fixed point becomes repulsive, and $u(s)$ quickly flows to the stable

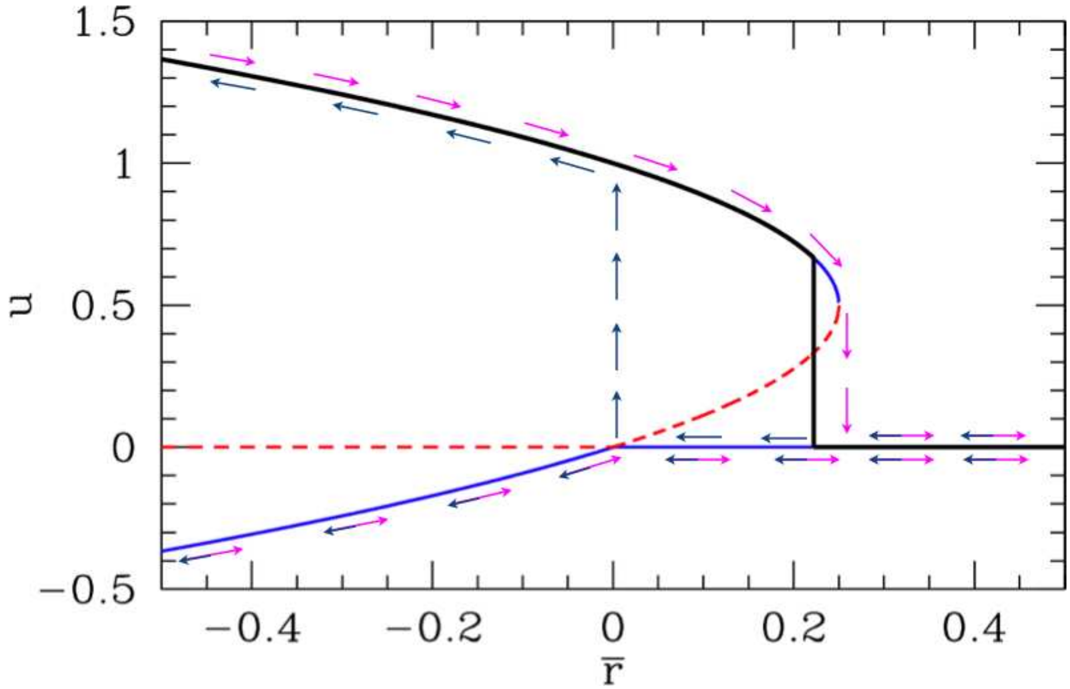

Figure 2.19: Fixed points for $\varphi(u) = \frac{1}{2}\bar{r}u^2 - \frac{1}{3}u^3 + \frac{1}{4}u^4$ and flow under the dynamics $\dot{u} = -\varphi'(u)$. Solid curves represent stable fixed points and dashed curves unstable fixed points. Magenta arrows show behavior under slowly increasing control parameter $\bar{r}$ and dark blue arrows show behavior under slowly decreasing $\bar{r}$. For $u > 0$ there is a hysteresis loop. The thick black curve shows the equilibrium thermodynamic value of $u(\bar{r})$, *i.e.* that value which minimizes the free energy $\varphi(u)$. There is a first order phase transition at $\bar{r} = \frac{2}{9}$, where the thermodynamic value of u jumps from $u = 0$ to $u = \frac{2}{3}$.

fixed point $u_+ = \frac{1}{2} + \sqrt{\frac{1}{4} - \bar{r}}$. Further decreasing r, the system remains on this branch. If $\bar{r}$ is later increased, then $u(s)$ remains on the upper branch past $r = 0$, until the u_+ fixed point annihilates with the unstable fixed point at $u_- = \frac{1}{2} - \sqrt{\frac{1}{4} - \bar{r}}$, at which time $u(s)$ quickly flows down to $u = 0^+$ again.

2.4.5 Sixth order Landau theory : tricritical point

Finally, consider a model with $\mathbb{Z}_2$ symmetry, with the Landau free energy

$$f = f_0 + \tfrac{1}{2}am^2 + \tfrac{1}{4}bm^4 + \tfrac{1}{6}cm^6 \ , \tag{2.69}$$

with $c > 0$ for stability. We seek the phase diagram in the (a, b) plane. Extremizing f with respect to m, we obtain

$$\frac{\partial f}{\partial m} = 0 = m\,(a + bm^2 + cm^4) \ , \tag{2.70}$$

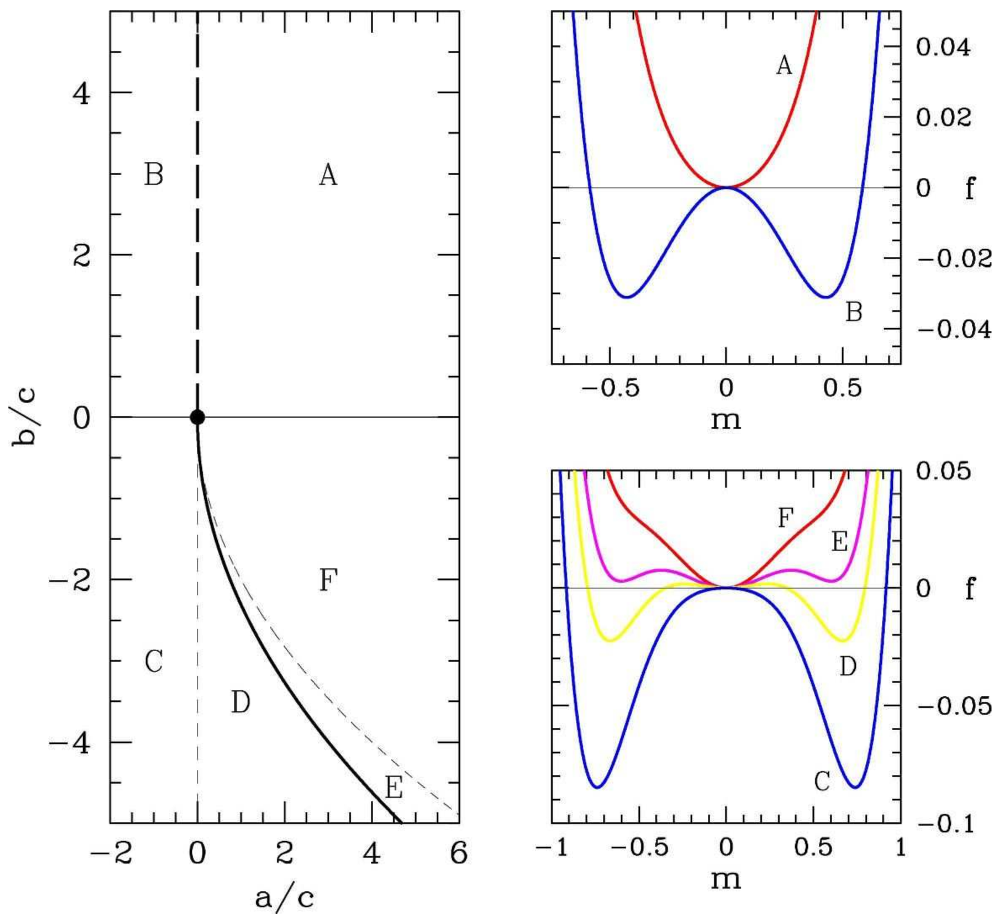

Figure 2.20: Behavior of the sextic free energy $f(m) = \frac{1}{2}am^2 + \frac{1}{4}bm^4 + \frac{1}{6}cm^6$. A: $a > 0$ and $b > 0$; B: $a < 0$ and $b > 0$; C: $a < 0$ and $b < 0$; D: $a > 0$ and $b < -\frac{4}{\sqrt{3}}\sqrt{ac}$; E: $a > 0$ and $-\frac{4}{\sqrt{3}}\sqrt{ac} < b < -2\sqrt{ac}$; F: $a > 0$ and $-2\sqrt{ac} < b < 0$. The thick dashed line is a line of second order transitions, which meets the thick solid line of first order transitions at the tricritical point, $(a, b) = (0, 0)$.

which is a quintic with five solutions over the complex m plane. One solution is obviously $m = 0$. The other four are

$$m = \pm\sqrt{-\frac{b}{2c} \pm \sqrt{\left(\frac{b}{2c}\right)^2 - \frac{a}{c}}} \; . \tag{2.71}$$

For each $\pm$ symbol in the above equation, there are two options, hence four roots in all.

If $a > 0$ and $b > 0$, then four of the roots are imaginary and there is a unique minimum at $m = 0$.

For $a < 0$, there are only three solutions to $f'(m) = 0$ for real m, since the $-$ choice for the $\pm$ sign under the radical leads to imaginary roots. One of the solutions is $m = 0$. The other two are

$$m = \pm\sqrt{-\frac{b}{2c} + \sqrt{\left(\frac{b}{2c}\right)^2 - \frac{a}{c}}} \ . \tag{2.72}$$

The most interesting situation is $a > 0$ and $b < 0$. If $a > 0$ and $b < -2\sqrt{ac}$, all five roots are real. There must be three minima, separated by two local maxima. Clearly if m^* is a solution, then so is $-m^*$. Thus, the only question is whether the outer minima are of lower energy than the minimum at $m = 0$. We assess this by demanding $f(m^*) = f(0)$, where m^* is the position of the largest root (*i.e.* the rightmost minimum). This gives a second quadratic equation,

$$0 = \tfrac{1}{2}a + \tfrac{1}{4}bm^2 + \tfrac{1}{6}cm^4 \ , \tag{2.73}$$

which together with equation 2.70 gives

$$b = -\tfrac{4}{\sqrt{3}}\,\sqrt{ac} \ . \tag{2.74}$$

Thus, we have the following, for fixed $a > 0$:

$$\begin{aligned}
b > -2\sqrt{ac} \quad &: \quad \text{1 real root } m = 0 \\
-2\sqrt{ac} > b > -\tfrac{4}{\sqrt{3}}\,\sqrt{ac} \quad &: \quad \text{5 real roots; minimum at } m = 0 \\
-\tfrac{4}{\sqrt{3}}\,\sqrt{ac} > b \quad &: \quad \text{5 real roots; minima at } m = \pm\sqrt{-\frac{b}{2c} + \sqrt{\left(\frac{b}{2c}\right)^2 - \frac{a}{c}}}
\end{aligned}$$

The point $(a, b) = (0, 0)$, which lies at the confluence of a first order line and a second order line, is known as a *tricritical point*.

2.4.6 Hysteresis for the sextic potential

Once again, we consider the dissipative dynamics $\dot{m} = -\Gamma\, f'(m)$. We adimensionalize by writing

$$m \equiv \sqrt{\frac{|b|}{c}} \cdot u \qquad , \qquad a \equiv \frac{b^2}{c} \cdot \bar{r} \qquad , \qquad t \equiv \frac{c}{\Gamma\, b^2} \cdot s \ . \tag{2.75}$$

Then we obtain once again the dimensionless equation

$$\frac{\partial u}{\partial s} = -\frac{\partial \varphi}{\partial u} \ , \tag{2.76}$$

where

$$\varphi(u) = \tfrac{1}{2}\bar{r}u^2 \pm \tfrac{1}{4}u^4 + \tfrac{1}{6}u^6 \ . \tag{2.77}$$

In the above equation, the coefficient of the quartic term is positive if $b > 0$ and negative if $b < 0$. That is, the coefficient is $\text{sgn}(b)$. When $b > 0$ we can ignore the sextic term for sufficiently small u, and we recover the quartic free energy studied earlier. There is then a second order transition at $r = 0$. .

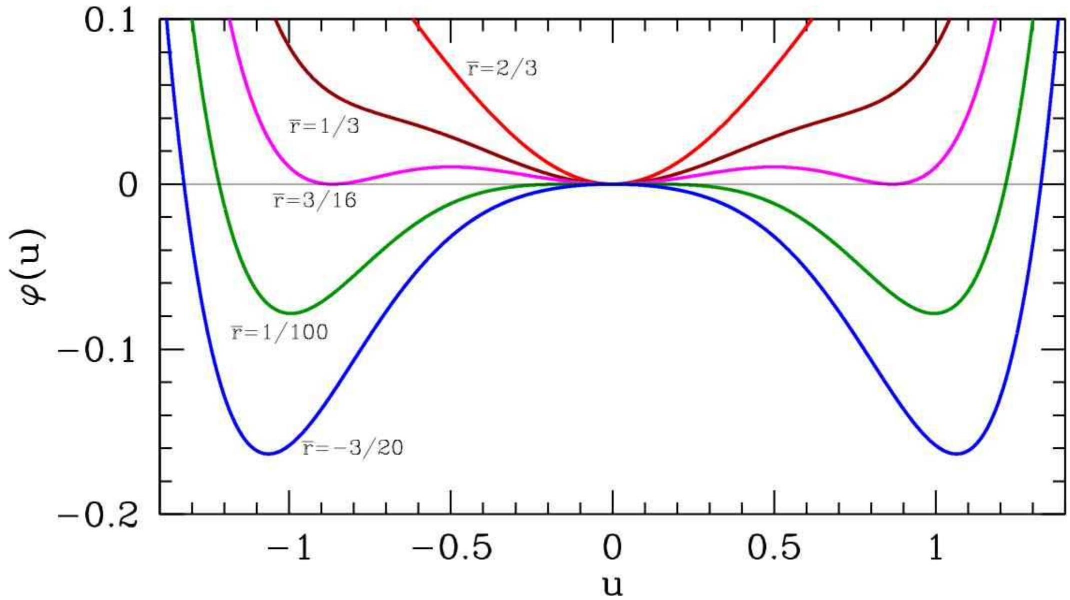

Figure 2.21: Free energy $\varphi(u) = \frac{1}{2}\bar{r}u^2 - \frac{1}{4}u^4 + \frac{1}{6}u^6$ for several different values of the control parameter $\bar{r}$.

New and interesting behavior occurs for $b > 0$. The fixed points of the dynamics are obtained by setting $\varphi'(u) = 0$. We have

$$\varphi(u) = \tfrac{1}{2}\bar{r}u^2 - \tfrac{1}{4}u^4 + \tfrac{1}{6}u^6 \tag{2.78}$$

$$\varphi'(u) = u\,(\bar{r} - u^2 + u^4)\ . \tag{2.79}$$

Thus, the equation $\varphi'(u) = 0$ factorizes into a linear factor u and a quartic factor $u^4 - u^2 + \bar{r}$ which is quadratic in u^2. Thus, we can easily obtain the roots:

$$\bar{r} < 0 \quad : \quad u^* = 0\ ,\ u^* = \pm\sqrt{\tfrac{1}{2} + \sqrt{\tfrac{1}{4} - \bar{r}}} \tag{2.80}$$

$$0 < \bar{r} < \tfrac{1}{4} \quad : \quad u^* = 0\ ,\ u^* = \pm\sqrt{\tfrac{1}{2} + \sqrt{\tfrac{1}{4} - \bar{r}}}\ ,\ u^* = \pm\sqrt{\tfrac{1}{2} - \sqrt{\tfrac{1}{4} - \bar{r}}} \tag{2.81}$$

$$\bar{r} > \tfrac{1}{4} \quad : \quad u^* = 0\ . \tag{2.82}$$

In fig. 2.22, we plot the fixed points and the hysteresis loops for this system. At $\bar{r} = \frac{1}{4}$, there are two symmetrically located saddle-node bifurcations at $u = \pm\frac{1}{\sqrt{2}}$. We find $\varphi(u = \pm\frac{1}{\sqrt{2}}, \bar{r} = \frac{1}{4}) = \frac{1}{48}$, which is positive, indicating that the stable fixed point $u^* = 0$ remains the thermodynamic minimum for the free energy $\varphi(u)$ as $\bar{r}$ is decreased through $\bar{r} = \frac{1}{4}$. Setting $\varphi(u) = 0$ and $\varphi'(u) = 0$ simultaneously, we obtain $\bar{r} = \frac{3}{16}$ and $u = \pm\frac{\sqrt{3}}{2}$. The thermodynamic value for u therefore jumps discontinuously from $u = 0$ to $u = \pm\frac{\sqrt{3}}{2}$ (either branch) at $\bar{r} = \frac{3}{16}$; this is a first order transition.

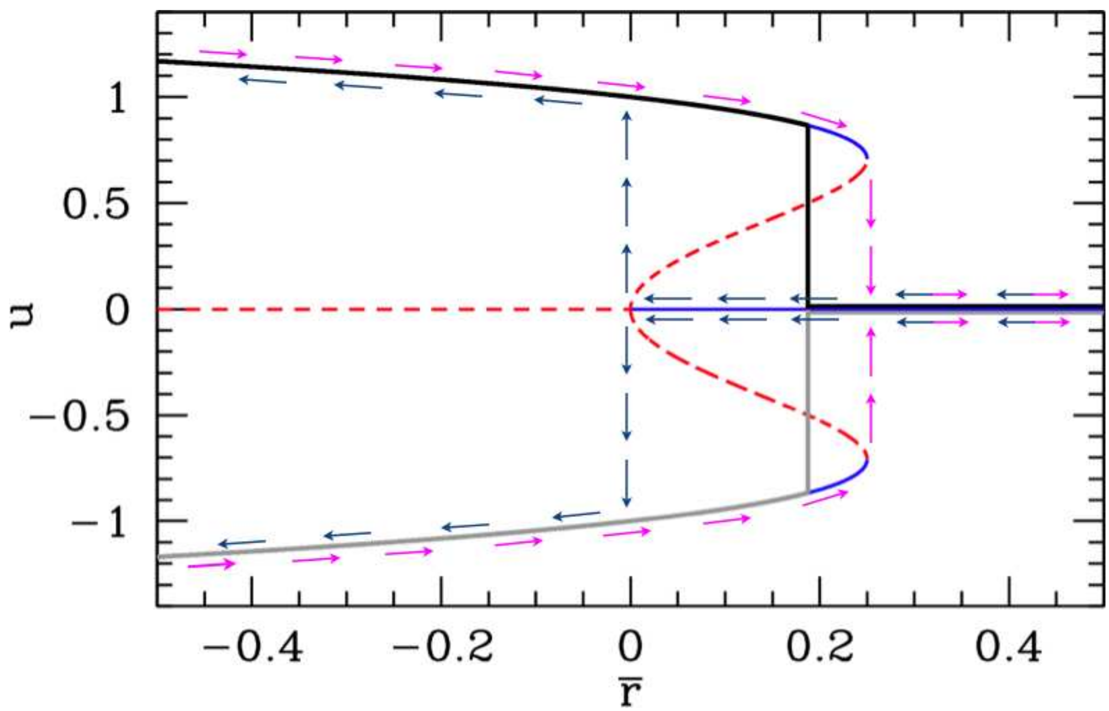

Figure 2.22: Fixed points $\varphi'(u^*) = 0$ for the sextic potential $\varphi(u) = \frac{1}{2}\bar{r}u^2 - \frac{1}{4}u^4 + \frac{1}{6}u^6$, and corresponding dynamical flow (arrows) under $\dot{u} = -\varphi'(u)$. Solid curves show stable fixed points and dashed curves show unstable fixed points. The thick solid black and solid grey curves indicate the equilibrium thermodynamic values for u; note the overall $u \to -u$ symmetry. Within the region $\bar{r} \in [0, \frac{1}{4}]$ the dynamics are irreversible and the system exhibits the phenomenon of hysteresis. There is a first order phase transition at $\bar{r} = \frac{3}{16}$.

Under the dissipative dynamics considered here, the system exhibits hysteresis, as indicated in the figure, where the arrows show the evolution of $u(s)$ for very slowly varying $\bar{r}(s)$. When the control parameter $\bar{r}$ is large and positive, the flow is toward the sole fixed point at $u^* = 0$. At $\bar{r} = \frac{1}{4}$, two simultaneous saddle-node bifurcations take place at $u^* = \pm\frac{1}{\sqrt{2}}$; the outer branch is stable and the inner branch unstable in both cases. At $r = 0$ there is a subcritical pitchfork bifurcation, and the fixed point at $u^* = 0$ becomes unstable.

Suppose one starts off with $\bar{r} \gg \frac{1}{4}$ with some value $u > 0$. The flow $\dot{u} = -\varphi'(u)$ then rapidly results in $u \to 0^+$. This is the 'high temperature phase' in which there is no magnetization. Now let r increase slowly, using s as the dimensionless time variable. The scaled magnetization $u(s) = u^*\big(\bar{r}(s)\big)$ will remain pinned at the fixed point $u^* = 0^+$. As $\bar{r}$ passes through $\bar{r} = \frac{1}{4}$, two new stable values of u^* appear, but our system remains at $u = 0^+$, since $u^* = 0$ is a stable fixed point. But after the subcritical pitchfork, $u^* = 0$ becomes unstable. The magnetization $u(s)$ then flows rapidly to the stable fixed point at $u^* = \frac{1}{\sqrt{2}}$, and follows the curve $u^*(\bar{r}) = \big(\frac{1}{2} + (\frac{1}{4} - \bar{r})^{1/2}\big)^{1/2}$ for all $r < 0$.

Now suppose we start increasing r (*i.e.* increasing temperature). The magnetization follows the stable fixed point $u^*(\bar{r}) = \left(\frac{1}{2} + (\frac{1}{4} - \bar{r})^{1/2}\right)^{1/2}$ past $\bar{r} = 0$, beyond the first order phase transition point at $\bar{r} = \frac{3}{16}$, and all the way up to $\bar{r} = \frac{1}{4}$, at which point this fixed point is annihilated at a saddle-node bifurcation. The flow then rapidly takes $u \to u^* = 0^+$, where it remains as r continues to be increased further.

Within the region $\bar{r} \in \left[0, \frac{1}{4}\right]$ of control parameter space, the dynamics are said to be *irreversible* and the behavior of $u(s)$ is said to be *hysteretic*.

Chapter 3

Two-Dimensional Phase Flows

We've seen how, for one-dimensional dynamical systems $\dot{u} = f(u)$, the possibilities in terms of the behavior of the system are in fact quite limited. Starting from an arbitrary initial condition $u(0)$, the phase flow is monotonically toward the first stable fixed point encountered. (That point may lie at infinity.) No oscillations are possible[1]. For $N = 2$ phase flows, a richer set of possibilities arises, as we shall now see.

3.1 Harmonic Oscillator and Pendulum

3.1.1 Simple harmonic oscillator

A one-dimensional harmonic oscillator obeys the equation of motion,

$$m\frac{d^2x}{dt^2} = -kx \ , \tag{3.1}$$

where m is the mass and k the force constant (of a spring). If we define $v = \dot{x}$, this may be written as the $N = 2$ system,

$$\frac{d}{dt}\begin{pmatrix} x \\ v \end{pmatrix} = \begin{pmatrix} 0 & 1 \\ -\Omega^2 & 0 \end{pmatrix}\begin{pmatrix} x \\ v \end{pmatrix} = \begin{pmatrix} v \\ -\Omega^2\, x \end{pmatrix} \ , \tag{3.2}$$

where $\Omega = \sqrt{k/m}$ has the dimensions of frequency (inverse time). The solution is well known:

$$x(t) = x_0\, \cos(\Omega t) + \frac{v_0}{\Omega}\, \sin(\Omega t) \tag{3.3}$$

$$v(t) = v_0\, \cos(\Omega t) - \Omega\, x_0\, \sin(\Omega t) \ . \tag{3.4}$$

[1]If phase space itself is multiply connected, *e.g.* a circle, then the system can oscillate by moving around the circle.

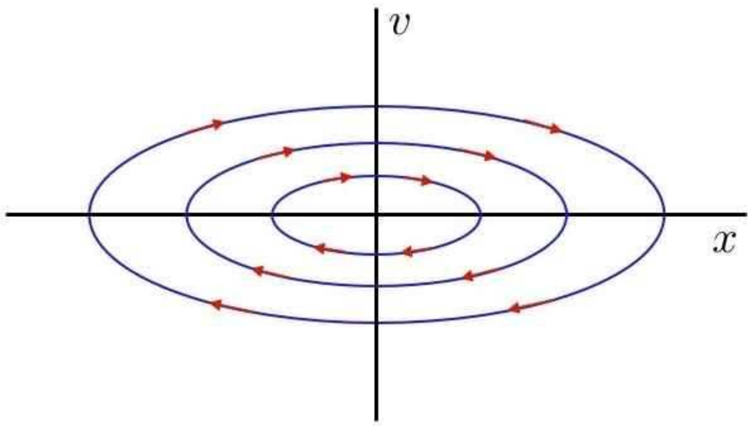

Figure 3.1: Phase curves for the harmonic oscillator.

The phase curves are ellipses:

$$\Omega\, x^2(t) + \Omega^{-1}\, v^2(t) = C \ , \tag{3.5}$$

where the constant $C = \Omega\, x_0^2 + \Omega^{-1}\, v_0^2$. A sketch of the phase curves and of the phase flow is shown in Fig. 3.1. Note that the x and v axes have different dimensions. Note also that the origin is a fixed point, however, unlike the $N = 1$ systems studied in the first lecture, here the phase flow can avoid the fixed points, and oscillations can occur.

Incidentally, eqn. 3.2 is linear, and may be solved by the following method. Write the equation as $\dot{\boldsymbol{\varphi}} = M\boldsymbol{\varphi}$, with

$$\boldsymbol{\varphi} = \begin{pmatrix} x \\ \dot{x} \end{pmatrix} \qquad \text{and} \qquad M = \begin{pmatrix} 0 & 1 \\ -\Omega^2 & 0 \end{pmatrix} \tag{3.6}$$

The formal solution to $\dot{\boldsymbol{\varphi}} = M\boldsymbol{\varphi}$ is

$$\boldsymbol{\varphi}(t) = e^{Mt}\, \boldsymbol{\varphi}(0) \ . \tag{3.7}$$

What do we mean by the exponential of a matrix? We mean its Taylor series expansion:

$$e^{Mt} = \mathbb{I} + Mt + \tfrac{1}{2!}\, M^2\, t^2 + \tfrac{1}{3!}\, M^3\, t^3 + \ldots \ . \tag{3.8}$$

Note that

$$\begin{aligned} M^2 &= \begin{pmatrix} 0 & 1 \\ -\Omega^2 & 0 \end{pmatrix} \begin{pmatrix} 0 & 1 \\ -\Omega^2 & 0 \end{pmatrix} \\ &= \begin{pmatrix} -\Omega^2 & 0 \\ 0 & -\Omega^2 \end{pmatrix} = -\Omega^2\, \mathbb{I} \ , \end{aligned} \tag{3.9}$$

hence

$$M^{2k} = (-\Omega^2)^k\, \mathbb{I} \qquad , \qquad M^{2k+1} = (-\Omega^2)^k\, M \ . \tag{3.10}$$

Thus,

$$
\begin{aligned}
e^{Mt} &= \sum_{k=0}^{\infty} \frac{1}{(2k)!}\,(-\Omega^2 t^2)^k \cdot \mathbb{I} + \sum_{k=0}^{\infty} \frac{1}{(2k+1)!}\,(-\Omega^2 t^2)^k \cdot Mt \\
&= \cos(\Omega t)\cdot \mathbb{I} + \Omega^{-1}\sin(\Omega t)\cdot M \\
&= \begin{pmatrix} \cos(\Omega t) & \Omega^{-1}\sin(\Omega t) \\ -\Omega\,\sin(\Omega t) & \cos(\Omega t) \end{pmatrix} \ . \qquad (3.11)
\end{aligned}
$$

Plugging this into eqn. 3.7, we obtain the desired solution.

For the damped harmonic oscillator, we have

$$
\ddot{x} + 2\beta\dot{x} + \Omega^2 x = 0 \qquad \Longrightarrow \qquad M = \begin{pmatrix} 0 & 1 \\ -\Omega^2 & -2\beta \end{pmatrix} \ . \qquad (3.12)
$$

The phase curves then spiral inward to the fixed point at $(0,0)$.

3.1.2 Pendulum

Next, consider the simple pendulum, composed of a mass point m affixed to a massless rigid rod of length ℓ.

$$
m\ell^2\,\ddot{\theta} = -mg\ell\sin\theta \ . \qquad (3.13)
$$

This is equivalent to

$$
\frac{d}{dt}\begin{pmatrix} \theta \\ \omega \end{pmatrix} = \begin{pmatrix} \omega \\ -\Omega^2\,\sin\theta \end{pmatrix} \ , \qquad (3.14)
$$

where $\omega = \dot{\theta}$ is the angular velocity, and where $\Omega = \sqrt{g/\ell}$ is the natural frequency of small oscillations.

The phase curves for the pendulum are shown in Fig. 3.2. The small oscillations of the pendulum are essentially the same as those of a harmonic oscillator. Indeed, within the small angle approximation, $\sin\theta \approx \theta$, and the pendulum equations of motion are exactly those of the harmonic oscillator. These oscillations are called *librations*. They involve a back-and-forth motion in real space, and the phase space motion is contractable to a point, in the topological sense. However, if the initial angular velocity is large enough, a qualitatively different kind of motion is observed, whose phase curves are *rotations*. In this case, the pendulum bob keeps swinging around in the same direction, because, as we'll see in a later lecture, the total energy is sufficiently large. The phase curve which separates these two topologically distinct motions is called a *separatrix*.

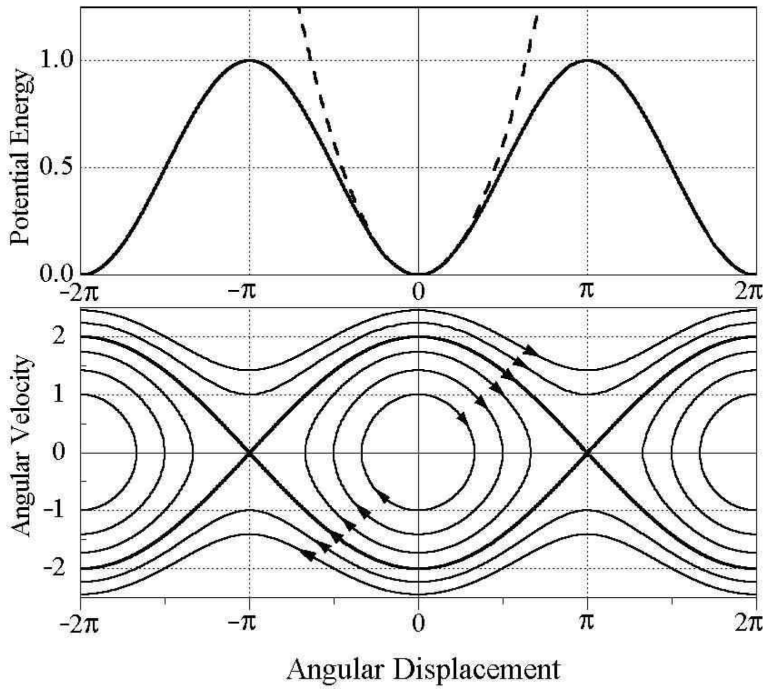

Figure 3.2: Phase curves for the simple pendulum. The *separatrix* divides phase space into regions of vibration and libration.

3.2 General $N = 2$ Systems

The general form to be studied is

$$\frac{d}{dt}\begin{pmatrix} x \\ y \end{pmatrix} = \begin{pmatrix} V_x(x,y) \\ V_y(x,y) \end{pmatrix} . \tag{3.15}$$

Special cases include autonomous second order ODEs, *viz.*

$$\ddot{x} = f(x,\dot{x}) \qquad \Longrightarrow \qquad \frac{d}{dt}\begin{pmatrix} x \\ v \end{pmatrix} = \begin{pmatrix} v \\ f(x,v) \end{pmatrix} , \tag{3.16}$$

of the type which occur in one-dimensional mechanics.

3.2.1 The damped driven pendulum

Another example is that of the damped and driven harmonic oscillator,

$$\frac{d^2\phi}{ds^2} + \gamma\,\frac{d\phi}{ds} + \sin\phi = j \ . \tag{3.17}$$

This is equivalent to a model of a resistively and capacitively shunted Josephson junction, depicted in fig. 3.3. If ϕ is the superconducting phase difference across the junction, the

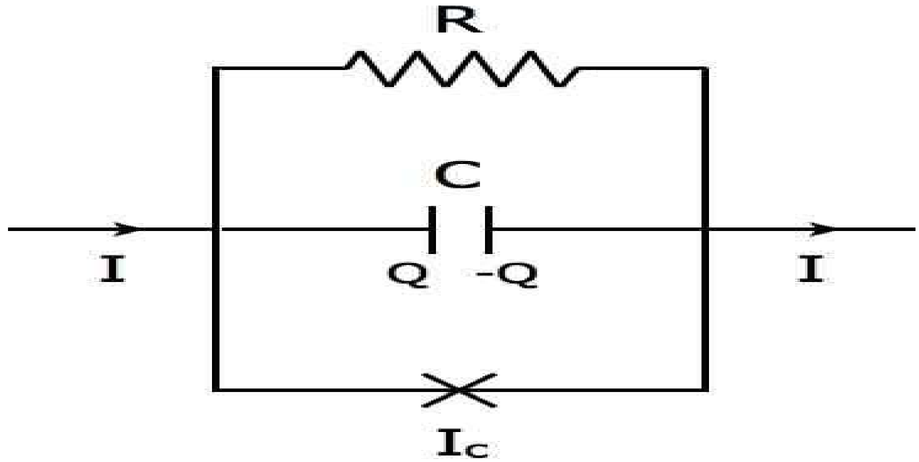

Figure 3.3: . The resistively and capacitively shunted Josephson junction. The Josephson junction is the X element at the bottom of the figure.

current through the junction is given by $I_J = I_c \sin\phi$, where I_c is the *critical current*. The current carried by the resistor is $I_R = V/R$ from Ohm's law, and the current from the capacitor is $I_C = \dot{Q}$. Finally, the *Josephson relation* relates the voltage V across the junction to the superconducting phase difference ϕ: $V = (\hbar/2e)\,\dot{\phi}$. Summing up the parallel currents, we have that the total current I is given by

$$I = \frac{\hbar C}{2e}\,\ddot{\phi} + \frac{\hbar}{2eR}\,\dot{\phi} + I_c\,\sin\phi\ , \tag{3.18}$$

which, again, is equivalent to a damped, driven pendulum.

This system also has a mechanical analog. Define the 'potential'

$$U(\phi) = -I_c\,\cos\phi - I\phi\ . \tag{3.19}$$

The equation of motion is then

$$\frac{\hbar C}{2e}\,\ddot{\phi} + \frac{\hbar}{2eR}\,\dot{\phi} = -\frac{\partial U}{\partial \phi}\ . \tag{3.20}$$

Thus, the combination $\hbar C/2e$ plays the role of the inertial term (mass, or moment of inertia), while the combination $\hbar/2eR$ plays the role of a damping coefficient. The potential $U(\phi)$ is known as the *tilted washboard potential*, for obvious reasons. (Though many of you have perhaps never seen a washboard.)

The model is adimensionalized by defining the Josephson plasma frequency ω_p and the RC time constant τ:

$$\omega_p \equiv \sqrt{\frac{2eI_c}{\hbar C}}\qquad ,\qquad \tau \equiv RC\ . \tag{3.21}$$

The dimensionless combination $\omega_p\tau$ then enters the adimensionalized equation as the sole control parameter:

$$\frac{I}{I_c} = \frac{d^2\phi}{ds^2} + \frac{1}{\omega_p\tau}\,\frac{d\phi}{ds} + \sin\phi\ , \tag{3.22}$$

where $s = \omega_{\rm p} t$. In the Josephson junction literature, the quantity $\beta \equiv 2eI_{\rm c}R^2C/\hbar = (\omega_{\rm p}\tau)^2$, known as the *McCumber-Stewart* parameter, is a dimensionless measure of the damping (large β means small damping). In terms of eqn. 3.17, we have $\gamma = (\omega_{\rm p}\tau)^{-1}$ and $j = I/I_{\rm c}$.

We can write the second order ODE of eqn. 3.17 as two coupled first order ODEs:

$$\frac{d}{dt}\begin{pmatrix}\phi\\ \omega\end{pmatrix} = \begin{pmatrix}\omega\\ j - \sin\phi - \gamma\,\omega\end{pmatrix} \ , \tag{3.23}$$

where $\omega = \dot\phi$. Phase space is a cylinder, $\mathbb{S}^1 \times \mathbb{R}^1$.

The quantity $\omega_{\rm p}\tau$ typically ranges from 10^{-3} to 10^3 in Josephson junction applications. If $\omega_{\rm p}\tau$ is small, then the system is heavily damped, and the inertial term $d^2\phi/ds^2$ can be neglected. One then obtains the $N = 1$ system

$$\gamma\,\frac{d\phi}{ds} = j - \sin\phi \ . \tag{3.24}$$

If $|j| < 1$, then $\phi(s)$ evolves to the first stable fixed point encountered, where $\phi^* = \sin^{-1}(j)$ and $\cos\phi^* = \sqrt{1-j^2}$. Since $\phi(s) \to \phi^*$ is asymptotically a constant, the voltage drop V must then vanish, as a consequence of the Josephson relation $V = (\hbar/2e)\,\dot\phi$. This, there is current flowing with no voltage drop!

If $|j| > 1$, the RHS never vanishes, in which case $\phi(s)$ is monotonic. We then can integrate the differential equation

$$dt = \frac{\hbar}{2eR}\cdot\frac{d\phi}{I - I_{\rm c}\,\sin\phi} \ . \tag{3.25}$$

Asymptotically the motion is periodic, with the period T obtained by integrating over the interval $\phi \in [0, 2\pi]$. One finds

$$T = \frac{\hbar}{2eR}\cdot\frac{2\pi}{\sqrt{I^2 - I_{\rm c}^2}} \ . \tag{3.26}$$

The time-averaged voltage drop is then

$$\langle V\rangle = \frac{\hbar}{2e}\,\langle\dot\phi\rangle = \frac{\hbar}{2e}\cdot\frac{2\pi}{T} = R\sqrt{I^2 - I_{\rm c}^2} \ . \tag{3.27}$$

This is the physics of the *current-biased resistively and capacitively shunted Josephson junction* in the strong damping limit. It is 'current-biased' because we are specifying the current I. Note that Ohm's law is recovered at large values of I.

For general $\omega_{\rm p}\tau$, we can still say quite a bit. At a fixed point, both components of the vector field $\boldsymbol{V}(\phi,\omega)$ must vanish. This requires $\omega = 0$ and $j = \sin\phi$. Therefore, there are two fixed points for $|j| < 1$, one a saddle point and the other a stable spiral. For $|j| > 1$ there are no fixed points, and asymptotically the function $\phi(t)$ tends to a periodic *limit cycle* $\phi_{\rm LC}(t)$. The flow is sketched for two representative values of j in Fig. 3.4.

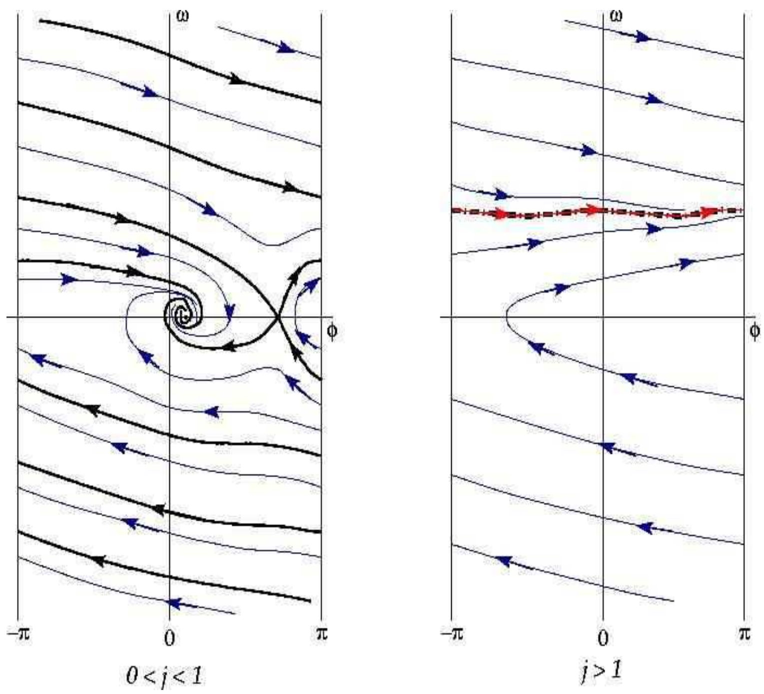

Figure 3.4: Phase flows for the equation $\ddot{\phi} + \gamma^{-1}\dot{\phi} + \sin\phi = j$. Left panel: $0 < j < 1$; note the separatrix (in black), which flows into the stable and unstable fixed points. Right panel: $j > 1$. The red curve overlying the thick black dot-dash curve is a *limit cycle*.

3.2.2 Classification of $N = 2$ fixed points

Suppose we have solved the fixed point equations $V_x(x^*, y^*) = 0$ and $V_y(x^*, y^*) = 0$. Let us now expand about the fixed point, writing

$$\dot{x} = \frac{\partial V_x}{\partial x}\bigg|_{(x^*,y^*)} (x - x^*) + \frac{\partial V_x}{\partial y}\bigg|_{(x^*,y^*)} (y - y^*) + \ldots \tag{3.28}$$

$$\dot{y} = \frac{\partial V_y}{\partial x}\bigg|_{(x^*,y^*)} (x - x^*) + \frac{\partial V_y}{\partial y}\bigg|_{(x^*,y^*)} (y - y^*) + \ldots \ . \tag{3.29}$$

We define

$$u_1 = x - x^* \qquad , \qquad u_2 = y - y^* \ , \tag{3.30}$$

which, to linear order, satisfy

$$\frac{d}{dt}\begin{pmatrix} u_1 \\ u_2 \end{pmatrix} = \overbrace{\begin{pmatrix} a & b \\ c & d \end{pmatrix}}^{M} \begin{pmatrix} u_1 \\ u_2 \end{pmatrix} + \mathcal{O}(u^2) \ . \tag{3.31}$$

The formal solution to $\dot{\boldsymbol{u}} = M\boldsymbol{u}$ is

$$\boldsymbol{u}(t) = \exp(Mt)\,\boldsymbol{u}(0) \ , \tag{3.32}$$

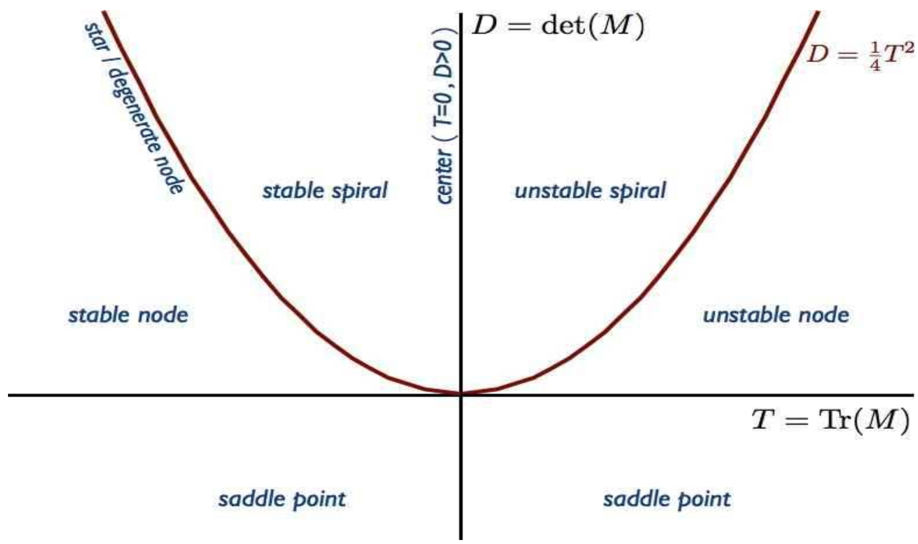

Figure 3.5: Complete classification of fixed points for the $N = 2$ system.

where $\exp(Mt) = \sum_{n=0}^{\infty} \frac{1}{n!}\,(Mt)^n$ is the exponential of the matrix Mt.

The behavior of the system is determined by the eigenvalues of M, which are roots of the characteristic equation $P(\lambda) = 0$, where

$$\begin{aligned} P(\lambda) &= \det(\lambda\mathbb{I} - M) \\ &= \lambda^2 - T\lambda + D \ , \end{aligned} \tag{3.33}$$

with $T = a + d = \mathrm{Tr}(M)$ and $D = ad - bc = \det(M)$. The two eigenvalues are therefore

$$\lambda_\pm = \tfrac{1}{2}\Big(T \pm \sqrt{T^2 - 4D}\Big) \ . \tag{3.34}$$

To see why the eigenvalues control the behavior, let us expand $\boldsymbol{u}(0)$ in terms of the eigenvectors of M. Since M is not necessarily symmetric, we should emphasize that we expand $\boldsymbol{u}(0)$ in terms of the *right* eigenvectors of M, which satisfy

$$M\boldsymbol{\psi}_a = \lambda_a \boldsymbol{\psi}_a \ , \tag{3.35}$$

where the label a runs over the symbols $+$ and $-$, as in (3.34). We write

$$\boldsymbol{u}(t) = \sum_a C_a(t)\,\boldsymbol{\psi}_a \ . \tag{3.36}$$

Since (we assume) the eigenvectors are *linearly independent*, the equation $\dot{\boldsymbol{u}} = M\boldsymbol{u}$ becomes

$$\dot{C}_a = \lambda_a\, C_a \ , \tag{3.37}$$

with solution

$$C_a(t) = e^{\lambda_a t}\, C_a(0) \ . \tag{3.38}$$

Thus, the coefficients of the eigenvectors $\boldsymbol{\psi}_a$ will *grow* in magnitude if $|\lambda_a| > 1$, and will *shrink* if $|\lambda_a| < 1$.

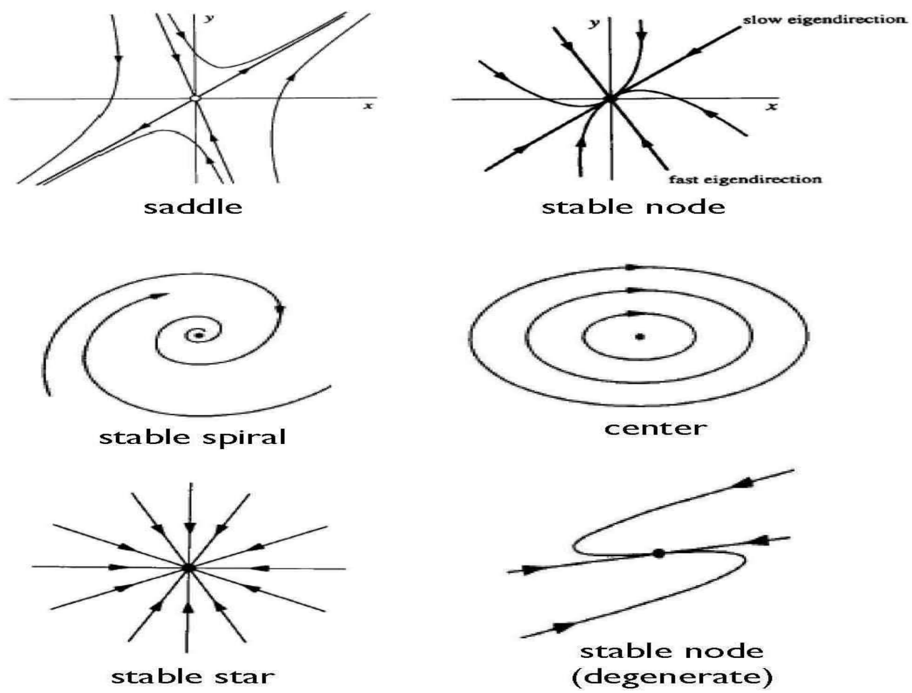

Figure 3.6: Fixed point zoo for $N = 2$ systems. Not shown: unstable versions of node, spiral, and star (reverse direction of arrows to turn stable into unstable).

3.2.3 The fixed point zoo

- **Saddles** : When $D < 0$, both eigenvalues are real; one is positive and one is negative, *i.e.* $\lambda_+ > 0$ and $\lambda_- < 0$. The right eigenvector $\boldsymbol{\psi}_-$ is thus the *stable direction* while $\boldsymbol{\psi}_+$ is the *unstable direction*.

- **Nodes** : When $0 < D < \frac{1}{4}T^2$, both eigenvalues are real and of the same sign. Thus, both right eigenvectors correspond to stable or to unstable directions, depending on whether $T < 0$ (stable; $\lambda_- < \lambda_+ < 0$) or $T < 0$ (unstable; $\lambda_+ > \lambda_- > 0$). If $\lambda_\pm$ are distinct, one can distinguish *fast* and *slow* eigendirections, based on the magnitude of the eigenvalues.

- **Spirals** : When $D > \frac{1}{4}T^2$, the discriminant $T^2 - 4D$ is negative, and the eigenvalues come in a complex conjugate pair: $\lambda_- = \lambda_+^*$. The real parts are given by $\mathrm{Re}(\lambda_\pm) = \frac{1}{2}T$, so the motion is stable (*i.e.* collapsing to the fixed point) if $T < 0$ and unstable (*i.e.* diverging from the fixed point) if $T > 0$. The motion is easily shown to correspond to a spiral. One can check that the spiral rotates counterclockwise for $a > d$ and clockwise for $a < d$.

- **Degenerate Cases** : When $T = 0$ we have $\lambda_\pm = \pm\sqrt{-D}$. For $D < 0$ we have a saddle, but for $D > 0$ both eigenvalues are imaginary: $\lambda_\pm = \pm i\sqrt{D}$. The orbits do not collapse to a point, nor do they diverge to infinity, in the $t \to \infty$ limit, as they do

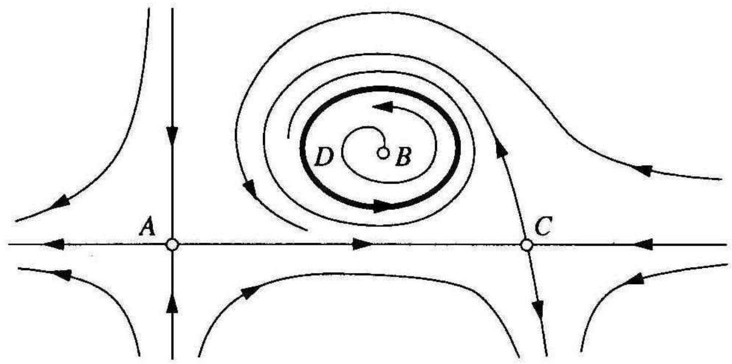

Figure 3.7: Phase portrait for an $N = 2$ flow including saddles (A,C), unstable spiral (B), and limit cycle (D).

in the case of the stable and unstable spiral. The fixed point is called a *center*, and it is surrounded by closed trajectories.

When $D = \frac{1}{4}T^2$, the discriminant vanishes and the eigenvalues are degenerate. If the rank of M is two, the fixed point is a stable ($T < 0$) or unstable ($T > 0$) *star*. If M is degenerate and of rank one, the fixed point is a *degenerate node*.

When $D = 0$, one of the eigenvalues vanishes. This indicates a *fixed line* in phase space, since any point on that line will not move. The fixed line can be stable or unstable, depending on whether the remaining eigenvalue is negative (stable, $T < 0$), or positive (unstable, $T > 0$).

Putting it all together, an example of a phase portrait is shown in Fig. 3.7. Note the presence of an *isolated, closed trajectory*, which is called a *limit cycle*. Many self-sustained physical oscillations, *i.e.* oscillations with no external forcing, exhibit limit cycle behavior. Limit cycles, like fixed points, can be stable or unstable, or partially stable. Limit cycles are inherently nonlinear. While the linear equation $\dot{\boldsymbol{\varphi}} = M\,\boldsymbol{\varphi}$ can have periodic solutions if M has purely imaginary eigenvalues, these periodic trajectories are not *isolated*, because $\lambda\,\boldsymbol{\varphi}(t)$ is also a solution. The amplitude of these linear oscillations is fixed by the initial conditions, whereas for limit cycles, the amplitude is inherent from the dynamics itself, and the initial conditions are irrelevant (for a stable limit cycle).

In fig. 3.8 we show simple examples of stable, unstable, and half-stable limit cycles. As we shall see when we study nonlinear oscillations, the Van der Pol oscillator,

$$\ddot{x} + \mu(x^2 - 1)\,\dot{x} + x = 0 \ , \tag{3.39}$$

with $\mu > 0$ has a stable limit cycle. The physics is easy to apprehend. The coefficient of the $\dot{x}$ term in the equation of motion is positive for $|x| > 1$ and negative for $|x| < 1$. Interpreting this as a coefficient of friction, we see that the friction is positive, *i.e.* dissipating energy, when $|x| > 1$ but *negative*, *i.e.* accumulating energy, for $|x| < 1$. Thus, any small motion with $|x| < 1$ is *amplified* due to the negative friction, and would increase without bound

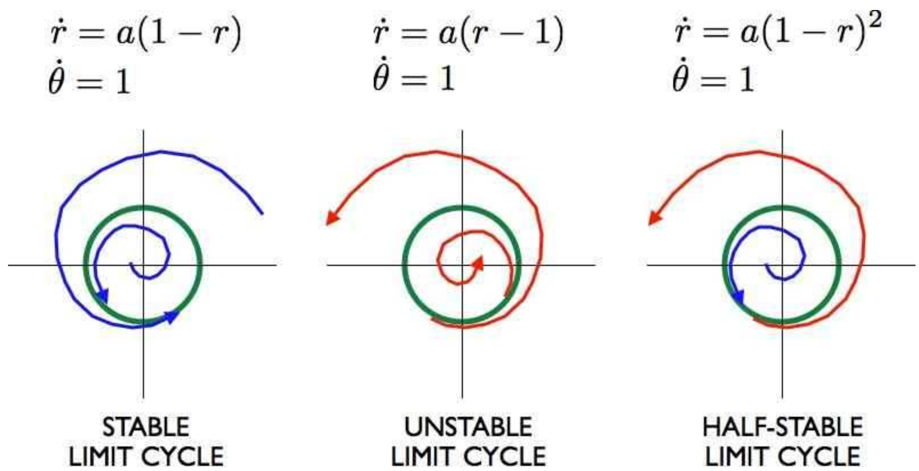

Figure 3.8: Stable, unstable, and half-stable limit cycles.

were it not for the fact that the friction term reverses its sign and becomes dissipative for $|x| > 1$. The limit cycle for $\mu \gg 1$ is shown in fig. 3.9.

3.2.4 Fixed points for $N = 3$ systems

For an $N = 2$ system, there are five generic types of fixed points. They are classified according to the eigenvalues of the linearized dynamics at the fixed point. For a real 2×2 matrix, the eigenvalues must be real or else must be a complex conjugate pair. The five types of fixed points are then

$$\begin{aligned}
\lambda_1 > 0 \ , \ \lambda_2 > 0 \quad &: \quad \text{(1) unstable node} \\
\lambda_1 > 0 \ , \ \lambda_2 < 0 \quad &: \quad \text{(2) saddle point} \\
\lambda_1 < 0 \ , \ \lambda_2 < 0 \quad &: \quad \text{(3) stable node} \\
\mathsf{Re}\,\lambda_1 > 0 \ , \ \lambda_2 = \lambda_1^* \quad &: \quad \text{(4) unstable spiral} \\
\mathsf{Re}\,\lambda_1 < 0 \ , \ \lambda_2 = \lambda_1^* \quad &: \quad \text{(5) stable spiral}
\end{aligned}$$

How many possible generic fixed points are there for an $N = 3$ system?

For a general real 3×3 matrix M, the characteristic polynomial $P(\lambda) = \det(\lambda - M)$ satisfies $P(\lambda^*) = P(\lambda)$. Thus, if λ is a root then so is λ^*. This means that the eigenvalues are either real or else come in complex conjugate pairs. There are then ten generic possibilities for

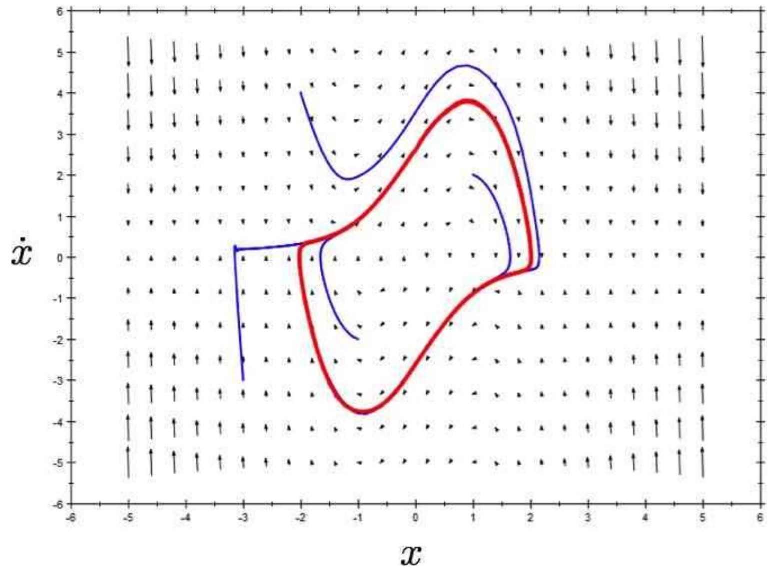

Figure 3.9: Limit cycle of the Van der Pol oscillator for $\mu \gg 1$. (Source: Wikipedia)

the three eigenvalues:

(1)	unstable node	:	$\lambda_1 > \lambda_2 > \lambda_3 > 0$
(2)	$(++-)$ saddle	:	$\lambda_1 > \lambda_2 > 0 > \lambda_3$
(3)	$(+--)$ saddle	:	$\lambda_1 > 0 > \lambda_2 > \lambda_3$
(4)	stable note	:	$0 > \lambda_1 > \lambda_2 > \lambda_3$
(5)	unstable spiral-node	:	$\lambda_1 > \mathsf{Re}\,\lambda_{2,3} > 0$; $\mathsf{Im}\,\lambda_2 = -\mathsf{Im}\,\lambda_3$
(6)	unstable spiral-node	:	$\mathsf{Re}\,\lambda_{1,2} > \lambda_3 > 0$; $\mathsf{Im}\,\lambda_1 = -\mathsf{Im}\,\lambda_2$
(7)	stable spiral-node	:	$0 > \lambda_1 > \mathsf{Re}\,\lambda_{2,3}$; $\mathsf{Im}\,\lambda_2 = -\mathsf{Im}\,\lambda_3$
(8)	stable spiral-node	:	$0 > \mathsf{Re}\,\lambda_{1,2} > \lambda_3$; $\mathsf{Im}\,\lambda_1 = -\mathsf{Im}\,\lambda_2$
(9)	$(+--)$ spiral-saddle	:	$\lambda_1 > 0 > \mathsf{Re}\,\lambda_{2,3}$; $\mathsf{Im}\,\lambda_2 = -\mathsf{Im}\,\lambda_3$
(10)	$(++-)$ spiral-saddle	:	$\mathsf{Re}\,\lambda_{1,2} > 0 > \lambda_3$; $\mathsf{Im}\,\lambda_1 = -\mathsf{Im}\,\lambda_2$.

3.3 Andronov-Hopf Bifurcation

A bifurcation between a spiral and a limit cycle is known as an *Andronov-Hopf bifurcation.* As a simple example, consider the $N = 2$ system,

$$\dot{x} = ax - by - C(x^2 + y^2)\, x \tag{3.40}$$

$$\dot{y} = bx + ay - C(x^2 + y^2)\, y \ , \tag{3.41}$$

where a, b, and C are real. Clearly the origin is a fixed point, at which one finds the eigenvalues $\lambda = a \pm ib$. Thus, the fixed point is a stable spiral if $a < 0$ and an unstable spiral if $a > 0$.

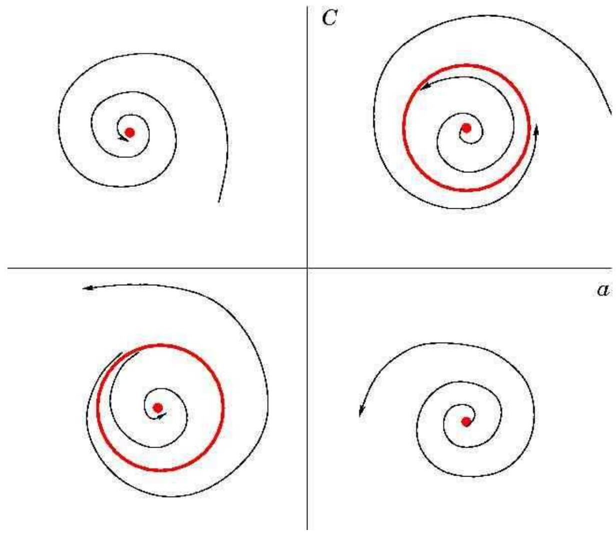

Figure 3.10: Hopf bifurcation: for $C > 0$ the bifurcation is supercritical, between stable spiral and stable limit cycle. For $C < 0$ the bifurcation is subcritical, between unstable spiral and unstable limit cycle. The bifurcation occurs at $a = 0$ in both cases.

Written in terms of the complex variable $z = x + iy$, these two equations collapse to the single equation

$$\dot{z} = (a + ib)\, z - C\, |z|^2\, z \ . \tag{3.42}$$

The dynamics are also simple in polar coordinates $r = |z|$, $\theta = \arg(z)$:

$$\dot{r} = ar - Cr^3 \tag{3.43}$$

$$\dot{\theta} = b \ . \tag{3.44}$$

The phase diagram, for fixed $b > 0$, is depicted in Fig. 3.10. For positive a/C, there is a limit cycle at $r = \sqrt{a/C}$. In both cases, the limit cycle disappears as a crosses the value $a^* = 0$ and is replaced by a stable $(a < 0, C > 0)$ or unstable $(a > 0, C < 0)$ spiral.

This example also underscores the following interesting point. Adding a small nonlinear term C has no fundamental effect on the fixed point behavior so long as $a \neq 0$, when the fixed point is a stable or unstable spiral. In general, fixed points which are attractors (stable spirals or nodes), repellers (unstable spirals or nodes), or saddles are *robust* with respect to the addition of a small nonlinearity. But the fixed point behavior in the marginal cases – centers, stars, degenerate nodes, and fixed lines – is strongly affected by the presence of even a small nonlinearity. In this example, the FP is a center when $a = 0$. But as the (r, θ) dynamics shows, a small nonlinearity will destroy the center and turn the FP into an attractor $(C > 0)$ or a repeller $(C < 0)$.

3.4 Population Biology : Lotka-Volterra Models

Consider two species with populations N_1 and N_2, respectively. We model the evolution of these populations by the coupled ODEs

$$\frac{dN_1}{dt} = aN_1 + bN_1N_2 + cN_1^2 \tag{3.45}$$

$$\frac{dN_2}{dt} = dN_2 + eN_1N_2 + fN_2^2 \ , \tag{3.46}$$

where $\{a, b, c, d, e, f\}$ are constants. We can eliminate some constants by rescaling $N_{1,2}$. This results in the following:

$$\dot{x} = x\big(r - \mu x - ky\big) \tag{3.47}$$

$$\dot{y} = y\big(r' - \mu' y - k' x\big) \ , \tag{3.48}$$

where μ, and μ' can each take on one of three possible values $\{0, \pm 1\}$. By rescaling time, we can eliminate the scale of either of r or r' as well. Typically, intra-species competition guarantees $\mu = \mu' = +1$. The remaining coefficients (r, k, k') are real may also be of either sign. The values and especially the signs of the various coefficients have a physical (or biological) significance. For example, if $k < 0$ it means that x grows due to the presence of y. The effect of y on x may be of the same sign $(kk' > 0)$ or of opposite sign $(kk' < 0)$.

3.4.1 Rabbits and foxes

As an example, consider the model

$$\dot{x} = x - xy \tag{3.49}$$

$$\dot{y} = -\beta y + xy \ . \tag{3.50}$$

The quantity x might represent the (scaled) population of rabbits and y the population of foxes in an ecosystem. There are two fixed points: at $(0, 0)$ and at $(\beta, 1)$. Linearizing the dynamics about these fixed points, one finds that $(0, 0)$ is a saddle while $(\beta, 1)$ is a center. Let's do this explicitly.

The first step is to find the fixed points (x^*, y^*). To do this, we set $\dot{x} = 0$ and $\dot{y} = 0$. From $\dot{x} = x(1 - y) = 0$ we have that $x = 0$ or $y = 1$. Suppose $x = 0$. The second equation, $\dot{y} = (x - \beta)y$ then requires $y = 0$. So $\boldsymbol{P}_1 = (0, 0)$ is a fixed point. The other possibility is that $y = 1$, which then requires $x = \beta$. So $\boldsymbol{P}_2 = (\beta, 1)$ is the second fixed point. Those are the only possibilities.

We now compute the linearized dynamics at these fixed points. The linearized dynamics are given by $\dot{\boldsymbol{\varphi}} = M\boldsymbol{\varphi}$, with

$$M = \begin{pmatrix} \partial\dot{x}/\partial x & \partial\dot{x}/\partial y \\ \partial\dot{y}/\partial x & \partial\dot{y}/\partial y \end{pmatrix} = \begin{pmatrix} 1 - y & -x \\ y & x - \beta \end{pmatrix} \ . \tag{3.51}$$

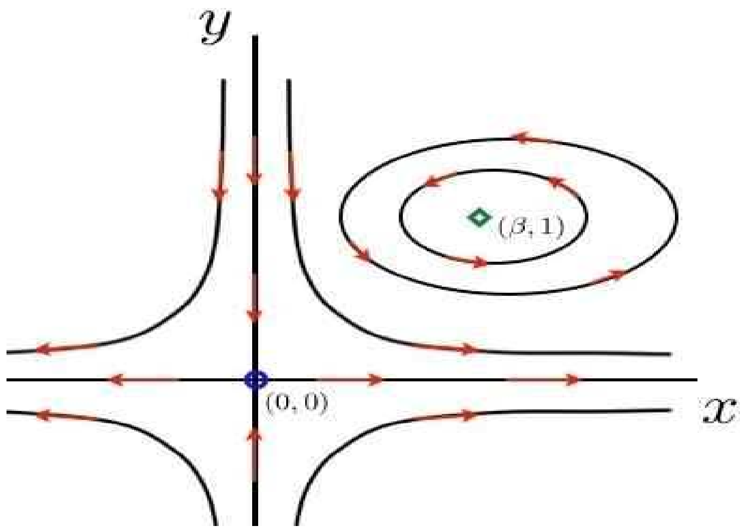

Figure 3.11: Phase flow for the rabbits *vs.* foxes Lotka-Volterra model of eqs. 3.49, 3.50.

Evaluating M at $\boldsymbol{P}_1$ and $\boldsymbol{P}_2$, we find

$$M_1 = \begin{pmatrix} 1 & 0 \\ 0 & -\beta \end{pmatrix} \quad , \qquad M_2 = \begin{pmatrix} 0 & -\beta \\ 1 & 0 \end{pmatrix} \ . \tag{3.52}$$

The eigenvalues are easily found:

$$\boldsymbol{P}_1 \ : \ \lambda_+ = 1 \qquad\qquad \boldsymbol{P}_2 \ : \ \lambda_+ = i\sqrt{\beta} \tag{3.53}$$

$$\lambda_- = -\beta \qquad\qquad \lambda_- = -i\sqrt{\beta} \ . \tag{3.54}$$

Thus $\boldsymbol{P}_1$ is a saddle point and $\boldsymbol{P}_2$ is a center.

3.4.2 Rabbits and sheep

In the rabbits and foxes model of eqs. 3.49, 3.50, the rabbits are the food for the foxes. This means $k = 1$ but $k' = -1$, *i.e.* the fox population is enhanced by the presence of rabbits, but the rabbit population is diminished by the presence of foxes. Consider now a model in which the two species (rabbits and sheep, say) compete for food:

$$\dot{x} = x\,(r - x - ky) \tag{3.55}$$

$$\dot{y} = y\,(1 - y - k'x) \ , \tag{3.56}$$

with r, k, and k' all positive. Note that when either population x or y vanishes, the remaining population is governed by the logistic equation, *i.e.* it will flow to a nonzero fixed point.

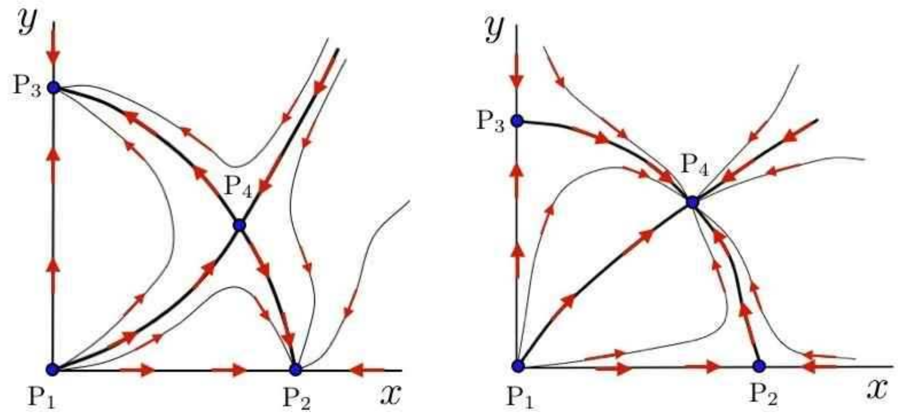

Figure 3.12: Two possible phase flows for the rabbits *vs.* sheep model of eqs. 3.55, 3.56. Left panel: $k > r > k'^{-1}$. Right panel: $k < r < k'^{-1}$.

The matrix of derivatives, which is to be evaluated at each fixed point in order to assess its stability, is

$$M = \begin{pmatrix} \partial\dot{x}/\partial x & \partial\dot{x}/\partial y \\ \partial\dot{y}/\partial x & \partial\dot{y}/\partial y \end{pmatrix} = \begin{pmatrix} r - 2x - ky & -kx \\ -k'y & 1 - 2y - k'x \end{pmatrix} . \tag{3.57}$$

At each fixed point, we must evaluate $D = \det(M)$ and $T = \mathrm{Tr}\,(M)$ and apply the classification scheme of Fig. 3.5.

- $\boldsymbol{P}_1 = (0,0)$: This is the trivial state with no rabbits ($x = 0$) and no sheep ($y = 0$). The linearized dynamics gives $M_1 = \begin{pmatrix} r & 0 \\ 0 & 1 \end{pmatrix}$, which corresponds to an unstable node.

- $\boldsymbol{P}_2 = (r,0)$: Here we have rabbits but no sheep. The linearized dynamics gives $M_2 = \begin{pmatrix} -r & -rk \\ 0 & 1 - rk' \end{pmatrix}$. For $rk' > 1$ this is a stable node; for $rk' < 1$ it is a saddle point.

- $\boldsymbol{P}_3 = (0,1)$: Here we have sheep but no rabbits. The linearized dynamics gives $M_3 = \begin{pmatrix} r - k & 0 \\ -k' & -1 \end{pmatrix}$. For $k > r$ this is a stable node; for $k < r$ it is a saddle.

- There is one remaining fixed point – a nontrivial one where both x and y are nonzero. To find it, we set $\dot{x} = \dot{y} = 0$, and divide out by x and y respectively, to get

$$x + ky = r \tag{3.58}$$
$$kx' + y = 1 \ . \tag{3.59}$$

This is a simple rank 2 inhomogeneous linear system. If the fixed point $\boldsymbol{P}_4$ is to lie in the physical quadrant ($x > 0, y > 0$), then either (i) $k > r$ and $k' > r^{-1}$ or (ii) $k < r$

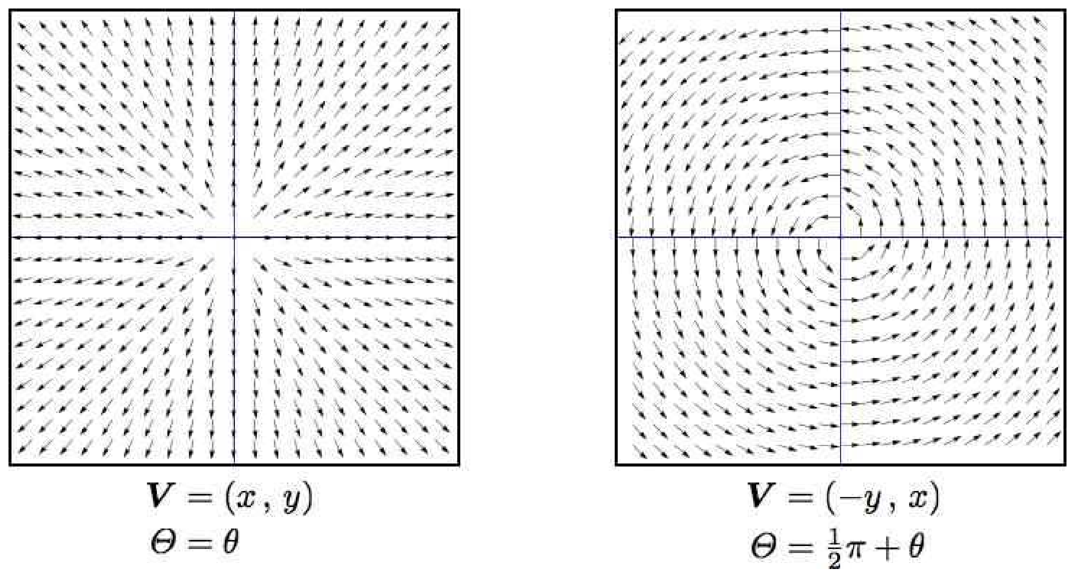

Figure 3.13: Two singularities with index +1. The direction field $\hat{\boldsymbol{V}} = \boldsymbol{V}/\big|\boldsymbol{V}\big|$ is shown in both cases.

and $k' < r^{-1}$. The solution is

$$\boldsymbol{P}_4 = \begin{pmatrix} 1 & k \\ k' & 1 \end{pmatrix}^{-1} \begin{pmatrix} r \\ 1 \end{pmatrix} = \frac{1}{1-kk'} \begin{pmatrix} r-k \\ 1-rk' \end{pmatrix} . \tag{3.60}$$

The linearized dynamics then gives

$$M_4 = \frac{1}{1-kk'} \begin{pmatrix} k-r & k(k-r) \\ \\ k'(rk'-1) & rk'-1 \end{pmatrix} , \tag{3.61}$$

yielding

$$T = \frac{rk'-1+k-r}{1-kk'} \tag{3.62}$$

$$D = \frac{(k-r)(rk'-1)}{1-kk'} . \tag{3.63}$$

The classification of this fixed point can vary with parameters. Consider the case $r = 1$. If $k = k' = 2$ then both $\boldsymbol{P}_2$ and $\boldsymbol{P}_3$ are stable nodes. At $\boldsymbol{P}_4$, one finds $T = -\frac{2}{3}$ and $D = -\frac{1}{3}$, corresponding to a saddle point. In this case it is the fate of one population to die out at the expense of the other, and which one survives depends on initial conditions. If instead we took $k = k' = \frac{1}{2}$, then $T = -\frac{4}{3}$ and $D = \frac{1}{3}$, corresponding to a stable node (node $D < \frac{1}{4}T^2$ in this case). The situation is depicted in Fig. 3.12.

3.5 Poincaré-Bendixson Theorem

Although $N = 2$ systems are much richer than $N = 1$ systems, they are still ultimately rather impoverished in terms of their long-time behavior. If an orbit does not flow off to infinity or asymptotically approach a stable fixed point (node or spiral or nongeneric example), the only remaining possibility is limit cycle behavior. This is the content of the *Poincaré-Bendixson theorem*, which states:

- *IF* Ω is a compact (*i.e.* closed and bounded) subset of phase space,
- *AND* $\dot{\boldsymbol{\varphi}} = \boldsymbol{V}(\boldsymbol{\varphi})$ is continuously differentiable on Ω,
- *AND* Ω contains no fixed points (*i.e.* $\boldsymbol{V}(\boldsymbol{\varphi})$ never vanishes in Ω),
- *AND* a phase curve $\boldsymbol{\varphi}(t)$ is always confined to Ω,

◇ *THEN* $\boldsymbol{\varphi}(t)$ is either closed or approaches a closed trajectory in the limit $t \to \infty$.

Thus, under the conditions of the theorem, Ω must contain a closed orbit.

One way to prove that $\boldsymbol{\varphi}(t)$ is confined to Ω is to establish that $\boldsymbol{V} \cdot \hat{\boldsymbol{n}} \leq 0$ everywhere on the boundary $\partial\Omega$, which means that the phase flow is always directed inward (or tangent) along the boundary. Let's analyze an example from the book by Strogatz. Consider the system

$$\dot{r} = r(1 - r^2) + \lambda\, r\, \cos\theta \tag{3.64}$$

$$\dot{\theta} = 1\ , \tag{3.65}$$

with $0 < \lambda < 1$. Then define

$$a \equiv \sqrt{1-\lambda} \quad , \quad b \equiv \sqrt{1+\lambda} \tag{3.66}$$

and

$$\Omega \equiv \Big\{ (r, \theta) \ \Big| \ a < r < b \ \Big\} \ . \tag{3.67}$$

On the boundaries of Ω, we have

$$r = a \qquad \Rightarrow \qquad \dot{r} = \lambda\, a \left(1 + \cos\theta\right) \tag{3.68}$$

$$r = b \qquad \Rightarrow \qquad \dot{r} = -\lambda\, b \left(1 - \cos\theta\right)\ . \tag{3.69}$$

We see that the radial component of the flow is inward along both $r = a$ and $r = b$. Thus, any trajectory which starts inside Ω can never escape. The Poincaré-Bendixson theorem tells us that the trajectory will approach a stable limit cycle in the limit $t \to \infty$.

It is only with $N \geq 3$ systems that the interesting possibility of chaotic behavior emerges.

3.6 Index Theory

Consider a smooth two-dimensional vector field $\boldsymbol{V}(\boldsymbol{\varphi})$. The angle that the vector $\boldsymbol{V}$ makes with respect to the $\hat{\boldsymbol{\varphi}}_1$ and $\hat{\boldsymbol{\varphi}}_2$ axes is a scalar field,

$$\Theta(\boldsymbol{\varphi}) = \tan^{-1}\left(\frac{V_2(\boldsymbol{\varphi})}{V_1(\boldsymbol{\varphi})}\right) . \tag{3.70}$$

So long as $\boldsymbol{V}$ has finite length, the angle Θ is well-defined. In particular, we expect that we can integrate $\boldsymbol{\nabla}\Theta$ over a closed curve $\mathcal{C}$ in phase space to get

$$\oint\limits_{\mathcal{C}} d\boldsymbol{\varphi} \cdot \boldsymbol{\nabla}\Theta = 0 . \tag{3.71}$$

However, this can fail if $\boldsymbol{V}(\boldsymbol{\varphi})$ vanishes (or diverges) at one or more points in the interior of $\mathcal{C}$. In general, if we define

$$\mathsf{W}_{\mathcal{C}}(\boldsymbol{V}) = \frac{1}{2\pi} \oint\limits_{\mathcal{C}} d\boldsymbol{\varphi} \cdot \boldsymbol{\nabla}\Theta , \tag{3.72}$$

then $\mathsf{W}_{\mathcal{C}}(\boldsymbol{V}) \in \mathbb{Z}$ is an integer valued function of $\mathcal{C}$, which is the change in Θ around the curve $\mathcal{C}$. This must be an integer, because Θ is well-defined only up to multiples of 2π. Note that *differential changes* of Θ are in general well-defined.

Thus, if $\boldsymbol{V}(\boldsymbol{\varphi})$ is finite, meaning neither infinite nor infinitesimal, *i.e.* $\boldsymbol{V}$ neither diverges nor vanishes anywhere in $\text{int}(\mathcal{C})$, then $\mathsf{W}_{\mathcal{C}}(\boldsymbol{V}) = 0$. Assuming that $\boldsymbol{V}$ never diverges, any singularities in Θ must arise from points where $\boldsymbol{V} = 0$, which in general occurs at isolated points, since it entails two equations in the two variables $(\varphi_1\, , \varphi_2)$.

The index of a two-dimensional vector field $\boldsymbol{V}(\boldsymbol{\varphi})$ at a *point* $\boldsymbol{\varphi}$ is the integer-valued winding of $\boldsymbol{V}$ about that point:

$$\underset{\boldsymbol{\varphi}_0}{\mathsf{ind}}\,(\boldsymbol{V}) = \lim_{a\to 0} \frac{1}{2\pi} \oint\limits_{\mathcal{C}_a(\boldsymbol{\varphi}_0)} d\boldsymbol{\varphi} \cdot \boldsymbol{\nabla}\Theta \tag{3.73}$$

$$= \lim_{a\to 0} \frac{1}{2\pi} \oint\limits_{\mathcal{C}_a(\boldsymbol{\varphi}_0)} d\boldsymbol{\varphi} \cdot \frac{V_1 \boldsymbol{\nabla} V_2 - V_2 \boldsymbol{\nabla} V_1}{V_1^2 + V_2^2} , \tag{3.74}$$

where $\mathcal{C}_a(\boldsymbol{\varphi}_0)$ is a circle of radius a surrounding the point $\boldsymbol{\varphi}_0$. The index of a closed curve $\mathcal{C}$ is given by the sum of the indices at all the singularities enclosed by the curve:[2]

$$\mathsf{W}_{\mathcal{C}}(\boldsymbol{V}) = \sum_{\boldsymbol{\varphi}_i \in \text{int}(\mathcal{C})} \underset{\boldsymbol{\varphi}_i}{\mathsf{ind}}\,(\boldsymbol{V}) . \tag{3.75}$$

[2]Technically, we should weight the index at each enclosed singularity by the signed number of times the curve $\mathcal{C}$ encloses that singularity. For simplicity and clarity, we assume that the curve $\mathcal{C}$ is homeomorphic to the circle $\mathbb{S}^1$.

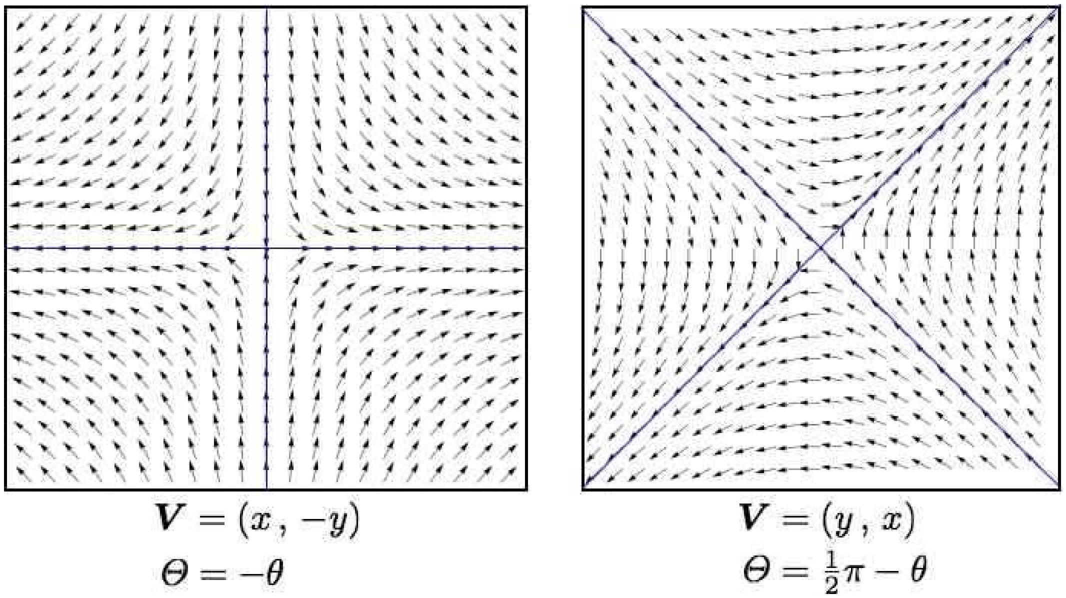

Figure 3.14: Two singularities with index -1.

As an example, consider the vector fields plotted in fig. 3.13. We have:

$$\boldsymbol{V} = (x\,,\,y) \qquad \Longrightarrow \qquad \Theta = \theta \tag{3.76}$$
$$\boldsymbol{V} = (-y\,,\,x) \qquad \Longrightarrow \qquad \Theta = \theta + \tfrac{1}{2}\pi\ . \tag{3.77}$$

The index is the same, $+1$, in both cases, even though the first corresponds to an unstable node and the second to a center. Any $N = 2$ fixed point with $\det M > 0$ has index $+1$.

Fig. 3.14 shows two vector fields, each with index -1:

$$\boldsymbol{V} = (x\,,\,-y) \qquad \Longrightarrow \qquad \Theta = -\theta \tag{3.78}$$
$$\boldsymbol{V} = (y\,,\,x) \qquad \Longrightarrow \qquad \Theta = -\theta + \tfrac{1}{2}\pi\ . \tag{3.79}$$

In both cases, the fixed point is a saddle.

As an example of the content of eqn. 3.75, consider the vector fields in eqn. 3.15. The left panel shows the vector field $\boldsymbol{V} = (x^2 - y^2\,,\,2xy)$, which has a single fixed point, at the origin $(0\,,\,0)$, of index $+2$. The right panel shows the vector field $\boldsymbol{V} = (1 + x^2 - y^2\,,\,x + 2xy)$, which has fixed points $(x^*\,,\,y^*)$ at $(0\,,\,1)$ and $(0\,,\,-1)$. The linearized dynamics is given by the matrix

$$M = \begin{pmatrix} \frac{\partial\dot{x}}{\partial x} & \frac{\partial\dot{x}}{\partial y} \\ \\ \frac{\partial\dot{y}}{\partial x} & \frac{\partial\dot{y}}{\partial y} \end{pmatrix} = \begin{pmatrix} 2x & -2y \\ \\ 1 + 2y & 2x \end{pmatrix} . \tag{3.80}$$

Thus,

$$M_{(0,1)} = \begin{pmatrix} 0 & -2 \\ 2 & 0 \end{pmatrix} \qquad , \qquad M_{(0,-1)} = \begin{pmatrix} 0 & 2 \\ -2 & 0 \end{pmatrix} . \tag{3.81}$$

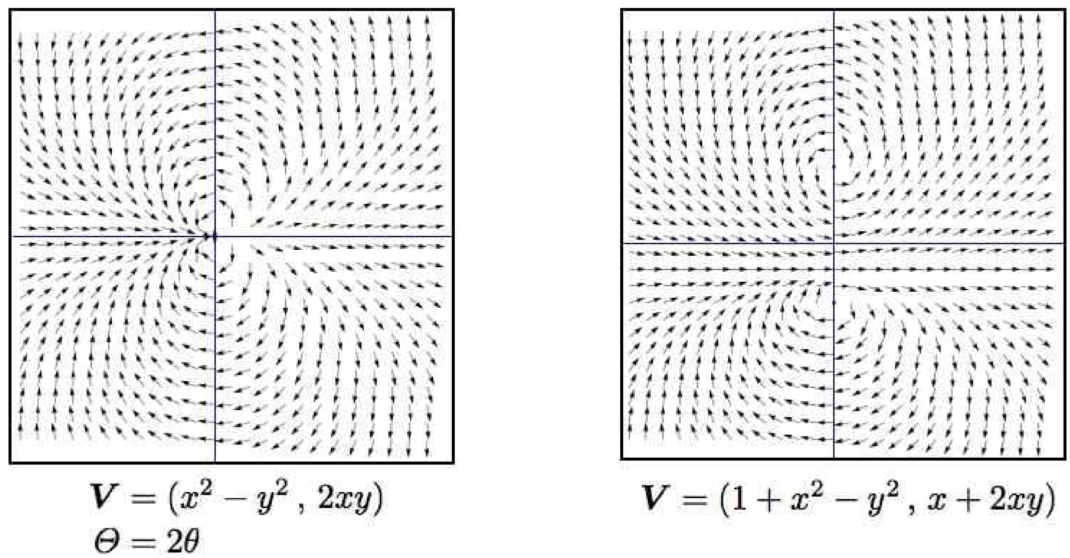

Figure 3.15: Left panel: a singularity with index +2. Right panel: two singularities each with index +1. Note that the long distance behavior of $\boldsymbol{V}$ is the same in both cases.

At each of these fixed points, we have $T = 0$ and $D = 4$, corresponding to a center, with index +1. If we consider a square-ish curve $\mathcal{C}$around the periphery of each figure, the vector field is almost the same along such a curve for both the left and right panels, and the winding number is $\mathsf{W}_{\mathcal{C}}(\boldsymbol{V}) = +2$.

Finally, consider the vector field shown in fig. 3.16, with $\boldsymbol{V} = (x^2 - y^2\,,\, -2xy)$. Clearly $\Theta = -2\theta$, and the index of the singularity at $(0\,,\,0)$ is -2.

To recapitulate some properties of the index / winding number:

- The index $\mathsf{ind}_{\varphi_0}(\boldsymbol{V})$ of an $N = 2$ vector field $\boldsymbol{V}$ at a point φ_0 is the winding number of $\boldsymbol{V}$ about that point.

- The winding number $\mathsf{W}_{\mathcal{C}}(\boldsymbol{V})$ of a curve $\mathcal{C}$ is the sum of the indices of the singularities enclosed by that curve.

- Smooth deformations of $\mathcal{C}$ do not change its winding number. One must instead "stretch" $\mathcal{C}$ over a fixed point singularity in order to change $\mathsf{W}_{\mathcal{C}}(\boldsymbol{V})$.

- Uniformly rotating each vector in the vector field by an angle β has the effect of sending $\Theta \to \Theta + \beta$; this leaves all indices and winding numbers invariant.

- Nodes and spirals, whether stable or unstable, have index +1 (ss do the special cases of centers, stars, and degenerate nodes). Saddle points have index -1.

- Clearly any closed orbit must lie on a curve $\mathcal{C}$ of index +1.

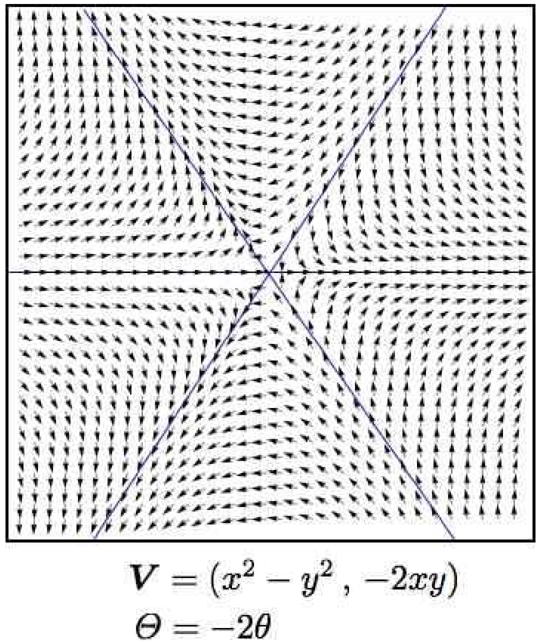

Figure 3.16: A vector field with index -2.

3.6.1 Gauss-Bonnet Theorem

There is a deep result in mathematics, the Gauss-Bonnet theorem, which connects the local *geometry* of a two-dimensional manifold to its global *topological structure*. The content of the theorem is as follows:

$$\int\limits_{\mathcal{M}} dA\, K = 2\pi\, \chi(\mathcal{M}) = 2\pi \sum_i \underset{\varphi_i}{\mathsf{ind}}\,(\boldsymbol{V})\ , \tag{3.82}$$

where $\mathcal{M}$ is a 2-manifold (a topological space locally homeomorphic to $\mathbb{R}^2$), κ is the local *Gaussian curvature* of $\mathcal{M}$, which is given by $K = (R_1\, R_2)^{-1}$, where $R_{1,2}$ are the principal radii of curvature at a given point, and dA is the differential area element. The quantity $\chi(\mathcal{M})$ is called the *Euler characteristic* of $\mathcal{M}$ and is given by $\chi(\mathcal{M}) = 2 - 2g$, where g is the *genus* of $\mathcal{M}$, which is the number of holes (or handles) of $\mathcal{M}$. Furthermore, $\boldsymbol{V}(\boldsymbol{\varphi})$ is *any* smooth vector field on $\mathcal{M}$, and $\boldsymbol{\varphi}_i$ are the singularity points of that vector field, which are fixed points of the dynamics $\dot{\boldsymbol{\varphi}} = \boldsymbol{V}(\boldsymbol{\varphi})$.

To apprehend the content of the Gauss-Bonnet theorem, it is helpful to consider an example. Let $\mathcal{M} = \mathbb{S}^2$ be the unit 2-sphere, as depicted in fig. 3.17. At any point on the unit 2-sphere, the radii of curvature are degenerate and both equal to $R = 1$, hence $K = 1$. If we integrate the Gaussian curvature over the sphere, we thus get $4\pi = 2\pi\,\chi\big(\mathbb{S}^2\big)$, which says $\chi(\mathbb{S}^2) = 2-2g = 2$, which agrees with $g = 0$ for the sphere. Furthermore, the Gauss-Bonnet theorem says that *any* smooth vector field on $\mathbb{S}^2$ *must* have a singularity or singularities, with the total index summed over the singularities equal to $+2$. The vector field sketched in the left panel of fig. 3.17 has two index $+1$ singularities, which could be taken at the

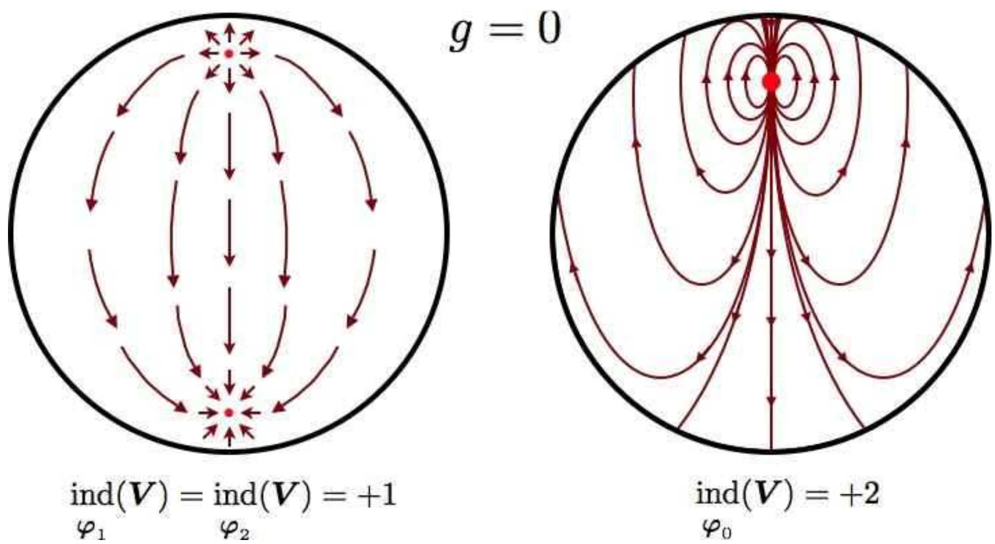

Figure 3.17: Two smooth vector fields on the sphere $\mathbb{S}^2$, which has genus $g = 0$. Left panel: two index +1 singularities. Right panel: one index +2 singularity.

north and south poles, but which could be anywhere. Another possibility, depicted in the right panel of fig. 3.17, is that there is a one singularity with index +2.

In fig. 3.18 we show examples of manifolds with genii $g = 1$ and $g = 2$. The case $g = 1$ is the familiar 2-torus, which is topologically equivalent to a product of circles: $\mathbb{T}^2 \simeq \mathbb{S}^1 \times \mathbb{S}^1$, and is thus coordinatized by two angles θ_1 and θ_2. A smooth vector field pointing in the direction of increasing θ_1 never vanishes, and thus has no singularities, consistent with $g = 1$ and $\chi\big(\mathbb{T}^2\big) = 0$. Topologically, one can define a torus as the quotient space $\mathbb{R}^2/\mathbb{Z}^2$, or as a square with opposite sides identified. This is what mathematicians call a 'flat torus' – one with curvature $K = 0$ everywhere. Of course, such a torus cannot be embedded in three-dimensional Euclidean space; a two-dimensional figure embedded in a three-dimensional Euclidean space inherits a metric due to the embedding, and for a physical torus, like the surface of a bagel, the Gaussian curvature is only zero *on average*.

The $g = 2$ surface $\mathcal{M}$ shown in the right panel of fig. 3.18 has Euler characteristic $\chi(\mathcal{M}) = -2$, which means that any smooth vector field on $\mathcal{M}$ must have singularities with indices totalling -2. One possibility, depicted in the figure, is to have two saddle points with index -1; one of these singularities is shown in the figure (the other would be on the opposite side).

3.6.2 Singularities and topology

For any $N = 1$ system $\dot{x} = f(x)$, we can identify a 'charge' Q with any generic fixed point x^* by setting

$$Q = \mathsf{sgn}\Big[f'(x^*)\Big] \ , \tag{3.83}$$

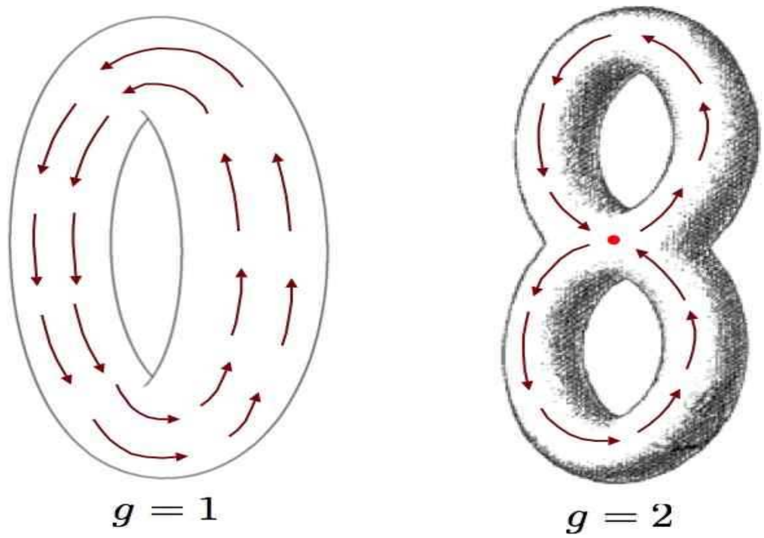

Figure 3.18: Smooth vector fields on the torus $\mathbb{T}^2$ ($g=1$), and on a 2-manifold $\mathcal{M}$ of genus $g=2$.

where $f(x^*)=0$. The total charge contained in a region $\big[x_1,x_2\big]$ is then

$$Q_{12} = \tfrac{1}{2}\,\mathsf{sgn}\Big[f(x_2)\Big] - \tfrac{1}{2}\,\mathsf{sgn}\Big[f(x_1)\Big] \ . \tag{3.84}$$

It is easy to see that Q_{12} is the sum of the charges of all the fixed points lying within the interval $\big[x_1,x_2\big]$.

In higher dimensions, we have the following general construction. Consider an N-dimensional dynamical system $\dot{\boldsymbol{x}} = \boldsymbol{V}(\boldsymbol{x})$, and let $\hat{\boldsymbol{n}}(\boldsymbol{x})$ be the unit vector field defined by

$$\hat{\boldsymbol{n}}(\boldsymbol{x}) = \frac{\boldsymbol{V}(\boldsymbol{x})}{|\boldsymbol{V}(\boldsymbol{x})|} \ . \tag{3.85}$$

Consider now a unit sphere in $\hat{\boldsymbol{n}}$ space, which is of dimension $(N-1)$. If we integrate over this surface, we obtain

$$\Omega_N = \oint d\sigma_a \, n^a = \frac{2\pi^{(N-1)/2}}{\Gamma\big(\frac{N-1}{2}\big)} \ , \tag{3.86}$$

which is the surface area of the unit sphere $\mathbb{S}^{N-1}$. Thus, $\Omega_2 = 2\pi$, $\Omega_3 = 4\pi$, $\Omega_4 = 2\pi^2$, *etc.*

Now consider a change of variables over the surface of the sphere, to the set $(\xi_1,\ldots,\xi_{N-1})$. We then have

$$\Omega_N = \oint\limits_{\mathbb{S}^{N-1}} d\sigma_a \, n^a = \oint d^{N-1}\xi \ \epsilon_{a_1\cdots a_N} \, n^{a_1} \, \frac{\partial n^{a_2}}{\partial \xi_1} \cdots \frac{\partial n^{a_N}}{\partial \xi_{N-1}} \tag{3.87}$$

The topological charge is then

$$Q = \frac{1}{\Omega_N} \oint d^{N-1}\xi \ \epsilon_{a_1\cdots a_N} \, n^{a_1} \, \frac{\partial n^{a_2}}{\partial \xi_1} \cdots \frac{\partial n^{a_N}}{\partial \xi_{N-1}} \tag{3.88}$$

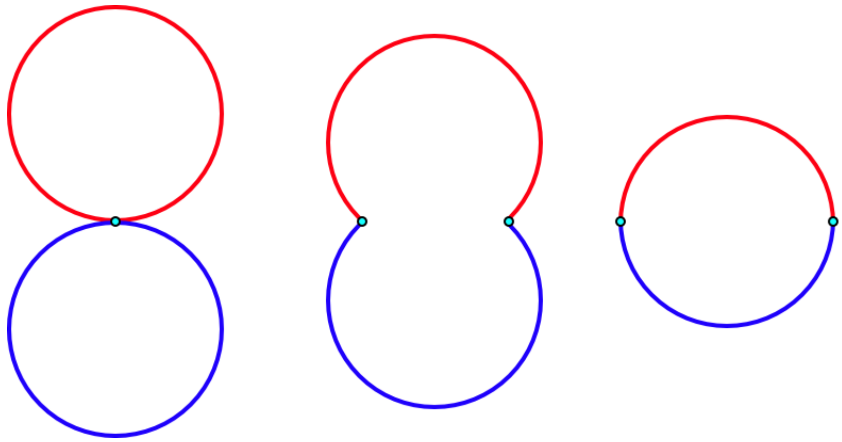

Figure 3.19: Composition of two circles. The same general construction applies to the merging of n-spheres $\mathbb{S}^n$, called the *wedge sum*.

The quantity Q is an *integer topological invariant* which characterizes the map from the surface $(\xi_1, \ldots, \xi_{N-1})$ to the unit sphere $|\hat{\boldsymbol{n}}| = 1$. In mathematical parlance, Q is known as the *Pontrjagin index* of this map.

This analytical development recapitulates some basic topology. Let $\mathcal{M}$ be a topological space and consider a map from the circle $\mathbb{S}^1$ to $\mathcal{M}$. We can compose two such maps by merging the two circles, as shown in fig. 3.19. Two maps are said to be *homotopic* if they can be smoothly deformed into each other. Any two homotopic maps are said to belong to the same *equivalence class* or *homotopy class*. For general $\mathcal{M}$, the homotopy classes may be multiplied using the composition law, resulting in a group structure. The group is called the *fundamental group* of the manifold $\mathcal{M}$, and is abbreviated $\pi_1(\mathcal{M})$. If $\mathcal{M} = \mathbb{S}^2$, then any such map can be smoothly contracted to a point on the 2-sphere, which is to say a trivial map. We then have $\pi_1(\mathcal{M}) = 0$. If $\mathcal{M} = \mathbb{S}^1$, the maps can wind nontrivially, and the homotopy classes are labeled by a single integer winding number: $\pi_1(\mathbb{S}^1) = \mathbb{Z}$. The winding number of the composition of two such maps is the sum of their individual winding numbers. If $\mathcal{M} = \mathbb{T}^2$, the maps can wind nontrivially around either of the two cycles of the 2-torus. We then have $\pi_1(\mathbb{T}^2) = \mathbb{Z}^2$, and in general $\pi_1(\mathbb{T}^n) = \mathbb{Z}^n$. This makes good sense, since an n-torus is topologically equivalent to a product of n circles. In some cases, $\pi_1(\mathcal{M})$ can be nonabelian, as is the case when $\mathcal{M}$ is the genus $g = 2$ structure shown in the right hand panel of fig. 3.18.

In general we define the n^{th} *homotopy group* $\pi_n(\mathcal{M})$ as the group under composition of maps from $\mathbb{S}^n$ to $\mathcal{M}$. For $n \geq 2$, $\pi_n(\mathcal{M})$ is abelian. If $\dim(\mathcal{M}) < n$, then $\pi_n(\mathcal{M}) = 0$. In general, $\pi_n(\mathbb{S}^n) = \mathbb{Z}$. These n^{th} homotopy classes of the n-sphere are labeled by their Pontrjagin index Q.

Finally, we ask what is Q in terms of the eigenvalues and eigenvectors of the linearized map

$$M_{ij} = \frac{\partial V_i}{\partial x_j}\bigg|_{\boldsymbol{x}^*} \,. \tag{3.89}$$

For simple cases where all the λ_i are nonzero, we have

$$Q = \mathsf{sgn}\left(\prod_{i=1}^{N} \lambda_i\right) . \tag{3.90}$$

3.7 Appendix : Example Problem

Consider the two-dimensional phase flow,

$$\dot{x} = \tfrac{1}{2}x + xy - 2x^3 \tag{3.91}$$

$$\dot{y} = \tfrac{5}{2}y + xy - y^2 . \tag{3.92}$$

`(a)` Find and classify all fixed points.

Solution : We have

$$\dot{x} = x\left(\tfrac{1}{2} + y - 2x^2\right) \tag{3.93}$$
$$\dot{y} = y\left(\tfrac{5}{2} + x - y\right) . \tag{3.94}$$

The matrix of first derivatives is

$$M = \begin{pmatrix} \frac{\partial \dot{x}}{\partial x} & \frac{\partial \dot{x}}{\partial y} \\ \frac{\partial \dot{y}}{\partial x} & \frac{\partial \dot{y}}{\partial y} \end{pmatrix} = \begin{pmatrix} \frac{1}{2} + y - 6x^2 & x \\ y & \frac{5}{2} + x - 2y \end{pmatrix} . \tag{3.95}$$

There are six fixed points.

$(x, y) = (0, 0)$: The derivative matrix is

$$M = \begin{pmatrix} \frac{1}{2} & 0 \\ 0 & \frac{5}{2} \end{pmatrix} . \tag{3.96}$$

The determinant is $D = \frac{5}{4}$ and the trace is $T = 3$. Since $D < \frac{1}{4}T^2$ and $T > 0$, this is an unstable node. (Duh! One can read off both eigenvalues are real and positive.) Eigenvalues: $\lambda_1 = \frac{1}{2}$, $\lambda_2 = \frac{5}{2}$.

$(x, y) = (0, \frac{5}{2})$: The derivative matrix is

$$M = \begin{pmatrix} 3 & 0 \\ \frac{5}{2} & -\frac{5}{2} \end{pmatrix} , \tag{3.97}$$

for which $D = -\frac{15}{2}$ and $T = \frac{1}{2}$. The determinant is negative, so this is a saddle. Eigenvalues: $\lambda_1 = -\frac{5}{2}$, $\lambda_2 = 3$.

$(x, y) = (-\frac{1}{2}, 0)$: The derivative matrix is

$$M = \begin{pmatrix} -1 & -\frac{1}{2} \\ 0 & 2 \end{pmatrix} , \tag{3.98}$$

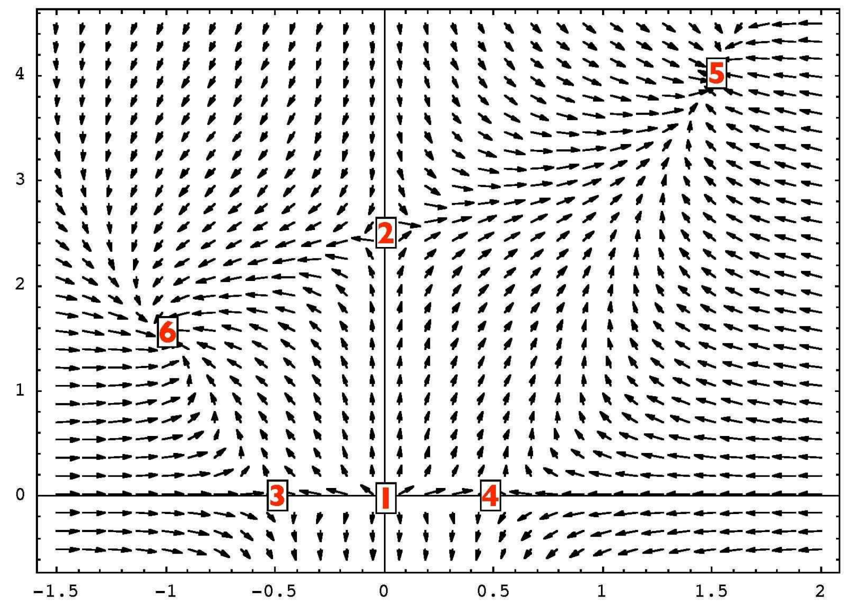

Figure 3.20: Sketch of phase flow for $\dot{x} = \frac{1}{2}x + xy - 2x^3$, $\dot{y} = \frac{5}{2}y + xy - y^2$. Fixed point classifications are in the text.

for which $D = -2$ and $T = +1$. The determinant is negative, so this is a saddle. Eigenvalues: $\lambda_1 = -1$, $\lambda_2 = 2$.

$(x, y) = (\frac{1}{2}, 0)$: The derivative matrix is

$$M = \begin{pmatrix} -1 & \frac{1}{2} \\ 0 & 3 \end{pmatrix} , \tag{3.99}$$

for which $D = -3$ and $T = +2$. The determinant is negative, so this is a saddle. Eigenvalues: $\lambda_1 = -1$, $\lambda_2 = 3$.

$(x, y) = (\frac{3}{2}, 4)$: This is one root obtained by setting $y = x + \frac{5}{2}$ and the solving $\frac{1}{2} + y - 2x^2 = 3 + x - 2x^2 = 0$, giving $x = -1$ and $x = +\frac{3}{2}$. The derivative matrix is

$$M = \begin{pmatrix} -9 & \frac{3}{2} \\ 4 & -4 \end{pmatrix} , \tag{3.100}$$

for which $D = 30$ and $T = -13$. Since $D < \frac{1}{4}T^2$ and $T < 0$, this corresponds to a stable node. Eigenvalues: $\lambda_1 = -10$, $\lambda_2 = -3$.

$(x, y) = (-1, \frac{3}{2})$: This is the second root obtained by setting $y = x + \frac{5}{2}$ and the solving $\frac{1}{2} + y - 2x^2 = 3 + x - 2x^2 = 0$, giving $x = -1$ and $x = +\frac{3}{2}$. The derivative matrix is

$$M = \begin{pmatrix} -4 & -1 \\ \frac{3}{2} & -\frac{3}{2} \end{pmatrix} , \tag{3.101}$$

for which $D = \frac{15}{2}$ and $T = -\frac{11}{2}$. Since $D < \frac{1}{4}T^2$ and $T < 0$, this corresponds to a stable node. Eigenvalues: $\lambda_1 = -3$, $\lambda_2 = -\frac{5}{2}$.

`(b)` Sketch the phase flow.

Solution : The flow is sketched in fig. 3.20. Thanks to Evan Bierman for providing the `Mathematica` code.

Chapter 4

Nonlinear Oscillators

4.1 Weakly Perturbed Linear Oscillators

Consider a nonlinear oscillator described by the equation of motion

$$\ddot{x} + \Omega_0^2\, x = \epsilon\, h(x) \ . \tag{4.1}$$

Here, ϵ is a dimensionless parameter, assumed to be small, and $h(x)$ is a nonlinear function of x. In general, we might consider equations of the form

$$\ddot{x} + \Omega_0^2\, x = \epsilon\, h(x, \dot{x}) \ , \tag{4.2}$$

such as the van der Pol oscillator,

$$\ddot{x} + \mu(x^2 - 1)\dot{x} + \Omega_0^2\, x = 0 \ . \tag{4.3}$$

First, we will focus on nondissipative systems, *i.e.* where we may write $m\ddot{x} = -\partial_x V$, with $V(x)$ some potential.

As an example, consider the simple pendulum, which obeys

$$\ddot{\theta} + \Omega_0^2 \sin\theta = 0 \ , \tag{4.4}$$

where $\Omega_0^2 = g/\ell$, with ℓ the length of the pendulum. We may rewrite his equation as

$$\begin{aligned} \ddot{\theta} + \Omega_0^2\, \theta &= \Omega_0^2\, (\theta - \sin\theta) \\ &= \tfrac{1}{6}\, \Omega_0^2\, \theta^3 - \tfrac{1}{120}\, \Omega_0^2\, \theta^5 + \ldots \end{aligned} \tag{4.5}$$

The RHS above is a nonlinear function of θ. We can define this to be $h(\theta)$, and take $\epsilon = 1$.

4.1.1 Naïve Perturbation theory and its failure

Let's assume though that ϵ is small, and write a formal power series expansion of the solution $x(t)$ to equation 4.1 as

$$x = x_0 + \epsilon\, x_1 + \epsilon^2\, x_2 + \ldots \ . \tag{4.6}$$

We now plug this into 4.1. We need to use Taylor's theorem,

$$h(x_0 + \eta) = h(x_0) + h'(x_0)\,\eta + \tfrac{1}{2}\,h''(x_0)\,\eta^2 + \ldots \tag{4.7}$$

with

$$\eta = \epsilon\, x_1 + \epsilon^2\, x_2 + \ldots \ . \tag{4.8}$$

Working out the resulting expansion in powers of ϵ is tedious. One finds

$$h(x) = h(x_0) + \epsilon\, h'(x_0)\, x_1 + \epsilon^2 \Big\{ h'(x_0)\, x_2 + \tfrac{1}{2}\, h''(x_0)\, x_1^2 \Big\} + \ldots \ . \tag{4.9}$$

Equating terms of the same order in ϵ, we obtain a hierarchical set of equations,

$$\ddot{x}_0 + \Omega_0^2\, x_0 = 0 \tag{4.10}$$

$$\ddot{x}_1 + \Omega_0^2\, x_1 = h(x_0) \tag{4.11}$$

$$\ddot{x}_2 + \Omega_0^2\, x_2 = h'(x_0)\, x_1 \tag{4.12}$$

$$\ddot{x}_3 + \Omega_0^2\, x_3 = h'(x_0)\, x_2 + \tfrac{1}{2}\, h''(x_0)\, x_1^2 \tag{4.13}$$

et cetera, where prime denotes differentiation with respect to argument. The first of these is easily solved: $x_0(t) = A\,\cos(\Omega_0 t + \varphi)$, where A and φ are constants. This solution then is plugged in at the next order, to obtain an inhomogeneous equation for $x_1(t)$. Solve for $x_1(t)$ and insert into the following equation for $x_2(t)$, *etc.* It looks straightforward enough.

The problem is that resonant forcing terms generally appear in the RHS of each equation of the hierarchy past the first. Define $\theta \equiv \Omega_0 t + \varphi$. Then $x_0(\theta)$ is an even periodic function of θ with period 2π, hence so is $h(x_0)$. We may then expand $h\big(x_0(\theta)\big)$ in a Fourier series:

$$h\big(A\cos\theta\big) = \sum_{n=0}^{\infty} h_n(A)\, \cos(n\theta) \ . \tag{4.14}$$

The $n = 1$ term leads to resonant forcing. Thus, the solution for $x_1(t)$ is

$$x_1(t) = \frac{1}{\Omega_0^2} \sum_{\substack{n=0\\(n\neq 1)}}^{\infty} \frac{h_n(A)}{1-n^2}\, \cos(n\Omega_0 t + n\varphi) + \frac{h_1(A)}{2\Omega_0}\, t\, \sin(\Omega_0 t + \varphi) \ , \tag{4.15}$$

which increases linearly with time. As an example, consider a cubic nonlinearity with $h(x) = r\,x^3$, where r is a constant. Then using

$$\cos^3\!\theta = \tfrac{3}{4}\cos\theta + \tfrac{1}{4}\cos(3\theta) \ , \tag{4.16}$$

we have $h_1 = \frac{3}{4}\, rA^3$ and $h_3 = \frac{1}{4}\, rA^3$.

4.1.2 Poincaré-Lindstedt method

The problem here is that the nonlinear oscillator has a different frequency than its linear counterpart. Indeed, if we assume the frequency Ω is a function of ϵ, with

$$\Omega(\epsilon) = \Omega_0 + \epsilon\,\Omega_1 + \epsilon^2\Omega_2 + \ldots\ , \tag{4.17}$$

then subtracting the unperturbed solution from the perturbed one and expanding in ϵ yields

$$\begin{aligned}\cos(\Omega t) - \cos(\Omega_0 t) &= -\sin(\Omega_0 t)\,(\Omega - \Omega_0)\,t - \tfrac{1}{2}\cos(\Omega_0 t)\,(\Omega-\Omega_0)^2\,t^2 + \ldots \\ &= -\epsilon\,\sin(\Omega_0 t)\,\Omega_1 t - \epsilon^2\Big\{\sin(\Omega_0 t)\,\Omega_2 t + \tfrac{1}{2}\cos(\Omega_0 t)\,\Omega_1^2 t^2\Big\} + \mathcal{O}(\epsilon^3)\ .\end{aligned} \tag{4.18}$$

What perturbation theory can do for us is to provide a good solution *up to a given time*, provided that ϵ is *sufficiently small*. It *will not* give us a solution that is close to the true answer for *all* time. We see above that in order to do that, and to recover the shifted frequency $\Omega(\epsilon)$, we would have to resum perturbation theory to all orders, which is a daunting task.

The Poincaré-Lindstedt method obviates this difficulty by assuming $\Omega = \Omega(\epsilon)$ from the outset. Define a dimensionless time $s \equiv \Omega t$ and write 4.1 as

$$\Omega^2\,\frac{d^2x}{ds^2} + \Omega_0^2\,x = \epsilon\,h(x)\ , \tag{4.19}$$

where

$$x = x_0 + \epsilon\,x_1 + \epsilon^2\,x_2 + \ldots \tag{4.20}$$

$$\Omega^2 = a_0 + \epsilon\,a_1 + \epsilon^2\,a_2 + \ldots\ . \tag{4.21}$$

We now plug the above expansions into 4.19:

$$\begin{aligned}\big(a_0 + \epsilon\,a_1 + \epsilon^2\,a_2 + \ldots\big)&\bigg(\frac{d^2x_0}{ds^2} + \epsilon\,\frac{d^2x_1}{ds^2} + \epsilon^2\,\frac{d^2x_2}{ds^2} + \ldots\bigg) \\ &+ \Omega_0^2\,\big(x_0 + \epsilon\,x_1 + \epsilon^2\,x_2 + \ldots\big) \\ &= \epsilon\,h(x_0) + \epsilon^2\,h'(x_0)\,x_1 + \epsilon^3\,\Big\{h'(x_0)\,x_2 + \tfrac{1}{2}\,h''(x_0)\,x_1^2\Big\} + \ldots\end{aligned} \tag{4.22}$$

Now let's write down equalities at each order in ϵ:

$$a_0\,\frac{d^2x_0}{ds^2} + \Omega_0^2\,x_0 = 0 \tag{4.23}$$

$$a_0\,\frac{d^2x_1}{ds^2} + \Omega_0^2\,x_1 = h(x_0) - a_1\,\frac{d^2x_0}{ds^2} \tag{4.24}$$

$$a_0\,\frac{d^2x_2}{ds^2} + \Omega_0^2\,x_2 = h'(x_0)\,x_1 - a_2\,\frac{d^2x_0}{ds^2} - a_1\,\frac{d^2x_1}{ds^2}\ , \tag{4.25}$$

et cetera.

The first equation of the hierarchy is immediately solved by

$$a_0 = \Omega_0^2 \qquad , \qquad x_0(s) = A\,\cos(s+\varphi)\ . \tag{4.26}$$

At $\mathcal{O}(\epsilon)$, then, we have

$$\frac{d^2x_1}{ds^2} + x_1 = \Omega_0^{-2}\,h\big(A\cos(s+\varphi)\big) + \Omega_0^{-2}\,a_1\,A\cos(s+\varphi)\ . \tag{4.27}$$

The LHS of the above equation has a natural frequency of unity (in terms of the dimensionless time s). We expect $h(x_0)$ to contain resonant forcing terms, per 4.14. However, we now have the freedom to adjust the undetermined coefficient a_1 to *cancel* any such resonant term. Clearly we must choose

$$a_1 = -\frac{h_1(A)}{A}\ . \tag{4.28}$$

The solution for $x_1(s)$ is then

$$x_1(s) = \frac{1}{\Omega_0^2}\sum_{\substack{n=0\\(n\neq 1)}}^{\infty}\frac{h_n(A)}{1-n^2}\,\cos(ns+n\varphi)\ , \tag{4.29}$$

which is periodic and hence does not increase in magnitude without bound, as does 4.15. The perturbed frequency is then obtained from

$$\Omega^2 = \Omega_0^2 - \frac{h_1(A)}{A}\,\epsilon + \mathcal{O}(\epsilon^2) \quad\Longrightarrow\quad \Omega(\epsilon) = \Omega_0 - \frac{h_1(A)}{2A\Omega_0}\,\epsilon + \mathcal{O}(\epsilon^2)\ . \tag{4.30}$$

Note that Ω depends on the amplitude of the oscillations.

As an example, consider an oscillator with a quartic nonlinearity in the potential, *i.e.* $h(x) = r\,x^3$. Then

$$h\big(A\cos\theta\big) = \tfrac{3}{4}rA^3\,\cos\theta + \tfrac{1}{4}rA^3\,\cos(3\theta)\ . \tag{4.31}$$

We then obtain, setting $\epsilon = 1$ at the end of the calculation,

$$\Omega = \Omega_0 - \frac{3\,rA^2}{8\,\Omega_0} + \ldots \tag{4.32}$$

where the remainder is higher order in the amplitude A. In the case of the pendulum,

$$\ddot\theta + \Omega_0^2\,\theta = \tfrac{1}{6}\Omega_0^2\,\theta^3 + \mathcal{O}\big(\theta^5\big)\ , \tag{4.33}$$

and with $r = \frac{1}{6}\,\Omega_0^2$ and $\theta_0(t) = \theta_0\sin(\Omega t)$, we find

$$T(\theta_0) = \frac{2\pi}{\Omega} = \frac{2\pi}{\Omega_0}\cdot\Big\{1 + \tfrac{1}{16}\,\theta_0^2 + \ldots\Big\}\ . \tag{4.34}$$

One can check that this is correct to lowest nontrivial order in the amplitude, using the exact result for the period,

$$T(\theta_0) = \frac{4}{\Omega_0}\,\mathbb{K}\big(\sin^2 \tfrac{1}{2}\theta_0\big) \ , \tag{4.35}$$

where $\mathbb{K}(x)$ is the complete elliptic integral.

The procedure can be continued to the next order, where the free parameter a_2 is used to eliminate resonant forcing terms on the RHS.

A good exercise to test one's command of the method is to work out the lowest order nontrivial corrections to the frequency of an oscillator with a quadratic nonlinearity, such as $h(x) = rx^2$. One finds that there are no resonant forcing terms at first order in ϵ, hence one must proceed to second order to find the first nontrivial corrections to the frequency.

4.2 Multiple Time Scale Method

Another method of eliminating secular terms (*i.e.* driving terms which oscillate at the resonant frequency of the unperturbed oscillator), and one which has applicability beyond periodic motion alone, is that of multiple time scale analysis. Consider the equation

$$\ddot{x} + x = \epsilon\, h(x,\dot{x}) \ , \tag{4.36}$$

where ϵ is presumed small, and $h(x,\dot{x})$ is a nonlinear function of position and/or velocity. We define a hierarchy of time scales: $T_n \equiv \epsilon^n\, t$. There is a normal time scale $T_0 = t$, slow time scale $T_1 = \epsilon t$, a 'superslow' time scale $T_2 = \epsilon^2 t$, *etc.* Thus,

$$\begin{aligned}\frac{d}{dt} &= \frac{\partial}{\partial T_0} + \epsilon\,\frac{\partial}{\partial T_1} + \epsilon^2\,\frac{\partial}{\partial T_2} + \ldots \\ &= \sum_{n=0}^\infty \epsilon^n\,\frac{\partial}{\partial T_n} \ .\end{aligned} \tag{4.37}$$

Next, we expand

$$x(t) = \sum_{n=0}^\infty \epsilon^n\, x_n(T_0\,,\,T_1,\ldots) \ . \tag{4.38}$$

Thus, we have

$$\bigg(\sum_{n=0}^\infty \epsilon^n\,\frac{\partial}{\partial T_n}\bigg)^{\!2}\bigg(\sum_{k=0}^\infty \epsilon^k\,x_k\bigg) + \sum_{k=0}^\infty \epsilon^k\,x_k = \epsilon\,h\bigg(\sum_{k=0}^\infty \epsilon^k\,x_k\ ,\ \sum_{n=0}^\infty \epsilon^n\,\frac{\partial}{\partial T_n}\bigg(\sum_{k=0}^\infty \epsilon^k\,x_k\bigg)\bigg) \ .$$

We now evaluate this order by order in ϵ:

$$\mathcal{O}(\epsilon^0)\ :\ \left(\frac{\partial^2}{\partial T_0^2}+1\right)x_0=0 \tag{4.39}$$

$$\mathcal{O}(\epsilon^1)\ :\ \left(\frac{\partial^2}{\partial T_0^2}+1\right)x_1=-2\,\frac{\partial^2 x_0}{\partial T_0\,\partial T_1}+h\bigg(x_0\,,\,\frac{\partial x_0}{\partial T_0}\bigg) \tag{4.40}$$

$$\mathcal{O}(\epsilon^2)\ :\ \left(\frac{\partial^2}{\partial T_0^2}+1\right)x_2=-2\,\frac{\partial^2 x_1}{\partial T_0\,\partial T_1}-2\,\frac{\partial^2 x_0}{\partial T_0\,\partial T_2}-\frac{\partial^2 x_0}{\partial T_1^2} + \frac{\partial h}{\partial x}\bigg|_{\{x_0,\dot{x}_0\}}x_1+\frac{\partial h}{\partial \dot{x}}\bigg|_{\{x_0,\dot{x}_0\}}\left(\frac{\partial x_1}{\partial T_0}+\frac{\partial x_0}{\partial T_1}\right)\ , \tag{4.41}$$

et cetera. The expansion gets more and more tedious with increasing order in ϵ.

Let's carry this procedure out to first order in ϵ. To order ϵ^0,

$$x_0=A\,\cos\big(T_0+\phi\big)\ , \tag{4.42}$$

where A and ϕ are arbitrary (at this point) functions of $\big\{T_1\,,\,T_2\,,\,\ldots\big\}$. Now we solve the next equation in the hierarchy, for x_1. Let $\theta\equiv T_0+\phi$. Then $\frac{\partial}{\partial T_0}=\frac{\partial}{\partial\theta}$ and we have

$$\left(\frac{\partial^2}{\partial\theta^2}+1\right)x_1=2\,\frac{\partial A}{\partial T_1}\,\sin\theta+2\,A\,\frac{\partial\phi}{\partial T_1}\,\cos\theta+h\big(A\cos\theta,-A\sin\theta\big)\ . \tag{4.43}$$

Since the arguments of h are periodic under $\theta\to\theta+2\pi$, we may expand h in a Fourier series:

$$h(\theta)\equiv h\big(A\cos\theta,-A\sin\theta\big)=\sum_{k=1}^{\infty}\alpha_k(A)\sin(k\theta)+\sum_{k=0}^{\infty}\beta_k(A)\cos(k\theta)\ . \tag{4.44}$$

The inverse of this relation is

$$\alpha_k(A)=\int\limits_0^{2\pi}\!\frac{d\theta}{\pi}\,h(\theta)\,\sin(k\theta)\qquad(k>0) \tag{4.45}$$

$$\beta_0(A)=\int\limits_0^{2\pi}\!\frac{d\theta}{2\pi}\,h(\theta) \tag{4.46}$$

$$\beta_k(A)=\int\limits_0^{2\pi}\!\frac{d\theta}{\pi}\,h(\theta)\,\cos(k\theta)\qquad(k>0)\ . \tag{4.47}$$

We now demand that the secular terms on the RHS – those terms proportional to $\cos\theta$ and $\sin\theta$ – must vanish. This means

$$2\,\frac{\partial A}{\partial T_1}+\alpha_1(A)=0 \tag{4.48}$$

$$2A\,\frac{\partial\phi}{\partial T_1}+\beta_1(A)=0\ . \tag{4.49}$$

These two first order equations require two initial conditions, which is sensible since our initial equation $\ddot{x} + x = \epsilon\, h(x, \dot{x})$ is second order in time.

With the secular terms eliminated, we may solve for x_1:

$$x_1 = \sum_{k \neq 1}^{\infty} \left\{ \frac{\alpha_k(A)}{1-k^2} \sin(k\theta) + \frac{\beta_k(A)}{1-k^2} \cos(k\theta) \right\} + C_0 \cos\theta + D_0 \sin\theta \ . \tag{4.50}$$

Note: (i) the $k = 1$ terms are excluded from the sum, and (ii) an arbitrary solution to the homogeneous equation, *i.e.* eqn. 4.43 with the right hand side set to zero, is included. The constants C_0 and D_0 are arbitrary functions of T_1, T_2, *etc.* .

The equations for A and ϕ are both first order in T_1. They will therefore involve two constants of integration – call them A_0 and ϕ_0. At second order, these constants are taken as dependent upon the superslow time scale T_2. *The method itself may break down at this order.* (See if you can find out why.)

Let's apply this to the nonlinear oscillator $\ddot{x} + \sin x = 0$, also known as the simple pendulum. We'll expand the sine function to include only the lowest order nonlinear term, and consider

$$\ddot{x} + x = \tfrac{1}{6}\, \epsilon\, x^3 \ . \tag{4.51}$$

We'll assume ϵ is small and take $\epsilon = 1$ at the end of the calculation. This will work provided the amplitude of the oscillation is itself small. To zeroth order, we have $x_0 = A\, \cos(t + \phi)$, as always. At first order, we must solve

$$\begin{aligned} \left(\frac{\partial^2}{\partial\theta^2} + 1 \right) x_1 &= 2\, \frac{\partial A}{\partial T_1} \sin\theta + 2\, A\, \frac{\partial\phi}{\partial T_1} \cos\theta + \tfrac{1}{6}\, A^2 \cos^3\theta \\ &= 2\, \frac{\partial A}{\partial T_1} \sin\theta + 2\, A\, \frac{\partial\phi}{\partial T_1} \cos\theta + \tfrac{1}{24}\, A^3\, \cos(3\theta) + \tfrac{1}{8}\, A^3\, \cos\theta \ . \end{aligned} \tag{4.52}$$

We eliminate the secular terms by demanding

$$\frac{\partial A}{\partial T_1} = 0 \qquad , \qquad \frac{\partial\phi}{\partial T_1} = -\tfrac{1}{16}\, A^2 \ , \tag{4.53}$$

hence $A = A_0$ and $\phi = -\frac{1}{16}\, A_0^2\, T_1 + \phi_0$, and

$$\begin{aligned} x(t) = A_0 \cos&\left(t - \tfrac{1}{16}\, \epsilon\, A_0^2\, t + \phi_0 \right) \\ &- \tfrac{1}{192}\, \epsilon\, A_0^3\, \cos\left(3t - \tfrac{3}{16}\, \epsilon A_0^2\, t + 3\phi_0 \right) + \ldots \ , \end{aligned} \tag{4.54}$$

which reproduces the result obtained from the Poincaré-Lindstedt method.

4.2.1 Duffing oscillator

Consider the equation

$$\ddot{x} + 2\epsilon\mu\dot{x} + x + \epsilon x^3 = 0 \ . \tag{4.55}$$

This describes a damped nonlinear oscillator. Here we assume both the damping coefficient $\tilde{\mu} \equiv \epsilon\mu$ as well as the nonlinearity both depend linearly on the small parameter ϵ. We may write this equation in our standard form $\ddot{x} + x = \epsilon\, h(x, \dot{x})$, with $h(x, \dot{x}) = -2\mu\dot{x} - x^3$.

For $\epsilon > 0$, which we henceforth assume, it is easy to see that the only fixed point is $(x, \dot{x}) = (0, 0)$. The linearized flow in the vicinity of the fixed point is given by

$$\frac{d}{dt}\begin{pmatrix} x \\ \dot{x} \end{pmatrix} = \begin{pmatrix} 0 & 1 \\ -1 & -2\epsilon\mu \end{pmatrix}\begin{pmatrix} x \\ \dot{x} \end{pmatrix} + \mathcal{O}(x^3) \ . \tag{4.56}$$

The determinant is $D = 1$ and the trace is $T = -2\epsilon\mu$. Thus, provided $\epsilon\mu < 1$, the fixed point is a stable spiral; for $\epsilon\mu > 1$ the fixed point becomes a stable node.

We employ the multiple time scale method to order ϵ. We have $x_0 = A\cos(T_0 + \phi)$ to zeroth order, as usual. The nonlinearity is expanded in a Fourier series in $\theta = T_0 + \phi$:

$$\begin{aligned} h\Big(x_0\,,\,\tfrac{\partial x_0}{\partial T_0}\Big) &= 2\mu A \sin\theta - A^3\cos^3\theta \\ &= 2\mu A\sin\theta - \tfrac{3}{4}A^3\cos\theta - \tfrac{1}{4}A^3\cos 3\theta \ . \end{aligned} \tag{4.57}$$

Thus, $\alpha_1(A) = 2\mu A$ and $\beta_1(A) = -\frac{3}{4}A^3$. We now solve the first order equations,

$$\frac{\partial A}{\partial T_1} = -\tfrac{1}{2}\,\alpha_1(A) = -\mu A \qquad \Longrightarrow \qquad A(T) = A_0\, e^{-\mu T_1} \tag{4.58}$$

as well as

$$\frac{\partial\phi}{\partial T_1} = -\frac{\beta_1(A)}{2A} = \tfrac{3}{8}A_0^2\, e^{-2\mu T_1} \qquad \Longrightarrow \qquad \phi(T_1) = \phi_0 + \frac{3A_0^2}{16\mu}\big(1 - e^{-2\mu T_1}\big) \ . \tag{4.59}$$

After elimination of the secular terms, we may read off

$$x_1(T_0\,,\,T_1) = \tfrac{1}{32}A^3(T_1)\cos\big(3T_0 + 3\phi(T_1)\big) \ . \tag{4.60}$$

Finally, we have

$$\begin{aligned} x(t) = A_0\, e^{-\epsilon\mu t}\, &\cos\bigg(t + \frac{3A_0^2}{16\mu}\big(1 - e^{-2\epsilon\mu t}\big) + \phi_0\bigg) \\ &+ \tfrac{1}{32}\epsilon A_0^3\, e^{-3\epsilon\mu t}\, \cos\bigg(3t + \frac{9A_0^2}{16\mu}\big(1 - e^{-2\epsilon\mu t}\big) + 3\phi_0\bigg) \ . \end{aligned} \tag{4.61}$$

4.2.2 Van der Pol oscillator

Let's apply this method to another problem, that of the van der Pol oscillator,

$$\ddot{x} + \epsilon\,(x^2 - 1)\,\dot{x} + x = 0 \ , \tag{4.62}$$

with $\epsilon > 0$. The nonlinear term acts as a frictional drag for $x > 1$, and as a 'negative friction' (*i.e.* increasing the amplitude) for $x < 1$. Note that the linearized equation at the fixed point $(x = 0, \dot{x} = 0)$ corresponds to an unstable spiral for $\epsilon < 2$.

For the van der Pol oscillator, we have $h(x, \dot{x}) = (1-x^2)\,\dot{x}$, and plugging in the zeroth order solution $x_0 = A\,\cos(t + \phi)$ gives

$$\begin{aligned} h\bigg(x_0\,,\,\frac{\partial x_0}{\partial T_0}\bigg) &= \big(1 - A^2\cos^2\theta\big)\,\big(-A\sin\theta\big) \\ &= \big(-A + \tfrac{1}{4}A^3\big)\,\sin\theta + \tfrac{1}{4}\,A^3\,\sin(3\theta)\ , \end{aligned} \tag{4.63}$$

with $\theta \equiv t + \phi$. Thus, $\alpha_1 = -A + \frac{1}{4}A^3$ and $\beta_1 = 0$, which gives $\phi = \phi_0$ and

$$2\,\frac{\partial A}{\partial T_1} = A - \tfrac{1}{4}A^3\ . \tag{4.64}$$

The equation for A is easily integrated:

$$\begin{aligned} dT_1 = -\frac{8\,dA}{A\,(A^2-4)} &= \bigg(\frac{2}{A} - \frac{1}{A-2} - \frac{1}{A+2}\bigg)\,dA = d\ln\bigg(\frac{A}{A^2-4}\bigg) \\ \Longrightarrow \qquad A(T_1) &= \frac{2}{\sqrt{1 - \big(1 - \frac{4}{A_0^2}\big)\,\exp(-T_1)}}\ . \end{aligned} \tag{4.65}$$

Thus,

$$x_0(t) = \frac{2\cos(t+\phi_0)}{\sqrt{1 - \big(1 - \frac{4}{A_0^2}\big)\,\exp(-\epsilon t)}}\ . \tag{4.66}$$

This behavior describes the approach to the limit cycle $2\cos(t + \phi_0)$. With the elimination of the secular terms, we have

$$x_1(t) = -\tfrac{1}{32}A^3\sin(3\theta) = -\frac{\frac{1}{4}\sin\big(3t + 3\phi_0\big)}{\Big[1 - \big(1 - \frac{4}{A_0^2}\big)\,\exp(-\epsilon t)\Big]^{3/2}}\ . \tag{4.67}$$

4.3 Forced Nonlinear Oscillations

The forced, damped linear oscillator,

$$\ddot{x} + 2\mu\dot{x} + x = f_0\cos\Omega t \tag{4.68}$$

has the solution

$$x(t) = x_{\rm h}(t) + C(\Omega)\,\cos\big(\Omega t + \delta(\Omega)\big)\ , \tag{4.69}$$

where

$$x_{\rm h}(t) = A_+\,e^{\lambda_+ t} + A_-\,e^{\lambda_- t}\ , \tag{4.70}$$

where $\lambda_\pm = -\mu \pm \sqrt{\mu^2 - 1}$ are the roots of $\lambda^2 + 2\mu\lambda + 1 = 0$. The 'susceptibility' C and phase shift δ are given by

$$C(\Omega) = \frac{1}{\sqrt{(\Omega^2-1)^2 + 4\mu^2\Omega^2}} \qquad , \qquad \delta(\Omega) = \tan^{-1}\bigg(\frac{2\mu\Omega}{1-\Omega^2}\bigg)\ . \tag{4.71}$$

The homogeneous solution, $x_{\mathrm{h}}(t)$, is a transient and decays exponentially with time, since $\mathrm{Re}(\lambda_{\pm}) < 0$. The asymptotic behavior is a phase-shifted oscillation at the driving frequency Ω.

Now let's add a nonlinearity. We study the equation

$$\ddot{x} + x = \epsilon\, h(x, \dot{x}) + \epsilon\, f_0\, \cos(t + \epsilon\nu t)\ . \tag{4.72}$$

Note that amplitude of the driving term, $\epsilon f_0 \cos(\Omega t)$, is assumed to be small, *i.e.* proportional to ϵ, and the driving frequency $\Omega = 1 + \epsilon\nu$ is assumed to be close to resonance. (The resonance frequency of the unperturbed oscillator is $\omega_{\mathrm{res}} = 1$.) Were the driving frequency far from resonance, it could be dealt with in the same manner as the non-secular terms encountered thus far. The situation when Ω is close to resonance deserves our special attention.

At order ϵ^0, we still have $x_0 = A\cos(T_0 + \phi)$. At order ϵ^1, we must solve

$$\begin{aligned}\bigg(\frac{\partial^2}{\partial\theta^2} + 1\bigg) x_1 &= 2A' \sin\theta + 2A\phi' \cos\theta + h\big(A\cos\theta\, ,\, -A\sin\theta\big) + f_0\, \cos(\theta - \psi) \\ &= \sum_{k\neq 1}\Big(\alpha_k \sin(k\theta) + \beta_k \cos(k\theta)\Big) + \Big(2A' + \alpha_1 + f_0 \sin\psi\Big) \sin\theta \\ &\qquad\qquad + \Big(2A\psi' + 2A\nu + \beta_1 + f_0 \cos\psi\Big) \cos\theta\ ,\end{aligned} \tag{4.73}$$

where $\psi \equiv \phi(T_1) - \nu T_1$, and where the prime denotes differentiation with respect to T_1. We must therefore solve

$$\frac{dA}{dT_1} = -\tfrac{1}{2}\alpha_1(A) - \tfrac{1}{2} f_0 \sin\psi \tag{4.74}$$

$$\frac{d\psi}{dT_1} = -\nu - \frac{\beta_1(A)}{2A} - \frac{f_0}{2A} \cos\psi\ . \tag{4.75}$$

If we assume that $\{A, \psi\}$ approaches a fixed point of these dynamics, then at the fixed point these equations provide a relation between the amplitude A, the 'detuning' parameter ν, and the drive f_0:

$$\Big[\alpha_1(A)\Big]^2 + \Big[2\nu A + \beta_1(A)\Big]^2 = f_0^2\ . \tag{4.76}$$

In general this is a nonlinear equation for $A(f_0, \nu)$.

4.3.1 Forced Duffing oscillator

Thus far our approach has been completely general. We now restrict our attention to the Duffing equation, for which

$$\alpha_1(A) = 2\mu A \qquad , \qquad \beta_1(A) = -\tfrac{3}{4}A^3\ , \tag{4.77}$$

which yields the cubic equation

$$A^6 - \tfrac{16}{3}\nu A^4 + \tfrac{64}{9}(\mu^2 + \nu^2) A^2 - \tfrac{16}{9} f_0^2 = 0\ . \tag{4.78}$$

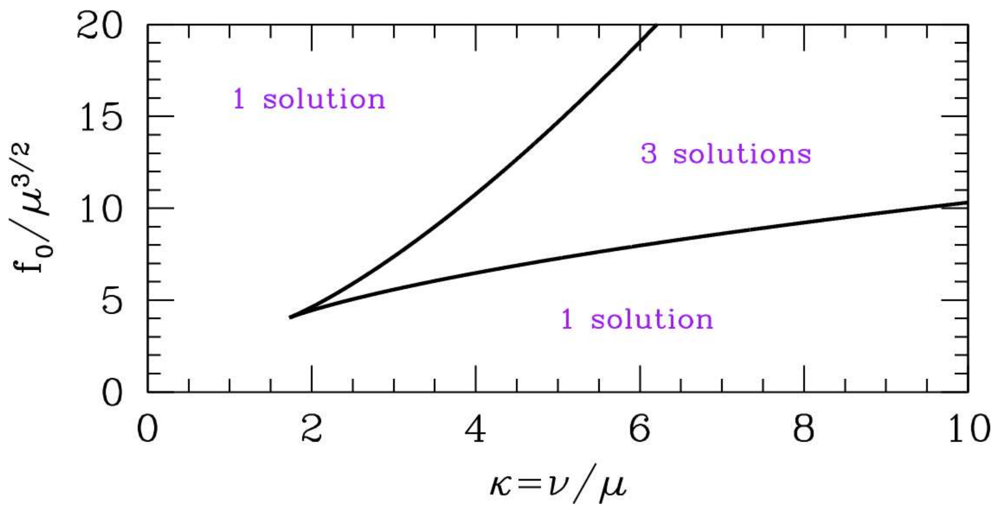

Figure 4.1: Phase diagram for the forced Duffing oscillator.

Analyzing the cubic is a good exercise. Setting $y = A^2$, we define

$$G(y) \equiv y^3 - \tfrac{16}{3}\nu\, y^2 + \tfrac{64}{9}(\mu^2 + \nu^2)\, y \ , \tag{4.79}$$

and we seek a solution to $G(y) = \frac{16}{9} f_0^2$. Setting $G'(y) = 0$, we find roots at

$$y_\pm = \tfrac{16}{9}\nu \pm \tfrac{8}{9}\sqrt{\nu^2 - 3\mu^2} \ . \tag{4.80}$$

If $\nu^2 < 3\mu^2$ the roots are imaginary, which tells us that $G(y)$ is monotonically increasing for real y. There is then a unique solution to $G(y) = \frac{16}{9} f_0^2$.

If $\nu^2 > 3\mu^2$, then the cubic $G(y)$ has a local maximum at $y = y_-$ and a local minimum at $y = y_+$. For $\nu < -\sqrt{3}\,\mu$, we have $y_- < y_+ < 0$, and since $y = A^2$ must be positive, this means that once more there is a unique solution to $G(y) = \frac{16}{9} f_0^2$.

For $\nu > \sqrt{3}\,\mu$, we have $y_+ > y_- > 0$. There are then three solutions for $y(\nu)$ for $f_0 \in \big[f_0^-, f_0^+\big]$, where $f_0^\pm = \frac{3}{4}\sqrt{G(y_\mp)}$. If we define $\kappa \equiv \nu/\mu$, then

$$f_0^\pm = \tfrac{8}{9}\,\mu^{3/2}\sqrt{\kappa^3 + 9\kappa \pm \sqrt{\kappa^2 - 3}} \ . \tag{4.81}$$

The phase diagram is shown in Fig. 4.1. The minimum value for f_0 is $f_{0,\mathrm{c}} = \frac{16}{3^{5/4}}\,\mu^{3/2}$, which occurs at $\kappa = \sqrt{3}$.

Thus far we have assumed that the (A, ψ) dynamics evolves to a fixed point. We should check to make sure that this fixed point is in fact stable. To do so, we evaluate the linearized dynamics at the fixed point. Writing $A = A^* + \delta A$ and $\psi = \psi^* + \delta\psi$, we have

$$\frac{d}{dT_1}\begin{pmatrix} \delta A \\ \delta\psi \end{pmatrix} = M \begin{pmatrix} \delta A \\ \delta\psi \end{pmatrix} \ , \tag{4.82}$$

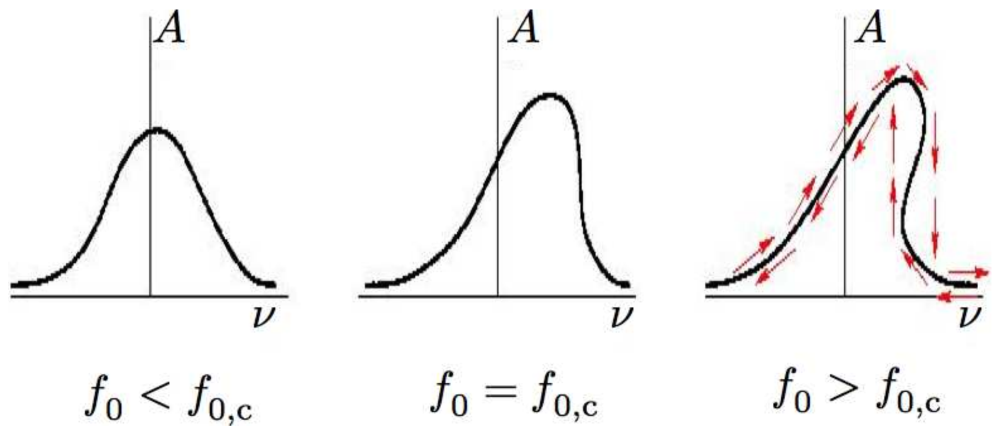

Figure 4.2: Amplitude A *versus* detuning ν for the forced Duffing oscillator for three values of the drive f_0. The critical drive is $f_{0,c} = \frac{16}{3^{5/4}}\,\mu^{3/2}$. For $f_0 > f_{0,c}$, there is hysteresis as a function of the detuning.

with

$$M = \begin{pmatrix} \frac{\partial \dot{A}}{\partial A} & \frac{\partial \dot{A}}{\partial \psi} \\ \\ \frac{\partial \dot{\psi}}{\partial A} & \frac{\partial \dot{\psi}}{\partial \psi} \end{pmatrix} = \begin{pmatrix} -\mu & -\frac{1}{2} f_0 \, \cos\psi \\ \\ \frac{3}{4}A + \frac{f_0}{2A^2}\,\cos\psi & \frac{f_0}{2A}\,\sin\psi \end{pmatrix}$$

$$= \begin{pmatrix} -\mu & \nu A - \frac{3}{8}A^3 \\ \\ \frac{9}{8}A - \frac{\nu}{A} & -\mu \end{pmatrix} \ . \tag{4.83}$$

One then has $T = -2\mu$ and

$$D = \mu^2 + \big(\nu - \tfrac{3}{8}A^2\big)\big(\nu - \tfrac{9}{8}A^2\big) \ . \tag{4.84}$$

Setting $D = \frac{1}{4}T^2 = \mu^2$ sets the boundary between stable spiral and stable node. Setting $D = 0$ sets the boundary between stable node and saddle. The fixed point structure is as shown in Fig. 4.3.

4.3.2 Forced van der Pol oscillator

Consider now a weakly dissipative, weakly forced van der Pol oscillator, governed by the equation

$$\ddot{x} + \epsilon\,(x^2 - 1)\,\dot{x} + x = \epsilon\, f_0\, \cos(t + \epsilon\nu t) \ , \tag{4.85}$$

where the forcing frequency is $\Omega = 1 + \epsilon\nu$, which is close to the natural frequency $\omega_0 = 1$. We apply the multiple time scale method, with $h(x, \dot{x}) = (1 - x^2)\,\dot{x}$. As usual, the lowest order solution is $x_0 = A(T_1)\cos\big(T_0 + \phi(T_1)\big)$, where $T_0 = t$ and $T_1 = \epsilon t$. Again, we define $\theta \equiv T_0 + \phi(T_1)$ and $\psi(T_1) \equiv \phi(T_1) - \nu T_1$. From

$$h(A\cos\theta, -A\sin\theta) = \big(\tfrac{1}{4}A^3 - A\big)\,\sin\theta + \tfrac{1}{4}A^3\sin(3\theta) \ , \tag{4.86}$$

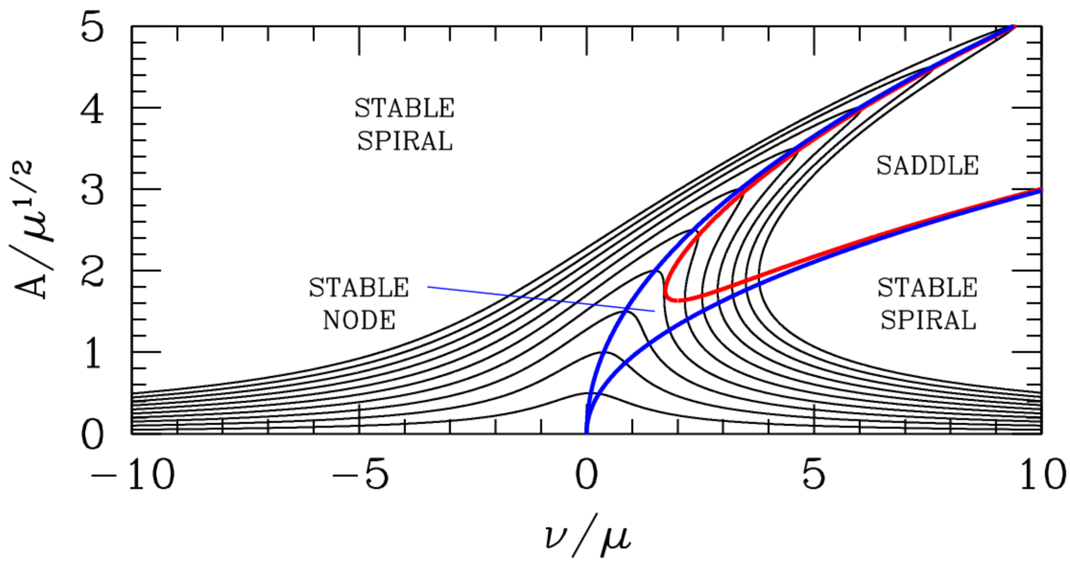

Figure 4.3: Amplitude *versus* detuning for the forced Duffing oscillator for ten equally spaced values of f_0 between $\mu^{3/2}$ and $10\,\mu^{3/2}$. The critical value is $f_{0,\mathrm{c}} = 4.0525\,\mu^{3/2}$. The red and blue curves are boundaries for the fixed point classification.

we arrive at

$$\begin{aligned}\bigg(\frac{\partial^2}{\partial\theta^2}+1\bigg)x_1 &= -2\frac{\partial^2 x_0}{\partial T_0\,\partial T_1} + h\bigg(x_0\,,\,\frac{\partial x_0}{\partial T_0}\bigg)\\ &= \big(\tfrac{1}{4}A^3 - A + 2A' + f_0\sin\psi\big)\sin\theta\\ &\qquad + \big(2A\,\psi' + 2\nu A + f_0\cos\psi\big)\cos\theta + \tfrac{1}{4}A^3\sin(3\theta)\ . \end{aligned} \tag{4.87}$$

We eliminate the secular terms, proportional to $\sin\theta$ and $\cos\theta$, by demanding

$$\frac{dA}{dT_1} = \tfrac{1}{2}A - \tfrac{1}{8}A^3 - \tfrac{1}{2}f_0\sin\psi \tag{4.88}$$

$$\frac{d\psi}{dT_1} = -\nu - \frac{f_0}{2A}\cos\psi\ . \tag{4.89}$$

Stationary solutions have $A' = \psi' = 0$, hence $\cos\psi = -2\nu\,A/f_0$, and hence

$$\begin{aligned}f_0^2 &= 4\nu^2A^2 + \big(1+\tfrac{1}{4}A^2\big)^2A^2\\ &= \tfrac{1}{16}A^6 - \tfrac{1}{2}A^4 + (1+4\nu^2)A^2\ .\end{aligned} \tag{4.90}$$

For this solution, we have

$$x_0 = A^*\cos(T_0 + \nu T_1 + \psi^*)\ , \tag{4.91}$$

and the oscillator's frequency is the forcing frequency Ω. This oscillator is thus *entrained*.

To proceed further, let $y = A^2$, and consider the cubic equation

$$F(y) = \tfrac{1}{16}y^3 - \tfrac{1}{2}y^2 + (1+4\nu^2)\,y - f_0^2 = 0\ . \tag{4.92}$$

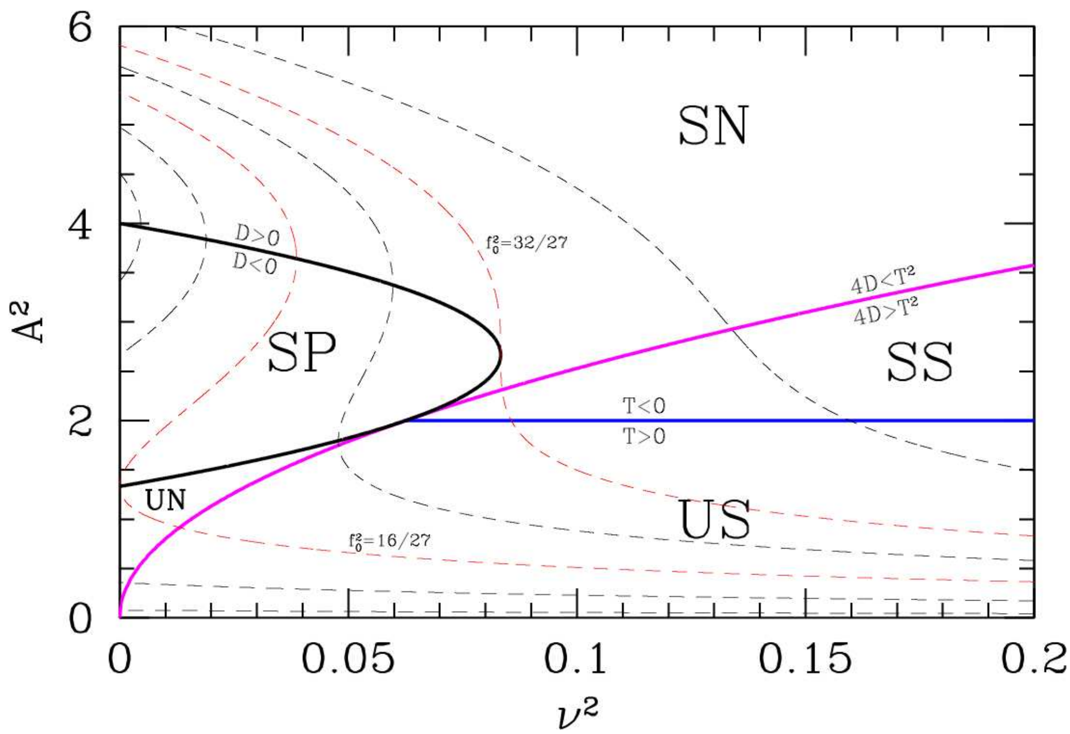

Figure 4.4: Amplitude *versus* detuning for the forced van der Pol oscillator. Fixed point classifications are abbreviated SN (stable node), SS (stable spiral), UN (unstable node), US (unstable spiral), and SP (saddle point).

Setting $F'(y) = 0$, we find the roots of $F'(y)$ lie at $y_\pm = \frac{4}{3}\,(2 \pm u)$, where $u = (1 - 12\,\nu^2)^{1/2}$. Thus, the roots are complex for $\nu^2 > \frac{1}{12}$, in which case $F(y)$ is monotonically increasing, and there is a unique solution to $F(y) = 0$. Since $F(0) = -f_0^2 < 0$, that solution satisfies $y > 0$. For $\nu^2 < \frac{1}{12}$, there are two local extrema at $y = y_\pm$. When $F_{\rm min} = F(y_+) < 0 < F(y_-) = F_{\rm max}$, the cubic $F(y)$ has three real, positive roots. This is equivalent to the condition

$$-\tfrac{8}{27}\,u^3 + \tfrac{8}{9}\,u^2 < \tfrac{32}{27} - f_0^2 < \tfrac{8}{27}\,u^3 + \tfrac{8}{9}\,u^2 \ . \tag{4.93}$$

We can say even more by exploring the behavior of (4.4,4.5) in the vicinity of the fixed points. Writing $A = A^* + \delta A$ and $\psi = \psi^* + \delta\psi$, we have

$$\frac{d}{dT_1}\begin{pmatrix} \delta A \\ \\ \delta\psi \end{pmatrix} = \begin{pmatrix} \frac{1}{2}\big(1 - \frac{3}{4}A^{*2}\big) & \nu A^* \\ \\ -\nu/A^* & \frac{1}{2}\big(1 - \frac{1}{4}A^{*2}\big) \end{pmatrix}\begin{pmatrix} \delta A \\ \\ \delta\psi \end{pmatrix} \ . \tag{4.94}$$

The eigenvalues of the linearized dynamics at the fixed point are given by $\lambda_\pm = \frac{1}{2}\big(T \pm \sqrt{T^2 - 4D}\big)$, where T and D are the trace and determinant of the linearized equation. Recall now the classification scheme for fixed points of two-dimensional phase flows, discussed in chapter 3. To recapitulate, when $D < 0$, we have $\lambda_- < 0 < \lambda_+$ and the fixed point is a saddle. For $0 < 4D < T^2$, both eigenvalues have the same sign, so the fixed point is a node.

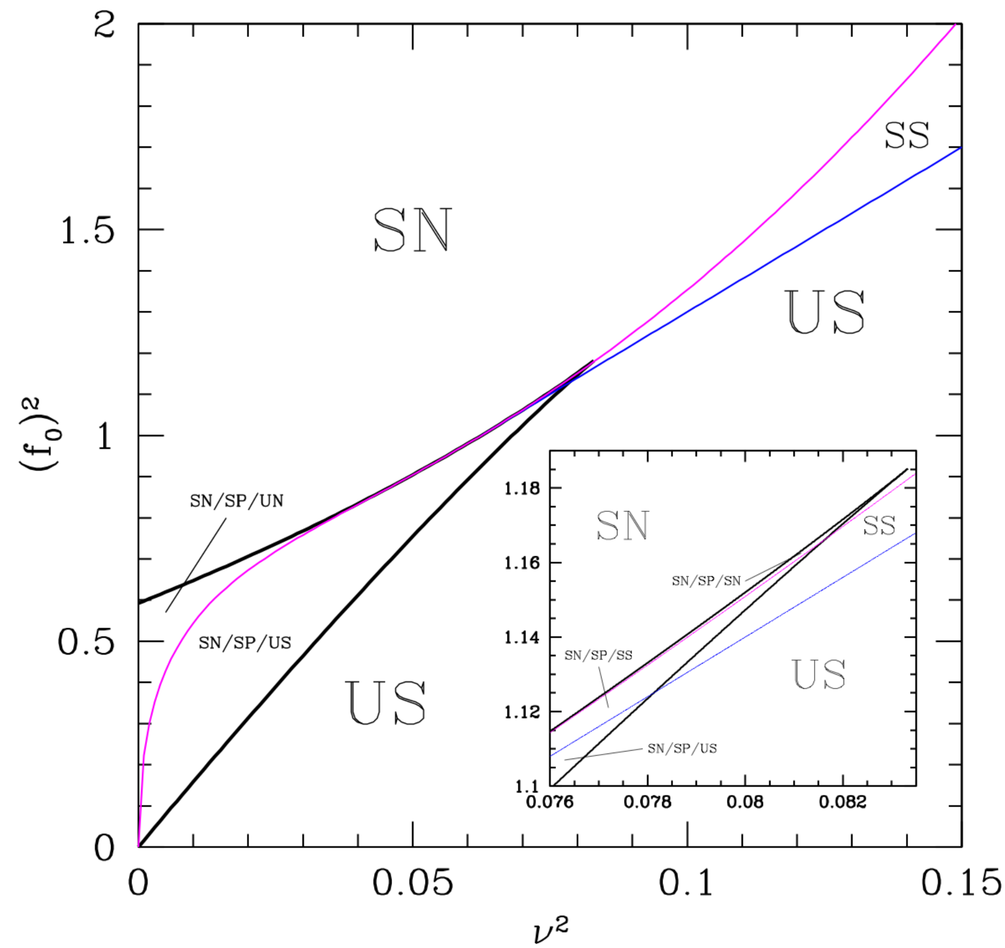

Figure 4.5: Phase diagram for the weakly forced van der Pol oscillator in the (ν^2, f_0^2) plane. Inset shows detail. Abbreviations for fixed point classifications are as in Fig. 4.4.

For $4D > T^2$, the eigenvalues form a complex conjugate pair, and the fixed point is a spiral. A node/spiral fixed point is stable if $T < 0$ and unstable if $T > 0$. For our forced van der Pol oscillator, we have

$$T = 1 - \tfrac{1}{2}A^{*2} \tag{4.95}$$

$$D = \tfrac{1}{4}\big(1 - A^{*2} + \tfrac{3}{16}A^{*4}\big) + \nu^2 \ . \tag{4.96}$$

From these results we can obtain the plot of Fig. 4.4, where amplitude is shown *versus* detuning. Note that for $f_0 < \sqrt{\frac{32}{27}}$ there is a region $\big[\nu_-, \nu_+\big]$ of hysteretic behavior in which varying the detuning parameter ν is not a reversible process. The phase diagram in the (ν^2, f_0^2) is shown in Fig. 4.5.

Finally, we can make the following statement about the *global* dynamics (*i.e.* not simply in

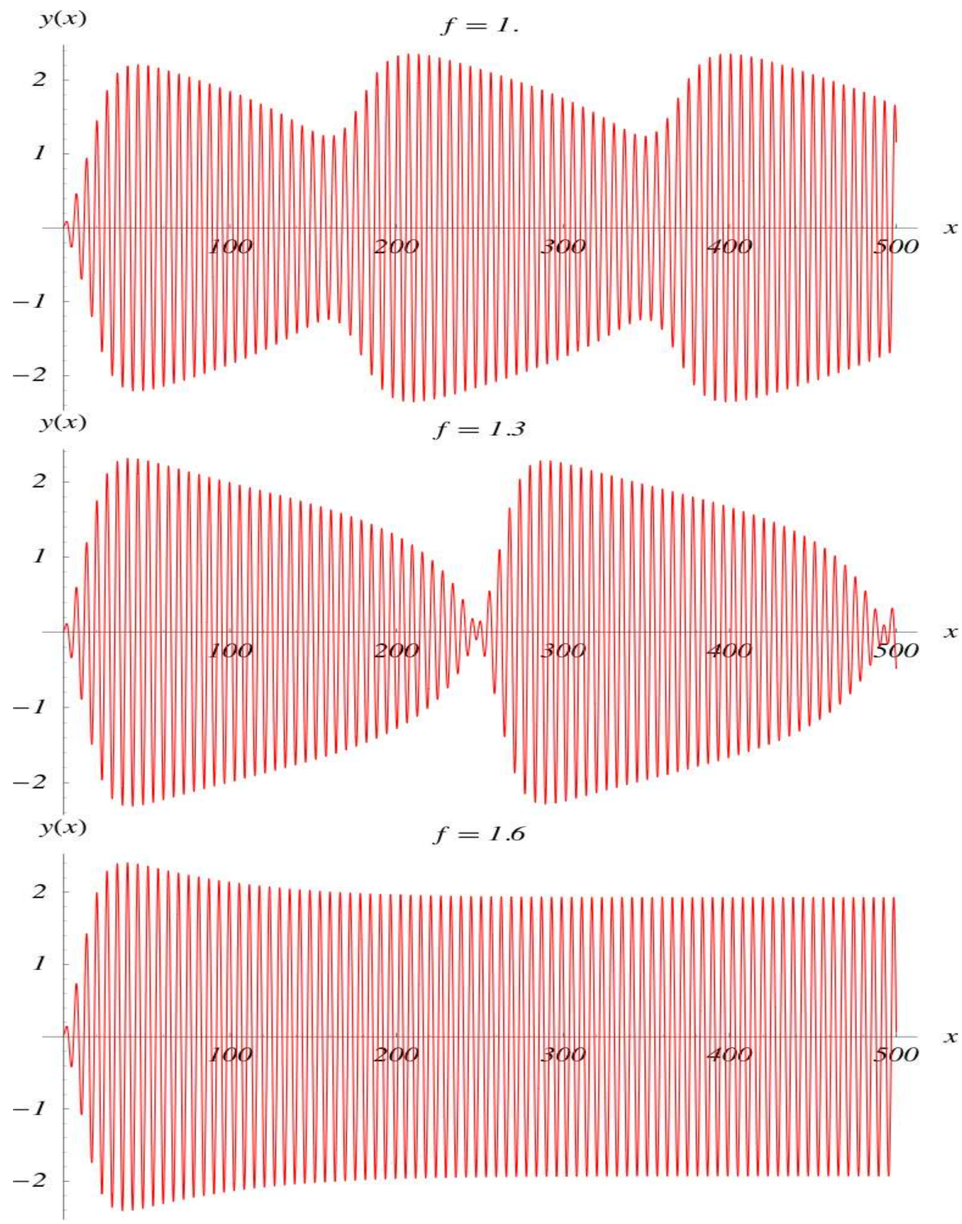

Figure 4.6: Forced van der Pol system with $\epsilon = 0.1$, $\nu = 0.4$ for three values of f_0. The limit entrained solution becomes unstable at $f_0 = 1.334$.

the vicinity of a fixed point). For large A, we have

$$\frac{dA}{dT_1} = -\tfrac{1}{8}A^3 + \ldots \qquad , \qquad \frac{d\psi}{dT_1} = -\nu + \ldots \; . \tag{4.97}$$

This flow is inward, hence if the flow is not to a stable fixed point, it must be attracted to a limit cycle. The limit cycle necessarily involves several frequencies. This result – the generation of new frequencies by nonlinearities – is called *heterodyning*.

We can see heterodyning in action in the van der Pol system. In Fig. 4.5, the blue line which separates stable and unstable spiral solutions is given by $f_0^2 = 8\nu^2 + \frac{1}{2}$. For example, if we take $\nu = 0.40$ then the boundary lies at $f_0 = 1.334$. For $f_0 < 1.334$, we expect heterodyning, as the entrained solution is unstable. For $f > 1.334$ the solution is entrained and oscillates at a fixed frequency. This behavior is exhibited in Fig. 4.6.

4.4 Relaxation Oscillations

We saw how to use multiple time scale analysis to identify the limit cycle of the van der Pol oscillator when ϵ is small. Consider now the opposite limit, where the coefficient of the damping term is very large. We generalize the van der Pol equation to

$$\ddot{x} + \mu\,\Phi(x)\,\dot{x} + x = 0 \ , \tag{4.98}$$

and suppose $\mu \gg 1$. Define now the variable

$$\begin{aligned} y &\equiv \frac{\dot{x}}{\mu} + \int\limits_0^x \! dx'\,\Phi(x') \\ &= \frac{\dot{x}}{\mu} + F(x) \ , \end{aligned} \tag{4.99}$$

where $F'(x) = \Phi(x)$. (y is sometimes called the *Liènard variable*, and (x, y) the *Liènard plane*.) Then the original second order equation may be written as two coupled first order equations:

$$\dot{x} = \mu\Big(y - F(x)\Big) \tag{4.100}$$

$$\dot{y} = -\frac{x}{\mu} \ . \tag{4.101}$$

Since $\mu \gg 1$, the first of these equations is *fast* and the second one *slow*. The dynamics rapidly achieves $y \approx F(x)$, and then slowly evolves along the curve $y = F(x)$, until it is forced to make a large, fast excursion.

A concrete example is useful. Consider $F(x)$ of the form sketched in Fig. 4.7. This is what one finds for the van der Pol oscillator, where $\Phi(x) = x^2 - 1$ and $F(x) = \frac{1}{3}x^3 - x$. The limit cycle behavior $x_{\text{LC}}(t)$ is sketched in Fig. 4.8. We assume $\Phi(x) = \Phi(-x)$ for simplicity.

Assuming $\Phi(x) = \Phi(-x)$ is symmetric, $F(x)$ is antisymmetric. For the van der Pol oscillator and other similar cases, $F(x)$ resembles the sketch in fig. 4.7. There are two local extrema: a local maximum at $x = -a$ and a local minimum at $x = +a$. We define b such that $F(b) = F(-a)$, as shown in the figure; antisymmetry then entails $F(-b) = F(+a)$. Starting from an arbitrary initial condition, the y dynamics are slow, since $\dot{y} = -\mu^{-1}x$ (we assume $\mu \gg x(0)$). So y can be regarded as essentially constant for the fast dynamics of eqn. 4.101, according to which $x(t)$ flows rapidly to the right if $y > F(x)$ and rapidly to the left if

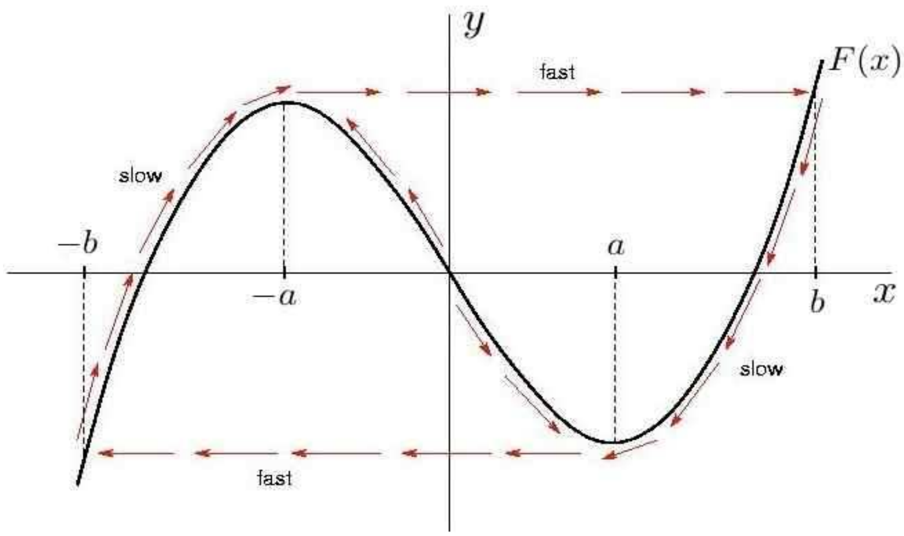

Figure 4.7: Relaxation oscillations in the so-called Liènard plane (x, y). The system rapidly flows to a point on the curve $y = F(x)$, and then crawls slowly along this curve. The slow motion takes x from $-b$ to $-a$, after which the system executes a rapid jump to $x = +b$, then a slow retreat to $x = +a$, followed by a rapid drop to $x = -b$.

$y < F(x)$. This fast motion stops when $x(t)$ reaches a point where $y = F(x)$. At this point, the slow dynamics takes over. Assuming $y \approx F(x)$, we have

$$y \approx F(x) \qquad \Rightarrow \qquad \dot{y} = -\frac{x}{\mu} \approx F'(x)\,\dot{x} \ , \tag{4.102}$$

which says that

$$\dot{x} \approx -\frac{x}{\mu\, F'(x)} \qquad \text{if } y \approx F(x) \tag{4.103}$$

over the slow segments of the motion, which are the regions $x \in [-b, -a]$ and $x \in [a, b]$. The relaxation oscillation is then as follows. Starting at $x = -b$, $x(t)$ increases slowly according to eqn. 4.103. At $x = -a$, the motion can no longer follow the curve $y = F(x)$, since $\dot{y} = -\mu^{-1}x$ is still positive. The motion thus proceeds quickly to $x = +b$, with

$$\dot{x} \approx \mu\Big(F(b) - F(x)\Big) \qquad x \in \big[-a, +b\big] \ . \tag{4.104}$$

After reaching $x = +b$, the motion once again is slow, and again follows eqn. 4.103, according to which $x(t)$ now decreases slowly until it reaches $x = +a$, at which point the motion is again fast, with

$$\dot{x} \approx \mu\Big(F(a) - F(x)\Big) \qquad x \in \big[-b, +a\big] \ . \tag{4.105}$$

The cycle then repeats.

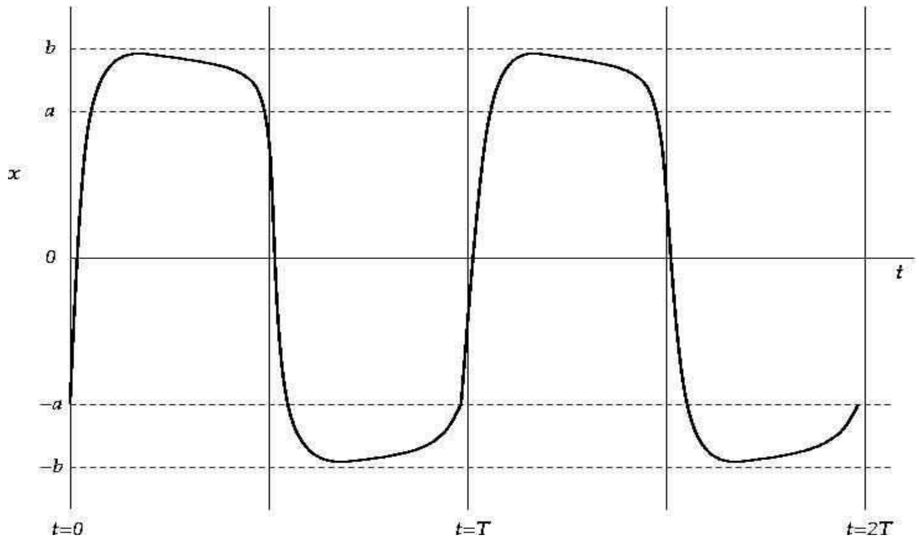

Figure 4.8: A sketch of the limit cycle for the relaxation oscillation studied in this section.

Thus, the limit cycle is given by the following segments:

$$x \in [\,-b,-a\,] \qquad (\dot{x}>0)\ : \qquad \dot{x} \approx -\frac{x}{\mu\, F'(x)} \tag{4.106}$$

$$x \in [\,-a,b\,] \qquad (\dot{x}>0)\ : \qquad \dot{x} \approx \mu\big[F(b)-F(x)\big] \tag{4.107}$$

$$x \in [\,a,b\,] \qquad (\dot{x}<0)\ : \qquad \dot{x} \approx -\frac{x}{\mu\, F'(x)} \tag{4.108}$$

$$x \in [\,-b,a\,] \qquad (\dot{x}<0)\ : \qquad \dot{x} \approx \mu\big[F(a)-F(x)\big]\ . \tag{4.109}$$

A sketch of the limit cycle is given in fig. 4.9, showing the slow and fast portions.

When $\mu \gg 1$ we can determine approximately the period of the limit cycle. Clearly the period is twice the time for either of the slow portions, hence

$$T \approx 2\mu \int\limits_a^b dx\, \frac{\Phi(x)}{x}\ , \tag{4.110}$$

where $F'(\pm a) = \Phi(\pm a) = 0$ and $F(\pm b) = F(\mp a)$. For the van der Pol oscillator, with $\Phi(x) = x^2 - 1$, we have $a = 1$, $b = 2$, and $T \simeq (3 - 2\ln 2)\,\mu$.

4.4.1 Example problem

Consider the equation

$$\ddot{x} + \mu\big(|x|-1\big)\dot{x} + x = 0\ . \tag{4.111}$$

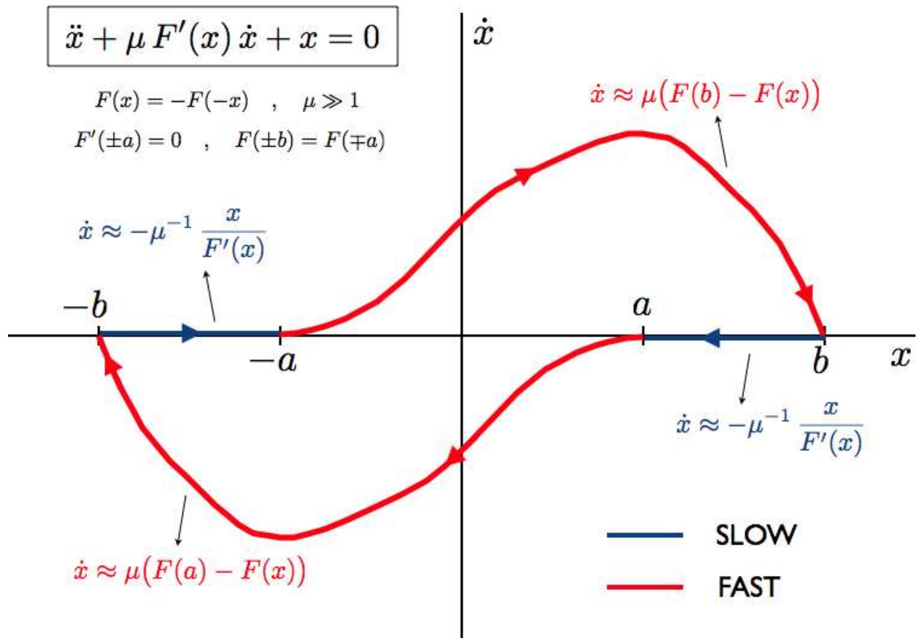

Figure 4.9: Limit cycle for large μ relaxation oscillations, shown in the phase plane $(x, \dot{x})$.

Sketch the trajectory in the Liènard plane, and find the approximate period of the limit cycle for $\mu \gg 1$.

Solution : We define

$$F'(x) = |x| - 1 \quad \Rightarrow \quad F(x) = \begin{cases} +\frac{1}{2}x^2 - x & \text{if } x > 0 \\ \\ -\frac{1}{2}x^2 - x & \text{if } x < 0 \ . \end{cases} \tag{4.112}$$

We therefore have

$$\dot{x} = \mu\big\{y - F(x)\big\} \quad , \quad \dot{y} = -\frac{x}{\mu} \ , \tag{4.113}$$

with $y \equiv \mu^{-1}\,\dot{x} + F(x)$.

Setting $F'(x) = 0$ we find $x = \pm a$, where $a = 1$ and $F(\pm a) = \mp\frac{1}{2}$. We also find $F(\pm b) = F(\mp a)$, where $b = 1 + \sqrt{2}$. Thus, the limit cycle is as follows: (i) fast motion from $x = -a$ to $x = +b$, (ii) slow relaxation from $x = +b$ to $x = +a$, (iii) fast motion from $x = +a$ to $x = -b$, and (iv) slow relaxation from $x = -b$ to $x = -a$. The period is approximately the time it takes for the slow portions of the cycle. Along these portions, we have $y \simeq F(x)$, and hence $\dot{y} \simeq F'(x)\,\dot{x}$. But $\dot{y} = -x/\mu$, so

$$F'(x)\,\dot{x} \simeq -\frac{x}{\mu} \quad \Rightarrow \quad dt = -\mu\,\frac{F'(x)}{x}\,dx \ , \tag{4.114}$$

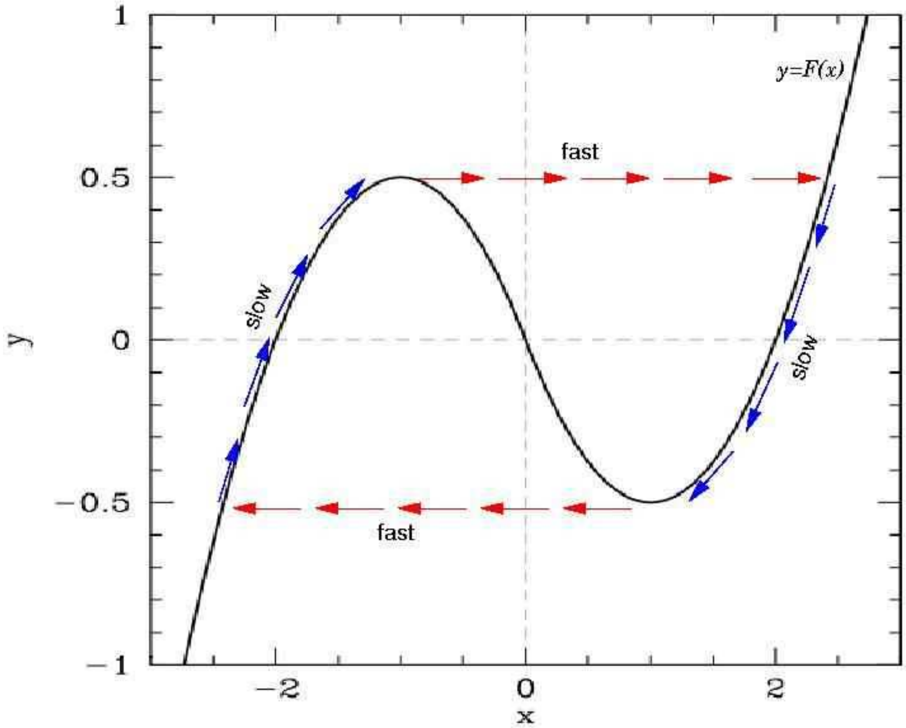

Figure 4.10: Relaxation oscillations for $\ddot{x} + \mu\big(|x| - 1\big)\,\dot{x} + x = 0$ plotted in the Liénard plane. The solid black curve is $y = F(x) = \frac{1}{2}x^2\,\mathrm{sgn}(x) - x$. The variable y is defined to be $y = \mu^{-1}\,\dot{x} + F(x)$. Along slow portions of the limit cycle, $y \simeq F(x)$.

which we integrate to obtain

$$T \simeq -2\mu\int\limits_b^a dx\,\frac{F'(x)}{x} = 2\mu\int\limits_1^{1+\sqrt{2}} dx\,\left(1 - \frac{1}{x}\right) \tag{4.115}$$

$$= 2\mu\Big[\sqrt{2} - \ln\big(1+\sqrt{2}\big)\Big] \simeq 1.066\,\mu\ . \tag{4.116}$$

4.4.2 Multiple limit cycles

For the equation

$$\ddot{x} + \mu\,F'(x)\,\dot{x} + x = 0\ , \tag{4.117}$$

it is illustrative to consider what sort of $F(x)$ would yield more than one limit cycle. Such an example is shown in fig. 4.11.

In polar coordinates, it is very easy to construct such examples. Consider, for example, the

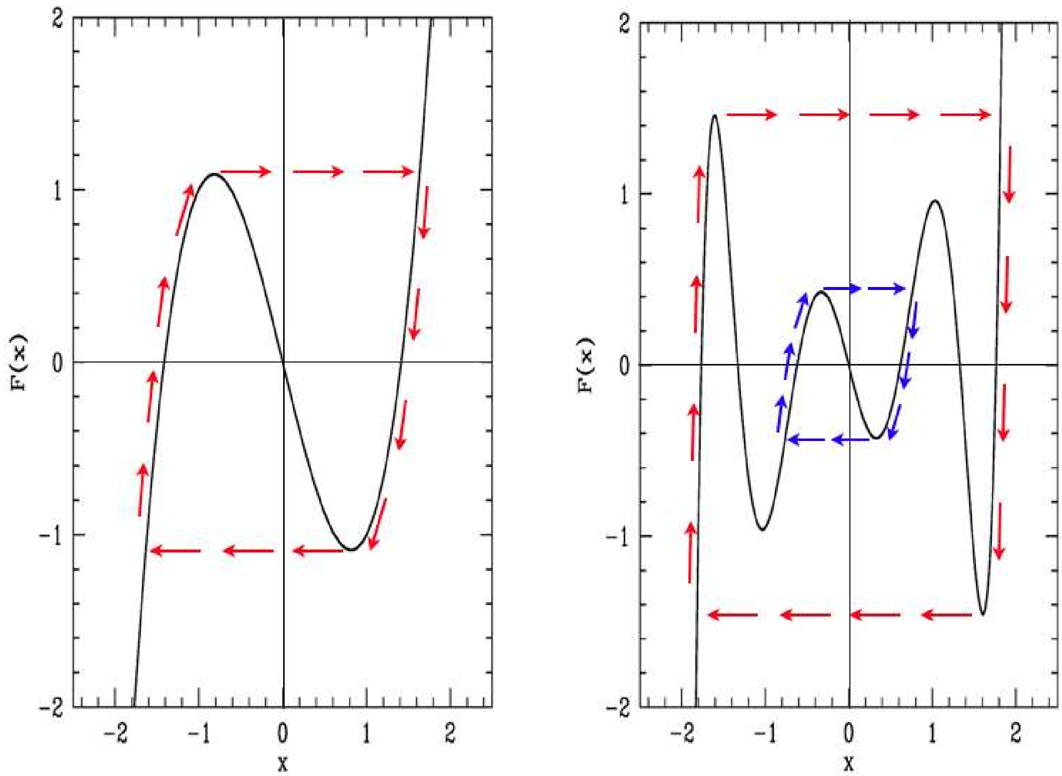

Figure 4.11: Liénard plots for systems with one (left) and two (right) relaxation oscillations.

system

$$\dot{r} = \sin(\pi r) + \epsilon \cos\theta \tag{4.118}$$

$$\dot{\theta} = b\,r \ , \tag{4.119}$$

with $|\epsilon| < 1$. First consider the case $\epsilon = 0$. Clearly the radial flow is outward for $\sin(\pi r) > 0$ and inward for $\sin(\pi r) < 0$. Thus, we have stable limit cycles at $r = 2n+1$ and unstable limit cycles at $r = 2n$, for all $n \in \mathbb{Z}$. With $0 < |\epsilon| < 1$, we have

$$\dot{r} > 0 \qquad \text{for} \qquad r \in \big[2n + \tfrac{1}{\pi}\sin^{-1}\epsilon\,,\, 2n+1 - \tfrac{1}{\pi}\sin^{-1}\epsilon\big] \tag{4.120}$$

$$\dot{r} < 0 \qquad \text{for} \qquad r \in \big[2n + 1 + \tfrac{1}{\pi}\sin^{-1}\epsilon\,,\, 2n+2 - \tfrac{1}{\pi}\sin^{-1}\epsilon\big] \tag{4.121}$$

The Poincaré-Bendixson theorem then guarantees the existence of stable and unstable limit cycles. We can put bounds on the radial extent of these limit cycles.

$$\text{stable limit cycle} \quad : \quad r \in \big[2n + 1 - \tfrac{1}{\pi}\sin^{-1}\epsilon\,,\, 2n+1 + \tfrac{1}{\pi}\sin^{-1}\epsilon\big] \tag{4.122}$$

$$\text{unstable limit cycle} \quad : \quad r \in \big[2n - \tfrac{1}{\pi}\sin^{-1}\epsilon\,,\, 2n + \tfrac{1}{\pi}\sin^{-1}\epsilon\big] \tag{4.123}$$

Note that an unstable limit cycle is a repeller, which is to say that it is stable (an attractor) if we run the dynamics backwards, sending $t \to -t$.

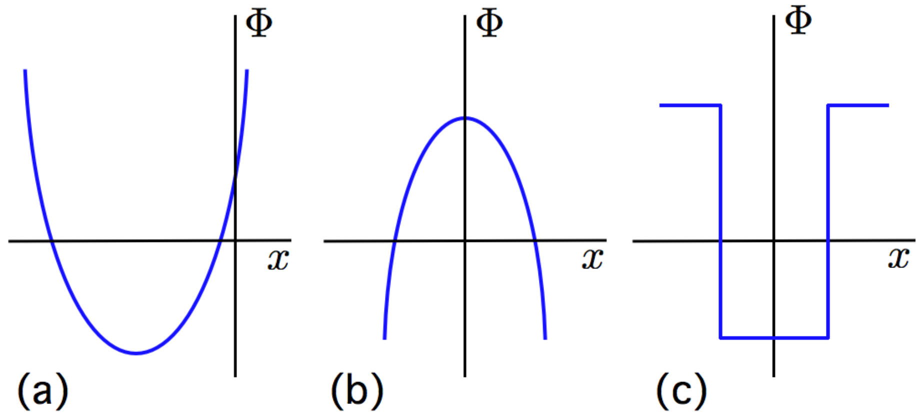

Figure 4.12: Three instances of $\Phi(x)$.

4.4.3 Example problem

Consider the nonlinear oscillator,

$$\ddot{x} + \mu\,\Phi(x)\,\dot{x} + x = 0\ ,$$

with $\mu \gg 1$. For each case in fig. 4.12, sketch the flow in the Liènard plane, starting with a few different initial conditions. For which case(s) do relaxation oscillations occur?

Solution : Recall the general theory of relaxation oscillations. We define

$$y \equiv \frac{\dot{x}}{\mu} + \int\limits_0^x \! dx'\,\Phi(x') = \frac{\dot{x}}{\mu} + F(x)\ ,$$

in which case the second order ODE for the oscillator may be written as two coupled first order ODEs:

$$\dot{y} = -\frac{x}{\mu} \quad , \quad \dot{x} = \mu\Big(y - F(x)\Big)\ .$$

Since $\mu \gg 1$, the first of these equations is *slow* and the second one *fast*. The dynamics rapidly achieves $y \approx F(x)$, and then slowly evolves along the curve $y = F(x)$, until it is forced to make a large, fast excursion.

To explore the dynamics in the Liènard plane, we plot $F(x)$ *versus* x, which means we must integrate $\Phi(x)$. This is done for each of the three cases in fig. 4.12.

Note that a fixed point corresponds to $x = 0$ and $\dot{x} = 0$. In the Liènard plane, this means $x = 0$ and $y = F(0)$. Linearizing by setting $x = \delta x$ and $y = F(0) + \delta y$, we have[1]

$$\frac{d}{dt}\begin{pmatrix} \delta x \\ \delta y \end{pmatrix} = \begin{pmatrix} \mu\,\delta y - \mu F'(0)\,\delta x \\ -\mu^{-1}\,\delta x \end{pmatrix} = \begin{pmatrix} -\mu F'(0) & \mu \\ -\mu^{-1} & 0 \end{pmatrix}\begin{pmatrix} \delta x \\ \delta y \end{pmatrix}\ .$$

[1] We could, of course, linearize about the fixed point in $(x, \dot{x})$ space and obtain the same results.

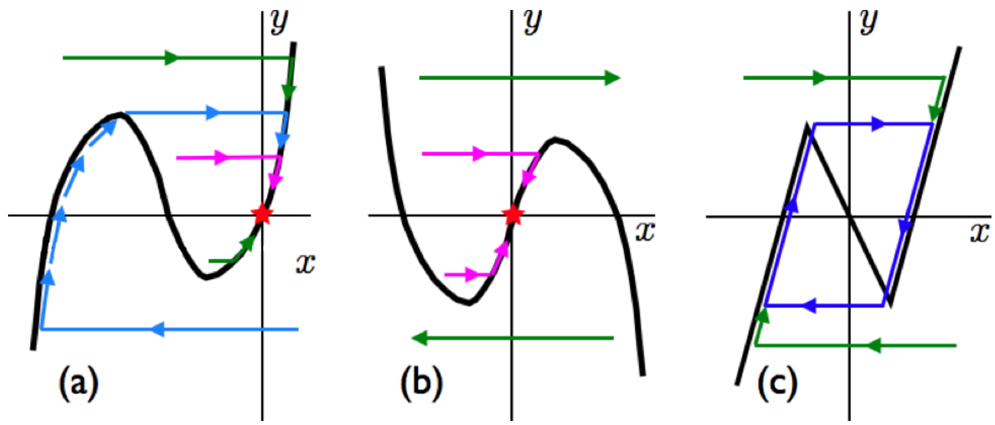

Figure 4.13: Phase flows in the Liénard plane for the three examples in fig. 4.12.

The linearized map has trace $T = -\mu\, F'(0)$ and determinant $D = 1$. Since $\mu \gg 1$ we have $0 < D < \frac{1}{4}T^2$, which means the fixed point is either a stable node, for $F'(0) > 0$, or an unstable node, for $F'(0) < 0$. In cases (a) and (b) the fixed point is a stable node, while in case (c) it is unstable. The flow in case (a) always collapses to the stable node. In case (b) the flow either is unbounded or else it collapses to the stable node. In case (c), all initial conditions eventually flow to a unique limit cycle exhibiting relaxation oscillations.

4.5 Parametric Oscillator

Consider the equation

$$\ddot{x} + \omega_0^2(t)\, x = 0 \ , \tag{4.124}$$

where the oscillation frequency is a function of time. Equivalently,

$$\frac{d}{dt}\begin{pmatrix} x \\ \dot{x} \end{pmatrix} = \overbrace{\begin{pmatrix} 0 & 1 \\ -\omega_0^2(t) & 0 \end{pmatrix}}^{M(t)} \overbrace{\begin{pmatrix} x \\ \dot{x} \end{pmatrix}}^{\varphi(t)} \ . \tag{4.125}$$

The formal solution is the path-ordered exponential,

$$\varphi(t) = \mathcal{P} \exp\left\{ \int_0^t dt'\, M(t') \right\} \varphi(0) \ . \tag{4.126}$$

Let's consider an example in which

$$\omega(t) = \begin{cases} (1+\epsilon)\,\omega_0 & \text{if } 2n\tau \le t \le (2n+1)\tau \\ \\ (1-\epsilon)\,\omega_0 & \text{if } (2n+1)\tau \le t \le (2n+2)\tau \ . \end{cases} \tag{4.127}$$

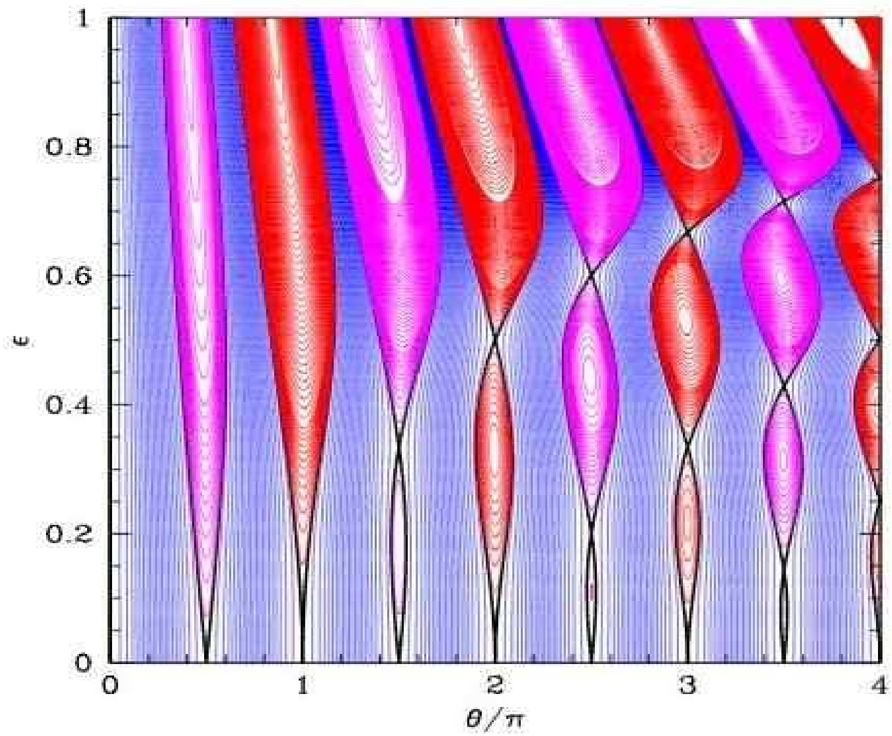

Figure 4.14: Phase diagram for the parametric oscillator in the (θ, ϵ) plane. Thick black lines correspond to $T = \pm 2$. Blue regions: $|T| < 2$. Red regions: $T > 2$. Magenta regions: $T < -2$.

Define $\boldsymbol{\varphi}_n \equiv \boldsymbol{\varphi}(2n\tau)$. Then

$$\boldsymbol{\varphi}_{n+1} = \exp(M_- \tau)\, \exp(M_+ \tau)\, \boldsymbol{\varphi}_n \ , \tag{4.128}$$

where

$$M_\pm = \begin{pmatrix} 0 & 1 \\ -\omega_\pm^2 & 0 \end{pmatrix} \ , \tag{4.129}$$

with $\omega_\pm \equiv (1 \pm \epsilon)\, \omega_0$. Note that $M_\pm^2 = -\omega_\pm^2 \cdot \mathbb{I}$ is a multiple of the identity. Evaluating the Taylor series for the exponential, one finds

$$\exp(M_\pm t) = \begin{pmatrix} \cos\omega_\pm \tau & \omega_\pm^{-1} \sin\omega_\pm \tau \\ -\omega_\pm \, \sin\omega_\pm \tau & \cos\omega_\pm \tau \end{pmatrix} \ , \tag{4.130}$$

from which we derive

$$\begin{aligned} \mathcal{Q} \equiv \begin{pmatrix} a & b \\ c & d \end{pmatrix} &= \exp(M_- \tau)\, \exp(M_+ \tau) \qquad (4.131) \\ &= \begin{pmatrix} \cos\omega_- \tau & \omega_-^{-1} \sin\omega_- \tau \\ -\omega_- \, \sin\omega_- \tau & \cos\omega_- \tau \end{pmatrix} \begin{pmatrix} \cos\omega_+ \tau & \omega_+^{-1} \sin\omega_+ \tau \\ -\omega_+ \, \sin\omega_+ \tau & \cos\omega_+ \tau \end{pmatrix} \end{aligned}$$

with

$$a = \cos\omega_-\tau\,\cos\omega_+\tau - \frac{\omega_+}{\omega_-}\,\sin\omega_-\tau\,\sin\omega_+\tau \tag{4.132}$$

$$b = \frac{1}{\omega_+}\,\cos\omega_-\tau\sin\omega_+\tau + \frac{1}{\omega_-}\,\sin\omega_-\tau\cos\omega_+\tau \tag{4.133}$$

$$c = -\omega_+\,\cos\omega_-\tau\sin\omega_+\tau - \omega_-\,\sin\omega_-\tau\cos\omega_+\tau \tag{4.134}$$

$$d = \cos\omega_-\tau\,\cos\omega_+\tau - \frac{\omega_-}{\omega_+}\,\sin\omega_-\tau\,\sin\omega_+\tau\ . \tag{4.135}$$

Note that $\det\exp(M_\pm\tau) = 1$, hence $\det\mathcal{Q} = 1$. Also note that

$$P(\lambda) = \det\big(\mathcal{Q} - \lambda\cdot\mathbb{I}\big) = \lambda^2 - T\lambda + \varDelta\ , \tag{4.136}$$

where

$$T = a + d = \mathrm{Tr}\,\mathcal{Q} \tag{4.137}$$

$$\varDelta = ad - bc = \det\mathcal{Q}\ . \tag{4.138}$$

The eigenvalues of $\mathcal{Q}$ are

$$\lambda_\pm = \tfrac{1}{2}T \pm \tfrac{1}{2}\sqrt{T^2 - 4\varDelta}\ . \tag{4.139}$$

In our case, $\varDelta = 1$. There are two cases to consider:

$$|T| < 2\ :\ \lambda_+ = \lambda_-^* = e^{i\delta}\quad,\quad \delta = \cos^{-1}\tfrac{1}{2}T \tag{4.140}$$

$$|T| > 2\ :\ \lambda_+ = \lambda_-^{-1} = \pm e^{\mu}\quad,\quad \mu = \cosh^{-1}\tfrac{1}{2}|T|\ . \tag{4.141}$$

When $|T| < 2$, $\boldsymbol{\varphi}$ remains bounded; when $|T| > 2$, $|\boldsymbol{\varphi}|$ increases exponentially with time. Note that phase space volumes are preserved by the dynamics.

To investigate more fully, let $\theta \equiv \omega_0\tau$. The period of the ω_0 oscillations is $\delta t = 2\tau$, *i.e.* $\omega_{\rm pump} = \pi/\tau$ is the frequency at which the system is 'pumped'. We compute the trace of $\mathcal{Q}$ and find

$$\tfrac{1}{2}T = \frac{\cos(2\theta) - \epsilon^2\cos(2\epsilon\theta)}{1-\epsilon^2}\ . \tag{4.142}$$

We are interested in the boundaries in the (θ,ϵ) plane where $|T| = 2$. Setting $T = +2$, we write $\theta = n\pi + \delta$, which means $\omega_0 \approx n\omega_{\rm pump}$. Expanding for small δ and ϵ, we obtain the relation

$$\delta^2 = \epsilon^4\,\theta^2 \quad\Rightarrow\quad \epsilon = \left|\frac{\delta}{n\pi}\right|^{1/2}\ . \tag{4.143}$$

Setting $T = -2$, we write $\theta = (n+\frac{1}{2})\pi + \delta$, *i.e.* $\omega_0 \approx (n+\frac{1}{2})\,\omega_{\rm pump}$. This gives

$$\delta^2 = \epsilon^2 \quad\Rightarrow\quad \epsilon = \pm\delta\ . \tag{4.144}$$

The full phase diagram in the (θ,ϵ) plane is shown in Fig. 4.14. A physical example is pumping a swing. By extending your legs periodically, you effectively change the length $\ell(t)$ of the pendulum, resulting in a time-dependent $\omega_0(t) = \sqrt{g/\ell(t)}$.

4.6 Appendix I : Multiple Time Scale Analysis to $\mathcal{O}(\epsilon^2)$

Problem : A particle of mass m moves in one dimension subject to the potential

$$U(x) = \tfrac{1}{2}m\,\omega_0^2\,x^2 + \tfrac{1}{3}\epsilon\,m\,\omega_0^2\,\frac{x^3}{a}\ , \tag{4.145}$$

where ϵ is a dimensionless parameter.

(a) Find the equation of motion for x. Show that by rescaling x and t you can write this equation in dimensionless form as

$$\frac{d^2u}{ds^2} + u = -\epsilon u^2\ . \tag{4.146}$$

Solution : The equation of motion is

$$m\ddot{x} = -U'(x) \tag{4.147}$$

$$= -m\omega_0^2 x - \epsilon m\omega_0^2\,\frac{x^2}{a}\ . \tag{4.148}$$

We now define $s \equiv \omega_0 t$ and $u \equiv x/a$, yielding

$$\frac{d^2u}{ds^2} + u = -\epsilon u^2\ . \tag{4.149}$$

(b) You are now asked to perform an $\mathcal{O}(\epsilon^2)$ multiple time scale analysis of this problem, writing

$$T_0 = s \qquad , \qquad T_1 = \epsilon s \qquad , \qquad T_2 = \epsilon^2 s\ ,$$

and

$$u = u_0 + \epsilon u_1 + \epsilon^2 u_2 + \ldots\ .$$

This results in a hierarchy of coupled equations for the functions $\{u_n\}$. Derive the first three equations in the hierarchy.

Solution : We have

$$\frac{d}{ds} = \frac{\partial}{\partial T_0} + \epsilon\,\frac{\partial}{\partial T_1} + \epsilon^2\,\frac{\partial}{\partial_2} + \ldots\ . \tag{4.150}$$

Therefore

$$\bigg(\frac{\partial}{\partial T_0} + \epsilon\,\frac{\partial}{\partial T_1} + \epsilon^2\,\frac{\partial}{\partial T_2} + \ldots\bigg)^2 \Big(u_0 + \epsilon\,u_1 + \epsilon^2\,u_2 + \ldots\Big) + \Big(u_0 + \epsilon\,u_1 + \epsilon^2\,u_2 + \ldots\Big)$$
$$= -\epsilon\,\Big(u_0 + \epsilon\,u_1 + \epsilon^2\,u_2 + \ldots\Big)^2\ . \tag{4.151}$$

Expanding and then collecting terms order by order in ϵ, we derive the hierarchy. The first three levels are

$$\frac{\partial^2 u_0}{\partial T_0^2} + u_0 = 0 \tag{4.152}$$

$$\frac{\partial^2 u_1}{\partial T_0^2} + u_1 = -2\,\frac{\partial^2 u_0}{\partial T_0\,\partial T_1} - u_0^2 \tag{4.153}$$

$$\frac{\partial^2 u_2}{\partial T_0^2} + u_2 = -2\,\frac{\partial^2 u_0}{\partial T_0\,\partial T_2} - \frac{\partial^2 u_0}{\partial T_1^2} - 2\,\frac{\partial^2 u_1}{\partial T_0\,\partial T_1} - 2\,u_0\,u_1\ . \tag{4.154}$$

(c) Show that there is no frequency shift to first order in ϵ.

Solution : At the lowest (first) level of the hierarchy, the solution is

$$u_0 = A(T_1, T_2)\,\cos\big(T_0 + \phi(T_1, T_2)\big)\ .$$

At the second level, then,

$$\frac{\partial^2 u_1}{\partial T_0^2} + u_1 = 2\,\frac{\partial A}{\partial T_1}\,\sin(T_0+\phi) + 2A\,\frac{\partial \phi}{\partial T_1}\,\cos(T_0+\phi) - A^2\cos^2(T_0+\phi)\ .$$

We eliminate the resonant forcing terms on the RHS by demanding

$$\frac{\partial A}{\partial T_1} = 0 \qquad \text{and} \qquad \frac{\partial \phi}{\partial T_1} = 0\ .$$

Thus, we must have $A = A(T_2)$ and $\phi = \phi(T_2)$. To $\mathcal{O}(\epsilon)$, then, ϕ is a constant, which means there is no frequency shift at this level of the hierarchy.

(d) Find $u_0(s)$ and $u_1(s)$.

Solution :The equation for u_1 is that of a non-resonantly forced harmonic oscillator. The solution is easily found to be

$$u_1 = -\tfrac{1}{2}A^2 + \tfrac{1}{6}A^2\cos(2T_0 + 2\phi)\ .$$

We now insert this into the RHS of the third equation in the hierarchy:

$$\begin{aligned}\frac{\partial^2 u_2}{\partial T_0^2} + u_2 &= -2\frac{\partial^2 u_0}{\partial T_0\,\partial T_2} - 2\,u_0\,u_1 \\ &= 2\,\frac{\partial A}{\partial T_2}\,\sin(T_0+\phi) + 2A\,\frac{\partial \phi}{\partial T_2}\,\cos(T_0+\phi) - 2A\cos(T_0+\phi)\Big\{-\tfrac{1}{2}A^2 + \tfrac{1}{6}A^2\cos(2T_0+2\phi)\Big\} \\ &= 2\,\frac{\partial A}{\partial T_2}\,\sin(T_0+\phi) + \Big(2A\,\frac{\partial \phi}{\partial T_2} + \tfrac{5}{6}A^3\Big)\cos(T_0+\phi) - \tfrac{1}{6}A^3\,\cos(3T_0+3\phi)\ .\end{aligned}$$

Setting the coefficients of the resonant terms on the RHS to zero yields

$$\frac{\partial A}{\partial T_2} = 0 \quad \Rightarrow \quad A = A_0$$

$$2A\,\frac{\partial \phi}{\partial T_2} + \tfrac{5}{6}A^3 = 0 \quad \Rightarrow \quad \phi = -\tfrac{5}{12}\,A_0^2\,T_2\ .$$

Therefore,

$$u(s) = \overbrace{A_0 \cos\big(s - \tfrac{5}{12}\,\epsilon^2 A_0^2\, s\big)}^{u_0(s)} + \overbrace{\tfrac{1}{6}\,\epsilon\, A_0^2 \cos\big(2s - \tfrac{5}{6}\,\epsilon^2 A_0^2\, s\big) - \tfrac{1}{2}\,\epsilon\, A_0^2}^{\epsilon\, u_1(s)} + \mathcal{O}(\epsilon^2)$$

4.7 Appendix II : MSA and Poincaré-Lindstedt Methods

4.7.1 Problem using multiple time scale analysis

Consider the central force law $F(r) = -k\, r^{\beta^2-3}$.

(a) Show that a stable circular orbit exists at radius $r_0 = (\ell^2/\mu k)^{1/\beta^2}$.

Solution : For a circular orbit, the effective radial force must vanish:

$$F_{\rm eff}(r) = \frac{\ell^2}{\mu r^3} + F(r) = \frac{\ell^2}{\mu r^3} - \frac{k}{r^{3-\beta^2}} = 0 \ . \tag{4.155}$$

Solving for $r = r_0$, we have $r_0 = (\ell^2/\mu k)^{1/\beta^2}$. The second derivative of $U_{\rm eff}(r)$ at this point is

$$U''_{\rm eff}(r_0) = -F'_{\rm eff}(r_0) = \frac{3\ell^2}{\mu r_0^4} + (\beta^2 - 3)\,\frac{k}{r_0^{4-\beta^2}} = \frac{\beta^2 \ell^2}{\mu r_0^4} \ , \tag{4.156}$$

which is manifestly positive. Thus, the circular orbit at $r = r_0$ is stable.

(b) Show that the geometric equation for the shape of the orbit may be written

$$\frac{d^2 s}{d\phi^2} + s = K(s) \tag{4.157}$$

where $s = 1/r$, and

$$K(s) = s_0 \left(\frac{s}{s_0}\right)^{1-\beta^2} \ , \tag{4.158}$$

with $s_0 = 1/r_0$.

Solution : We have previously derived (*e.g.* in the notes) the equation

$$\frac{d^2 s}{d\phi^2} + s = -\frac{\mu}{\ell^2 s^2}\, F(s^{-1}) \ . \tag{4.159}$$

From the given $F(r)$, we then have

$$\frac{d^2 s}{d\phi^2} + s = \frac{\mu k}{\ell^2}\, s^{1-\beta^2} \equiv K(s) \ , \tag{4.160}$$

where $s_0 \equiv (\mu k/\ell^2)^{1/\beta^2} = 1/r_0$, and where

$$K(s) = s_0 \left(\frac{s}{s_0}\right)^{1-\beta^2} \ . \tag{4.161}$$

(c) Writing $s \equiv (1+u)\,s_0$, show that u satisfies

$$\frac{1}{\beta^2}\,\frac{d^2u}{d\phi^2} + u = a_1\,u^2 + a_2\,u^3 + \ldots \ . \tag{4.162}$$

Find a_1 and a_2.

Solution : Writing $s \equiv s_0\,(1+u)$, we have

$$\begin{aligned}\frac{d^2u}{d\phi^2} + 1 + u &= (1+u)^{1-\beta^2} \\ &= 1 + (1-\beta^2)\,u + \tfrac{1}{2}(-\beta^2)(1-\beta^2)\,u^2 \\ &\qquad + \tfrac{1}{6}(-1-\beta^2)(-\beta^2)(1-\beta^2)\,u^3 + \ldots \ .\end{aligned} \tag{4.163}$$

Thus,

$$\frac{1}{\beta^2}\,\frac{d^2u}{d\phi^2} + u = a_1\,u^2 + a_2\,u^3 + \ldots \ , \tag{4.164}$$

where

$$a_1 = -\tfrac{1}{2}(1-\beta^2) \quad , \quad a_2 = \tfrac{1}{6}(1-\beta^4) \ . \tag{4.165}$$

(d) Now let us associate a power of ε with each power of the deviation u and write

$$\frac{1}{\beta^2}\,\frac{d^2u}{d\phi^2} + u = \varepsilon\,a_1\,u^2 + \varepsilon^2\,a_2\,u^3 + \ldots \ , \tag{4.166}$$

Solve this equation using the method of multiple scale analysis (MSA). You will have to go to second order in the multiple scale expansion, writing

$$X \equiv \beta\phi \quad , \quad Y \equiv \varepsilon\,\beta\phi \quad , \quad Z \equiv \varepsilon^2\,\beta\phi \tag{4.167}$$

and hence

$$\frac{1}{\beta}\,\frac{d}{d\phi} = \frac{\partial}{\partial X} + \varepsilon\,\frac{\partial}{\partial Y} + \varepsilon^2\,\frac{\partial}{\partial Z} + \ldots \ . \tag{4.168}$$

Further writing

$$u = u_0 + \varepsilon\,u_1 + \varepsilon^2\,u_2 + \ldots \ , \tag{4.169}$$

derive the equations for the multiple scale analysis, up to second order in ε.

Solution : We now associate one power of ε with each additional power of u beyond order u^1. In this way, a uniform expansion in terms of ε will turn out to be an expansion in powers of the amplitude of the oscillations. We'll see how this works below. We then have

$$\frac{1}{\beta^2}\,\frac{d^2u}{d\phi^2} + u = a_1\,\varepsilon\,u^2 + a_2\,\varepsilon^2\,u^3 + \ldots \ , \tag{4.170}$$

with $\varepsilon = 1$. We now perform a multiple scale analysis, writing

$$X \equiv \beta\phi \quad , \quad Y \equiv \varepsilon\,\beta\phi \quad , \quad Z \equiv \varepsilon^2\,\beta\phi \ . \tag{4.171}$$

This entails

$$\frac{1}{\beta}\,\frac{d}{d\phi} = \frac{\partial}{\partial X} + \varepsilon\,\frac{\partial}{\partial Y} + \varepsilon^2\,\frac{\partial}{\partial Z} + \ldots \ . \tag{4.172}$$

We also expand u in powers of ε, as

$$u = u_0 + \varepsilon\,u_1 + \varepsilon^2\,u_2 + \ldots \ . \tag{4.173}$$

Thus, we obtain

$$\begin{aligned}\big(\partial_X + \varepsilon\,\partial_Y + \varepsilon^2\,\partial_Z + \ldots\big)^2\,(u_0 + \varepsilon u_1 + \varepsilon^2 u_2 + \ldots) + (u_0 + \varepsilon u_1 + \varepsilon^2 u_2 + \ldots)&\\ = \varepsilon\,a_1\,(u_0 + \varepsilon u_1 + \varepsilon^2 u_2 + \ldots)^2 + \varepsilon^2\,a_2\,(u_0 + \varepsilon u_1 + \varepsilon^2 u_2 + \ldots)^3 + \ldots \ .&\end{aligned} \tag{4.174}$$

We now extract a hierarchy of equations, order by order in powers of ε.

We find, out to order ε^2,

$$\mathcal{O}(\varepsilon^0): \quad \frac{\partial^2 u_0}{\partial X^2} + u_0 = 0 \tag{4.175}$$

$$\mathcal{O}(\varepsilon^1): \quad \frac{\partial^2 u_1}{\partial X^2} + u_1 = -2\frac{\partial^2 u_0}{\partial Y\,\partial X} + a_1\,u_0^2 \tag{4.176}$$

$$\mathcal{O}(\varepsilon^2): \quad \frac{\partial^2 u_2}{\partial X^2} + u_2 = -2\frac{\partial^2 u_0}{\partial Z\,\partial X} - \frac{\partial^2 u_0}{\partial Y^2} - 2\frac{\partial^2 u_1}{\partial Z\,\partial X} + 2a_1\,u_0\,u_1 + a_2\,u_0^3\ . \tag{4.177}$$

(e) Show that there is no shift of the angular period $\Delta\phi = 2\pi/\beta$ if one works only to leading order in ε.

Solution : The $\mathcal{O}(\varepsilon^0)$ equation in the hierarchy is solved by writing

$$u_0 = A\,\cos(X + \psi)\ , \tag{4.178}$$

where

$$A = A(Y,Z) \quad , \quad \psi = \psi(Y,Z)\ . \tag{4.179}$$

We define $\theta \equiv X + \psi(Y,Z)$, so we may write $u_0 = A\cos\theta$. At the next order, we obtain

$$\begin{aligned}\frac{\partial^2 u_1}{\partial\theta^2} + u_1 &= 2\frac{\partial A}{\partial Y}\,\sin\theta + 2A\,\frac{\partial\psi}{\partial Y}\,\cos\theta + a_1\,A^2\cos\theta\\ &= 2\frac{\partial A}{\partial Y}\,\sin\theta + 2A\,\frac{\partial\psi}{\partial Y}\,\cos\theta + \tfrac{1}{2}a_1 A^2 + \tfrac{1}{2}a_1 A^2\,\cos 2\theta\ .\end{aligned} \tag{4.180}$$

In order that there be no resonantly forcing terms on the RHS of eqn. 5.37, we demand

$$\frac{\partial A}{\partial Y} = 0 \quad , \quad \frac{\partial\psi}{\partial Y} = 0 \quad \Rightarrow \quad A = A(Z) \quad , \quad \psi = \psi(Z)\ . \tag{4.181}$$

The solution for u_1 is then

$$u_1(\theta) = \tfrac{1}{2} a_1 A^2 - \tfrac{1}{6} a_1 A^2 \cos 2\theta \ . \tag{4.182}$$

Were we to stop at this order, we could ignore $Z = \varepsilon^2 \beta \phi$ entirely, since it is of order ε^2, and the solution would be

$$u(\phi) = A_0 \cos(\beta\phi + \psi_0) + \tfrac{1}{2}\varepsilon a_1 A_0^2 - \tfrac{1}{6}\varepsilon a_1 A_0^2 \cos(2\beta\phi + 2\psi_0) \ . \tag{4.183}$$

The angular period is still $\Delta\phi = 2\pi/\beta$, and, starting from a small amplitude solution at order ε^0 we find that to order ε we must add a constant shift proportional to A_0^2, as well as a second harmonic term, also proportional to A_0^2.

(f) Carrying out the MSA to second order in ε, show that the shift of the angular period vanishes only if $\beta^2 = 1$ or $\beta^2 = 4$.

Solution : Carrying out the MSA to the next order, $\mathcal{O}(\varepsilon^2)$, we obtain

$$\begin{aligned}
\frac{\partial^2 u_2}{\partial\theta^2} + u_2 &= 2\frac{\partial A}{\partial Z}\sin\theta + 2A\,\frac{\partial\psi}{\partial Z}\cos\theta + 2a_1 A\cos\theta\,\big(\tfrac{1}{2}a_1 A^2 - \tfrac{1}{6}a_1 A^2\cos 2\theta\big) + a_2 A^3\cos^3\!\theta \\
&= 2\frac{\partial A}{\partial Z}\sin\theta + 2A\,\frac{\partial\psi}{\partial Z}\cos\theta + \big(\tfrac{5}{6}a_1^2 + \tfrac{3}{4}a_2\big)\,A^3\cos\theta + \big(-\tfrac{1}{6}a_1^2 + \tfrac{1}{4}a_2\big)\,A^3\cos 3\theta \ .
\end{aligned} \tag{4.184}$$

Now in order to make the resonant forcing terms on the RHS vanish, we must choose

$$\frac{\partial A}{\partial Z} = 0 \tag{4.185}$$

as well as

$$\frac{\partial\psi}{\partial Z} = -\big(\tfrac{5}{12}a_1^2 + \tfrac{3}{8}a_2\big)\,A^2 \tag{4.186}$$

$$= -\tfrac{1}{24}(\beta^2 - 4)(\beta^2 - 1) \ . \tag{4.187}$$

The solutions to these equations are trivial:

$$A(Z) = A_0 \quad , \quad \psi(Z) = \psi_0 - \tfrac{1}{24}(\beta^2 - 1)(\beta^2 - 4)A_0^2\, Z \ . \tag{4.188}$$

With the resonant forcing terms eliminated, we may write

$$\frac{\partial^2 u_2}{\partial\theta^2} + u_2 = \big(-\tfrac{1}{6}a_1^2 + \tfrac{1}{4}a_2\big)\,A^3\cos 3\theta \ , \tag{4.189}$$

with solution

$$\begin{aligned}
u_2 &= \tfrac{1}{96}(2a_1^2 - 3a_2)\,A^3\,\cos 3\theta \\
&= \tfrac{1}{96}\,\beta^2\,(\beta^2 - 1)\,A_0^2\,\cos\big(3X + 3\psi(Z)\big) \ .
\end{aligned} \tag{4.190}$$

The full solution to second order in this analysis is then

$$u(\phi) = A_0 \cos(\beta'\phi + \psi_0) + \tfrac{1}{2}\varepsilon a_1 A_0^2 - \tfrac{1}{6}\varepsilon a_1 A_0^2 \cos(2\beta'\phi + 2\psi_0)$$
$$+ \tfrac{1}{96}\varepsilon^2 \left(2a_1^2 - 3a_2\right) A_0^3 \cos(3\beta'\phi + 3\psi_0) \ . \tag{4.191}$$

with

$$\beta' = \beta \cdot \Big\{1 - \tfrac{1}{24}\,\varepsilon^2\,(\beta^2 - 1)(\beta^2 - 4)A_0^2\Big\} \ . \tag{4.192}$$

The angular period shifts:

$$\Delta\phi = \frac{2\pi}{\beta'} = \frac{2\pi}{\beta} \cdot \Big\{1 + \tfrac{1}{24}\,\varepsilon^2\,(\beta^2 - 1)(\beta^2 - 4)A_0^2\Big\} + \mathcal{O}(\varepsilon^3) \ . \tag{4.193}$$

Note that there is no shift in the period, for any amplitude, if $\beta^2 = 1$ (*i.e.* Kepler potential) or $\beta^2 = 4$ (*i.e.* harmonic oscillator).

4.7.2 Solution using Poincaré-Lindstedt method

Recall that geometric equation for the shape of the (relative coordinate) orbit for the two body central force problem is

$$\frac{d^2 s}{d\phi^2} + s = K(s) \tag{4.194}$$

$$K(s) = s_0 \left(\frac{s}{s_0}\right)^{1-\beta^2} \tag{4.195}$$

where $s = 1/r$, $s_0 = (l^2/\mu k)^{1/\beta^2}$ is the inverse radius of the stable circular orbit, and $f(r) = -kr^{\beta^2-3}$ is the central force. Expanding about the stable circular orbit, one has

$$\frac{d^2 y}{d\phi^2} + \beta^2\, y = \tfrac{1}{2}K''(s_0)\, y^2 + \tfrac{1}{6}K'''(s_0)\, y^3 + \ldots \ , \tag{4.196}$$

where $s = s_0(1 + y)$, with

$$K'(s) = (1 - \beta^2)\left(\frac{s_0}{s}\right)^{\beta^2} \tag{4.197}$$

$$K''(s) = -\beta^2\,(1 - \beta^2)\left(\frac{s_0}{s}\right)^{1+\beta^2} \tag{4.198}$$

$$K'''(s) = \beta^2\,(1 - \beta^2)\,(1 + \beta^2)\left(\frac{s_0}{s}\right)^{2+\beta^2} \ . \tag{4.199}$$

Thus,

$$\frac{d^2 y}{d\phi^2} + \beta^2\, y = \epsilon\, a_1\, y^2 + \epsilon^2\, a_2\, y^3 \ , \tag{4.200}$$

with $\epsilon = 1$ and

$$a_1 = -\tfrac{1}{2}\,\beta^2\,(1-\beta^2) \tag{4.201}$$

$$a_2 = +\tfrac{1}{6}\,\beta^2\,(1-\beta^2)\,(1+\beta^2)\ . \tag{4.202}$$

Note that we assign one factor of ϵ for each order of nonlinearity beyond order y^1. Note also that while y here corresponds to u in eqn. 4.164, the constants $a_{1,2}$ here are a factor of β^2 larger than those defined in eqn. 4.165.

We now apply the Poincaré-Lindstedt method, by defining $\theta = \Omega\,\phi$, with

$$\Omega^2 = \Omega_0^2 + \epsilon\,\Omega_1^2 + \epsilon^2\,\Omega_2^2 + \ldots \tag{4.203}$$

and

$$y(\theta) = y_0(\theta) + \epsilon\,y_1(\theta) + \epsilon^2\,y_2(\theta) + \ldots\ . \tag{4.204}$$

We therefore have

$$\frac{d}{d\phi} = \Omega\,\frac{d}{d\theta} \tag{4.205}$$

and

$$\big(\Omega_0^2 + \epsilon\,\Omega_1^2 + \epsilon^2\,\Omega_2^2 + \ldots\big)\big(y_0'' + \epsilon\,y_1'' + \epsilon^2\,y_2'' + \ldots\big) + \beta^2\,\big(y_0 + \epsilon\,y_1 + \epsilon^2\,y_2 + \ldots\big) \tag{4.206}$$

$$= \epsilon\,a_1\,\big(y_0 + \epsilon\,y_1 + \epsilon^2\,y_2 + \ldots\big)^2 + \epsilon^2\,a_2\,\big(y_0 + \epsilon\,y_1 + \epsilon^2\,y_2 + \ldots\big)^3\ . \tag{4.207}$$

We now extract equations at successive orders of ϵ. The first three in the hierarchy are

$$\Omega_0^2\,y_0'' + \beta^2\,y_0 = 0 \tag{4.208}$$

$$\Omega_1^2\,y_0'' + \Omega_0^2\,y_1'' + \beta^2\,y_1 = a_1 y_0^2 \tag{4.209}$$

$$\Omega_2^2\,y_0'' + \Omega_1^2\,y_1'' + \Omega_0^2\,y_2'' + \beta^2\,y_2 = 2\,a_1\,y_0\,y_1 + a_2\,y_0^3\ , \tag{4.210}$$

where prime denotes differentiation with respect to θ.

To order ϵ^0, the solution is $\Omega_0^2 = \beta^2$ and

$$y_0(\theta) = A\,\cos(\theta + \delta)\ , \tag{4.211}$$

where A and δ are constants.

At order ϵ^1, we have

$$\begin{aligned}\beta^2\big(y_1'' + y_1\big) &= -\Omega_1^2\,y_0'' + a_1\,y_0^2\\ &= \Omega_1^2\,A\,\cos(\theta+\delta) + a_1 A^2\cos^2(\theta+\delta)\\ &= \Omega_1^2\,A\,\cos(\theta+\delta) + \tfrac{1}{2}\,a_1 A^2 + \tfrac{1}{2}\,a_1 A^2\cos(2\theta+2\delta)\ .\end{aligned} \tag{4.212}$$

The secular forcing terms on the RHS are eliminated by the choice $\Omega_1^2 = 0$. The solution is then

$$y_1(\theta) = \frac{a_1 A^2}{2\,\beta^2}\Big\{1 - \tfrac{1}{3}\cos(2\theta + 2\delta)\Big\}\ . \tag{4.213}$$

At order ϵ^2, then, we have

$$\begin{aligned}\beta^2\big(y_2'' + y_2\big) &= -\Omega_2^2\, y_0'' - \Omega_1^2\, y_1'' + 2\,a_1\,y_1\,y_1 + a_2\,y_0^3 \\ &= \Omega_2^2\, A\cos(\theta+\delta) + \frac{a_1^2 A^3}{\beta^2}\,\Big\{1 - \tfrac{1}{3}\cos(2\theta+2\delta)\Big\}\cos(\theta+\delta) + a_2 A^3\cos^2(\theta+\delta) \\ &= \bigg\{\Omega_2^2 + \frac{5\,a_1^2 A^3}{6\beta^2} + \tfrac{3}{4}\,a_2 A^3\bigg\}A\cos(\theta+\delta) + \bigg\{-\frac{a_1^2 A^3}{6\beta^2} + \tfrac{1}{4}\,a_2 A^3\bigg\}\cos(3\theta+3\delta)\ .\end{aligned} \tag{4.214}$$

The resonant forcing terms on the RHS are eliminated by the choice

$$\begin{aligned}\Omega_2^2 &= -\Big(\tfrac{5}{6}\,\beta^{-2}\,a_1^2 + \tfrac{3}{4}\,a_2\Big)A^3 \\ &= -\tfrac{1}{24}\,\beta^2\,(1-\beta^2)\,\Big[5\,(1-\beta^2) + 3\,(1+\beta^2)\Big] \\ &= -\tfrac{1}{12}\,\beta^2\,(1-\beta^2)\,(4-\beta^2)\ .\end{aligned} \tag{4.215}$$

Thus, the frequency shift to this order vanishes whenever $\beta^2 = 0$, $\beta^2 = 1$, or $\beta^2 = 4$. Recall the force law is $F(r) = -C\,r^{\beta^2-3}$, so we see that there is no shift – hence no precession – for inverse cube, inverse square, or linear forces.

4.8 Appendix III : Modified van der Pol Oscillator

Consider the nonlinear oscillator

$$\ddot{x} + \epsilon\,(x^4 - 1)\,\dot{x} + x = 0\ . \tag{4.216}$$

Analyze this using the same approach we apply to the van der Pol oscillator.

(a) Sketch the vector field $\dot{\boldsymbol{\varphi}}$ for this problem. It may prove convenient to first identify the *nullclines*, which are the curves along which $\dot{x} = 0$ or $\dot{v} = 0$ (with $v = \dot{x}$). Argue that a limit cycle exists.

Solution : There is a single fixed point, at the origin $(0,0)$, for which the linearized dynamics obeys

$$\frac{d}{dt}\begin{pmatrix} x \\ v\end{pmatrix} = \begin{pmatrix} 0 & 1 \\ -1 & \epsilon\end{pmatrix}\begin{pmatrix} x \\ v\end{pmatrix} + \mathcal{O}(x^4\,v)\ . \tag{4.217}$$

One finds $T = \epsilon$ and $D = 1$ for the trace and determinant, respectively. The origin is an unstable spiral for $0 < \epsilon < 2$ and an unstable node for $\epsilon > 2$.

The nullclines are sketched in Fig. 4.15. One has

$$\dot{x} = 0 \ \leftrightarrow\ v = 0 \qquad , \qquad \dot{v} = 0 \ \leftrightarrow\ v = \frac{1}{\epsilon}\,\frac{x}{1 - x^4}\ . \tag{4.218}$$

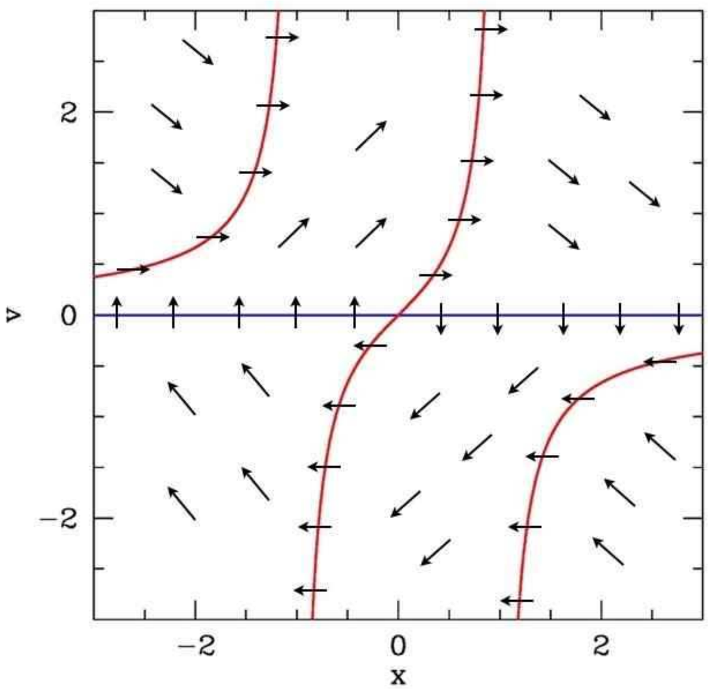

Figure 4.15: Sketch of phase flow and nullclines for the oscillator $\ddot{x} + \epsilon\,(x^4 - 1)\,\dot{x} + x = 0$. Red nullclines: $\dot{v} = 0$; blue nullcline: $\dot{x} = 0$.

The flow at large distances from the origin winds once around the origin and spirals in. The flow close to the origin spirals out ($\epsilon < 2$) or flows radially out ($\epsilon > 2$). Ultimately the flow must collapse to a limit cycle, as can be seen in the accompanying figures.

(b) In the limit $0 < \varepsilon \ll 1$, use multiple time scale analysis to obtain a solution which reveals the approach to the limit cycle.

Solution : We seek to solve the equation

$$\ddot{x} + x = \epsilon\, h(x, \dot{x}) \ , \tag{4.219}$$

with

$$h(x, \dot{x}) = (1 - x^4)\,\dot{x} \ . \tag{4.220}$$

Employing the multiple time scale analysis to lowest nontrivial order, we write $T_0 \equiv t$, $T_1 \equiv \epsilon t$,

$$x = x_0 + \epsilon x_1 + \ldots \tag{4.221}$$

and identify terms order by order in ϵ. At $\mathcal{O}(\epsilon^0)$, this yields

$$\frac{\partial^2 x_0}{\partial T_0^2} + x_0 = 0 \qquad \Rightarrow \qquad x_0 = A\cos(T_0 + \phi) \ , \tag{4.222}$$

where $A = A(T_1)$ and $\phi = \phi(T_1)$. At $\mathcal{O}(\epsilon^1)$, we have

$$\begin{aligned}\frac{\partial^2 x_1}{\partial T_0^2} + x_1 &= -2\,\frac{\partial^2 x_0}{\partial T_0\,\partial T_1} + h\bigg(x_0\,,\,\frac{\partial x_0}{\partial T_0}\bigg) \\ &= 2\,\frac{\partial A}{\partial T_1}\,\sin\theta + 2A\,\frac{\partial \phi}{\partial T_1}\,\cos\theta + h\big(A\cos\theta, -A\sin\theta\big)\end{aligned} \tag{4.223}$$

with $\theta = T_0 + \phi(T_1)$ as usual. We also have

$$\begin{aligned}h(A\cos\theta, -A\sin\theta\big) &= A^5\sin\theta\cos\theta - A\sin\theta \\ &= \big(\tfrac{1}{8}A^5 - A\big)\,\sin\theta + \tfrac{3}{16}\,A^5\sin 3\theta + \tfrac{1}{16}\,A^5\sin 5\theta\ .\end{aligned} \tag{4.224}$$

To eliminate the resonant terms in eqn. 4.223, we must choose

$$\frac{\partial A}{\partial T_1} = \tfrac{1}{2}A - \tfrac{1}{16}A^5 \qquad , \qquad \frac{\partial\phi}{\partial T_1} = 0\ . \tag{4.225}$$

The A equation is similar to the logistic equation. Clearly $A = 0$ is an unstable fixed point, and $A = 8^{1/4} \approx 1.681793$ is a stable fixed point. Thus, the amplitude of the oscillations will asymptotically approach $A^* = 8^{1/4}$. (Recall the asymptotic amplitude in the van der Pol case was $A^* = 2$.)

To integrate the A equation, substitute $y = \frac{1}{\sqrt{8}}A^2$, and obtain

$$dT_1 = \frac{dy}{y\,(1-y^2)} = \tfrac{1}{2}d\ln\frac{y^2}{1-y^2} \qquad\Rightarrow\qquad y^2(T_1) = \frac{1}{1 + (y_0^{-2} - 1)\,\exp(-2T_1)}\ . \tag{4.226}$$

We then have

$$A(T_1) = 8^{1/4}\,\sqrt{y(T_1)} = \bigg(\frac{8}{1 + (8A_0^{-4} - 1)\,\exp(-2T_1)}\bigg)^{1/4}\ . \tag{4.227}$$

(c) In the limit $\epsilon \gg 1$, find the period of relaxation oscillations, using Liénard plane analysis. Sketch the orbit of the relaxation oscillation in the Liénard plane.

Solution : Our nonlinear oscillator may be written in the form

$$\ddot{x} + \epsilon\,\frac{dF(x)}{dt} + x = 0\ , \tag{4.228}$$

with

$$F(x) = \tfrac{1}{5}x^5 - x\ . \tag{4.229}$$

Note $\dot{F} = (x^4 - 1)\,\dot{x}$. Now we define the Liénard variable

$$y \equiv \frac{\dot{x}}{\epsilon} + F(x)\ , \tag{4.230}$$

and in terms of (x,y) we have

$$\dot{x} = \epsilon\Big[y - F(x)\Big] \qquad , \qquad \dot{y} = -\frac{x}{\epsilon} \ . \tag{4.231}$$

As we have seen in the notes, for large ϵ the motion in the (x,y) plane is easily analyzed. $x(t)$ must move quickly over to the curve $y = F(x)$, at which point the motion slows down and slowly creeps along this curve until it can no longer do so, at which point another big fast jump occurs. The jumps take place between the local extrema of $F(x)$, which occur for $F'(a) = a^4 - 1 = 0$, *i.e.* at $a = \pm 1$, and points on the curve with the same values of $F(a)$. Thus, we solve $F(-1) = \frac{4}{5} = \frac{1}{5}b^5 - b$ and find the desired root at $b^* \approx 1.650629$. The period of the relaxation oscillations, for large ϵ, is

$$T \approx 2\epsilon \int\limits_a^b \! dx \, \frac{F'(x)}{x} = \epsilon \cdot \Big[\tfrac{1}{2}x^4 - 2\ln x\Big]_a^b \approx 2.20935\,\epsilon \ . \tag{4.232}$$

(d) Numerically integrate the equation (4.216) starting from several different initial conditions.

Solution : The accompanying `Mathematica` plots show $x(t)$ and $v(t)$ for this system for two representative values of ϵ.

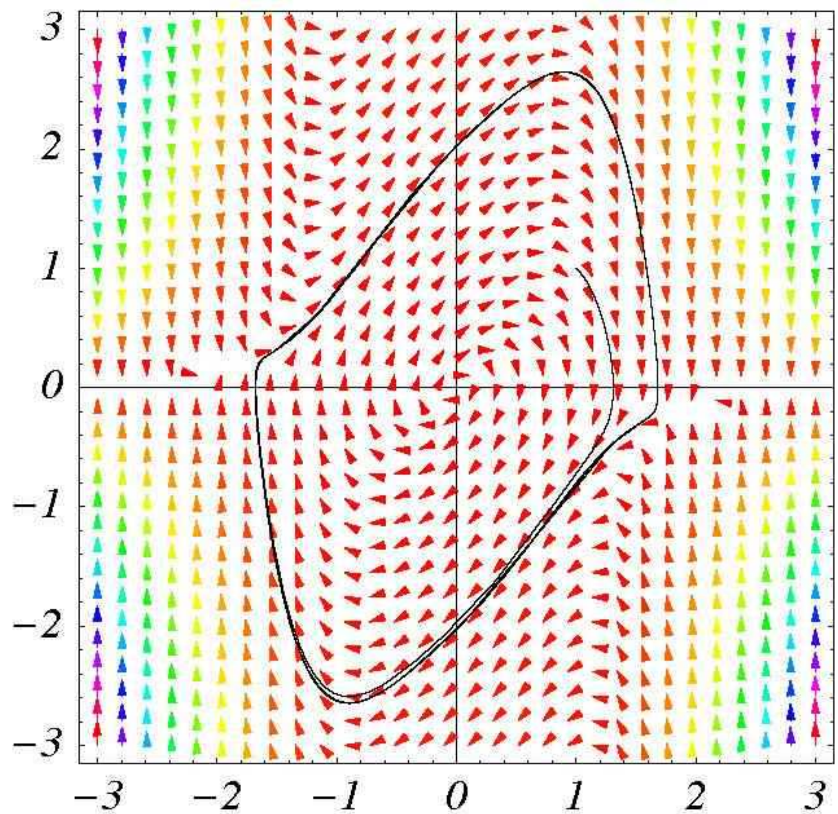

Figure 4.16: Vector field and phase curves for the oscillator $\ddot{x} + \epsilon\,(x^4 - 1)\,\dot{x} + x = 0$, with $\epsilon = 1$ and starting from $(x_0, v_0) = (1, 1)$.

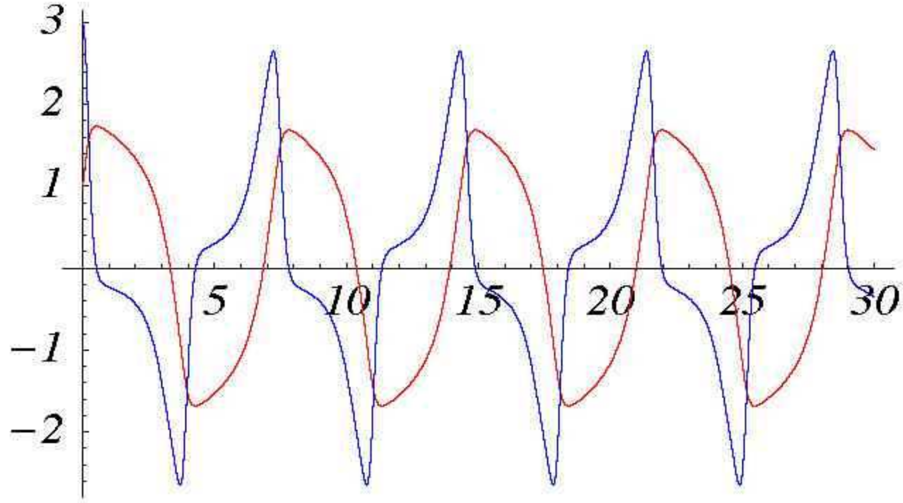

Figure 4.17: Solution to the oscillator equation $\ddot{x} + \epsilon\,(x^4 - 1)\,\dot{x} + x = 0$ with $\epsilon = 1$ and initial conditions $(x_0, v_0) = (1, 3)$. $x(t)$ is shown in red and $v(t)$ in blue. Note that $x(t)$ resembles a relaxation oscillation for this moderate value of ϵ.

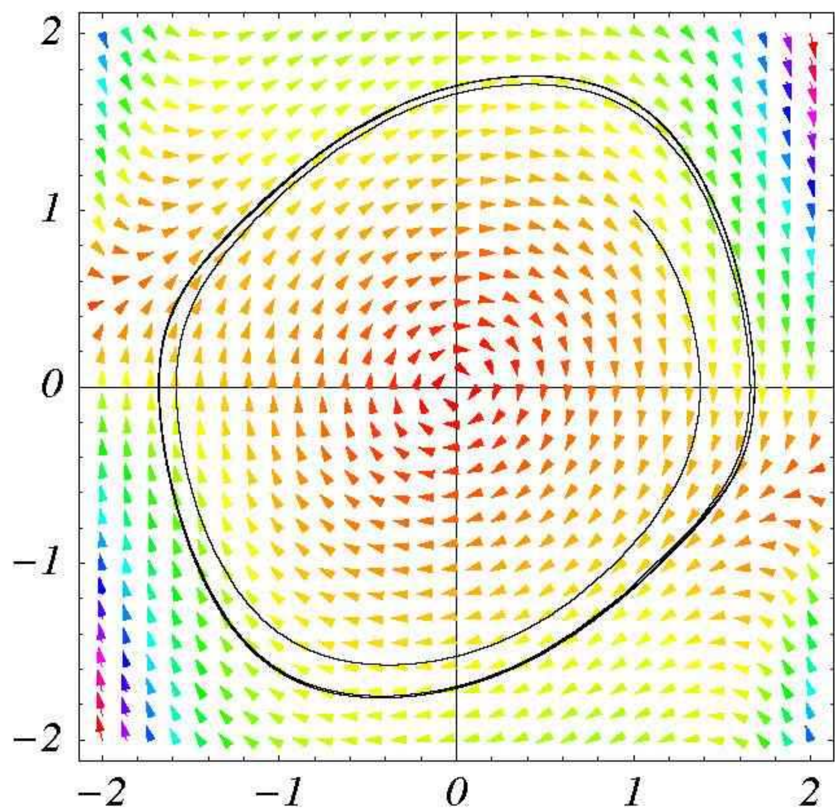

Figure 4.18: Vector field and phase curves for the oscillator $\ddot{x} + \epsilon\,(x^4 - 1)\,\dot{x} + x = 0$, with $\epsilon = 0.25$ and starting from $(x_0, v_0) = (1, 1)$. As $\epsilon \to 0$, the limit cycle is a circle of radius $A^* = 8^{1/4} \approx 1.682$.

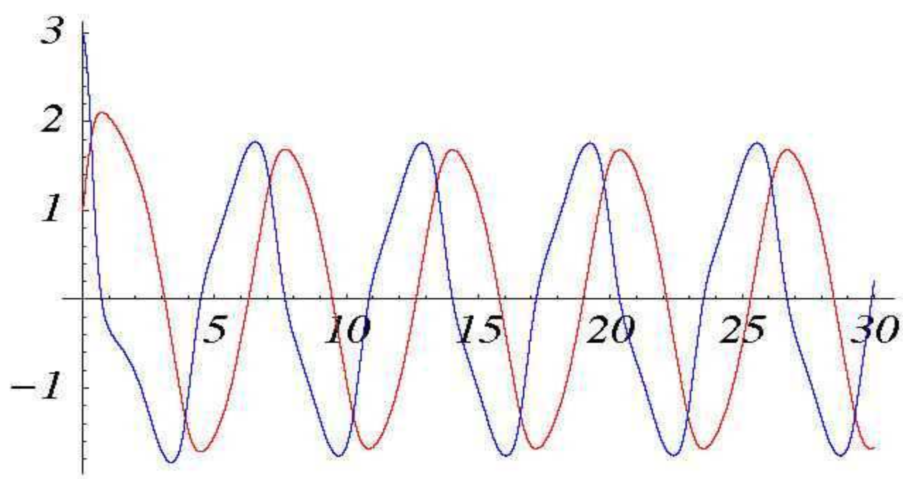

Figure 4.19: Solution to the oscillator equation $\ddot{x} + \epsilon\,(x^4 - 1)\,\dot{x} + x = 0$ with $\epsilon = 0.25$ and initial conditions $(x_0, v_0) = (1, 3)$. $x(t)$ is shown in red and $v(t)$ in blue. As $\epsilon \to 0$, the amplitude of the oscillations tends to $A^* = 8^{1/4} \approx 1.682$.

Chapter 5

Hamiltonian Mechanics

5.1 The Hamiltonian

Recall that $L = L(q, \dot{q}, t)$, and

$$p_\sigma = \frac{\partial L}{\partial \dot{q}_\sigma} \ . \tag{5.1}$$

The Hamiltonian, $H(q, p)$ is obtained by a Legendre transformation,

$$H(q, p) = \sum_{\sigma=1}^{n} p_\sigma \, \dot{q}_\sigma - L \ . \tag{5.2}$$

Note that

$$\begin{aligned} dH &= \sum_{\sigma=1}^{n} \bigg(p_\sigma \, d\dot{q}_\sigma + \dot{q}_\sigma \, dp_\sigma - \frac{\partial L}{\partial q_\sigma} \, dq_\sigma - \frac{\partial L}{\partial \dot{q}_\sigma} \, d\dot{q}_\sigma \bigg) - \frac{\partial L}{\partial t} \, dt \\ &= \sum_{\sigma=1}^{n} \bigg(\dot{q}_\sigma \, dp_\sigma - \frac{\partial L}{\partial q_\sigma} \, dq_\sigma \bigg) - \frac{\partial L}{\partial t} \, dt \ . \end{aligned} \tag{5.3}$$

Thus, we obtain Hamilton's equations of motion,

$$\frac{\partial H}{\partial p_\sigma} = \dot{q}_\sigma \quad , \quad \frac{\partial H}{\partial q_\sigma} = -\frac{\partial L}{\partial q_\sigma} = -\dot{p}_\sigma \tag{5.4}$$

and

$$\frac{dH}{dt} = \frac{\partial H}{\partial t} = -\frac{\partial L}{\partial t} \ . \tag{5.5}$$

Some remarks:

- As an example, consider a particle moving in three dimensions, described by spherical polar coordinates (r, θ, ϕ). Then

$$L = \tfrac{1}{2} m \left(\dot{r}^2 + r^2 \, \dot{\theta}^2 + r^2 \sin^2\!\theta \, \dot{\phi}^2 \right) - U(r, \theta, \phi) \ . \tag{5.6}$$

We have

$$p_r = \frac{\partial L}{\partial \dot{r}} = m\dot{r} \quad , \quad p_\theta = \frac{\partial L}{\partial \dot{\theta}} = mr^2\,\dot{\theta} \quad , \quad p_\phi = \frac{\partial L}{\partial \dot{\phi}} = mr^2\,\sin^2\!\theta\,\dot{\phi}\ , \tag{5.7}$$

and thus

$$\begin{aligned} H &= p_r\,\dot{r} + p_\theta\,\dot{\theta} + p_\phi\,\dot{\phi} - L \\ &= \frac{p_r^2}{2m} + \frac{p_\theta^2}{2mr^2} + \frac{p_\phi^2}{2mr^2\sin^2\!\theta} + U(r,\theta,\phi)\ . \end{aligned} \tag{5.8}$$

Note that H is time-independent, hence $\frac{\partial H}{\partial t} = \frac{dH}{dt} = 0$, and therefore H is a constant of the motion.

- In order to obtain $H(q,p)$ we must invert the relation $p_\sigma = \frac{\partial L}{\partial \dot{q}_\sigma} = p_\sigma(q,\dot{q})$ to obtain $\dot{q}_\sigma(q,p)$. This is possible if the Hessian,

$$\frac{\partial p_\alpha}{\partial \dot{q}_\beta} = \frac{\partial^2 L}{\partial \dot{q}_\alpha\,\partial \dot{q}_\beta} \tag{5.9}$$

is nonsingular. This is the content of the 'inverse function theorem' of multivariable calculus.

- Define the rank $2n$ vector, ξ, by its components,

$$\xi_i = \begin{cases} q_i & \text{if } 1 \le i \le n \\ p_{i-n} & \text{if } n \le i \le 2n\ . \end{cases} \tag{5.10}$$

Then we may write Hamilton's equations compactly as

$$\dot{\xi}_i = J_{ij}\,\frac{\partial H}{\partial \xi_j}\ , \tag{5.11}$$

where

$$J = \begin{pmatrix} \mathbb{O}_{n\times n} & \mathbb{I}_{n\times n} \\ -\mathbb{I}_{n\times n} & \mathbb{O}_{n\times n} \end{pmatrix} \tag{5.12}$$

is a rank $2n$ matrix. Note that $J^{\rm t} = -J$, *i.e.* J is antisymmetric, and that $J^2 = -\mathbb{I}_{2n\times 2n}$. We shall utilize this 'symplectic structure' to Hamilton's equations shortly.

5.2 Modified Hamilton's Principle

We have that

$$
\begin{aligned}
0 = \delta \int\limits_{t_a}^{t_b} \! dt\, L = \delta \int\limits_{t_a}^{t_b} \! dt\, \big(p_\sigma \, \dot q_\sigma - H\big) \qquad (5.13) \\
= \int\limits_{t_a}^{t_b} \! dt\, \bigg\{ p_\sigma \, \delta \dot q_\sigma + \dot q_\sigma \, \delta p_\sigma - \frac{\partial H}{\partial q_\sigma}\, \delta q_\sigma - \frac{\partial H}{\partial p_\sigma}\, \delta p_\sigma \bigg\} \\
= \int\limits_{t_a}^{t_b} \! dt\, \Bigg\{ - \bigg(\dot p_\sigma + \frac{\partial H}{\partial q_\sigma}\bigg)\, \delta q_\sigma + \bigg(\dot q_\sigma - \frac{\partial H}{\partial p_\sigma}\bigg)\, \delta p_\sigma \Bigg\} + \big(p_\sigma \, \delta q_\sigma\big)\Big|_{t_a}^{t_b} \ ,
\end{aligned}
$$

assuming $\delta q_\sigma(t_a) = \delta q_\sigma(t_b) = 0$. Setting the coefficients of δq_σ and δp_σ to zero, we recover Hamilton's equations.

5.3 Phase Flow is Incompressible

A flow for which $\boldsymbol{\nabla} \cdot \boldsymbol{v} = 0$ is *incompressible* – we shall see why in a moment. Let's check that the divergence of the phase space velocity does indeed vanish:

$$
\begin{aligned}
\boldsymbol{\nabla} \cdot \dot{\boldsymbol{\xi}} &= \sum_{\sigma=1}^{n} \bigg\{ \frac{\partial \dot q_\sigma}{\partial q_\sigma} + \frac{\partial \dot p_\sigma}{\partial p_\sigma} \bigg\} \\
&= \sum_{i=1}^{2n} \frac{\partial \dot \xi_i}{\partial \xi_i} = \sum_{i,j} J_{ij} \, \frac{\partial^2 H}{\partial \xi_i \, \partial \xi_j} = 0 \ . \qquad (5.14)
\end{aligned}
$$

Now let $\rho(\boldsymbol{\xi}, t)$ be a distribution on phase space. Continuity implies

$$
\frac{\partial \rho}{\partial t} + \boldsymbol{\nabla} \cdot (\rho \, \dot{\boldsymbol{\xi}}) = 0 \ . \qquad (5.15)
$$

Invoking $\boldsymbol{\nabla} \cdot \dot{\boldsymbol{\xi}} = 0$, we have that

$$
\frac{D\rho}{Dt} = \frac{\partial \rho}{\partial t} + \dot{\boldsymbol{\xi}} \cdot \boldsymbol{\nabla} \rho = 0 \ , \qquad (5.16)
$$

where $D\rho/Dt$ is sometimes called the *convective derivative* – it is the total derivative of the function $\rho\big(\boldsymbol{\xi}(t), t\big)$, evaluated at a point $\xi(t)$ in phase space which moves according to the dynamics. This says that the density in the "comoving frame" is locally constant.

5.4 Poincaré Recurrence Theorem

Let g_τ be the 'τ-advance mapping' which evolves points in phase space according to Hamilton's equations

$$\dot{q}_i = +\frac{\partial H}{\partial p_i} \quad , \quad \dot{p}_i = -\frac{\partial H}{\partial q_i} \tag{5.17}$$

for a time interval $\Delta t = \tau$. Consider a region Ω in phase space. Define $g_\tau^n \Omega$ to be the $n^{\rm th}$ image of Ω under the mapping g_τ. Clearly g_τ is invertible; the inverse is obtained by integrating the equations of motion backward in time. We denote the inverse of g_τ by g_τ^{-1}. By Liouville's theorem, g_τ is volume preserving when acting on regions in phase space, since the evolution of any given point is Hamiltonian. This follows from the continuity equation for the phase space density,

$$\frac{\partial \varrho}{\partial t} + \nabla \cdot (\boldsymbol{u}\varrho) = 0 \tag{5.18}$$

where $\boldsymbol{u} = \{\dot{\boldsymbol{q}}, \dot{\boldsymbol{p}}\}$ is the velocity vector in phase space, and Hamilton's equations, which say that the phase flow is incompressible, *i.e.* $\nabla \cdot \boldsymbol{u} = 0$:

$$\begin{aligned} \nabla \cdot \boldsymbol{u} &= \sum_{i=1}^n \left\{ \frac{\partial \dot{q}_i}{\partial q_i} + \frac{\partial \dot{p}_i}{\partial p_i} \right\} \\ &= \sum_{i=1}^n \left\{ \frac{\partial}{\partial q_i}\left(\frac{\partial H}{\partial p_i}\right) + \frac{\partial}{\partial p_i}\left(-\frac{\partial H}{\partial q_i}\right) \right\} = 0 \ . \end{aligned} \tag{5.19}$$

Thus, we have that the convective derivative vanishes, *viz.*

$$\frac{D\varrho}{Dt} \equiv \frac{\partial \varrho}{\partial t} + \boldsymbol{u} \cdot \nabla \varrho = 0 \ , \tag{5.20}$$

which guarantees that the density remains constant in a frame moving with the flow.

The proof of the recurrence theorem is simple. Assume that g_τ is invertible and volume-preserving, as is the case for Hamiltonian flow. Further assume that phase space volume is finite. Since the energy is preserved in the case of time-independent Hamiltonians, we simply ask that the volume of phase space *at fixed total energy* E be finite, *i.e.*

$$\int \! d\mu \, \delta\big(E - H(\boldsymbol{q}, \boldsymbol{p})\big) < \infty \ , \tag{5.21}$$

where $d\mu = d\boldsymbol{q}\, d\boldsymbol{p}$ is the phase space uniform integration measure.

Theorem: In any finite neighborhood Ω of phase space there exists a point $\boldsymbol{\varphi}_0$ which will return to Ω after n applications of g_τ, where n is finite.

Proof: Assume the theorem fails; we will show this assumption results in a contradiction. Consider the set Υ formed from the union of all sets $g_\tau^m \, \Omega$ for all m:

$$\Upsilon = \bigcup_{m=0}^{\infty} g_\tau^m \, \Omega \tag{5.22}$$

We assume that the set $\{g_\tau^m\,\Omega \,|\, m \in \mathbb{Z}\,, m \geq 0\}$ is disjoint. The volume of a union of disjoint sets is the sum of the individual volumes. Thus,

$$\begin{aligned} \mathrm{vol}(\Upsilon) &= \sum_{m=0}^{\infty} \mathrm{vol}(g_\tau^m\,\Omega) \\ &= \mathrm{vol}(\Omega) \cdot \sum_{m=1}^{\infty} 1 = \infty \ , \end{aligned} \tag{5.23}$$

since $\mathrm{vol}(g_\tau^m\,\Omega) = \mathrm{vol}(\Omega)$ from volume preservation. But clearly Υ is a subset of the entire phase space, hence we have a contradiction, because by assumption phase space is of finite volume.

Thus, the assumption that the set $\{g_\tau^m\,\Omega \,|\, m \in \mathbf{Z}\,, m \geq 0\}$ is disjoint fails. This means that there exists some pair of integers k and l, with $k \neq l$, such that $g_\tau^k\,\Omega \cap g_\tau^l\,\Omega \neq \emptyset$. Without loss of generality we may assume $k > l$. Apply the inverse g_τ^{-1} to this relation l times to get $g_\tau^{k-l}\,\Omega \cap \Omega \neq \emptyset$. Now choose any point $\boldsymbol{\varphi} \in g_\tau^n\,\Omega \cap \Omega$, where $n = k - l$, and define $\boldsymbol{\varphi}_0 = g_\tau^{-n}\boldsymbol{\varphi}$. Then by construction both $\boldsymbol{\varphi}_0$ and $g_\tau^n\,\boldsymbol{\varphi}_0$ lie within Ω and the theorem is proven.

Each of the two central assumptions – invertibility and volume preservation – is crucial. Without either of them, the proof fails. Consider, for example, a volume-preserving map which is not invertible. An example might be a mapping $f\colon \mathbb{R} \to \mathbb{R}$ which takes any real number to its fractional part. Thus, $f(\pi) = 0.14159265\ldots$. Let us restrict our attention to intervals of width less than unity. Clearly f is then volume preserving. The action of f on the interval $[2,3)$ is to map it to the interval $[0,1)$. But $[0,1)$ remains fixed under the action of f, so no point within the interval $[2,3)$ will ever return under repeated iterations of f. Thus, f does not exhibit Poincaré recurrence.

Consider next the case of the damped harmonic oscillator. In this case, phase space volumes contract. For a one-dimensional oscillator obeying $\ddot{x} + 2\beta\dot{x} + \Omega_0^2 x = 0$ one has $\nabla\cdot\boldsymbol{u} = -2\beta < 0$ ($\beta > 0$ for damping). Thus the convective derivative obeys $D_t\varrho = -(\nabla\cdot\boldsymbol{u})\varrho = +2\beta\varrho$ which says that the density increases exponentially in the comoving frame, as $\varrho(t) = e^{2\beta t}\,\varrho(0)$. Thus, phase space volumes collapse, and are not preserved by the dynamics. In this case, it is possible for the set Υ to be of finite volume, even if it is the union of an infinite number of sets $g_\tau^n\,\Omega$, because the volumes of these component sets themselves decrease exponentially, as $\mathrm{vol}(g_\tau^n\,\Omega) = e^{-2n\beta\tau}\,\mathrm{vol}(\Omega)$. A damped pendulum, released from rest at some small angle θ_0, will not return arbitrarily close to these initial conditions.

5.5 Poisson Brackets

The time evolution of any function $F(q,p)$ over phase space is given by

$$\begin{aligned} \frac{d}{dt}\,F\big(q(t),p(t),t\big) &= \frac{\partial F}{\partial t} + \sum_{\sigma=1}^{n} \left\{ \frac{\partial F}{\partial q_\sigma}\,\dot{q}_\sigma + \frac{\partial F}{\partial p_\sigma}\,\dot{p}_\sigma \right\} \\ &\equiv \frac{\partial F}{\partial t} + \big\{F,H\big\} \ , \end{aligned} \tag{5.24}$$

where the *Poisson bracket* $\{\cdot\,,\cdot\}$ is given by

$$\big\{A,B\big\} \equiv \sum_{\sigma=1}^{n}\left(\frac{\partial A}{\partial q_\sigma}\,\frac{\partial B}{\partial p_\sigma} - \frac{\partial A}{\partial p_\sigma}\,\frac{\partial B}{\partial q_\sigma}\right) \tag{5.25}$$

$$= \sum_{i,j=1}^{2n} J_{ij}\,\frac{\partial A}{\partial \xi_i}\,\frac{\partial B}{\partial \xi_j}\ . \tag{5.26}$$

Properties of the Poisson bracket:

- Antisymmetry:

$$\big\{f,g\big\} = -\big\{g,f\big\}\ . \tag{5.27}$$

- Bilinearity: if λ is a constant, and f, g, and h are functions on phase space, then

$$\big\{f+\lambda\,g,h\big\} = \big\{f,h\big\} + \lambda\{g,h\big\}\ . \tag{5.28}$$

  Linearity in the second argument follows from this and the antisymmetry condition.

- Associativity:

$$\big\{fg,h\big\} = f\big\{g,h\big\} + g\big\{f,h\big\}\ . \tag{5.29}$$

- Jacobi identity:

$$\big\{f,\{g,h\}\big\} + \big\{g,\{h,f\}\big\} + \big\{h,\{f,g\}\big\} = 0\ . \tag{5.30}$$

Some other useful properties:

- If $\{A,H\}=0$ and $\frac{\partial A}{\partial t}=0$, then $\frac{dA}{dt}=0$, *i.e.* $A(q,p)$ is a constant of the motion.
- If $\{A,H\}=0$ and $\{B,H\}=0$, then $\big\{\{A,B\},H\big\}=0$. If in addition A and B have no explicit time dependence, we conclude that $\{A,B\}$ is a constant of the motion.
- It is easily established that

$$\{q_\alpha,q_\beta\}=0 \quad , \quad \{p_\alpha,p_\beta\}=0 \quad , \quad \{q_\alpha,p_\beta\}=\delta_{\alpha\beta}\ . \tag{5.31}$$

5.6 Canonical Transformations

5.6.1 Point transformations in Lagrangian mechanics

In Lagrangian mechanics, we are free to redefine our generalized coordinates, *viz.*

$$Q_\sigma = Q_\sigma(q_1,\ldots,q_n,t)\ . \tag{5.32}$$

This is called a "point transformation." The transformation is invertible if

$$\det\left(\frac{\partial Q_\alpha}{\partial q_\beta}\right) \neq 0 \; . \tag{5.33}$$

The transformed Lagrangian, $\tilde{L}$, written as a function of the new coordinates Q and velocities $\dot{Q}$, is

$$\tilde{L}\big(Q, \dot{Q}, t\big) = L\big(q(Q,t), \dot{q}(Q,\dot{Q},t)\big) \; . \tag{5.34}$$

Finally, Hamilton's principle,

$$\delta \int\limits_{t_1}^{t_b} dt\, \tilde{L}(Q, \dot{Q}, t) = 0 \tag{5.35}$$

with $\delta Q_\sigma(t_a) = \delta Q_\sigma(t_b) = 0$, still holds, and the form of the Euler-Lagrange equations remains unchanged:

$$\frac{\partial \tilde{L}}{\partial Q_\sigma} - \frac{d}{dt}\left(\frac{\partial \tilde{L}}{\partial \dot{Q}_\sigma}\right) = 0 \; . \tag{5.36}$$

The invariance of the equations of motion under a point transformation may be verified explicitly. We first evaluate

$$\frac{d}{dt}\left(\frac{\partial \tilde{L}}{\partial \dot{Q}_\sigma}\right) = \frac{d}{dt}\left(\frac{\partial L}{\partial \dot{q}_\alpha}\,\frac{\partial \dot{q}_\alpha}{\partial \dot{Q}_\sigma}\right) = \frac{d}{dt}\left(\frac{\partial L}{\partial \dot{q}_\alpha}\,\frac{\partial q_\alpha}{\partial Q_\sigma}\right) \; , \tag{5.37}$$

where the relation

$$\frac{\partial \dot{q}_\alpha}{\partial \dot{Q}_\sigma} = \frac{\partial q_\alpha}{\partial Q_\sigma} \tag{5.38}$$

follows from

$$\dot{q}_\alpha = \frac{\partial q_\alpha}{\partial Q_\sigma}\,\dot{Q}_\sigma + \frac{\partial q_\alpha}{\partial t} \; . \tag{5.39}$$

Now we compute

$$\begin{aligned}
\frac{\partial \tilde{L}}{\partial Q_\sigma} &= \frac{\partial L}{\partial q_\alpha}\,\frac{\partial q_\alpha}{\partial Q_\sigma} + \frac{\partial L}{\partial \dot{q}_\alpha}\,\frac{\partial \dot{q}_\alpha}{\partial Q_\sigma} \\
&= \frac{\partial L}{\partial q_\alpha}\,\frac{\partial q_\alpha}{\partial Q_\sigma} + \frac{\partial L}{\partial \dot{q}_\alpha}\left(\frac{\partial^2 q_\alpha}{\partial Q_\sigma\,\partial Q_{\sigma'}}\,\dot{Q}_{\sigma'} + \frac{\partial^2 q_\alpha}{\partial Q_\sigma\,\partial t}\right) \\
&= \frac{d}{dt}\left(\frac{\partial L}{\partial \dot{q}_\sigma}\right)\frac{\partial q_\alpha}{\partial Q_\sigma} + \frac{\partial L}{\partial \dot{q}_\alpha}\,\frac{d}{dt}\left(\frac{\partial q_\alpha}{\partial Q_\sigma}\right) \\
&= \frac{d}{dt}\left(\frac{\partial L}{\partial \dot{q}_\sigma}\,\frac{\partial q_\alpha}{\partial Q_\sigma}\right) = \frac{d}{dt}\left(\frac{\partial \tilde{L}}{\partial \dot{Q}_\sigma}\right) \; ,
\end{aligned} \tag{5.40}$$

where the last equality is what we obtained earlier in eqn. 5.37.

5.6.2 Canonical transformations in Hamiltonian mechanics

In Hamiltonian mechanics, we will deal with a much broader class of transformations – ones which mix all the $q's$ and $p's$. The general form for a canonical transformation (CT) is

$$q_\sigma = q_\sigma\big(Q_1, \ldots, Q_n; P_1, \ldots, P_n; t\big) \tag{5.41}$$

$$p_\sigma = p_\sigma\big(Q_1, \ldots, Q_n; P_1, \ldots, P_n; t\big) \ , \tag{5.42}$$

with $\sigma \in \{1, \ldots, n\}$. We may also write

$$\xi_i = \xi_i\big(\Xi_1, \ldots, \Xi_{2n}; t\big) \ , \tag{5.43}$$

with $i \in \{1, \ldots, 2n\}$. The transformed Hamiltonian is $\tilde{H}(Q, P, t)$.

What sorts of transformations are allowed? Well, if Hamilton's equations are to remain invariant, then

$$\dot{Q}_\sigma = \frac{\partial \tilde{H}}{\partial P_\sigma} \quad , \quad \dot{P}_\sigma = -\frac{\partial \tilde{H}}{\partial Q_\sigma} \ , \tag{5.44}$$

which gives

$$\frac{\partial \dot{Q}_\sigma}{\partial Q_\sigma} + \frac{\partial \dot{P}_\sigma}{\partial P_\sigma} = 0 = \frac{\partial \dot{\Xi}_i}{\partial \Xi_i} \ . \tag{5.45}$$

I.e. the flow remains incompressible in the new (Q, P) variables. We will also require that phase space volumes are preserved by the transformation, *i.e.*

$$\det\bigg(\frac{\partial \Xi_i}{\partial \xi_j}\bigg) = \left|\left| \frac{\partial(Q, P)}{\partial(q, p)} \right|\right| = 1 \ . \tag{5.46}$$

Additional conditions will be discussed below.

5.6.3 Hamiltonian evolution

Hamiltonian evolution itself defines a canonical transformation. Let $\xi_i = \xi_i(t)$ and $\xi'_i = \xi_i(t + dt)$. Then from the dynamics $\dot{\xi}_i = J_{ij} \frac{\partial H}{\partial \xi_j}$, we have

$$\xi_i(t + dt) = \xi_i(t) + J_{ij} \frac{\partial H}{\partial \xi_j} \, dt + \mathcal{O}\big(dt^2\big) \ . \tag{5.47}$$

Thus,

$$\begin{aligned} \frac{\partial \xi'_i}{\partial \xi_j} &= \frac{\partial}{\partial \xi_j}\bigg(\xi_i + J_{ik} \frac{\partial H}{\partial \xi_k} \, dt + \mathcal{O}\big(dt^2\big)\bigg) \\ &= \delta_{ij} + J_{ik} \frac{\partial^2 H}{\partial \xi_j \, \partial \xi_k} \, dt + \mathcal{O}\big(dt^2\big) \ . \end{aligned} \tag{5.48}$$

Now, using the result

$$\det\big(1 + \epsilon M\big) = 1 + \epsilon \, \mathrm{Tr}\, M + \mathcal{O}(\epsilon^2) \ , \tag{5.49}$$

we have

$$\left|\left|\frac{\partial\xi'_i}{\partial\xi_j}\right|\right| = 1 + J_{jk}\,\frac{\partial^2 H}{\partial\xi_j\,\partial\xi_k}\,dt + \mathcal{O}\big(dt^2\big) \tag{5.50}$$

$$= 1 + \mathcal{O}\big(dt^2\big)\ . \tag{5.51}$$

5.6.4 Symplectic structure

We have that

$$\dot\xi_i = J_{ij}\,\frac{\partial H}{\partial\xi_j}\ . \tag{5.52}$$

Suppose we make a time-independent canonical transformation to new phase space coordinates, $\varXi_a = \varXi_a(\xi)$. We then have

$$\dot\varXi_a = \frac{\partial\varXi_a}{\partial\xi_j}\,\dot\xi_j = \frac{\partial\varXi_a}{\partial\xi_j}\,J_{jk}\,\frac{\partial H}{\partial\xi_k}\ . \tag{5.53}$$

But if the transformation is canonical, then the equations of motion are preserved, and we also have

$$\dot\varXi_a = J_{ab}\,\frac{\partial\tilde H}{\partial\varXi_b} = J_{ab}\,\frac{\partial\xi_k}{\partial\varXi_b}\,\frac{\partial H}{\partial\xi_k}\ . \tag{5.54}$$

Equating these two expressions, we have

$$M_{aj}\,J_{jk}\,\frac{\partial H}{\partial\xi_k} = J_{ab}\,M^{-1}_{kb}\,\frac{\partial H}{\partial\xi_k}\ , \tag{5.55}$$

where

$$M_{aj} \equiv \frac{\partial\varXi_a}{\partial\xi_j} \tag{5.56}$$

is the Jacobian of the transformation. Since the equality must hold for all ξ, we conclude

$$MJ = J\big(M^{\rm t}\big)^{-1} \quad\Longrightarrow\quad MJM^{\rm t} = J\ . \tag{5.57}$$

A matrix M satisfying $MM^{\rm t} = \mathbb{I}$ is of course an *orthogonal* matrix. A matrix M satisfying $MJM^{\rm t} = J$ is called *symplectic*. We write $M \in {\rm Sp}(2n)$, *i.e.* M is an element of the group of *symplectic matrices*[1] of rank $2n$.

The symplectic property of M guarantees that the Poisson brackets are preserved under a

[1]Note that the rank of a symplectic matrix is always even. Note also $MJM^{\rm t} = J$ implies $M^{\rm t}JM = J$.

canonical transformation:

$$
\begin{aligned}
\big\{A,B\big\}_\xi &= J_{ij}\,\frac{\partial A}{\partial \xi_i}\,\frac{\partial B}{\partial \xi_j} \\
&= J_{ij}\,\frac{\partial A}{\partial \Xi_a}\,\frac{\partial \Xi_a}{\partial \xi_i}\,\frac{\partial B}{\partial \Xi_b}\,\frac{\partial \Xi_b}{\partial \xi_j} \\
&= \big(M_{ai}\,J_{ij}\,M^{\rm t}_{jb}\big)\,\frac{\partial A}{\partial \Xi_a}\,\frac{\partial B}{\partial \Xi_b} \\
&= J_{ab}\,\frac{\partial A}{\partial \Xi_a}\,\frac{\partial B}{\partial \Xi_b} \\
&= \big\{A,B\big\}_\Xi \ .
\end{aligned}
\tag{5.58}
$$

5.6.5 Generating functions for canonical transformations

For a transformation to be canonical, we require

$$
\delta\int\limits_{t_a}^{t_b}\!dt\,\Big\{p_\sigma\,\dot q_\sigma - H(q,p,t)\Big\} = 0 = \delta\int\limits_{t_a}^{t_b}\!dt\,\Big\{P_\sigma\,\dot Q_\sigma - \tilde H(Q,P,t)\Big\} \ . \tag{5.59}
$$

This is satisfied provided

$$
\Big\{p_\sigma\,\dot q_\sigma - H(q,p,t)\Big\} = \lambda\,\bigg\{P_\sigma\,\dot Q_\sigma - \tilde H(Q,P,t) + \frac{dF}{dt}\bigg\} \ , \tag{5.60}
$$

where λ is a constant. For canonical transformations, $\lambda=1$.[2] Thus,

$$
\begin{aligned}
\tilde H(Q,P,t) = H(q,p,t) + P_\sigma\,\dot Q_\sigma - p_\sigma\,\dot q_\sigma &+ \frac{\partial F}{\partial q_\sigma}\,\dot q_\sigma + \frac{\partial F}{\partial Q_\sigma}\,\dot Q_\sigma \\
&+ \frac{\partial F}{\partial p_\sigma}\,\dot p_\sigma + \frac{\partial F}{\partial P_\sigma}\,\dot P_\sigma + \frac{\partial F}{\partial t} \ .
\end{aligned}
\tag{5.61}
$$

Thus, we require

$$
\frac{\partial F}{\partial q_\sigma} = p_\sigma \quad , \quad \frac{\partial F}{\partial Q_\sigma} = -P_\sigma \quad , \quad \frac{\partial F}{\partial p_\sigma} = 0 \quad , \quad \frac{\partial F}{\partial P_\sigma} = 0 \ . \tag{5.62}
$$

The transformed Hamiltonian is

$$
\tilde H(Q,P,t) = H(q,p,t) + \frac{\partial F}{\partial t} \ . \tag{5.63}
$$

[2] Solutions of eqn. 5.60 with $\lambda \neq 1$ are known as *extended* canonical transformations. We can always rescale coordinates and/or momenta to achieve $\lambda = 1$.

There are four possibilities, corresponding to the freedom to make Legendre transformations with respect to each of the arguments of $F(q,Q)$:

$$F(q,Q,t) = \begin{cases} F_1(q,Q,t) & ; \quad p_\sigma = +\frac{\partial F_1}{\partial q_\sigma} \quad , \quad P_\sigma = -\frac{\partial F_1}{\partial Q_\sigma} \quad \text{(type I)} \\ \\ F_2(q,P,t) - P_\sigma\, Q_\sigma & ; \quad p_\sigma = +\frac{\partial F_2}{\partial q_\sigma} \quad , \quad Q_\sigma = +\frac{\partial F_2}{\partial P_\sigma} \quad \text{(type II)} \\ \\ F_3(p,Q,t) + p_\sigma\, q_\sigma & ; \quad q_\sigma = -\frac{\partial F_3}{\partial p_\sigma} \quad , \quad P_\sigma = -\frac{\partial F_3}{\partial Q_\sigma} \quad \text{(type III)} \\ \\ F_4(p,P,t) + p_\sigma\, q_\sigma - P_\sigma\, Q_\sigma & ; \quad q_\sigma = -\frac{\partial F_4}{\partial p_\sigma} \quad , \quad Q_\sigma = +\frac{\partial F_4}{\partial P_\sigma} \quad \text{(type IV)} \end{cases}$$

In each case $(\gamma = 1,2,3,4)$, we have

$$\tilde{H}(Q,P,t) = H(q,p,t) + \frac{\partial F_\gamma}{\partial t} \ . \tag{5.64}$$

Let's work out some examples:

- Consider the type-II transformation generated by

$$F_2(q,P) = A_\sigma(q)\, P_\sigma \ , \tag{5.65}$$

where $A_\sigma(q)$ is an arbitrary function of the $\{q_\sigma\}$. We then have

$$Q_\sigma = \frac{\partial F_2}{\partial P_\sigma} = A_\sigma(q) \qquad , \qquad p_\sigma = \frac{\partial F_2}{\partial q_\sigma} = \frac{\partial A_\alpha}{\partial q_\sigma}\, P_\alpha \ . \tag{5.66}$$

Thus,

$$Q_\sigma = A_\sigma(q) \qquad , \qquad P_\sigma = \frac{\partial q_\alpha}{\partial Q_\sigma}\, p_\alpha \ . \tag{5.67}$$

This is a general point transformation of the kind discussed in eqn. 5.32. For a general linear point transformation, $Q_\alpha = M_{\alpha\beta}\, q_\beta$, we have $P_\alpha = p_\beta\, M^{-1}_{\beta\alpha}$, *i.e.* $Q = Mq$, $P = p\, M^{-1}$. If $M_{\alpha\beta} = \delta_{\alpha\beta}$, this is the identity transformation. $F_2 = q_1 P_3 + q_3 P_1$ interchanges labels 1 and 3, *etc.*

- Consider the type-I transformation generated by

$$F_1(q,Q) = A_\sigma(q)\, Q_\sigma \ . \tag{5.68}$$

We then have

$$p_\sigma = \frac{\partial F_1}{\partial q_\sigma} = \frac{\partial A_\alpha}{\partial q_\sigma}\, Q_\alpha \tag{5.69}$$

$$P_\sigma = -\frac{\partial F_1}{\partial Q_\sigma} = -A_\sigma(q) \ . \tag{5.70}$$

Note that $A_\sigma(q) = q_\sigma$ generates the transformation

$$\begin{pmatrix} q \\ p \end{pmatrix} \longrightarrow \begin{pmatrix} -P \\ +Q \end{pmatrix} \ . \tag{5.71}$$

- A mixed transformation is also permitted. For example,

$$F(q,Q) = q_1\,Q_1 + (q_3 - Q_2)\,P_2 + (q_2 - Q_3)\,P_3 \tag{5.72}$$

is of type-I with respect to index $\sigma = 1$ and type-II with respect to indices $\sigma = 2, 3$. The transformation effected is

$$Q_1 = p_1 \qquad Q_2 = q_3 \qquad Q_3 = q_2 \tag{5.73}$$

$$P_1 = -q_1 \qquad P_2 = p_3 \qquad P_3 = p_2\ . \tag{5.74}$$

- Consider the harmonic oscillator,

$$H(q,p) = \frac{p^2}{2m} + \tfrac{1}{2}kq^2\ . \tag{5.75}$$

If we could find a time-independent canonical transformation such that

$$p = \sqrt{2mf(P)}\,\cos Q \quad , \quad q = \sqrt{\frac{2\,f(P)}{k}}\,\sin Q\ , \tag{5.76}$$

where $f(P)$ is some function of P, then we'd have $\tilde{H}(Q,P) = f(P)$, which is cyclic in Q. To find this transformation, we take the ratio of p and q to obtain

$$p = \sqrt{mk}\,q\ \mathrm{ctn}\,Q\ , \tag{5.77}$$

which suggests the type-I transformation

$$F_1(q,Q) = \tfrac{1}{2}\sqrt{mk}\,q^2\ \mathrm{ctn}\,Q\ . \tag{5.78}$$

This leads to

$$p = \frac{\partial F_1}{\partial q} = \sqrt{mk}\,q\ \mathrm{ctn}\,Q \quad , \quad P = -\frac{\partial F_1}{\partial Q} = \frac{\sqrt{mk}\,q^2}{2\,\sin^2\!Q}\ . \tag{5.79}$$

Thus,

$$q = \frac{\sqrt{2P}}{\sqrt[4]{mk}}\,\sin Q \quad \Longrightarrow \quad f(P) = \sqrt{\frac{k}{m}}\,P = \omega P\ , \tag{5.80}$$

where $\omega = \sqrt{k/m}$ is the oscillation frequency. We therefore have

$$\tilde{H}(Q,P) = \omega P\ , \tag{5.81}$$

whence $P = E/\omega$. The equations of motion are

$$\dot{P} = -\frac{\partial \tilde{H}}{\partial Q} = 0 \quad , \quad \dot{Q} = \frac{\partial \tilde{H}}{\partial P} = \omega\ , \tag{5.82}$$

which yields

$$Q(t) = \omega t + \varphi_0 \quad , \quad q(t) = \sqrt{\frac{2E}{m\omega^2}}\,\sin\big(\omega t + \varphi_0\big)\ . \tag{5.83}$$

5.7 Hamilton-Jacobi Theory

We've stressed the great freedom involved in making canonical transformations. Coordinates and momenta, for example, may be interchanged – the distinction between them is purely a matter of convention! We now ask: is there any specially preferred canonical transformation? In this regard, one obvious goal is to make the Hamiltonian $\tilde{H}(Q,P,t)$ and the corresponding equations of motion as simple as possible.

Recall the general form of the canonical transformation:

$$\tilde{H}(Q,P) = H(q,p) + \frac{\partial F}{\partial t} \ , \tag{5.84}$$

with

$$\frac{\partial F}{\partial q_\sigma} = p_\sigma \qquad\qquad \frac{\partial F}{\partial p_\sigma} = 0 \tag{5.85}$$

$$\frac{\partial F}{\partial Q_\sigma} = -P_\sigma \qquad\qquad \frac{\partial F}{\partial P_\sigma} = 0 \ . \tag{5.86}$$

We now demand that this transformation result in the simplest Hamiltonian possible, that is, $\tilde{H}(Q,P,t) = 0$. This requires we find a function F such that

$$\frac{\partial F}{\partial t} = -H \quad , \quad \frac{\partial F}{\partial q_\sigma} = p_\sigma \ . \tag{5.87}$$

The remaining functional dependence may be taken to be either on Q (type I) or on P (type II). As it turns out, the generating function F we seek is in fact the action, S, which is the integral of L with respect to time, expressed as a function of its endpoint values.

5.7.1 The action as a function of coordinates and time

We have seen how the action $S[\eta(\tau)]$ is a *functional* of the path $\eta(\tau)$ and a *function* of the endpoint values $\{q_a, t_a\}$ and $\{q_b, t_b\}$. Let us define the action *function* $S(q,t)$ as

$$S(q,t) = \int\limits_{t_a}^{t} d\tau\, L\big(\eta, \dot{\eta}, \tau\big) \ , \tag{5.88}$$

where $\eta(\tau)$ starts at (q_a, t_a) and ends at (q,t). We also require that $\eta(\tau)$ satisfy the Euler-Lagrange equations,

$$\frac{\partial L}{\partial \eta_\sigma} - \frac{d}{d\tau}\left(\frac{\partial L}{\partial \dot{\eta}_\sigma}\right) = 0 \tag{5.89}$$

Let us now consider a new path, $\tilde{\eta}(\tau)$, also starting at (q_a, t_a), but ending at $(q+dq, t+dt)$, and also satisfying the equations of motion. The differential of S is

$$\begin{aligned}
dS &= S\big[\tilde\eta(\tau)\big] - S\big[\eta(\tau)\big] \\
&= \int\limits_{t_a}^{t+dt} d\tau\, L(\tilde\eta,\dot{\tilde\eta},\tau) - \int\limits_{t_a}^{t} d\tau\, L\big(\eta,\dot\eta,\tau\big) \qquad (5.90) \\
&= \int\limits_{t_a}^{t} d\tau \left\{ \frac{\partial L}{\partial \eta_\sigma}\Big[\tilde\eta_\sigma(\tau)-\eta_\sigma(\tau)\Big] + \frac{\partial L}{\partial \dot\eta_\sigma}\Big[\dot{\tilde\eta}_\sigma(\tau)-\dot\eta_\sigma(\tau)\Big]\right\} + L\big(\tilde\eta(t),\dot{\tilde\eta}(t),t\big)\,dt \\
&= \int\limits_{t_a}^{t} d\tau \left\{ \frac{\partial L}{\partial \eta_\sigma} - \frac{d}{d\tau}\bigg(\frac{\partial L}{\partial \dot\eta_\sigma}\bigg)\right\}\Big[\tilde\eta_\sigma(\tau)-\eta_\sigma(\tau)\Big] \\
&\qquad\qquad + \frac{\partial L}{\partial \dot\eta_\sigma}\bigg|_t \Big[\tilde\eta_\sigma(t)-\eta_\sigma(t)\Big] + L\big(\tilde\eta(t),\dot{\tilde\eta}(t),t\big)\,dt \\
&= 0 + \pi_\sigma(t)\,\delta\eta_\sigma(t) + L\big(\eta(t),\dot\eta(t),t\big)\,dt + \mathcal{O}(\delta q\cdot dt)\ , \qquad (5.91)
\end{aligned}$$

where we have defined

$$\pi_\sigma = \frac{\partial L}{\partial \dot\eta_\sigma}\ , \qquad (5.92)$$

and

$$\delta\eta_\sigma(\tau) \equiv \tilde\eta_\sigma(\tau) - \eta_\sigma(\tau)\ . \qquad (5.93)$$

Note that the differential dq_σ is given by

$$\begin{aligned}
dq_\sigma &= \tilde\eta_\sigma(t+dt) - \eta_\sigma(t) \qquad (5.94) \\
&= \tilde\eta_\sigma(t+dt) - \tilde\eta_\sigma(t) + \tilde\eta_\sigma(t) - \eta_\sigma(t) \\
&= \dot{\tilde\eta}_\sigma(t)\,dt + \delta\eta_\sigma(t) \\
&= \dot q_\sigma(t)\,dt + \delta\eta_\sigma(t) + \mathcal{O}(\delta q\cdot dt)\ . \qquad (5.95)
\end{aligned}$$

Thus, with $\pi_\sigma(t)\equiv p_\sigma$, we have

$$\begin{aligned}
dS &= p_\sigma\,dq_\sigma + \big(L - p_\sigma\,\dot q_\sigma\big)\,dt \\
&= p_\sigma\,dq_\sigma - H\,dt\ . \qquad (5.96)
\end{aligned}$$

We therefore obtain

$$\frac{\partial S}{\partial q_\sigma} = p_\sigma \quad , \quad \frac{\partial S}{\partial t} = -H \quad , \quad \frac{dS}{dt} = L\ . \qquad (5.97)$$

What about the lower limit at t_a? Clearly there are $n+1$ constants associated with this limit: $\big\{q_1(t_a),\ldots,q_n(t_a);t_a\big\}$. Thus, we may write

$$S = S(q_1,\ldots,q_n;\Lambda_1,\ldots,\Lambda_n,t) + \Lambda_{n+1}\ , \qquad (5.98)$$

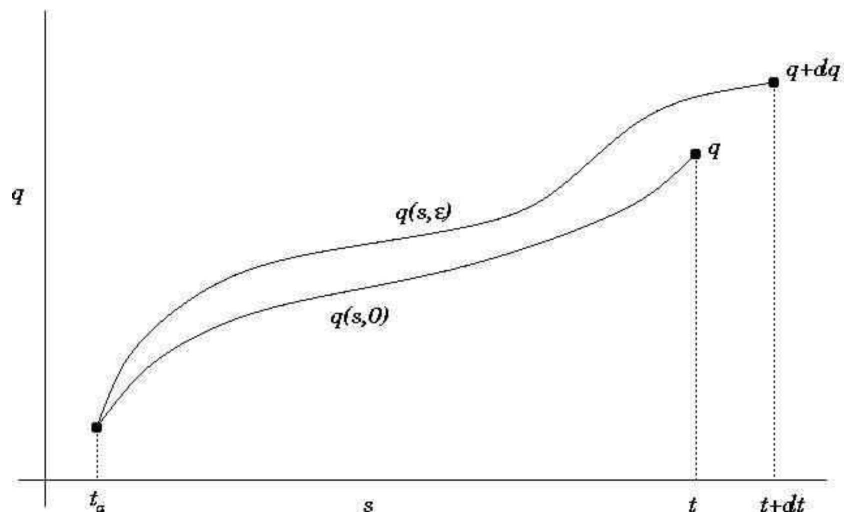

Figure 5.1: A one-parameter family of paths $q(s;\epsilon)$.

where our $n+1$ constants are $\{\Lambda_1,\ldots,\Lambda_{n+1}\}$. If we regard S as a mixed generator, which is type-I in some variables and type-II in others, then each Λ_σ for $1\le\sigma\le n$ may be chosen to be either Q_σ or P_σ. We will define

$$\Gamma_\sigma = \frac{\partial S}{\partial \Lambda_\sigma} = \begin{cases} +Q_\sigma & \text{if } \Lambda_\sigma = P_\sigma \\ -P_\sigma & \text{if } \Lambda_\sigma = Q_\sigma \end{cases} \tag{5.99}$$

For each σ, the two possibilities $\Lambda_\sigma = Q_\sigma$ or $\Lambda_\sigma = P_\sigma$ are of course rendered equivalent by a canonical transformation $(Q_\sigma, P_\sigma) \to (P_\sigma, -Q_\sigma)$.

5.7.2 The Hamilton-Jacobi equation

Since the action $S(q,\Lambda,t)$ has been shown to generate a canonical transformation for which $\tilde{H}(Q,P)=0$. This requirement may be written as

$$H\Big(q_1,\ldots,q_n,\frac{\partial S}{\partial q_1},\ldots,\frac{\partial S}{\partial q_n},t\Big) + \frac{\partial S}{\partial t} = 0 \ . \tag{5.100}$$

This is the *Hamilton-Jacobi equation* (HJE). It is a first order partial differential equation in $n+1$ variables, and in general is nonlinear (since kinetic energy is generally a quadratic function of momenta). Since $\tilde{H}(Q,P,t)=0$, the equations of motion are trivial, and

$$Q_\sigma(t) = \text{const.} \quad , \quad P_\sigma(t) = \text{const.} \tag{5.101}$$

Once the HJE is solved, one must invert the relations $\Gamma_\sigma = \partial S(q,\Lambda,t)/\partial\Lambda_\sigma$ to obtain $q(Q,P,t)$. This is possible only if

$$\det\bigg(\frac{\partial^2 S}{\partial q_\alpha\,\partial\Lambda_\beta}\bigg) \neq 0 \ , \tag{5.102}$$

which is known as the *Hessian condition*.

It is worth noting that the HJE may have several solutions. For example, consider the case of the free particle, with $H(q,p) = p^2/2m$. The HJE is

$$\frac{1}{2m}\left(\frac{\partial S}{\partial q}\right)^2 + \frac{\partial S}{\partial t} = 0 \ . \tag{5.103}$$

One solution of the HJE is

$$S(q,\Lambda,t) = \frac{m\,(q-\Lambda)^2}{2t} \ . \tag{5.104}$$

For this we find

$$\Gamma = \frac{\partial S}{\partial \Lambda} = -\frac{m}{t}\,(q-\Lambda) \quad \Rightarrow \quad q(t) = \Lambda - \frac{\Gamma}{m}\,t \ . \tag{5.105}$$

Here $\Lambda = q(0)$ is the initial value of q, and $\Gamma = -p$ is minus the momentum.

Another equally valid solution to the HJE is

$$S(q,\Lambda,t) = q\,\sqrt{2m\Lambda} - \Lambda\,t \ . \tag{5.106}$$

This yields

$$\Gamma = \frac{\partial S}{\partial \Lambda} = q\,\sqrt{\frac{2m}{\Lambda}} - t \quad \Rightarrow \quad q(t) = \sqrt{\frac{\Lambda}{2m}}\,(t+\Gamma) \ . \tag{5.107}$$

For this solution, Λ is the energy and Γ may be related to the initial value of $q(t) = \Gamma\sqrt{\Lambda/2m}$.

5.7.3 Time-independent Hamiltonians

When H has no explicit time dependence, we may reduce the order of the HJE by one, writing

$$S(q,\Lambda,t) = W(q,\Lambda) + T(\Lambda,t) \ . \tag{5.108}$$

The HJE becomes

$$H\left(q, \frac{\partial W}{\partial q}\right) = -\frac{\partial T}{\partial t} \ . \tag{5.109}$$

Note that the LHS of the above equation is independent of t, and the RHS is independent of q. Therefore, each side must only depend on the constants Λ, which is to say that each side must be a constant, which, without loss of generality, we take to be Λ_1. Therefore

$$S(q,\Lambda,t) = W(q,\Lambda) - \Lambda_1 t \ . \tag{5.110}$$

The function $W(q,\Lambda)$ is called *Hamilton's characteristic function*. The HJE now takes the form

$$H\left(q_1,\ldots,q_n, \frac{\partial W}{\partial q_1},\ldots,\frac{\partial W}{\partial q_n}\right) = \Lambda_1 \ . \tag{5.111}$$

Note that adding an arbitrary constant C to S generates the same equation, and simply shifts the last constant $\Lambda_{n+1} \rightarrow \Lambda_{n+1} + C$. This is equivalent to replacing t by $t - t_0$ with $t_0 = C/\Lambda_1$, *i.e.* it just redefines the zero of the time variable.

5.7.4 Example: one-dimensional motion

As an example of the method, consider the one-dimensional system,

$$H(q,p) = \frac{p^2}{2m} + U(q) \ . \tag{5.112}$$

The HJE is

$$\frac{1}{2m}\left(\frac{\partial S}{\partial q}\right)^2 + U(q) = \Lambda \ . \tag{5.113}$$

which may be recast as

$$\frac{\partial S}{\partial q} = \sqrt{2m\big[\Lambda - U(q)\big]} \ , \tag{5.114}$$

with solution

$$S(q,\Lambda,t) = \sqrt{2m}\int^{q}\! dq' \, \sqrt{\Lambda - U(q')} - \Lambda \, t \ . \tag{5.115}$$

We now have

$$p = \frac{\partial S}{\partial q} = \sqrt{2m\big[\Lambda - U(q)\big]} \ , \tag{5.116}$$

as well as

$$\Gamma = \frac{\partial S}{\partial \Lambda} = \sqrt{\frac{m}{2}}\int^{q(t)} \frac{dq'}{\sqrt{\Lambda - U(q')}} - t \ . \tag{5.117}$$

Thus, the motion $q(t)$ is given by quadrature:

$$\Gamma + t = \sqrt{\frac{m}{2}}\int^{q(t)} \frac{dq'}{\sqrt{\Lambda - U(q')}} \ , \tag{5.118}$$

where Λ and Γ are constants. The lower limit on the integral is arbitrary and merely shifts t by another constant. Note that Λ is the total energy.

5.7.5 Separation of variables

It is convenient to first work an example before discussing the general theory. Consider the following Hamiltonian, written in spherical polar coordinates:

$$H = \frac{1}{2m}\left(p_r^2 + \frac{p_\theta^2}{r^2} + \frac{p_\phi^2}{r^2 \sin^2\!\theta}\right) + \overbrace{A(r) + \frac{B(\theta)}{r^2} + \frac{C(\phi)}{r^2\sin^2\!\theta}}^{\text{potential } U(r,\theta,\phi)} \ . \tag{5.119}$$

We seek a solution with the characteristic function

$$W(r,\theta,\phi) = W_r(r) + W_\theta(\theta) + W_\phi(\phi) \ . \tag{5.120}$$

The HJE is then

$$\frac{1}{2m}\left(\frac{\partial W_r}{\partial r}\right)^2 + \frac{1}{2mr^2}\left(\frac{\partial W_\theta}{\partial \theta}\right)^2 + \frac{1}{2mr^2\sin^2\!\theta}\left(\frac{\partial W_\phi}{\partial \phi}\right)^2 + A(r) + \frac{B(\theta)}{r^2} + \frac{C(\phi)}{r^2\sin^2\!\theta} = \Lambda_1 = E \ . \tag{5.121}$$

Multiply through by $r^2\sin^2\!\theta$ to obtain

$$\frac{1}{2m}\left(\frac{\partial W_\phi}{\partial \phi}\right)^2 + C(\phi) = -\sin^2\!\theta\left\{\frac{1}{2m}\left(\frac{\partial W_\theta}{\partial \theta}\right)^2 + B(\theta)\right\} - r^2\sin^2\!\theta\left\{\frac{1}{2m}\left(\frac{\partial W_r}{\partial r}\right)^2 + A(r) - \Lambda_1\right\} \ . \tag{5.122}$$

The LHS is independent of (r,θ), and the RHS is independent of ϕ. Therefore, we may set

$$\frac{1}{2m}\left(\frac{\partial W_\phi}{\partial \phi}\right)^2 + C(\phi) = \Lambda_2 \ . \tag{5.123}$$

Proceeding, we replace the LHS in eqn. 5.122 with Λ_2, arriving at

$$\frac{1}{2m}\left(\frac{\partial W_\theta}{\partial \theta}\right)^2 + B(\theta) + \frac{\Lambda_2}{\sin^2\!\theta} = -r^2\left\{\frac{1}{2m}\left(\frac{\partial W_r}{\partial r}\right)^2 + A(r) - \Lambda_1\right\} \ . \tag{5.124}$$

The LHS of this equation is independent of r, and the RHS is independent of θ. Therefore,

$$\frac{1}{2m}\left(\frac{\partial W_\theta}{\partial \theta}\right)^2 + B(\theta) + \frac{\Lambda_2}{\sin^2\!\theta} = \Lambda_3 \ . \tag{5.125}$$

We're left with

$$\frac{1}{2m}\left(\frac{\partial W_r}{\partial r}\right)^2 + A(r) + \frac{\Lambda_3}{r^2} = \Lambda_1 \ . \tag{5.126}$$

The full solution is therefore

$$S(q,\Lambda,t) = \sqrt{2m}\int^r\! dr'\,\sqrt{\Lambda_1 - A(r') - \frac{\Lambda_3}{r'^2}} \tag{5.127}$$

$$+\sqrt{2m}\int^\theta\! d\theta'\,\sqrt{\Lambda_3 - B(\theta') - \frac{\Lambda_2}{\sin^2\!\theta'}}$$

$$+\sqrt{2m}\int^\phi\! d\phi'\,\sqrt{\Lambda_2 - C(\phi')} - \Lambda_1 t \ . \tag{5.128}$$

We then have

$$\varGamma_1 = \frac{\partial S}{\partial \varLambda_1} = \int^{r(t)} \frac{\sqrt{\frac{m}{2}}\, dr'}{\sqrt{\varLambda_1 - A(r') - \varLambda_3\, r'^{-2}}} - t \tag{5.129}$$

$$\varGamma_2 = \frac{\partial S}{\partial \varLambda_2} = -\int^{\theta(t)} \frac{\sqrt{\frac{m}{2}}\, d\theta'}{\sin^2\!\theta' \sqrt{\varLambda_3 - B(\theta') - \varLambda_2 \csc^2\!\theta'}} + \int^{\phi(t)} \frac{\sqrt{\frac{m}{2}}\, d\phi'}{\sqrt{\varLambda_2 - C(\phi')}} \tag{5.130}$$

$$\varGamma_3 = \frac{\partial S}{\partial \varLambda_3} = -\int^{r(t)} \frac{\sqrt{\frac{m}{2}}\, dr'}{r'^2 \sqrt{\varLambda_1 - A(r') - \varLambda_3\, r'^{-2}}} + \int^{\theta(t)} \frac{\sqrt{\frac{m}{2}}\, d\theta'}{\sqrt{\varLambda_3 - B(\theta') - \varLambda_2 \csc^2\!\theta'}} \ . \tag{5.131}$$

The game plan here is as follows. The first of the above trio of equations is inverted to yield $r(t)$ in terms of t and constants. This solution is then invoked in the last equation (the upper limit on the first integral on the RHS) in order to obtain an implicit equation for $\theta(t)$, which is invoked in the second equation to yield an implicit equation for $\phi(t)$. The net result is the motion of the system in terms of time t and the six constants $(\varLambda_1, \varLambda_2, \varLambda_3, \varGamma_1, \varGamma_2, \varGamma_3)$. A seventh constant, associated with an overall shift of the zero of t, arises due to the arbitrary lower limits of the integrals.

In general, the separation of variables method begins with[3]

$$W(q, \varLambda) = \sum_{\sigma=1}^{n} W_\sigma(q_\sigma, \varLambda) \ . \tag{5.132}$$

Each $W_\sigma(q_\sigma, \varLambda)$ may be regarded as a function of the single variable q_σ, and is obtained by satisfying an ODE of the form[4]

$$H_\sigma\bigg(q_\sigma, \frac{dW_\sigma}{dq_\sigma}\bigg) = \varLambda_\sigma \ . \tag{5.133}$$

We then have

$$p_\sigma = \frac{\partial W_\sigma}{\partial q_\sigma} \quad , \quad \varGamma_\sigma = \frac{\partial W}{\partial \varLambda_\sigma} + \delta_{\sigma,1}\, t \ . \tag{5.134}$$

Note that while each W_σ depends on only a single q_σ, it may depend on several of the $\varLambda_\sigma$.

5.7.6 Example #2 : point charge plus electric field

Consider a potential of the form

$$U(r) = \frac{k}{r} - Fz \ , \tag{5.135}$$

which corresponds to a charge in the presence of an external point charge plus an external electric field. This problem is amenable to separation in parabolic coordinates, (ξ, η, φ):

$$x = \sqrt{\xi\eta}\,\cos\varphi \quad , \quad y = \sqrt{\xi\eta}\,\sin\varphi \quad , \quad z = \tfrac{1}{2}(\xi - \eta) \ . \tag{5.136}$$

[3] Here we assume *complete separability*. A given system may only be *partially* separable.

[4] $H_\sigma(q_\sigma, p_\sigma)$ may also depend on several of the $\varLambda_\alpha$. See *e.g.* eqn. 5.126, which is of the form $H_r\big(r, \partial_r W_r, \varLambda_3\big) = \varLambda_1$.

Note that

$$\rho \equiv \sqrt{x^2+y^2} = \sqrt{\xi\eta} \tag{5.137}$$

$$r = \sqrt{\rho^2+z^2} = \tfrac{1}{2}(\xi+\eta) \ . \tag{5.138}$$

The kinetic energy is

$$\begin{aligned} T &= \tfrac{1}{2}m\big(\dot\rho^2 + \rho^2\,\dot\varphi^2 + \dot z^2\big) \\ &= \tfrac{1}{8}m\,(\xi+\eta)\bigg(\frac{\dot\xi^2}{\xi} + \frac{\dot\eta^2}{\eta}\bigg) + \tfrac{1}{2}m\,\xi\eta\,\dot\varphi^2 \ , \end{aligned} \tag{5.139}$$

and hence the Lagrangian is

$$L = \tfrac{1}{8}m\,(\xi+\eta)\bigg(\frac{\dot\xi^2}{\xi} + \frac{\dot\eta^2}{\eta}\bigg) + \tfrac{1}{2}m\,\xi\eta\,\dot\varphi^2 - \frac{2k}{\xi+\eta} + \tfrac{1}{2}F\,(\xi-\eta) \ . \tag{5.140}$$

Thus, the conjugate momenta are

$$p_\xi = \frac{\partial L}{\partial\dot\xi} = \tfrac{1}{4}m\,(\xi+\eta)\,\frac{\dot\xi}{\xi} \tag{5.141}$$

$$p_\eta = \frac{\partial L}{\partial\dot\eta} = \tfrac{1}{4}m\,(\xi+\eta)\,\frac{\dot\eta}{\eta} \tag{5.142}$$

$$p_\varphi = \frac{\partial L}{\partial\dot\varphi} = m\,\xi\eta\,\dot\varphi \ , \tag{5.143}$$

and the Hamiltonian is

$$H = p_\xi\,\dot\xi + p_\eta\,\dot\eta + p_\varphi\,\dot\varphi \tag{5.144}$$

$$= \frac{2}{m}\bigg(\frac{\xi\,p_\xi^2 + \eta\,p_\eta^2}{\xi+\eta}\bigg) + \frac{p_\varphi^2}{2m\xi\eta} + \frac{2k}{\xi+\eta} - \tfrac{1}{2}F\,(\xi-\eta) \ . \tag{5.145}$$

Notice that $\partial H/\partial t = 0$, which means $dH/dt = 0$, *i.e.* $H = E \equiv \varLambda_1$ is a constant of the motion. Also, φ is cyclic in H, so its conjugate momentum p_φ is a constant of the motion.

We write

$$S(q,\varLambda) = W(q,\varLambda) - Et \tag{5.146}$$

$$= W_\xi(\xi,\varLambda) + W_\eta(\eta,\varLambda) + W_\varphi(\varphi,\varLambda) - Et \ . \tag{5.147}$$

with $E = \varLambda_1$. Clearly we may take

$$W_\varphi(\varphi,\varLambda) = P_\varphi\,\varphi \ , \tag{5.148}$$

where $P_\varphi = \Lambda_2$. Multiplying the Hamilton-Jacobi equation by $\frac{1}{2}m\,(\xi+\eta)$ then gives

$$\begin{aligned}\xi\left(\frac{dW_\xi}{d\xi}\right)^2 + \frac{P_\varphi^2}{4\xi} + mk - \tfrac{1}{4}F\xi^2 - \tfrac{1}{2}mE\xi \\ = -\eta\left(\frac{dW_\eta}{d\eta}\right)^2 - \frac{P_\varphi^2}{4\eta} - \tfrac{1}{4}F\eta^2 + \tfrac{1}{2}mE\eta \equiv \Upsilon \ ,\end{aligned} \tag{5.149}$$

where $\Upsilon = \Lambda_3$ is the third constant: $\Lambda = (E, P_\varphi, \Upsilon)$. Thus,

$$\begin{aligned}S(\overbrace{\xi,\eta,\varphi}^{q};\underbrace{E,P_\varphi,\Upsilon}_{\Lambda}) &= \int^\xi d\xi' \sqrt{\tfrac{1}{2}mE + \frac{\Upsilon - mk}{\xi'} + \tfrac{1}{4}mF\xi' - \frac{P_\varphi^2}{4\xi'^2}} \\ &\quad + \int^\eta d\eta' \sqrt{\tfrac{1}{2}mE - \frac{\Upsilon}{\eta'} - \tfrac{1}{4}mF\eta' - \frac{P_\varphi^2}{4\eta'^2}} \\ &\quad + P_\varphi\,\varphi - Et \ .\end{aligned} \tag{5.150}$$

5.7.7 Example #3 : Charged Particle in a Magnetic Field

The Hamiltonian is

$$H = \frac{1}{2m}\Big(\boldsymbol{p} - \frac{e}{c}\boldsymbol{A}\Big)^2 \ . \tag{5.151}$$

We choose the gauge $\boldsymbol{A} = Bx\hat{\boldsymbol{y}}$, and we write

$$S(x,y,P_1,P_2) = W_x(x,P_1,P_2) + W_y(y,P_1,P_2) - P_1\,t \ . \tag{5.152}$$

Note that here we will consider S to be a function of $\{q_\sigma\}$ and $\{P_\sigma\}$.

The Hamilton-Jacobi equation is then

$$\left(\frac{\partial W_x}{\partial x}\right)^2 + \left(\frac{\partial W_y}{\partial y} - \frac{eBx}{c}\right)^2 = 2mP_1 \ . \tag{5.153}$$

We solve by writing

$$W_y = P_2\,y \qquad \Rightarrow \qquad \left(\frac{dW_x}{dx}\right)^2 + \left(P_2 - \frac{eBx}{c}\right)^2 = 2mP_1 \ . \tag{5.154}$$

This equation suggests the substitution

$$x = \frac{cP_2}{eB} + \frac{c}{eB}\sqrt{2mP_1}\,\sin\theta \ . \tag{5.155}$$

in which case

$$\frac{\partial x}{\partial\theta} = \frac{c}{eB}\sqrt{2mP_1}\,\cos\theta \tag{5.156}$$

and

$$\frac{\partial W_x}{\partial x} = \frac{\partial W_x}{\partial \theta} \cdot \frac{\partial \theta}{\partial x} = \frac{eB}{c\sqrt{2mP_1}} \, \frac{1}{\cos\theta} \, \frac{\partial W_x}{\partial \theta} \ . \tag{5.157}$$

Substitution this into eqn. 5.154, we have

$$\frac{\partial W_x}{\partial \theta} = \frac{2mcP_1}{eB} \, \cos^2\!\theta \ , \tag{5.158}$$

with solution

$$W_x = \frac{mcP_1}{eB} \, \theta + \frac{mcP_1}{2eB} \, \sin(2\theta) \ . \tag{5.159}$$

We then have

$$p_x = \frac{\partial W_x}{\partial x} = \frac{\partial W_x}{\partial \theta} \bigg/ \frac{\partial x}{\partial \theta} = \sqrt{2mP_1} \, \cos\theta \tag{5.160}$$

and

$$p_y = \frac{\partial W_y}{\partial y} = P_2 \ . \tag{5.161}$$

The type-II generator we seek is then

$$S(q,P,t) = \frac{mcP_1}{eB} \, \theta + \frac{mcP_1}{2eB} \, \sin(2\theta) + P_2 \, y - P_1 \, t \ , \tag{5.162}$$

where

$$\theta = \frac{eB}{c\sqrt{2mP_1}} \, \sin^{-1}\!\left(x - \frac{cP_2}{eB}\right) \ . \tag{5.163}$$

Note that, from eqn. 5.155, we may write

$$dx = \frac{c}{eB} \, dP_2 + \frac{mc}{eB} \, \frac{1}{\sqrt{2mP_1}} \, \sin\theta \, dP_1 + \frac{c}{eB} \, \sqrt{2mP_1} \, \cos\theta \, d\theta \ , \tag{5.164}$$

from which we derive

$$\frac{\partial \theta}{\partial P_1} = -\frac{\tan\theta}{2P_1} \qquad , \qquad \frac{\partial \theta}{\partial P_2} = -\frac{1}{\sqrt{2mP_1} \, \cos\theta} \ . \tag{5.165}$$

These results are useful in the calculation of Q_1 and Q_2:

$$\begin{aligned} Q_1 &= \frac{\partial S}{\partial P_1} \\ &= \frac{mc}{eB} \, \theta + \frac{mcP_1}{eB} \, \frac{\partial \theta}{\partial P_1} + \frac{mc}{2eB} \, \sin(2\theta) + \frac{mcP_1}{eB} \, \cos(2\theta) \, \frac{\partial \theta}{\partial P_1} - t \\ &= \frac{mc}{eB} \, \theta - t \end{aligned} \tag{5.166}$$

and

$$\begin{aligned} Q_2 &= \frac{\partial S}{\partial P_2} \\ &= y + \frac{mcP_1}{eB} \big[1 + \cos(2\theta)\big] \, \frac{\partial \theta}{\partial P_2} \\ &= y - \frac{c}{eB} \, \sqrt{2mP_1} \, \cos\theta \ . \end{aligned} \tag{5.167}$$

Now since $\tilde{H}(P, Q) = 0$, we have that $\dot{Q}_\sigma = 0$, which means that each Q_σ is a constant. We therefore have the following solution:

$$x(t) = x_0 + A \sin(\omega_c t + \delta) \tag{5.168}$$

$$y(t) = y_0 + A \cos(\omega_c t + \delta) \ , \tag{5.169}$$

where $\omega_c = eB/mc$ is the 'cyclotron frequency', and

$$x_0 = \frac{cP_2}{eB} \quad , \quad y_0 = Q_2 \quad , \quad \delta \equiv \omega_c \, Q_1 \quad , \quad A = \frac{c}{eB} \sqrt{2mP_1} \ . \tag{5.170}$$

5.8 Action-Angle Variables

5.8.1 Circular Phase Orbits: Librations and Rotations

In a completely integrable system, the Hamilton-Jacobi equation may be solved by separation of variables. Each momentum p_σ is a function of only its corresponding coordinate q_σ plus constants – no other coordinates enter:

$$p_\sigma = \frac{\partial W_\sigma}{\partial q_\sigma} = p_\sigma(q_\sigma, \Lambda) \ . \tag{5.171}$$

The motion satisfies

$$H_\sigma(q_\sigma, p_\sigma) = \Lambda_\sigma \ . \tag{5.172}$$

The level sets of H_σ are curves $\mathcal{C}_\sigma$. In general, these curves each depend on all of the constants Λ, so we write $\mathcal{C}_\sigma = \mathcal{C}_\sigma(\Lambda)$. The curves $\mathcal{C}_\sigma$ are the *projections* of the full motion onto the (q_σ, p_σ) plane. In general we will assume the motion, and hence the curves $\mathcal{C}_\sigma$, is *bounded*. In this case, two types of projected motion are possible: librations and rotations. Librations are periodic oscillations about an equilibrium position. Rotations involve the advancement of an angular variable by 2π during a cycle. This is most conveniently illustrated in the case of the simple pendulum, for which

$$H(p_\phi, \phi) = \frac{p_\phi^2}{2I} + \tfrac{1}{2} I \omega^2 \left(1 - \cos\phi\right) \ . \tag{5.173}$$

- When $E < I\,\omega^2$, the momentum p_ϕ vanishes at $\phi = \pm\cos^{-1}(2E/I\omega^2)$. The system executes librations between these extreme values of the angle ϕ.
- When $E > I\,\omega^2$, the kinetic energy is always positive, and the angle advances monotonically, executing rotations.

In a completely integrable system, each $\mathcal{C}_\sigma$ is either a libration or a rotation[5]. Both librations and rotations are closed curves. Thus, each $\mathcal{C}_\sigma$ is in general homotopic to (= "can be

[5] $\mathcal{C}_\sigma$ may correspond to a separatrix, but this is a nongeneric state of affairs.

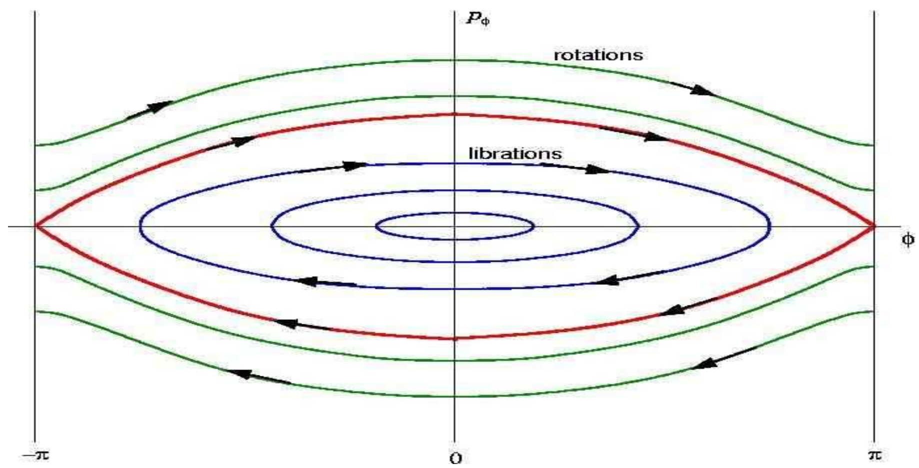

Figure 5.2: Phase curves for the simple pendulum, showing librations (in blue), rotations (in green), and the separatrix (in red). This phase flow is most correctly viewed as taking place on a cylinder, obtained from the above sketch by identifying the lines $\phi = \pi$ and $\phi = -\pi$.

continuously distorted to yield") a circle, $\mathbb{S}^1$. For n freedoms, the motion is therefore confined to an n-torus, $\mathbb{T}^n$:

$$\mathbb{T}^n = \overbrace{\mathbb{S}^1 \times \mathbb{S}^1 \times \cdots \times \mathbb{S}^1}^{n \text{ times}} \ . \tag{5.174}$$

These are called *invariant tori* (or *invariant manifolds*). There are many such tori, as there are many $\mathcal{C}_\sigma$ curves in each of the n two-dimensional submanifolds.

Invariant tori never intersect! This is ruled out by the uniqueness of the solution to the dynamical system, expressed as a set of coupled ordinary differential equations.

Note also that phase space is of dimension $2n$, while the invariant tori are of dimension n. Phase space is 'covered' by the invariant tori, but it is in general difficult to conceive of how this happens. Perhaps the most accessible analogy is the $n = 1$ case, where the '1-tori' are just circles. Two-dimensional phase space is covered noninteracting circular orbits. (The orbits are *topologically* equivalent to circles, although *geometrically* they may be distorted.) It is challenging to think about the $n = 2$ case, where a four-dimensional phase space is filled by nonintersecting 2-tori.

5.8.2 Action-Angle Variables

For a completely integrable system, one can transform canonically from (q, p) to new coordinates (ϕ, J) which specify a particular n-torus $\mathbb{T}^n$ as well as the location on the torus, which is specified by n angle variables. The $\{J_\sigma\}$ are 'momentum' variables which specify the torus itself; they are constants of the motion since the tori are invariant. They are called *action variables*. Since $\dot{J}_\sigma = 0$, we must have

$$\dot{J}_\sigma = -\frac{\partial H}{\partial \phi_\sigma} = 0 \quad \Longrightarrow \quad H = H(J) \ . \tag{5.175}$$

The $\{\phi_\sigma\}$ are the *angle variables*.

The coordinate ϕ_σ describes the projected motion along $\mathcal{C}_\sigma$, and is normalized by

$$\oint\limits_{\mathcal{C}_\sigma} d\phi_\sigma = 2\pi \qquad (\text{once around } \mathcal{C}_\sigma) \ . \tag{5.176}$$

The dynamics of the angle variables are given by

$$\dot{\phi}_\sigma = \frac{\partial H}{\partial J_\sigma} \equiv \nu_\sigma(J) \ . \tag{5.177}$$

Thus,

$$\phi_\sigma(t) = \phi_\sigma(0) + \nu_\sigma(J)\, t \ . \tag{5.178}$$

The $\big\{\nu_\sigma(J)\big\}$ are *frequencies* describing the rate at which the $\mathcal{C}_\sigma$ are traversed; $T_\sigma(J) = 2\pi/\nu_\sigma(J)$ is the period.

5.8.3 Canonical Transformation to Action-Angle Variables

The $\{J_\sigma\}$ determine the $\{\mathcal{C}_\sigma\}$; each q_σ determines a point on $\mathcal{C}_\sigma$. This suggests a type-II transformation, with generator $F_2(q, J)$:

$$p_\sigma = \frac{\partial F_2}{\partial q_\sigma} \quad , \quad \phi_\sigma = \frac{\partial F_2}{\partial J_\sigma} \ . \tag{5.179}$$

Note that[6]

$$2\pi = \oint\limits_{\mathcal{C}_\sigma} d\phi_\sigma = \oint\limits_{\mathcal{C}_\sigma} d\bigg(\frac{\partial F_2}{\partial J_\sigma}\bigg) = \oint\limits_{\mathcal{C}_\sigma} \frac{\partial^2 F_2}{\partial J_\sigma\, \partial q_\sigma}\, dq_\sigma = \frac{\partial}{\partial J_\sigma} \oint\limits_{\mathcal{C}_\sigma} p_\sigma\, dq_\sigma \ , \tag{5.180}$$

which suggests the definition

$$J_\sigma = \frac{1}{2\pi} \oint\limits_{\mathcal{C}_\sigma} p_\sigma\, dq_\sigma \ . \tag{5.181}$$

I.e. J_σ is $(2\pi)^{-1}$ times the area enclosed by $\mathcal{C}_\sigma$.

If, separating variables,

$$W(q, \Lambda) = \sum_\sigma W_\sigma(q_\sigma, \Lambda) \tag{5.182}$$

[6] In general, we should write $d\big(\frac{\partial F_2}{\partial J_\sigma}\big) = \frac{\partial^2 F_2}{\partial J_\sigma\, \partial q_\alpha}\, dq_\alpha$ with a sum over α. However, in eqn. 5.180 all coordinates and momenta other than q_σ and p_σ are held fixed. Thus, $\alpha = \sigma$ is the only term in the sum which contributes.

is Hamilton's characteristic function for the transformation $(q,p) \to (Q,P)$, then

$$J_\sigma = \frac{1}{2\pi} \oint\limits_{\mathcal{C}_\sigma} \frac{\partial W_\sigma}{\partial q_\sigma}\, dq_\sigma = J_\sigma(\Lambda) \tag{5.183}$$

is a function only of the $\{\Lambda_\alpha\}$ and not the $\{\Gamma_\alpha\}$. We then invert this relation to obtain $\Lambda(J)$, to finally obtain

$$F_2(q,J) = W\big(q,\Lambda(J)\big) = \sum_\sigma W_\sigma\big(q_\sigma,\Lambda(J)\big) \ . \tag{5.184}$$

Thus, the recipe for canonically transforming to action-angle variable is as follows:

(1) Separate and solve the Hamilton-Jacobi equation for $W(q,\Lambda) = \sum_\sigma W_\sigma(q_\sigma,\Lambda)$.

(2) Find the orbits $\mathcal{C}_\sigma$ – the level sets of satisfying $H_\sigma(q_\sigma,p_\sigma) = \Lambda_\sigma$.

(3) Invert the relation $J_\sigma(\Lambda) = \frac{1}{2\pi} \oint\limits_{\mathcal{C}_\sigma} \frac{\partial W_\sigma}{\partial q_\sigma}\, dq_\sigma$ to obtain $\Lambda(J)$.

(4) $F_2(q,J) = \sum_\sigma W_\sigma\big(q_\sigma,\Lambda(J)\big)$ is the desired type-II generator[7].

5.8.4 Example : Harmonic Oscillator

The Hamiltonian is

$$H = \frac{p^2}{2m} + \tfrac{1}{2} m\omega_0^2 q^2 \ , \tag{5.185}$$

hence the Hamilton-Jacobi equation is

$$\left(\frac{dW}{dq}\right)^2 + m^2\omega_0^2 q^2 = 2m\Lambda \ . \tag{5.186}$$

Thus,

$$p = \frac{dW}{dq} = \pm\sqrt{2m\Lambda - m^2\omega_0^2 q^2} \ . \tag{5.187}$$

We now define

$$q \equiv \left(\frac{2\Lambda}{m\omega_0^2}\right)^{1/2} \sin\theta \quad \Rightarrow \quad p = \sqrt{2m\Lambda}\, \cos\theta \ , \tag{5.188}$$

in which case

$$J = \frac{1}{2\pi} \oint p\, dq = \frac{1}{2\pi} \cdot \frac{2\Lambda}{\omega_0} \cdot \int\limits_0^{2\pi} d\theta\, \cos^2\!\theta = \frac{\Lambda}{\omega_0} \ . \tag{5.189}$$

[7] Note that $F_2(q,J)$ is time-independent. *I.e.* we are not transforming to $\tilde{H} = 0$, but rather to $\tilde{H} = \tilde{H}(J)$.

Solving the HJE, we write

$$\frac{dW}{d\theta} = \frac{\partial q}{\partial \theta} \cdot \frac{dW}{dq} = 2J\cos^2\!\theta \ . \tag{5.190}$$

Integrating,

$$W = J\theta + \tfrac{1}{2} J \sin 2\theta \ , \tag{5.191}$$

up to an irrelevant constant. We then have

$$\phi = \frac{\partial W}{\partial J}\bigg|_q = \theta + \tfrac{1}{2}\sin 2\theta + J\big(1+\cos 2\theta\big)\,\frac{\partial\theta}{\partial J}\bigg|_q \ . \tag{5.192}$$

To find $(\partial\theta/\partial J)_q$, we differentiate $q = \sqrt{2J/m\omega_0}\,\sin\theta$:

$$dq = \frac{\sin\theta}{\sqrt{2m\omega_0 J}}\,dJ + \sqrt{\frac{2J}{m\omega_0}}\,\cos\theta\,d\theta \qquad \Rightarrow \qquad \frac{\partial\theta}{\partial J}\bigg|_q = -\frac{1}{2J}\,\tan\theta \ . \tag{5.193}$$

Plugging this result into eqn. 5.192, we obtain $\phi = \theta$. Thus, the full transformation is

$$q = \bigg(\frac{2J}{m\omega_0}\bigg)^{1/2} \sin\phi \quad , \quad p = \sqrt{2m\omega_0 J}\,\cos\phi \ . \tag{5.194}$$

The Hamiltonian is

$$H = \omega_0\, J \ , \tag{5.195}$$

hence $\dot\phi = \frac{\partial H}{\partial J} = \omega_0$ and $\dot J = -\frac{\partial H}{\partial \phi} = 0$, with solution $\phi(t) = \phi(0) + \omega_0\, t$ and $J(t) = J(0)$.

5.8.5 Example : Particle in a Box

Consider a particle in an open box of dimensions $L_x \times L_y$ moving under the influence of gravity. The bottom of the box lies at $z = 0$. The Hamiltonian is

$$H = \frac{p_x^2}{2m} + \frac{p_y^2}{2m} + \frac{p_z^2}{2m} + mgz \ . \tag{5.196}$$

Step one is to solve the Hamilton-Jacobi equation via separation of variables. The Hamilton-Jacobi equation is written

$$\frac{1}{2m}\bigg(\frac{\partial W_x}{\partial x}\bigg)^2 + \frac{1}{2m}\bigg(\frac{\partial W_y}{\partial y}\bigg)^2 + \frac{1}{2m}\bigg(\frac{\partial W_z}{\partial z}\bigg)^2 + mgz = E \equiv \varLambda_z \ . \tag{5.197}$$

We can solve for $W_{x,y}$ by inspection:

$$W_x(x) = \sqrt{2m\varLambda_x}\,x \quad , \quad W_y(y) = \sqrt{2m\varLambda_y}\,y \ . \tag{5.198}$$

We then have[8]

$$W_z'(z) = -\sqrt{2m\big(\varLambda_z - \varLambda_x - \varLambda_y - mgz\big)} \tag{5.199}$$

$$W_z(z) = \frac{2\sqrt{2}}{3\sqrt{m}\,g}\big(\varLambda_z - \varLambda_x - \varLambda_y - mgz\big)^{3/2} \ . \tag{5.200}$$

[8]Our choice of signs in taking the square roots for W_x', W_y', and W_z' is discussed below.

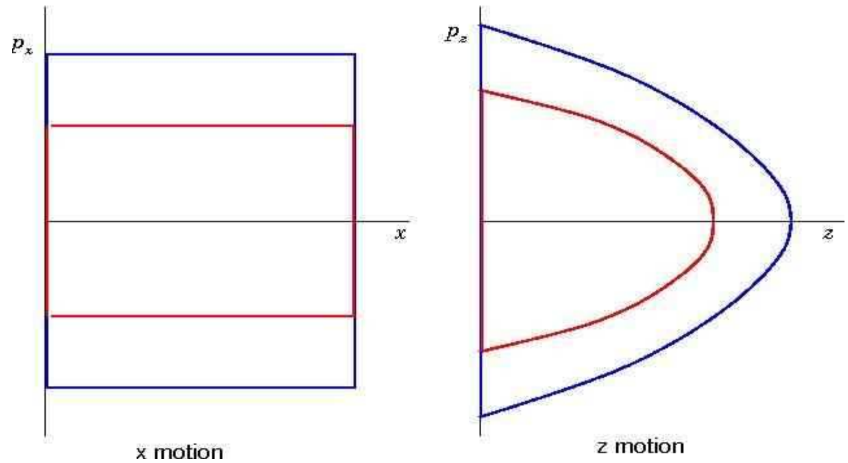

Figure 5.3: The librations $\mathcal{C}_z$ and $\mathcal{C}_x$. Not shown is $\mathcal{C}_y$, which is of the same shape as $\mathcal{C}_x$.

Step two is to find the $\mathcal{C}_\sigma$. Clearly $p_{x,y} = \sqrt{2m\Lambda_{x,y}}$. For fixed p_x, the x motion proceeds from $x = 0$ to $x = L_x$ and back, with corresponding motion for y. For x, we have

$$p_z(z) = W_z'(z) = \sqrt{2m\big(\Lambda_z - \Lambda_x - \Lambda_y - mgz\big)}\ , \tag{5.201}$$

and thus $\mathcal{C}_z$ is a truncated parabola, with $z_{\text{max}} = (\Lambda_z - \Lambda_x - \Lambda_y)/mg$.

Step three is to compute $J(\Lambda)$ and invert to obtain $\Lambda(J)$. We have

$$J_x = \frac{1}{2\pi} \oint\limits_{\mathcal{C}_x} p_x\, dx = \frac{1}{\pi} \int\limits_0^{L_x} dx \sqrt{2m\Lambda_x} = \frac{L_x}{\pi} \sqrt{2m\Lambda_x} \tag{5.202}$$

$$J_y = \frac{1}{2\pi} \oint\limits_{\mathcal{C}_y} p_y\, dy = \frac{1}{\pi} \int\limits_0^{L_y} dy \sqrt{2m\Lambda_y} = \frac{L_y}{\pi} \sqrt{2m\Lambda_y} \tag{5.203}$$

and

$$\begin{aligned} J_z &= \frac{1}{2\pi} \oint\limits_{\mathcal{C}_z} p_z\, dz = \frac{1}{\pi} \int\limits_0^{z_{\text{max}}} dx\, \sqrt{2m\big(\Lambda_z - \Lambda_x - \Lambda_y - mgz\big)} \\ &= \frac{2\sqrt{2}}{3\pi\sqrt{m}\, g} \big(\Lambda_z - \Lambda_x - \Lambda_y\big)^{3/2}\ . \end{aligned} \tag{5.204}$$

We now invert to obtain

$$\Lambda_x = \frac{\pi^2}{2mL_x^2}\, J_x^2 \qquad , \qquad \Lambda_y = \frac{\pi^2}{2mL_y^2}\, J_y^2 \tag{5.205}$$

$$\Lambda_z = \left(\frac{3\pi\sqrt{m}\, g}{2\sqrt{2}}\right)^{2/3} J_z^{2/3} + \frac{\pi^2}{2mL_x^2}\, J_x^2 + \frac{\pi^2}{2mL_y^2}\, J_y^2\ . \tag{5.206}$$

$$F_2\big(x,y,z,J_x,J_y,J_z\big) = \frac{\pi x}{L_x}\,J_x + \frac{\pi y}{L_y}\,J_y + \pi\bigg(J_z^{2/3} - \frac{2m^{2/3}g^{1/3}z}{(3\pi)^{2/3}}\bigg)^{3/2} \quad . \tag{5.207}$$

We now find

$$\phi_x = \frac{\partial F_2}{\partial J_x} = \frac{\pi x}{L_x} \quad , \quad \phi_y = \frac{\partial F_2}{\partial J_y} = \frac{\pi y}{L_y} \tag{5.208}$$

and

$$\phi_z = \frac{\partial F_2}{\partial J_z} = \pi\sqrt{1 - \frac{2m^{2/3}g^{1/3}z}{(3\pi J_z)^{2/3}}} = \pi\sqrt{1 - \frac{z}{z_{\rm max}}} \ , \tag{5.209}$$

where

$$z_{\rm max}(J_z) = \frac{(3\pi J_z)^{2/3}}{2m^{2/3}g^{1/3}} \ . \tag{5.210}$$

The momenta are

$$p_x = \frac{\partial F_2}{\partial x} = \frac{\pi J_x}{L_x} \quad , \quad p_y = \frac{\partial F_2}{\partial y} = \frac{\pi J_y}{L_y} \tag{5.211}$$

and

$$p_z = \frac{\partial F_2}{\partial z} = -\sqrt{2m}\,\Bigg(\bigg(\frac{3\pi\sqrt{m}\,g}{2\sqrt{2}}\bigg)^{2/3} J_z^{2/3} - mgz\Bigg)^{1/2} \ . \tag{5.212}$$

We note that the angle variables $\phi_{x,y,z}$ seem to be restricted to the range $[0,\pi]$, which seems to be at odds with eqn. 5.180. Similarly, the momenta $p_{x,y,z}$ all seem to be positive, whereas we know the momenta reverse sign when the particle bounces off a wall. The origin of the apparent discrepancy is that when we solved for the functions $W_{x,y,z}$, we had to take a square root in each case, and we chose a particular branch of the square root. So rather than $W_x(x) = \sqrt{2m\Lambda_x}\,x$, we should have taken

$$W_x(x) = \begin{cases} \sqrt{2m\Lambda_x}\,x & \text{if } p_x > 0 \\ \sqrt{2m\Lambda_x}\,(2L_x - x) & \text{if } p_x < 0 \ . \end{cases} \tag{5.213}$$

The relation $J_x = (L_x/\pi)\sqrt{2m\Lambda_x}$ is unchanged, hence

$$W_x(x) = \begin{cases} (\pi x/L_x)\,J_x & \text{if } p_x > 0 \\ 2\pi J_x - (\pi x/L_x)\,J_x & \text{if } p_x < 0 \ . \end{cases} \tag{5.214}$$

and

$$\phi_x = \begin{cases} \pi x/L_x & \text{if } p_x > 0 \\ \pi(2L_x - x)/L_x & \text{if } p_x < 0 \ . \end{cases} \tag{5.215}$$

Now the angle variable ϕ_x advances by 2π during the cycle $\mathcal{C}_x$. Similar considerations apply to the y and z sectors.

5.8.6 Kepler Problem in Action-Angle Variables

This is discussed in detail in standard texts, such as Goldstein. The potential is $V(r) = -k/r$, and the problem is separable. We write[9]

$$W(r,\theta,\phi) = W_r(r) + W_\theta(\theta) + W_\varphi(\varphi) \ , \tag{5.216}$$

hence

$$\frac{1}{2m}\bigg(\frac{\partial W_r}{\partial r}\bigg)^2 + \frac{1}{2mr^2}\bigg(\frac{\partial W_\theta}{\partial \theta}\bigg)^2 + \frac{1}{2mr^2\sin^2\!\theta}\bigg(\frac{\partial W_\varphi}{\partial \varphi}\bigg)^2 + V(r) = E \equiv \Lambda_r \ . \tag{5.217}$$

Separating, we have

$$\frac{1}{2m}\bigg(\frac{dW_\varphi}{d\varphi}\bigg)^2 = \Lambda_\varphi \quad \Rightarrow \quad J_\varphi = \oint\limits_{\mathcal{C}_\varphi} d\varphi\, \frac{dW_\varphi}{d\varphi} = 2\pi\sqrt{2m\Lambda_\varphi} \ . \tag{5.218}$$

Next we deal with the θ coordinate:

$$\begin{aligned}
\frac{1}{2m}\bigg(\frac{dW_\theta}{d\theta}\bigg)^2 = \Lambda_\theta - \frac{\Lambda_\varphi}{\sin^2\!\theta} \qquad &\Rightarrow \\
J_\theta &= 4\sqrt{2m\Lambda_\theta}\int\limits_0^{\theta_0} d\theta\, \sqrt{1 - \big(\Lambda_\varphi/\Lambda_\theta\big)\csc^2\!\theta} \\
&= 2\pi\sqrt{2m}\Big(\sqrt{\Lambda_\theta} - \sqrt{\Lambda_\varphi}\Big) \ ,
\end{aligned} \tag{5.219}$$

where $\theta_0 = \sin^{-1}(\Lambda_\varphi/\Lambda_\theta)$. Finally, we have[10]

$$\begin{aligned}
\frac{1}{2m}\bigg(\frac{dW_r}{dr}\bigg)^2 = E + \frac{k}{r} - \frac{\Lambda_\theta}{r^2} \quad &\Rightarrow \\
J_r &= \oint\limits_{\mathcal{C}_r} dr\, \sqrt{2m\bigg(E + \frac{k}{r} - \frac{\Lambda_\theta}{r^2}\bigg)} \\
&= -(J_\theta + J_\varphi) + \pi k\sqrt{\frac{2m}{|E|}} \ ,
\end{aligned} \tag{5.220}$$

where we've assumed $E < 0$, *i.e.* bound motion.

Thus, we find

$$H = E = -\frac{2\pi^2 mk^2}{\big(J_r + J_\theta + J_\varphi\big)^2} \ . \tag{5.221}$$

Note that the frequencies are completely degenerate:

$$\nu \equiv \nu_{r,\theta,\varphi} = \frac{\partial H}{\partial J_{r,\theta,\varphi}} = \frac{4\pi^2 mk^2}{\big(J_r + J_\theta + J_\varphi\big)^3} = \bigg(\frac{\pi^2 mk^2}{2|E|^3}\bigg)^{1/2} \ . \tag{5.222}$$

[9] We denote the azimuthal angle by φ to distinguish it from the AA variable ϕ.

[10] The details of performing the integral around $\mathcal{C}_r$ are discussed in *e.g.* Goldstein.

This threefold degeneracy may be removed by a transformation to new AA variables,

$$\Big\{(\phi_r, J_r),\ (\phi_\theta, J_\theta),\ (\phi_\varphi, J_\varphi)\Big\} \longrightarrow \Big\{(\phi_1, J_1),\ (\phi_2, J_2),\ (\phi_3, J_3)\Big\} \ , \tag{5.223}$$

using the type-II generator

$$F_2(\phi_r, \phi_\theta, \phi_\varphi; J_1, J_2, J_3) = (\phi_\varphi - \phi_\theta)\, J_1 + (\phi_\theta - \phi_r)\, J_2 + \phi_r\, J_3 \ , \tag{5.224}$$

which results in

$$\phi_1 = \frac{\partial F_2}{\partial J_1} = \phi_\varphi - \phi_\theta \qquad\qquad J_r = \frac{\partial F_2}{\partial \phi_r} = J_3 - J_2 \tag{5.225}$$

$$\phi_2 = \frac{\partial F_2}{\partial J_2} = \phi_\theta - \phi_r \qquad\qquad J_\theta = \frac{\partial F_2}{\partial \phi_\theta} = J_2 - J_1 \tag{5.226}$$

$$\phi_3 = \frac{\partial F_2}{\partial J_3} = \phi_r \qquad\qquad J_\varphi = \frac{\partial F_2}{\partial \phi_\varphi} = J_1 \ . \tag{5.227}$$

The new Hamiltonian is

$$H(J_1, J_2, J_3) = -\frac{2\pi^2 m k^2}{J_3^2} \ , \tag{5.228}$$

whence $\nu_1 = \nu_2 = 0$ and $\nu_3 = \nu$.

5.8.7 Charged Particle in a Magnetic Field

For the case of the charged particle in a magnetic field, studied above in section 5.7.7, we found

$$x = \frac{cP_2}{eB} + \frac{c}{eB}\sqrt{2mP_1}\,\sin\theta \tag{5.229}$$

and

$$p_x = \sqrt{2mP_1}\,\cos\theta \qquad , \qquad p_y = P_2 \ . \tag{5.230}$$

The action variable J is then

$$J = \oint p_x\, dx = \frac{2mcP_1}{eB}\int\limits_0^{2\pi} d\theta\, \cos^2\!\theta = \frac{mcP_1}{eB} \ . \tag{5.231}$$

We then have

$$W = J\theta + \tfrac{1}{2} J \sin(2\theta) + Py \ , \tag{5.232}$$

where $P \equiv P_2$. Thus,

$$\begin{aligned}
\phi &= \frac{\partial W}{\partial J} \\
&= \theta + \tfrac{1}{2}\sin(2\theta) + J\big[1 + \cos(2\theta)\big]\,\frac{\partial\theta}{\partial J} \\
&= \theta + \tfrac{1}{2}\sin(2\theta) + 2J\cos^2\!\theta \cdot \left(-\frac{\tan\theta}{2J}\right) \\
&= \theta \ .
\end{aligned} \tag{5.233}$$

The other canonical pair is (Q, P), where

$$Q = \frac{\partial W}{\partial P} = y - \sqrt{\frac{2cJ}{eB}}\,\cos\phi\ . \tag{5.234}$$

Therefore, we have

$$x = \frac{cP}{eB} + \sqrt{\frac{2cJ}{eB}}\,\sin\phi \qquad , \qquad y = Q + \sqrt{\frac{2cJ}{eB}}\,\cos\phi \tag{5.235}$$

and

$$p_x = \sqrt{\frac{2eBJ}{c}}\,\cos\phi \qquad , \qquad p_y = P\ . \tag{5.236}$$

The Hamiltonian is

$$\begin{aligned} H &= \frac{p_x^2}{2m} + \frac{1}{2m}\bigg(p_y - \frac{eBx}{c}\bigg)^2 \\ &= \frac{eBJ}{mc}\,\cos^2\!\phi + \frac{eBJ}{mc}\,\sin^2\!\phi \\ &= \omega_{\rm c}\,J\ , \end{aligned} \tag{5.237}$$

where $\omega_{\rm c} = eB/mc$. The equations of motion are

$$\dot\phi = \frac{\partial H}{\partial J} = \omega_{\rm c} \qquad , \qquad \dot J = -\frac{\partial H}{\partial \phi} = 0 \tag{5.238}$$

and

$$\dot Q = \frac{\partial H}{\partial P} = 0 \qquad , \qquad \dot P = -\frac{\partial H}{\partial Q} = 0\ . \tag{5.239}$$

Thus, Q, P, and J are constants, and $\phi(t) = \phi_0 + \omega_{\rm c}\,t$.

5.8.8 Motion on Invariant Tori

The angle variables evolve as

$$\phi_\sigma(t) = \nu_\sigma(J)\,t + \phi_\sigma(0)\ . \tag{5.240}$$

Thus, they wind around the invariant torus, specified by $\{J_\sigma\}$ at constant rates. In general, while each ϕ_σ executed periodic motion around a circle, the motion of the system as a whole is not periodic, since the frequencies $\nu_\sigma(J)$ are not, in general, commensurate. In order for the motion to be periodic, there must exist a set of integers, $\{l_\sigma\}$, such that

$$\sum_{\sigma=1}^n l_\sigma\,\nu_\sigma(J) = 0\ . \tag{5.241}$$

This means that the ratio of any two frequencies ν_σ/ν_α must be a rational number. On a given torus, there are several possible orbits, depending on initial conditions $\phi(0)$. However, since the frequencies are determined by the action variables, which specify the tori, on a given torus either all orbits are periodic, or none are.

In terms of the original coordinates q, there are two possibilities:

$$\begin{aligned} q_\sigma(t) &= \sum_{\ell_1=-\infty}^{\infty} \cdots \sum_{\ell_n=-\infty}^{\infty} A^{(\sigma)}_{\ell_1\ell_2\cdots\ell_n}\, e^{i\ell_1\phi_1(t)} \cdots e^{i\ell_n\phi_n(t)} \\ &\equiv \sum_{\boldsymbol{\ell}} A^\sigma_{\boldsymbol{\ell}}\, e^{i\boldsymbol{\ell}\cdot\boldsymbol{\phi}(t)} \qquad \text{(libration)} \end{aligned} \tag{5.242}$$

or

$$q_\sigma(t) = q^\circ_\sigma\, \phi_\sigma(t) + \sum_{\boldsymbol{\ell}} B^\sigma_{\boldsymbol{\ell}}\, e^{i\boldsymbol{\ell}\cdot\boldsymbol{\phi}(t)} \qquad \text{(rotation)}\ . \tag{5.243}$$

For rotations, the variable $q_\sigma(t)$ increased by $\Delta q_\sigma = 2\pi\, q^\circ_\sigma$. R

5.9 Canonical Perturbation Theory

5.9.1 Canonical Transformations and Perturbation Theory

Suppose we have a Hamiltonian

$$H(\xi,t) = H_0(\xi,t) + \epsilon\, H_1(\xi,t)\ , \tag{5.244}$$

where ϵ is a small dimensionless parameter. Let's implement a type-II transformation, generated by $S(q,P,t)$:[11]

$$\tilde{H}(Q,P,t) = H(q,p,t) + \frac{\partial}{\partial t} S(q,P,t)\ . \tag{5.245}$$

Let's expand everything in powers of ϵ:

$$q_\sigma = Q_\sigma + \epsilon\, q_{1,\sigma} + \epsilon^2\, q_{2,\sigma} + \ldots \tag{5.246}$$

$$p_\sigma = P_\sigma + \epsilon\, p_{1,\sigma} + \epsilon^2\, p_{2,\sigma} + \ldots \tag{5.247}$$

$$\tilde{H} = \tilde{H}_0 + \epsilon\, \tilde{H}_1 + \epsilon^2\, \tilde{H}_2 + \ldots \tag{5.248}$$

$$S = \underbrace{q_\sigma\, P_\sigma}_{\substack{\text{identity}\\ \text{transformation}}} + \epsilon\, S_1 + \epsilon^2\, S_2 + \ldots\ . \tag{5.249}$$

Then

$$\begin{aligned} Q_\sigma = \frac{\partial S}{\partial P_\sigma} &= q_\sigma + \epsilon\, \frac{\partial S_1}{\partial P_\sigma} + \epsilon^2\, \frac{\partial S_2}{\partial P_\sigma} + \ldots \\ &= Q_\sigma + \bigg(q_{1,\sigma} + \frac{\partial S_1}{\partial P_\sigma}\bigg)\epsilon + \bigg(q_{2,\sigma} + \frac{\partial S_2}{\partial P_\sigma}\bigg)\epsilon^2 + \ldots \end{aligned} \tag{5.250}$$

[11] $Here, S(q,P,t)$ is not meant to signify Hamilton's principal function.

and

$$p_\sigma = \frac{\partial S}{\partial q_\sigma} = P_\sigma + \epsilon\,\frac{\partial S_1}{\partial q_\sigma} + \epsilon^2\,\frac{\partial S_2}{\partial q_\sigma} + \ldots \tag{5.251}$$

$$= P_\sigma + \epsilon\, p_{1,\sigma} + \epsilon^2\, p_{2,\sigma} + \ldots\ . \tag{5.252}$$

We therefore conclude, order by order in ϵ,

$$q_{k,\sigma} = -\frac{\partial S_k}{\partial P_\sigma} \quad , \quad p_{k,\sigma} = +\frac{\partial S_k}{\partial q_\sigma}\ . \tag{5.253}$$

Now let's expand the Hamiltonian:

$$\tilde H(Q,P,t) = H_0(q,p,t) + \epsilon\, H_1(q,p,t) + \frac{\partial S}{\partial t} \tag{5.254}$$

$$\begin{aligned}
&= H_0(Q,P,t) + \frac{\partial H_0}{\partial Q_\sigma}\,(q_\sigma - Q_\sigma) + \frac{\partial H_0}{\partial P_\sigma}\,(p_\sigma - P_\sigma) \\
&\qquad + \epsilon H_1(Q,P,t) + \epsilon\,\frac{\partial}{\partial t}\,S_1(Q,P,t) + \mathcal{O}(\epsilon^2) \\
&= H_0(Q,P,t) + \Bigg(- \frac{\partial H_0}{\partial Q_\sigma}\,\frac{\partial S_1}{\partial P_\sigma} + \frac{\partial H_0}{\partial P_\sigma}\,\frac{\partial S_1}{\partial Q_\sigma} + \frac{\partial S_1}{\partial t} + H_1\Bigg)\,\epsilon + \mathcal{O}(\epsilon^2) \\
&= H_0(Q,P,t) + \bigg(H_1 + \big\{S_1, H_0\big\} + \frac{\partial S_1}{\partial t}\bigg)\,\epsilon + \mathcal{O}(\epsilon^2)\ .
\end{aligned} \tag{5.255}$$

In the above expression, we evaluate $H_k(q,p,t)$ and $S_k(q,P,t)$ at $q = Q$ and $p = P$ and expand in the differences $q - Q$ and $p - P$. Thus, we have derived the relation

$$\tilde H(Q,P,t) = \tilde H_0(Q,P,t) + \epsilon \tilde H_1(Q,P,t) + \ldots \tag{5.256}$$

with

$$\tilde H_0(Q,P,t) = H_0(Q,P,t) \tag{5.257}$$

$$\tilde H_1(Q,P,t) = H_1 + \big\{S_1, H_0\big\} + \frac{\partial S_1}{\partial t}\ . \tag{5.258}$$

The problem, though, is this: we have one equation, eqn, 5.258, for the two unknowns $\tilde H_1$ and S_1. Thus, the problem is underdetermined. Of course, we could choose $\tilde H_1 = 0$, which basically recapitulates standard Hamilton-Jacobi theory. But we might just as well demand that $\tilde H_1$ satisfy some other requirement, such as that $\tilde H_0 + \epsilon\, \tilde H_1$ being integrable.

Incidentally, this treatment is paralleled by one in quantum mechanics, where a unitary transformation may be implemented to eliminate a perturbation to lowest order in a small parameter. Consider the Schrödinger equation,

$$i\hbar\frac{\partial \psi}{\partial t} = (\mathcal{H}_0 + \epsilon\, \mathcal{H}_1)\, \psi\ , \tag{5.259}$$

and define χ by

$$\psi \equiv e^{iS/\hbar}\,\chi \ , \tag{5.260}$$

with

$$S = \epsilon\, S_1 + \epsilon^2\, S_2 + \ldots \ . \tag{5.261}$$

As before, the transformation $U \equiv \exp(iS/\hbar)$ collapses to the identity in the $\epsilon \to 0$ limit. Now let's write the Schrödinger equation for χ. Expanding in powers of ϵ, one finds

$$i\hbar \frac{\partial \chi}{\partial t} = \mathcal{H}_0\,\chi + \epsilon\left(\mathcal{H}_1 + \frac{1}{i\hbar}\big[S_1, \mathcal{H}_0\big] + \frac{\partial S_1}{\partial t}\right)\chi + \ldots \equiv \tilde{\mathcal{H}}\,\chi \ , \tag{5.262}$$

where $[A, B] = AB - BA$ is the commutator. Note the classical-quantum correspondence,

$$\{A, B\} \longleftrightarrow \frac{1}{i\hbar}\,[A, B] \ . \tag{5.263}$$

Again, what should we choose for S_1? Usually the choice is made to make the $\mathcal{O}(\epsilon)$ term in $\tilde{\mathcal{H}}$ vanish. But this is not the only possible simplifying choice.

5.9.2 Canonical Perturbation Theory for $n = 1$ Systems

Henceforth we shall assume $H(\xi, t) = H(\xi)$ is time-independent, and we write the perturbed Hamiltonian as

$$H(\xi) = H_0(\xi) + \epsilon H_1(\xi) \ . \tag{5.264}$$

Let (ϕ_0, J_0) be the action-angle variables for H_0. Then

$$\tilde{H}_0(\phi_0, J_0) = H_0\big(q(\phi_0, J_0), p(\phi_0, J_0)\big) = \tilde{H}_0(J_0) \ . \tag{5.265}$$

We define

$$\tilde{H}_1(\phi_0, J_0) = H_1\big(q(\phi_0, J_0), p(\phi_0, J_0)\big) \ . \tag{5.266}$$

We assume that $\tilde{H} = \tilde{H}_0 + \epsilon\,\tilde{H}_1$ is integrable[12], so it, too, possesses action-angle variables, which we denote by (ϕ, J)[13]. Thus, there must be a canonical transformation taking $(\phi_0, J_0) \to (\phi, J)$, with

$$\tilde{H}\big(\phi_0(\phi, J), J_0(\phi, J)\big) \equiv K(J) = E(J) \ . \tag{5.267}$$

We solve via a type-II canonical transformation:

$$S(\phi_0, J) = \phi_0 J + \epsilon\, S_1(\phi_0, J) + \epsilon^2\, S_2(\phi_0, J) + \ldots \ , \tag{5.268}$$

where $\phi_0 J$ is the identity transformation. Then

$$J_0 = \frac{\partial S}{\partial \phi_0} = J + \epsilon\,\frac{\partial S_1}{\partial \phi_0} + \epsilon^2\,\frac{\partial S_2}{\partial \phi_0} + \ldots \tag{5.269}$$

$$\phi = \frac{\partial S}{\partial J} = \phi_0 + \epsilon\,\frac{\partial S_1}{\partial J} + \epsilon^2\,\frac{\partial S_2}{\partial J} + \ldots \ , \tag{5.270}$$

[12] This is always true, in fact, for $n = 1$.

[13] We assume the motion is bounded, so action-angle variables may be used.

and

$$\begin{aligned} E(J) &= E_0(J) + \epsilon\, E_1(J) + \epsilon^2\, E_2(J) + \ldots && (5.271) \\ &= \tilde{H}_0(\phi_0, J_0) + \tilde{H}_1(\phi_0, J_0)\ . && (5.272) \end{aligned}$$

We now expand $\tilde{H}(\phi_0, J_0)$ in powers of $J_0 - J$:

$$\begin{aligned} \tilde{H}(\phi_0, J_0) &= \tilde{H}_0(\phi_0, J_0) + \epsilon\, \tilde{H}_1(\phi_0, J_0) && (5.273) \\ &= \tilde{H}_0(J) + \frac{\partial \tilde{H}_0}{\partial J}\,(J_0 - J) + \tfrac{1}{2}\,\frac{\partial^2 \tilde{H}_0}{\partial J^2}\,(J_0 - J)^2 + \ldots \\ &\qquad + \epsilon\, \tilde{H}_1(\phi_0, J_0) + \epsilon\, \frac{\partial \tilde{H}_1}{\partial J}\,(J_0 - J) + \ldots \\ &= \tilde{H}_0(J) + \bigg(\tilde{H}_1(\phi_0, J_0) + \frac{\partial \tilde{H}_0}{\partial J}\,\frac{\partial S_1}{\partial \phi_0}\bigg)\,\epsilon && (5.274) \\ &\qquad + \bigg(\frac{\partial \tilde{H}_0}{\partial J}\,\frac{\partial S_2}{\partial \phi_0} + \frac{1}{2}\,\frac{\partial^2 \tilde{H}_0}{\partial J^2}\,\bigg(\frac{\partial S_1}{\partial \phi_0}\bigg)^2 + \frac{\partial \tilde{H}_1}{\partial J}\,\frac{\partial S_1}{\partial \phi_0}\bigg)\,\epsilon^2 + \ldots\ . \end{aligned}$$

Equating terms, then,

$$\begin{aligned} E_0(J) &= \tilde{H}_0(J) && (5.275) \\ E_1(J) &= \tilde{H}_1(\phi_0, J) + \frac{\partial \tilde{H}_0}{\partial J}\,\frac{\partial S_1}{\partial \phi_0} && (5.276) \\ E_2(J) &= \frac{\partial \tilde{H}_0}{\partial J}\,\frac{\partial S_2}{\partial \phi_0} + \frac{1}{2}\,\frac{\partial^2 \tilde{H}_0}{\partial J^2}\,\bigg(\frac{\partial S_1}{\partial \phi_0}\bigg)^2 + \frac{\partial \tilde{H}_1}{\partial J}\,\frac{\partial S_1}{\partial \phi_0}\ . && (5.277) \end{aligned}$$

How, one might ask, can we be sure that the LHS of each equation in the above hierarchy depends only on J when each RHS seems to depend on ϕ_0 as well? The answer is that we use the freedom to choose each S_k to make this so. We demand each RHS be independent of ϕ_0, which means it must be equal to its average, $\langle\, \mathrm{RHS}(\phi_0)\, \rangle$, where

$$\big\langle f\big(\phi_0\big) \big\rangle = \int\limits_0^{2\pi} \frac{d\phi_0}{2\pi}\, f\big(\phi_0\big)\ . \qquad (5.278)$$

The average is performed *at fixed* J and *not* at fixed J_0. In this regard, we note that holding J constant and increasing ϕ_0 by 2π also returns us to the same starting point. Therefore, J is a periodic function of ϕ_0. We must then be able to write

$$S_k(\phi_0, J) = \sum_{m=-\infty}^{\infty} S_k(J; m)\, e^{im\phi_0} \qquad (5.279)$$

for each $k > 0$, in which case

$$\bigg\langle \frac{\partial S_k}{\partial \phi_0} \bigg\rangle = \frac{1}{2\pi}\big[S_k(2\pi) - S_k(0)\big] = 0\ . \qquad (5.280)$$

Let's see how this averaging works to the first two orders of the hierarchy. Since $\tilde{H}_0(J)$ is independent of ϕ_0 and since $\partial S_1/\partial\phi_0$ is periodic, we have

$$E_1(J) = \big\langle \tilde{H}_1(\phi_0, J)\big\rangle + \frac{\partial \tilde{H}_0}{\partial J} \overbrace{\left\langle \frac{\partial S_1}{\partial \phi_0} \right\rangle}^{\text{this vanishes!}} \tag{5.281}$$

and hence S_1 must satisfy

$$\frac{\partial S_1}{\partial \phi_0} = \frac{\langle \tilde{H}_1 \rangle - \tilde{H}_1}{\nu_0(J)} \ , \tag{5.282}$$

where $\nu_0(J) = \partial \tilde{H}_0/\partial J$. Clearly the RHS of eqn. 5.282 has zero average, and must be a periodic function of ϕ_0. The solution is $S_1 = S_1(\phi_0, J) + g(J)$, where $g(J)$ is an arbitrary function of J. However, $g(J)$ affects only the difference $\phi - \phi_0$, changing it by a constant value $g'(J)$. So there is no harm in taking $g(J) = 0$.

Next, let's go to second order in ϵ. We have

$$E_2(J) = \left\langle \frac{\partial \tilde{H}_1}{\partial J}\, \frac{\partial S_1}{\partial \phi_0} \right\rangle + \tfrac{1}{2} \frac{\partial \nu_0}{\partial J} \left\langle \left(\frac{\partial S_1}{\partial \phi_1} \right)^2 \right\rangle + \nu_0(J) \overbrace{\left\langle \frac{\partial S_2}{\partial \phi_0} \right\rangle}^{\text{this vanishes!}} \quad . \tag{5.283}$$

The equation for S_2 is then

$$\begin{aligned} \frac{\partial S_2}{\partial \phi_0} = \frac{1}{\nu_0^2(J)} \Bigg\{ & \left\langle \frac{\partial \tilde{H}_1}{\partial J} \right\rangle \langle \tilde{H}_0 \rangle - \left\langle \frac{\partial \tilde{H}_1}{\partial J}\, \tilde{H}_0 \right\rangle - \frac{\partial \tilde{H}_1}{\partial J}\, \langle \tilde{H}_1 \rangle + \frac{\partial \tilde{H}_1}{\partial J}\, \tilde{H}_1 \\ & + \frac{1}{2}\, \frac{\partial \ln \nu_0}{\partial J} \left(\langle \tilde{H}_1^2 \rangle - 2 \langle \tilde{H}_1 \rangle^2 + 2 \langle \tilde{H}_1 \rangle - \tilde{H}_1^2 \right) \Bigg\} \ . \end{aligned} \tag{5.284}$$

The expansion for the energy $E(J)$ is then

$$\begin{aligned} E(J) = \tilde{H}_0(J) + \epsilon \langle \tilde{H}_1 \rangle + \frac{\epsilon^2}{\nu_0(J)} \Bigg\{ & \left\langle \frac{\partial \tilde{H}_1}{\partial J} \right\rangle \langle \tilde{H}_1 \rangle - \left\langle \frac{\partial \tilde{H}_1}{\partial J}\, \tilde{H}_1 \right\rangle \\ & + \frac{1}{2}\, \frac{\partial \ln \nu_0}{\partial J} \left(\langle \tilde{H}_1^2 - \langle \tilde{H}_1 \rangle^2 \right) \Bigg\} + \mathcal{O}(\epsilon^3) \ . \end{aligned} \tag{5.285}$$

Note that we don't need S to find $E(J)$! The perturbed frequencies are

$$\nu(J) = \frac{\partial E}{\partial J} \ . \tag{5.286}$$

Sometimes the frequencies are all that is desired. However, we can of course obtain the full motion of the system via the succession of canonical transformations,

$$(\phi, J) \longrightarrow (\phi_0, J_0) \longrightarrow (q, p) \ . \tag{5.287}$$

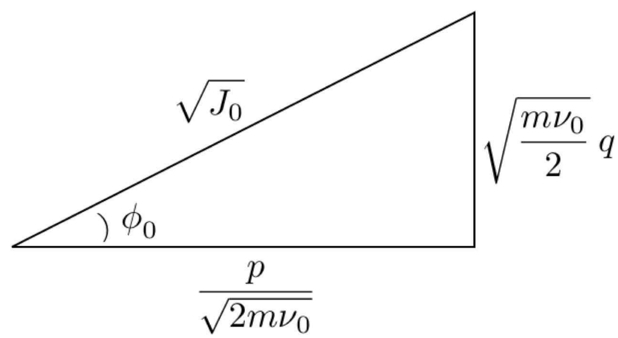

Figure 5.4: Action-angle variables for the harmonic oscillator.

5.9.3 Example : Nonlinear Oscillator

Consider the nonlinear oscillator with Hamiltonian

$$H(q,p) = \overbrace{\frac{p^2}{2m} + \tfrac{1}{2}m\nu_0^2 q^2}^{H_0} + \tfrac{1}{4}\epsilon\alpha q^4 \ . \tag{5.288}$$

The action-angle variables for the harmonic oscillator Hamiltonian H_0 are

$$\phi_0 = \tan^{-1}\!\big(mvq/p\big) \quad , \quad J_0 = \frac{p^2}{2m\nu_0} + \tfrac{1}{2}m\nu_0 q^2 \ , \tag{5.289}$$

and the relation between (ϕ_0, J_0) and (q,p) is further depicted in fig. 5.4. Note $H_0 = \nu_0\, J_0$. For the full Hamiltonian, we have

$$\begin{aligned}\tilde{H}(\phi_0, J_0) &= \nu_0 J_0 + \tfrac{1}{4}\epsilon\,\alpha\bigg(\sqrt{\frac{2J_0}{m\nu_0}}\ \sin\phi_0\bigg)^4 \\ &= \nu_0 J_0 + \frac{\epsilon\alpha}{m^2\nu_0^2}\, J_0^2\, \sin^4\!\phi_0 \ . \end{aligned} \tag{5.290}$$

We may now evaluate

$$E_1(J) = \big\langle \tilde{H}_1 \big\rangle = \frac{\alpha J^2}{m^2\nu_0^2}\int\limits_0^{2\pi}\frac{d\phi_0}{2\pi}\,\sin^4\!\phi_0 = \frac{3\alpha J^2}{8m^2\nu_0^2} \ . \tag{5.291}$$

The frequency, to order ϵ, is

$$\nu(J) = \nu_0 + \frac{3\,\epsilon\,\alpha J}{4m^2\nu_0^2} \ . \tag{5.292}$$

Now to lowest order in ϵ, we may replace J by $J_0 = \frac{1}{2}m\nu_0 A^2$, where A is the amplitude of the q motion. Thus,

$$\nu(A) = \nu_0 + \frac{3\epsilon\alpha}{8m\nu_0} \ . \tag{5.293}$$

This result agrees with that obtained via heavier lifting, using the Poincaré-Lindstedt method.

Next, let's evaluate the canonical transformation $(\phi_0, J_0) \to (\phi, J)$. We have

$$\nu_0 \, \frac{\partial S_1}{\partial \phi_0} = \frac{\alpha J^2}{m^2 \nu_0^2} \left(\tfrac{3}{8} - \sin^4\!\phi_0 \right) \qquad \Rightarrow$$

$$S(\phi_0, J) = \phi_0 \, J + \frac{\epsilon \alpha J^2}{8m^2 \nu_0^3} \left(3 + 2\sin^2\!\phi_0\right) \, \sin\phi_0 \, \cos\phi_0 + \mathcal{O}(\epsilon^2) \ . \tag{5.294}$$

Thus,

$$\phi = \frac{\partial S}{\partial J} = \phi_0 + \frac{\epsilon \alpha J}{4m^2 \nu_0^3} \left(3 + 2\sin^2\!\phi_0\right) \, \sin\phi_0 \, \cos\phi_0 + \mathcal{O}(\epsilon^2) \tag{5.295}$$

$$J_0 = \frac{\partial S}{\partial \phi_0} = J + \frac{\epsilon \alpha J^2}{8m^2 \nu_0^3} \left(4\cos 2\phi_0 - \cos 4\phi_0\right) + \mathcal{O}(\epsilon^2) \ . \tag{5.296}$$

Again, to lowest order, we may replace J by J_0 in the above, whence

$$J = J_0 - \frac{\epsilon \alpha J_0^2}{8m^2 \nu_0^3} \left(4\cos 2\phi_0 - \cos 4\phi_0\right) + \mathcal{O}(\epsilon^2) \tag{5.297}$$

$$\phi = \phi_0 + \frac{\epsilon \alpha J_0}{8m^2 \nu_0^3} \left(3 + 2\sin^2\!\phi_0\right) \, \sin 2\phi_0 + \mathcal{O}(\epsilon^2) \ . \tag{5.298}$$

To obtain (q, p) in terms of (ϕ, J) is not analytically tractable – the relations cannot be analytically inverted.

5.9.4 $n > 1$ Systems : Degeneracies and Resonances

Generalizing the procedure we derived for $n = 1$, we obtain

$$J_0^\alpha = \frac{\partial S}{\partial \phi_0^\alpha} = J^\alpha + \epsilon \, \frac{\partial S_1}{\partial \phi_0^\alpha} + \epsilon^2 \, \frac{\partial S_2}{\partial \phi_0^\alpha} + \ldots \tag{5.299}$$

$$\phi^\alpha = \frac{\partial S}{\partial J^\alpha} = \phi_0^\alpha + \epsilon \, \frac{\partial S_1}{\partial J^\alpha} + \epsilon^2 \, \frac{\partial S_2}{\partial J^\alpha} + \ldots \tag{5.300}$$

and

$$E_0(\boldsymbol{J}) = \tilde{H}_0(\boldsymbol{J}) \tag{5.301}$$

$$E_1(\boldsymbol{J}) = \tilde{H}_0(\boldsymbol{\phi}_0, \boldsymbol{J}) + \nu_0^\alpha(\boldsymbol{J}) \, \frac{\partial S_1}{\partial \phi_0^\alpha} \tag{5.302}$$

$$E_2(\boldsymbol{J}) = \frac{\partial \tilde{H}_0}{\partial J_\alpha} \, \frac{\partial S_2}{\partial \phi_0^\alpha} + \frac{1}{2} \, \frac{\partial \nu_0^\alpha}{\partial J^\beta} \, \frac{\partial S_1}{\partial \phi_0^\alpha} \, \frac{\partial S_1}{\partial \phi_0^\beta} + \nu_0^\alpha \, \frac{\partial S_1}{\partial \phi_0^\alpha} \ . \tag{5.303}$$

We now implement the averaging procedure, with

$$\big\langle f(J^1, \ldots, J^n) \big\rangle = \int\limits_0^{2\pi} \frac{d\phi_0^1}{2\pi} \, \cdots \int\limits_0^{2\pi} \frac{d\phi_0^n}{2\pi} \, f\big(\phi_0^1, \ldots, \phi_0^n, J^1, \ldots, J^n\big) \ . \tag{5.304}$$

The equation for S_1 is

$$\nu_0^\alpha \, \frac{\partial S_1}{\partial \phi_0^\alpha} = \big\langle \tilde{H}_1 \big\rangle - \tilde{H}_1 \equiv -{\sum_{\boldsymbol{\ell}}}' V_{\boldsymbol{\ell}} \, e^{i\boldsymbol{\ell}\cdot\boldsymbol{\phi}} \ , \tag{5.305}$$

where $\boldsymbol{\ell} = \{\ell^1, \ell^2, \ldots, \ell^n\}$, with each ℓ^σ an integer, and with $\boldsymbol{\ell} \neq 0$. The solution is

$$S_1(\boldsymbol{\phi}_0, \boldsymbol{J}) = i \, {\sum_l}' \frac{V_{\boldsymbol{\ell}}}{\boldsymbol{\ell}\cdot\boldsymbol{\nu}_0} \, e^{i\boldsymbol{\ell}\cdot\boldsymbol{\phi}} \ . \tag{5.306}$$

where $\boldsymbol{\ell}\cdot\boldsymbol{\nu}_0 = l^\alpha \nu_0^\alpha$. When two or more of the frequencies $\nu_\alpha(J)$ are *commensurate*, there exists a set of integers l such that the denominator of $D(l)$ vanishes. But even when the frequencies are not rationally related, one can approximate the ratios $\nu_0^\alpha / \nu_0^{\alpha'}$ by rational numbers, and for large enough l the denominator can become arbitrarily small.

Periodic time-dependent perturbations present a similar problem. Consider the system

$$H(\boldsymbol{\phi}, \boldsymbol{J}, t) = H_0(\boldsymbol{J}) + \epsilon \, V(\boldsymbol{\phi}, \boldsymbol{J}, t) \ , \tag{5.307}$$

where $V(t+T) = V(t)$. This means we may write

$$\begin{aligned} V(\boldsymbol{\phi}, \boldsymbol{J}, t) &= \sum_k V_k(\boldsymbol{\phi}, \boldsymbol{J}) \, e^{-ik\Omega t} &(5.308)\\ &= \sum_{\boldsymbol{k}} \sum_{\boldsymbol{\ell}} \hat{V}_{k,\boldsymbol{\ell}}(\boldsymbol{J}) \, e^{i\boldsymbol{\ell}\cdot\boldsymbol{\phi}} \, e^{-ik\Omega t} \ . &(5.309)\end{aligned}$$

by Fourier transforming from both time and angle variables; here $\Omega = 2\pi/T$. Note that $V(\boldsymbol{\phi}, \boldsymbol{J}, t)$ is real if $V^*_{k,\boldsymbol{\ell}} = V_{-\boldsymbol{k},-l}$. The equations of motion are

$$\begin{aligned} \dot{J}^\alpha &= -\frac{\partial H}{\partial \phi^\alpha} = -i\epsilon \sum_{k,\boldsymbol{\ell}} l^\alpha \, \hat{V}_{k,\boldsymbol{\ell}}(\boldsymbol{J}) \, e^{i\boldsymbol{\ell}\cdot\boldsymbol{\phi}} \, e^{-ik\Omega t} &(5.310)\\ \dot{\phi}^\alpha &= +\frac{\partial H}{\partial J^\alpha} = \nu_0^\alpha(\boldsymbol{J}) + \epsilon \sum_{k,\boldsymbol{\ell}} \frac{\partial \hat{V}_{k,\boldsymbol{\ell}}(\boldsymbol{J})}{\partial J^\alpha} \, e^{i\boldsymbol{\ell}\cdot\boldsymbol{\phi}} \, e^{-ik\Omega t} \ . &(5.311)\end{aligned}$$

We now expand in ϵ:

$$\begin{aligned} \phi^\alpha &= \phi_0^\alpha + \epsilon \, \phi_1^\alpha + \epsilon^2 \, \phi_2^\alpha + \ldots &(5.312)\\ J^\alpha &= J_0^\alpha + \epsilon \, J_1^\alpha + \epsilon^2 \, J_2^\alpha + \ldots \ . &(5.313)\end{aligned}$$

To order ϵ^0, $J^\alpha = J_0^\alpha$ and $\phi_0^\alpha = \nu_0^\alpha \, t + \beta_0^\alpha$. To order ϵ^1,

$$\dot{J}_1^\alpha = -i \sum_{k,l} l^\alpha \, \hat{V}_{k,\boldsymbol{\ell}}(\boldsymbol{J}_0) \, e^{i(\boldsymbol{\ell}\cdot\boldsymbol{\nu}_0 - k\Omega)t} \, e^{i\boldsymbol{\ell}\cdot\boldsymbol{\beta}_0} \tag{5.314}$$

and

$$\dot{\phi}_1^\alpha = \frac{\partial \nu_0^\alpha}{\partial J^\beta} \, J_1^\beta + \sum_{k,\boldsymbol{\ell}} \frac{\partial \hat{V}_{k,\boldsymbol{\ell}}(\boldsymbol{J})}{\partial J^\alpha} \, e^{i(\boldsymbol{\ell}\cdot\boldsymbol{\nu}_0 - k\Omega)t} \, e^{i\boldsymbol{\ell}\cdot\boldsymbol{\beta}_0} \ , \tag{5.315}$$

where derivatives are evaluated at $\boldsymbol{J} = \boldsymbol{J}_0$. The solution is:

$$J_1^\alpha = \sum_{k,\boldsymbol{\ell}} \frac{l^\alpha \, \hat{V}_{k,\boldsymbol{\ell}}(J_0)}{k\Omega - \boldsymbol{\ell}\cdot\boldsymbol{\nu}_0} \, e^{i(\boldsymbol{\ell}\cdot\boldsymbol{\nu}_0 - k\Omega)t} \, e^{i\boldsymbol{\ell}\cdot\boldsymbol{\beta}_0} \tag{5.316}$$

$$\phi_1^\alpha = \left\{ \frac{\partial\nu_0^\alpha}{\partial J^\beta} \, \frac{l^\beta \, \hat{V}_{k,\boldsymbol{\ell}}(J_0)}{(k\Omega - \boldsymbol{\ell}\cdot\boldsymbol{\nu}_0)^2} + \frac{\partial\hat{V}_{k,\boldsymbol{\ell}}(J)}{\partial J^\alpha} \, \frac{1}{k\Omega - \boldsymbol{\ell}\cdot\boldsymbol{\nu}_0} \right\} e^{i(\boldsymbol{\ell}\cdot\boldsymbol{\nu}_0 - k\Omega)t} \, e^{i\boldsymbol{\ell}\cdot\boldsymbol{\beta}_0} \ . \tag{5.317}$$

When the resonance condition,

$$k\Omega = \boldsymbol{\ell}\cdot\boldsymbol{\nu}_0(\boldsymbol{J}_0) \ , \tag{5.318}$$

holds, the denominators vanish, and the perturbation theory breaks down.

5.9.5 Particle-Wave Interaction

Consider a particle of charge e moving in the presence of a constant magnetic field $\boldsymbol{B} = B\hat{\boldsymbol{z}}$ and a space- and time-varying electric field $\boldsymbol{E}(\boldsymbol{x},t)$, described by the Hamiltonian

$$H = \frac{1}{2m}\big(\boldsymbol{p} - \tfrac{e}{c}\boldsymbol{A}\big)^2 + \epsilon \, eV_0 \, \cos(k_\perp x + k_z z - \omega t) \ , \tag{5.319}$$

where ϵ is a dimensionless expansion parameter. Working in the gauge $\boldsymbol{A} = Bx\hat{\boldsymbol{y}}$, from our earlier discussions in section 5.7.7, we may write

$$H = \omega_{\rm c} J + \frac{p_z^2}{2m} + \epsilon \, eV_0 \, \cos\left(k_z z + \frac{k_\perp P}{m\omega_{\rm c}} + k_\perp \sqrt{\frac{2J}{m\omega_{\rm c}}} \, \sin\phi - \omega t \right) \ . \tag{5.320}$$

Here,

$$x = \frac{P}{m\omega_{\rm c}} + \sqrt{\frac{2J}{m\omega_{\rm c}}} \, \sin\phi \qquad , \qquad y = Q + \sqrt{\frac{2J}{m\omega_{\rm c}}} \, \cos\phi \ , \tag{5.321}$$

with $\omega_{\rm c} = eB/mc$, the cyclotron frequency. We now make a mixed canonical transformation, generated by

$$F = \phi J' + \Big(k_z z + \frac{k_\perp P}{m\omega_{\rm c}} - \omega t \Big) K' - PQ' \ , \tag{5.322}$$

where the new sets of conjugate variables are $\big\{ (\phi', J') \, , \, (Q', P') \, , \, (\psi', K') \big\}$. We then have

$$\phi' = \frac{\partial F}{\partial J'} = \phi \qquad\qquad J = \frac{\partial F}{\partial \phi} = J' \tag{5.323}$$

$$Q = -\frac{\partial F}{\partial P} = -\frac{k_\perp K'}{m\omega_{\rm c}} + Q' \qquad\qquad P' = -\frac{\partial F}{\partial Q'} = P \tag{5.324}$$

$$\psi' = \frac{\partial F}{\partial K'} = k_z z + \frac{k_\perp P}{m\omega_{\rm c}} - \omega t \qquad\qquad p_z = \frac{\partial F}{\partial z} = k_z K' \ . \tag{5.325}$$

The transformed Hamiltonian is

$$\begin{aligned} H' &= H + \frac{\partial F}{\partial t} \\ &= \omega_{\rm c} J' + \frac{k_z^2}{2m} \, K'^2 - \omega K' + \epsilon \, eV_0 \, \cos\left(\psi' + k_\perp \sqrt{\frac{2J'}{m\omega_{\rm c}}} \, \sin\phi' \right) \ . \end{aligned} \tag{5.326}$$

We will now drop primes and simply write $H = H_0 + \epsilon\, H_1$, with

$$H_0 = \omega_c J + \frac{k_z^2}{2m}\, K^2 - \omega K \tag{5.327}$$

$$H_1 = eV_0 \,\cos\bigg(\psi + k_\perp \sqrt{\frac{2J}{m\omega_c}}\, \sin\phi\bigg) \ . \tag{5.328}$$

When $\epsilon = 0$, the frequencies associated with the ϕ and ψ motion are

$$\omega_\phi^0 = \frac{\partial H_0}{\partial \phi} = \omega_c \qquad , \qquad \omega_\psi^0 = \frac{\partial H_0}{\partial \psi} = \frac{k_z^2 K}{m} - \omega = k_z v_z - \omega \ , \tag{5.329}$$

where $v_z = p_z/m$ is the z-component of the particle's velocity. Now let us solve eqn. 5.305:

$$\omega_\phi^0\, \frac{\partial S_1}{\partial \phi} + \omega_\psi^0\, \frac{\partial S_1}{\partial \psi} = \langle\, H_1 \,\rangle - H_1 \ . \tag{5.330}$$

This yields

$$\begin{aligned}\omega_c\, \frac{\partial S_1}{\partial \phi} + \bigg(\frac{k_z^2 K}{m} - \omega\bigg) \frac{\partial S_1}{\partial \psi} &= -eA_0 \cos\bigg(\psi + k_\perp \sqrt{\frac{2J}{m\omega_c}}\, \sin\phi\bigg) \\ &= -eA_0 \sum_{n=-\infty}^{\infty} J_n\bigg(k_\perp \sqrt{\frac{2J}{m\omega_c}}\bigg)\, \cos(\psi + n\phi) \ ,\end{aligned} \tag{5.331}$$

where we have used the result

$$e^{iz\sin\theta} = \sum_{n=-\infty}^{\infty} J_n(z)\, e^{in\theta} \ . \tag{5.332}$$

The solution for S_1 is

$$S_1 = \sum_n \frac{eV_0}{\omega - n\omega_c - k_z^2 \bar{K}/m}\, J_n\bigg(k_\perp \sqrt{\frac{2\bar{J}}{m\omega_c}}\bigg)\, \sin(\psi + n\phi) \ . \tag{5.333}$$

We then have new action variables $\bar{J}$ and $\bar{K}$, where

$$J = \bar{J} + \epsilon\, \frac{\partial S_1}{\partial \phi} + \mathcal{O}(\epsilon^2) \tag{5.334}$$

$$K = \bar{K} + \epsilon\, \frac{\partial S_1}{\partial \psi} + \mathcal{O}(\epsilon^2) \ . \tag{5.335}$$

Defining the dimensionless variable

$$\lambda \equiv k_\perp \sqrt{\frac{2J}{m\omega_c}} \ , \tag{5.336}$$

we obtain the result

$$\bigg(\frac{m\omega_c^2}{2eV_0 k_\perp^2}\bigg) \bar{\lambda}^2 = \bigg(\frac{m\omega_c^2}{2eV_0 k_\perp^2}\bigg) \lambda^2 - \epsilon \sum_n \frac{nJ_n(\lambda)\cos(\psi + n\phi)}{\frac{\omega}{\omega_c} - n - \frac{k_z^2 K}{m\omega_c}} + \mathcal{O}(\epsilon^2) \ , \tag{5.337}$$

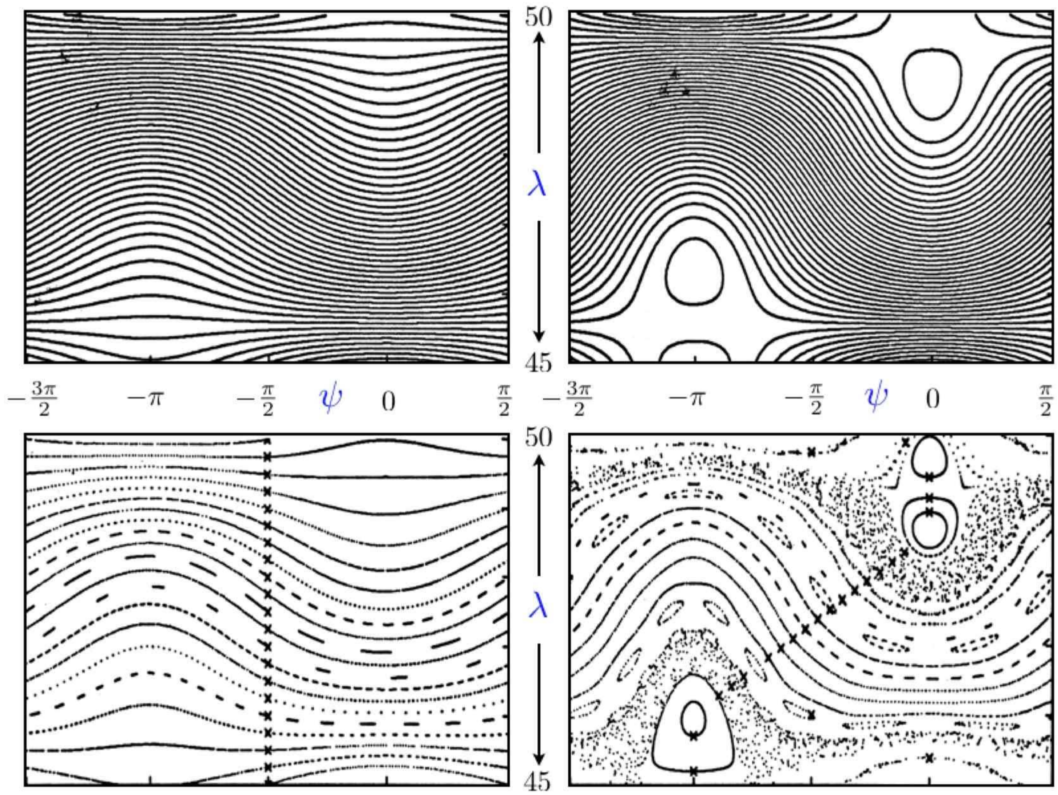

Figure 5.5: Plot of λ *versus* ψ for $\phi = 0$ (Poincaré section) for $\omega = 30.11\,\omega_c$ Top panels are nonresonant invariant curves calculated to first order. Bottom panels are exact numerical dynamics, with x symbols marking the initial conditions. Left panels: weak amplitude (no trapping). Right panels: stronger amplitude (shows trapping). From Lichtenberg and Lieberman (1983).

where $\bar{\lambda} = k_\perp \sqrt{2\bar{J}/m\omega_c}$.[14]

We see that resonances occur whenever

$$\frac{\omega}{\omega_c} - \frac{k_z^2 K}{m\omega_c} = n \;, \tag{5.338}$$

for any integer n. Let us consider the case $k_z = 0$, in which the resonance condition is $\omega = n\omega_c$. We then have

$$\frac{\bar{\lambda}^2}{2\alpha} = \frac{\lambda^2}{2\alpha} - \sum_n \frac{n\, J_n(\lambda)\cos(\psi + n\phi)}{\frac{\omega}{\omega_c} - n} \;, \tag{5.339}$$

where

$$\alpha = \frac{E_0}{B} \cdot \frac{ck_\perp}{\omega_c} \tag{5.340}$$

[14]Note that the argument of J_n in eqn. 5.337 is λ and not $\bar{\lambda}$. This arises because we are computing the new action $\bar{J}$ in terms of the old variables (ϕ, J) and (ψ, K).

is a dimensionless measure of the strength of the perturbation, with $E_0 \equiv k_\perp V_0$. In Fig. 5.5 we plot the level sets for the RHS of the above equation $\lambda(\psi)$ for $\phi = 0$, for two different values of the dimensionless amplitude α, for $\omega/\omega_c = 30.11$ (*i.e.* off resonance). Thus, when the amplitude is small, the level sets are far from a primary resonance, and the analytical and numerical results are very similar (left panels). When the amplitude is larger, resonances may occur which are not found in the lowest order perturbation treatment. However, as is apparent from the plots, the gross features of the phase diagram are reproduced by perturbation theory. What is missing is the existence of 'chaotic islands' which initially emerge in the vicinity of the trapping regions.

5.10 Adiabatic Invariants

Adiabatic perturbations are slow, smooth, time-dependent perturbations to a dynamical system. A classic example: a pendulum with a slowly varying length $l(t)$. Suppose $\lambda(t)$ is the adiabatic parameter. We write $H = H\big(q, p; \lambda(t)\big)$. All explicit time-dependence to H comes through $\lambda(t)$. Typically, a dimensionless parameter ϵ may be associated with the perturbation:

$$\epsilon = \frac{1}{\omega_0}\left|\frac{d\ln\lambda}{dt}\right| \ , \tag{5.341}$$

where ω_0 is the natural frequency of the system when λ is constant. We require $\epsilon \ll 1$ for adiabaticity. In adiabatic processes, the action variables are conserved to a high degree of accuracy. These are the *adiabatic invariants*. For example, for the harmonix oscillator, the action is $J = E/\nu$. While E and ν may vary considerably during the adiabatic process, their ratio is very nearly fixed. As a consequence, assuming small oscillations,

$$E = \nu J = \tfrac{1}{2} mgl\,\theta_0^2 \quad \Rightarrow \quad \theta_0(l) \approx \frac{2J}{m\sqrt{g}\,l^{3/2}} \ , \tag{5.342}$$

so $\theta_0(\ell) \propto l^{-3/4}$.

Suppose that for fixed λ the Hamiltonian is transformed to action-angle variables via the generator $S(q, J; \lambda)$. The transformed Hamiltonian is

$$\tilde{H}(\phi, J, t) = H(\phi, J; \lambda) + \frac{\partial S}{\partial \lambda}\,\frac{d\lambda}{dt} \ , \tag{5.343}$$

where

$$H(\phi, J; \lambda) = H\big(q(\phi, J; \lambda), p(\phi, J; \lambda); \lambda\big) \ . \tag{5.344}$$

We assume $n = 1$ here. Hamilton's equations are now

$$\dot{\phi} = +\frac{\partial \tilde{H}}{\partial J} = \nu(J; \lambda) + \frac{\partial^2 S}{\partial \lambda\, \partial J}\,\frac{d\lambda}{dt} \tag{5.345}$$

$$\dot{J} = -\frac{\partial \tilde{H}}{\partial \phi} = -\frac{\partial^2 S}{\partial \lambda\, \partial \phi}\,\frac{d\lambda}{dt} \ . \tag{5.346}$$

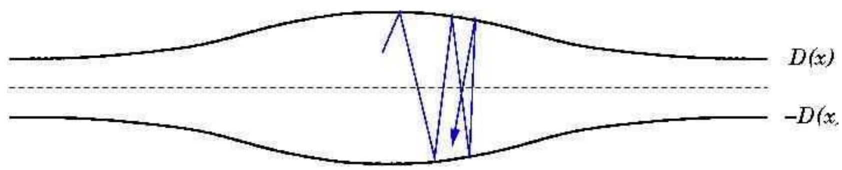

Figure 5.6: A mechanical mirror.

The second of these may be Fourier decomposed as

$$\dot{J} = -i\dot{\lambda} \sum_m m \, \frac{\partial S_m(J;\lambda)}{\partial \lambda} \, e^{im\phi} \ , \tag{5.347}$$

hence

$$\Delta J = J(t=+\infty) - J(t=-\infty) = -i \sum_m m \int_{-\infty}^{\infty} \! dt \, \frac{\partial S_m(J;\lambda)}{\partial \lambda} \, \frac{d\lambda}{dt} \, e^{im\phi} \ . \tag{5.348}$$

Since $\dot{\lambda}$ is small, we have $\phi(t) = \nu\, t + \beta$, to lowest order. We must therefore evaluate integrals such as

$$\mathcal{I}_m = \int_{-\infty}^{\infty} \! dt \, \frac{\partial S_m(J;\lambda)}{\partial \lambda} \, \frac{d\lambda}{dt} \, e^{im\nu t} \ . \tag{5.349}$$

The term in curly brackets is a smooth, slowly varying function of t. Call it $f(t)$. We presume $f(t)$ can be analytically continued off the real t axis, and that its closest singularity in the complex t plane lies at $t = \pm i\tau$, in which case $\mathcal{I}$ behaves as $\exp(-|m|\nu\tau)$. Consider, for example, the Lorentzian,

$$f(t) = \frac{\mathcal{C}}{1 + (t/\tau)^2} \qquad \Rightarrow \qquad \int_{-\infty}^{\infty} \! dt \, f(t) \, e^{im\nu t} = \pi\tau \, e^{-|m|\nu\tau} \ , \tag{5.350}$$

which is exponentially small in the time scale τ. Because of this, only $m = \pm 1$ need be considered. What this tells us is that the change ΔJ may be made arbitrarily small by a sufficiently slowly varying $\lambda(t)$.

5.10.1 Example: mechanical mirror

Consider a two-dimensional version of a mechanical mirror, depicted in fig. 5.6. A particle bounces between two curves, $y = \pm D(x)$, where $|D'(x)| << 1$. The bounce time is $\tau_{\mathrm{b}\perp} = 2D/v_y$. We assume $\tau \ll L/v_x$, where $v_{x,y}$ are the components of the particle's velocity, and L is the total length of the system. There are, therefore, many bounces, which means the particle gets to sample the curvature in $D(x)$.

The adiabatic invariant is the action,

$$J = \frac{1}{2\pi} \int\limits_{-D}^{D} dy\, m\, v_y + \frac{1}{2\pi} \int\limits_{D}^{-D} dy\, m\,(-v_y) = \frac{2}{\pi}\, m v_y\, D(x) \ . \tag{5.351}$$

Thus,

$$E = \tfrac{1}{2} m \big(v_x^2 + v_y^2\big) = \tfrac{1}{2} m v_x^2 + \frac{\pi^2 J^2}{8 m D^2(x)} \ , \tag{5.352}$$

or

$$v_x^2 = \frac{2E}{m} - \bigg(\frac{\pi J}{2 m D(x)}\bigg)^2 \ . \tag{5.353}$$

The particle is reflected in the throat of the device at horizontal coordinate x^*, where

$$D(x^*) = \frac{\pi J}{\sqrt{8 m E}} \ . \tag{5.354}$$

5.10.2 Example: magnetic mirror

Consider a particle of charge e moving in the presence of a uniform magnetic field $\boldsymbol{B} = B\hat{\boldsymbol{z}}$. Recall the basic physics: velocity in the parallel direction v_z is conserved, while in the plane perpendicular to $\boldsymbol{B}$ the particle executes circular 'cyclotron orbits', satisfying

$$\frac{m v_\perp^2}{\rho} = \frac{e}{c}\, v_\perp B \quad \Rightarrow \quad \rho = \frac{m c v_\perp}{eB} \ , \tag{5.355}$$

where ρ is the radial coordinate in the plane perpendicular to $\boldsymbol{B}$. The period of the orbits is $T = 2\pi\rho . v_\perp = 2\pi mc/eB$, hence their frequency is the cyclotron frequency $\omega_{\rm c} = eB/mc$.

Now assume that the magnetic field is spatially dependent. Note that a spatially varying $\boldsymbol{B}$-field cannot be unidirectional:

$$\boldsymbol{\nabla} \cdot \boldsymbol{B} = \boldsymbol{\nabla}_\perp \cdot \boldsymbol{B}_\perp + \frac{\partial B_z}{\partial z} = 0 \ . \tag{5.356}$$

The non-collinear nature of $\boldsymbol{B}$ results in the *drift* of the cyclotron orbits. Nevertheless, if the field $\boldsymbol{B}$ felt by the particle varies slowly on the time scale $T = 2\pi/\omega_{\rm c}$, then the system possesses an adiabatic invariant:

$$J = \frac{1}{2\pi} \oint\limits_{\mathcal{C}} \boldsymbol{p} \cdot d\boldsymbol{\ell} = \frac{1}{2\pi} \oint\limits_{\mathcal{C}} \big(m\boldsymbol{v} + \tfrac{e}{c}\, \boldsymbol{A}\big) \cdot d\boldsymbol{\ell} \tag{5.357}$$

$$= \frac{m}{2\pi} \oint\limits_{\mathcal{C}} \boldsymbol{v} \cdot d\boldsymbol{\ell} + \frac{e}{2\pi c} \oint\limits_{\text{int}(\mathcal{C})} \boldsymbol{B} \cdot \hat{\boldsymbol{n}}\, d\Sigma \ . \tag{5.358}$$

The last two terms are of opposite sign, and one has

$$J = -\frac{m}{2\pi} \cdot \frac{\rho e B_z}{mc} \cdot 2\pi\rho + \frac{e}{2\pi c} \cdot B_z \cdot \pi\rho^2 \tag{5.359}$$

$$= -\frac{e B_z \rho^2}{2c} = -\frac{e}{2\pi c} \cdot \Phi_B(\mathcal{C}) = -\frac{m^2 v_\perp^2 c}{2 e B_z} \ , \tag{5.360}$$

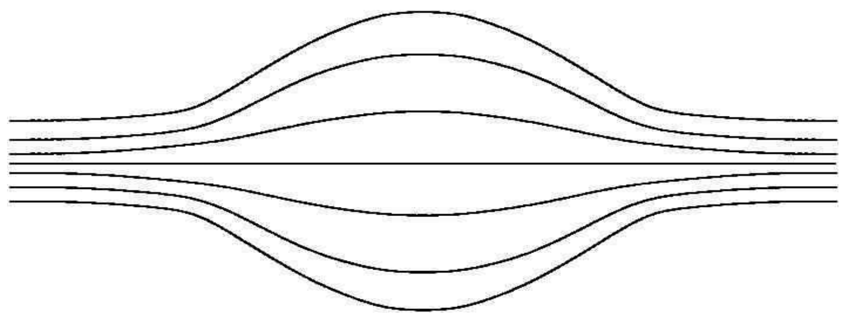

Figure 5.7: $\boldsymbol{B}$ field lines in a magnetic bottle.

where $\Phi_B(\mathcal{C})$ is the magnetic flux enclosed by $\mathcal{C}$.

The energy is

$$E = \tfrac{1}{2}mv_\perp^2 + \tfrac{1}{2}mv_z^2 \ , \tag{5.361}$$

hence we have

$$v_z = \sqrt{\frac{2}{m}\big(E - MB\big)} \ . \tag{5.362}$$

where

$$M \equiv -\frac{e}{mc}\,J = \frac{e^2}{2\pi mc^2}\,\Phi_{\rm B}(\mathcal{C}) \tag{5.363}$$

is the *magnetic moment*. Note that v_z vanishes when $B = B_{\rm max} = E/M$. When this limit is reached, the particle turns around. This is a *magnetic mirror*. A pair of magnetic mirrors may be used to confine charged particles in a *magnetic bottle*, depicted in fig. 5.7.

Let $v_{\|,0}$, $\boldsymbol{v}_{\perp,0}$, and $B_{\|,0}$ be the longitudinal particle velocity, transverse particle velocity, and longitudinal component of the magnetic field, respectively, at the point of injection. Our two conservation laws (J and E) guarantee

$$v_\|^2(z) + v_\perp^2(z) = v_{\|,0}^2 + v_{\perp,0}^2 \tag{5.364}$$

$$\frac{v_\perp(z)^2}{B_\|(z)} = \frac{v_{\perp,0}^2}{B_{\|,0}} \ . \tag{5.365}$$

This leads to reflection at a longitudinal coordinate z^*, where

$$B_\|(z^*) = B_{\|,0}\sqrt{1 + \frac{v_{\|,0}^2}{v_{\perp,0}^2}} \ . \tag{5.366}$$

The physics is quite similar to that of the mechanical mirror.

5.10.3 Resonances

When $n > 1$, we have

$$\dot{J}^\alpha = -i\dot{\lambda} \sum_{\boldsymbol{m}} m^\alpha \, \frac{\partial S_m(J;\lambda)}{\partial \lambda} \, e^{i\boldsymbol{m}\cdot\boldsymbol{\phi}} \tag{5.367}$$

$$\Delta J = -i \sum_{\boldsymbol{m}} m^\alpha \int\limits_{-\infty}^{\infty} \! dt \, \frac{\partial S_{\boldsymbol{m}}(J;\lambda)}{\partial \lambda} \, \frac{d\lambda}{dt} \, e^{i\boldsymbol{m}\cdot\boldsymbol{\nu} t} \, e^{i\boldsymbol{m}\cdot\boldsymbol{\beta}} \; . \tag{5.368}$$

Therefore, when $\boldsymbol{m}\cdot\boldsymbol{\nu}(J) = 0$ we have a resonance, and the integral grows linearly with time – a violation of the adiabatic invariance of J^α.

5.11 Appendix : Canonical Perturbation Theory

Consider the Hamiltonian

$$H = \frac{p^2}{2m} + \tfrac{1}{2} m\,\omega_0^2\, q^2 + \tfrac{1}{3}\epsilon\, m\,\omega_0^2\, \frac{q^3}{a} \; ,$$

where ϵ is a small dimensionless parameter.

(a) Show that the oscillation frequency satisfies $\nu(J) = \omega_0 + \mathcal{O}(\epsilon^2)$. That is, show that the first order (in ϵ) frequency shift vanishes.

Solution: It is good to recall the basic formulae

$$q = \sqrt{\frac{2J_0}{m\omega_0}} \, \sin\phi_0 \qquad , \qquad p = \sqrt{2m\,\omega_0\, J_0} \, \cos\phi_0 \tag{5.369}$$

as well as the results

$$J_0 = \frac{\partial S}{\partial \phi_0} = J + \epsilon\, \frac{\partial S_1}{\partial \phi_0} + \epsilon^2\, \frac{\partial S_2}{\partial \phi_0} + \ldots \tag{5.370}$$

$$\phi = \frac{\partial S}{\partial J} = \phi_0 + \epsilon\, \frac{\partial S_1}{\partial J} + \epsilon^2\, \frac{\partial S_2}{\partial J} + \ldots \; , \tag{5.371}$$

and

$$E_0(J) = \tilde{H}_0(J) \tag{5.372}$$

$$E_1(J) = \tilde{H}_1(\phi_0, J) + \frac{\partial \tilde{H}_0}{\partial J}\, \frac{\partial S_1}{\partial \phi_0} \tag{5.373}$$

$$E_2(J) = \frac{\partial \tilde{H}_0}{\partial J}\, \frac{\partial S_2}{\partial \phi_0} + \frac{1}{2}\, \frac{\partial^2 \tilde{H}_0}{\partial J^2} \left(\frac{\partial S_1}{\partial \phi_0}\right)^{\!2} + \frac{\partial \tilde{H}_1}{\partial J}\, \frac{\partial S_1}{\partial \phi_0} \; . \tag{5.374}$$

Expressed in action-angle variables,

$$\tilde{H}_0(\phi_0, J) = \omega_0\, J \tag{5.375}$$

$$\tilde{H}_1(\phi_0, J) = \frac{2}{3}\sqrt{\frac{2\omega_0}{ma^2}}\, J^{3/2}\, \sin^3\!\phi_0 \ . \tag{5.376}$$

Thus, $\nu_0 = \frac{\partial \tilde{H}_0}{\partial J} = \omega_0$.

Averaging the equation for $E_1(J)$ yields

$$E_1(J) = \big\langle \tilde{H}_1(\phi_0, J)\big\rangle = \frac{2}{3}\sqrt{\frac{2\omega_0}{ma^2}}\, J^{3/2}\, \big\langle \sin^3\!\phi_0\big\rangle = 0 \ . \tag{5.377}$$

(b) Compute the frequency shift $\nu(J)$ to second order in ϵ.

Solution : From the equation for E_1, we also obtain

$$\frac{\partial S_1}{\partial \phi_0} = \frac{1}{\nu_0}\Big(\big\langle \tilde{H}_1\big\rangle - \tilde{H}_1\Big) \ . \tag{5.378}$$

Inserting this into the equation for $E_2(J)$ and averaging then yields

$$E_2(J) = \frac{1}{\nu_0}\bigg\langle \frac{\partial \tilde{H}_1}{\partial J}\Big(\big\langle \tilde{H}_1\big\rangle - \tilde{H}_1\Big)\bigg\rangle = -\frac{1}{\nu_0}\bigg\langle \tilde{H}_1\, \frac{\partial \tilde{H}_1}{\partial J}\bigg\rangle \tag{5.379}$$

$$= -\frac{4\nu_0 J^2}{3ma^2}\, \big\langle \sin^6\!\phi_0\big\rangle \tag{5.380}$$

In computing the average of $\sin^6\!\phi_0$, it is good to recall the binomial theorem, or the Fibonacci tree. The sixth order coefficents are easily found to be $\{1, 6, 15, 20, 15, 6, 1\}$, whence

$$\sin^6\!\phi_0 = \frac{1}{(2i)^6}\big(e^{i\phi_0} - e^{-i\phi_0}\big)^6 \tag{5.381}$$

$$= \tfrac{1}{64}\big(- 2\sin 6\phi_0 + 12\sin 4\phi_0 - 30\sin 2\phi_0 + 20\big) \ . \tag{5.382}$$

Thus,

$$\big\langle \sin^6\!\phi_0\big\rangle = \tfrac{5}{16} \ , \tag{5.383}$$

whence

$$E(J) = \omega_0\, J - \tfrac{5}{12}\epsilon^2\, \frac{J^2}{ma^2} \tag{5.384}$$

and

$$\nu(J) = \frac{\partial E}{\partial J} = \omega_0 - \tfrac{5}{6}\epsilon^2\, \frac{J}{ma^2} \ . \tag{5.385}$$

(c) Find $q(t)$ to order ϵ. Your result should be finite for all times.

Solution : From the equation for $E_1(J)$, we have

$$\frac{\partial S_1}{\partial \phi_0} = -\frac{2}{3}\sqrt{\frac{2J^3}{m\omega_0 a^2}}\, \sin^3\!\phi_0 \ . \tag{5.386}$$

Integrating, we obtain

$$S_1(\phi_0, J) = \frac{2}{3}\sqrt{\frac{2J^3}{m\omega_0 a^2}}\,\big(\cos\phi_0 - \tfrac{1}{3}\cos^3\phi_0\big) \tag{5.387}$$

$$= \frac{J^{3/2}}{\sqrt{2m\omega_0 a^2}}\,\big(\cos\phi_0 - \tfrac{1}{9}\cos 3\phi_0\big)\ . \tag{5.388}$$

Thus, with

$$S(\phi_0, J) = \phi_0\, J + \epsilon\, S_1(\phi_0, J) + \ldots\ , \tag{5.389}$$

we have

$$\phi = \frac{\partial S}{\partial J} = \phi_0 + \frac{3}{2}\frac{\epsilon\, J^{1/2}}{\sqrt{2m\omega_0 a^2}}\,\big(\cos\phi_0 - \tfrac{1}{9}\cos 3\phi_0\big) \tag{5.390}$$

$$J_0 = \frac{\partial S}{\partial \phi_0} = J - \frac{\epsilon\, J^{3/2}}{\sqrt{2m\omega_0 a^2}}\,\big(\sin\phi_0 - \tfrac{1}{3}\sin 3\phi_0\big)\ . \tag{5.391}$$

Inverting, we may write ϕ_0 and J_0 in terms of ϕ and J:

$$\phi_0 = \phi + \frac{3}{2}\frac{\epsilon\, J^{1/2}}{\sqrt{2m\omega_0 a^2}}\,\big(\tfrac{1}{9}\cos 3\phi - \cos\phi\big) \tag{5.392}$$

$$J_0 = J + \frac{\epsilon\, J^{3/2}}{\sqrt{2m\omega_0 a^2}}\,\big(\tfrac{1}{3}\sin 3\phi - \sin\phi\big)\ . \tag{5.393}$$

Thus,

$$q(t) = \sqrt{\frac{2J_0}{m\omega_0}}\ \sin\phi_0 \tag{5.394}$$

$$= \sqrt{\frac{2J}{m\omega_0}}\ \sin\phi\cdot\Big(1 + \frac{\delta J}{2J} + \ldots\Big)\Big(\sin\phi + \delta\phi\ \cos\phi + \ldots\Big) \tag{5.395}$$

$$= \sqrt{\frac{2J}{m\omega_0}}\ \sin\phi - \frac{\epsilon\, J}{m\omega_0 a}\,\big(1 + \tfrac{1}{3}\cos 2\phi\big) + \mathcal{O}\big(\epsilon^2\big)\ , \tag{5.396}$$

with

$$\phi(t) = \phi(0) + \nu(J)\, t\ . \tag{5.397}$$

Chapter 6

Ergodicity and the Approach to Equilibrium

6.1 Equilibrium

Recall that a thermodynamic system is one containing an enormously large number of constituent particles, a typical 'large number' being Avogadro's number, $N_{\mathrm{A}} = 6.02 \times 10^{23}$. Nevertheless, in *equilibrium*, such a system is characterized by a relatively small number of thermodynamic state variables. Thus, while a complete description of a (classical) system would require us to account for $\mathcal{O}\big(10^{23}\big)$ evolving degrees of freedom, with respect to the physical quantities in which we are interested, the details of the initial conditions are effectively forgotten over some microscopic time scale τ, called the collision time, and over some microscopic distance scale, ℓ, called the mean free path[1]. The equilibrium state is time-independent.

6.2 The Master Equation

Relaxation to equilibrium is often modeled with something called the *master equation*. Let $P_i(t)$ be the probability that the system is in a quantum or classical state i at time t. Then write

$$\frac{dP_i}{dt} = \sum_j \big(W_{ji}\, P_j - W_{ij}\, P_i\big) \ . \tag{6.1}$$

Here, W_{ij} is the rate at which i makes a transition to j. Note that we can write this equation as

$$\frac{dP_i}{dt} = -\sum_j \Gamma_{ij}\, P_j \ , \tag{6.2}$$

[1]Exceptions involve quantities which are conserved by collisions, such as overall particle number, momentum, and energy. These quantities relax to equilibrium in a special way called *hydrodynamics*.

where

$$\Gamma_{ij} = \begin{cases} -W_{ji} & \text{if } i \neq j \\ \sum_k' W_{jk} & \text{if } i = j \ , \end{cases} \tag{6.3}$$

where the prime on the sum indicates that $k = j$ is to be excluded. The constraints on the W_{ij} are that $W_{ij} \geq 0$ for all i, j, and we may take $W_{ii} \equiv 0$ (no sum on i). Fermi's Golden Rule of quantum mechanics says that

$$W_{ji} = \frac{2\pi}{\hbar} \left| \langle\, i \,|\, \hat{V} \,|\, j \,\rangle \right|^2 \rho(E_i) \ , \tag{6.4}$$

where $\hat{H}_0 \big|\, i \,\big\rangle = E_i \big|\, i \,\big\rangle$, $\hat{V}$ is an additional potential which leads to transitions, and $\rho(E_i)$ is the density of final states at energy E_i.

If the transition rates W_{ij} are themselves time-independent, then we may formally write

$$P_i(t) = \left(e^{-\Gamma t}\right)_{ij} P_j(0) \ . \tag{6.5}$$

Here we have used the Einstein 'summation convention' in which repeated indices are summed over (in this case, the j index). Note that

$$\sum_i \Gamma_{ij} = 0 \ , \tag{6.6}$$

which says that the total probability $\sum_i P_i$ is conserved:

$$\frac{d}{dt} \sum_i P_i = -\sum_{i,j} \Gamma_{ij} \, P_j = -\sum_j \Big(\sum_i \Gamma_{ij} \Big) P_j = 0 \ . \tag{6.7}$$

Suppose we have a time-independent solution to the master equation, P_i^{eq}. Then we must have

$$\Gamma_{ij} \, P_j^{\text{eq}} = 0 \qquad \Longrightarrow \qquad P_j^{\text{eq}} \, W_{ji} = P_i^{\text{eq}} \, W_{ij} . \tag{6.8}$$

This is called the condition of *detailed balance*. Assuming $W_{ij} \neq 0$ and $P_j^{\text{eq}} = 0$, we can divide to obtain

$$\frac{W_{ji}}{W_{ij}} = \frac{P_i^{\text{eq}}}{P_j^{\text{eq}}} \ . \tag{6.9}$$

6.2.1 Example: radioactive decay

Consider a group of atoms, some of which are in an excited state which can undergo nuclear decay. Let $P_n(t)$ be the probability that n atoms are excited at some time t. We then model the decay dynamics by

$$W_{nm} = \begin{cases} 0 & \text{if } m \geq n \\ n\gamma & \text{if } m = n - 1 \\ 0 & \text{if } m < n - 1 \ . \end{cases} \tag{6.10}$$

Here, γ is the decay rate of an individual atom, which can be determined from quantum mechanics. The master equation then tells us

$$\frac{dP_n}{dt} = (n+1)\,\gamma\,P_{n+1} - n\,\gamma\,P_n \ . \tag{6.11}$$

The interpretation here is as follows: let $\big|\,n\,\big\rangle$ denote a state in which n atoms are excited. Then $P_n(t) = \big|\langle\,\psi(t)\,|\,n\,\rangle\big|^2$. Then $P_n(t)$ will increase due to spontaneous transitions from $|\,n{+}1\,\rangle$ to $|\,n\,\rangle$, and will decrease due to spontaneous transitions from $|\,n\,\rangle$ to $|\,n{-}1\,\rangle$.

The average number of particles in the system is

$$N(t) = \sum_{n=0}^{\infty} n\,P_n(t) \ . \tag{6.12}$$

Note that

$$\begin{aligned} \frac{dN}{dt} &= \sum_{n=0}^{\infty} n\Big[(n+1)\,\gamma\,P_{n+1} - n\,\gamma\,P_n\Big] \\ &= \gamma\sum_{n=0}^{\infty}\Big[n(n-1)\,P_n - n^2 P_n\Big] \\ &= -\gamma\sum_{n=0}^{\infty} n\,P_n = -\gamma\,N \ . \end{aligned} \tag{6.13}$$

Thus,

$$N(t) = N(0)\,e^{-\gamma t} \ . \tag{6.14}$$

The relaxation time is $\tau = \gamma^{-1}$, and the equilibrium distribution is

$$P_n^{\rm eq} = \delta_{n,0} \ . \tag{6.15}$$

Note that this satisfies detailed balance.

We can go a bit farther here. Let us define

$$P(z,t) \equiv \sum_{n=0}^{\infty} z^n\,P_n(t) \ . \tag{6.16}$$

This is sometimes called a *generating function*. Then

$$\begin{aligned} \frac{\partial P}{\partial t} &= \gamma\sum_{n=0}^{\infty} z^n\Big[(n+1)\,P_{n+1} - n\,P_n\Big] \\ &= \gamma\,\frac{\partial P}{\partial z} - \gamma z\,\frac{\partial P}{\partial z} \ . \end{aligned} \tag{6.17}$$

Thus,

$$\frac{1}{\gamma}\,\frac{\partial P}{\partial t} - (1-z)\,\frac{\partial P}{\partial z} = 0 \ . \tag{6.18}$$

We now see that any function $f(\xi)$ satisfies the above equation, where $\xi = \gamma t - \ln(1-z)$. Thus, we can write

$$P(z,t) = f\big(\gamma t - \ln(1-z)\big) \ . \tag{6.19}$$

Setting $t=0$ we have $P(z,0) = f\big(-\ln(1-z)\big)$, and inverting this result we obtain $f(u) = P(1-e^{-u},0)$, *i.e.*

$$P(z,t) = P\big(1 + (z-1)\, e^{-\gamma t} \, , \, 0\big) \ . \tag{6.20}$$

The total probability is $P(z{=}1,t) = \sum_{n=0}^\infty P_n$, which clearly is conserved: $P(1,t) = P(1,0)$. The average particle number is

$$N(t) = \sum_{n=0}^\infty n\, P_n(t) = \frac{\partial P}{\partial z}\bigg|_{z=1} = \ e^{-\gamma t}\, P(1,0) = N(0)\, e^{-\gamma t} \ . \tag{6.21}$$

6.2.2 Decomposition of Γ_{ij}

The matrix Γ_{ij} is real but not necessarily symmetric. For such a matrix, the left eigenvectors ϕ^α_i and the right eigenvectors ψ^β_j are not the same: general different:

$$\phi^\alpha_i \, \Gamma_{ij} = \lambda_\alpha \, \phi^\alpha_j \tag{6.22}$$

$$\Gamma_{ij} \, \psi^\beta_j = \lambda_\beta \, \psi^\beta_i \ . \tag{6.23}$$

Note that the eigenvalue equation for the right eigenvectors is $\Gamma\psi = \lambda\psi$ while that for the left eigenvectors is $\Gamma^{\rm t}\phi = \lambda\phi$. The characteristic polynomial is the same in both cases:

$$\det\,(\lambda - \Gamma) = \det\,(\lambda - \Gamma^{\rm t}) \ , \tag{6.24}$$

which means that the left and right eigenvalues are the same. Multiplying the eigenvector equation for ϕ^α on the right by ψ^β_j and summing over j, and multiplying the eigenvector equation for ψ^β on the left by ϕ^α_i and summing over i, and subtracting the two results yields

$$\big(\lambda_\alpha - \lambda_\beta\big)\, \langle\, \phi^\alpha \,|\, \psi^\beta \,\rangle = 0 \ , \tag{6.25}$$

where the inner product is

$$\langle\, \phi \,|\, \psi \,\rangle = \sum_i \phi_i\, \psi_i \ . \tag{6.26}$$

We can now demand

$$\langle\, \phi^\alpha \,|\, \psi^\beta \,\rangle = \delta_{\alpha\beta} \ , \tag{6.27}$$

in which case we can write

$$\Gamma = \sum_\alpha \lambda_\alpha \,|\, \psi^\alpha \,\rangle\langle\, \phi^\beta \,| \qquad \Longleftrightarrow \qquad \Gamma_{ij} = \sum_\alpha \lambda_\alpha \, \psi^\alpha_i \, \phi^\alpha_j \ . \tag{6.28}$$

We note that $\vec{\phi} = (1,1,\ldots,1)$ is a left eigenvector with eigenvalue $\lambda=0$, since $\sum_i \Gamma_{ij} = 0$. We do not know *a priori* the corresponding right eigenvector, which depends on other details of Γ_{ij}. Now let's expand $P_i(t)$ in the right eigenvectors of Γ, writing

$$P_i(t) = \sum_\alpha C_\alpha(t)\, \psi^\alpha_i \ . \tag{6.29}$$

Then

$$\begin{aligned}\frac{dP_i}{dt} &= \sum_\alpha \frac{dC_\alpha}{dt}\,\psi_i^\alpha \\ &= -\Gamma_{ij}\,P_j = -\sum_\alpha C_\alpha\,\Gamma_{ij}\,\psi_j^\alpha \\ &= -\sum_\alpha \lambda_\alpha\,C_\alpha\,\psi_i^\alpha \ .\end{aligned} \tag{6.30}$$

This allows us to write

$$\frac{dC_\alpha}{dt} = -\lambda_\alpha\,C_\alpha \qquad \Longrightarrow \qquad C_\alpha(t) = C_\alpha(0)\,e^{-\lambda_\alpha t} \ . \tag{6.31}$$

Hence, we can write

$$P_i(t) = \sum_\alpha C_\alpha(0)\,e^{-\lambda_\alpha t}\,\psi_i^\alpha \ . \tag{6.32}$$

It is now easy to see that $\mathrm{Re}\,(\lambda_\alpha) \geq 0$ for all λ, or else the probabilities will become negative. For suppose $\mathrm{Re}\,(\lambda_\alpha) < 0$ for some α. Then as $t \to \infty$, the sum in eqn. 6.32 will be dominated by the term for which λ_α has the largest negative real part; all other contributions will be subleading. But we must have $\sum_i \psi_i^\alpha = 0$ since $\big|\,\psi^\alpha\,\big\rangle$ must be orthogonal to the left eigenvector $\vec{\phi}^{\alpha=0} = (1,1,\ldots,1)$. The eigenvectors can also be chosen to be real, since Γ_{ij} itself is real. Therefore, at least one component of ψ_i^α (*i.e.* for some value of i) must be negative, which means a negative probability!

We conclude that $P_i(t) \to P_i^{\mathrm{eq}}$ as $t \to \infty$, relaxing to the $\lambda = 0$ right eigenvector, with $\mathrm{Re}\,(\lambda_\alpha) \geq 0$ for all α.

6.3 Boltzmann's H-theorem

Suppose for the moment that Γ is a symmetric matrix, *i.e.* $\Gamma_{ij} = \Gamma_{ji}$. Then construct the function

$$H(t) = \sum_i P_i(t)\,\ln P_i(t) \ . \tag{6.33}$$

Then

$$\begin{aligned}\frac{dH}{dt} &= \sum_i \frac{dP_i}{dt}\big(1 + \ln P_i\big) = \sum_i \frac{dP_i}{dt}\,\ln P_i \\ &= -\sum_{i,j} \Gamma_{ij}\,P_j \ln P_i \\ &= \sum_{i,j} \Gamma_{ij}\,P_j\big(\ln P_j - \ln P_i\big) \ ,\end{aligned} \tag{6.34}$$

where we have used $\sum_i \varGamma_{ij} = 0$. Now switch $i \leftrightarrow j$ in the above sum and add the terms to get

$$\frac{dH}{dt} = \frac{1}{2} \sum_{i,j} \varGamma_{ij} \big(P_i - P_j\big) \big(\ln P_i - \ln P_j\big) \ . \tag{6.35}$$

Note that the $i = j$ term does not contribute to the sum. For $i \neq j$ we have $\varGamma_{ij} = -W_{ji} \leq 0$, and using the result

$$(x - y)\,(\ln x - \ln y) \geq 0 \ , \tag{6.36}$$

we conclude

$$\frac{dH}{dt} \leq 0 \ . \tag{6.37}$$

In equilibrium, $P_i^{\rm eq}$ is a constant, independent of i. We write

$$P_i^{\rm eq} = \frac{1}{\Omega} \quad , \quad \Omega = \sum_i 1 \quad \Longrightarrow \quad H = -\ln \Omega \ . \tag{6.38}$$

If $\varGamma_{ij} \neq \varGamma_{ji}$,we can still prove a version of the H-theorem. Define a new symmetric matrix

$$\overline{W}_{ij} \equiv P_i^{\rm eq}\, W_{ij} = P_j^{\rm eq}\, W_{ji} = \overline{W}_{ji} \ , \tag{6.39}$$

and the generalized H-function,

$$H(t) \equiv \sum_i P_i(t)\, \ln\!\left(\frac{P_i(t)}{P_i^{\rm eq}}\right) \ . \tag{6.40}$$

Then

$$\frac{dH}{dt} = -\frac{1}{2} \sum_{i,j} \overline{W}_{ij} \left(\frac{P_i}{P_i^{\rm eq}} - \frac{P_j}{P_j^{\rm eq}}\right) \left[\ln\!\left(\frac{P_i}{P_i^{\rm eq}}\right) - \ln\!\left(\frac{P_j}{P_j^{\rm eq}}\right)\right] \leq 0 \ . \tag{6.41}$$

6.4 Hamiltonian Evolution

The master equation provides us with a semi-phenomenological description of a dynamical system's relaxation to equilibrium. It explicitly breaks time reversal symmetry. Yet the microscopic laws of Nature are (approximately) time-reversal symmetric. How can a system which obeys Hamilton's equations of motion come to equilibrium?

Let's start our investigation by reviewing the basics of Hamiltonian dynamics. Recall the Lagrangian $L = L(q, \dot{q}, t) = T - V$. The Euler-Lagrange equations of motion for the action $S\big[q(t)\big] = \int dt\, L$ are

$$\dot{p}_\sigma = \frac{d}{dt}\left(\frac{\partial L}{\partial \dot{q}_\sigma}\right) = \frac{\partial L}{\partial q_\sigma} \ , \tag{6.42}$$

where p_σ is the canonical momentum conjugate to the generalized coordinate q_σ:

$$p_\sigma = \frac{\partial L}{\partial \dot{q}_\sigma} \ . \tag{6.43}$$

The Hamiltonian, $H(q,p)$ is obtained by a Legendre transformation,

$$H(q,p) = \sum_{\sigma=1}^{r} p_\sigma \, \dot{q}_\sigma - L \ . \tag{6.44}$$

Note that

$$\begin{aligned} dH &= \sum_{\sigma=1}^{r} \left(p_\sigma \, d\dot{q}_\sigma + \dot{q}_\sigma \, dp_\sigma - \frac{\partial L}{\partial q_\sigma} \, dq_\sigma - \frac{\partial L}{\partial \dot{q}_\sigma} \, d\dot{q}_\sigma \right) - \frac{\partial L}{\partial t} \, dt \\ &= \sum_{\sigma=1}^{r} \left(\dot{q}_\sigma \, dp_\sigma - \frac{\partial L}{\partial q_\sigma} \, dq_\sigma \right) - \frac{\partial L}{\partial t} \, dt \ . \end{aligned} \tag{6.45}$$

Thus, we obtain Hamilton's equations of motion,

$$\frac{\partial H}{\partial p_\sigma} = \dot{q}_\sigma \quad , \quad \frac{\partial H}{\partial q_\sigma} = -\frac{\partial L}{\partial q_\sigma} = -\dot{p}_\sigma \tag{6.46}$$

and

$$\frac{dH}{dt} = \frac{\partial H}{\partial t} = -\frac{\partial L}{\partial t} \ . \tag{6.47}$$

Define the rank $2r$ vector $\boldsymbol{\varphi}$ by its components,

$$\varphi_i = \begin{cases} q_i & \text{if } 1 \le i \le r \\ \\ p_{i-r} & \text{if } r \le i \le 2r \ . \end{cases} \tag{6.48}$$

Then we may write Hamilton's equations compactly as

$$\dot{\varphi}_i = J_{ij} \, \frac{\partial H}{\partial \varphi_j} \ , \tag{6.49}$$

where

$$J = \begin{pmatrix} 0_{r\times r} & 1_{r\times r} \\ -1_{r\times r} & 0_{r\times r} \end{pmatrix} \tag{6.50}$$

is a rank $2r$ matrix. Note that $J^{\rm t} = -J$, *i.e.* J is antisymmetric, and that $J^2 = -1_{2r\times 2r}$.

6.5 Evolution of Phase Space Volumes

Consider a general dynamical system,

$$\frac{d\boldsymbol{\varphi}}{dt} = \boldsymbol{V}(\boldsymbol{\varphi}) \ , \tag{6.51}$$

where $\boldsymbol{\varphi}(t)$ is a point in an n-dimensional phase space. Consider now a compact[2] region $\mathcal{R}_0$ in phase space, and consider its evolution under the dynamics. That is, $\mathcal{R}_0$ consists of

[2]'Compact' in the parlance of mathematical analysis means 'closed and bounded'.

a set of points $\{\boldsymbol{\varphi} \,|\, \boldsymbol{\varphi} \in \mathcal{R}_0\}$, and if we regard each $\boldsymbol{\varphi} \in \mathcal{R}_0$ as an initial condition, we can define the time-dependent set $\mathcal{R}(t)$ as the set of points $\boldsymbol{\varphi}(t)$ that *were* in $\mathcal{R}_0$ at time $t = 0$:

$$\mathcal{R}(t) = \big\{\boldsymbol{\varphi}(t) \,\big|\, \boldsymbol{\varphi}(0) \in \mathcal{R}_0\big\} \ . \tag{6.52}$$

Now consider the volume $\Omega(t)$ of the set $\mathcal{R}(t)$. We have

$$\Omega(t) = \int\limits_{\mathcal{R}(t)} d\mu \tag{6.53}$$

where

$$d\mu = d\varphi_1\, d\varphi_2 \, \cdots \, d\varphi_n \ , \tag{6.54}$$

for an n-dimensional phase space. We then have

$$\Omega(t+dt) = \int\limits_{\mathcal{R}(t+dt)} d\mu' = \int\limits_{\mathcal{R}(t)} d\mu \left| \frac{\partial\varphi_i(t+dt)}{\partial\varphi_j(t)} \right| \ , \tag{6.55}$$

where

$$\left| \frac{\partial\varphi_i(t+dt)}{\partial\varphi_j(t)} \right| \equiv \frac{\partial(\varphi'_1, \ldots, \varphi'_n)}{\partial(\varphi_1, \ldots, \varphi_n)} \tag{6.56}$$

is a determinant, which is the Jacobean of the transformation from the set of coordinates $\{\varphi_i = \varphi_i(t)\}$ to the coordinates $\{\varphi'_i = \varphi_i(t+dt)\}$. But according to the dynamics, we have

$$\varphi_i(t+dt) = \varphi_i(t) + V_i\big(\boldsymbol{\varphi}(t)\big)\, dt + \mathcal{O}(dt^2) \tag{6.57}$$

and therefore

$$\frac{\partial\varphi_i(t+dt)}{\partial\varphi_j(t)} = \delta_{ij} + \frac{\partial V_i}{\partial\varphi_j}\, dt + \mathcal{O}(dt^2) \ . \tag{6.58}$$

We now make use of the equality

$$\ln\det M = \mathrm{Tr}\ln M \ , \tag{6.59}$$

for any matrix M, which gives us[3], for small ε,

$$\det\big(1+\varepsilon A\big) = \exp \mathrm{Tr}\, \ln\big(1+\varepsilon A\big) = 1 + \varepsilon\, \mathrm{Tr}\, A + \tfrac{1}{2}\,\varepsilon^2 \Big(\big(\mathrm{Tr}\, A\big)^2 - \mathrm{Tr}\,(A^2)\Big) + \ldots \tag{6.60}$$

Thus,

$$\Omega(t+dt) = \Omega(t) + \int\limits_{\mathcal{R}(t)} d\mu\, \boldsymbol{\nabla}\!\cdot\! \boldsymbol{V}\, dt + \mathcal{O}(dt^2) \ , \tag{6.61}$$

which says

$$\frac{d\Omega}{dt} = \int\limits_{\mathcal{R}(t)} d\mu\, \boldsymbol{\nabla}\!\cdot\! \boldsymbol{V} = \int\limits_{\partial\mathcal{R}(t)} dS\, \hat{\boldsymbol{n}} \cdot \boldsymbol{V} \tag{6.62}$$

[3]The equality $\ln\det M = \mathrm{Tr}\ln M$ is most easily proven by bringing the matrix to diagonal form via a similarity transformation, and proving the equality for diagonal matrices.

Here, the divergence is the *phase space divergence*,

$$\boldsymbol{\nabla}\cdot\boldsymbol{V} = \sum_{i=1}^{n} \frac{\partial V_i}{\partial \varphi_i} \ , \tag{6.63}$$

and we have used Stokes' theorem to convert the volume integral of the divergence to a surface integral of $\hat{\boldsymbol{n}}\cdot\boldsymbol{V}$, where $\hat{\boldsymbol{n}}$ is the surface normal and dS is the differential element of surface area, and $\partial\mathcal{R}$ denotes the boundary of the region $\mathcal{R}$. We see that if $\boldsymbol{\nabla}\cdot\boldsymbol{V} = 0$ everywhere in phase space, then $\Omega(t)$ is a constant, and phase space volumes are *preserved* by the evolution of the system.

For an alternative derivation, consider a function $\varrho(\boldsymbol{\varphi}, t)$ which is defined to be the *density* of some collection of points in phase space at phase space position $\boldsymbol{\varphi}$ and time t. This must satisfy the continuity equation,

$$\frac{\partial\varrho}{\partial t} + \boldsymbol{\nabla}\cdot(\varrho\boldsymbol{V}) = 0 \ . \tag{6.64}$$

This is called the *continuity equation*. It says that 'nobody gets lost'. If we integrate it over a region of phase space $\mathcal{R}$, we have

$$\frac{d}{dt}\int\limits_{\mathcal{R}} d\mu\, \varrho = -\int\limits_{\mathcal{R}} d\mu\, \boldsymbol{\nabla}\cdot(\varrho\boldsymbol{V}) = -\int\limits_{\partial\mathcal{R}} dS\, \hat{\boldsymbol{n}}\cdot(\varrho\boldsymbol{V}) \ . \tag{6.65}$$

It is perhaps helpful to think of ϱ as a charge density, in which case $\boldsymbol{J} = \varrho\boldsymbol{V}$ is the current density. The above equation then says

$$\frac{dQ_{\mathcal{R}}}{dt} = -\int\limits_{\partial\mathcal{R}} dS\, \hat{\boldsymbol{n}}\cdot\boldsymbol{J} \ , \tag{6.66}$$

where $Q_{\mathcal{R}}$ is the total charge contained inside the region $\mathcal{R}$. In other words, the rate of increase or decrease of the charge within the region $\mathcal{R}$ is equal to the total integrated current flowing in or out of $\mathcal{R}$ at its boundary.

The Leibniz rule lets us write the continuity equation as

$$\frac{\partial\varrho}{\partial t} + \boldsymbol{V}\cdot\boldsymbol{\nabla}\varrho + \varrho\,\boldsymbol{\nabla}\cdot\boldsymbol{V} = 0 \ . \tag{6.67}$$

But now suppose that the phase flow is divergenceless, *i.e.* $\boldsymbol{\nabla}\cdot\boldsymbol{V} = 0$. Then we have

$$\frac{D\varrho}{Dt} \equiv \left(\frac{\partial}{\partial t} + \boldsymbol{V}\cdot\boldsymbol{\nabla}\right)\varrho = 0 \ . \tag{6.68}$$

The combination inside the brackets above is known as the *convective derivative*. It tells us the total rate of change of ϱ for an observer *moving with the phase flow*. That is

$$\begin{aligned} \frac{d}{dt}\,\varrho\big(\boldsymbol{\varphi}(t), t\big) &= \frac{\partial\varrho}{\partial\varphi_i}\,\frac{d\varphi_i}{dt} + \frac{\partial\varrho}{\partial t} \\ &= \sum_{i=1}^{n} V_i\,\frac{\partial\rho}{\partial\varphi_i} + \frac{\partial\varrho}{\partial t} = \frac{D\varrho}{Dt} \ . \end{aligned} \tag{6.69}$$

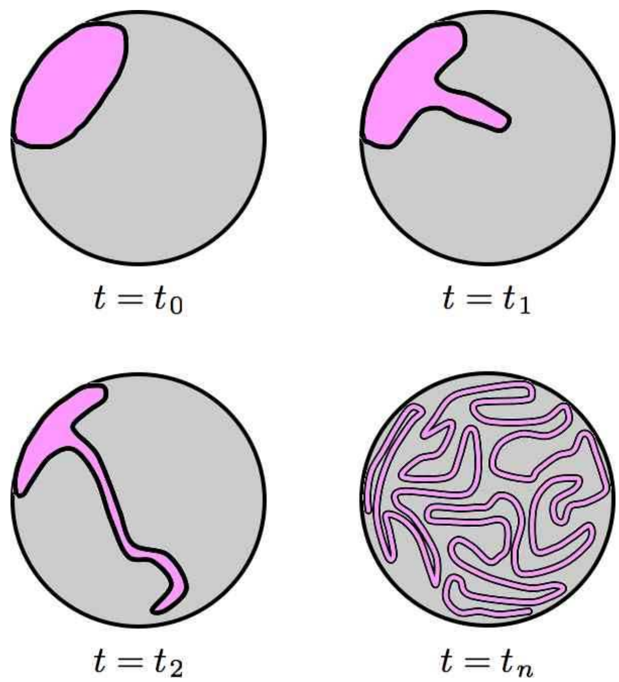

Figure 6.1: Time evolution of two immiscible fluids. The local density remains constant.

If $D\varrho/Dt = 0$, the local density remains the same during the evolution of the system. If we consider the 'characteristic function'

$$\varrho(\boldsymbol{\varphi}, t = 0) = \begin{cases} 1 & \text{if } \boldsymbol{\varphi} \in \mathcal{R}_0 \\ 0 & \text{otherwise} \end{cases} \tag{6.70}$$

then the vanishing of the convective derivative means that the image of the set $\mathcal{R}_0$ under time evolution will always have the same volume.

Hamiltonian evolution in classical mechanics is volume preserving. The equations of motion are

$$\dot{q}_i = +\frac{\partial H}{\partial p_i} \quad , \quad \dot{p}_i = -\frac{\partial H}{\partial q_i} \tag{6.71}$$

A point in phase space is specified by r positions q_i and r momenta p_i, hence the dimension of phase space is $n = 2r$:

$$\boldsymbol{\varphi} = \begin{pmatrix} \boldsymbol{q} \\ \boldsymbol{p} \end{pmatrix} \quad , \quad \boldsymbol{V} = \begin{pmatrix} \dot{\boldsymbol{q}} \\ \dot{\boldsymbol{p}} \end{pmatrix} = \begin{pmatrix} \partial H/\partial \boldsymbol{p} \\ -\partial H/\partial \boldsymbol{q} \end{pmatrix} . \tag{6.72}$$

Hamilton's equations of motion guarantee that the phase space flow is divergenceless:

$$\begin{aligned} \nabla\cdot\boldsymbol{V} &= \sum_{i=1}^{r} \left\{ \frac{\partial \dot{q}_i}{\partial q_i} + \frac{\partial \dot{p}_i}{\partial p_i} \right\} \\ &= \sum_{i=1}^{r} \left\{ \frac{\partial}{\partial q_i} \left(\frac{\partial H}{\partial p_i} \right) + \frac{\partial}{\partial p_i} \left(-\frac{\partial H}{\partial q_i} \right) \right\} = 0 \, . \end{aligned} \tag{6.73}$$

Thus, we have that the convective derivative vanishes, *viz.*

$$\frac{D\varrho}{Dt} \equiv \frac{\partial\varrho}{\partial t} + \boldsymbol{V} \cdot \nabla\varrho = 0 \ , \tag{6.74}$$

for any distribution $\varrho(\boldsymbol{\varphi}, t)$ on phase space. Thus, the value of the density $\varrho(\boldsymbol{\varphi}(t), t)$ is constant, which tells us that the phase flow is *incompressible*. In particular, phase space volumes are preserved.

6.5.1 Liouville's Equation

Let $\varrho(\boldsymbol{\varphi}) = \varrho(\boldsymbol{q}, \boldsymbol{p})$ be a distribution on phase space. Assuming the evolution is Hamiltonian, we can write

$$\begin{aligned}\frac{\partial\varrho}{\partial t} &= -\dot{\boldsymbol{\varphi}} \cdot \boldsymbol{\nabla}\varrho = -\sum_{k=1}^{r} \left(\dot{q}_k \frac{\partial}{\partial q_k} + \dot{p}_k \frac{\partial}{\partial p_k} \right) \varrho \\ &= -i\hat{L}\varrho \ ,\end{aligned} \tag{6.75}$$

where $\hat{L}$ is a differential operator known as the *Liouvillian*:

$$\hat{L} = -i \sum_{k=1}^{r} \left\{ \frac{\partial H}{\partial p_k} \frac{\partial}{\partial q_k} - \frac{\partial H}{\partial q_k} \frac{\partial}{\partial p_k} \right\} . \tag{6.76}$$

Eqn. 6.75, known as *Liouville's equation*, bears an obvious resemblance to the Schrödinger equation from quantum mechanics.

Suppose that $\Lambda_a(\boldsymbol{\varphi})$ is conserved by the dynamics of the system. Typical conserved quantities include the components of the total linear momentum (if there is translational invariance), the components of the total angular momentum (if there is rotational invariance), and the Hamiltonian itself (if the Lagrangian is not explicitly time-dependent). Now consider a distribution $\varrho(\boldsymbol{\varphi}, t) = \varrho(\Lambda_1, \Lambda_2, \ldots, \Lambda_k)$ which is a function only of these various conserved quantities. Then from the chain rule, we have

$$\dot{\boldsymbol{\varphi}} \cdot \boldsymbol{\nabla}\varrho = \sum_a \frac{\partial\varrho}{\partial\Lambda_a} \, \dot{\boldsymbol{\varphi}} \cdot \boldsymbol{\nabla}\Lambda_a = 0 \ , \tag{6.77}$$

since for each a we have

$$\frac{d\Lambda_a}{dt} = \sum_{\sigma=1}^{r} \left(\frac{\partial\Lambda_a}{\partial q_\sigma} \, \dot{q}_\sigma + \frac{\partial\Lambda_a}{\partial p_\sigma} \, \dot{p}_\sigma \right) = \dot{\boldsymbol{\varphi}} \cdot \boldsymbol{\nabla}\Lambda_a = 0 \ . \tag{6.78}$$

We conclude that any distribution $\varrho(\boldsymbol{\varphi}, t) = \varrho(\Lambda_1, \Lambda_2, \ldots, \Lambda_k)$ which is a function solely of conserved dynamical quantities is a stationary solution to Liouville's equation.

Clearly the microcanonical distribution,

$$\varrho_E(\boldsymbol{\varphi}) = \frac{\delta\big(E - H(\boldsymbol{\varphi})\big)}{\Sigma(E)} = \frac{\delta\big(E - H(\boldsymbol{\varphi})\big)}{\int\! d\mu \, \delta\big(E - H(\boldsymbol{\varphi})\big)} \ , \tag{6.79}$$

is a fixed point solution of Liouville's equation.

6.6 Irreversibility and Poincaré Recurrence

The dynamics of the master equation describe an approach to equilibrium. These dynamics are irreversible: $(dH/dt) \le 0$. However, the microscopic laws of physics are (almost) time-reversal invariant[4], so how can we understand the emergence of irreversibility? Furthermore, any dynamics which are deterministic and volume-preserving in a finite phase space exhibits the phenomenon of *Poincaré recurrence*, which guarantees that phase space trajectories are arbitrarily close to periodic if one waits long enough.

6.6.1 Poincaré recurrence theorem

The proof of the recurrence theorem is simple. Let g_τ be the 'τ-advance mapping' which evolves points in phase space according to Hamilton's equations. Assume that g_τ is invertible and volume-preserving, as is the case for Hamiltonian flow. Further assume that phase space volume is finite. Since the energy is preserved in the case of time-independent Hamiltonians, we simply ask that the volume of phase space *at fixed total energy E* be finite, *i.e.*

$$\int\! d\mu\, \delta\big(E - H(\boldsymbol{q},\boldsymbol{p})\big) < \infty \ , \tag{6.80}$$

where $d\mu = d\boldsymbol{q}\, d\boldsymbol{p}$ is the phase space uniform integration measure.

Theorem: In any finite neighborhood $\mathcal{R}_0$ of phase space there exists a point $\boldsymbol{\varphi}_0$ which will return to $\mathcal{R}_0$ after m applications of g_τ, where m is finite.

Proof: Assume the theorem fails; we will show this assumption results in a contradiction. Consider the set Υ formed from the union of all sets $g_\tau^k\,\mathcal{R}$ for all m:

$$\Upsilon = \bigcup_{k=0}^{\infty} g_\tau^k\,\mathcal{R}_0 \tag{6.81}$$

We assume that the set $\{g_\tau^k\,\mathcal{R}_0 \,|\, k \in {}_{+}\}$ is disjoint. The volume of a union of disjoint sets is the sum of the individual volumes. Thus,

$$\begin{aligned} \mathrm{vol}(\Upsilon) &= \sum_{k=0}^{\infty} \mathrm{vol}\big(g_\tau^k\,\mathcal{R}_0\big) \\ &= \mathrm{vol}(\mathcal{R}_0)\cdot \sum_{k=0}^{\infty} 1 = \infty \ , \end{aligned} \tag{6.82}$$

since $\mathrm{vol}\big(g_\tau^k\,\mathcal{R}_0\big) = \mathrm{vol}\big(\mathcal{R}_0\big)$ from volume preservation. But clearly Υ is a subset of the entire phase space, hence we have a contradiction, because by assumption phase space is of finite volume.

[4]Actually, the microscopic laws of physics are *not* time-reversal invariant, but rather are invariant under the product PCT, where P is parity, C is charge conjugation, and T is time reversal.

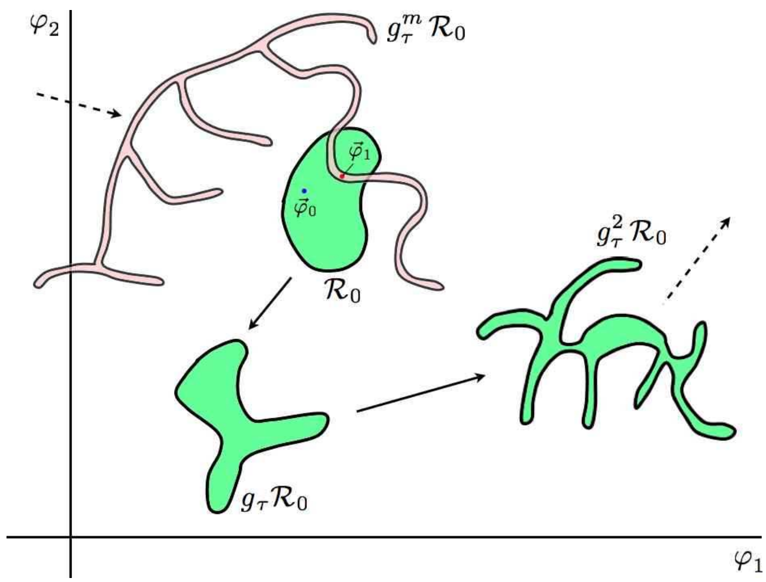

Figure 6.2: Successive images of a set $\mathcal{R}_0$ under the τ-advance mapping g_τ, projected onto a two-dimensional phase plane. The Poincaré recurrence theorem guarantees that if phase space has finite volume, and g_τ is invertible and volume preserving, then for any set $\mathcal{R}_0$ there exists an integer m such that $\mathcal{R}_0 \cap g_\tau^m \mathcal{R}_0 \neq \emptyset$.

Thus, the assumption that the set $\{g_\tau^k \mathcal{R}_0 \,|\, k \in \mathbb{Z}_+\}$ is disjoint fails. This means that there exists some pair of integers k and l, with $k \neq l$, such that $g_\tau^k \mathcal{R}_0 \cap g_\tau^l \mathcal{R}_0 \neq \emptyset$. Without loss of generality we may assume $k < l$. Apply the inverse g_τ^{-1} to this relation k times to get $g_\tau^{l-k} \mathcal{R}_0 \cap \mathcal{R}_0 \neq \emptyset$. Now choose any point $\boldsymbol{\varphi}_1 \in g_\tau^m \mathcal{R}_0 \cap \mathcal{R}_0$, where $m = l - k$, and define $\boldsymbol{\varphi}_0 = g_\tau^{-m} \boldsymbol{\varphi}_1$. Then by construction both $\boldsymbol{\varphi}_0$ and $g_\tau^m \boldsymbol{\varphi}_0$ lie within $\mathcal{R}_0$ and the theorem is proven.

Poincaré recurrence has remarkable implications. Consider a bottle of perfume which is opened in an otherwise evacuated room, as depicted in fig. 6.3. The perfume molecules evolve according to Hamiltonian evolution. The positions are bounded because physical space is finite. The momenta are bounded because the total energy is conserved, hence no single particle can have a momentum such that $T(\boldsymbol{p}) > E_{\text{TOT}}$, where $T(\boldsymbol{p})$ is the single particle kinetic energy function[5]. Thus, phase space, however large, is still bounded. Hamiltonian evolution, as we have seen, is invertible and volume preserving, therefore the system is recurrent. All the molecules must eventually return to the bottle. What's more, they all must return with momenta arbitrarily close to their initial momenta! In this case, we could define the region $\mathcal{R}_0$ as

$$\mathcal{R}_0 = \big\{ (q_1, \ldots, q_r, p_1, \ldots, p_r) \,\big|\, |q_i - q_i^0| \leq \Delta q \text{ and } |p_j - p_j^0| \leq \Delta p \;\forall\; i,j \big\} \ , \tag{6.83}$$

which specifies a hypercube in phase space centered about the point $(\boldsymbol{q}^0, \boldsymbol{p}^0)$.

Each of the three central assumptions – finite phase space, invertibility, and volume preser-

[5]In the nonrelativistic limit, $T = p^2/2m$. For relativistic particles, we have $T = (p^2c^2 + m^2c^4)^{1/2} - mc^2$.

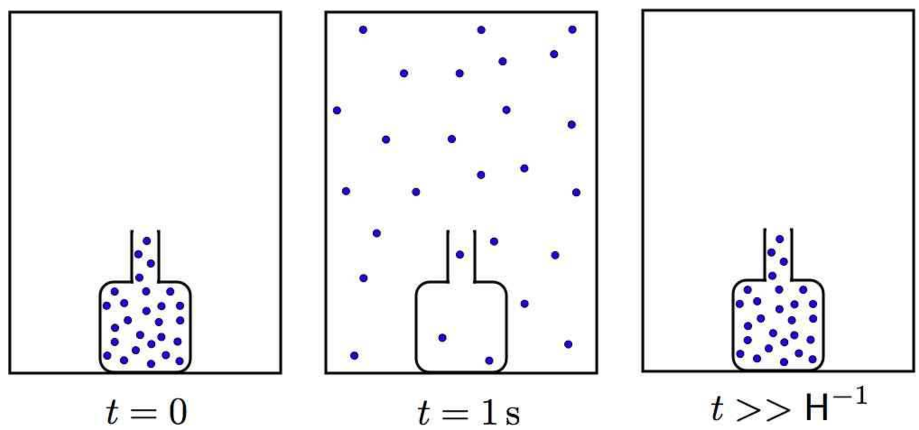

Figure 6.3: Poincaré recurrence guarantees that if we remove the cap from a bottle of perfume in an otherwise evacuated room, all the perfume molecules will eventually return to the bottle!

vation – is crucial. If any one of these assumptions does not hold, the proof fails. Obviously if phase space is infinite the flow needn't be recurrent since it can keep moving off in a particular direction. Consider next a volume-preserving map which is not invertible. An example might be a mapping $f : \mathbb{R} \to \mathbb{R}$ which takes any real number to its fractional part. Thus, $f(\pi) = 0.14159265\ldots$. Let us restrict our attention to intervals of width less than unity. Clearly f is then volume preserving. The action of f on the interval $[2, 3)$ is to map it to the interval $[0, 1)$. But $[0, 1)$ remains fixed under the action of f, so no point within the interval $[2, 3)$ will ever return under repeated iterations of f. Thus, f does not exhibit Poincaré recurrence.

Consider next the case of the damped harmonic oscillator. In this case, phase space volumes contract. For a one-dimensional oscillator obeying $\ddot{x} + 2\beta\dot{x} + \Omega_0^2\, x = 0$ one has $\nabla\cdot\boldsymbol{V} = -2\beta < 0$, since $\beta > 0$ for physical damping. Thus the convective derivative is $D_t\varrho = -(\nabla\cdot\boldsymbol{V})\varrho = 2\beta\varrho$ which says that the density increases exponentially in the comoving frame, as $\varrho(t) = e^{2\beta t}\,\varrho(0)$. Thus, phase space volumes collapse: $\Omega(t) = e^{-2\beta 2}\,\Omega(0)$, and are not preserved by the dynamics. The proof of recurrence therefore fails. In this case, it is possible for the set Υ to be of finite volume, even if it is the union of an infinite number of sets $g_\tau^k\,\mathcal{R}_0$, because the volumes of these component sets themselves decrease exponentially, as $\mathrm{vol}(g_\tau^n\,\mathcal{R}_0) = e^{-2n\beta\tau}\,\mathrm{vol}(\mathcal{R}_0)$. A damped pendulum, released from rest at some small angle θ_0, will not return arbitrarily close to these initial conditions.

6.7 Kac Ring Model

The implications of the Poincaré recurrence theorem are surprising – even shocking. If one takes a bottle of perfume in a sealed, evacuated room and opens it, the perfume molecules will diffuse throughout the room. The recurrence theorem guarantees that after some finite time T all the molecules will go back inside the bottle (and arbitrarily close to their initial

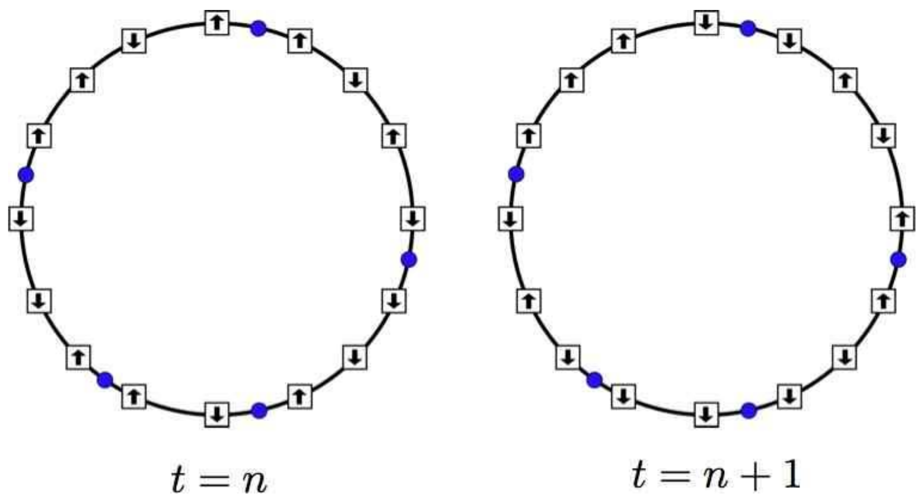

Figure 6.4: Left: A configuration of the Kac ring with $N = 16$ sites and $F = 4$ flippers. The flippers, which live on the links, are represented by blue dots. Right: The ring system after one time step. Evolution proceeds by clockwise rotation. Spins passing through flippers are flipped.

velocities as well). The hitch is that this could take a very long time, *e.g.* much much longer than the age of the Universe.

On less absurd time scales, we know that most systems come to thermodynamic equilibrium. But how can a system both exhibit equilibration *and* Poincaré recurrence? The two concepts seem utterly incompatible!

A beautifully simple model due to Kac shows how a recurrent system can exhibit the phenomenon of equilibration. Consider a ring with N sites. On each site, place a 'spin' which can be in one of two states: up or down. Along the N links of the system, F of them contain 'flippers'. The configuration of the flippers is set at the outset and never changes. The dynamics of the system are as follows: during each time step, every spin moves clockwise a distance of one lattice spacing. Spins which pass through flippers reverse their orientation: up becomes down, and down becomes up.

The 'phase space' for this system consists of 2^N discrete configurations. Since each configuration maps onto a unique image under the evolution of the system, phase space 'volume' is preserved. The evolution is invertible; the inverse is obtained simply by rotating the spins counterclockwise. Figure 6.4 depicts an example configuration for the system, and its first iteration under the dynamics.

Suppose the flippers were not fixed, but moved about randomly. In this case, we could focus on a single spin and determine its configuration probabilistically. Let p_n be the probability that a given spin is in the up configuration at time n. The probability that it is up at time $(n + 1)$ is then

$$p_{n+1} = (1 - x)\, p_n + x\,(1 - p_n) \ , \tag{6.84}$$

where $x = F/N$ is the fraction of flippers in the system. In words: a spin will be up at

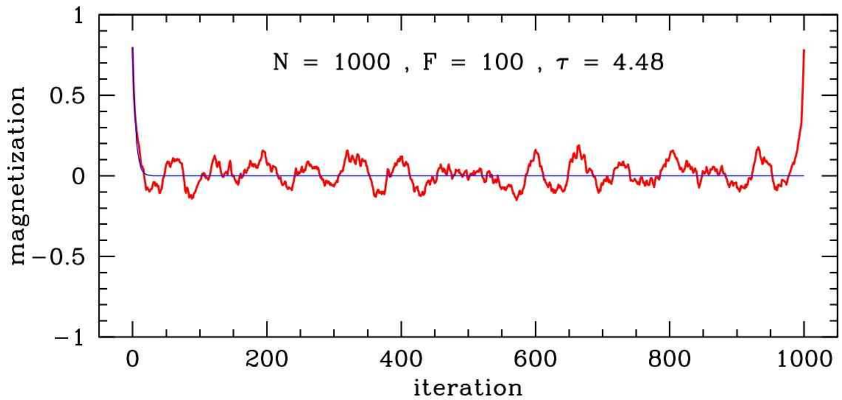

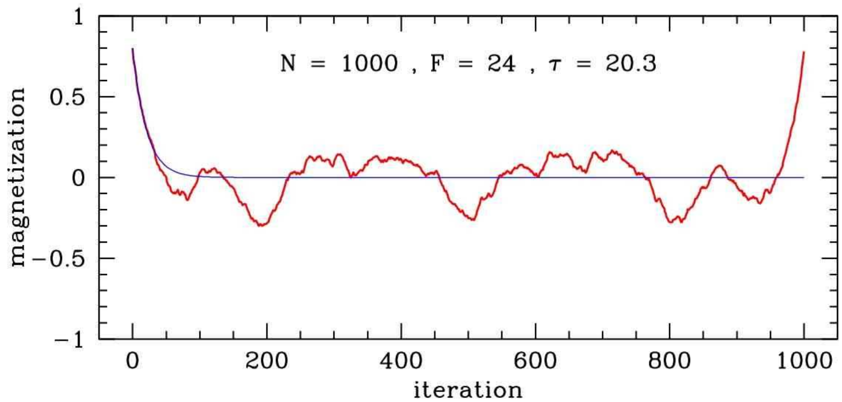

Figure 6.5: Two simulations of the Kac ring model, each with $N = 1000$ sites and with $F = 100$ flippers (top panel) and $F = 24$ flippers (bottom panel). The red line shows the magnetization as a function of time, starting from an initial configuration in which 90% of the spins are up. The blue line shows the prediction of the *Stosszahlansatz*, which yields an exponentially decaying magnetization with time constant τ.

time $(n + 1)$ if it was up at time n and did not pass through a flipper, or if it was down at time n and did pass through a flipper. If the flipper locations are randomized at each time step, then the probability of flipping is simply $x = F/N$. Equation 6.84 can be solved immediately:

$$p_n = \tfrac{1}{2} + (1 - 2x)^n \, (p_0 - \tfrac{1}{2}) \ , \tag{6.85}$$

which decays exponentially to the equilibrium value of $p_{\text{eq}} = \frac{1}{2}$ with time scale

$$\tau(x) = -\frac{1}{\ln|1 - 2x|} \ . \tag{6.86}$$

We identify $\tau(x)$ as the microscopic relaxation time over which local equilibrium is established. If we define the magnetization $m \equiv (N_\uparrow - N_\downarrow)/N$, then $m = 2p - 1$, so $m_n = (1 - 2x)^n \, m_0$. The equilibrium magnetization is $m_{\text{eq}} = 0$. Note that for $\frac{1}{2} < x < 1$ that the magnetization reverses sign each time step, as well as decreasing exponentially in magnitude.

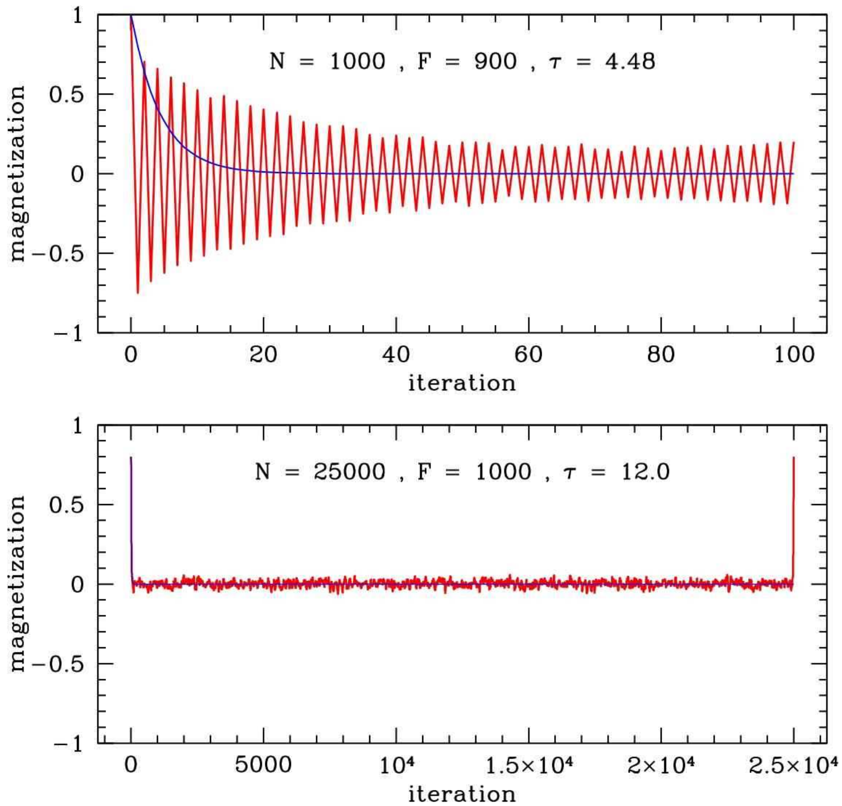

Figure 6.6: Simulations of the Kac ring model. Top: $N = 1000$ sites with $F = 900$ flippers. The flipper density $x = F/N$ is greater than $\frac{1}{2}$, so the magnetization reverses sign every time step. Only 100 iterations are shown, and the blue curve depicts the absolute value of the magnetization within the *Stosszahlansatz*. Bottom: $N = 25,000$ sites with $F = 1000$ flippers. Note that the fluctuations about the 'equilibrium' magnetization $m = 0$ are much smaller than in the $N = 1000$ site simulations.

The assumption that leads to equation 6.84 is called the *Stosszahlansatz*[6], a long German word meaning, approximately, 'assumption on the counting of hits'. The resulting dynamics are irreversible: the magnetization inexorably decays to zero. However, the Kac ring model is purely deterministic, and the *Stosszahlansatz* can at best be an approximation to the true dynamics. Clearly the *Stosszahlansatz* fails to account for correlations such as the following: if spin i is flipped at time n, then spin $i + 1$ will have been flipped at time $n - 1$. Also if spin i is flipped at time n, then it also will be flipped at time $n + N$. Indeed, since the dynamics of the Kac ring model are invertible and volume preserving, it must exhibit Poincaré recurrence. We see this most vividly in figs. 6.5 and 6.6.

The model is trivial to simulate. The results of such a simulation are shown in figure 6.5 for a ring of $N = 1000$ sites, with $F = 100$ and $F = 24$ flippers. Note how the magnetization

[6]Unfortunately, many important physicists were German and we have to put up with a legacy of long German words like *Gedankenexperiment*, *Zitterbewegung*, *Brehmsstrahlung*, *Stosszahlansatz*, *Kartoffelsalat*, *etc.*

decays and fluctuates about the equilibrium value $_{\text{eq}} = 0$, but that after N iterations m recovers its initial value: $m_N = m_0$. The recurrence time for this system is simply N if F is even, and $2N$ if F is odd, since every spin will then have flipped an even number of times.

In figure 6.6 we plot two other simulations. The top panel shows what happens when $x > \frac{1}{2}$, so that the magnetization wants to reverse its sign with every iteration. The bottom panel shows a simulation for a larger ring, with $N = 25000$ sites. Note that the fluctuations in m about equilibrium are smaller than in the cases with $N = 1000$ sites. Why?

6.8 Remarks on Ergodic Theory

A mechanical system evolves according to Hamilton's equations of motion. We have seen how such a system is *recurrent* in the sense of Poincaré.

There is a level beyond recurrence called *ergodicity*. In an ergodic system, time averages over intervals $[0, T]$ with $T \to \infty$ may be replaced by phase space averages. The time average of a function $f(\boldsymbol{\varphi})$ is defined as

$$\big\langle f(\boldsymbol{\varphi}) \big\rangle_T = \lim_{T\to\infty} \frac{1}{T} \int\limits_0^T dt\, f\big(\boldsymbol{\varphi}(t)\big) \ . \tag{6.87}$$

For a Hamiltonian system, the *phase space average* of the same function is defined by

$$\big\langle f(\boldsymbol{\varphi}) \big\rangle_S = \int d\mu\, f(\boldsymbol{\varphi})\, \delta\big(E - H(\boldsymbol{\varphi})\big) \bigg/ \int d\mu\, \delta\big(E - H(\boldsymbol{\varphi})\big) \ , \tag{6.88}$$

where $H(\boldsymbol{\varphi}) = H(\boldsymbol{q}, \boldsymbol{p})$ is the Hamiltonian, and where $\delta(x)$ is the Dirac δ-function. Thus,

$$\text{ergodicity} \quad \Longleftrightarrow \quad \big\langle f(\boldsymbol{\varphi}) \big\rangle_T = \big\langle f(\boldsymbol{\varphi}) \big\rangle_S \ , \tag{6.89}$$

for all smooth functions $f(\boldsymbol{\varphi})$ for which $\big\langle f(\boldsymbol{\varphi}) \big\rangle_S$ exists and is finite. Note that we do not average over *all* of phase space. Rather, we average only over a hypersurface along which $H(\boldsymbol{\varphi}) = E$ is fixed, *i.e.* over one of the *level sets* of the Hamiltonian function. This is because the dynamics *preserves the energy*. Ergodicity means that almost all points $\boldsymbol{\varphi}$ will, upon Hamiltonian evolution, move in such a way as to eventually pass through every finite neighborhood on the energy surface, and will spend equal time in equal regions of phase space.

Let $\chi_{\mathcal{R}}(\boldsymbol{\varphi})$ be the characteristic function of a region $\mathcal{R}$:

$$\chi_{\mathcal{R}}(\boldsymbol{\varphi}) = \begin{cases} 1 & \text{if } \boldsymbol{\varphi} \in \mathcal{R} \\ 0 & \text{otherwise,} \end{cases} \tag{6.90}$$

where $H(\boldsymbol{\varphi}) = E$ for all $\boldsymbol{\varphi} \in \mathcal{R}$. Then

$$\big\langle \chi_{\mathcal{R}}(\boldsymbol{\varphi}) \big\rangle_T = \lim_{T\to\infty} \left(\frac{\text{time spent in } \mathcal{R}}{T} \right) . \tag{6.91}$$

If the system is ergodic, then

$$\big\langle \chi_{\mathcal{R}}(\boldsymbol{\varphi})\big\rangle_T = P(\mathcal{R}) = \frac{\Sigma_{\mathcal{R}}(E)}{\Sigma(E)} \ , \tag{6.92}$$

where $P(\mathcal{R})$ is the *a priori* probability to find $\boldsymbol{\varphi} \in \mathcal{R}$, based solely on the relative volumes of $\mathcal{R}$ and of the entire phase space. The latter is given by

$$\Sigma(E) = \int d\mu \, \delta\big(E - H(\boldsymbol{\varphi})\big) \tag{6.93}$$

is the surface area of phase space at energy E, and

$$\Sigma_{\mathcal{R}}(E) = \int\limits_{\mathcal{R}} d\mu \, \delta\big(E - H(\boldsymbol{\varphi})\big) \ . \tag{6.94}$$

is the surface area of phase space at energy E contained in $\mathcal{R}$.

Note that

$$\Sigma(E) \equiv \int d\mu \, \delta\big(E - H(\boldsymbol{\varphi})\big) = \int\limits_{\mathcal{S}_E} \frac{dS}{|\boldsymbol{\nabla} H|} \tag{6.95}$$

$$= \frac{d}{dE} \int d\mu \, \Theta\big(E - \mathcal{H}(\boldsymbol{\varphi})\big) = \frac{d\Omega(E)}{dE} \ . \tag{6.96}$$

Here, dS is the differential surface element, $\mathcal{S}_E$ is the constant H hypersurface $H(\boldsymbol{\varphi}) = E$, and $\Omega(E)$ is the volume of phase space over which $H(\boldsymbol{\varphi}) < E$. Note also that we may write

$$d\mu = dE \, d\Sigma_E \ , \tag{6.97}$$

where

$$d\Sigma_E = \frac{dS}{|\boldsymbol{\nabla} H|}\bigg|_{H(\boldsymbol{\varphi})=E} \tag{6.98}$$

is the the *invariant surface element*.

6.8.1 The microcanonical ensemble

The distribution,

$$\varrho_E(\boldsymbol{\varphi}) = \frac{\delta\big(E - H(\boldsymbol{\varphi})\big)}{\Sigma(E)} = \frac{\delta\big(E - H(\boldsymbol{\varphi})\big)}{\int d\mu \, \delta\big(E - H(\boldsymbol{\varphi})\big)} \ , \tag{6.99}$$

defines the *microcanonical ensemble* (μCE) of Gibbs.

We could also write

$$\big\langle f(\boldsymbol{\varphi})\big\rangle_S = \frac{1}{\Sigma(E)} \int\limits_{\mathcal{S}_E} d\Sigma_E \, f(\boldsymbol{\varphi}) \ , \tag{6.100}$$

integrating over the hypersurface $\mathcal{S}_E$ rather than the entire phase space.

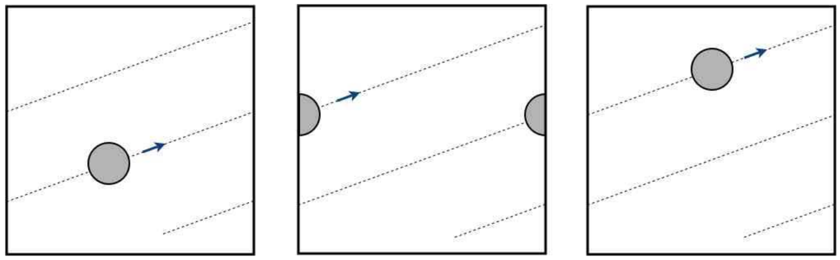

Figure 6.7: Constant phase space velocity at an irrational angle over a toroidal phase space is ergodic, but not mixing. A circle remains a circle, and a blob remains a blob.

6.8.2 Ergodicity and mixing

Just because a system is ergodic, it doesn't necessarily mean that $\varrho(\varphi,t) \to \varrho^{\rm eq}(\boldsymbol{\varphi})$, for consider the following motion on the toroidal space $\big(\boldsymbol{\varphi} = (q,p) \,\big|\, 0 \le q < 1 \ ,\ 0 \le p < 1\big\}$, where we identify opposite edges, *i.e.* we impose periodic boundary conditions. We also take q and p to be dimensionless, for simplicity of notation. Let the dynamics be given by

$$\dot q = 1 \qquad , \qquad \dot p = \alpha \ . \tag{6.101}$$

The solution is

$$q(t) = q_0 + t \qquad , \qquad p(t) = p_0 + \alpha t \ , \tag{6.102}$$

hence the phase curves are given by

$$p = p_0 + \alpha (q - q_0) \ . \tag{6.103}$$

Now consider the average of some function $f(q,p)$. We can write $f(q,p)$ in terms of its Fourier transform,

$$f(q,p) = \sum_{m,n} \hat f_{mn} \, e^{2\pi i (mq+np)} \ . \tag{6.104}$$

We have, then,

$$f\big(q(t),p(t)\big) = \sum_{m,n} \hat f_{mn} \, e^{2\pi i (mq_0+np_0)} \, e^{2\pi i (m+\alpha n)t} \ . \tag{6.105}$$

We can now perform the time average of f:

$$\begin{aligned} \big\langle f(q,p)\big\rangle_T &= \hat f_{00} + \lim_{T\to\infty} \frac{1}{T} {\sum_{m,n}}' e^{2\pi i (mq_0+np_0)} \, \frac{e^{2\pi i (m+\alpha n)T} - 1}{2\pi i (m+\alpha n)} \\ &= \hat f_{00} \quad \text{if } \alpha \text{ irrational.} \end{aligned} \tag{6.106}$$

Clearly,

$$\big\langle f(q,p)\big\rangle_S = \int\limits_0^1 \! dq \int\limits_0^1 \! dp \, f(q,p) = \hat f_{00} = \big\langle f(q,p)\big\rangle_T \ , \tag{6.107}$$

so the system is ergodic.

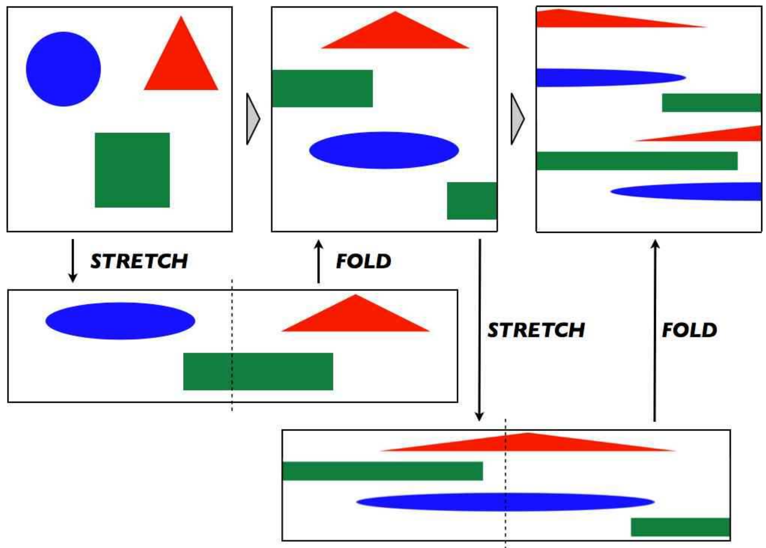

Figure 6.8: The baker's transformation is a successive stretching, cutting, and restacking.

The situation is depicted in fig. 6.7. If we start with the characteristic function of a disc,

$$\varrho(q,p,t=0) = \Theta\big(a^2 - (q-q_0)^2 - (p-p_0)^2\big) \ , \tag{6.108}$$

then it remains the characteristic function of a disc:

$$\varrho(q,p,t) = \Theta\big(a^2 - (q-q_0-t)^2 - (p-p_0-\alpha t)^2\big) \ , \tag{6.109}$$

A stronger condition one could impose is the following. Let A and B be subsets of $\mathcal{S}_E$. Define the *measure*

$$\nu(A) = \int\! d\Sigma_E \, \chi_A(\boldsymbol{\varphi}) \Big/ \!\! \int\! d\Sigma_E = \frac{\Sigma_A(E)}{\Sigma(E)} \ , \tag{6.110}$$

where $\chi_A(\boldsymbol{\varphi})$ is the characteristic function of A. The measure of a set A is the fraction of the energy surface $\mathcal{S}_E$ covered by A. This means $\nu(\mathcal{S}_E)=1$, since $\mathcal{S}_E$ is the entire phase space at energy E. Now let g be a volume-preserving map on phase space. Given two measurable sets A and B, we say that a system is *mixing* if

$$\text{mixing} \qquad \Longleftrightarrow \qquad \lim_{n\to\infty} \nu\Big(g^n A \cap B\Big) = \nu(A)\,\nu(B) \ . \tag{6.111}$$

In other words, the fraction of B covered by the n^{th} iterate of A, *i.e.* $g^n A$, is, as $n\to\infty$, simply the fraction of $\mathcal{S}_E$ covered by A. The iterated map g^n distorts the region A so severely that it eventually spreads out 'evenly' over the entire energy hypersurface. Of course by 'evenly' we mean 'with respect to any finite length scale', because at the very smallest scales, the phase space density is still locally constant as one evolves with the dynamics.

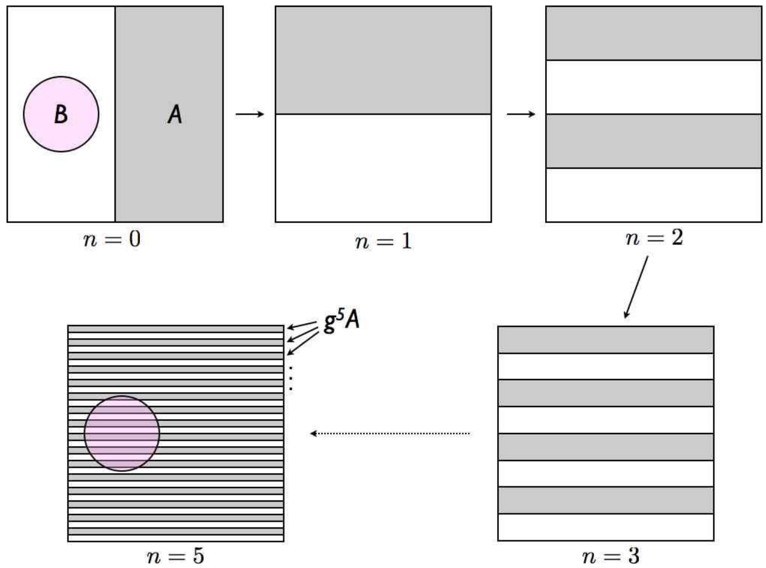

Figure 6.9: The multiply iterated baker's transformation. The set A covers half the phase space and its area is preserved under the map. Initially, the fraction of B covered by A is zero. After many iterations, the fraction of B covered by g^nA approaches $\frac{1}{2}$.

Mixing means that

$$\begin{aligned}\big\langle f(\boldsymbol{\varphi})\big\rangle &= \int\! d\mu\; \varrho(\boldsymbol{\varphi},t)\, f(\boldsymbol{\varphi}) \\ &\xrightarrow[t\to\infty]{} \int\! d\mu\, f(\boldsymbol{\varphi})\, \delta\big(E-H(\boldsymbol{\varphi})\big)\Big/\!\int\! d\mu\, \delta\big(E-H(\boldsymbol{\varphi})\big) \\ &\equiv \mathrm{Tr}\Big[f(\boldsymbol{\varphi})\,\delta\big(E-H(\boldsymbol{\varphi})\big)\Big]\Big/\mathrm{Tr}\Big[\delta\big(E-H(\boldsymbol{\varphi})\big)\Big]\ . \end{aligned} \tag{6.112}$$

Physically, we can imagine regions of phase space being successively stretched and folded. During the stretching process, the volume is preserved, so the successive stretch and fold operations map phase space back onto itself.

An example of a mixing system is the *baker's transformation*, depicted in fig. 6.8. The baker map is defined by

$$g(q,p) = \begin{cases} \big(2q\,,\,\frac{1}{2}p\big) & \text{if} \quad 0 \le q < \frac{1}{2} \\ \\ \big(2q-1\,,\,\frac{1}{2}p+\frac{1}{2}\big) & \text{if} \quad \frac{1}{2} \le q < 1\ . \end{cases} \tag{6.113}$$

Note that g is invertible and volume-preserving. The baker's transformation consists of an initial stretch in which q is expanded by a factor of two and p is contracted by a factor of two, which preserves the total volume. The system is then mapped back onto the original area by cutting and restacking, which we can call a 'fold'. The inverse transformation is accomplished by stretching first in the vertical (p) direction and squashing in the horizontal

Figure 6.10: The Arnold cat map applied to an image of 150×150 pixels. After 300 iterations, the image repeats itself. (*Source: Wikipedia*)

(q) direction, followed by a slicing and restacking. Explicitly,

$$g^{-1}(q,p) = \begin{cases} \left(\frac{1}{2}q\,,\,2p\right) & \text{if} \quad 0 \le p < \frac{1}{2} \\ \\ \left(\frac{1}{2}q + \frac{1}{2}\,,\,2p-1\right) & \text{if} \quad \frac{1}{2} \le p < 1\ . \end{cases} \tag{6.114}$$

Another example of a mixing system is Arnold's 'cat map'[7]

$$g(q,p) = \big(\,[q+p]\,,\,[q+2p]\,\big)\ , \tag{6.115}$$

where $[x]$ denotes the fractional part of x. One can write this in matrix form as

$$\begin{pmatrix} q' \\ p' \end{pmatrix} = \overbrace{\begin{pmatrix} 1 & 1 \\ 1 & 2 \end{pmatrix}}^{M} \begin{pmatrix} q \\ p \end{pmatrix} \mod \mathbb{Z}^2\ . \tag{6.116}$$

The matrix M is very special because it has integer entries and its determinant is $\det M = 1$. This means that the inverse also has integer entries. The inverse transformation is then

$$\begin{pmatrix} q \\ p \end{pmatrix} = \overbrace{\begin{pmatrix} 2 & -1 \\ -1 & 1 \end{pmatrix}}^{M^{-1}} \begin{pmatrix} q' \\ p' \end{pmatrix} \mod \mathbb{Z}^2\ . \tag{6.117}$$

Now for something cool. Suppose that our image consists of a set of discrete points located at $(n_1/k\,,\,n_2/k)$, where the denominator $k \in \mathbb{Z}$ is fixed, and where n_1 and n_2 range over the set $\{1,\ldots,k\}$. Clearly g and its inverse preserve this set, since the entries of M and M^{-1} are

[7]The cat map gets its name from its initial application, by Arnold, to the image of a cat's face.

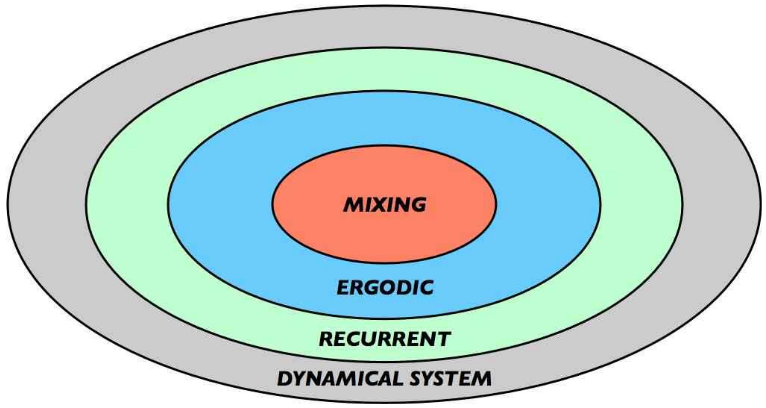

Figure 6.11: The hierarchy of dynamical systems.

integers. If there are two possibilities for each pixel (say off and on, or black and white), then there are $2^{(k^2)}$ possible images, and the cat map will map us invertibly from one image to another. Therefore it must exhibit Poincaré recurrence! This phenomenon is demonstrated vividly in fig. 6.10, which shows a $k = 150$ pixel (square) image of a cat subjected to the iterated cat map. The image is stretched and folded with each successive application of the cat map, but after 300 iterations the image is restored! How can this be if the cat map is mixing? The point is that only the discrete set of points $(n_1/k\,,\,n_2/k)$ is periodic. Points with different denominators will exhibit a different periodicity, and points with irrational coordinates will in general never return to their exact initial conditions, although recurrence says they will come arbitrarily close, given enough iterations. The baker's transformation is also different in this respect, since the denominator of the p coordinate is doubled upon each successive iteration.

The student should now contemplate the hierarchy of dynamical systems depicted in fig. 6.11, understanding the characteristic features of each successive refinement[8].

[8]There is something beyond mixing, called a *K-system*. A K-system has positive Kolmogorov-Sinai entropy. For such a system, closed orbits separate exponentially in time, and consequently the Liouvillian L has a Lebesgue spectrum with denumerably infinite multiplicity.

Chapter 7

Maps, Strange Attractors, and Chaos

7.1 Maps

Earlier we studied the parametric oscillator $\ddot{x} + \omega^2(t)\, x = 0$, where $\omega(t+T) = \omega(t)$ is periodic. If we define $x_n = x(nT)$ and $\dot{x}_n = \dot{x}(nT)$, then we have

$$\begin{pmatrix} x_{n+1} \\ \dot{x}_{n+1} \end{pmatrix} = A \begin{pmatrix} x_n \\ \dot{x}_n \end{pmatrix} \ , \tag{7.1}$$

where the matrix M is the path ordered exponential

$$A = \mathcal{P} \,\exp \int\limits_0^T \! dt\, M(t) \ , \tag{7.2}$$

where

$$M(t) = \begin{pmatrix} 0 & 1 \\ -\omega^2(t) & 0 \end{pmatrix} \ . \tag{7.3}$$

Eqn. 7.1 defines a discrete linear map from phase space to itself.

A related model is described by the *kicked dynamics* of the Hamiltonian

$$H(t) = \frac{p^2}{2m} + V(q)\, K(t) \ , \tag{7.4}$$

where

$$K(t) = \tau \sum_{n=-\infty}^{\infty} \delta(t - n\tau) \tag{7.5}$$

is the kicking function. The potential thus winks on and off with period τ. Note that

$$\lim_{\tau \to 0} K(t) = 1 \ . \tag{7.6}$$

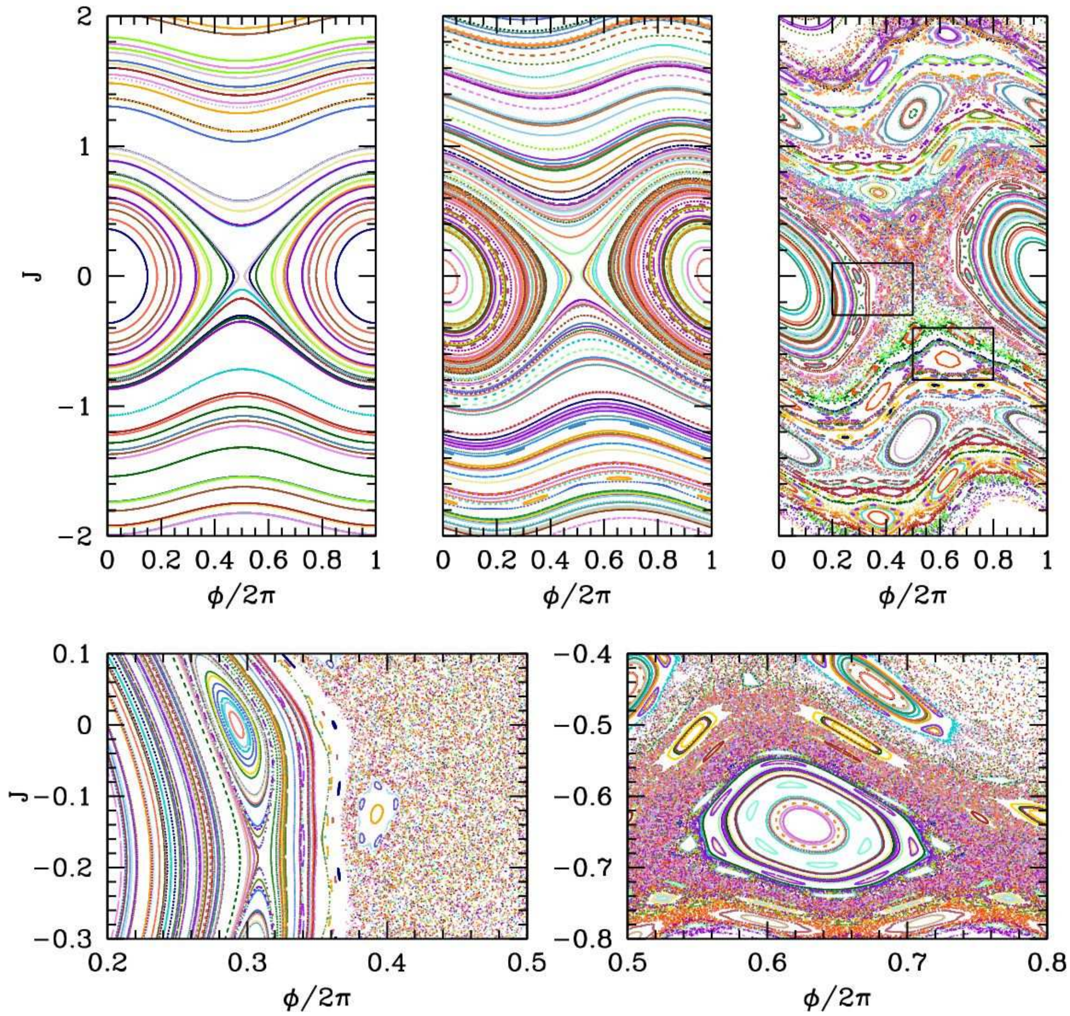

Figure 7.1: Top: the standard map, as defined in the text. Four values of the ϵ parameter are shown: $\epsilon = 0.01$ (left), $\epsilon = 0.2$ (center), and $\epsilon = 0.4$ (right). Bottom: details of the $\epsilon = 0.4$ map.

In the $\tau \to 0$ limit, the system is continuously kicked, and is equivalent to motion in a time-independent external potential $V(q)$.

The equations of motion are

$$\dot{q} = \frac{p}{m} \qquad , \qquad \dot{p} = -V'(q)\,K(t) \; . \tag{7.7}$$

Integrating these equations, we obtain the map

$$q_{n+1} = q_n + \frac{\tau}{m}\,p_n \tag{7.8}$$

$$p_{n+1} = p_n - \tau\,V'(q_n) \; . \tag{7.9}$$

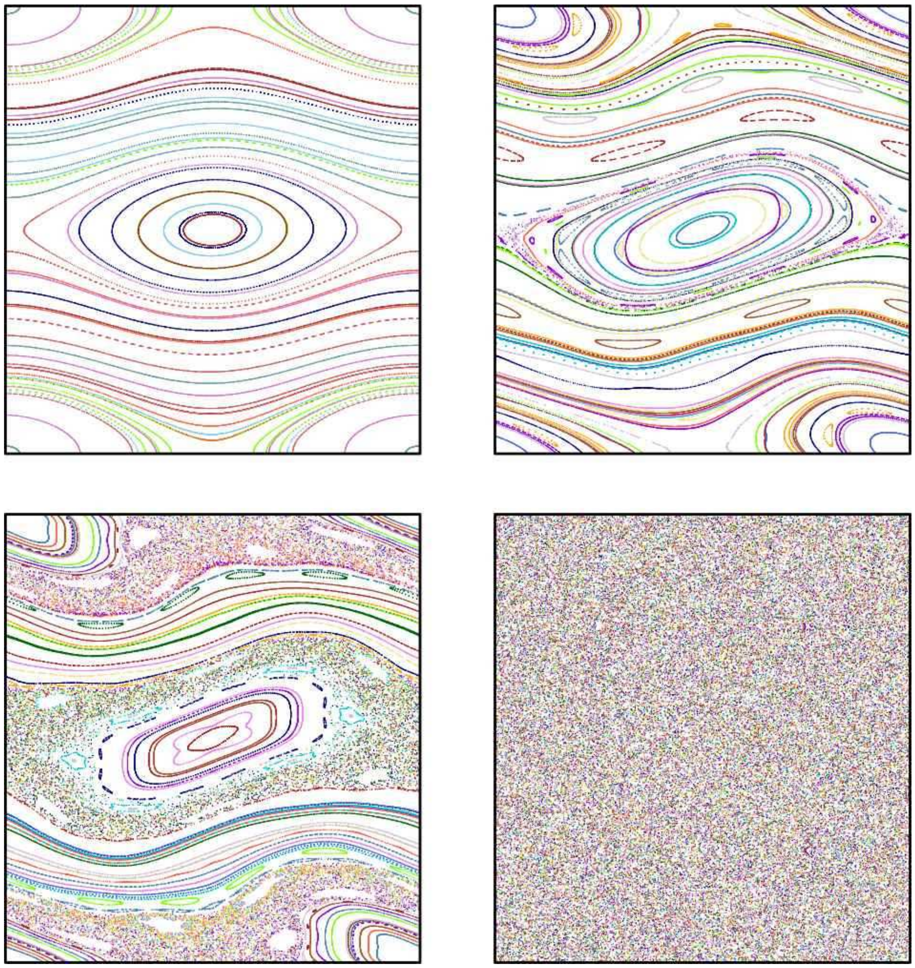

Figure 7.2: The kicked harper map, with $\alpha = 2$, and with $\epsilon = 0.01$, 0.125, 0.2, and 5.0 (clockwise from upper left). The phase space here is the unit torus, $\mathbb{T}^2 = [0,1] \times [0,1]$.

Note that the determinant of Jacobean of the map is unity:

$$\frac{\partial(q_{n+1}\,,\,p_{n+1})}{\partial(q_n\,,\,p_n)} = \begin{pmatrix} 1 & \frac{\tau}{m} \\ -\tau\,V''(q_{n+1}) & 1 - \frac{\tau^2}{m}\,V''(q_{n+1}) \end{pmatrix} . \tag{7.10}$$

This means that the map preserves phase space volumes.

Consider, for example, the Hamiltonian $H(t) = \frac{L^2}{2I} - V\cos(\phi)\,K(t)$, where L is the angular momentum conjugate to ϕ. This results in the map

$$\phi_{n+1} = \phi_n + 2\pi\epsilon\,J_n \tag{7.11}$$

$$J_{n+1} = J_n - \epsilon \sin\phi_{n+1} \ , \tag{7.12}$$

where $J_n = L_n/\sqrt{2\pi I V}$ and $\epsilon = \tau\sqrt{V/2\pi I}$. This is known as the *standard map*[1]. In the

[1] The standard map us usually written in the form $x_{n+1} = x_n + \mathcal{J}_n$ and $\mathcal{J}_{n+1} = \mathcal{J}_n - k\sin(2\pi x_{n+1})$. We can recover our version by rescaling $\phi_n = 2\pi x_n$, $\mathcal{J}_n \equiv \sqrt{k}\,J_n$ and defining $\epsilon \equiv \sqrt{k}$.

limit $\epsilon \to 0$, we may define $\dot{x} = (x_{n+1} - x_n)/\epsilon$ and $\dot{J} = (J_{n+1} - J_n)/\epsilon$, and we recover the continuous time dynamics $\dot{\phi} = 2\pi J$ and $\dot{J} = -\sin\phi$. These dynamics preserve the energy function $E = \pi J^2 - \cos\phi$. There is a separatrix at $E = 1$, given by $J(\phi) = \pm\frac{2}{\pi}\big|\cos(\phi/2)\big|$. We see from fig. 7.1 that this separatrix is the first structure to be replaced by a chaotic fuzz as ϵ increases from zero to a small finite value.

Another well-studied system is the *kicked Harper model*, for which

$$H(t) = -V_1 \cos\left(\frac{2\pi p}{P}\right) - V_2 \cos\left(\frac{2\pi q}{Q}\right) K(t) \ . \tag{7.13}$$

With $x = q/Q$ and $y = p/P$, Hamilton's equations generate the map

$$x_{n+1} = x_n + \epsilon\,\alpha\,\sin(2\pi y_n) \tag{7.14}$$

$$y_{n+1} = y_n - \frac{\epsilon}{\alpha}\,\sin(2\pi x_{n+1}) \ , \tag{7.15}$$

where $\epsilon = 2\pi\tau\sqrt{V_1 V_2}/PQ$ and $\alpha = \sqrt{V_1/V_2}$ are dimensionless parameters. In this case, the conserved energy is

$$E = -\alpha^{-1}\cos(2\pi x) - \alpha\cos(2\pi y) \ . \tag{7.16}$$

There are then two separatrices, at $E = \pm(\alpha - \alpha^{-1})$, with equations $\alpha\cos(\pi y) = \pm\sin(\pi x)$ and $\alpha\sin(\pi y) = \pm\cos(\pi x)$. Again, as is apparent from fig. 7.2, the separatrix is the first structure to be destroyed at finite ϵ. We shall return to discuss this phenomenon below.

7.2 One-dimensional Maps

Consider now an even simpler case of a purely one-dimensional map,

$$x_{n+1} = f(x_n) \ , \tag{7.17}$$

or, equivalently, $x' = f(x)$. A fixed point of the map satisfies $x = f(x)$. Writing the solution as x^* and expanding about the fixed point, we write $x = x^* + u$ and obtain

$$u' = f'(x^*)\,u + \mathcal{O}(u^2) \ . \tag{7.18}$$

Thus, the fixed point is stable if $\big|f'(x^*)\big| < 1$, since successive iterates of u then get smaller and smaller. The fixed point is unstable if $\big|f'(x^*)\big| > 1$.

Perhaps the most important and most studied of the one-dimensional maps is the logistic map, where $f(x) = rx(1-x)$, defined on the interval $x \in [0,1]$. This has a fixed point at $x^* = 1 - r^{-1}$ if $r > 1$. We then have $f'(x^*) = 2 - r$, so the fixed point is stable if $r \in (1,3)$. What happens for $r > 3$? We can explore the behavior of the iterated map by drawing a *cobweb diagram*, shown in fig. 7.3. We sketch, on the same graph, the curves $y = x$ (in blue) and $y = f(x)$ (in black). Starting with a point x on the line $y = x$, we move vertically until we reach the curve $y = f(x)$. To iterate, we then move horizontally to the line $y = x$

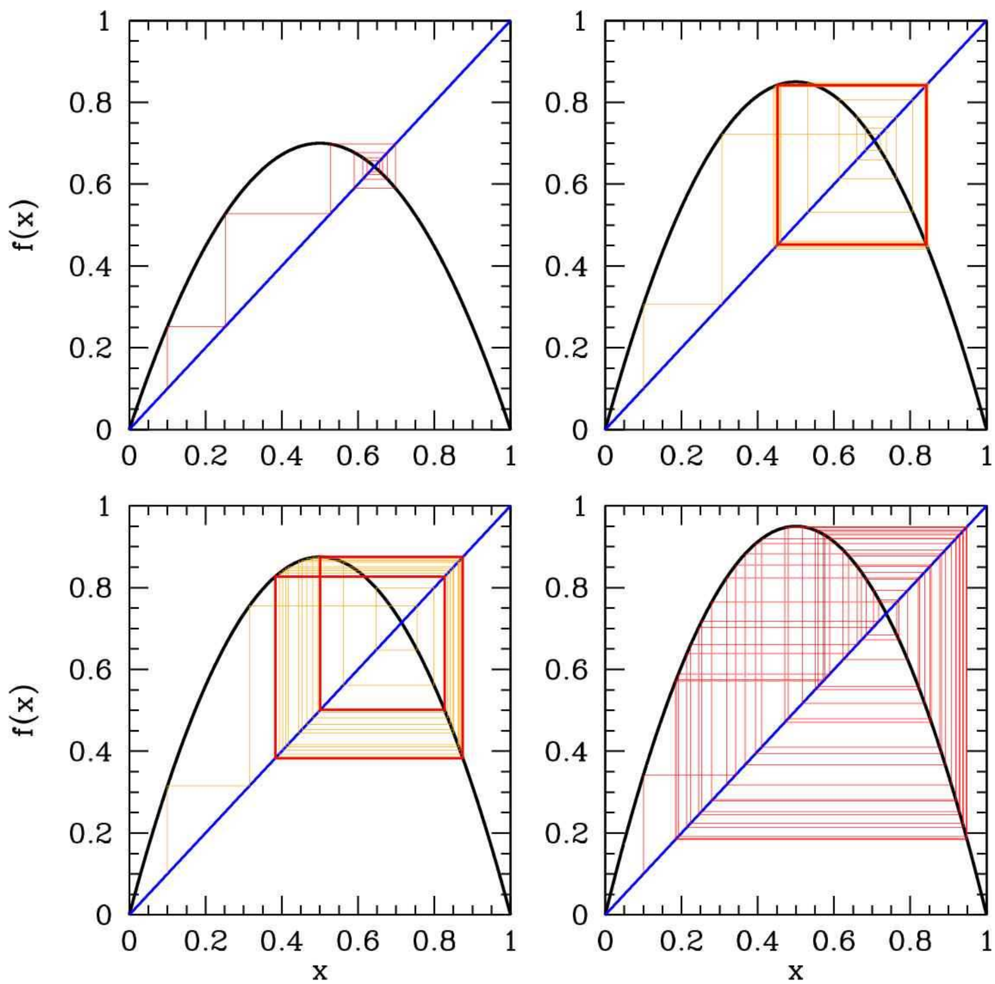

Figure 7.3: Cobweb diagram showing iterations of the logistic map $f(x) = rx(1-x)$ for $r = 2.8$ (upper left), $r = 3.4$ (upper right), $r = 3.5$ (lower left), and $r = 3.8$ (lower right). Note the single stable fixed point for $r = 2.8$, the stable two-cycle for $r = 3.4$, the stable four-cycle for $r = 3.5$, and the chaotic behavior for $r = 3.8$.

and repeat the process. We see that for $r = 3.4$ the fixed point x^* is unstable, but there is a stable two-cycle, defined by the equations

$$x_2 = rx_1(1-x_1) \tag{7.19}$$

$$x_1 = rx_2(1-x_2) \ . \tag{7.20}$$

The second iterate of $f(x)$ is then

$$f^{(2)}(x) = f\big(f(x)\big) = r^2 x(1-x)\big(1 - rx + rx^2\big) \ . \tag{7.21}$$

Setting $x = f^{(2)}(x)$, we obtain a cubic equation. Since $x - x^*$ must be a factor, we can divide out by this monomial and obtain a quadratic equation for x_1 and x_2. We find

$$x_{1,2} = \frac{1 + r \pm \sqrt{(r+1)(r-3)}}{2r} \ . \tag{7.22}$$

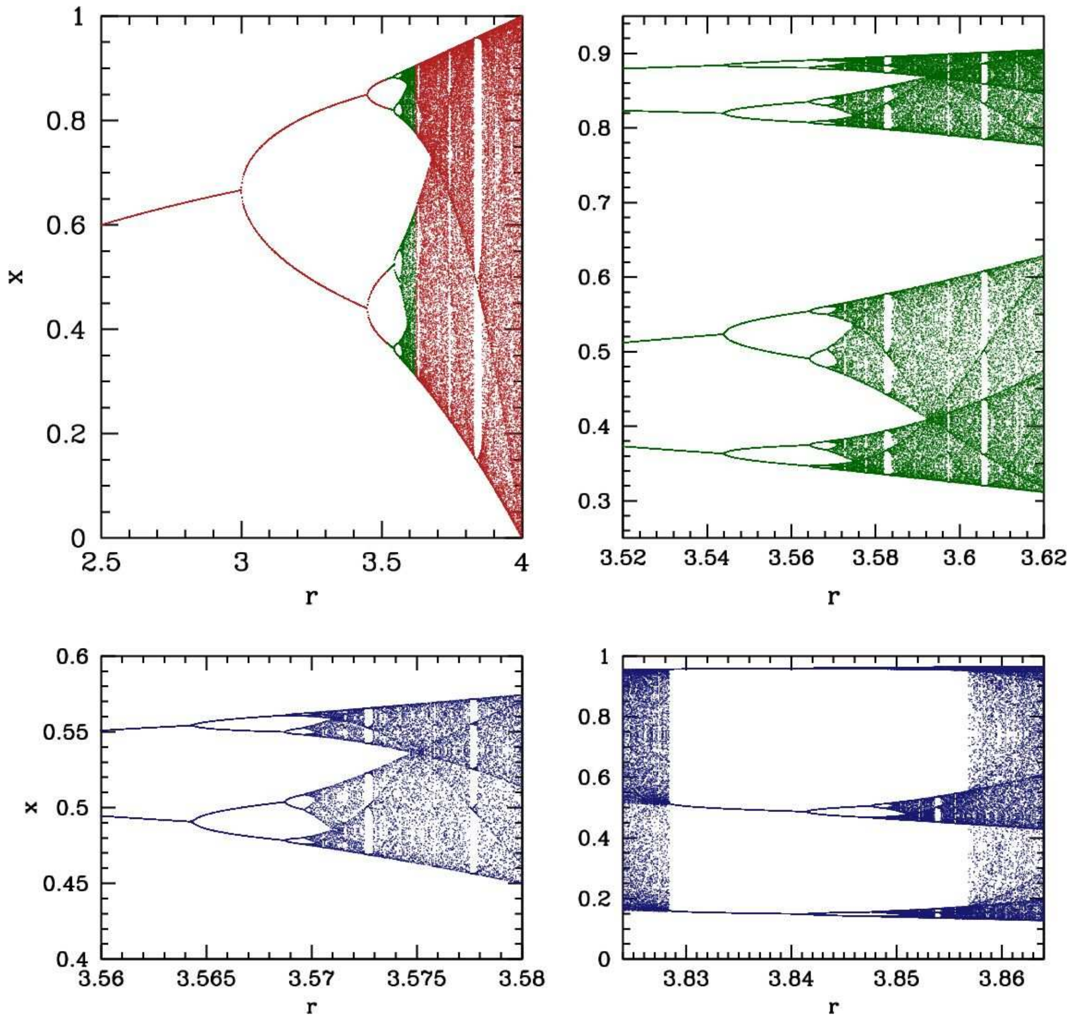

Figure 7.4: Iterates of the logistic map $f(x) = rx(1-x)$.

How stable is this 2-cycle? We find

$$\frac{d}{dx} f^{(2)}(x) = r^2(1-2x_1)(1-2x_2) = -r^2 + 2r + 4 \ . \tag{7.23}$$

The condition that the 2-cycle be stable is then

$$-1 < r^2 - 2r - 4 < 1 \qquad \Longrightarrow \qquad r \in \big[3\,,\,1+\sqrt{6}\,\big] \ . \tag{7.24}$$

At $r = 1 + \sqrt{6} = 3.4494897\ldots$ there is a bifurcation to a 4-cycle, as can be seen in fig. 7.4.

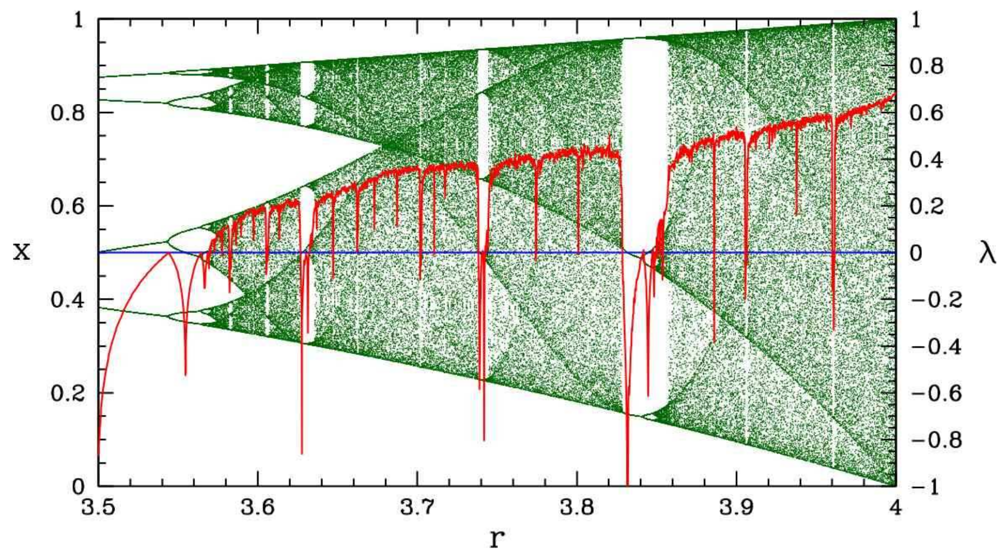

Figure 7.5: Lyapunov exponent for the logistic map.

7.2.1 Lyapunov Exponents

The *Lyapunov exponent* $\lambda(x)$ of the iterated map $f(x)$ at point x is defined to be

$$\lambda(x) = \lim_{n\to\infty} \frac{1}{n} \ln\left(\frac{df^{(n)}(x)}{dx}\right) = \lim_{n\to\infty} \frac{1}{n} \sum_{j=1}^{n} \ln\big(f'(x_j)\big) \ , \tag{7.25}$$

where $x_{j+1} \equiv f(x_j)$. The significance of the Lyapunov exponent is the following. If $\mathsf{Re}\big(\lambda(x)\big) > 0$ then two initial conditions near x will exponentially separate under the iterated map. For the *tent map*,

$$f(x) = \begin{cases} 2rx & \text{if } x < \frac{1}{2} \\ 2r(1-x) & \text{if } x \geq \frac{1}{2} \ , \end{cases} \tag{7.26}$$

one easily finds $\lambda(x) = \ln(2r)$ independent of x. Thus, if $r > \frac{1}{2}$ the Lyapunov exponent is positive, meaning that every neighboring pair of initial conditions will eventually separate exponentially under repeated application of the map. The Lyapunov exponent for the logistic map is depicted in fig. 7.5.

7.2.2 Chaos in the logistic map

What happens in the logistic map for $r > 1 + \sqrt{6}$? At this point, the 2-cycle becomes unstable and a stable 4-cycle develops. However, this soon goes unstable and is replaced by a stable 8-cycle, as the right hand panel of fig. 7.4 shows. The first eight values of r where

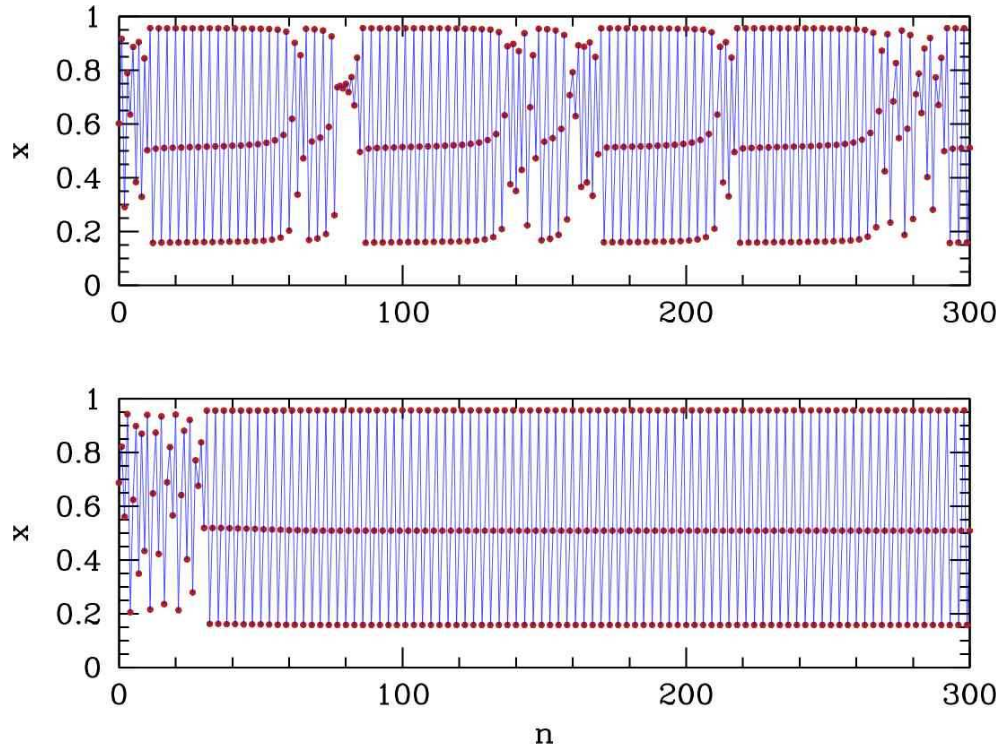

Figure 7.6: Intermittency in the logistic map in the vicinity of the 3-cycle Top panel: $r = 3.828$, showing intermittent behavior. Bottom panel: $r = 3.829$, showing a stable 3-cycle.

bifurcations occur are given by

$$r_1 = 3 \ , \ r_2 = 1 + \sqrt{6} = 3.4494897 \ , \ r_3 = 3.544096 \ , \ r_4 = 3.564407 \ ,$$
$$r_5 = 3.568759 \ , \ r_6 = 3.569692 \ , \ r_7 = 3.569891 \ , \ r_8 = 3.569934 \ , \ \ldots$$

Feigenbaum noticed that these numbers seemed to be converging exponentially. With the *Ansatz*

$$r_\infty - r_k = \frac{c}{\delta^k} \ , \tag{7.27}$$

one finds

$$\delta = \frac{r_k - r_{k-1}}{r_{k+1} - r_k} \ , \tag{7.28}$$

and taking the limit $k \to \infty$ from the above data one finds

$$\delta = 4.669202 \quad , \quad c = 2.637 \quad , \quad r_\infty = 3.5699456 \ . \tag{7.29}$$

There's a very nifty way of thinking about the chaos in the logistic map at the special value $r = 4$. If we define $x_n \equiv \sin^2\theta_n$, then we find

$$\theta_{n+1} = 2\theta_n \ . \tag{7.30}$$

Now let us write

$$\theta_0 = \pi \sum_{k=1}^{\infty} \frac{b_k}{2^k} \ , \tag{7.31}$$

where each b_k is either 0 or 1. In other words, the $\{b_k\}$ are the digits in the binary decimal expansion of θ_0/π. Now $\theta_n = 2^n \theta_0$, hence

$$\theta_n = \pi \sum_{k=1}^{\infty} \frac{b_{n+k}}{2^k} \ . \tag{7.32}$$

We now see that the logistic map has the effect of *shifting* to the left the binary digits of θ_n/π to yield θ_{n+1}/π. The last digit falls off the edge of the world, as it were, since it results in an overall contribution to θ_{n+1} which is zero modulo 2π. This very emphatically demonstrates the sensitive dependence on initial conditions which is the hallmark of chaotic behavior, for eventually two very close initial conditions, differing by $\Delta\theta \sim 2^{-m}$, will, after m iterations of the logistic map, come to differ by $\mathcal{O}(1)$.

7.2.3 Intermittency

Successive period doubling is one route to chaos, as we've just seen. Another route is *intermittency*. Intermittency works like this. At a particular value of our control parameter r, the map exhibits a stable periodic cycle, such as the stable 3-cycle at $r = 3.829$, as shown in the bottom panel of fig. 7.6. If we then vary the control parameter slightly in a certain direction, the periodic behavior persists for a finite number of iterations, followed by a *burst*, which is an interruption of the regular periodicity, followed again by periodic behavior, *ad infinitum*. There are three types of intermittent behavior, depending on whether the Lyapunov exponent λ goes through $\mathsf{Re}(\lambda) = 0$ while $\mathsf{Im}(\lambda) = 0$ (type-I intermittency), or with $\mathsf{Im}(\lambda) = \pi$ (type-III intermittency, or, as is possible for two-dimensional maps, with $\mathsf{Im}(\lambda) = \eta$, a general real number.

7.3 Attractors

An *attractor* of a dynamical system $\dot{\boldsymbol{\varphi}} = \boldsymbol{V}(\boldsymbol{\varphi})$ is the set of $\boldsymbol{\varphi}$ values that the system evolves to after a sufficiently long time. For $N = 1$ the only possible attractors are stable fixed points. For $N = 2$, we have stable nodes and spirals, but also stable limit cycles. For $N > 2$ the situation is qualitatively different, and a fundamentally new type of set, the *strange attractor,* emerges.

A strange attractor is basically a bounded set on which nearby orbits diverge exponentially (*i.e.* there exists at least one positive Lyapunov exponent). To envision such a set, consider a flat rectangle, like a piece of chewing gum. Now fold the rectangle over, stretch it, and squash it so that it maintains its original volume. Keep doing this. Two points which started out nearby to each other will eventually, after a sufficiently large number of folds and stretches, grow far apart. Formally, a strange attractor is a *fractal*, and may have *noninteger Hausdorff dimension.* (We won't discuss fractals and Hausdorff dimension here.)

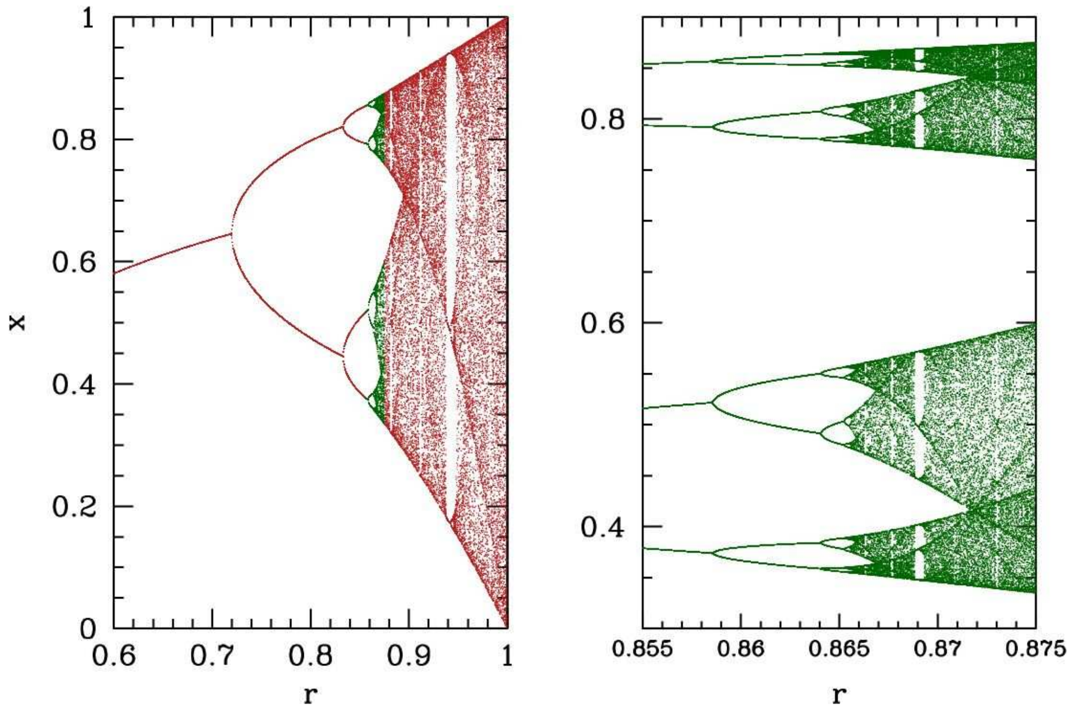

Figure 7.7: Iterates of the sine map $f(x) = r\sin(\pi x)$.

7.4 The Lorenz Model

The canonical example of an $N = 3$ strange attractor is found in the Lorenz model. E. N. Lorenz, in a seminal paper from the early 1960's, reduced the essential physics of the

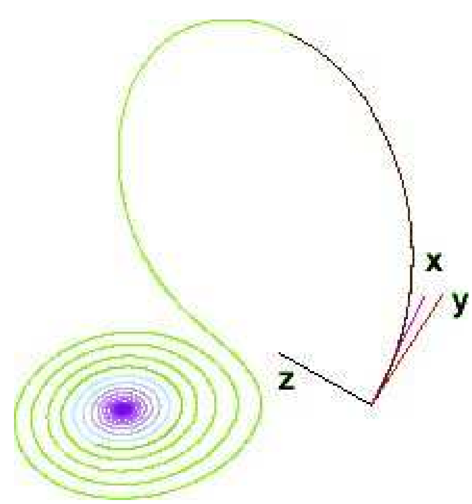

Figure 7.8: Evolution of the Lorenz equations for $\sigma = 10$, $b = \frac{8}{3}$, and $r = 15$, with initial conditions $(x, y, z) = (0, 1, 0)$, projected onto the (x, z) plane. The system is attracted by a stable spiral. (Source: Wikipedia)

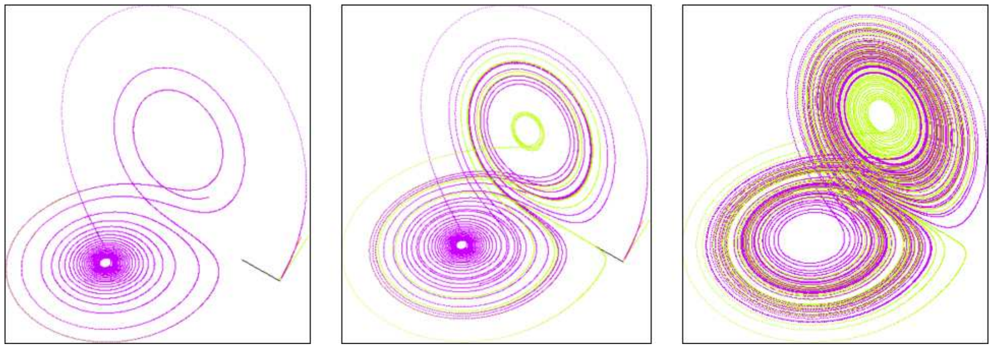

Figure 7.9: Evolution of the Lorenz equations showing sensitive dependence on initial conditions. The magenta and green curves differ in their initial X coordinate by 10^{-5}. (Source: Wikipedia)

coupled *partial* differential equations describing Rayleigh-Benard convection (a fluid slab of finite thickness, heated from below – in Lorenz's case a model of the atmosphere warmed by the ocean) to a set of twelve coupled nonlinear *ordinary* differential equations. Lorenz's intuition was that his weather model should exhibit recognizable patterns over time. What he found instead was that in some cases, changing his initial conditions by a part in a thousand rapidly led to totally different behavior. This *sensitive dependence on initial conditions* is a hallmark of chaotic systems.

The essential physics (or mathematics?) of Lorenz's $N = 12$ system is elicited by the reduced $N = 3$ system,

$$\dot{X} = -\sigma X + \sigma Y \tag{7.33}$$

$$\dot{Y} = rX - Y - XZ \tag{7.34}$$

$$\dot{Z} = XY - bZ \ , \tag{7.35}$$

where σ, r, and b are all real and positive. Here t is the familiar time variable (appropriately scaled), and (X, Y, Z) represent linear combinations of physical fields, such as global wind current and poleward temperature gradient. These equations possess a symmetry under $(X, Y, Z) \to (-X, -Y, Z)$, but what is most important is the presence of nonlinearities in the second and third equations.

The Lorenz system is *dissipative* because phase space volumes contract:

$$\boldsymbol{\nabla}\cdot\boldsymbol{V} = \frac{\partial \dot{X}}{\partial X} + \frac{\partial \dot{Y}}{\partial Y} + \frac{\partial \dot{Z}}{\partial Z} = -(\sigma + b + 1) \ . \tag{7.36}$$

Thus, volumes contract under the flow. Another property is the following. Let

$$F(X, Y, Z) = \tfrac{1}{2}X^2 + \tfrac{1}{2}Y^2 + \tfrac{1}{2}(Z - r - \sigma)^2 \ . \tag{7.37}$$

Then

$$\begin{aligned} \dot{F} &= X\dot{X} + Y\dot{Y} + (Z - r - \sigma)\dot{Z} \\ &= -\sigma X^2 - Y^2 - b\big(Z - \tfrac{1}{2}r - \tfrac{1}{2}\sigma\big)^2 + \tfrac{1}{4}b(r + \sigma)^2 \ . \end{aligned} \tag{7.38}$$

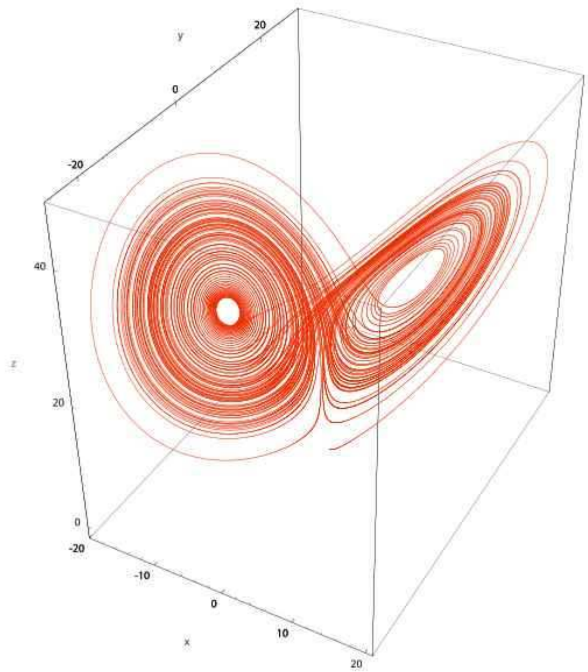

Figure 7.10: Evolution of the Lorenz equations for $\sigma = 10$, $b = \frac{8}{3}$, and $r = 28$, with initial conditions $(X_0, Y_0, Z_0) = (0, 1, 0)$, showing the 'strange attractor'. (Source: Wikipedia)

Thus, $\dot{F} < 0$ outside an ellipsoid, which means that all solutions must remain bounded in phase space for all times.

7.4.1 Fixed point analysis

Setting $\dot{x} = \dot{y} = \dot{z} = 0$, we have three possible solutions. One solution, which is always present, is $x^* = y^* = z^* = 0$. If we linearize about this solution, we obtain

$$\frac{d}{dt}\begin{pmatrix}\delta X\\ \delta Y\\ \delta Z\end{pmatrix} = \begin{pmatrix}-\sigma & \sigma & 0\\ r & -1 & 0\\ 0 & 0 & -b\end{pmatrix}\begin{pmatrix}\delta X\\ \delta Y\\ \delta Z\end{pmatrix} . \tag{7.39}$$

The eigenvalues of the linearized dynamics are found to be

$$\begin{aligned}\lambda_{1,2} &= -\tfrac{1}{2}(1+\sigma) \pm \tfrac{1}{2}\sqrt{(1+\sigma)^2 + 4\sigma(r-1)} \\ \lambda_3 &= -b \ ,\end{aligned} \tag{7.40}$$

and thus if $0 < r < 1$ all three eigenvalues are negative, and the fixed point is a stable node. If, however, $r > 1$, then $\lambda_2 > 0$ and the fixed point is attractive in two directions but repulsive in a third, corresponding to a three-dimensional version of a saddle point.

For $r > 1$, a new pair of solutions emerges, with

$$X^* = Y^* = \pm\sqrt{b(r-1)} \quad , \quad Z^* = r - 1 \ . \tag{7.41}$$

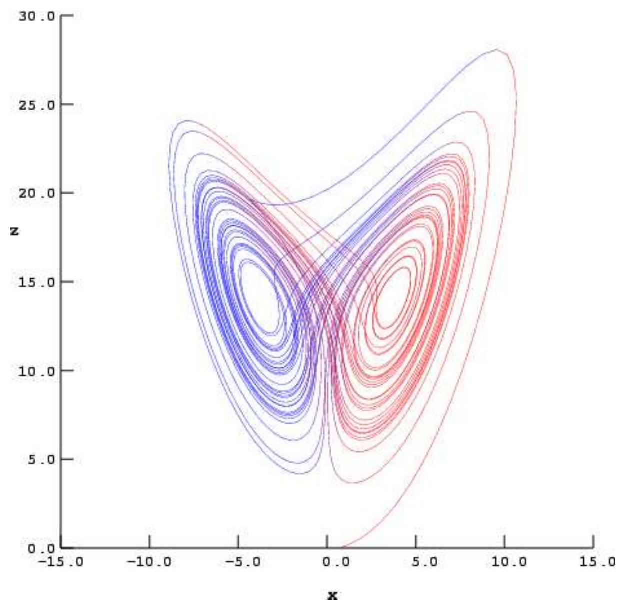

Figure 7.11: The Lorenz attractor, projected onto the (X, Z) plane.

Linearizing about either one of these fixed points, we find

$$\frac{d}{dt}\begin{pmatrix}\delta X\\ \delta Y\\ \delta Z\end{pmatrix} = \begin{pmatrix}-\sigma & \sigma & 0\\ 1 & -1 & -X^*\\ X^* & X^* & -b\end{pmatrix}\begin{pmatrix}\delta X\\ \delta Y\\ \delta Z\end{pmatrix} \ . \tag{7.42}$$

The characteristic polynomial of the linearized map is

$$P(\lambda) = \lambda^3 + (b+\sigma+1)\,\lambda^2 + b(\sigma+r)\,\lambda + 2b(r-1) \ . \tag{7.43}$$

Since b, σ, and r are all positive, $P'(\lambda) > 0$ for all $\lambda \geq 0$. Since $P(0) = 2b(r-1) > 0$, we may conclude that there is always at least one eigenvalue λ_1 which is real and negative. The remaining two eigenvalues are either both real and negative, or else they occur as a complex conjugate pair: $\lambda_{2,3} = \alpha \pm i\beta$. The fixed point is stable provided $\alpha < 0$. The stability boundary lies at $\alpha = 0$. Thus, we set

$$P(i\beta) = \Big[2b(r-1) - (b+\sigma+1)\beta^2\Big] + i\Big[b(\sigma+r) - \beta^2\Big]\beta = 0 \ , \tag{7.44}$$

which results in two equations. Solving these two equations for $r(\sigma, b)$, we find

$$r_{\rm c} = \frac{\sigma(\sigma+b+3)}{\sigma-b-1} \ . \tag{7.45}$$

The fixed point is stable for $r \in \big[1, r_{\rm c}\big]$. These fixed points correspond to steady convection. The approach to this fixed point is shown in Fig. 7.8.

The Lorenz system has commonly been studied with $\sigma = 10$ and $b = \frac{8}{3}$. This means that the volume collapse is very rapid, since $\boldsymbol{\nabla}\cdot \boldsymbol{V} = -\frac{41}{3} \approx -13.67$, leading to a volume contraction

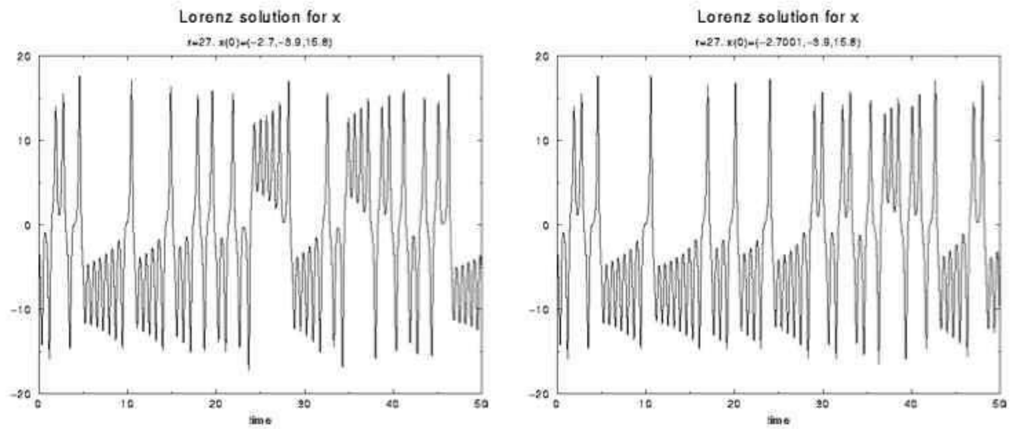

Figure 7.12: $X(t)$ for the Lorenz equations with $\sigma = 10$, $b = \frac{8}{3}$, $r = 28$, and initial conditions $(X_0, Y_0, Z_0) = (-2.7, -3.9, 15.8)$, and initial conditions $(X_0, Y_0, Z_0) = (-2.7001, -3.9, 15.8)$.

of $e^{-41/3} \simeq 1.16 \times 10^{-6}$ per unit time. For these parameters, one also has $r_{\rm c} = \frac{470}{19} \approx 24.74$. The capture by the strange attractor is shown in Fig. 7.10.

In addition to the new pair of fixed points, a strange attractor appears for $r > r_{\rm s} \simeq 24.06$. In the narrow interval $r \in [24.06, 24.74]$ there are then *three* stable attractors, two of which correspond to steady convection and the third to chaos. Over this interval, there is also hysteresis. *I.e.* starting with a convective state for $r < 24.06$, the system remains in the convective state until $r = 24.74$, when the convective fixed point becomes unstable. The system is then driven to the strange attractor, corresponding to chaotic dynamics. Reversing the direction of r, the system remains chaotic until $r = 24.06$, when the strange attractor loses its own stability.

7.4.2 Poincaré section

One method used by Lorenz in analyzing his system was to plot its *Poincaré section*. This entails placing one constraint on the coordinates (X, Y, Z) to define a two-dimensional surface Σ, and then considering the intersection of this surface Σ with a given phase curve for the Lorenz system. Lorenz chose to set $\dot{Z} = 0$, which yields the surface $Z = b^{-1}XY$. Note that since $\dot{Z} = 0$, $Z(t)$ takes its maximum and minimum values on this surface; see fig. 7.13. By plotting the values of the maxima Z_N as the integral curve successively passed through this surface, Lorenz obtained results such as those shown in fig. 7.14, which has the form of a one-dimensional map and may be analyzed as such. Thus, chaos in the Lorenz attractor can be related to chaos in a particular one-dimensional map, known as the *return map* for the Lorenz system.

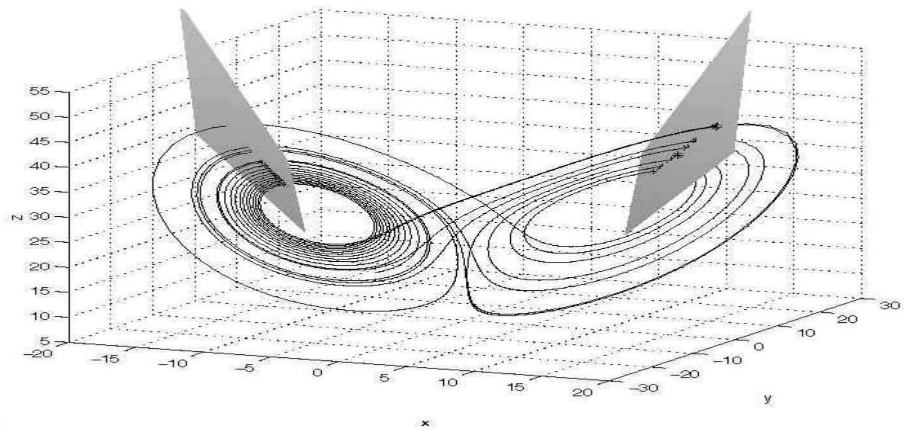

Figure 7.13: Lorenz attractor for $b = \frac{8}{3}$, $\sigma = 10$, and $r = 28$. Maxima of Z are depicted by stars.

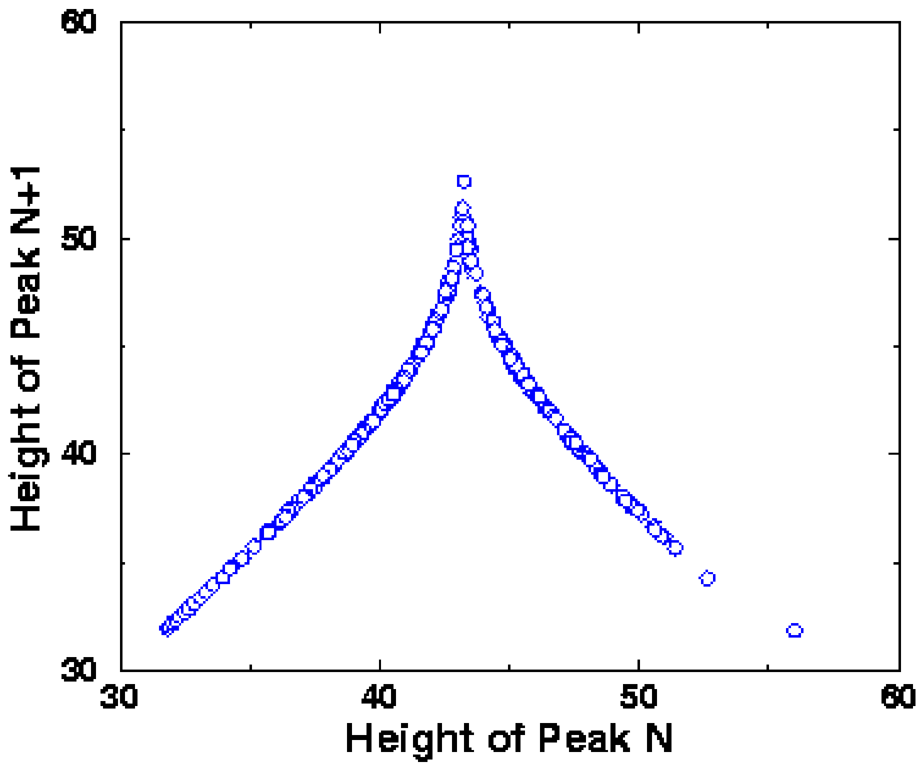

Figure 7.14: Plot of relation between successive maxima Z_N along the strange attractor for the Lorenz system.

7.4.3 Rössler System

Another simple $N = 3$ system which possesses a strange attractor is the Rössler system,

$$\dot{X} = -Y - Z \tag{7.46}$$

$$\dot{Y} = Z + aY \tag{7.47}$$

$$\dot{Z} = b + Z(X - c) \ , \tag{7.48}$$

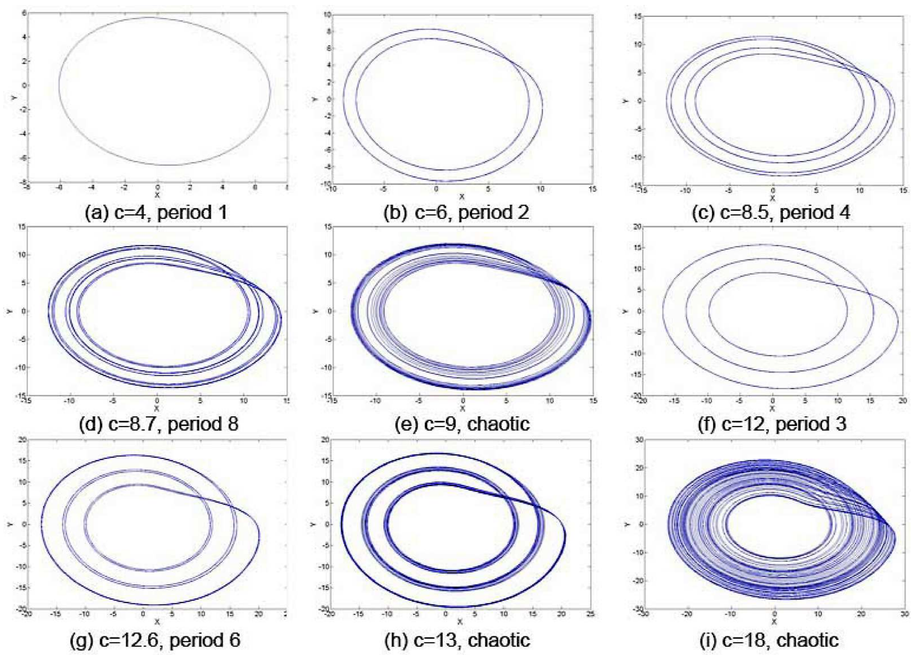

Figure 7.15: Period doubling bifurcations of the Rössler attractor, projected onto the (x, y) plane, for nine values of c, with $a = b = \frac{1}{10}$.

typically studied as a function of c for $a = b = \frac{1}{5}$. In Fig. 7.16, we present results from work by Crutchfield *et al.* (1980). The transition from simple limit cycle to strange attractor proceeds via a sequence of period-doubling bifurcations, as shown in the figure. A convenient diagnostic for examining this period-doubling route to chaos is the *power spectral density,* or PSD, defined for a function $F(t)$ as

$$\Phi_F(\omega) = \left| \int\limits_{-\infty}^{\infty} \frac{d\omega}{2\pi}\, F(t)\, e^{-i\omega t} \right|^2 = \big|\hat{F}(\omega)\big|^2 \ . \tag{7.49}$$

As one sees in Fig. 7.16, as c is increased past each critical value, the PSD exhibits a series of frequency halvings (*i.e.* period doublings). All harmonics of the lowest frequency peak are present. In the chaotic region, where $c > c_\infty \approx 4.20$, the PSD also includes a noisy broadband background.

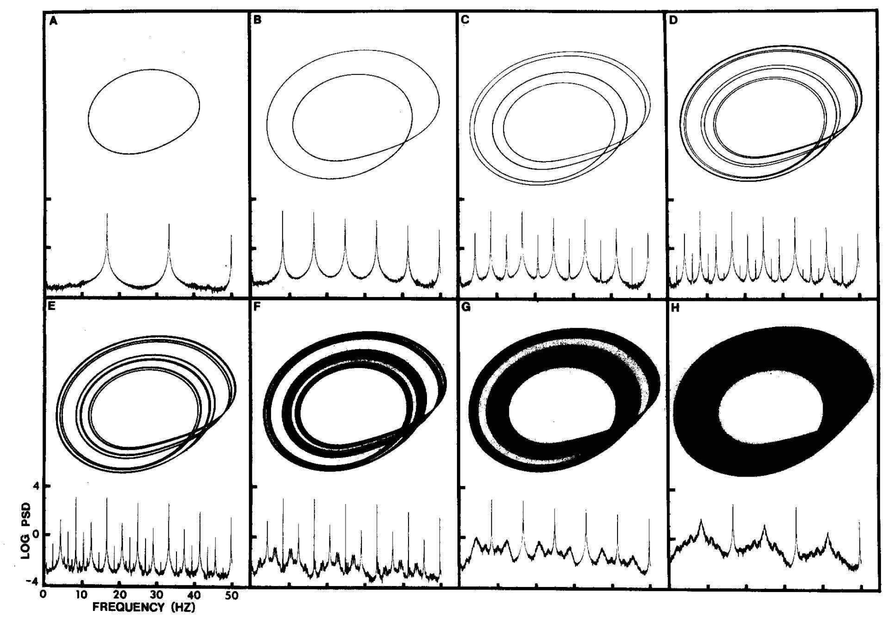

Figure 7.16: Period doubling bifurcations of the Rössler attractor with $a = b = \frac{1}{5}$, projected onto the (X,Y) plane, for eight values of c, and corresponding power spectral density for Z(t). (a) $c = 2.6$; (b) $c = 3.5$; (c) $c = 4.1$; (d) $c = 4.18$; (e) $c = 4.21$; (f) $c = 4.23$; (g) $c = 4.30$; (h) $c = 4.60$.

Chapter 8

Front Propagation

8.1 Reaction-Diffusion Systems

We've studied simple $N = 1$ dynamical systems of the form

$$\frac{du}{dt} = R(u) \ . \tag{8.1}$$

Recall that the dynamics evolves $u(t)$ monotonically toward the first stable fixed point encountered. Now let's extend the function $u(t)$ to the spatial domain as well, *i.e.* $u(\boldsymbol{x}, t)$, and add a diffusion term:

$$\frac{\partial u}{\partial t} = D\, \boldsymbol{\nabla}^2 u + R(u) \ , \tag{8.2}$$

where D is the diffusion constant. This is an example of a *reaction-diffusion system*. If we extend $u(\boldsymbol{x}, t)$ to a multicomponent field $\boldsymbol{u}(\boldsymbol{x}, t)$, we obtain the general reaction-diffusion equation (RDE)

$$\frac{\partial u_i}{\partial t} = D_{ij}\, \boldsymbol{\nabla}^2 u_i + R_i(u_1, \ldots, u_N) \ . \tag{8.3}$$

Here, $\boldsymbol{u}$ is interpreted as a *vector of reactants*, $\boldsymbol{R}(\boldsymbol{u})$ describes the *nonlinear local reaction kinetics*, and D_{ij} is the *diffusivity matrix*. If diffusion is negligible, this PDE reduces to decoupled local ODEs of the form $\dot{\boldsymbol{u}} = \boldsymbol{R}(\boldsymbol{u})$, which is to say a dynamical system at each point in space. Thus, any fixed point $\boldsymbol{u}^*$ of the local reaction dynamics also describes a spatially homogeneous, time-independent solution to the RDE. These solutions may be characterized as dynamically stable or unstable, depending on the eigenspectrum of the Jacobian matrix $J_{ij} = \partial_i R_j(\boldsymbol{u}^*)$. At a stable fixed point, $\mathsf{Re}(\lambda_i) < 0$ for all eigenvalues.

8.1.1 Single component systems

We first consider the single component system,

$$\frac{\partial u}{\partial t} = D\boldsymbol{\nabla}^2 u + R(u) \ . \tag{8.4}$$

Note that the right hand side can be expressed as the functional derivative of a *Lyapunov functional*,

$$L[u] = \int d^dx \left[\tfrac{1}{2} D(\boldsymbol{\nabla} u)^2 - U(u) \right] , \tag{8.5}$$

where

$$U(u) = \int_0^u du' \, R(u') . \tag{8.6}$$

(The lower limit in the above equation is arbitrary.) Thus, eqn. 8.4 is equivalent to

$$\frac{\partial u}{\partial t} = -\frac{\delta L}{\delta u(\boldsymbol{x},t)} . \tag{8.7}$$

Thus, the Lyapunov functional runs strictly downhill, *i.e.* $\dot{L} < 0$, except where $u(\boldsymbol{x},t)$ solves the RDE, at which point $\dot{L} = 0$.

8.1.2 Propagating front solutions

Suppose the dynamical system $\dot{u} = R(u)$ has two or more fixed points. Each such fixed point represents a static, homogeneous solution to the RDE. We now seek a dynamical, inhomogeneous solution to the RDE in the form of a *propagating front*, described by

$$u(x,t) = u(x - Vt) , \tag{8.8}$$

where V is the (as yet unknown) front propagation speed. With this *Ansatz*, the PDE of eqn. 8.4 is converted to an ODE,

$$D \frac{d^2u}{d\xi^2} + V \frac{du}{d\xi} + R(u) = 0 , \tag{8.9}$$

where $\xi = x - Vt$. With $R(u) \equiv U'(u)$ as in eqn. 8.6, we have the following convenient interpretation. If we substitute $u \to q$, $\xi \to t$, $D \to m$, and $v \to \gamma$, this equation describes the damped motion of a massive particle under friction: $m\ddot{q} + \gamma\dot{q} = -U'(q)$. The fixed points q^* satisfy $U'(q^*) = 0$ and are hence local extrema of $U(q)$. The propagating front solution we seek therefore resembles the motion of a massive particle rolling between extrema of the potential $U(q)$. Note that the stable fixed points of the local reaction kinetics have $R'(q) = U''(q) < 0$, corresponding to *unstable* mechanical equilibria. Conversely, unstable fixed points of the local reaction kinetics have $R'(q) = U''(q) > 0$, corresponding to *stable* mechanical equilibria.

A front solution corresponds to a mechanical motion interpolating between two equilibria at $u(\xi = \pm\infty)$. If the front propagates to the right then $V > 0$, corresponding to a positive (*i.e.* usual) friction coefficient γ. Any solution, therefore must start from an unstable equilibrium point u^*_{I} and end at another equilibrium u^*_{II}. The final state, however, may be either a stable or an unstable equilibrium for the potential $U(q)$. Consider the functions $R(u)$ and $U(u)$ in the left panels of fig. 8.1. Starting at 'time' $\xi = -\infty$ with $u = u^*_{\mathrm{I}} = 1$, a particle with

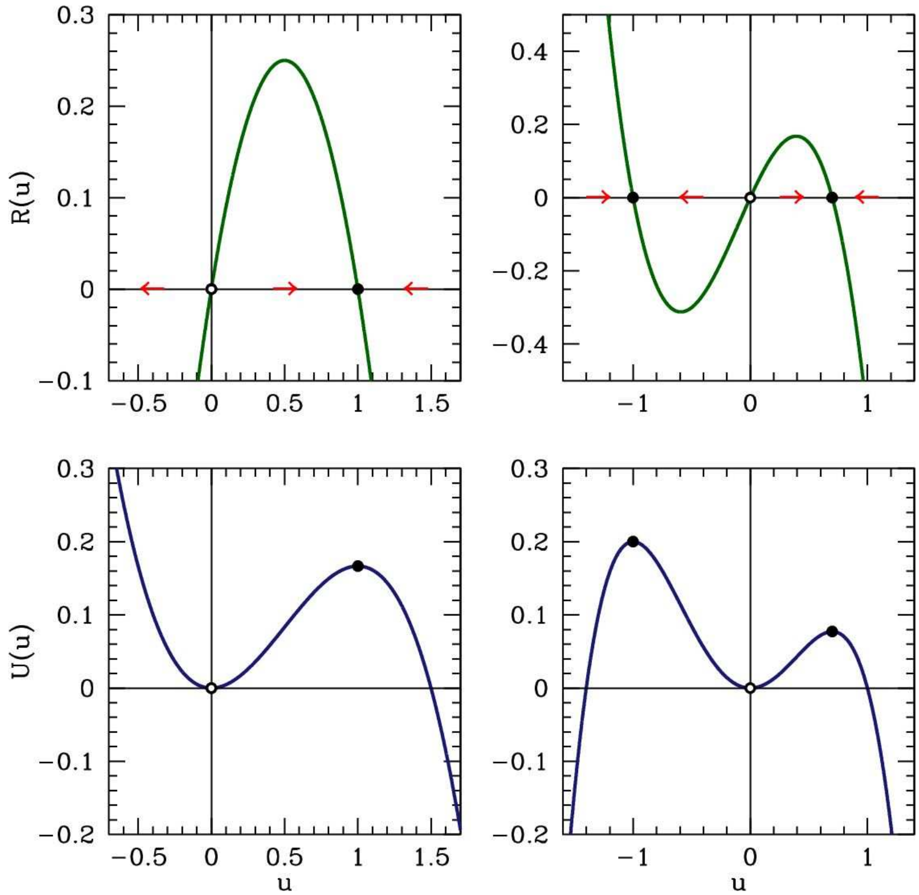

Figure 8.1: Upper panels : reaction functions $R(u) = ru(a - u)$ with $r = a = 1$ (left) and $R(u) = -ru(u - a)(u - b)$ with $r = 1$, $a = -1$, $b = 0.7$ (right), along with corresponding potentials $U(u)$ (bottom panels). Stable fixed points for the local reaction kinetic are shown with a solid black dot, and unstable fixed points as a hollow black dot. Note that $R(u) = U'(u)$, so stable fixed points for the local reaction kinetics have $R'(u) = U''(u) < 0$, and thus correspond to *unstable* mechanical equilibria in the potential $U(u)$. Similarly, unstable fixed points for the local reaction kinetics correspond to stable mechanical equilibria.

positive friction rolls down hill and eventually settles at position $u^*_{\rm II} = 0$. If the motion is underdamped, it will oscillate as it approaches its final value, but there will be a solution connecting the two fixed points for an entire range of V values. Consider a model where

$$R(u) = ru(u - a)(b - u) \tag{8.10}$$

$$U(u) = -\frac{r}{4}\,u^4 + \frac{r}{3}(a + b)u^3 - \frac{r}{2}abu^2 \tag{8.11}$$

which is depicted in the right panels of fig. 8.1. Assuming $r > 0$, there are two stable fixed points for the local reaction kinetics: $u^* = a$ and $u^* = b$. Since $U(a) - U(b) = \frac{1}{12}(a - b)^2(a^2 - b^2)$, the fixed point which is farther from $u = 0$ has the higher value. Without loss of generality, let us assume $a^2 > b^2$. One can then roll off the peak at $u^* = a$

and eventually settle in at the local minimum $u^* = 0$ for a range of c values, provided c is sufficiently large that the motion does not take u beyond the other fixed point at $u^* = b$. If we start at $u^* = b$, then a solution interpolating between this value and $u^* = 0$ exists for any positive value of V. As we shall see, this makes the issue of velocity selection a subtle one, as at this stage it appears a continuous family of propagating front solutions are possible. At any rate, for this type of front we have $u(\xi = -\infty) = u^*_{\mathrm{I}}$ and $u(\xi = +\infty) = u^*_{\mathrm{II}}$, where $u^*_{\mathrm{I,II}}$ correspond to stable and unstable fixed points of the local dynamics. If we fix x and examine what happens as a function of t, we have $\xi \to \mp\infty$ as $t \to \pm\infty$, since $c > 0$, meaning that we start out in the unstable fixed point and eventually as the front passes over our position we transition to the stable fixed point. Accordingly, this type of front describes a *propagation into an unstable phase*. Note that for $V < 0$, corresponding to left-moving fronts, we have negative friction, meaning we move uphill in the potential $U(u)$. Thus, we start at $\xi = -\infty$ with $u(-\infty) = 0$ and end up at $u(+\infty) = u^*_{\mathrm{I,II}}$. But now we have $\xi \to \pm\infty$ as $t \to \pm\infty$, hence once again *the stable phase invades the unstable phase*.

Another possibility is that one stable phase invades another. For the potential in the lower right panel of fig. 8.1, this means starting at the leftmost fixed point where $u(-\infty) = a$ and, with $V > 0$ and positive friction, rolling down hill past $u = 0$, then back up the other side, asymptotically coming to a perfect stop at $u(+\infty) = b$. Clearly this requires that V be finely tuned to a specific value so that the system dissipates an energy exactly equal to $U(a) - U(b)$ to friction during its motion. If $c < 0$ we have the time reverse of this motion. The fact that V is finely tuned to a specific value in order to have a solution means that we have a *velocity selection* taking place. Thus, if $R(a) = R(b) = 0$, then defining

$$\Delta U = \int_a^b du\, R(u) = U(b) - U(a) \ , \tag{8.12}$$

we have that $u^* = a$ invades $u^* = b$ if $\Delta U > 0$, and $u^* = b$ invades $u^* = a$ if $\Delta U < 0$. The front velocity in either case is fixed by the selection criterion that we asymptotically approach both local maxima of $U(u)$ as $t \to \pm\infty$.

For the equation

$$Du'' + Vu' = ru(u-a)(u-b) \ , \tag{8.13}$$

we can find an exact solution of the form

$$u(\xi) = \left(\frac{a+b}{2}\right) + \left(\frac{a-b}{2}\right) \tanh(A\xi) \ . \tag{8.14}$$

Direct substitution shows this is a solution when

$$A = \frac{(a-b)^2 r}{8D} \tag{8.15}$$

$$V = 2D\left(\frac{b-a}{b+a}\right) \ . \tag{8.16}$$

8.1.3 Fisher's equation

If we take $R(u) = ru(1-u)$, the local reaction kinetics are those of the logistic equation $\dot{u} = ru(1-u)$. With $r > 0$, this system has an unstable fixed point at $u = 0$ and a stable fixed point at $u = 1$. Rescaling time to eliminate the rate constant r, and space to eliminate the diffusion constant D, the corresponding one-dimensional RDE is

$$\frac{\partial u}{\partial t} = \frac{\partial^2 u}{\partial x^2} + u(1-u) \ , \tag{8.17}$$

which is known as Fisher's equation (1937), originally proposed to describe the spreading of biological populations. Note that the physical length scale is $\ell = (D/r)^{1/2}$ and the physical time scale is $\tau = r^{-1}$. Other related RDEs are the Newell-Whitehead Segel equation, for which $R(u) = u(1-u^2)$, and the Zeldovich equation, for which $R(u) = u(1-u)(a-u)$ with $0 < a < 1$.

To study front propagation, we assume $u(x,t) = u(x - Vt)$, resulting in

$$\frac{d^2u}{d\xi^2} + V\frac{du}{d\xi} = -U'(u) \ , \tag{8.18}$$

where

$$U(u) = -\tfrac{1}{2}u^2 + \tfrac{1}{3}u^3 \ . \tag{8.19}$$

Let $v = du/d\xi$. Then we have the $N = 2$ dynamical system

$$\frac{du}{d\xi} = v \tag{8.20}$$

$$\frac{dv}{d\xi} = -u(1-u) - Vv \ , \tag{8.21}$$

with fixed points at $(u^*, v^*) = (0,0)$ and $(u^*, v^*) = (1,0)$. The Jacobian matrix is

$$J = \begin{pmatrix} 0 & 1 \\ 2u^* - 1 & -V \end{pmatrix} \tag{8.22}$$

At $(u^*, v^*) = (1,0)$, we have $\det(J) = -1$ and $\mathrm{Tr}(J) = -V$, corresponding to a saddle. At $(u^*, v^*) = (0,0)$, we have $\det(J) = 1$ and $\mathrm{Tr}(J) = -V$, corresponding to a stable node if $V > 2$ and a stable spiral if $0 < V < 2$. If $u(x,t)$ describes a density, then we must have $u(x,t) \geq 0$ for all x and t, and this rules out $0 < V < 2$ since the approach to the $u^* = 0$ fixed point is oscillating (and damped).

8.1.4 Velocity selection and stability

Is there a preferred velocity V? According to our analysis thus far, any $V \geq 2$ will yield an acceptable front solution with $u(x,t) > 0$. However, Kolmogorov and collaborators proved that starting with the initial conditions $u(x, t = 0) = \Theta(-x)$, the function $u(x,t)$ evolves

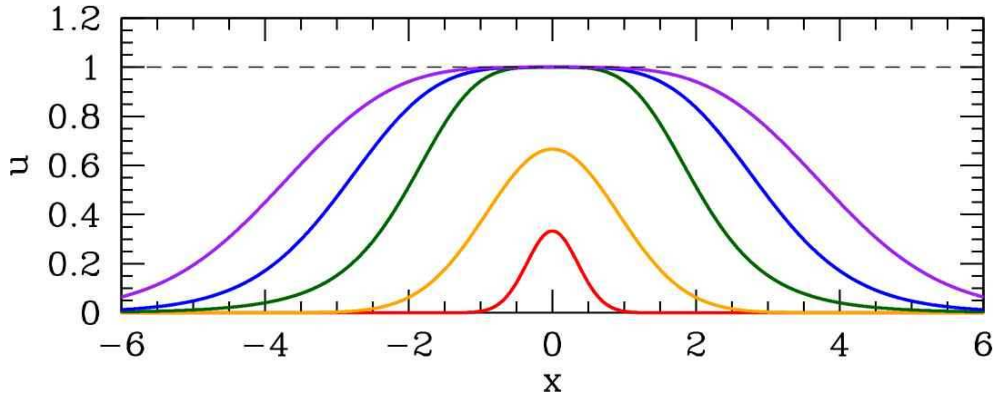

Figure 8.2: Evolution of a blip in the Fisher equation. The initial configuration is shown in red. Progressive configurations are shown in orange, green, blue, and purple. Asymptotically the two fronts move with speed $V = 2$.

to a traveling wave solution with $V = 2$, which is the minimum allowed propagation speed. That is, the system exhibits *velocity selection*.

We can begin to see why if we assume an asymptotic solution $u(\xi) = A\,e^{-\kappa\xi}$ as $\xi \to \infty$. Then since $u^2 \ll u$ we have the linear equation

$$u'' + Vu' + u = 0 \qquad \Rightarrow \qquad V = \kappa + \kappa^{-1} \ . \tag{8.23}$$

Thus, any $\kappa > 0$ yields a solution, with $V = V(\kappa)$. Note that the minimum allowed value is $V_{\rm min} = 2$, achieved at $\kappa = 1$. If $\kappa < 1$, the solution falls off more slowly than for $\kappa = 1$, and we apparently have a propagating front with $V > 2$. However, if $\kappa > 1$, the solution decays more rapidly than for $\kappa = 1$, and the $\kappa = 1$ solution will dominate.

We can make further progress by deriving a formal asymptotic expansion. We start with the front equation

$$u'' + Vu' + u(1-u) = 0 \ , \tag{8.24}$$

and we define $z = \xi/V$, yielding

$$\epsilon\,\frac{d^2u}{dz^2} + \frac{du}{dz} + u(1-u) = 0 \ , \tag{8.25}$$

with $\epsilon = V^{-2} \le \frac{1}{4}$. We now develop a perturbation expansion:

$$u(z\,;\,\epsilon) = u_0(z) + \epsilon\,u_1(z) + \ldots \ , \tag{8.26}$$

and isolating terms of equal order in ϵ, we obtain a hierarchy. At order $\mathcal{O}(\epsilon^0)$, we have

$$u_0' + u_0\,(1-u_0) = 0 \ , \tag{8.27}$$

which is to say

$$\frac{du_0}{u_0(u_0-1)} = d\ln\big(u_0^{-1} - 1\big) = dz \ . \tag{8.28}$$

Thus,

$$u_0(z) = \frac{1}{\exp(z-a)+1} \ , \tag{8.29}$$

where a is a constant of integration. At level k of the hierarchy, with $k > 1$ we have

$$u''_{k-1} + u'_k + u_k - \sum_{l=0}^{k} u_l \, u_{k-l} = 0 \ , \tag{8.30}$$

which is a first order ODE relating u_k at level k to the set $\{u_j\}$ at levels $j < k$. Separating out the terms, we can rewrite this as

$$u'_k + (1-2u_0)\, u_k = -u''_{k-1} - \sum_{l=1}^{k-1} u_l \, u_{k-l} \ . \tag{8.31}$$

At level $k = 1$, we have

$$u'_1 + (1-2u_0)\, u_1 = -u''_0 \ . \tag{8.32}$$

Plugging in our solution for $u_0(z)$, this inhomogeneous first order ODE may be solved via elementary means. The solution is

$$u_1(z) = -\frac{\ln\cosh\big(\frac{z-a}{2}\big)}{2\cosh^2\big(\frac{z-a}{2}\big)} \ . \tag{8.33}$$

Here we have adjusted the constant of integration so that $u_1(a) \equiv 0$. Without loss of generality we may set $a = 0$, and we obtain

$$u(\xi) = \frac{1}{\exp(\xi/V)+1} - \frac{1}{2V^2}\,\frac{\ln\cosh(\xi/2V)}{\cosh^2(\xi/2V)} + \mathcal{O}(V^{-4}) \ . \tag{8.34}$$

At $\xi = 0$, where the front is steepest, we have

$$-u'(0) = \frac{1}{4V} + \mathcal{O}(V^{-3}) \ . \tag{8.35}$$

Thus, the *slower* the front moves, the *steeper* it gets. Recall that we are assuming $V \geq 2$ here.

8.1.5 Stability calculation

Recall that we began with the Fisher equation, which is a PDE, and any proper assessment of the stability of a solution must proceed from this original PDE. To this end, we write

$$u(x,t) = F(x - Vt) + \delta u(x,t) \ , \tag{8.36}$$

where $f(\xi)$ is a solution to $F'' + VF' + F\,(1-F) = 0$. Linearizing in δu, we obtain the PDE

$$\frac{\partial\, \delta u}{\partial t} = \frac{\partial^2 \delta u}{\partial x^2} + (1-2F)\,\delta u \ . \tag{8.37}$$

While this equation is linear, it is not autonomous, due to the presence of $F = F(x - Vt)$. Let's shift to a moving frame defined by $\xi = x - Vt$ and $s = t$. Then

$$\frac{\partial}{\partial x} = \frac{\partial \xi}{\partial x}\,\frac{\partial}{\partial \xi} + \frac{\partial s}{\partial x}\,\frac{\partial}{\partial s} = \frac{\partial}{\partial \xi} \tag{8.38}$$

$$\frac{\partial}{\partial t} = \frac{\partial \xi}{\partial t}\,\frac{\partial}{\partial \xi} + \frac{\partial s}{\partial t}\,\frac{\partial}{\partial s} = -V\frac{\partial}{\partial \xi} + \frac{\partial}{\partial s} \ . \tag{8.39}$$

So now we have the equation

$$\frac{\partial\,\delta u}{\partial s} = \frac{\partial^2 \delta u}{\partial \xi^2} + \big(1 - 2F(\xi)\big)\,\delta u \ . \tag{8.40}$$

This equation, unlike eqn. 8.37, is linear and autonomous, hence the solutions may be written in the form

$$u(\xi, s) = g(\xi)\, e^{-\lambda s} \ , \tag{8.41}$$

where

$$g'' + V g' + \Big\{\lambda + 1 - 2\,F(\xi)\Big\} g = 0 \ . \tag{8.42}$$

With the boundary conditions $g(\pm\infty) = 0$, this becomes an *eigenvalue equation* for λ. Note that $g(\xi) = F'(\xi)$ is an eigenfunction with eigenvalue $\lambda = 0$. This is because translational invariance requires that

$$F(\xi + \delta\xi) = F(\xi) + F'(\xi)\,\delta\xi \tag{8.43}$$

must also be a solution to the front equation. Equivalently, we can differentiate the front equation $F'' + VF' + F(1 - F)$ to obtain

$$F''' + VF'' + (1 - 2F)\,F' = 0 \ , \tag{8.44}$$

which shows explicitly that $g = F'$ is a zero mode.

Finally, if we write

$$g(\xi) = \psi(\xi)\, e^{-V\xi/2} \ , \tag{8.45}$$

we obtain a Schrödinger equation

$$-\frac{d^2\psi}{d\xi^2} + W(\xi)\,\psi = \lambda\psi \ , \tag{8.46}$$

where the 'potential' is

$$W(\xi) = 2F(\xi) + \tfrac{1}{4}V^2 - 1 \ . \tag{8.47}$$

If $|V| > 2$, then $W(\xi) = 2F(\xi) > 0$ and the potential $W(\xi)$ is always positive. This precludes bound states, which means all the eigenvalues are positive[1]. If $|V| < 2$, we have negative eigenvalues, since the potential is negative for sufficiently large values of ξ. Thus, we conclude that solutions with $|V| < 2$ are *unstable*.

[1]Note that by making the shift from $g(\xi)$ to $\psi(\xi)$, the zero mode solution becomes unnormalizable, and is excluded from the spectrum of the transformed equation.

8.2 Multi-Species Reaction-Diffusion Systems

We've already introduced the general multi-species RDE,

$$\frac{\partial u_i}{\partial t} = D_{ij} \boldsymbol{\nabla}^2 u_i + R_i(u_1, \ldots, u_N) \ . \tag{8.48}$$

We will be interested in stable traveling wave solutions to these coupled nonlinear PDEs. We'll start with a predator-prey model,

$$\frac{\partial N_1}{\partial t} = r N_1 \bigg(1 - \frac{N_1}{K}\bigg) - \alpha N_1 N_2 + D_1 \, \frac{\partial^2 N_1}{\partial x^2} \tag{8.49}$$

$$\frac{\partial N_2}{\partial t} = \beta N_1 N_2 - \gamma N_2 + D_2 \frac{\partial^2 N_2}{\partial x^2} \ . \tag{8.50}$$

Rescaling x, t, N_1, and N_2, this seven parameter system can be reduced to one with only three parameters, all of which are assumed to be positive:

$$\frac{\partial u}{\partial t} = u\,(1 - u - v) + \mathcal{D} \, \frac{\partial^2 u}{\partial x^2} \tag{8.51}$$

$$\frac{\partial v}{\partial t} = av\,(u - b) + \frac{\partial^2 v}{\partial x^2} \ . \tag{8.52}$$

The interpretation is as follows. According to the local dynamics, species v is parasitic in that it decays as $\dot{v} = -abv$ in the absence of u. The presence of u increases the growth rate for v. Species u on the other hand will grow in the absence of v, and the presence of v decreases its growth rate and can lead to its extinction. Thus, v is the predator and u is the prey.

Before analyzing this reaction-diffusion system, we take the opportunity to introduce some notation on partial derivatives. We will use subscripts to denote partial differentiation, so *e.g.*

$$\phi_t = \frac{\partial \phi}{\partial t} \quad , \quad \phi_{xx} = \frac{\partial^2 \phi}{\partial x^2} \quad , \quad \phi_{xxt} = \frac{\partial^3 \phi}{\partial x^2 \, \partial t} \quad , \quad \textit{etc.} \tag{8.53}$$

Thus, our two-species RDE may be written

$$u_t = u\,(1 - u - v) + \mathcal{D}\, u_{xx} \tag{8.54}$$

$$v_t = av\,(u - b) + v_{xx} \ . \tag{8.55}$$

We assume $0 < b < 1$, in which case there are three fixed points:

$$\text{empty state: } (u^*, v^*) = (0,0)$$

$$\text{prey at capacity: } (u^*, v^*) = (1,0)$$

$$\text{coexistence: } (u^*, v^*) = (b, 1-b) \ .$$

We now compute the Jacobian for the local dynamics:

$$J = \begin{pmatrix} \dot{u}_u & \dot{u}_v \\ \dot{v}_u & \dot{v}_v \end{pmatrix} = \begin{pmatrix} 1-2u-v & -u \\ av & a(u-b) \end{pmatrix} . \tag{8.56}$$

We now examine the three fixed points.

- At $(u^*, v^*) = (0,0)$ we have

$$J_{(0,0)} = \begin{pmatrix} 1 & 0 \\ 0 & -b \end{pmatrix} \qquad \Rightarrow \qquad T = 1-b \ , \ D = -b \ , \tag{8.57}$$

  corresponding to a saddle.

- At $(u^*, v^*) = (1,0)$,

$$J_{(1,0)} = \begin{pmatrix} -1 & -1 \\ 0 & a(1-b) \end{pmatrix} \qquad \Rightarrow \qquad T = a(1-b) - 1 \ , \ D = -a(1-b) \ , \tag{8.58}$$

  which is also a saddle, since $0 < b < 1$.

- Finally, at $(u^*, v^*) = (b, 1-b)$,

$$J_{(b,1-b)} = \begin{pmatrix} -b & -b \\ a(1-b) & 0 \end{pmatrix} \qquad \Rightarrow \qquad T = -b \ , \ D = ab(1-b) \ . \tag{8.59}$$

  Since $T < 0$ and $D > 0$ this fixed point is stable. For $D > \frac{1}{4}T^2$ it corresponds to a spiral, and otherwise a node. In terms of a and b, this transition occurs at $a = b/4(1-b)$. That is,

$$\text{stable node: } a < \frac{b}{4(1-b)} \qquad , \qquad \text{stable spiral: } a > \frac{b}{4(1-b)} . \tag{8.60}$$

The local dynamics has an associated Lyapunov function,

$$L(u,v) = ab\left[\frac{u}{b} - 1 - \ln\left(\frac{u}{v}\right)\right] + (1-b)\left[\frac{v}{1-b} - 1 - \ln\left(\frac{v}{1-b}\right)\right] . \tag{8.61}$$

The constants in the above Lyapunov function are selected to take advantage of the relation $x - 1 - \ln x \geq 0$; thus, $L(u,v) \geq 0$, and $L(u,v)$ achieves its minimum $L = 0$ at the stable fixed point $(b, 1-b)$. Ignoring diffusion, under the local dynamics we have

$$\frac{dL}{dt} = -a(u-b)^2 \leq 0 \ . \tag{8.62}$$

8.2.1 Propagating front solutions

We now look for a propagating front solution of the form

$$u(x,t) = u(x - Vt) \qquad , \qquad v(x,t) = v(x - Vt) \ . \tag{8.63}$$

This results in the coupled ODE system,

$$\mathcal{D}\, u'' + V u' + u(1 - u - v) = 0 \tag{8.64}$$

$$v'' + V v' + av(u - b) = 0 \ , \tag{8.65}$$

where once again the independent variable is $\xi = x - Vt$. These two coupled second order ODEs may be written as an $N = 4$ system.

We will make a simplifying assumption and take $\mathcal{D} = D_1/D_2 = 0$. This is appropriate if one species diffuses very slowly. An example might be plankton ($D_1 \approx 0$) and an herbivorous species ($D_2 > 0$). We then have $\mathcal{D} = 0$, which results in the $N = 3$ dynamical system,

$$\frac{du}{d\xi} = -V^{-1}\, u\,(1 - u - v) \tag{8.66}$$

$$\frac{dv}{d\xi} = w \tag{8.67}$$

$$\frac{dw}{d\xi} = -av\,(u - b) - Vw \ , \tag{8.68}$$

where $w = v'$. In terms of the $N = 3$ phase space $\boldsymbol{\varphi} = (u, v, w)$, the three fixed points are

$$(u^*, v^*, w^*) = (0, 0, 0) \tag{8.69}$$

$$(u^*, v^*, w^*) = (1, 0, 0) \tag{8.70}$$

$$(u^*, v^*, w^*) = (b, 1 - b, 0) \ . \tag{8.71}$$

The first two are unstable and the third is stable. We will look for solutions where the stable solution invades one of the two unstable solutions. Since the front is assumed to propagate to the right, we must have the stable solution at $\xi = -\infty$, *i.e.* $\boldsymbol{\varphi}(-\infty) = (b, 1 - b, 0)$. There are then two possibilities: either (i) $\boldsymbol{\varphi}(+\infty) = (0, 0, 0)$, or (ii) $\boldsymbol{\varphi}(+\infty) = (1, 0, 0)$. We will call the former a type-I front and the latter a type-II front.

For our analysis, we will need to evaluate the Jacobian of the system at the fixed point. In general, we have

$$J = \begin{pmatrix} -V^{-1}(1 - 2u^* - v^*) & V^{-1}u^* & 0 \\ 0 & 0 & 1 \\ -av^* & -a(u^* - b) & -V \end{pmatrix} \ . \tag{8.72}$$

We now evaluate the behavior at the fixed points.

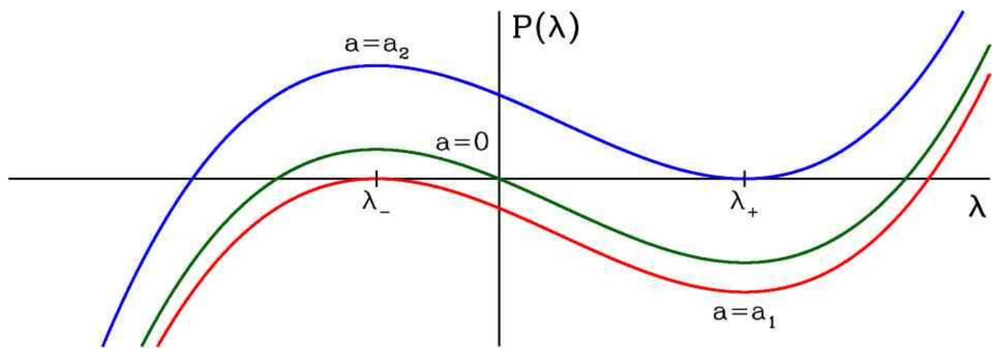

Figure 8.3: Analysis of the characteristic polynomial for the Jacobian of the linearized map at the fixed point $(u^*, v^*, w^*) = (b, 1-b, 0)$.

- Let's first look in the vicinity of $\boldsymbol{\varphi} = (0,0,0)$. The linearized dynamics then give

$$\frac{d\boldsymbol{\eta}}{d\xi} = J\boldsymbol{\eta} \quad , \quad J = \begin{pmatrix} -V^{-1} & 0 & 0 \\ 0 & 0 & 1 \\ 0 & ab & -c \end{pmatrix} \ , \tag{8.73}$$

where $\boldsymbol{\varphi} = \boldsymbol{\varphi}^* + \boldsymbol{\eta}$. The eigenvalues are

$$\lambda_1 = -V^{-1} \quad , \quad \lambda_{2,3} = -\tfrac{1}{2}c \pm \tfrac{1}{2}\sqrt{V^2 + 4ab} \ . \tag{8.74}$$

We see that $\lambda_{1,2} < 0$ while $\lambda_3 > 0$.

- In the vicinity of $\boldsymbol{\varphi} = (1,0,0)$, we have

$$\frac{d\boldsymbol{\eta}}{d\xi} = J\boldsymbol{\eta} \quad , \quad J = \begin{pmatrix} c^{-1} & c^{-1} & 0 \\ 0 & 0 & 1 \\ 0 & ab & -V \end{pmatrix} \ , \tag{8.75}$$

The eigenvalues are

$$\lambda_1 = V^{-1} \quad , \quad \lambda_{2,3} = \tfrac{1}{2}c \pm \tfrac{1}{2}\sqrt{c^2 - 4a(1-b)} \ . \tag{8.76}$$

We now have $\lambda_1 > 0$ and $\mathsf{Re}(\lambda_{2,3}) > 0$. If we exclude oscillatory solutions, then we must have

$$V > V_{\text{min}} = 2\sqrt{a(1-b)} \ . \tag{8.77}$$

- Finally, let's examine the structure of the fixed point at $\boldsymbol{\varphi} = (b, 1-b, 0)$, where

$$\frac{d\boldsymbol{\eta}}{d\xi} = J\boldsymbol{\eta} \quad , \quad J = \begin{pmatrix} b\,V^{-1} & b\,V^{-1} & 0 \\ 0 & 0 & 1 \\ -a\,(1-b) & 0 & -V \end{pmatrix} \ , \tag{8.78}$$

The characteristic polynomial is

$$\begin{aligned} P(\lambda) &= \det\big(\lambda \cdot \mathbb{I} - J\big) \\ &= \lambda^3 + \big(V - b\,V^{-1}\big)\lambda^2 - b\,\lambda + ab(1-b)V^{-1} \ . \end{aligned} \tag{8.79}$$

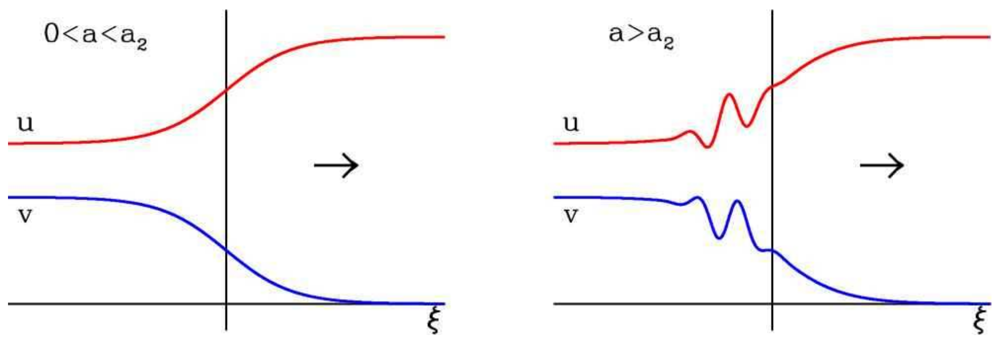

Figure 8.4: Sketch of the type-II front. Left panel: $0 < a < a_2$, for which the trailing edge of the front is monotonic. Right panel: $a > a_2$, for which the trailing edge of the front is oscillatory. In both cases, $\frac{1}{2} < b < 1$, and the front propagates to the right.

To analyze this cubic, note that it has extrema when $P'(\lambda) = 0$, which is to say at

$$\lambda = \lambda_\pm = -\tfrac{1}{3}\big(V - b\,V^{-1}\big) \pm \tfrac{1}{3}\sqrt{\big(V - b\,V^{-1}\big)^2 + 3b}\ . \tag{8.80}$$

Note that $\lambda_- < 0 < \lambda_+$. Since the sign of the cubic term in $P(\lambda)$ is positive, we must have that λ_- is a local maximum and λ_+ a local minimum. Note furthermore that both λ_+ and λ_- are independent of the constant a, and depend only on b and c. Thus, the situation is as depicted in fig. 8.3. The constant a merely shifts the cubic $P(\lambda)$ uniformly up or down. When $a = 0$, $P(0) = 0$ and the curve runs through the origin. There exists an $a_1 < 0$ such that for $a = a_1$ we have $P(\lambda_-) = 0$. Similarly, there exists an $a_2 > 0$ such that for $a = a_2$ we have $P(\lambda_+) = 0$. Thus,

$$a < a_1 < 0 \quad : \quad \mathsf{Re}\,(\lambda_{1,2}) < 0 < \lambda_3 \tag{8.81}$$
$$a_1 < a < 0 \quad : \quad \lambda_1 < \lambda_2 < 0 < \lambda_3 \tag{8.82}$$
$$a = 0 \quad : \quad \lambda_1 < \lambda_2 = 0 < \lambda_3 \tag{8.83}$$
$$0 < a < a_2 \quad : \quad \lambda_1 < 0 < \lambda_2 < \lambda_3 \tag{8.84}$$
$$0 < a_2 < a \quad : \quad \lambda_1 < 0 < \mathsf{Re}\,(\lambda_{2,3})\ . \tag{8.85}$$

Since this is the fixed point approached as $\xi \to -\infty$, we must approach it along one of its *unstable* manifolds, *i.e.* along a direction corresponding to a positive eigenvalue. Thus, we conclude that if $a > a_2$ that the approach is oscillatory, while for $0 < a < a_2$ the approach is monotonic.

In fig. 8.4 we sketch the solution for a type-II front, where the stable coexistence phase invades the unstable 'prey at capacity' phase.

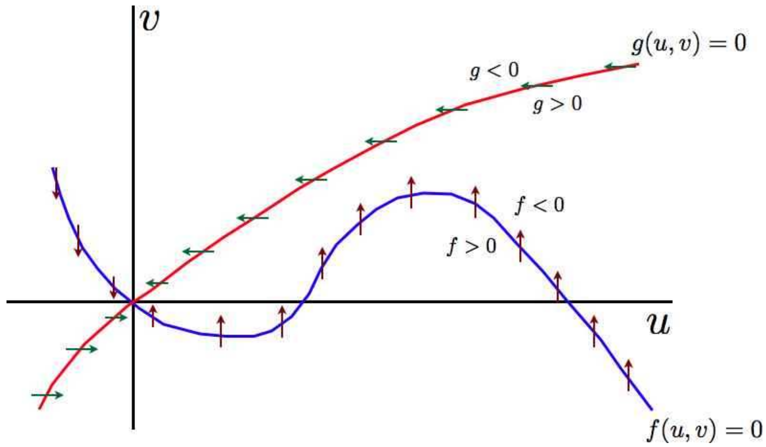

Figure 8.5: Sketch of the nullclines for the dynamical system described in the text.

8.3 Excitable Media

Consider the following $N = 2$ system:

$$\dot{u} = f(u,v) \tag{8.86}$$
$$\dot{v} = \epsilon\, g(u,v) \ , \tag{8.87}$$

where $0 < \epsilon \ll 1$. The first equation is 'fast' and the second equation 'slow'. We assume the nullclines for $f = 0$ and $g = 0$ are as depicted in fig. 8.5. As should be clear from the figure, the origin is a stable fixed point. In the vicinity of the origin, we can write

$$f(u,v) = -au - bv + \ldots \tag{8.88}$$
$$g(u,v) = +cu - dv + \ldots \ , \tag{8.89}$$

where a, b, c, and d are all positive real numbers. The equation for the nullclines in the vicinity of the origin is then $au + bv = 0$ for the $f = 0$ nullcline, and $cu - dv = 0$ for the $g = 0$ nullcline. Note that

$$M \equiv \frac{\partial(f,g)}{\partial(u,v)}\bigg|_{(0,0)} = \begin{pmatrix} -a & -b \\ c & -d \end{pmatrix} \ , \tag{8.90}$$

and therefore $\mathrm{Tr}\, M = -(a+d)$ and $\det M = ad + bc > 0$. SInce the trace is negative and the determinant positive, the fixed point is stable. The boundary between spiral and node solutions is $\det M = \frac{1}{4}(\mathrm{Tr}\, M)^2$, which means

$$|a - d| > 2\sqrt{bc} \ : \ \text{stable node} \tag{8.91}$$
$$|a - d| < 2\sqrt{bc} \ : \ \text{stable spiral} \ . \tag{8.92}$$

Although the trivial fixed point $(u^*, v^*) = (0,0)$ is stable, it is still *excitable* in the sense that a large enough perturbation will result in a big excursion. Consider the sketch in fig. 8.6.

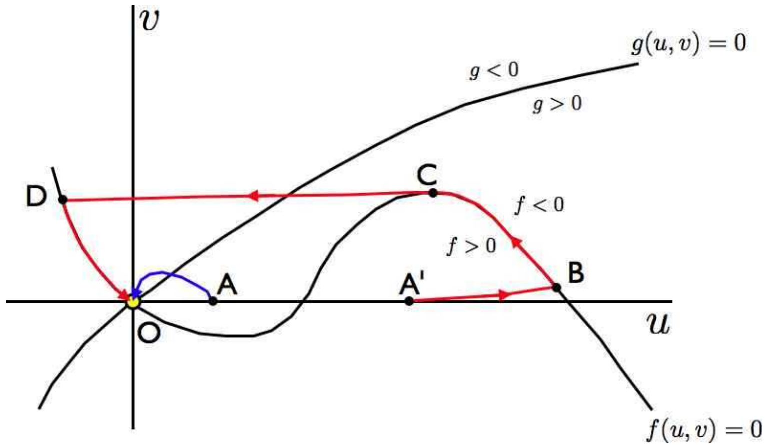

Figure 8.6: Sketch of the fizzle, which starts from A, and the burst, which starts from A′.

Starting from A, v initially increases as u decreases, but eventually both u and v get sucked into the stable fixed point at O. We call this path the *fizzle*. Starting from A′, however, u begins to increase rapidly and v increases slowly until the $f = 0$ nullcline is reached. At this point the fast dynamics has played itself out. The phase curve follows the nullcline, since any increase in v is followed by an immediate readjustment of u back to the nullcline. This state of affairs continues until C is reached, at which point the phase curve makes a large rapid excursion to D, following which it once again follows the $f = 0$ nullcline to the origin O. We call this path a *burst*. The behavior of $u(t)$ and $v(t)$ during these paths is depicted in fig. 8.7.

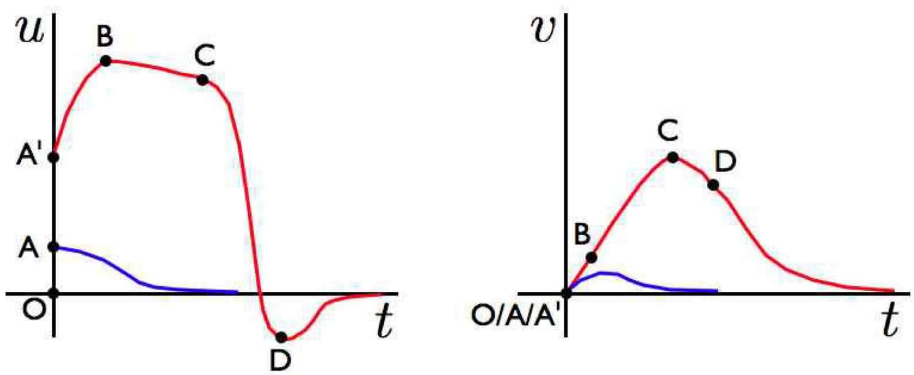

Figure 8.7: Sketch of $u(t)$ and $v(t)$ for the fizzle and burst.

It is also possible for there to be multiple bursts. Consider for example the situation depicted in fig. 8.8, in which the $f = 0$ and $g = 0$ nullclines cross three times. Two of these crossings correspond to stable (attractive) fixed points, while the third is unstable. There are now two different large scale excursion paths, depending on which stable fixed point one ends up at[2].

[2]For a more egregious example of a sentence ending in several prepositions: "What did you bring that

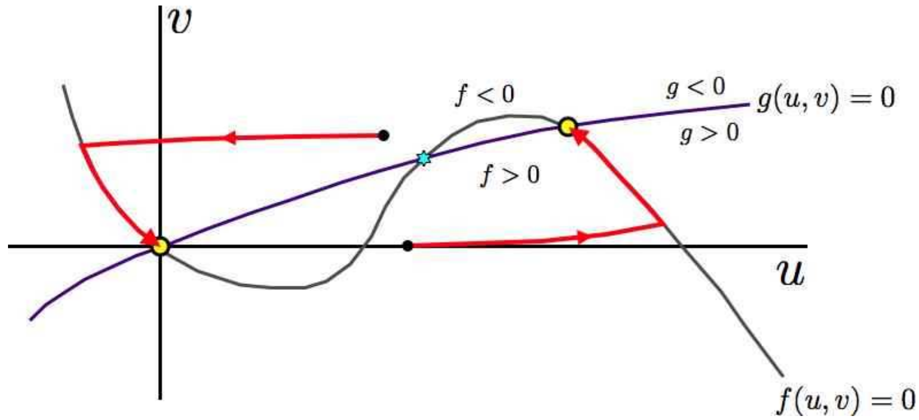

Figure 8.8: With three nullcline crossings, there are two stable fixed points, and hence two types of burst. The yellow-centered circles denote stable fixed points, and the blue-centered star denotes an unstable fixed point.

8.3.1 Front propagation in excitable media

Now let's add in diffusion:

$$u_t = D_1\, u_{xx} + f(u, v) \tag{8.93}$$

$$v_t = D_2\, v_{xx} + \epsilon\, g(u, v)\ . \tag{8.94}$$

We will consider a specific model,

$$u_t = u(a - u)(u - 1) - v + D\, u_{xx} \tag{8.95}$$

$$v_t = b\, u - \gamma\, v\ . \tag{8.96}$$

This is known as the *FitzHugh-Nagumo model* of nerve conduction (1961-2). It represents a tractable simplification and reduction of the famous Hodgkin-Huxley model (1952) of electrophysiology. Very briefly, u represents the membrane potential, and v the contributions to the membrane current from Na^+ and K^+ ions. We have $0 < a < 1$, $b > 0$, and $\gamma > 0$. The nullclines for the local dynamics resemble those in fig. 8.5, with the nullcline for the slow reaction perfectly straight.

We are interested in wave (front) solutions, which might describe wave propagation in muscle (*e.g.* heart) tissue. Let us once again define $\xi = x - Vt$ and assume a propagating front solution. We then arrive at the coupled ODEs,

$$D\, u'' + V u' + h(u) - v = 0 \tag{8.97}$$

$$V v' + b\, u - \gamma\, v = 0\ , \tag{8.98}$$

where

$$h(u) = u(a - u)(u - 1)\ . \tag{8.99}$$

---

book I didn't want to be read to out of up around for?"

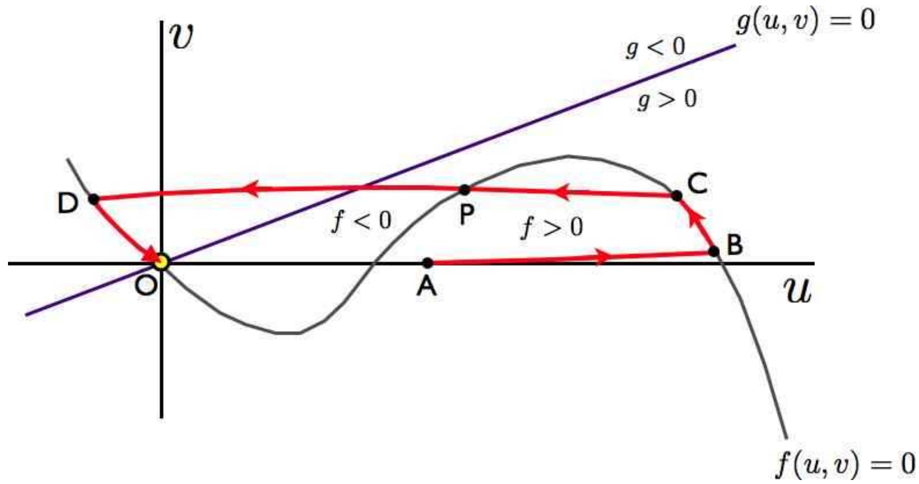

Figure 8.9: Excitation cycle for the FitzHugh-Nagumo model.

Once again, we have an $N = 3$ dynamical system:

$$\frac{du}{d\xi} = w \tag{8.100}$$

$$\frac{dv}{d\xi} = -b\,V^{-1}\,u + \gamma\,V^{-1}\,v \tag{8.101}$$

$$\frac{dw}{d\xi} = -D^{-1}\,h(u) + D^{-1}\,v - V D^{-1}\,w\ , \tag{8.102}$$

where $w = u'$.

We assume that b and γ are both small, so that the v dynamics are slow. Furthermore, v remains small throughout the motion of the system. Then, assuming an initial value $(u_0, 0, 0)$, we may approximate

$$u_t \approx D\,u_{xx} + h(u)\ . \tag{8.103}$$

With $D = 0$, the points $u = 1$ and $u = 1$ are both linearly stable and $u = a$ is linearly unstable. For finite D there is a wave connecting the two stable fixed points with a unique speed of propagation.

The equation $Du'' + Vu' = -h(u)$ may again be interpreted mechanically, with $h(u) = U'(u)$. Then since the cubic term in $h(u)$ has a negative sign, the potential $U(u)$ resembles an inverted asymmetric double well, with local maxima at $u = 0$ and $u = 1$, and a local minimum somewhere in between at $u = a$. Since

$$U(0) - U(1) = \int\limits_0^1 du\, h(u) = \tfrac{1}{12}(1 - 2a)\ , \tag{8.104}$$

hence if $V > 0$ we must have $a < \frac{1}{2}$ in order for the left maximum to be higher than the

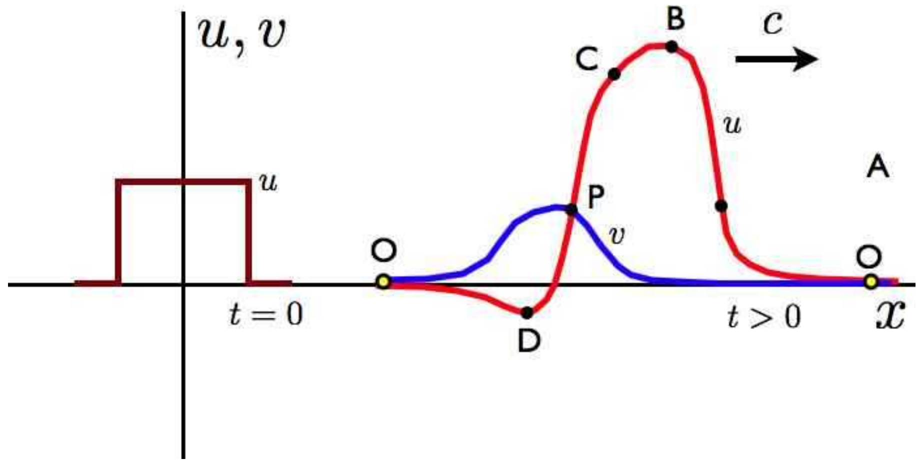

Figure 8.10: Sketch of the excitation pulse of the FitzHugh-Nagumo model..

right maximum. The constant V is adjusted so as to yield a solution. This entails

$$V\int\limits_{-\infty}^{\infty} d\xi\, u_\xi^2 = V\int\limits_0^1 du\, u_\xi = U(0) - U(1)\ . \qquad (8.105)$$

The solution makes use of some very special properties of the cubic $h(u)$ and is astonishingly simple:

$$V = (D/2)^{1/2}\,(1-2a)\ . \qquad (8.106)$$

We next must find the speed of propagation on the CD leg of the excursion. There we have

$$u_t \approx D\,u_{xx} + h(u) - v_{\rm C}\ , \qquad (8.107)$$

with $u(-\infty) = u_{\rm D}$ and $u(+\infty) = u_{\rm C}$. The speed of propagation is

$$\tilde V = (D/2)^{1/2}\,\big(u_{\rm C} - 2u_{\rm P} + u_{\rm D}\big)\ . \qquad (8.108)$$

We then set $V = \tilde V$ to determine the location of C. The excitation pulse is sketched in fig. 8.10

Calculation of the wave speed

Consider the second order ODE,

$$\mathcal{L}(u) \equiv D\,u'' + V u' + A(u-u_1)(u_2-u)(u-u_3) = 0\ . \qquad (8.109)$$

We may, with almost no loss of generality[3], assume $u_1 < u_2 < u_3$. Remarkably, a solution may be found. We claim that if

$$u' = \alpha(u-u_1)(u-u_3)\ , \qquad (8.110)$$

[3]We assume that each of $u_{1,2,3}$ is distinct.

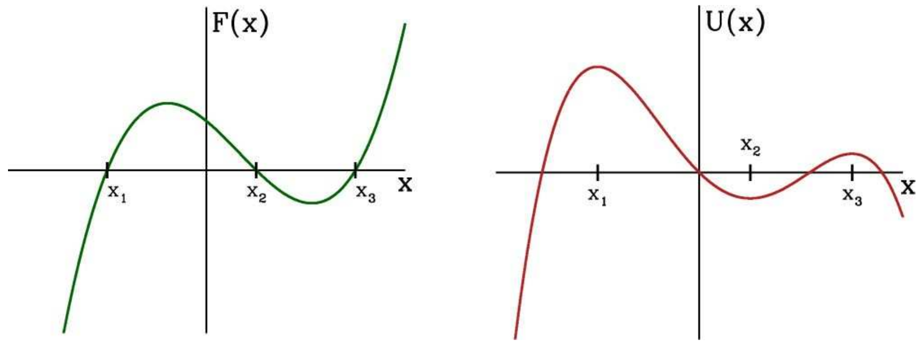

Figure 8.11: Mechanical analog for the front solution, showing force $F(x)$ and corresponding potential $U(x)$.

then, by suitably adjusting α, the solution to eqn. 8.110 also solves eqn. 8.109. To show this, note that under the assumption of eqn. 8.110 we have

$$\begin{aligned} u'' &= \frac{du'}{du} \cdot \frac{du}{d\xi} \\ &= \alpha\,(2u - u_1 - u_3)\,u' \\ &= \alpha^2 (u-u_1)(u-u_3)(2u-u_1-u_3) \ . \end{aligned} \tag{8.111}$$

Thus,

$$\begin{aligned} \mathcal{L}(u) &= (u-u_1)(u-u_3)\Big[\alpha^2 D(2u-u_1-u_3) + \alpha V + A(u_2-u)\Big] \\ &= (u-u_1)(u-u_3)\Big[\big(2\alpha^2 D - A\big)u + \big(\alpha V + A u_2 - \alpha^2 D(u_1+u_3)\big)\Big] \ . \end{aligned} \tag{8.112}$$

Therefore, if we choose

$$\alpha = \pm\sqrt{\frac{A}{2D}} \qquad , \qquad V = \pm\sqrt{\frac{AD}{2}}\,\big(u_1 - 2u_2 + u_3\big) \quad , \tag{8.113}$$

we obtain a solution to $\mathcal{L}(u) = 0$. Note that the velocity V has been *selected*.

The integration of eqn. 8.110 is elementary, yielding the kink solution

$$u(\xi) = \frac{u_3 + \sigma\, u_1 e^{\alpha(u_3-u_1)\xi}}{1 + \sigma\, e^{\alpha(u_3-u_1)\xi}} \ , \tag{8.114}$$

where $\sigma > 0$ is a constant which determines the location of the center of the kink. Recall we have assumed $u_1 < u_2 < u_3$, so if $\alpha > 0$ we have $u(-\infty) = u_3$ and $u(+\infty) = u_1$. Conversely, if $\alpha < 0$ then $u(-\infty) = u_1$ and $u(+\infty) = u_3$.

It is instructive to consider the analogue mechanical setting of eqn. 8.109. We write $D \to M$ and $V \to \gamma$, and $u \to x$, giving

$$M\ddot{x} + \gamma\,\dot{x} = A(x-x_1)(x-x_2)(x-x_3) \equiv F(x) \ . \tag{8.115}$$

Mechanically, the points $x = x_{1,3}$ are unstable equilibria. The front solution interpolates between these two stationary states. If $\gamma = V > 0$, the friction is of the usual sign, and the path starts from the equilibrium at which the potential $U(x)$ is greatest. Note that

$$U(x_1) - U(x_3) = \int\limits_{x_1}^{x_3} \! dx \, F(x) \tag{8.116}$$

$$= \tfrac{1}{12}(x_3 - x_1)^2 \Big[(x_2 - x_1)^2 - (x_3 - x_2)^2 \Big] \ . \tag{8.117}$$

so if, for example, the integral of $F(x)$ between x_1 and x_3 is positive, then $U(x_1) > U(x_3)$. For our cubic force $F(x)$, this occurs if $x_2 > \frac{1}{2}(x_1 + x_3)$.

Chapter 9

Pattern Formation

Patterning is a common occurrence found in a wide variety of physical systems, including chemically active media, fluids far from equilibrium, liquid crystals, *etc.* In this chapter we will touch very briefly on the basic physics of patterning instabilities.

9.0.2 Reaction-Diffusion Dynamics Revisited

Let $\big\{\phi_i(\boldsymbol{r},t)\big\}$ denote a set of scalar fields satisfying

$$\partial_t\,\phi_i + \boldsymbol{\nabla}\!\cdot\!\boldsymbol{J}_i = R_i \ , \tag{9.1}$$

where

$$J_i^\alpha = -D_{ij}^{\alpha\beta}\,\partial_\beta\,\phi_j \tag{9.2}$$

is the α component of the current density of species i. We assume that the local reaction kinetics is given by

$$R_i = R_i\big(\{\phi_j\},\lambda\big) \ , \tag{9.3}$$

where λ is a control parameter, or possibly a set of control parameters. Thus,

$$\partial_t\phi_i = \partial_\alpha\,D_{ij}^{\alpha\beta}\,\partial_\beta\,\phi_j + R_i\big(\{\phi_j\},\lambda\big) \ . \tag{9.4}$$

Let us expand about a homogeneous solution to the local dynamics, $R\big(\{\phi_i^*\},\lambda\big)=0$, writing

$$\phi_i(\boldsymbol{r},t) = \phi_i^* + \eta_i(\boldsymbol{r},t) \ . \tag{9.5}$$

We then have

$$\partial_t\,\eta_i = \frac{\partial R_i}{\partial \phi_j}\bigg|_{\boldsymbol{\phi}^*}\eta_j + \partial_\alpha\,D_{ij}^{\alpha\beta}\,\partial_\beta\,\eta_j \ . \tag{9.6}$$

Assuming $D_{ij}^{\alpha\beta}$ is constant in space, we obtain the linear equation

$$\partial_t\,\hat\eta(\boldsymbol{q},t) = L_{ij}(\boldsymbol{q}\,;\lambda)\,\hat\eta_j(\boldsymbol{q},t) \ , \tag{9.7}$$

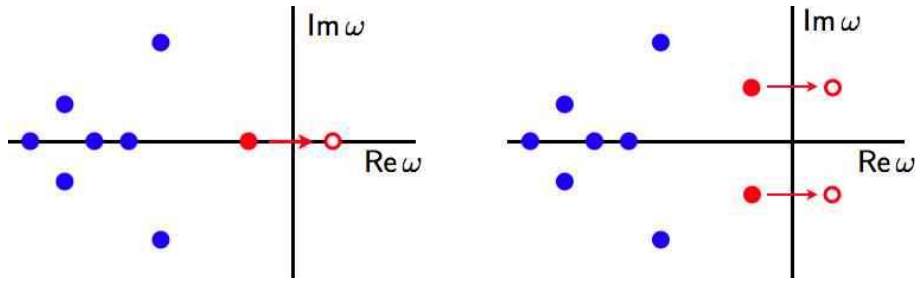

Figure 9.1: Instabilities in linear systems $\dot{\boldsymbol{\eta}} = L\boldsymbol{\eta}$ occur when the real part of the largest eigenvalue of L crosses zero. If L is a real operator, its eigenvalues are either real or come in complex conjugate pairs.

where

$$L_{ij}(\boldsymbol{q}\,;\lambda) = \frac{\partial R_i}{\partial \phi_j}\bigg|_{\boldsymbol{\phi}^*} - D_{ij}^{\alpha\beta}\, q_\alpha q_\beta \ . \tag{9.8}$$

Let

$$P(\omega) = \det\big(\omega\,\mathbb{I} - L\big) \tag{9.9}$$

be the characteristic polynomial for $L(\boldsymbol{q}\,;\lambda)$. The eigenvalues $\omega_a(\boldsymbol{q}\,;\lambda)$ satisfy $P(\omega_a) = 0$. If we assume that $L_{ij}(\boldsymbol{q}\,;\lambda) \in \mathbb{R}$ is real, then $P(\omega^*) = \big[P(\omega)\big]^*$, which means that the eigenvalues ω_a are either purely real or else come in complex conjugate pairs $\omega_{a,1} \pm i\omega_{a,2}$. The eigenvectors $\psi_i^a(\boldsymbol{q}\,;\lambda)$ need not be real, since L is not necessarily Hermitian. The general solution is then

$$\eta_i(\boldsymbol{q}\,t) = \sum_a C_a\, \psi_i^a(\boldsymbol{q}\,;\lambda)\, e^{\omega_a(\boldsymbol{q}\,;\lambda)\,t} \ . \tag{9.10}$$

Modes with $\mathsf{Re}\,\omega_a > 0$ are stabilized by nonlinear terms, *e.g.* $\dot{A} = rA - A^3$.

Let's assume the eigenvalues are ordered so that $\mathsf{Re}\,(\omega_a) \geq \mathsf{Re}\,(\omega_{a+1})$, and that $\mathsf{Re}\,(\omega_1) \leq 0$ for $\lambda \leq \lambda_{\rm c}$.

- If $\omega_1(\boldsymbol{q} = 0\,;\lambda_{\rm c}) = 0$, we expect a transition between homogeneous ($\boldsymbol{q} = 0$) states at $\lambda = \lambda_{\rm c}$.
- If $\omega_1(\boldsymbol{q} = \boldsymbol{Q}\,;\lambda_{\rm c}) = 0$, we expect a transition to a spatially modulated structure with wavevector $\boldsymbol{Q}$.
- If $\mathsf{Re}\ \omega_1(\boldsymbol{q} = 0\,;\lambda_{\rm c}) = 0$ but $\mathsf{Im}\ \omega_1(\boldsymbol{q} = 0\,;\lambda_{\rm c}) \neq 0$ we expect a Hopf bifurcation and limit cycle behavior.
- If $\mathsf{Re}\ \omega_1(\boldsymbol{q} = \boldsymbol{Q}\,;\lambda_{\rm c}) = 0$ but $\mathsf{Im}\ \omega_1(\boldsymbol{q} = \boldsymbol{Q}\,;\lambda_{\rm c}) \neq 0$ we expect a Hopf bifurcation to a spatiotemporal pattern structure.

In the vicinity of a bifurcation, space and time scales associated with the unstable mode(s) tend to infinity. This indicates a *critical slowing down*. If the unstable modes evolve very slowly, the faster, non-critical modes may be averaged over (*i.e.* 'adiabatically eliminated').

For the most unstable mode $\omega \equiv \omega_1$, we envisage the following possibilities:

$\omega = \epsilon - A\,\boldsymbol{q}^2$	homogeneous states ; $q = 0$ least stable
$\omega = \epsilon - A\big(\boldsymbol{q}^2 - Q^2\big)^2$	modulated: $q = Q$ is least stable
$\omega = \epsilon - A\big(\boldsymbol{q}^2 - Q^2\big)^2 - B\,\boldsymbol{q}^2\,\sin^2\theta_{\boldsymbol{q}}$	$\theta_{\boldsymbol{q}}$ between $\boldsymbol{q}$ and symmetry axis
$\omega = \epsilon - A\,\boldsymbol{q}^2 \pm i\Omega_0$	Hopf, to homogeneous state
$\omega = \epsilon - A\big(\boldsymbol{q}^2 - Q^2\big)^2 \pm i\Omega_0$	Hopf, to modulated state

where

$$\epsilon \propto \frac{\lambda - \lambda_c}{\lambda_c}\ . \tag{9.11}$$

9.1 Turing and Hopf Instabilities

As an explicit example in $d = 1$ dimension, consider the coupled RDEs,

$$u_t = D_u\, u_{xx} + f(u, v) \tag{9.12}$$

$$v_t = D_v\, v_{xx} + g(u, v)\ . \tag{9.13}$$

We linearize about the fixed point $u = v = 0$, obtaining

$$\begin{pmatrix} \delta\hat{u}_t \\ \delta\hat{v}_t \end{pmatrix} = \overbrace{\begin{pmatrix} f_u - D_u\, q^2 & f_v \\ g_u & g_v - D_v\, q^2 \end{pmatrix}}^{L(q)} \begin{pmatrix} \delta\hat{u} \\ \delta\hat{v} \end{pmatrix} + \ldots \tag{9.14}$$

for the Fourier transforms

$$\begin{pmatrix} \delta\hat{u}(q,t) \\ \delta\hat{v}(q,t) \end{pmatrix} = \int\limits_{-\infty}^{\infty} dx \begin{pmatrix} \delta u(x,t) \\ \delta v(x,t) \end{pmatrix} e^{-iqx}\ . \tag{9.15}$$

We now examine the eigenvalues of L. Clearly we have

$$\mathcal{T} \equiv \mathrm{Tr}(L) = f_u + g_v - (D_u + D_v)\, q^2 \tag{9.16}$$

$$\mathcal{D} \equiv \det(L) = D_u\, D_v\, q^4 - (D_u\, g_v + D_v\, f_u)\, q^2 + \Delta\ , \tag{9.17}$$

where

$$\Delta = f_u\, g_v - f_v\, g_u \tag{9.18}$$

is the determinant at $q = 0$. The eigenvalues are

$$\omega_\pm = \tfrac{1}{2}\mathcal{T} \pm \sqrt{\tfrac{1}{4}\mathcal{T}^2 - \mathcal{D}}\ . \tag{9.19}$$

Recall that in the $(\mathcal{T}, \mathcal{D})$ plane, it is the upper left quadrant, with $\mathcal{T} < 0$ and $\mathcal{D} > 0$, where the fixed point is stable. There are then two instability boundary, both of which are straight lines. The first boundary is the positive $\mathcal{D}$ axis, *i.e.* $(\mathcal{T} = 0\,,\mathcal{D} > 0)$, which separates the stable spiral from the unstable spiral, corresponding to the onset of an *oscillatory (Hopf) instability*. Since the q^2 term in $\mathcal{T}$ has a negative coefficient[1], this instability first occurs at $q = 0$, *i.e.* in the spatially homogeneous mode. The condition for the Hopf instability is then

$$f_u + g_v = 0 \ . \tag{9.20}$$

The second instability boundary is the half-line $(\mathcal{T} < 0\,,\mathcal{D} = 0)$, which forms the border with the saddle point region. If the coefficient of the q^2 term in $\mathcal{D}$ is negative, *i.e.* if $(D_u\, g_v + D_v\, f_u) > 0$, then the minimum of $\mathcal{D}(q)$ occurs at a finite value, $q = \pm Q$, where

$$Q^2 = \frac{D_u\, g_v + D_v\, f_u}{2D_u D_v} \ . \tag{9.21}$$

In this case, the instability is to a spatially inhomogeneous state. This is the *Turing instability*. This requires that at least one of f_u and g_v is positive, or *autocatalytic*. However, if both are positive, then the condition for the Hopf instability will already have been satisfied. So for the Turing instability we must require $f_u + g_v < 0$, which says that only one of the species is autocatalytic. Setting $\mathcal{D}(Q) = 0$, we eliminate Q and obtain the condition

$$D_u\, g_v + D_v\, f_u = 2\sqrt{\Delta D_u D_v} \ , \tag{9.22}$$

hence, at the threshold of instability, the ordering wavevector is

$$Q^2 = \sqrt{\frac{\Delta}{D_u D_v}} \ . \tag{9.23}$$

For the Turing instability, we may assume, without loss of generality, that $g_v < 0 < f_u$. The Turing instabilty *preempts* the Hopf instability when eqn. 9.22 is satisfied before eqn. 9.20. It is therefore a necessary (but not sufficient) condition that $D_v > D_u$. *The Turing instability preempts the Hopf instability when only one species is autocatalytic, and the autocatalytic species is less diffusive.* This requires a slowly diffusing *activator* and a more rapidly diffusing *inhibitor*.

9.2 The Brusselator

Consider the so-called Brusselator model of Prigogine and Lefever (1968). The Brusselator is a model for two fictitious chemical reactions,

$$\begin{aligned} \mathrm{A} &\longrightarrow \mathrm{B} \\ 2\mathrm{A} + \mathrm{B} &\longrightarrow 3\mathrm{A} \ . \end{aligned}$$

[1] We assume both diffusion constants are positive: $D_{u,v} > 0$.

The species A is assumed to be supplied and removed from the system, in which case, after adding diffusion, we have two coupled RDEs with

$$f(u,v) = a - (1+b)\,u + u^2 v \tag{9.24}$$

$$g(u,v) = b\,u - u^2 v \ . \tag{9.25}$$

The fixed point $f = g = 0$ occurs at $(u^*\,, v^*) = (a\,, b/a)$. Linearizing the local dynamics about the fixed point, we obtain

$$\begin{pmatrix} f_u & f_v \\ g_u & g_v \end{pmatrix} = \begin{pmatrix} b-1 & a^2 \\ -b & -a^2 \end{pmatrix} \ . \tag{9.26}$$

Thus, $\Delta = a^2 > 0$. The Hopf instability sets in when $f_u + g_v = 0$, *i.e.* when $b = b_{\rm H}$, where

$$b_{\rm H} = 1 + a^2 \ . \tag{9.27}$$

For the Turing instability, eqn. 9.22 gives $b = b_{\rm T}$, where

$$b_{\rm T} = (1+c)^2 \ , \tag{9.28}$$

where we have defined

$$c \equiv a\sqrt{\frac{D_u}{D_v}} \ . \tag{9.29}$$

Note that $c < a$ for the Turing instability. These two curves intersect at

$$c^* = -1 + \sqrt{1+a^2} \ . \tag{9.30}$$

Note that

$$Q^2 = \frac{a}{\sqrt{D_u D_v}} \qquad \Rightarrow \qquad D_u Q^2 = c \quad , \quad D_v Q^2 = \frac{a^2}{c} \ . \tag{9.31}$$

Suppose we are close to the Turing instability, and we write $b = b_{\rm T} + \epsilon$ with $|\epsilon| \ll 1$. We first expand the coupled RDEs about the fixed point, writing

$$u = u^* + \delta u \tag{9.32}$$

$$v = v^* + \delta v \ , \tag{9.33}$$

with $u^* = a$ and $v^* = \frac{b}{a}$. Written in terms of δu and δv, the coupled RDEs take the form

$$\delta u_t = D_u\,\delta u_{xx} - \delta u + \Big(b\,\delta u + a^2\,\delta v\Big) + \bigg(\frac{b}{a}\,(\delta u)^2 + 2a\,\delta u\,\delta v + (\delta u)^2 \delta v\bigg) \tag{9.34}$$

$$\delta v_t = D_v\,\delta v_{xx} - \Big(b\,\delta u + a^2\,\delta v\Big) - \bigg(\frac{b}{a}\,(\delta u)^2 + 2a\,\delta u\,\delta v + (\delta u)^2 \delta v\bigg) \ . \tag{9.35}$$

If we ignore the nonlinear terms, we obtain a linear equation which has a solution

$$\delta u(x,t) = U_{11}\,A(t)\,\cos(Qx) \tag{9.36}$$

$$\delta v(x,t) = V_{11}\,A(t)\,\cos(Qx) \ , \tag{9.37}$$

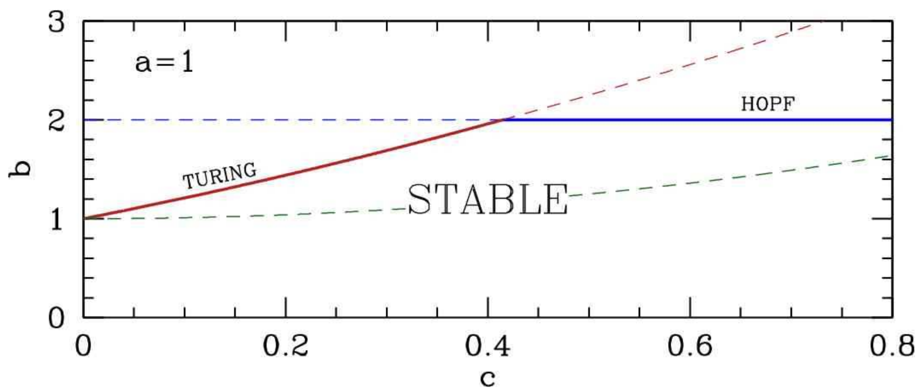

Figure 9.2: Instability lines for the Brusselator. The thick blue line denotes a Hopf instability and the thick red line a Turing instability. The dashed light green line is the locus of points for which $Q^2 > 0$.

where $A(t) = A_0 \exp(\omega t)$ is an amplitude, and where the eigenvector $(U_{11}\ V_{11})^{\mathrm{t}}$ satisfies

$$\begin{pmatrix} b-c-1 & a^2 \\ -b & -a^2-\frac{a^2}{c} \end{pmatrix} \begin{pmatrix} U_{11} \\ V_{11} \end{pmatrix} = \omega \begin{pmatrix} U_{11} \\ V_{11} \end{pmatrix} \ . \tag{9.38}$$

If $b > b_{\mathrm{T}}$, then there exists an eigenvalue ω which is real and positive, in which case the amplitude $A(t)$ grows exponentially.

The amplitude equation has a fixed point when $A_t = 0$, which says $\eta = gA^2$.

9.2.1 The amplitude equation

The exponential growth of the amplitude $A(t)$ is valid only insofar as the nonlinear terms in the dynamics are small. Our goal here will be to develop a nonlinear ODE governing the growth of $A(t)$, assuming $|b - b_{\mathrm{T}}| \ll 1$. We follow the treatment of Kessler and Levine (2009, unpublished).

We assume one Fourier mode will be excited, with $q = \pm Q$, along with its harmonics. We therefore write

$$\delta u = \sum_{m=1}^{\infty} \sum_{n=0}^{\infty} U_{mn}\, A^m \cos(nQx) \tag{9.39}$$

$$\delta v = \sum_{m=1}^{\infty} \sum_{n=0}^{\infty} V_{mn}\, A^m \cos(nQx) \ . \tag{9.40}$$

We shall only need the first few terms:

$$\delta u = \big(U_{11} A + U_{31} A^3\big) \cos(Qx) + U_{20} A^2 + U_{22} A^2 \cos(2Qx) + \ldots \tag{9.41}$$

$$\delta v = \big(V_{11} A + V_{31} A^3\big) \cos(Qx) + V_{20} A^2 + V_{22} A^2 \cos(2Qx) + \ldots \ . \tag{9.42}$$

Note that we assume $U_{10} = V_{10} = 0$ because the leading behavior is in the U_{11} and V_{11} terms. It is through the quadratic nonlinearities that terms with $n = 0$ are generated.

We now undertake the tedious process of working out the RHS of eqns. 9.34 and 9.35 to order A^3. Throughout our derivation, we shall include only the $n = 0$, $n = 1$ and $n = 2$ harmonics and drop all other terms. We will also assume $b = b_{\mathrm{T}}$ whenever it multiplies A^m with $m > 1$, since $\epsilon = b - b_{\mathrm{T}}$ is presumed small, and, as we shall see, the amplitude itself will be proportional to $\sqrt{\epsilon}$. Let's roll up our sleeves and get to work!

The first terms we need are all the ones linear in δu and δv. Thus, we need

$$\begin{aligned} D_u\, \delta u_{xx} - \delta u &= -(1+c)\Big(U_{11} A + U_{31} A^3\Big) \cos(Qx) - U_{20} A^2 \\ &\qquad - (1+4c)\, U_{22} A^2 \cos(2Qx) \end{aligned} \tag{9.43}$$

$$D_v\, \delta v_{xx} = -\frac{a^2}{c}\left(V_{11} A + V_{31} A^3\right) \cos(Qx) - \frac{4a^2}{c}\, V_{22} A^2 \cos(2Qx) \tag{9.44}$$

as well as

$$\begin{aligned} b\, \delta u + a^2\, \delta v &= \left\{ b\left(U_{11} A + U_{31} A^3\right) + a^2 \left(V_{11} A + V_{31} A^3\right)\right\} \cos(Qx) \\ &\qquad + \Big(b\, U_{20} + a^2\, V_{20}\Big) A^2 + \Big(b\, U_{22} + a^2\, V_{22}\Big) A^2 \cos(2Qx)\ . \end{aligned} \tag{9.45}$$

Next, we need the nonlinear terms, starting with

$$(\delta u)^2 = \tfrac{1}{2} U_{11}^2 A^2 + \tfrac{1}{2} U_{11}^2 A^2 \cos(2Qx) + U_{11}\big(2\, U_{20} + U_{22}\big) A^3 \cos(Qx) + \ldots\ , \tag{9.46}$$

where the remaining terms are of $\mathcal{O}(A^4)$ or are proportional to $\cos(3Qx)$. We also require

$$\begin{aligned} 2\, \delta u\, \delta v &= U_{11} V_{11} A^2 + U_{11} V_{11} A^2 \cos(2Qx) \\ &\qquad + \Big(2\, U_{11} V_{20} + 2\, V_{11} U_{20} + U_{11} V_{22} + V_{11} U_{22}\Big) A^3 \cos(Qx) + \ldots\ . \end{aligned} \tag{9.47}$$

Finally, we need

$$(\delta u)^2\, \delta v = \tfrac{3}{4}\, U_{11}^2 V_{11} \cos(Qx) + \ldots\ . \tag{9.48}$$

On the left hand side of eqns. 9.34 and 9.35, we have the time derivative terms. Again, as we shall see, the amplitude A will be proportional to $\sqrt{\epsilon}$, where $\epsilon = b - b_{\mathrm{T}}$ is presumed small. Its time derivative A_t will be proportional to $\epsilon^{3/2}$. Therefore, terms such as $(A^2)_t = 2AA_t$ will be negligible and we shall drop them from the outset. Thus,

$$\delta u_t = U_{11}\, A_t\, \cos(Qx) + \ldots \tag{9.49}$$

$$\delta v_t = V_{11}\, A_t\, \cos(Qx) + \ldots\ . \tag{9.50}$$

The linear terms in A comprise a zero mode for the system with $b = b_{\mathrm{T}}$. Thus,

$$\begin{pmatrix} b_{\mathrm{T}} - c - 1 & a^2 \\ -b_{\mathrm{T}} & -a^2 - \frac{a^2}{c} \end{pmatrix} \begin{pmatrix} U_{11} \\ V_{11} \end{pmatrix} = 0\ . \tag{9.51}$$

We may, without loss of generality, set $U_{11} \equiv 1$. We then have

$$U_{11} = 1 \qquad , \qquad V_{11} = -\frac{c\,(1+c)}{a^2} \ . \tag{9.52}$$

We now set to zero the coefficients of $\cos(nQx)$ for $n = 0$, 1, and 2 in each of eqns. 9.34 and 9.35. Setting the $n = 0$ terms on the RHS of these equations to zero, we obtain

$$U_{20} = 0 \tag{9.53}$$

$$\frac{b}{2a}\,U_{11}^2 + a\,U_{11}V_{11} + a^2\,V_{20} = 0 \ . \tag{9.54}$$

Doing the same for the $n = 2$ terms, we get

$$\frac{b}{2a}\,U_{11}^2 + a\,U_{11}V_{11} + b\,U_{22} + a^2\big(1 + 4c^{-1}\big)V_{22} = 0 \tag{9.55}$$

$$(1+4c)\,U_{22} + \frac{4a^2}{c}\,V_{22} = 0 \ . \tag{9.56}$$

Solving, we obtain

$$U_{20} = 0 \qquad\qquad U_{22} = \frac{2\,(1-c^2)}{9\,ac} \tag{9.57}$$

$$V_{20} = -\frac{1-c^2}{2\,a^3} \qquad\qquad V_{22} = -\frac{(1-c^2)\,(1+4c)}{18\,a^3} \ . \tag{9.58}$$

Finally, we need the $n = 1$ terms. There are three contributions. One comes from the linear terms, restoring the small differences proportional to $\epsilon = b - b_{\mathrm{T}}$. These terms contribute a coefficient for $\cos(Qx)$ of $\epsilon\,A$ in the RHS of eqn. 9.34 and $-\epsilon\,A$ on the RHS of eqn. 9.35. A second contribution comes from the nonlinear terms. We invoke eqns. 9.46 and 9.47, multiplying the former by $\frac{b}{a}$ and the latter by a. The term we seek is proportional to $A^3\cos(Qx)$, with a coefficient

$$\frac{b}{a}\,U_{22} + a\,\big(2\,V_{20} + V_{22} + V_{11}U_{22}\big) + \tfrac{3}{4}\,V_{11} = \frac{(1+c)\,(2+c)\,(8c^2 - 21c + 4)}{36\,a^2 c} \ . \tag{9.59}$$

We define

$$\lambda = -\frac{(1+c)\,(2+c)\,(8c^2 - 21c + 4)}{36\,a^2 c} \ . \tag{9.60}$$

Note that $\lambda > 0$ for $c \in \big[c_-\,,\,c_+\big]$, where $c_\pm = \frac{1}{16}\big(21 \pm \sqrt{313}\,\big)$. Numerically, $c_- \approx 0.20676$ and $c_+ \approx 2.4182$. Finally, we have the U_{31} and V_{31} terms themselves. Thus, dividing out the common $\cos(Qx)$ factor on both sides of both equations, we have

$$A_t = \epsilon\,A + \Big[c\,(1+c)\,U_{31} + a^2\,V_{31} - \lambda\Big]A^3 \tag{9.61}$$

$$-\frac{c\,(1+c)}{a^2}\,A_t = -\epsilon\,A - \Big[(1+c)^2\,U_{31} + \frac{a^2}{c}\,(1+c)\,V_{31} + \lambda\Big]A^3 \ . \tag{9.62}$$

We can rewrite these equations as a linear system for the coefficients U_{31} and V_{31}, *viz.*

$$A^3 \overbrace{\begin{pmatrix} c\,(1+c) & a^2 \\ -(1+c)^2 & -a^2 - \frac{a^2}{c} \end{pmatrix}}^{M} \begin{pmatrix} U_{31} \\ V_{31} \end{pmatrix} = \begin{pmatrix} A_t - \epsilon\, A + \lambda\, A^3 \\ -a^{-2}\, c\,(1+c)\, A_t + \epsilon\, A - \lambda\, A^3 \end{pmatrix} \ . \tag{9.63}$$

In order to be able to satisfy the above equation, the RHS must be orthogonal to the left eigenvector of the matrix M corresponding to the zero eigenvalue. This is called the *solvability condition*. It is easy to see that this zero left eigenvector is proportional to

$$\phi = \begin{pmatrix} 1+c & c \end{pmatrix} \ . \tag{9.64}$$

Thus, we demand

$$(1+c)\Big(A_t - \epsilon\, A + \lambda\, A^3\Big) - c\,\Big(a^{-2}\, c\,(1+c)\, A_t - \epsilon\, A + \lambda\, A^3\Big) = 0 \ . \tag{9.65}$$

This, at long last, yields our amplitude equation:

$$A_t = \eta A - g A^3 \ , \tag{9.66}$$

where

$$\eta = \frac{a^2\,(b - b_{\rm T})}{(1+c)\,(a^2 - c^2)} \qquad , \qquad g = -\frac{a^2\,(2+c)\,(8c^2 - 21c + 4)}{36\, a^2\, c\,(a^2 - c^2)} \ . \tag{9.67}$$

Since $c < a$, we have that η is positive for $b > b_{\rm T}$ and negative for $b < b_{\rm T}$. Furthermore g is positive for $c \in \big[c_- \, , \, c_+\big]$ and negative outside this region. Thus, A has a fixed point $A^* = \sqrt{\eta/g}$ (in addition to the one at $A = 0$) if both η and g are positive, or if both η and g are negative. In the former case, $A = 0$ is unstable and $A = A^*$ is stable. In the latter case, $A = 0$ is stable and $A = A^*$ is unstable.

9.3 Rayleigh-Bénard Instability

Consider a layer of fluid between two horizontal plates, as depicted in fig. 9.3. The top plate is held at temperature T_1 and the bottom plate at temperature T_2, with $\Delta T = T_2 - T_1 > 0$. As the fluid near the bottom plate is heated, it expands, and an upward buoyancy force per unit volume $f_{\rm buoy} = \rho g\, \alpha\, \Delta T$ results, where $\alpha = \frac{1}{V} \frac{\partial V}{\partial T}$ is the thermal expansion coefficient and ρ is the fluid density. This buoyancy force is a destabilizing effect, and is opposed by a stabilizing dissipative force per unit volume $f_{\rm diss} = \nu \kappa \rho / d^3$, where ν is the kinematic viscosity, κ the thermal diffusivity, and d the distance between the plates. The dimensionless ratio of these two force densities is known as the *Rayleigh number*,

$$\mathcal{R} = \frac{f_{\rm buoy}}{f_{\rm diss}} = \frac{g\, d^3\, \alpha\, \Delta T}{\nu\, \kappa} \ . \tag{9.68}$$

When $\mathcal{R} > \mathcal{R}_{\rm c} \approx 1708$, the destabilizing effects are sufficient to destroy the homogeneous state. Due to mass conservation, the entire fluid cannot rise uniformly, hence the instability

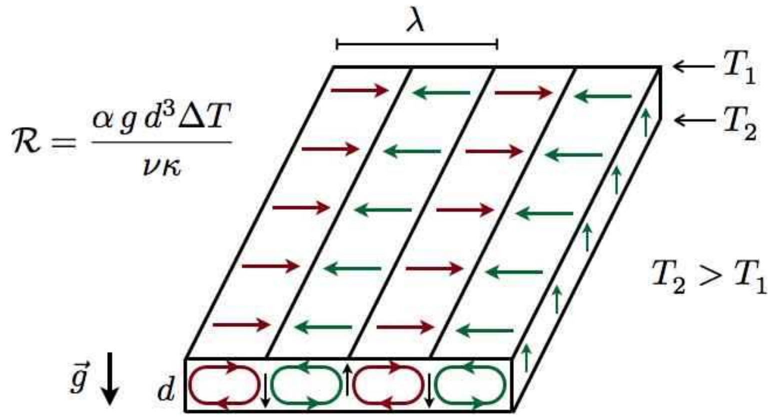

Figure 9.3: Bénard convection cells in a fluid heated from below.

occurs at a finite wavelength λ, owing to the formation of *convective rolls* known as *Bénard cells* (see fig. 9.3).

Swift and Hohenberg (1977) showed that the dynamics for this problem reduces to the following equation for the real field $\sigma(\boldsymbol{r},t)$[2]:

$$\frac{\partial\sigma}{\partial t} = \Big[\varepsilon - \big(Q^2 + \boldsymbol{\nabla}^2\big)^2\Big]\sigma - \sigma^3 \ . \tag{9.69}$$

Here,

$$\varepsilon \propto \mathcal{R} - \mathcal{R}_{\rm c} \tag{9.70}$$

measures the distance from the instability, and $\boldsymbol{\nabla} = \hat{\boldsymbol{x}}\,\partial_x + \hat{\boldsymbol{y}}\,\partial_y$ is the in-plane gradient. Distances are measured in units of d, and the maximally unstable wavevector is $Q \approx 3.12$.

We assume a plane wave disturbance, and we first separate out the oscillating features of $\sigma(\boldsymbol{r},t)$ so that we may talk of a slowly varying amplitude function $A(\boldsymbol{r},t)$:

$$\sigma(\boldsymbol{r},t) = A(\boldsymbol{r},t)\, e^{iQx} + A^*(\boldsymbol{r},t)\, e^{-iQx} \ , \tag{9.71}$$

where $\hat{\boldsymbol{n}}$ is a unit vector which we henceforth assume to be $\hat{\boldsymbol{n}} = \hat{\boldsymbol{x}}$. We then have

$$\sigma^3 = A^3\, e^{3iQx} + 3\,|A|^2\, A\, e^{iQx} + 3\,|A|^2\, A^*\, e^{-iQx} + A^{*3}\, e^{-3IQx} \tag{9.72}$$

$$\big(Q^2 + \boldsymbol{\nabla}^2\big)\, A\, e^{iQx} = e^{iQx} \cdot \big(2iQ\,\partial_x + \partial_x^2 + \partial_y^2\big) A \ . \tag{9.73}$$

Matching coefficients of e^{iQx}, we find

$$\partial_t\, A = \bigg\{\varepsilon - \Big(2iQ\,\partial_x + \partial_x^2 + \partial_y^2\Big)^2\bigg\} A - 3\,|A|^2\, A \ . \tag{9.74}$$

If we assume that the solution for A is such that $\partial_x \propto \epsilon^{1/2}$ and $\partial_y \propto \epsilon^{1/4}$ when acting on A, then the ∂_x^2 term is subleading relative to $Q\,\partial_x$ and ∂_y^2, and we may drop it for $|\epsilon| \ll 1$ and write

$$\partial_t\, A = \bigg\{\varepsilon - \Big(2iQ\,\partial_x + \partial_y^2\Big)^2\bigg\} A - 3\,|A|^2\, A \ . \tag{9.75}$$

[2]The field σ is actually a combination of temperature and vertical velocity fields.

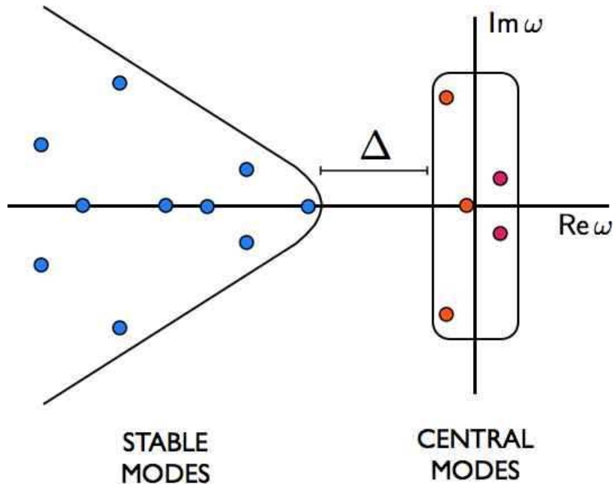

Figure 9.4: Sketch showing separation of frequency scales owing to gap Δ. The fast, stable modes are to the left, and the slow central modes all have $\mathsf{Re}\,\omega_a \approx 0$.

For $\varepsilon > 0$ there is a family of stationary solutions of the form

$$A(x,y) = A_{\boldsymbol{q}}\, e^{i\boldsymbol{q}\cdot\boldsymbol{r}}\, e^{i\delta} \ , \tag{9.76}$$

where

$$A_{\boldsymbol{q}} = \frac{1}{\sqrt{3}}\Big(\varepsilon - \big(2Qq_x + q_y^2\big)^2\Big)^{1/2} \ . \tag{9.77}$$

The instability first occurs at $\boldsymbol{q} = 0$, at $\varepsilon = 0$. As we shall see, the nonlinearity severely limits what multimode structures may form.

The derivation of the Swift-Hohenberg equation utilizes something called the *Boussinesq approximation*, in which the density variation of the fluid enters only in the buoyancy equation. For *non-Boussinesq* fluids, the symmetry $\sigma \to -\sigma$ is broken, and one has

$$\partial_t\, \sigma = \Big[\varepsilon - \big(Q^2 + \boldsymbol{\nabla}^2\big)^2\Big]\sigma + v\,\sigma^2 - \sigma^3 \ , \tag{9.78}$$

for which the bifurcation is subcritical. This is called the *Haken model*.

9.4 Center Manifold Reduction

Consider a dynamical system in the vicinity of a fixed point: $\dot{\phi}_i = L_{ij}\,\phi_j + \mathcal{O}(\phi^2)$. If we expand the variables ϕ_i in terms of the eigenvectors ψ_i^a of L, writing $\phi_i = \sum_a A_a\,\psi_i^a$, then we can treat the A_a as new variables. Furthermore, we assume that the eigenspectrum $\{\omega_a\}$ exhibits a gap Δ, as shown in fig. 9.4, which allows us to classify these normal modes as either stable or central. The stable normal modes have large ($\mathsf{Re}\,\omega_a < -\Delta$) negative real parts to their frequencies, and hence relax rapidly. On this time scales $\tau \lesssim \Delta^{-1}$, the central modes are roughly constant. We label these modes as $A^{\rm c}_a$ and $A^{\rm s}_a$, respectively. The dynamics of these modes may be written as

$$\frac{dA^{\rm c}_a}{dt} = J_{ab}\, A^{\rm c}_b + M_a(\boldsymbol{A}^{\rm c}, \boldsymbol{A}^{\rm s}) \tag{9.79}$$

$$\frac{dA^{\rm s}_a}{dt} = K_{ab}\, A^{\rm s}_b + N_a(\boldsymbol{A}^{\rm c}, \boldsymbol{A}^{\rm s}) \ , \tag{9.80}$$

where M_a and N_a are nonlinear. If we assume that the fast, stable modes come to equilibrium, we set $\dot{A}^{\rm s}_a = 0$ and solve the nonlinear equations $K_{ab} A^{\rm s}_b + N_a(\boldsymbol{A}^{\rm c}, \boldsymbol{A}^{\rm s}) = 0$ to obtain $A^{\rm s}_a = A^{\rm s}_a(\boldsymbol{A}^{\rm c})$. Inserting this into the first of the previous sets of equations, we arrive at a new set of equations for the central modes alone. These new equations, obtained by substituting the solution for the stable modes, which are slaved to the slower central modes, into the function $M_a(\boldsymbol{A}^{\rm c}, \boldsymbol{A}^{\rm s})$, are of the form

$$\frac{dA^{\rm c}_a}{dt} = L_{ab}\, A^{\rm c}_b + P_a(\boldsymbol{A}^{\rm c}) \ . \tag{9.81}$$

where P_a is nonlinear.

It is convenient to consider a nonlinear change of variables $(\boldsymbol{A}^{\rm c}, \boldsymbol{A}^{\rm s}) \to (\boldsymbol{B}^{\rm c}, \boldsymbol{B}^{\rm s})$ so that the center manifold is described by $\boldsymbol{B}^{\rm s} = 0$. To this end, we write $\boldsymbol{B} = \boldsymbol{A} + \boldsymbol{F}(\boldsymbol{A})$, or, equivalently, $\boldsymbol{A} = \boldsymbol{B} + \boldsymbol{G}(\boldsymbol{B})$. Note that to linear order the transformation is the identity $\boldsymbol{A} = \boldsymbol{B}$ because we wish to preserve the identification of the stable and central modes.

As a simple example, consider the system

$$\frac{dA_1}{dt} = 2A_1 A_2 \tag{9.82}$$

$$\frac{dA_2}{dt} = -5A_2 - A_1^2 \ . \tag{9.83}$$

We identify A_1 as the central mode and A_2 as the stable fast mode. We now try a nonlinear transformation of the form

$$A_1 = B_1 + \alpha\, B_1^2 + \beta\, B_1 B_2 + \gamma\, B_2^2 \tag{9.84}$$

$$A_2 = B_2 + \alpha'\, B_1^2 + \beta'\, B_1 B_2 + \gamma'\, B_2^2 \ . \tag{9.85}$$

We then have

$$\frac{dA_2}{dt} = \frac{dB_2}{dt} + 2\alpha'\, B_1\, \frac{dB_1}{dt} + \beta'\, B_1\, \frac{dB_2}{dt} + \beta'\, B_2\, \frac{dB_1}{dt} + 2\gamma'\, B_2\, \frac{dB_2}{dt} \ . \tag{9.86}$$

Setting $\beta' = 0$ we obtain the equation

$$\big(1 + 2\gamma' B_2\big)\, \frac{dB_2}{dt} = -5B_2 - (1 + 5\alpha')\, B_1^2 - 5\gamma'\, B_2^2 + \mathcal{O}(B^3) \tag{9.87}$$

We see that B_2 becomes isolated from B_1 if we choose $\alpha' = -\frac{1}{5}$. We are free to choose any value of γ' we please; for simplicity we choose $\gamma' = 0$. The B_2 equation is then

$$\frac{dB_2}{dt} = -5B_2 \ . \tag{9.88}$$

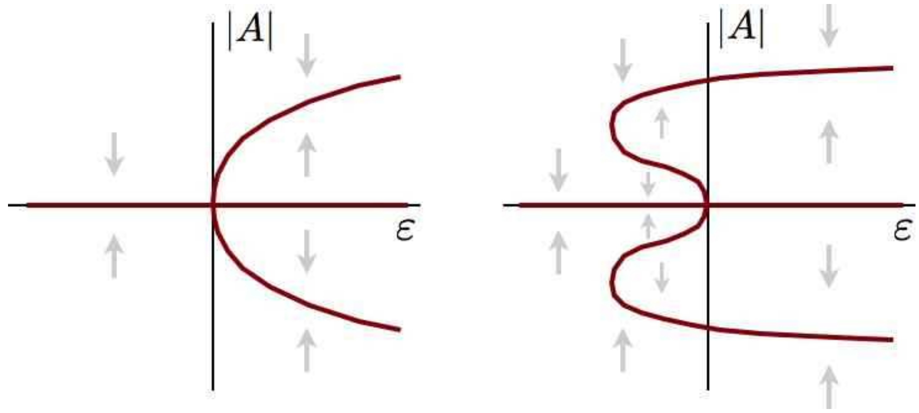

Figure 9.5: Flow diagrams for one-dimensional bifurcations $\dot{A} = \varepsilon\, A - g\,|A|^2 A$ with $g > 0$ (left) and $\dot{A} = \varepsilon\, A - g_1\,|A|^2 A - g_2\,|A|^4 A$ with $g_1 < 0$ and $g_2 > 0$ (right).

The fixed point is $B_2 = 0$. Note that

$$A_2 = B_2 - \tfrac{1}{5} B_1^2 \tag{9.89}$$

and so at the fixed point we conclude

$$A_2 = -\tfrac{1}{5} A_1^2 + \mathcal{O}(A_1^3) \ , \tag{9.90}$$

which is obvious from inspection of eqn. 9.83 as well.

9.5 Selection and Stability of Spatial Patterns

Consider the spatiotemporal dynamics for a real field $\sigma(\boldsymbol{r}, t)$ close to an instability which lies at $|\boldsymbol{q}| = Q$. We assume a form

$$\sigma(\boldsymbol{r}, t) = \sum_{\ell=1}^{M} \Big(A_\ell(t)\, e^{i\boldsymbol{q}_\ell \cdot \boldsymbol{r}} + A_\ell^*(t)\, e^{-i\boldsymbol{q}_\ell \cdot \boldsymbol{r}} \Big) \ , \tag{9.91}$$

where $\boldsymbol{q}_\ell = Q\, \hat{\boldsymbol{n}}_\ell$ and $\hat{\boldsymbol{n}}_\ell^2 = 1$. By assuming $A_\ell = A_\ell(t)$, *i.e.* with no spatial ($\boldsymbol{r}$) dependence, we are considering a system whose spatial structure is 'perfect' and whose growth rate is maximum. We now consider the amplitude equations for the $A_\ell(t)$. Note that the set of allowed wavevectors in the Fourier decomposition of $\sigma(\boldsymbol{r}, t)$ consists of $2M$ elements, which we can order $\big\{\boldsymbol{q}_1 \,,\, \ldots \,,\, \boldsymbol{q}_M \,,\, -\boldsymbol{q}_1 \,,\, \ldots \,,\, -\boldsymbol{q}_M\big\}$. With this ordering, we have $\boldsymbol{q}_{\ell+M} = -\boldsymbol{q}_\ell$ and $A_{\ell+M} = A_\ell^*$, where $1 \le \ell \le M$. We will use indices i, j, *etc.* to refer to the entire set: $1 \le j \le 2M$.

9.5.1 $d = 1$

For systems in one spatial dimension, the amplitude equation is quite limited, since $\hat{\boldsymbol{n}} = \hat{\boldsymbol{x}}$ is the only possibility, and consequently $M = 1$. The simplest case is the logistic type equation,

$$\frac{dA}{dt} = \varepsilon\, A - g\, |A|^2\, A \ . \tag{9.92}$$

Here, $\varepsilon \propto \lambda - \lambda_c$ is a measure of the system's proximity to an instability, where λ is a control parameter. There are fixed points at $A = 0$ and, for $g > 0$, at $|A| = \sqrt{\varepsilon/g}$. Fixed points at finite A are in fact fixed *rings* in the Cartesian space $(\mathsf{Re}\, A\,, \mathsf{Im}\, A)$, since the phase of A is undetermined and amplitude remains fixed if the phase is varied globally.

With $g > 0$, eqn. 9.92 describes a *supercritical pitchfork bifurcation*. The flow is sketched in the left panel of fig. 9.5. If $g < 0$, the bifurcation is *subcritical*, and the finite A fixed point occurs for $\varepsilon < 0$ and is unstable. In such a case, we must proceed to the next order in the amplitude equation,

$$\frac{dA}{dt} = \varepsilon\, A - g_1\, |A|^2\, A - g_2\, |A|^4\, A \ , \tag{9.93}$$

with $g_1 < 0$ and $g_2 > 0$. The bifurcation diagram for this equation is sketched in the right panel of fig. 9.5.

9.5.2 Remarks on the amplitude equations for $d > 1$

In dimensions $d > 1$ we have the possibility for nonlinear mixing of K different modes, provided

$$\sum_{j=1}^{K} \boldsymbol{q}_j = Q \sum_{j=1}^{K} \hat{\boldsymbol{n}}_j = 0 \ . \tag{9.94}$$

Recall also that A_j is associated with $e^{i\boldsymbol{q}_j\cdot\boldsymbol{r}}$ and A^*_j with $e^{-i\boldsymbol{q}_j\cdot\boldsymbol{r}}$. Under these conditions, the amplitude equations take the following general form:

$$\begin{aligned}\frac{dA_i}{dt} = \varepsilon\, A_i + v \sum_{j,k} A^*_j\, A^*_k\ \delta_{\hat{\boldsymbol{n}}_i+\hat{\boldsymbol{n}}_j+\hat{\boldsymbol{n}}_k\,,0} - g\, |A_i|^2 A_i - g {\sum_j}' \gamma_{ij}\, |A_j|^2\, A_i \\ - \sum_{j,k,l} \lambda_{ijkl}\, A^*_j\, A^*_k\, A^*_l\ \delta_{\hat{\boldsymbol{n}}_i+\hat{\boldsymbol{n}}_j+\hat{\boldsymbol{n}}_k+\hat{\boldsymbol{n}}_l\,,0} + \mathcal{O}(A^4) \ .\end{aligned} \tag{9.95}$$

The prime on the sum indicates that the term with $j = i$ is excluded. Taking the complex conjugate, we obtain the equation with index i replaced by $i + M$. The couplings γ_{ij} and λ_{ijkl} are functions of the relative angles:

$$\gamma_{ij} = \gamma(\hat{\boldsymbol{n}}_i\cdot\hat{\boldsymbol{n}}_j) \tag{9.96}$$

$$\lambda_{ijkl} = \lambda(\hat{\boldsymbol{n}}_i\cdot\hat{\boldsymbol{n}}_j\,,\, \hat{\boldsymbol{n}}_i\cdot\hat{\boldsymbol{n}}_k\,,\, \ldots) \ . \tag{9.97}$$

Note that if we associate A_j with $e^{i\boldsymbol{q}_j\cdot\boldsymbol{r}}$ we can define $A_{-j} \equiv A^*_j$, associated with $e^{-i\boldsymbol{q}_j\cdot\boldsymbol{r}}$. Also note that v is a constant independent of j and k because the dot products in that case necessarily are all identical: $\hat{\boldsymbol{n}}_i\cdot\hat{\boldsymbol{n}}_j = \hat{\boldsymbol{n}}_j\cdot\hat{\boldsymbol{n}}_k = \hat{\boldsymbol{n}}_k\cdot\hat{\boldsymbol{n}}_i$.

9.5.3 $d = 2$

For $d = 2$ systems all the allowed wavevectors lie on the circle $|\boldsymbol{q}_j| = Q$. Let's consider the cases $M = 1$, $M = 2$, and $M = 3$.

For $M = 1$ we recapitulate the $d = 1$ case. We have $\boldsymbol{q}_1 = Q\hat{\boldsymbol{x}}$ and $\boldsymbol{q}_2 = -Q\hat{\boldsymbol{x}}$ (up to continuous rotations). The amplitude equation is of the form $\dot{A} = \varepsilon\, A - g\,|A|^2 A$, and the patterned state is one with bands (stripes). This is not the last word, however, since we must check its stability with respect to $M = 2$ and $M = 3$ patterns.

$M = 2$ case

For $M = 2$, we write

$$\sigma(x, y, t) = A_1(t)\, e^{iQx} + A_1^*(t)\, e^{-iQx} + A_2(t)\, e^{iQy} + A_2^*(t)\, e^{-iQy} \ . \tag{9.98}$$

The amplitude equations are

$$\dot{A}_1 = \varepsilon\, A_1 - g\,|A_1|^2 A_1 - \gamma\, g\,|A_2|^2 A_1 \tag{9.99}$$

$$\dot{A}_2 = \varepsilon\, A_2 - g\,|A_2|^2 A_2 - \gamma\, g\,|A_1|^2 A_2 \ . \tag{9.100}$$

We assume $g > 0$. There are four possible fixed points $(\mathcal{A}_1, \mathcal{A}_2)$:

$$\begin{array}{ll}
(\mathcal{A}_1, \mathcal{A}_2) = (0\,, 0) & \text{(I: trivial state)} \\
(\mathcal{A}_1, \mathcal{A}_2) = \sqrt{\varepsilon/g} \cdot (e^{i\alpha_1}, 0) & \text{(II: } y\text{-directed bands)} \\
(\mathcal{A}_1, \mathcal{A}_2) = \sqrt{\varepsilon/g} \cdot (0\,,\, e^{i\alpha_2}) & \text{(III: } x\text{-directed bands)} \\
(\mathcal{A}_1, \mathcal{A}_2) = \sqrt{\varepsilon/g\,(1+\gamma)} \cdot (e^{i\alpha_1}, e^{i\alpha_2}) & \text{(IV: squares)}
\end{array}$$

Note that $\mathcal{A}_1 \to \mathcal{A}_1\, e^{-i\beta}$ is equivalent to a translation of the pattern in the $\hat{\boldsymbol{x}}$-direction by $\Delta x = \beta/Q$.

To assess the stability of these fixed points, we write

$$A_j = \mathcal{A}_j\,(1 + \eta_j) \ , \tag{9.101}$$

and we find

$$\begin{pmatrix} \dot{\eta}_1 \\ \dot{\eta}_2 \end{pmatrix} = \overbrace{\begin{pmatrix} \varepsilon - 3g\,|\mathcal{A}_1|^2 - \gamma\, g\,|\mathcal{A}_2|^2 & -2\gamma\, g\,|\mathcal{A}_2|^2 \\ -2\gamma\, g\,|\mathcal{A}_1|^2 & \varepsilon - \gamma\, g\,|\mathcal{A}_1|^2 - 3g\,|\mathcal{A}_2|^2 \end{pmatrix}}^{L} \begin{pmatrix} \eta_1 \\ \eta_2 \end{pmatrix} + \mathcal{O}(\eta^2) \ . \tag{9.102}$$

Evaluating L at the four fixed points, we find

$$L_{\mathrm{I}} = \begin{pmatrix} \varepsilon & 0 \\ 0 & \varepsilon \end{pmatrix} \quad , \quad L_{\mathrm{II}} = \begin{pmatrix} -2\varepsilon & 0 \\ -2\gamma\,\varepsilon & (1-\gamma)\,\varepsilon \end{pmatrix} \tag{9.103}$$

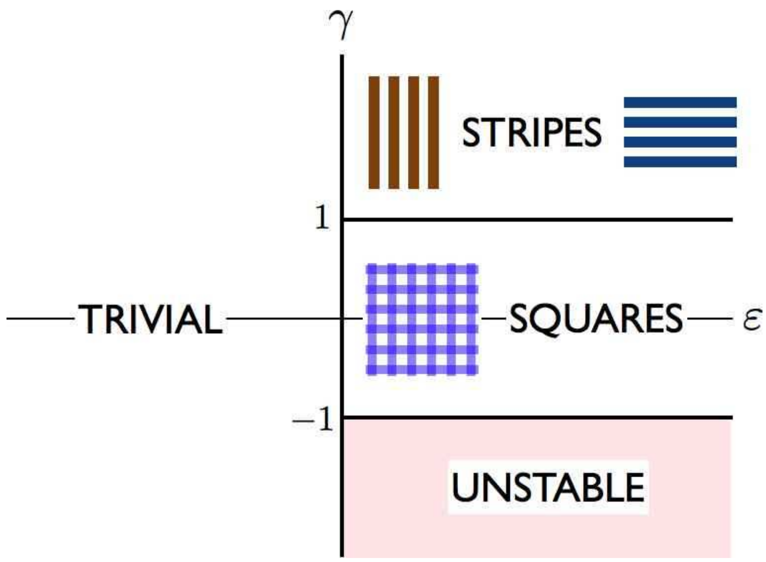

Figure 9.6: Phase diagram for the $M = 2$ system.

and

$$L_{\rm III} = \begin{pmatrix} (1-\gamma)\,\varepsilon & -2\gamma\,\varepsilon \\ \\ 0 & -2\varepsilon \end{pmatrix} \quad , \quad L_{\rm IV} = -\frac{2\varepsilon}{1+\gamma} \begin{pmatrix} 1 & \gamma \\ \\ \gamma & 1 \end{pmatrix} \quad . \tag{9.104}$$

Computing $\mathcal{T} = \mathrm{Tr}(L)$ and $\mathcal{D} = \det(L)$, we find:

(I) In the trivial phase, we have $\mathcal{T} = 2\varepsilon$ and $\mathcal{D} = \varepsilon^2$. This fixed point is stable star if $\varepsilon < 0$ and an unstable star if $\varepsilon > 0$.[3]

(II) In the striped phase, we have $\mathcal{T} = -(1+\gamma)\,\varepsilon$ and $\mathcal{D} = 2(\gamma-1)\,\varepsilon^2$. Thus, if $\gamma < 1$ the stripes are unstable as the fixed point is a saddle. Now suppose $\gamma > 1$, meaning $\mathcal{D} > 0$. The fixed point is therefore stable since $\varepsilon > 0$. If $\varepsilon < 0$, there is no solution for the fixed point at all. We next compute $\mathcal{D} - \frac{1}{4}\mathcal{T}^2 = -\frac{1}{4}(\gamma-3)^2\,\varepsilon^2$ which is always negative, indicating that the fixed point is always a stable node.

(III) Same as case II.

(IV) We find $\mathcal{T} = -4\varepsilon/(\gamma+1)$ and $\mathcal{D} = 4\varepsilon^2\,(1-\gamma)/(1+\gamma)$. The condition $\mathcal{D} > 0$ is equivalent to $|\gamma| < 1$. For $|\gamma| > 1$, this fixed point is a saddle, and is unstable. Note that $|\mathcal{A}_{1,2}|^2 = -\mathcal{T}/4g$ at the fixed point, so if a solution exists we must have $\mathcal{T} < 0$. If $|\gamma| < 1$ then, the fixed point is stable, and we find $\mathcal{D} - \frac{1}{4}\mathcal{T}^2 = -4\varepsilon^2\gamma^2/(1+\gamma)^2 < 0$, indicating a stable node. Note that a fixed point solution exists for $\varepsilon < 0$ if $1+\gamma < 0$, which means $\gamma < -1$, which is a saddle and unstable.

The phase diagram is shown in fig. 9.6.

[3]The star is a nongeneric fixed point, arising here because the eigenspace is degenerate. Note that $\mathcal{D} = \frac{1}{4}\mathcal{T}^2$ for the type I case.

$M = 3$ case

For $M = 3$ we write

$$\hat{\boldsymbol{n}}_1 = \hat{\boldsymbol{x}} \qquad , \qquad \hat{\boldsymbol{n}}_2 = -\tfrac{1}{2}\,\hat{\boldsymbol{x}} + \tfrac{\sqrt{3}}{2}\,\hat{\boldsymbol{y}} \qquad , \qquad \hat{\boldsymbol{n}}_3 = -\tfrac{1}{2}\,\hat{\boldsymbol{x}} - \tfrac{\sqrt{3}}{2}\,\hat{\boldsymbol{y}} \ , \tag{9.105}$$

with $\boldsymbol{q}_j = Q\,\hat{\boldsymbol{n}}_j$, with $\hat{\boldsymbol{n}}_{r+3} = -\hat{\boldsymbol{n}}_\ell$. The σ field is then given by the sum

$$\sigma(\boldsymbol{r},t) = A_1\,e^{i\boldsymbol{q}_1\cdot\boldsymbol{r}} + A_2\,e^{i\boldsymbol{q}_2\cdot\boldsymbol{r}} + A_3\,e^{i\boldsymbol{q}_3\cdot\boldsymbol{r}} + A_1^*\,e^{-i\boldsymbol{q}_1\cdot\boldsymbol{r}} + A_2^*\,e^{-i\boldsymbol{q}_2\cdot\boldsymbol{r}} + A_3^*\,e^{-i\boldsymbol{q}_3\cdot\boldsymbol{r}} \ . \tag{9.106}$$

Let's suppose the $\sigma \to -\sigma$ symmetry is broken, leaving us with the Haken model,

$$\frac{\partial\sigma}{\partial t} = \left[\varepsilon - \Big(Q^2 + \boldsymbol{\nabla}^2\Big)^2\right]\sigma + v\sigma^2 - \sigma^3 \ . \tag{9.107}$$

The resulting amplitude equations are then

$$\frac{dA_\ell}{dt} = \varepsilon\,A_\ell + v\,A_{\ell-1}^*\,A_{\ell+1}^* - g\,|A_\ell|^2 A_\ell - \gamma\,g\,\Big(|A_{\ell-1}|^2 + |A_{\ell+1}|^2\Big)\,A_\ell \ , \tag{9.108}$$

Our notation is cyclic in ℓ mod 3, so $A_{\ell+1} = A_1$ when $\ell = 3$, and $A_{\ell-1} = A_3$ when $\ell = 1$.

We now convert to amplitude and phase variables, writing

$$A_\ell = R_\ell\,e^{i\phi_\ell} \ . \tag{9.109}$$

Plugging this into the amplitude equations and taking the real part, we obtain

$$\frac{dR_\ell}{dt} = \varepsilon R_\ell + vR_{\ell-1}R_{\ell+1}\,\cos\phi - gR_\ell^3 - \gamma g\big(R_{\ell-1}^2 + R_{\ell+1}^2\big)R_\ell \tag{9.110}$$

where

$$\phi = \phi_1 + \phi_2 + \phi_3 \ . \tag{9.111}$$

The imaginary part yields the equations

$$\frac{d\phi_\ell}{dt} = -\frac{R_{\ell-1}R_{\ell+1}}{R_\ell}\cdot v\,\sin\phi \ . \tag{9.112}$$

Adding these last three equations, we obtain a single equation for the total phase angle ϕ:

$$\frac{d\phi}{dt} = -\frac{R_1^2\,R_2^2 + R_2^2\,R_3^2 + R_3^2\,R_1^2}{R_1R_2R_3}\cdot v\sin\phi \ . \tag{9.113}$$

Thus, $\sin\phi = 0$ is a fixed point for these dynamics, and in steady state, we have

$$\begin{aligned} v < 0 \quad &\Rightarrow \quad \phi = \pi \\ v > 0 \quad &\Rightarrow \quad \phi = 0 \ . \end{aligned}$$

Thus, $v\,\cos\phi > 0$ in steady state, *i.e.* $v\,\cos\phi = |v|$. Assuming the phase angle has reached its steady state value, the amplitude equations are given by

$$\frac{dR_1}{dt} = \varepsilon R_1 + |v| R_2 R_3 - g R_1^3 - \gamma g \big(R_2^2 + R_3^2\big) R_1 \tag{9.114}$$

$$\frac{dR_2}{dt} = \varepsilon R_2 + |v| R_3 R_1 - g R_2^3 - \gamma g \big(R_3^2 + R_1^2\big) R_2 \tag{9.115}$$

$$\frac{dR_3}{dt} = \varepsilon R_3 + |v| R_1 R_2 - g R_3^3 - \gamma g \big(R_1^2 + R_2^2\big) R_3 \ . \tag{9.116}$$

Subtracting the first equation from the second gives

$$\frac{d}{dt}\big(R_1 - R_2\big) = \Bigg[\varepsilon - |v| R_3 - g\big(R_1^2 + R_1 R_2 + R_2^2\big) - \gamma g R_3^2 + \gamma g R_1 R_2\Bigg]\big(R_1 - R_2\big) \ . \tag{9.117}$$

For sufficiently small ε, we suspect that the term in brackets is negative, indicating that the difference $R_1 - R_2$ tends to zero. As we could have chosen any two distinct values of r, we are motivated to consider the symmetric case $R_1 = R_2 = R_3 = R$. This results in the equation

$$\frac{dR}{dt} = \varepsilon R + |v| R^2 - g\,(1 + 2\gamma) R^3 \ . \tag{9.118}$$

The fixed points $\dot{R} = 0$ occur at $R = 0$ and at $R = R_\pm$, where

$$R_\pm = \frac{|v| \pm \sqrt{v^2 + 4\varepsilon\, g\,(1 + 2\gamma)}}{2g\,(1 + 2\gamma)} \ . \tag{9.119}$$

This solution describes a hexagonal structure.

To assess the stability of these solutions, it is *incorrect* to analyze the stability of eqn. 9.118. Rather, we must go back to the full $N = 4$ system (R_1, R_2, R_3, ϕ). Since the partial derivatives $\partial\dot{R}_\ell/\partial\phi = -v R_{\ell-1} R_{\ell+1} \sin\phi$ all vanish at the fixed point, we only need consider the $N = 3$ system (R_1, R_2, R_3) in eqns. 9.114, 9.115, and 9.116. We must examine the Jacobian

$$\begin{aligned} J_{\ell\ell'} = \frac{\partial\dot{R}_\ell}{\partial R_{\ell'}} &= \begin{pmatrix} a & b & b \\ b & a & b \\ b & b & a \end{pmatrix} \\ &= (a - b)\,\mathbb{I} + 3b\,|\psi\rangle\langle\psi| \ , \end{aligned} \tag{9.120}$$

where $\psi^{\rm t} = \frac{1}{\sqrt{3}}(1,1,1)$. Thus, $|\psi\rangle$ is an eigenvector with eigenvalue $\lambda_+ = a + 2b$, while the two-dimensional subspace orthogonal to $|\psi\rangle$ has the (doubly degenerate) eigenvalue $\lambda_- = a - b$. Thus,

$$\begin{aligned} \lambda_+ &= \varepsilon + 2|v| R - 3(1 + 2\gamma) g R^2 \\ &= -2\varepsilon - |v| R \end{aligned} \tag{9.121}$$

and

$$\begin{aligned}\lambda_- &= \varepsilon - |v|R - 3gR^2 \\ &= \frac{2}{1+2\gamma}\Big((\gamma-1)\,\varepsilon - (2+\gamma)\,|v|R\Big) \ .\end{aligned} \tag{9.122}$$

We have used the fixed point equation

$$g(1+2\gamma)\,R^2 - |v|R - \varepsilon = 0 \tag{9.123}$$

to eliminate the quadratic terms in R in these expressions for $\lambda_\pm$.

Consider the $R = R_+$ fixed point. Plugging the expression for R_+ into the expressions for $\lambda_\pm$, the stability criteria $\lambda_\pm < 0$ can be investigated. that the $R = R_+$ solution is stable for

$$-\frac{v^2}{4g(1+2\gamma)} \ < \ \varepsilon \ < \ \frac{(2+\gamma)\,v^2}{g(\gamma-1)^2} \ . \tag{9.124}$$

The lower limit for ϵ is set by the condition $\lambda_+ < 0$, and the upper limit by $\lambda_- < 0$. The $R = R_0$ solution and all other fixed points (such as when $v\cos\phi < 0$) are unstable. For example, there are so-called mixed modes, where

$$R_1 = \frac{|v|}{g\,(\gamma-1)} \qquad , \qquad R_2 = R_3 = \sqrt{\frac{\varepsilon - gR_1^2}{g\,(\gamma+1)}} \ . \tag{9.125}$$

These are also unstable.

The hexagonal pattern is described by

$$\sigma(\boldsymbol{r},t) = 2R(t)\Big[\cos(Q\,\hat{\boldsymbol{n}}_1\cdot\boldsymbol{r} + \phi_1) + \cos(Q\,\hat{\boldsymbol{n}}_2\cdot\boldsymbol{r} + \phi_2) \pm \cos(Q\,\hat{\boldsymbol{n}}_3\cdot\boldsymbol{r} - \phi_1 - \phi_2)\Big] \ . \tag{9.126}$$

where the upper sign is taken when $v > 0$ ($\phi = 0$), and the lower sign when $v < 0$ ($\phi = \pi$). Let us define the primitive *reciprocal lattice vectors*

$$\boldsymbol{b}_1 = Q\,\hat{\boldsymbol{x}} \qquad , \qquad \boldsymbol{b}_2 = Q\left(\tfrac{1}{2}\hat{\boldsymbol{x}} + \tfrac{\sqrt{3}}{2}\,\hat{\boldsymbol{y}}\right) \ . \tag{9.127}$$

With this definition, we have

$$\begin{aligned} &\boldsymbol{q}_1 = \boldsymbol{b}_1 && \boldsymbol{q}_2 = \boldsymbol{b}_2 - \boldsymbol{b}_1 && \boldsymbol{q}_3 = -\boldsymbol{b}_2 \\ &\boldsymbol{q}_4 = -\boldsymbol{b}_1 && \boldsymbol{q}_5 = \boldsymbol{b}_1 - \boldsymbol{b}_2 && \boldsymbol{q}_6 = \boldsymbol{b}_2 \ . \end{aligned}$$

We also define the primitive *direct lattice vectors*

$$\boldsymbol{a}_1 = \frac{4\pi}{\sqrt{3}\,Q}\left(\tfrac{\sqrt{3}}{2}\hat{\boldsymbol{x}} - \tfrac{1}{2}\hat{\boldsymbol{y}}\right) \qquad , \qquad \boldsymbol{a}_2 = \frac{4\pi}{\sqrt{3}\,Q}\,\hat{\boldsymbol{y}} \ . \tag{9.128}$$

Note that

$$\boldsymbol{a}_\mu\cdot\boldsymbol{b}_\nu = 2\pi\,\delta_{\mu\nu} \ . \tag{9.129}$$

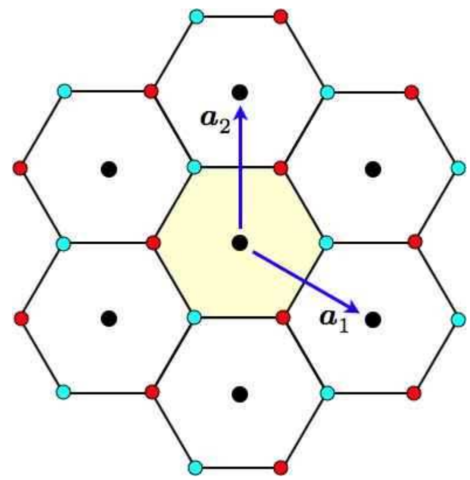

Figure 9.7: Points of high symmetry in the honeycomb lattice. The black dots label the Γ sublattice, the blue dots the K sublattice, and the red dots the K′ sublattice.

We can expand $\boldsymbol{r}$ in the basis of primitive direct lattice vectors as

$$\boldsymbol{r} \equiv \frac{\zeta_1}{2\pi}\,\boldsymbol{a}_1 + \frac{\zeta_2}{2\pi}\,\boldsymbol{a}_2 \ . \tag{9.130}$$

Then

$$\begin{aligned}\sigma(\boldsymbol{r},t) &= 2R(t)\Big[\cos\big(\boldsymbol{b}_1\cdot\boldsymbol{r}+\phi_1\big)+\cos\big((\boldsymbol{b}_2-\boldsymbol{b}_1)\cdot\boldsymbol{r}+\phi_2\big)\pm\cos\big(\boldsymbol{b}_2\cdot\boldsymbol{r}+\phi_1+\phi_2\big)\Big]\\ &= 2R(t)\,\Big[\cos\big(\zeta_1+\phi_1\big)+\cos\big(\zeta_2-\zeta_1+\phi_2\big)\pm\cos\big(\zeta_2+\phi_1+\phi_2\big)\Big]\ .\end{aligned} \tag{9.131}$$

If we now shift the origin of coordinates, defining

$$\tilde{\zeta}_1 = \begin{cases}\zeta_1+\phi_1 & \text{if } v>0\\ \zeta_1+\phi_1+\pi & \text{if } v<0\end{cases} \quad , \qquad \tilde{\zeta}_2 = \zeta_2+\phi_2 \ , \tag{9.132}$$

then we have

$$\sigma(\boldsymbol{r},t) = \pm 2R(t)\Big[\cos\tilde{\zeta}_1+\cos\big(\tilde{\zeta}_2-\tilde{\zeta}_1\big)+\cos\tilde{\zeta}_2\Big]\ , \tag{9.133}$$

where again the upper sign is for $v>0$ and the lower sign for $v<0$. Consider the case $v>0$. At a fixed time t, the function $\sigma(\boldsymbol{r},t)$ achieves its maxima $\sigma_{\text{max}}=6R$ when $\tilde{\zeta}_1=0$ modulo 2π and $\tilde{\zeta}_2=0$ modulo 2π, which is to say when $\boldsymbol{r}$ lies on a triangular lattice of points, which we call the Γ sublattice. This pattern is known as the H0 hexagonal pattern. The minima lie on a honeycomb lattice, which can be described as two interpenetrating triangular lattices. The K sublattice is defined by the set of points equivalent to $\tilde{\zeta}_1=\frac{4\pi}{3}$ and $\tilde{\zeta}_2=\frac{2\pi}{3}$, while the K′ sublattice consists of the points equivalent to $\tilde{\zeta}_1=\frac{2\pi}{3}$ and $\tilde{\zeta}_2=\frac{4\pi}{3}$, again modulo 2π in either component. The sum of the three cosines is then $-\frac{3}{2}$, hence $\sigma_{\text{min}}=-3R$. For $v<0$ the roles of minima and maxima are reversed, and the maxima lie on the vertices of a honeycomb lattice; this is the Hπ structure. See figs. 9.7 and 9.8.

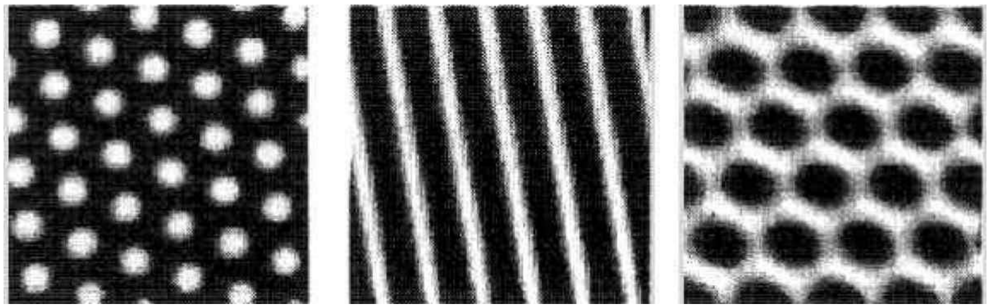

Figure 9.8: Two-dimensional stationary Turing patterns, showing H0 (left), striped (center), and Hπ (right) structures. White areas correspond to local maxima of the concentration field. From A. De Wit, *Adv. Chem. Phys.* **109**, 435 (1999).

Hexagons are not the only stable pattern, however. We can find stripe solutions where $R_1 = R$ and $R_2 = R_3 = 0$. Nontrivial solutions occur for $\varepsilon > 0$, where $R = \sqrt{\varepsilon/g}$, as in the one-dimensional case. The Jacobian at this fixed point is given by

$$J_{\ell\ell'} = \begin{pmatrix} -2\varepsilon & 0 & 0 \\ 0 & (1-\gamma)\,\varepsilon & |v|\sqrt{\frac{\varepsilon}{g}} \\ 0 & |v|\sqrt{\frac{\varepsilon}{g}} & (1-\gamma)\,\varepsilon \end{pmatrix} . \tag{9.134}$$

The eigenvalues are $\lambda_1 = -2\varepsilon$ and $\lambda_{2,3} = (1-\gamma)\,\varepsilon \pm |v|\sqrt{\frac{\varepsilon}{g}}$. Since $\varepsilon > 0$ in order to have a nontrivial solution, $\lambda_1 < 0$ and we can focus on $\lambda_{2,3}$. If $\gamma < 1$ then $\lambda_2 > 0$, so stripes are unstable for $\gamma < 1$. If $\gamma > 1$, we have that $\lambda_3 < 0$, and the condition $\lambda_2 < 0$ requires

$$\varepsilon > \frac{v^2}{g(1-\gamma)^2} \tag{9.135}$$

for the stripes to be stable, along with $\gamma > 1$.

It is convenient to rescale, defining

$$|v| \equiv u \cdot \sqrt{4g(1+2\gamma)} \quad , \quad R \equiv S \cdot \frac{u}{\sqrt{g}} \quad , \quad \varepsilon \equiv \eta \cdot u^2 \, . \tag{9.136}$$

Then we find

$$S_{\text{HEX}}(\eta) = \frac{1 \pm \sqrt{1+\eta}}{\sqrt{1+2\gamma}} \qquad , \qquad S_{\text{STRIPE}}(\eta) = \sqrt{\eta} \, . \tag{9.137}$$

The upper solution for the hexagons is stable for $\eta_- < \eta < \eta_+$, whereas the stripe solution is stable for $\eta > \eta_{\text{s}}$, where

$$\eta_- = -1 \qquad , \qquad \eta_{\text{s}} = \frac{4\,(1+2\gamma)}{(\gamma-1)^2} \qquad , \qquad \eta_+ = \frac{4\,(1+2\gamma)\,(2+\gamma)}{(\gamma-1)^2} \, . \tag{9.138}$$

These results are plotted in fig. 9.9.

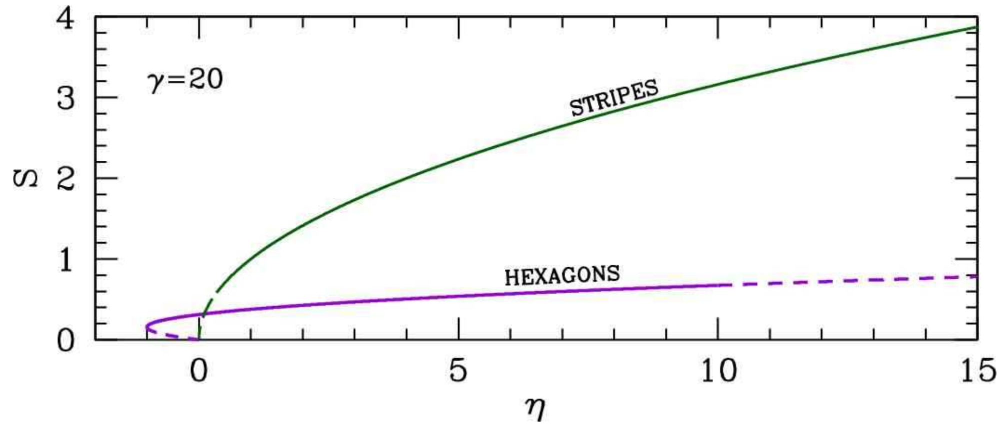

Figure 9.9: Dimensionless amplitude S *versus* dimensionless coupling η for the $M = 3$ system discussed in the text, showing stable (solid) and unstable (dashed) solutions.

9.5.4 $d = 3$

We can extend the previous $d = 2$ results to $d = 3$ dimensions simply by assuming there is no variation in the along z, the coordinate in the third direction. Thus, stripes in $d = 2$ become lamellae in $d = 3$. New structures emerge as well:

$$\begin{aligned} M &= 3 \;:\; 2M = 6 \quad \Rightarrow \text{ simple cubic in reciprocal and real space} \\ M &= 4 \;:\; 2M = 8 \quad \Rightarrow \text{ BCC reciprocal lattice, FCC direct lattice} \\ M &= 6 \;:\; 2M = 12 \quad \Rightarrow \text{ FCC reciprocal lattice, BCC direct lattice .} \end{aligned}$$

For a description of the many patterned structures which can form under these periodicities, see T. K. Callahan and E. Knobloch, *Nonlinearity* **10**, 1179 (1997) and *idem*, *Physica D* **132**, 339 (1999).

9.6 Anisotropy

Many physical systems exhibit intrinsic spatial anisotropies. To see how these might affect patterning, consider a modification of the Brusselator with anisotropic diffusion:

$$u_t = D_{u,\parallel}\, u_{xx} + D_{u,\perp}\, u_{yy} + a - (b+1)\, u + u^2 v \tag{9.139}$$

$$v_t = D_{v,\parallel}\, v_{xx} + D_{v,\perp}\, v_{yy} + b\, u - u^2 v \ . \tag{9.140}$$

The linearized dynamics, from eqn. 9.14, are given by the matrix

$$L(q) = \begin{pmatrix} b - 1 - \widetilde{D}_u(\phi)\, q^2 & a^2 \\ & \\ -b & -a^2 - \widetilde{D}_v(\phi)\, q^2 \end{pmatrix} \ . \tag{9.141}$$

where

$$q_x = q\cos\phi \qquad , \qquad q_y = q\sin\phi \tag{9.142}$$

and

$$\widetilde{D}_u(\phi) = D_{u,\parallel}\,\cos^2\!\phi - D_{u,\perp}\,\sin^2\!\phi \tag{9.143}$$

$$\widetilde{D}_v(\phi) = D_{v,\parallel}\,\cos^2\!\phi - D_{v,\perp}\,\sin^2\!\phi \ . \tag{9.144}$$

We identify the maximally unstable wavevector for the Turing instability $\det(L) = 0$ as before, *i.e.* by minimizing $\det(L)$ with respect to q^2. We then invoke $\det(L) = 0$, which gives us a second equation. From these two equations we obtain the critical value of b at the transition and the critical wavevector at the transition:

$$b_{\rm T}(\phi) = \left(1 + a\sqrt{\frac{\widetilde{D}_u(\phi)}{\widetilde{D}_v(\phi)}}\right)^2 \tag{9.145}$$

$$Q^2(\phi) = \frac{a}{\sqrt{\widetilde{D}_u(\phi)\,\widetilde{D}_v(\phi)}} \ . \tag{9.146}$$

We have thus described a one-parameter family of Turing instabilities, as a function of the angle ϕ. The earliest (smallest $b_{\rm T}(\phi)$ value) of these will preempt the others. Examining $b_{\rm T}(\phi)$, we find

$$\frac{D_{u,\perp}}{D_{u,\parallel}} > \frac{D_{v,\parallel}}{D_{v,\perp}} \quad \Rightarrow \quad \phi = 0 \tag{9.147}$$

$$\frac{D_{u,\perp}}{D_{u,\parallel}} < \frac{D_{v,\parallel}}{D_{v,\perp}} \quad \Rightarrow \quad \phi = \frac{\pi}{2} \ . \tag{9.148}$$

9.7 Phase Diffusion : Eckhaus and Zigzag Instabilities

Starting from the Swift-Hohenberg equation, the dynamics of a striped configuration, with $\sigma(x,y,t) = 2\,\mathsf{Re}\left[A(x,y,t)\,e^{iQx}\right]$ are governed by the Newell-Whitehead-Segel equation,

$$\frac{\partial A}{\partial T} = \mu\,A + \left(\frac{\partial}{\partial X} + \frac{i}{2}\frac{\partial^2}{\partial Y^2}\right)^2 A - |A|^2 A \ , \tag{9.149}$$

where X, Y, and T are scaled 'slow variables', $X = \varepsilon_0 Qx$, $Y = |\varepsilon_0|^{1/2} Qy$, $T = 4Q^2|\varepsilon_0|t$, and $\varepsilon = 4Q^2|\varepsilon_0|\,\mu$, where $|\varepsilon_0| \ll 1$. The amplitude has also been scaled by a factor of $\frac{2}{\sqrt{3}}Q^2|\varepsilon_0|^{1/2}$.

The optimal pattern is given by the constant solution $A = \sqrt{\mu}$, for $\mu > 0$, corresponding to $\sigma(x) = 2\sqrt{\mu}\cos(Qx)$. However, for $\varepsilon > 0$ an entire band of wavevectors is linearly unstable, since $\varepsilon - (Q^2 + \boldsymbol{\nabla}^2)^2$ acting on any plane wave $e^{i\boldsymbol{q}\cdot\boldsymbol{r}}$ will yield a positive growth rate so long as $|q^2 - Q^2| < \sqrt{\varepsilon}$. Thus the Newell-Whitehead-Segel (NWS) equation admits a band of static solutions,

$$A(X,Y) = \sqrt{\mu - k^2}\; e^{ikX} \ , \tag{9.150}$$

for $|k| < \sqrt{\mu}$. We now investigate the stability of these solutions, writing

$$A(X,Y,T) = \Big(\sqrt{\mu - k^2} + \rho(X,Y,T)\Big)\, e^{ikX}\, e^{i\phi(X,Y,T)} \ , \tag{9.151}$$

and linearizing in the amplitude and phase variations ρ and ϕ.

We start by defining $\Lambda = kX + \phi$. Then

$$e^{-i\Lambda}\,\frac{\partial}{\partial X}\,e^{i\Lambda} = \frac{\partial}{\partial X} + ik + i\,\frac{\partial\phi}{\partial X} \tag{9.152}$$

$$e^{-i\Lambda}\,\frac{\partial}{\partial Y}\,e^{i\Lambda} = \frac{\partial}{\partial Y} + i\,\frac{\partial\phi}{\partial Y} \ . \tag{9.153}$$

Thus,

$$e^{-i\Lambda}\Big(\partial_X - \tfrac{i}{2}\partial_Y^2\Big)\,e^{i\Lambda} = ik + \partial_X - \tfrac{i}{2}\partial_Y^2 + i\phi_X + \tfrac{1}{2}\phi_{YY} + \phi_Y\partial_Y + \tfrac{i}{2}\phi_Y^2 \tag{9.154}$$

We need to square the RHS and then apply it to $\big(\sqrt{\mu - k^2} + \rho\big)$, and then keep only terms up to linear order in ρ, ϕ, and their derivatives. Clearly we can drop the last two terms on the RHS above since $\phi_Y\partial_Y$ will be nonzero only when acting on ρ or ϕ, resulting in a nonlinear contribution; the last term ϕ_Y^2 is already nonlinear. Even with the reduction from seven to five terms, squaring is a slightly tedious process, and we skip the intermediate steps. Multiplying the NWS equation on the left by $e^{-i\Lambda}$ and then collecting real and imaginary terms, we obtain the coupled equations

$$\rho_T = -2(\mu - k^2)\,\rho - 2k\sqrt{\mu - k^2}\;\phi_X + \rho_{XX} + k\,\rho_{YY} + \sqrt{\mu - k^2}\;\phi_{XYY} - \tfrac{1}{4}\,\rho_{YYYY} \tag{9.155}$$

$$\phi_T = \frac{2k}{\sqrt{\mu - k^2}}\,\rho_X + \phi_{XX} + k\,\phi_{YY} - \frac{1}{2\sqrt{\mu - k^2}}\,\rho_{XYY} - \tfrac{1}{4}\,\phi_{YYYY} \ . \tag{9.156}$$

The terms on the RHS of these equations are ordered by increasing powers of derivatives. We assume a long wavelength disturbance, meaning we can neglect all but the lowest nontrivial terms. From the RHS of the first equation, we take the first two terms, which yield

$$\rho = -\frac{k}{\sqrt{\mu - k^2}}\,\phi_X \ . \tag{9.157}$$

Note that $\rho \propto \phi_X$, which means that the LHS of the first equation is $\rho_T \propto \phi_{XT}$, which has one more derivative. Substituting this result into the second equation, we obtain

$$\phi_T = \left(\frac{\mu - 3k^2}{\mu - k^2}\right)\phi_{XX} + k\,\phi_{YY} \ . \tag{9.158}$$

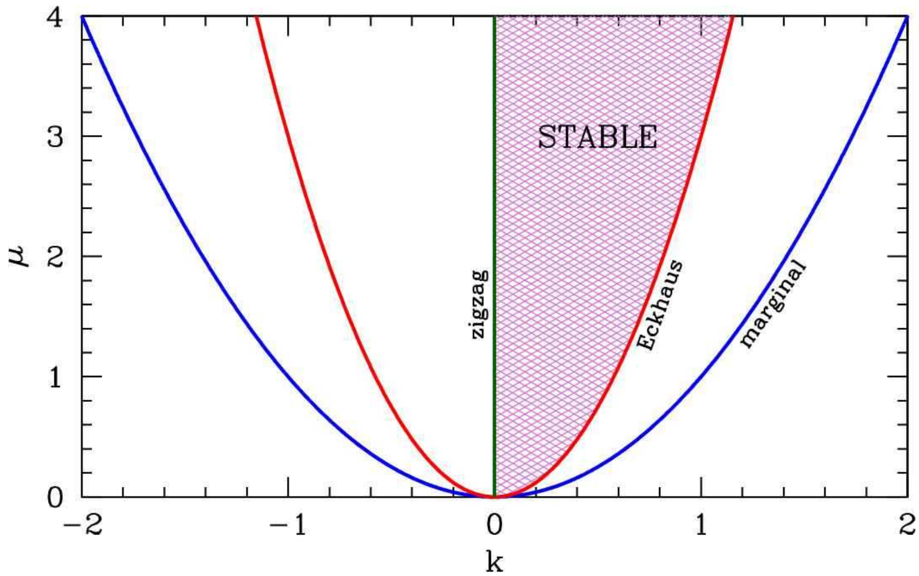

Figure 9.10: Boundary curves for Eckhaus and zigzag instabilities. Structures within the shaded region are stable.

This is an anisotropic diffusion equation. We identify

$$D_{\phi,X} = \frac{\mu - 3k^2}{\mu - k^2} \qquad , \qquad D_{\phi,Y} = k \ . \tag{9.159}$$

An instability occurs when either diffusion constant is negative. Note that $\mu = k^2$ is the so-called *marginal stability boundary* and that no patterned solution exists for $k^2 > \mu$. The condition $D_{\phi,X} < 0$ corresponds to the *Eckhaus instability* and $D_{\phi,Y} < 0$ to the *zigzag instability*. A sketch of the stability boundaries is provided in fig. 9.10.

These are many other patterning instabilities, several of which are discussed in detail in the book by R. Hoyle, listed in chapter 0 of these notes.

Chapter 10

Solitons

Starting in the 19$^{\rm th}$ century, researchers found that certain nonlinear PDEs admit exact solutions in the form of solitary waves, known today as *solitons*. There's a famous story of the Scottish engineer, John Scott Russell, who in 1834 observed a hump-shaped disturbance propagating undiminished down a canal. In 1844, he published this observation[1], writing,

> "I was observing the motion of a boat which was rapidly drawn along a narrow channel by a pair of horses, when the boat suddenly stopped - not so the mass of water in the channel which it had put in motion; it accumulated round the prow of the vessel in a state of violent agitation, then suddenly leaving it behind, rolled forward with great velocity, assuming the form of a large solitary elevation, a rounded, smooth and well-defined heap of water, which continued its course along the channel apparently without change of form or diminution of speed. I followed it on horseback, and overtook it still rolling on at a rate of some eight or nine miles an hour, preserving its original figure some thirty feet long and a foot to a foot and a half in height. Its height gradually diminished, and after a chase of one or two miles I lost it in the windings of the channel. Such, in the month of August 1834, was my first chance interview with that singular and beautiful phenomenon which I have called the Wave of Translation".

Russell was so taken with this phenomenon that subsequent to his discovery he built a thirty foot wave tank in his garden to reproduce the effect, which was precipitated by an initial sudden displacement of water. Russell found empirically that the velocity obeyed $v \simeq \sqrt{g(h+u_{\rm m})}$, where h is the average depth of the water and $u_{\rm m}$ is the maximum vertical displacement of the wave. He also found that a sufficiently large initial displacement would generate two solitons, and, remarkably, that solitons can pass through one another undisturbed. It was not until 1890 that Korteweg and deVries published a theory of shallow water waves and obtained a mathematical description of Russell's soliton.

[1] J. S. Russell, *Report on Waves*, 14$^{\rm th}$ Meeting of the British Association for the Advancement of Science, pp. 311-390.

Nonlinear PDEs which admit soliton solutions typically contain two important classes of terms which feed off each other to produce the effect:

$$\text{DISPERSION} \quad \rightleftharpoons \quad \text{NONLINEARITY}$$

The effect of dispersion is to spread out pulses, while the effect of nonlinearities is, often, to draw in the disturbances. We saw this in the case of front propagation, where dispersion led to spreading and nonlinearity to steepening.

In the 1970's it was realized that several of these nonlinear PDEs yield entire families of exact solutions, and not just isolated solitons. These families contain solutions with arbitrary numbers of solitons of varying speeds and amplitudes, and undergoing mutual collisions. The three most studied systems have been

- The *Korteweg-deVries equation*,

$$u_t + 6uu_x + u_{xxx} = 0 \ . \tag{10.1}$$

  This is a generic equation for 'long waves' in a dispersive, energy-conserving medium, to lowest order in the nonlinearity.

- The *Sine-Gordon equation*,

$$\phi_{tt} - \phi_{xx} + \sin\phi = 0 \ . \tag{10.2}$$

  The name is a play on the Klein-Gordon equation, $\phi_{tt} - \phi_{xx} + \phi = 0$. Note that the Sine-Gordon equation is periodic under $\phi \to \phi + 2\pi$.

- The *nonlinear Schrödinger equation*,

$$i\psi_t \pm \psi_{xx} + 2|\psi|^2\psi = 0 \ . \tag{10.3}$$

  Here, ψ is a complex scalar field. Depending on the sign of the second term, we denote this equation as either NLS(+) or NLS(−), corresponding to the so-called *focusing* (+) and *defocusing* (−) cases.

Each of these three systems supports soliton solutions, including exact N-soliton solutions, and nonlinear periodic waves.

10.1 The Korteweg-deVries Equation

Let h_0 denote the resting depth of water in a one-dimensional channel, and $y(x,t)$ the vertical displacement of the water's surface. Let L be a typical horizontal scale of the wave. When $|y| \ll h_0$, $h_0^2 \ll L^2$, and $v \approx 0$, the evolution of an x-directed wave is described by the KdV equation,

$$y_t + c_0\, y_x + \frac{3c_0}{2h_0}\, yy_x + \tfrac{1}{6} c_0\, h_0^2\; y_{xxx} = 0 \ , \tag{10.4}$$

where $c_0 = \sqrt{g h_0}$. For small amplitude disturbances, only the first two terms are consequential, and we have

$$y_t + c_0\, y_x \approx 0 \ , \tag{10.5}$$

the solution to which is

$$y(x,t) = f(x - c_0 t) \ , \tag{10.6}$$

where $f(\xi)$ is an *arbitrary* shape; the disturbance propagates with velocity c_0. When the dispersion and nonlinearity are included, only a *particular* pulse shape can propagate in an undistorted manner; this is the soliton.

It is convenient to shift to a moving frame of reference:

$$\tilde{x} = x - c_0 t \qquad , \qquad \tilde{t} = t \ , \tag{10.7}$$

hence

$$\frac{\partial}{\partial x} = \frac{\partial}{\partial \tilde{x}} \qquad , \qquad \frac{\partial}{\partial t} = \frac{\partial}{\partial \tilde{t}} - c_0\, \frac{\partial}{\partial \tilde{x}} \ . \tag{10.8}$$

Thus,

$$y_{\tilde{t}} + c_0\, y_{\tilde{x}} + \frac{3c_0}{2h_0}\, y\, y_{\tilde{x}} + \tfrac{1}{6} c_0\, h_0^2\, y_{\tilde{x}\tilde{x}\tilde{x}} = 0 \ . \tag{10.9}$$

Finally, rescaling position, time, and displacement, we arrive at the KdV equation ,

$$u_t + 6 u u_x + u_{xxx} = 0 \ , \tag{10.10}$$

which is a convenient form.

10.1.1 KdV solitons

We seek a solution to the KdV equation of the form $u(x,t) = u(x - Vt)$. Then with $\xi \equiv x - Vt$, we have $\partial_x = \partial_\xi$ and $\partial_t = -V\partial_\xi$ when acting on $u(x,t) = u(\xi)$. Thus, we have

$$-Vu' + 6uu' + u''' = 0 \ . \tag{10.11}$$

Integrating once, we have

$$-Vu + 3u^2 + u'' = A \ , \tag{10.12}$$

where A is a constant. We can integrate once more, obtaining

$$-\tfrac{1}{2} V u^2 + u^3 + \tfrac{1}{2} (u')^2 = Au + B \ , \tag{10.13}$$

where now both A and B are constants. We assume that u and all its derivatives vanish in the limit $\xi \to \pm\infty$, which entails $A = B = 0$. Thus,

$$\frac{du}{d\xi} = \pm\, u\, \sqrt{V - 2u} \ . \tag{10.14}$$

With the substitution

$$u = \tfrac{1}{2} V \operatorname{sech}^2 \theta \ , \tag{10.15}$$

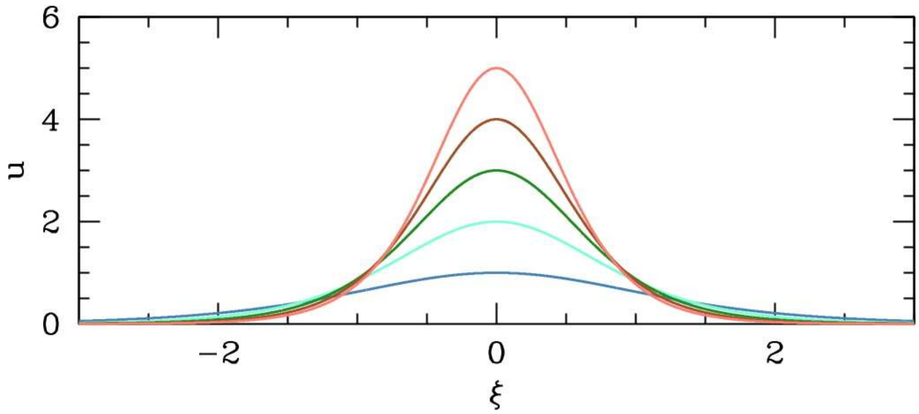

Figure 10.1: Soliton solutions to the KdV equation, with five evenly spaced V values ranging from $V = 2$ (blue) to $V = 10$ (orange). The greater the speed, the narrower the shape.

we find $d\theta = \mp\frac{1}{2}\sqrt{V}\,d\xi$, hence we have the solution

$$u(x,t) = \tfrac{1}{2}V\,\text{sech}^2\Big(\tfrac{\sqrt{V}}{2}\,(x - Vt - \xi_0)\Big) \ . \tag{10.16}$$

Note that the maximum amplitude of the soliton is $u_{\text{max}} = \frac{1}{2}V$, which is proportional to its velocity V. The KdV equation imposes no limitations on V other than $V \geq 0$.

10.1.2 Periodic solutions : soliton trains

If we relax the condition $A = B = 0$, new solutions to the KdV equation arise. Define the cubic

$$\begin{aligned} P(u) &= 2u^3 - Vu^2 - 2Au - 2B \\ &\equiv 2(u-u_1)(u-u_2)(u-u_3) \ , \end{aligned} \tag{10.17}$$

where $u_i = u_i(A,B,V)$. We presume that A, B, and V are such that all three roots $u_{1,2,3}$ are real and nondegenerate. Without further loss of generality, we may then assume $u_1 < u_2 < u_3$. Then

$$\frac{du}{d\xi} = \pm\sqrt{-P(u)} \ . \tag{10.18}$$

Since $P(u) < 0$ for $u_2 < u < u_3$, we conclude $u(\xi)$ must lie within this range. Therefore, we have

$$\begin{aligned} \xi - \xi_0 &= \pm\int\limits_{u_2}^{u} \frac{ds}{\sqrt{-P(s)}} \\ &= \pm\bigg(\frac{2}{u_3 - u_1}\bigg)^{1/2} \int\limits_0^{\phi} \frac{d\theta}{\sqrt{1 - k^2\sin^2\!\theta}} \ , \end{aligned} \tag{10.19}$$

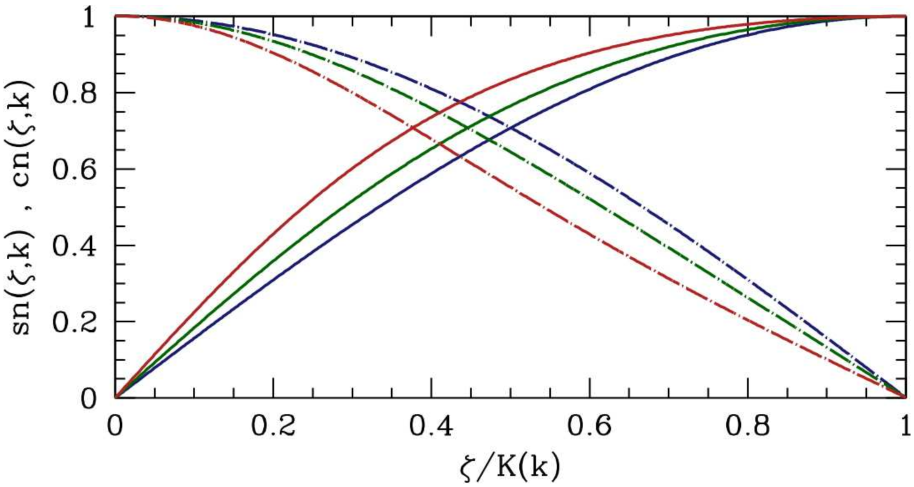

Figure 10.2: The Jacobi elliptic functions $\mathrm{sn}(\zeta,k)$ (solid) and $\mathrm{cn}(\zeta,k)$ (dot-dash) *versus* $\zeta/\mathrm{K}(k)$, for $k=0$ (blue), $k=\frac{1}{\sqrt{2}}$ (green), and $k=0.9$ (red).

where

$$u \equiv u_3 - (u_3 - u_2)\,\sin^2\!\phi \tag{10.20}$$

$$k^2 \equiv \frac{u_3-u_2}{u_3-u_1}\ . \tag{10.21}$$

The solution for $u(\xi)$ is then

$$u(\xi) = u_3 - (u_3-u_2)\,\mathrm{sn}^2(\zeta,k)\ , \tag{10.22}$$

where

$$\zeta = \sqrt{\frac{u_3-u_1}{2}}\,\big(\xi-\xi_0\big) \tag{10.23}$$

and $\mathrm{sn}(\zeta,k)$ is the Jacobi elliptic function.

10.1.3 Interlude: primer on elliptic functions

We assume $0 \le k^2 \le 1$ and we define

$$\zeta(\phi,k) = \int\limits_0^\phi \frac{d\theta}{\sqrt{1-k^2\sin^2\!\theta}}\ . \tag{10.24}$$

The sn and cn functions are defined by the relations

$$\mathrm{sn}(\zeta,k) = \sin\phi \tag{10.25}$$

$$\mathrm{cn}(\zeta,k) = \cos\phi\ . \tag{10.26}$$

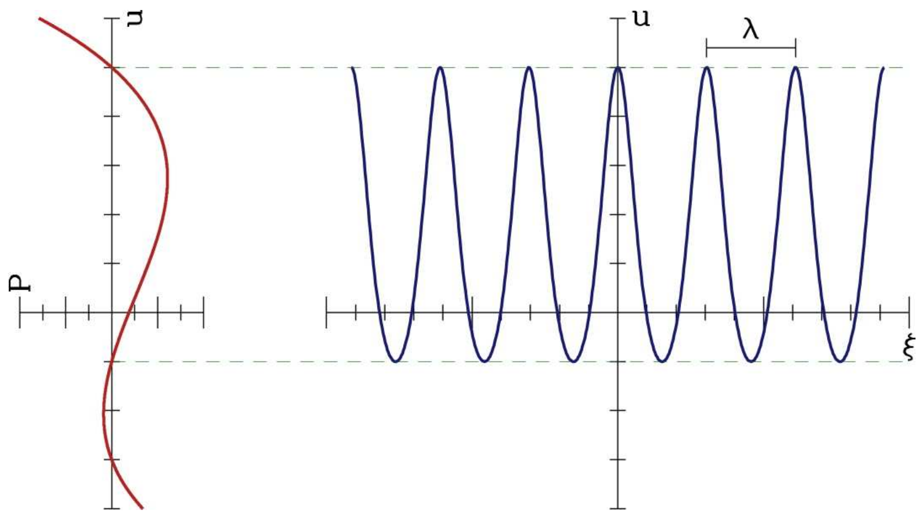

Figure 10.3: The cubic function $P(u)$ (left), and the soliton lattice (right) for the case $u_1 = -1.5$, $u_2 = -0.5$, and $u_3 = 2.5$.

Note that $\text{sn}^2(\zeta,k) + \text{cn}^2(\zeta,k) = 1$. One also defines the function $\text{dn}(\zeta,k)$ from the relation

$$\text{dn}^2(\zeta,k) + k^2\,\text{sn}^2(\zeta,k) = 1 \ . \tag{10.27}$$

When ϕ advances by one period, we have $\Delta\phi = 2\pi$, and therefore $\Delta\zeta = Z$, where

$$Z = \int\limits_0^{2\pi} \frac{d\theta}{\sqrt{1 - k^2 \sin^2\!\theta}} = 4\,\mathbb{K}(k) \ , \tag{10.28}$$

where $\mathbb{K}(k)$ is the complete elliptic integral of the first kind. Thus, $\text{sn}(\zeta + Z, k) = \text{sn}(\zeta, k)$, and similarly for the cn function. In fig. 10.2, we sketch the behavior of the elliptic functions over one quarter of a period. Note that for $k = 0$ we have $\text{sn}(\zeta, 0) = \sin\zeta$ and $\text{cn}(\zeta, 0) = \cos\zeta$.

10.1.4 The soliton lattice

Getting back to our solution in eqn. 10.22, we see that the solution describes a *soliton lattice* with a wavelength

$$\lambda = \frac{\sqrt{8}\,\mathrm{K}(k)}{\sqrt{u_3 - u_1}} \ . \tag{10.29}$$

Note that our definition of $P(u)$ entails

$$V = 2(u_1 + u_2 + u_3) \ . \tag{10.30}$$

There is a simple mechanical analogy which merits illumination. Suppose we define

$$W(u) \equiv u^3 - \tfrac{1}{2} V u^2 - A u \ , \tag{10.31}$$

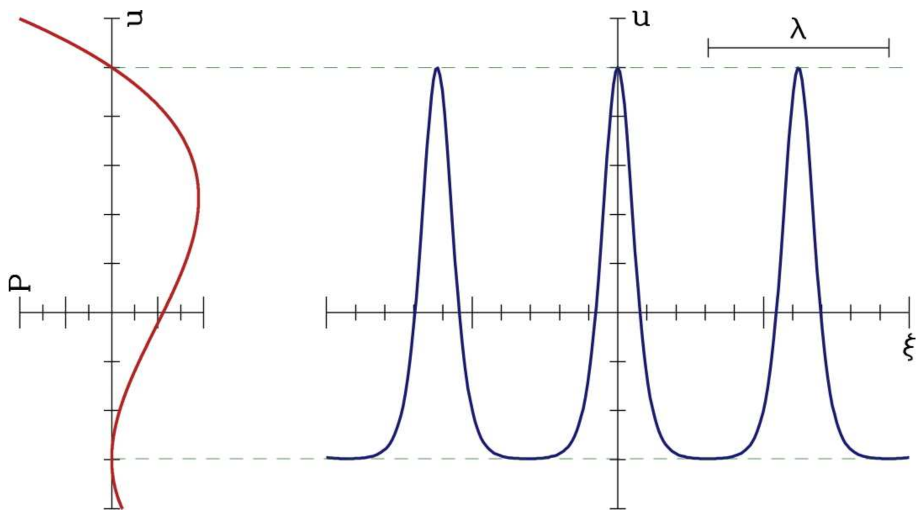

Figure 10.4: The cubic function $P(u)$ (left), and the soliton lattice (right) for the case $u_1 = -1.5$, $u_2 = -1.49$, and $u_3 = 2.50$.

and furthermore $E \equiv B$. Then

$$\frac{1}{2}\bigg(\frac{du}{d\xi}\bigg)^2 + W(u) = E \ , \tag{10.32}$$

which takes the form of a one-dimensional Newtonian mechanical system, if we replace $\xi \to t$ and interpret u_ξ as a velocity. The potential is $W(u)$ and the total energy is E. In terms of the polynomial $P(u)$, we have $P = 2(W - E)$. Accordingly, the 'motion' $u(\xi)$ is flattest for the lowest values of u, near $u = u_2$, which is closest to the local maximum of $W(u)$.

Note that specifying $u_{\rm min} = u_2$, $u_{\rm max} = u_3$, and the velocity V specifies all the parameters. Thus, we have a three parameter family of soliton lattice solutions.

10.1.5 N-soliton solutions to KdV

In 1971, Ryogo Hirota[2] showed that exact N-soliton solutions to the KdV equation exist. Here we discuss the Hirota solution, following the discussion in the book by Whitham.

The KdV equation may be written as

$$u_t + \big\{3u^2 + u_{xx}\big\}_x = 0 \ , \tag{10.33}$$

which is in the form of the one-dimensional continuity equation $u_t + j_x = 0$, where the current is $j = 3u^2 + u_{xx}$. Let us define $u = p_x$. Then our continuity equation reads $p_{tx} + j_x = 0$, which can be integrated to yield $p_t + j = C$, where C is a constant. Demanding that u and

[2]R. Hirota, *Phys. Rev. Lett.* **27**, 1192 (1971).

its derivatives vanish at spatial infinity requires $C = 0$. Hence, we have

$$p_t + 3p_x^2 + p_{xxx} = 0 \ . \tag{10.34}$$

Now consider the nonlinear transformation

$$p = 2\,(\ln F)_x = \frac{2F_x}{F} \ . \tag{10.35}$$

We then have

$$p_t = \frac{2F_{xt}}{F} - \frac{2F_x F_t}{F^2} \tag{10.36}$$

$$p_x = \frac{2F_{xx}}{F} - \frac{2F_x^2}{F^2} \tag{10.37}$$

and

$$p_{xx} = \frac{2F_{xxx}}{F} - \frac{6F_x F_{xx}}{F^2} + \frac{4F_x^3}{F^3} \tag{10.38}$$

$$p_{xxx} = \frac{2F_{xxxx}}{F} - \frac{8F_x F_{xxx}}{F^2} - \frac{6F_x x^2}{F^2} + \frac{24F_x^2 F_{xx}}{F^3} - \frac{12F_x^4}{F^4} \ . \tag{10.39}$$

When we add up the combination $p_t + 3p_x^2 + p_{xxx} = 0$, we find, remarkably, that the terms with F^3 and F^4 in the denominator cancel. We are then left with

$$F\big(F_t + F_{xxx}\big)_x - F_x\big(F_t + F_{xxx}\big) + 3\big(F_{xx}^2 - F_x F_{xxx}\big) = 0 \ . \tag{10.40}$$

This equation has the two-parameter family of solutions

$$F(x,t) = 1 + e^{\phi(x,t)} \ . \tag{10.41}$$

where

$$\phi(x,t) = \alpha\,(x - b - \alpha^2\,t) \ , \tag{10.42}$$

with α and b constants. Note that these solutions are all annihilated by the operator $\partial_t + \partial_x^3$, and also by the last term in eqn. 10.40 because of the homogeneity of the derivatives. Converting back to our original field variable $u(x,t)$, we have that these solutions are single solitons:

$$u = p_x = \frac{2(FF_{xx} - F_x^2)}{F^2} = \frac{\alpha^2\,f}{(1+f)^2} = \tfrac{1}{2}\alpha^2\,\mathrm{sech}^2(\tfrac{1}{2}\phi) \ . \tag{10.43}$$

The velocity for these solutions is $V = \alpha^2$.

If eqn. 10.40 were linear, our job would be done, and we could superpose solutions. We will meet up with such a felicitous situation when we discuss the Cole-Hopf transformation for the one-dimensional Burgers' equation. But for KdV the situation is significantly more difficult. We will write

$$F = 1 + F^{(1)} + F^{(2)} + \ldots + F^{(N)} \ , \tag{10.44}$$

with

$$F^{(1)} = f_1 + f_2 + \ldots + f_N \ , \tag{10.45}$$

where

$$f_j(x,t) = e^{\phi_j(x,t)} \tag{10.46}$$

$$\phi_j(x,t) = \alpha_j \, (x - \alpha_j^2 \, t - b_j) \ . \tag{10.47}$$

We may then derive a hierarchy of equations, the first two levels of which are

$$\big(F_t^{(1)} + F_{xxx}^{(1)}\big)_x = 0 \tag{10.48}$$

$$\big(F_t^{(2)} + F_{xxx}^{(2)}\big)_x = -3\big(F_{xx}^{(1)} F_{xx}^{(1)} - F_x^{(1)} F_{xxx}^{(1)}\big) \ . \tag{10.49}$$

Let's explore the case $N = 2$. The equation for $F^{(2)}$ becomes

$$\big(F_t^{(2)} + F_{xxx}^{(2)}\big)_x = 3 \, \alpha_1 \alpha_2 \, (\alpha_2 - \alpha_1)^2 \, f_1 f_2 \ , \tag{10.50}$$

with solution

$$F^{(2)} = \left(\frac{\alpha_1 - \alpha_2}{\alpha_1 + \alpha_2}\right)^2 f_1 f_2 \ . \tag{10.51}$$

Remarkably, this completes the hierarchy for $N = 2$. Thus,

$$\begin{aligned} F &= 1 + f_1 + f_2 + \left(\frac{\alpha_1 - \alpha_2}{\alpha_1 + \alpha_2}\right)^2 f_1 f_2 \\ &= \det \begin{pmatrix} 1 + f_1 & \frac{2\sqrt{\alpha_1 \alpha_2}}{\alpha_1 + \alpha_2} \, f_1 \\ \frac{2\sqrt{\alpha_1 \alpha_2}}{\alpha_1 + \alpha_2} \, f_2 & 1 + f_2 \end{pmatrix} \ . \end{aligned} \tag{10.52}$$

What Hirota showed, quite amazingly, is that this result generalizes to the N-soliton case,

$$F = \det \mathsf{Q} \ , \tag{10.53}$$

where Q is the symmetric matrix,

$$\mathsf{Q}_{mn} = \delta_{mn} + \frac{2\sqrt{\alpha_m \alpha_n}}{\alpha_m + \alpha_n} \, f_m \, f_n \ . \tag{10.54}$$

Thus, N-soliton solutions to the KdV equation may be written in the form

$$u(x,t) = 2 \, \frac{\partial^2}{\partial x^2} \, \ln \det \mathsf{Q}(x,t) \ . \tag{10.55}$$

Consider the case $N = 2$. Direct, if tedious, calculations lead to the expression

$$u = 2 \, \frac{\alpha_1^2 f_1 + \alpha_2^2 f_2 + 2\,(\alpha_1 - \alpha_2)^2 f_1 f_2 + \left(\frac{\alpha_1 - \alpha_2}{\alpha_1 + \alpha_2}\right)^2 \big(\alpha_1^2 f_1 f_2^2 + \alpha_2^2 f_1^2 f_2\big)}{\left[1 + f_1 + f_2 + \left(\frac{\alpha_1 - \alpha_2}{\alpha_1 + \alpha_2}\right)^2 f_1 f_2\right]^2} \ . \tag{10.56}$$

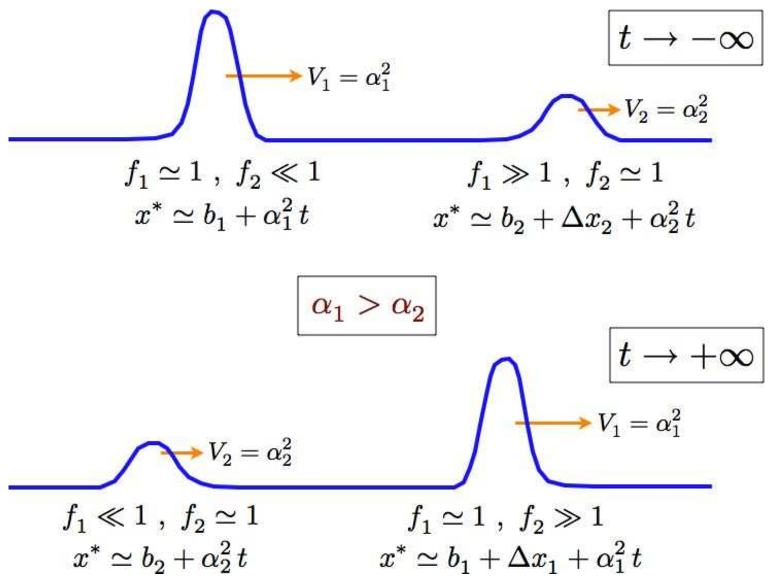

Figure 10.5: Early and late time configuration of the two soliton solution to the KdV equation.

Recall that

$$f_j(x,t) = \exp\big[\alpha_j\,(x_j - \alpha_j^2\, t - b_j)\big] \ . \tag{10.57}$$

Let's consider (x,t) values for which $f_1 \simeq 1$ is neither large nor small, and investigate what happens in the limits $f_2 \ll 1$ and $f_2 \gg 1$. In the former case, we find

$$u \simeq \frac{2\alpha_1^2\, f_1}{(1+f_1)^2} \qquad (f_2 \ll 1) \quad , \tag{10.58}$$

which is identical to the single soliton case of eqn. 10.43. In the opposite limit, we have

$$u \simeq \frac{2\alpha_1^2\, g_1}{(1+g_1)^2} \qquad (f_2 \gg 1) \quad , \tag{10.59}$$

where

$$g_1 = \left(\frac{\alpha_1 - \alpha_2}{\alpha_1 + \alpha_2}\right)^{\!2} f_1 \tag{10.60}$$

But multiplication of f_j by a constant C is equivalent to a translation:

$$C\, f_j(x,t) = f_j(x + \alpha_j^{-1} \ln C\,, t) \equiv f_j(x - \Delta x_j\,, t) \ . \tag{10.61}$$

Thus, depending on whether f_2 is large or small, the solution either acquires or does not acquire a spatial shift Δx_1, where

$$\Delta x_j = \frac{2}{\alpha_j}\, \ln\left|\frac{\alpha_1 + \alpha_2}{\alpha_1 - \alpha_2}\right| \ . \tag{10.62}$$

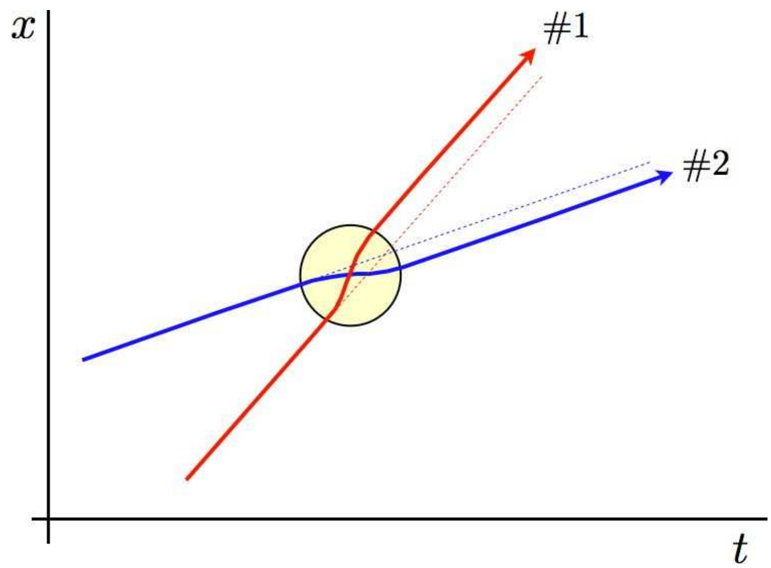

Figure 10.6: Spacetime diagram for the collision of two KdV solitons. The strong, fast soliton (#1) is shifted forward and the weak slow one (#2) is shifted backward. The red and blue lines indicate the centers of the two solitons. The yellow shaded circle is the 'interaction region' where the solution is not simply a sum of the two single soliton waveforms.

The function $f(x,t) = \exp\big[\alpha(x - \alpha^2 t - b)\big]$ is monotonically increasing in x (assuming $\alpha > 0$). Thus, if at fixed t the spatial coordinate x is such that $f \ll 1$, this means that the soliton lies to the right. Conversely, if $f \gg 1$ the soliton lies to the left. Suppose $\alpha_1 > \alpha_2$, in which case soliton #1 is stronger (*i.e.* greater amplitude) and faster than soliton #2. The situation is as depicted in figs. 10.5 and 10.6. Starting at early times, the strong soliton lies to the left of the weak soliton. It moves faster, hence it eventually overtakes the weak soliton. As the strong soliton passes through the weak one, it is shifted *forward*, and the weak soliton is shifted *backward*. It hardly seems fair that the strong fast soliton gets pushed even further ahead at the expense of the weak slow one, but sometimes life is just like that.

10.1.6 Bäcklund transformations

For certain nonlinear PDEs, a given solution may be used as a 'seed' to generate an entire hierarchy of solutions. This is familiar from the case of Riccati equations, which are nonlinear and nonautonomous ODEs, but for PDEs it is even more special. The general form of the Bäcklund transformation (BT) is

$$u_{1,t} = P(u_1\,,\,u_0\,,\,u_{0,t}\,,\,u_{0,x}) \tag{10.63}$$

$$u_{1,x} = Q(u_1\,,\,u_0\,,\,u_{0,t}\,,\,u_{0,x})\ , \tag{10.64}$$

where $u_0(x,t)$ is the known solution.

Figure 10.7: "Wrestling's living legend" Bob Backlund, in a 1983 match, is subjected to a devastating *camel clutch* by the Iron Sheikh. The American Bob Backlund has nothing to do with the Bäcklund transformations discussed in the text, which are named for the 19th century Swedish mathematician Albert Bäcklund. Note that Bob Backlund's manager has thrown in the towel (lower right).

A Bäcklund transformation for the KdV equation was first obtained in 1973[3]. This provided a better understanding of the Hirota hierarchy. To proceed, following the discussion in the book by Scott, we consider the earlier (1968) result of Miura[4], who showed that if $v(x,t)$ satisfies the modified KdV (MKdV) equation[5],

$$v_t - 6v^2 v_x + v_{xxx} = 0 \ , \tag{10.65}$$

then

$$u = -(v^2 + v_x) \tag{10.66}$$

solves KdV:

$$\begin{aligned} u_t + 6uu_x + u_{xxx} &= -(v^2 + v_x)_t + 6(v^2 + v_x)(v^2 + v_x)_x - (v^2 + v_x)_{xxx} \\ &= -\big(2v + \partial_x\big)\big(v_t - 6v^2 v_x + v_{xxx}\big) = 0 \ . \end{aligned} \tag{10.67}$$

From this result, we have that if

$$v_t - 6(v^2 + \lambda)\, v_x + v_{xxx} = 0 \ , \tag{10.68}$$

then

$$u = -(v^2 + v_x + \lambda) \tag{10.69}$$

solves KdV. The MKdV equation, however, is symmetric under $v \to -v$, hence

$$u_0 = -v_x - v^2 - \lambda \tag{10.70}$$

$$u_1 = +v_x - v^2 - \lambda \tag{10.71}$$

[3] H. D. Wahlquist and F. B. Eastabrook, *Phys. Rev. Lett.* **31**, 1386 (1973).

[4] R. M. Miura, *J. Math. Phys.* **9**, 1202 (1968).

[5] Note that the second term in the MKdV equation is proportional to $v^2 v_x$, as opposed to uu_x which appears in KdV.

both solve KdV. Now define $u_0 \equiv -w_{0,x}$ and $u_1 \equiv -w_{1,x}$. Subtracting the above two equations, we find

$$u_0 - u_1 = -2v_x \quad \Rightarrow \quad w_0 - w_1 = 2v \ . \tag{10.72}$$

Adding the equations instead gives

$$\begin{aligned} w_{0,x} + w_{1,x} &= 2(v^2 + \lambda) \\ &= \tfrac{1}{2}(w_0 - w_1)^2 + 2\lambda \ . \end{aligned} \tag{10.73}$$

Substituting for $v = \frac{1}{2}(w_0 - w_1)$ and $v^2 + \lambda - \frac{1}{2}(w_{0,x} + w_{1,x})$ into the MKdV equation, we have

$$(w_0 - w_1)_t - 3\big(w_{0,x}^2 - w_{1,x}^2\big) + (w_0 - w_1)_{xxx} = 0 \ . \tag{10.74}$$

This last equation is a Bäcklund transformation (BT), although in a somewhat nonstandard form, since the RHS of eqn. 10.63, for example, involves only the 'new' solution u_1 and the 'old' solution u_0 and its first derivatives. Our equation here involves third derivatives. However, we can use eqn. 10.73 to express $w_{1,x}$ in terms of w_0, $w_{0,x}$, and w_1.

Starting from the trivial solution $w_0 = 0$, eqn. 10.73 gives

$$w_{1,x} = \tfrac{1}{2} w_1^2 + \lambda \ . \tag{10.75}$$

With the choice $\lambda = -\frac{1}{4}\alpha^2 < 0$, we integrate and obtain

$$w_1(x,t) = -2\alpha \, \tanh\big(\tfrac{1}{2}\alpha x + \varphi(t)\big) \ , \tag{10.76}$$

were $\varphi(t)$ is at this point arbitrary. We fix $\varphi(t)$ by invoking eqn. 10.74, which says

$$w_{1,t} = 3w_{1,x}^2 - w_{1,xxx} = 0 \ . \tag{10.77}$$

Invoking $w_{1,x} = \frac{1}{2}w_1^2 + \lambda$ and differentiating twice to obtain $w_{1,xxx}$, we obtain an expression for the RHS of the above equation. The result is $w_{1,t} + \alpha^2 w_{1,x} = 0$, hence

$$w_1(x,t) = -\alpha \, \tanh\Big[\tfrac{1}{2}\alpha\,(x - \alpha^2 t - b)\Big] \tag{10.78}$$

$$u_1(x,t) = \tfrac{1}{2}\alpha^2 \, \mathrm{sech}^2\Big[\tfrac{1}{2}\alpha\,(x - \alpha^2 t - b)\Big] \ , \tag{10.79}$$

which recapitulates our earlier result. Of course we would like to do better, so let's try to insert this solution into the BT and the turn the crank and see what comes out. This is unfortunately a rather difficult procedure. It becomes tractable if we assume that successive Bäcklund transformations commute, which is the case, but which we certainly have not yet proven. That is, we assume that $w_{12} = w_{21}$, where

$$w_0 \xrightarrow{\lambda_1} w_1 \xrightarrow{\lambda_2} w_{12} \tag{10.80}$$

$$w_0 \xrightarrow{\lambda_2} w_2 \xrightarrow{\lambda_1} w_{21} \ . \tag{10.81}$$

Invoking this result, we find that the Bäcklund transformation gives

$$w_{12} = w_{21} = w_0 - \frac{4(\lambda_1 - \lambda_2)}{w_1 - w_2} \ . \tag{10.82}$$

Successive applications of the BT yield Hirota's multiple soliton solutions:

$$w_0 \xrightarrow{\lambda_1} w_1 \xrightarrow{\lambda_2} w_{12} \xrightarrow{\lambda_3} w_{123} \xrightarrow{\lambda_4} \cdots \ . \tag{10.83}$$

10.2 Sine-Gordon Model

Consider transverse electromagnetic waves propagating down a superconducting transmission line, shown in fig. 10.8. The transmission line is modeled by a set of inductors, capacitors, and Josephson junctions such that for a length dx of the transmission line, the capacitance is $dC = \mathcal{C}\,dx$, the inductance is $dL = \mathcal{L}\,dx$, and the critical current is $dI_0 = \mathcal{I}_0\,dx$. Dividing the differential voltage drop dV and shunt current dI by dx, we obtain

$$\frac{\partial V}{\partial x} = -\mathcal{L}\,\frac{\partial I}{\partial t} \tag{10.84}$$

$$\frac{\partial I}{\partial x} = -\mathcal{C}\,\frac{\partial V}{\partial t} - \mathcal{I}_0\,\sin\phi\ , \tag{10.85}$$

where ϕ is the difference $\phi = \phi_{\text{upper}} - \phi_{\text{lower}}$ in the superconducting phases. The voltage is related to the rate of change of ϕ through the Josephson equation,

$$\frac{\partial\phi}{\partial t} = \frac{2eV}{\hbar}\ , \tag{10.86}$$

and therefore

$$\frac{\partial\phi}{\partial x} = -\frac{2e\mathcal{L}}{\hbar}\,I\ . \tag{10.87}$$

Thus, we arrive at the equation

$$\frac{1}{c^2}\frac{\partial^2\phi}{\partial t^2} - \frac{\partial^2\phi}{\partial x^2} + \frac{1}{\lambda_{\text{J}}^2}\,\sin\phi = 0\ , \tag{10.88}$$

where $c = (\mathcal{L}\,\mathcal{C})^{-1/2}$ is the *Swihart velocity* and $\lambda_{\text{J}} = (\hbar/2e\mathcal{L}\mathcal{I}_0)^{1/2}$ is the *Josephson length*. We may now rescale lengths by λ_{J} and times by λ_{J}/c to arrive at the *sine-Gordon equation*,

$$\phi_{tt} - \phi_{xx} + \sin\phi = 0\ . \tag{10.89}$$

This equation of motion may be derived from the Lagrangian density

$$\mathcal{L} = \tfrac{1}{2}\phi_t^2 - \tfrac{1}{2}\phi_x^2 - U(\phi)\ . \tag{10.90}$$

We then obtain

$$\phi_{tt} - \phi_{xx} = -\frac{\partial U}{\partial\phi}\ , \tag{10.91}$$

and the sine-Gordon equation follows for $U(\phi) = 1 - \cos\phi$.

Assuming $\phi(x,t) = \phi(x - Vt)$ we arrive at $(1 - V^2)\,\phi_{\xi\xi} = U'(\xi)$, and integrating once we obtain

$$\tfrac{1}{2}(1 - V^2)\,\phi_\xi^2 - U(\phi) = E\ . \tag{10.92}$$

This describes a particle of mass $M = 1 - V^2$ moving in the *inverted potential* $-U(\phi)$. Assuming $V^2 < 1$, we may solve for ϕ_ξ:

$$\phi_\xi^2 = \frac{2(E + U(\phi))}{1 - V^2}\ , \tag{10.93}$$

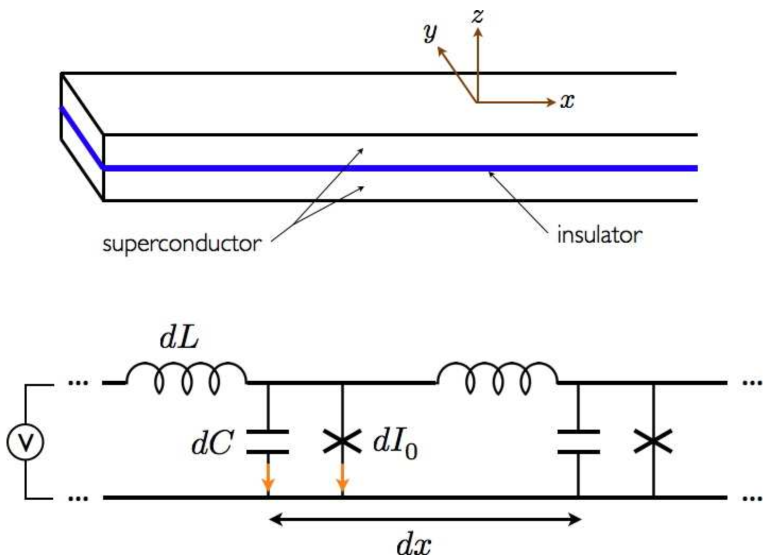

Figure 10.8: A superconducting transmission line is described by a capacitance per unit length $\mathcal{C}$, an inductance per unit length $\mathcal{L}$, and a critical current per unit length $\mathcal{I}_0$. Based on fig. 3.4 of A. Scott, *Nonlinear Science*.

which requires $E \geq -U_{\rm max}$ in order for a solution to exist. For $-U_{\rm max} < E < -U_{\rm min}$, the motion is bounded by turning points. The situation for the sine-Gordon (SG) model is sketched in fig. 10.9. For the SG model, the turning points are at $\phi^*_\pm = \pm\cos^{-1}(E+1)$, with $-2 < E < 0$. We can write

$$\phi^*_\pm = \pi \pm \delta \qquad , \qquad \delta = 2\cos^{-1}\sqrt{-\frac{E}{2}}\ . \tag{10.94}$$

This class of solutions describes periodic waves. From

$$\frac{\sqrt{2}\,d\xi}{\sqrt{1-V^2}} = \frac{d\phi}{\sqrt{E+U(\phi)}}\ , \tag{10.95}$$

we have that the spatial period λ is given by

$$\lambda = \sqrt{2\,(1-V^2)}\int\limits_{\phi^*_-}^{\phi^*_+}\frac{d\phi}{\sqrt{E+U(\phi)}}\ . \tag{10.96}$$

If $E > -U_{\rm min}$, then ϕ_ξ is always of the same sign, and $\phi(\xi)$ is a monotonic function of ξ. If $U(\phi) = U(\phi + 2\pi)$ is periodic, then the solution is a 'soliton lattice' where the spatial period of ϕ mod 2π is

$$\widetilde{\lambda} = \sqrt{\frac{1-V^2}{2}}\int\limits_0^{2\pi}\frac{d\phi}{\sqrt{E+U(\phi)}}\ . \tag{10.97}$$

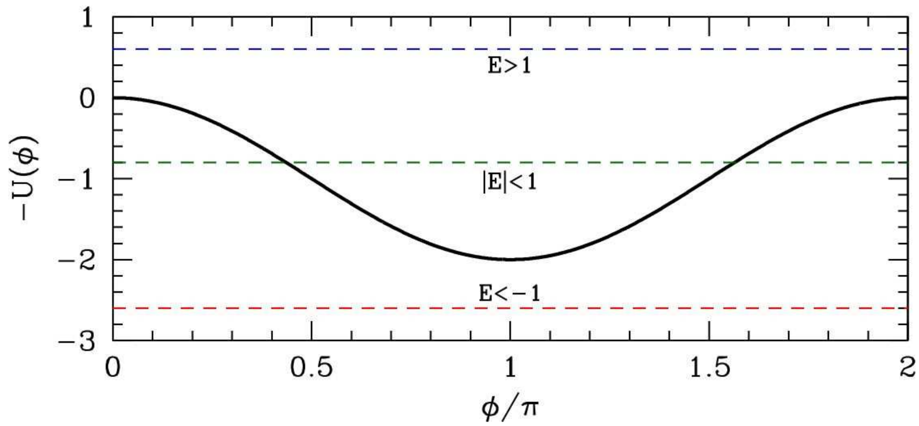

Figure 10.9: The inverted potential $-U(\phi) = \cos\phi - 1$ for the sine-Gordon problem.

For the sine-Gordon model, with $U(\phi) = 1 - \cos\phi$, one finds

$$\lambda = \sqrt{-\frac{\pi\,(1-V^2)}{E(E+2)}} \qquad , \qquad \widetilde{\lambda} = \sqrt{\frac{8\,(1-V^2)}{E+2}}\;\mathbb{K}\Bigg(\sqrt{\frac{2}{E+2}}\Bigg) \ . \tag{10.98}$$

10.2.1 Tachyon solutions

When $V^2 > 1$, we have

$$\tfrac{1}{2}(V^2-1)\,\phi_\xi^2 + U(\phi) = -E \ . \tag{10.99}$$

Such solutions are called *tachyonic*. There are again three possibilities:

- $E > U_{\rm min}$: no solution.
- $-U_{\rm max} < E < -U_{\rm min}$: periodic $\phi(\xi)$ with oscillations about $\phi = 0$.
- $E < -U_{\rm max}$: tachyon lattice with monotonic $\phi(\xi)$.

It turns out that the tachyon solution is unstable.

10.2.2 Hamiltonian formulation

The Hamiltonian density is

$$\mathcal{H} = \pi\,\phi_t - \mathcal{L} \ , \tag{10.100}$$

where

$$\pi = \frac{\partial\mathcal{L}}{\partial\phi_t} = \phi_t \tag{10.101}$$

is the momentum density conjugate to the field ϕ. Then

$$\mathcal{H}(\pi,\phi) = \tfrac{1}{2}\pi^2 + \tfrac{1}{2}\phi_x^2 + U(\phi) \ . \tag{10.102}$$

Note that the total momentum in the field is

$$\begin{aligned} P &= \int\limits_{-\infty}^{\infty} dx\, \pi = \int\limits_{-\infty}^{\infty} dx\, \phi_t = -V \int\limits_{-\infty}^{\infty} dx\, \phi_x \\ &= -V\Big[\phi(\infty) - \phi(-\infty)\Big] = -2\pi n V \ , \end{aligned} \tag{10.103}$$

where $n = \big[\phi(\infty) - \phi(-\infty)\big]/2\pi$ is the *winding number*.

10.2.3 Phonons

The Hamiltonian density for the SG system is minimized when $U(\phi) = 0$ everywhere. The ground states are then classified by an integer $n \in \mathbb{Z}$, where $\phi(x,t) = 2\pi n$ for ground state n. Suppose we linearize the SG equation about one of these ground states, writing

$$\phi(x,t) = 2\pi n + \eta(x,t) \ , \tag{10.104}$$

and retaining only the first order term in η from the nonlinearity. The result is the Klein-Gordon (KG) equation,

$$\eta_{tt} - \eta_{xx} + \eta = 0 \ . \tag{10.105}$$

This is a linear equation, whose solutions may then be superposed. Fourier transforming from (x,t) to (k,ω), we obtain the equation

$$\big(-\omega^2 + k^2 + 1\big)\, \hat{\eta}(k,\omega) = 0 \ , \tag{10.106}$$

which entails the dispersion relation $\omega = \pm\omega(k)$, where

$$\omega(k) = \sqrt{1+k^2} \ . \tag{10.107}$$

Thus, the most general solution to the $(1+1)$-dimensional KG equation is

$$\eta(x,t) = \int\limits_{-\infty}^{\infty} \frac{dk}{2\pi} \left\{ A(k)\, e^{ikx}\, e^{-i\sqrt{1+k^2}\,t} + B(k)\, e^{ikx}\, e^{i\sqrt{1+k^2}\,t} \right\} . \tag{10.108}$$

For the Helmholtz equation $\eta_{tt} - \eta_{xx} = 0$, the dispersion is $\omega(k) = |k|$, and the solution may be written as $\eta(x,t) = f(x-t) + g(x+t)$, which is the sum of arbitrary right-moving and left-moving components. The fact that the Helmholtz equation preserves the shape of the wave is a consequence of the absence of dispersion, *i.e.* the phase velocity $v_{\rm p}(k) = \frac{\omega}{k}$ is the same as the group velocity $v_{\rm g}(k) = \frac{\partial\omega}{\partial k}$. This is not the case for the KG equation, obviously, since

$$v_{\rm p}(k) = \frac{\omega}{k} = \frac{\sqrt{1+k^2}}{k} \qquad , \qquad v_{\rm g}(k) = \frac{\partial\omega}{\partial k} = \frac{k}{\sqrt{1+k^2}} \ , \tag{10.109}$$

hence $v_{\rm p} v_{\rm g} = 1$ for KG.

10.2.4 Mechanical realization

The sine-Gordon model can be realized mechanically by a set of pendula elastically coupled. The kinetic energy T and potential energy U are given by

$$T = \sum_n \tfrac{1}{2} m\ell^2 \dot{\phi}_n^2 \tag{10.110}$$

$$U = \sum_n \Big[\tfrac{1}{2}\kappa\big(\phi_{n+1} - \phi_n\big)^2 + mg\ell\big(1 - \cos\phi_n\big) \Big] \ . \tag{10.111}$$

Here ℓ is the distance from the hinge to the center-of-mass of the pendulum, and κ is the torsional coupling. From the Euler-Lagrange equations we obtain

$$m\ell^2 \ddot{\phi}_n = -\kappa\big(\phi_{n+1} + \phi_{n-1} - 2\phi_n\big) - mg\ell \sin\phi_n \ . \tag{10.112}$$

Let a be the horizontal spacing between the pendula. Then we can write the above equation as

$$\ddot{\phi}_n = \overbrace{\frac{\kappa a^2}{m\ell^2}}^{\equiv c^2} \cdot \overbrace{\frac{1}{a}\Bigg[\bigg(\frac{\phi_{n+1} - \phi_n}{a}\bigg) - \bigg(\frac{\phi_n - \phi_{n-1}}{a}\bigg)\Bigg]}^{\approx \phi_n''} - \frac{g}{\ell}\sin\phi_n \ . \tag{10.113}$$

The continuum limit of these coupled ODEs yields the PDE

$$\frac{1}{c^2}\,\phi_{tt} - \phi_{xx} + \frac{1}{\lambda^2}\,\sin\phi = 0 \ , \tag{10.114}$$

which is the sine-Gordon equation, with $\lambda = (\kappa a^2/mg\ell)^{1/2}$.

10.2.5 Kinks and antikinks

Let us return to eqn. 10.92 and this time set $E = -U_{\rm min}$. With $U(\phi) = 1 - \cos\phi$, we have $U_{\rm min} = 0$, and thus

$$\frac{d\phi}{d\xi} = \pm\frac{2}{\sqrt{1-V^2}}\,\sin\big(\tfrac{1}{2}\phi\big) \ . \tag{10.115}$$

This equation may be integrated:

$$\pm\frac{d\xi}{\sqrt{1-V^2}} = \frac{d\phi}{2\sin\frac{1}{2}\phi} = d\ln\tan\tfrac{1}{4}\phi \ . \tag{10.116}$$

Thus, the solution is

$$\phi(x,t) = 4\tan^{-1}\exp\bigg(\pm\frac{x - Vt - x_0}{\sqrt{1-V^2}}\bigg) \ . \tag{10.117}$$

where ξ_0 is a constant of integration. This describes either a kink (with $d\phi/dx > 0$) or an antikink (with $d\phi/dx < 0$) propagating with velocity V, instantaneously centered at $x = x_0 + Vt$. Unlike the KdV soliton, the amplitude of the SG soliton is independent of its

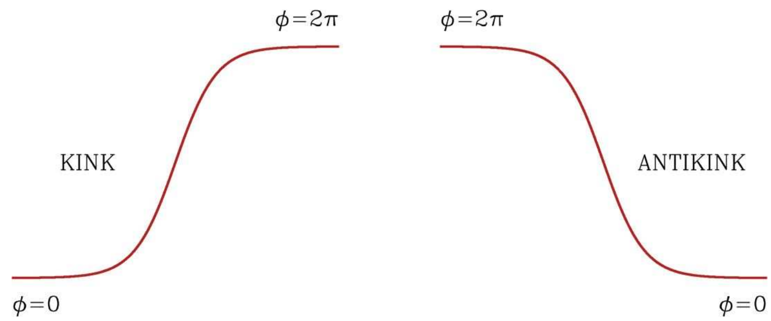

Figure 10.10: Kink and antikink solutions to the sine-Gordon equation.

velocity. The SG soliton is *topological*, interpolating between two symmetry-related vacuum states, namely $\phi = 0$ and $\phi = 2\pi$.

Note that the width of the kink and antikink solutions decreases as V increases. This is a Lorentz contraction, and should have been expected since the SG equation possesses a Lorentz invariance under transformations

$$x = \frac{x' + vt'}{\sqrt{1-v^2}} \tag{10.118}$$

$$t = \frac{t' + vx'}{\sqrt{1-v^2}} \ . \tag{10.119}$$

One then readily finds

$$\partial_t^2 - \partial_x^2 = \partial_{t'}^2 - \partial_{x'}^2 \ . \tag{10.120}$$

The moving soliton solutions may then be obtained by a Lorentz transformation of the stationary solution,

$$\phi(x,t) = 4\tan^{-1} e^{\pm(x-x_0)} \ . \tag{10.121}$$

The field ϕ itself is a Lorentz scalar, and hence does not change in magnitude under a Lorentz transformation.

10.2.6 Bäcklund transformation for the sine-Gordon system

Recall D'Alembert's method of solving the Helmholtz equation, by switching to variables

$$\zeta = \tfrac{1}{2}(x-t) \qquad\qquad \partial_x = \tfrac{1}{2}\partial_\zeta + \tfrac{1}{2}\partial_t \tag{10.122}$$

$$\tau = \tfrac{1}{2}(x+t) \qquad\qquad \partial_t = -\tfrac{1}{2}\partial_\zeta + \tfrac{1}{2}\partial_t \ . \tag{10.123}$$

The D'Alembertian operator then becomes

$$\partial_t^2 - \partial_x^2 = -\,\partial_\zeta\,\partial_\tau \ . \tag{10.124}$$

This transforms the Helmholtz equation $\phi_{tt} - \phi_{xx} = 0$ to $\phi_{\zeta\tau} = 0$, with solutions $\phi(\zeta,\tau) = f(\zeta) + g(\tau)$, with f and g arbitrary functions of their arguments. As applied to the SG equation, we have

$$\phi_{\zeta\tau} = \sin\phi \ . \tag{10.125}$$

Suppose we have a solution ϕ_0 to this equation. Suppose further that ϕ_1 satisfies the pair of equations,

$$\phi_{1,\zeta} = 2\lambda\,\sin\left(\frac{\phi_1+\phi_0}{2}\right) + \phi_{0,\zeta} \tag{10.126}$$

$$\phi_{1,\tau} = \frac{2}{\lambda}\,\sin\left(\frac{\phi_1-\phi_0}{2}\right) - \phi_{0,\tau}\ . \tag{10.127}$$

Thus,

$$\begin{aligned}\phi_{1,\zeta\tau}-\phi_{0,\zeta\tau} &= \lambda\cos\left(\frac{\phi_1+\phi_0}{2}\right)\left(\phi_{1,\tau}-\phi_{0,\tau}\right)\\ &= 2\cos\left(\frac{\phi_1+\phi_0}{2}\right)\,\sin\left(\frac{\phi_1-\phi_0}{2}\right)\\ &= \sin\phi_1-\sin\phi_0\ .\end{aligned} \tag{10.128}$$

Thus, if $\phi_{0,\zeta\tau}=\sin\phi_0$, then $\phi_{1,\zeta\tau}=\sin\phi_1$ as well, and ϕ_1 satisfies the SG equation. Eqns. 10.126 and 10.127 constitute a Bäcklund transformation for the SG system.

Let's give the 'Bäcklund crank' one turn, starting with the trivial solution $\phi_0=0$. We then have

$$\phi_{1,\zeta} = 2\lambda\,\sin\tfrac{1}{2}\phi_1 \tag{10.129}$$

$$\phi_{1,\tau} = 2\lambda^{-1}\sin\tfrac{1}{2}\phi_1\ . \tag{10.130}$$

The solution to these equations is easily found by direct integration:

$$\phi(\zeta,\tau) = 4\tan^{-1} e^{\lambda\zeta}\,e^{\tau/\lambda}\ . \tag{10.131}$$

In terms of our original independent variables (x,t), we have

$$\lambda\zeta+\lambda^{-1}\tau = \tfrac{1}{2}\big(\lambda+\lambda^{-1}\big)\,x-\tfrac{1}{2}\big(\lambda-\lambda^{-1}\big)\,t = \pm\,\frac{x-vt}{\sqrt{1-v^2}}\ , \tag{10.132}$$

where

$$v\equiv\frac{\lambda^2-1}{\lambda^2+1}\qquad\Longleftrightarrow\qquad\lambda=\pm\left(\frac{1+v}{1-v}\right)^{1/2}\ . \tag{10.133}$$

Thus, we generate the kink/antikink solution

$$\phi_1(x,t) = 4\tan^{-1}\exp\left(\pm\,\frac{x-vt}{\sqrt{1-v^2}}\right)\ . \tag{10.134}$$

As was the case with the KdV system, successive Bäcklund transformations commute. Thus,

$$\phi_0 \xrightarrow{\lambda_1} \phi_1 \xrightarrow{\lambda_2} \phi_{12} \tag{10.135}$$

$$\phi_0 \xrightarrow{\lambda_2} \phi_2 \xrightarrow{\lambda_1} \phi_{21}\ , \tag{10.136}$$

with $\phi_{12} = \phi_{21}$. This allows one to eliminate the derivatives and write

$$\tan\left(\frac{\phi_{12} - \phi_0}{4}\right) = \left(\frac{\lambda_1 + \lambda_2}{\lambda_1 - \lambda_2}\right) \tan\left(\frac{\phi_2 - \phi_1}{4}\right) . \tag{10.137}$$

We can now create new solutions from individual kink pairs (KK), or kink-antikink pairs ($\mathrm{K}\overline{\mathrm{K}}$). For the KK system, taking $v_1 = v_2 = v$ yields

$$\phi_{\mathrm{KK}}(x,t) = 4 \tan^{-1}\left(\frac{v \sinh(\gamma x)}{\cosh(\gamma v t)}\right) , \tag{10.138}$$

where γ is the Lorentz factor,

$$\gamma = \frac{1}{\sqrt{1 - v^2}} . \tag{10.139}$$

Note that $\phi_{\mathrm{KK}}(\pm\infty, t) = \pm 2\pi$ and $\phi_{\mathrm{KK}}(0,t) = 0$, so there is a phase increase of 2π on each of the negative and positive half-lines for x, and an overall phase change of $+4\pi$. For the $\mathrm{K}\overline{\mathrm{K}}$ system, if we take $v_1 = -v_2 = v$, we obtain the solution

$$\phi_{\mathrm{K}\overline{\mathrm{K}}}(x,t) = 4 \tan^{-1}\left(\frac{\sinh(\gamma v t)}{v \cosh(\gamma x)}\right) . \tag{10.140}$$

In this case, analytically continuing to imaginary v with

$$v = \frac{i\omega}{\sqrt{1 - \omega^2}} \qquad \Longrightarrow \qquad \gamma = \sqrt{1 - \omega^2} \tag{10.141}$$

yields the *stationary breather* solution,

$$\phi_{\mathrm{B}}(x,t) = 4 \tan^{-1}\left(\frac{\sqrt{1 - \omega^2}\, \sin(\omega t)}{\omega \cosh(\sqrt{1 - \omega^2}\, x)}\right) . \tag{10.142}$$

The breather is a localized solution to the SG system which oscillates in time. By applying a Lorentz transformation of the spacetime coordinates, one can generate a moving breather solution as well.

Please note, in contrast to the individual kink/antikink solutions, the solutions ϕ_{KK}, $\phi_{\mathrm{K}\overline{\mathrm{K}}}$, and ϕ_{B} are not functions of a single variable $\xi = x - Vt$. Indeed, a given multisoliton solution may involve components moving at several different velocities. Therefore the total momentum P in the field is no longer given by the simple expression $P = V\big(\phi(-\infty) - \phi(+\infty)\big)$. However, in cases where the multikink solutions evolve into well-separated solitions, as happens when the individual kink velocities are distinct, the situation simplifies, as we may consider each isolated soliton as linearly independent. We then have

$$P = -2\pi \sum_i n_i \, V_i \ , \tag{10.143}$$

where $n_i = +1$ for kinks and $n_i = -1$ for antikinks.

10.3 Nonlinear Schrödinger Equation

The Nonlinear Schrödinger (NLS) equation arises in several physical contexts. One is the Gross-Pitaevskii action for an interacting bosonic field,

$$S[\psi,\psi^*]=\int\!dt\!\int\!d^d\!x\bigg\{i\psi^*\,\frac{\partial\psi}{\partial t}-\frac{\hbar^2}{2m}\,\boldsymbol{\nabla}\psi^*\!\cdot\!\boldsymbol{\nabla}\psi-U\big(\psi^*\psi\big)+\mu\,\psi^*\psi\bigg\}\ , \tag{10.144}$$

where $\psi(\boldsymbol{x},t)$ is a complex scalar field. The local interaction $U\big(|\psi|^2\big)$ is taken to be quartic,

$$U\big(|\psi|^2\big)=\tfrac{1}{2}g\,|\psi|^4\ . \tag{10.145}$$

Note that

$$U\big(|\psi|^2\big)-\mu\,|\psi|^2=\tfrac{1}{2}g\bigg(|\psi|^2-\frac{\mu}{g}\bigg)^2-\frac{\mu^2}{2g}\ . \tag{10.146}$$

Extremizing the action with respect to ψ^* yields the equation

$$\frac{\delta S}{\delta\psi^*}=0=i\,\frac{\partial\psi}{\partial t}+\frac{\hbar^2}{2m}\,\boldsymbol{\nabla}^2\psi-U'\big(\psi^*\psi\big)\,\psi+\mu\,\psi\ . \tag{10.147}$$

Extremization with respect to ψ yields the complex conjugate equation. In $d=1$, we have

$$i\psi_t=-\frac{\hbar^2}{2m}\,\psi_{xx}+U'\big(\psi^*\psi\big)\,\psi-\mu\,\psi\ . \tag{10.148}$$

We can absorb the chemical potential by making a time-dependent gauge transformation

$$\psi(x,t)\longrightarrow e^{i\mu t}\,\psi(x,t)\ . \tag{10.149}$$

Further rescalings of the field and independent variables yield the generic form

$$i\psi_t\pm\psi_{xx}+2\,|\psi|^2\,\psi=0\ , \tag{10.150}$$

where the $+$ sign pertains for the case $g<0$ (attactive interaction), and the $-$ sign for the case $g>0$ (repulsive interaction). These cases are known as *focusing*, or NLS($+$), and *defocusing*, or NLS($-$), respectively.

10.3.1 Amplitude-phase representation

We can decompose the complex scalar ψ into its amplitude and phase:

$$\psi=A\,e^{i\phi}\ . \tag{10.151}$$

We then find

$$\psi_t=\big(A_t+iA\phi_t\big)\,e^{i\phi} \tag{10.152}$$

$$\psi_x=\big(A_x+iA\phi_x\big)\,e^{i\phi} \tag{10.153}$$

$$\psi_{xx}=\big(A_{xx}-A\phi_x^2+2iA_x\phi_x+iA\phi_{xx}\big)\,e^{i\phi}\ . \tag{10.154}$$

Multiplying the NLS($\pm$) equations by $e^{-i\phi}$ and taking real and imaginary parts, we obtain the coupled nonlinear PDEs,

$$-A\phi_t \pm \big(A_{xx} - A\phi_x^2\big) + 2A^3 = 0 \tag{10.155}$$

$$A_t \pm \big(2A_x\phi_x + A\phi_{xx}\big) = 0 \ . \tag{10.156}$$

Note that the second of these equations may be written in the form of a continuity equation,

$$\rho_t + j_x = 0 \ , \tag{10.157}$$

where

$$\rho = A^2 \tag{10.158}$$

$$j = \pm\, 2A^2\phi_x \ . \tag{10.159}$$

10.3.2 Phonons

One class of solutions to NLS($\pm$) is the spatially uniform case

$$\psi_0(x,t) = A_0\, e^{2iA_0^2\, t} \ , \tag{10.160}$$

with $A = A_0$ and $\phi = 2A_0^2\, t$. Let's linearize about these solutions, writing

$$A(x,t) = A_0 + \delta A(x,t) \tag{10.161}$$

$$\phi(x,t) = 2A_0^2\, t + \delta\phi(x,t) \ . \tag{10.162}$$

Our coupled PDEs then yield

$$4A_0^2\,\delta A \pm \delta A_{xx} - A_0\,\delta\phi_t = 0 \tag{10.163}$$

$$\delta A_t \pm A_0\,\delta\phi_{xx} = 0 \ . \tag{10.164}$$

Fourier transforming, we obtain

$$\begin{pmatrix} 4A_0^2 \mp k^2 & iA_0\,\omega \\ -i\omega & \mp A_0 k^2 \end{pmatrix} \begin{pmatrix} \delta\hat{A}(k,\omega) \\ \delta\hat{\phi}(k,\omega) \end{pmatrix} = 0 \ . \tag{10.165}$$

Setting the determinant to zero, we obtain

$$\omega^2 = \mp 4A_0^2\, k^2 + k^4 \ . \tag{10.166}$$

For NLS($-$), we see that $\omega^2 \geq 0$ for all k, meaning that the initial solution $\psi_0(x,t)$ is stable. For NLS($+$), however, we see that wavevectors $k \in \big[-2A_0\,,\, 2A_0\big]$ are *unstable*. This is known as the *Benjamin-Feir instability*.

10.3.3 Soliton solutions for NLS(+)

Let's consider moving soliton solutions for NLS(+). We try a two-parameter solution of the form

$$
\begin{aligned}
A(x,t) &= A(x-ut) && (10.167)\\
\phi(x,t) &= \phi(x-vt)\ . && (10.168)
\end{aligned}
$$

This results in the coupled ODEs

$$
\begin{aligned}
A_{xx} - A\,\phi_x^2 + vA\,\phi_x + 2A^3 &= 0 && (10.169)\\
A\,\phi_{xx} + 2A_x\phi_x - uA_x &= 0\ . && (10.170)
\end{aligned}
$$

Multiplying the second equation by $2A$ yields

$$
\Big((2\phi_x - u)A^2\Big)_x = 0 \quad \Longrightarrow \quad \phi_x = \tfrac{1}{2}u + \frac{P}{2A^2}\ , \tag{10.171}
$$

where P is a constant of integration. Inserting this in the first equation results in

$$
A_{xx} + 2A^3 + \tfrac{1}{4}(2uv - u^2)A + \tfrac{1}{2}(v-u)PA^{-1} - \tfrac{1}{4}PA^{-3} = 0\ . \tag{10.172}
$$

We may write this as

$$
A_{xx} + W'(A) = 0\ , \tag{10.173}
$$

where

$$
W(A) = \tfrac{1}{2}A^4 + \tfrac{1}{8}(2uv - u^2)A^2 + \tfrac{1}{2}(v-u)P\ln A + \tfrac{1}{8}PA^{-2} \tag{10.174}
$$

plays the role of a potential. We can integrate eqn. 10.173 to yield

$$
\tfrac{1}{2}A_x^2 + W(A) = E\ , \tag{10.175}
$$

where E is second constant of integration. This may be analyzed as a one-dimensional mechanics problem.

The simplest case to consider is $P=0$, in which case

$$
W(A) = \tfrac{1}{2}\big(A^2 + \tfrac{1}{2}uv - \tfrac{1}{4}u^2\big)A^2\ . \tag{10.176}
$$

If $u^2 < 2uv$, then $W(A)$ is everywhere nonnegative and convex, with a single global minimum at $A=0$, where $W(0)=0$. The analog mechanics problem tells us that A will oscillate between $A=0$ and $A=A^*$, where $W(A^*)=E>0$. There are no solutions with $E<0$. If $u^2 > 2uv$, then $W(A)$ has a double well shape[6]. If $E>0$ then the oscillations are still between $A=0$ and $A=A^*$, but if $E<0$ then there are two positive solutions to $W(A)=E$. In this latter case, we may write

$$
F(A) \equiv 2\big[E - W(A)\big] = \big(A^2 - A_0^2\big)\big(A_1^2 - A^2\big)\ , \tag{10.177}
$$

[6]Although we have considered $A>0$ to be an amplitude, there is nothing wrong with allowing $A<0$. When $A(t)$ crosses $A=0$, the phase $\phi(t)$ jumps by $\pm\pi$.

where $A_0 < A_1$ and

$$E = -\tfrac{1}{2} A_0^2 \, A_1^2 \tag{10.178}$$

$$\tfrac{1}{4} u^2 - \tfrac{1}{2} uv = A_0^2 + A_1^2 \; . \tag{10.179}$$

The amplitude oscillations are now between $A = A_0^*$ and $A = A_1^*$. The solution is given in terms of Jacobi elliptic functions:

$$\psi(x,t) = A_1 \, \exp\left[\tfrac{i}{2} u \, (x - vt)\right] \mathrm{dn}\big(A_1 (x - ut - \xi_0) \, , \, k\big) \; , \tag{10.180}$$

where

$$k^2 = 1 - \frac{A_0^2}{A_1^2} \; . \tag{10.181}$$

The simplest case is $E = 0$, for which $A_0 = 0$. We then obtain

$$\psi(x,t) = A^* \, \exp\left[\tfrac{i}{2} u \, (x - vt)\right] \mathrm{sech}\big(A^* (x - ut - \xi_0)\big) \; , \tag{10.182}$$

where $4 A^{*2} = u^2 - 2uv$. When $v = 0$ we obtain the stationary breather solution, for which the entire function $\psi(x,t)$ oscillates uniformly.

10.3.4 Dark solitons for NLS(−)

The small oscillations of NLS(−) are stable, as we found in our phonon calculation. It is therefore perhaps surprising to note that this system also supports solitons. We write

$$\psi(x,t) = \sqrt{\rho_0} \, e^{2i\rho_0 t} \, Z(x,t) \; , \tag{10.183}$$

which leads to

$$i Z_t = Z_{xx} + 2\rho_0 \big(1 - |Z|^2\big) Z \; . \tag{10.184}$$

We then write $Z = X + iY$, yielding

$$X_t = Y_{xx} + 2\rho_0 \big(1 - X^2 - Y^2\big) Y \tag{10.185}$$

$$-Y_t = X_{xx} + 2\rho_0 \big(1 - X^2 - Y^2\big) X \; . \tag{10.186}$$

We try $Y = Y_0$, a constant, and set $X(x,t) = X(x - Vt)$. Then

$$-V X_\xi = 2\rho_0 Y_0 \big(1 - Y_0^2 - X^2\big) \tag{10.187}$$

$$0 = X_{\xi\xi} + 2\rho_0 \big(1 - Y_0^2 - X^2\big) X \tag{10.188}$$

Thus,

$$X_\xi = -\frac{2\rho_0 Y_0}{V} \big(1 - Y_0^2 - X^2\big) \tag{10.189}$$

from which it follows that

$$\begin{aligned} X_{\xi\xi} &= \frac{4\rho_0 Y_0}{V}\, X X_\xi \\ &= -\frac{8\rho_0^2 Y_0^2}{V}\big(1 - Y_0^2 - X^2\big)X = \frac{4\rho_0 Y_0^2}{V^2}\, X_{\xi\xi} \ . \end{aligned} \tag{10.190}$$

Thus, in order to have a solution, we must have

$$V = \pm 2\sqrt{\rho_0}\, Y_0 \ . \tag{10.191}$$

We now write $\xi = x - Vt$, in which case

$$\pm\sqrt{\rho_0}\, d\xi = \frac{dX}{1 - Y_0^2 - X^2} \ . \tag{10.192}$$

From this point, the derivation is elementary. One writes $X = \sqrt{1 - Y_0^2}\, \widetilde{X}$, and integrates to obtain

$$\widetilde{X}(\xi) = \mp \tanh\Big(\sqrt{1 - Y_0^2}\ \sqrt{\rho_0}\,(\xi - \xi_0)\Big) \ . \tag{10.193}$$

We simplify the notation by writing $Y_0 = \sin\beta$. Then

$$\psi(x,t) = \sqrt{\rho_0}\, e^{i\alpha}\, e^{2i\rho_0 t}\bigg[\cos\beta\ \tanh\Big(\sqrt{\rho_0}\ \cos\big(\beta(x - Vt - \xi_0)\big)\Big) - i\sin\beta\bigg] \ , \tag{10.194}$$

where α is a constant. The density $\rho = |\psi|^2$ is then given by

$$\rho(x,t) = \rho_0\bigg[1 - \cos^2\!\beta\ \mathrm{sech}^2\Big(\sqrt{\rho_0}\ \cos\big(\beta(x - Vt - \xi_0)\big)\Big)\bigg] \ . \tag{10.195}$$

This is called a *dark soliton* because the density $\rho(x,t)$ is minimized at the center of the soliton, where $\rho = \rho_0 \sin^2\!\beta$, which is smaller than the asymptotic $|x| \to \infty$ value of $\rho(\pm\infty, t) = \rho_0$.

Chapter 11

Shock Waves

Here we shall follow closely the pellucid discussion in chapter 2 of the book by G. Whitham, beginning with the simplest possible PDE,

$$\rho_t + c_0\, \rho_x = 0\ . \tag{11.1}$$

The solution to this equation is an arbitrary right-moving wave (assuming $c_0 > 0$), with profile

$$\rho(x,t) = f(x - c_0 t)\ , \tag{11.2}$$

where the initial conditions on eqn. 11.1 are $\rho(x, t = 0) = f(x)$. Nothing to see here, so move along.

11.1 Nonlinear Continuity Equation

The simplest nonlinear PDE is a generalization of eqn. 11.1,

$$\rho_t + c(\rho)\, \rho_x = 0\ . \tag{11.3}$$

This equation arises in a number of contexts. One example comes from the theory of vehicular traffic flow along a single lane roadway. Starting from the continuity equation,

$$\rho_t + j_x = 0\ , \tag{11.4}$$

one posits a constitutive relation $j = j(\rho)$, in which case $c(\rho) = j'(\rho)$. If the individual vehicles move with a velocity $v = v(\rho)$, then

$$j(\rho) = \rho\, v(\rho) \quad \Rightarrow \quad c(\rho) = v(\rho) + \rho\, v'(\rho)\ . \tag{11.5}$$

It is natural to assume a form $v(\rho) = c_0\,(1 - a\rho)$, so that at low densities one has $v \approx c_0$, with $v(\rho)$ decreasing monotonically to $v = 0$ at a critical density $\rho = a^{-1}$, presumably corresponding to bumper-to-bumper traffic. The current $j(\rho)$ then takes the form of an inverted parabola. Note the difference between the individual vehicle velocity $v(\rho)$ and what turns out to be the group velocity of a traffic wave, $c(\rho)$. For $v(\rho) = c_0\,(1 - a\rho)$, one has $c(\rho) = c_0\,(1 - 2a\rho)$, which is *negative* for $\rho \in \big[\frac{1}{2}a^{-1}, a^{-1}\big]$. For vehicular traffic, we have $c'(\rho) = j''(\rho) < 0$ but in general $j(\rho)$ and thus $c(\rho)$ can be taken to be arbitrary.

Another example comes from the study of chromatography, which refers to the spatial separation of components in a mixture which is forced to flow through an immobile absorbing 'bed'. Let $\rho(x,t)$ denote the density of the desired component in the fluid phase and $n(x,t)$ be its density in the solid phase. Then continuity requires

$$n_t + \rho_t + V\rho_x = 0 \ , \tag{11.6}$$

where V is the velocity of the flow, which is assumed constant. The net rate at which the component is deposited from the fluid onto the solid is given by an equation of the form

$$n_t = F(n,\rho) \ . \tag{11.7}$$

In equilibrium, we then have $F(n,\rho) = 0$, which may in principle be inverted to yield $n = n_{\rm eq}(\rho)$. If we assume that the local deposition processes run to equilibrium on fast time scales, then we may substitute $n(x,t) \approx n_{\rm eq}\big(\rho(x,t)\big)$ into eqn. 11.6 and obtain

$$\rho_t + c(\rho)\,\rho_x = 0 \quad , \quad c(\rho) = \frac{V}{1 + n'_{\rm eq}(\rho)} \ . \tag{11.8}$$

We solve eqn. 11.3 using the *method of characteristics*. Suppose we have the solution $\rho = \rho(x,t)$. Consider then the family of curves obeying the ODE

$$\frac{dx}{dt} = c\big(\rho(x,t)\big) \ . \tag{11.9}$$

This is a family of curves, rather than a single curve, because it is parameterized by the initial condition $x(0) \equiv \zeta$. Now along any one of these curves we must have

$$\frac{d\rho}{dt} = \frac{\partial\rho}{\partial t} + \frac{\partial\rho}{\partial x}\,\frac{dx}{dt} = \frac{\partial\rho}{\partial t} + c(\rho)\,\frac{\partial\rho}{\partial x} = 0 \ . \tag{11.10}$$

Thus, $\rho(x,t)$ is a constant along each of these curves, which are called *characteristics*. For eqn. 11.3, the family of characteristics is a set of straight lines[1],

$$x_\zeta(t) = \zeta + c(\rho)\,t \ . \tag{11.11}$$

The initial conditions for the function $\rho(x,t)$ are

$$\rho(x=\zeta, t=0) = f(\zeta) \ , \tag{11.12}$$

[1]The existence of straight line characteristics is a special feature of the equation $\rho_t + c(\rho)\,\rho_x = 0$. For more general hyperbolic first order PDEs to which the method of characteristics may be applied, the characteristics are curves. See the discussion in the Appendix.

where $f(\zeta)$ is arbitrary. Thus, in the (x,t) plane, if the characteristic curve $x(t)$ intersects the line $t=0$ at $x=\zeta$, then its slope is constant and equal to $c\big(f(\zeta)\big)$. We then define

$$g(\zeta) \equiv c\big(f(\zeta)\big) \ . \tag{11.13}$$

This is a known function, computed from $c(\rho)$ and $f(\zeta)=\rho(x=\zeta,t=0)$. The equation of the characteristic $x_\zeta(t)$ is then

$$x_\zeta(t) = \zeta + g(\zeta)\,t \ . \tag{11.14}$$

Do not confuse the subscript in $x_\zeta(t)$ for a derivative!

To find $\rho(x,t)$, we follow this prescription:

(i) Given any point in the (x,t) plane, we find the characteristic $x_\zeta(t)$ on which it lies. This means we invert the equation $x=\zeta+g(\zeta)\,t$ to find $\zeta(x,t)$.

(ii) The value of $\rho(x,t)$ is then $\rho = f\big(\zeta(x,t)\big)$.

(iii) This procedure yields a unique value for $\rho(x,t)$ provided the characteristics do not cross, *i.e.* provided that there is a unique ζ such that $x=\zeta+g(\zeta)\,t$. If the characteristics do cross, then $\rho(x,t)$ is either *multi-valued*, or else the method has otherwise broken down. As we shall see, the crossing of characteristics, under the conditions of single-valuedness for $\rho(x,t)$, means that a *shock* has developed, and that $\rho(x,t)$ is *discontinuous*.

We can verify that this procedure yields a solution to the original PDE of eqn. 11.3 in the following manner. Suppose we invert

$$x = \zeta + g(\zeta)\,t \qquad \Longrightarrow \qquad \zeta = \zeta(x,t) \ . \tag{11.15}$$

We then have

$$\rho(x,t) = f\big(\zeta(x,t)\big) \qquad \Longrightarrow \qquad \begin{cases} \rho_t = f'(\zeta)\,\zeta_t \\ \\ \rho_x = f'(\zeta)\,\zeta_x \end{cases} \tag{11.16}$$

To find ζ_t and ζ_x, we invoke $x=\zeta+g(\zeta)\,t$, hence

$$0 = \frac{\partial}{\partial t}\big[\zeta + g(\zeta)\,t - x\big] = \zeta_t + \zeta_t\, g'(\zeta)\,t + g(\zeta) \tag{11.17}$$

$$0 = \frac{\partial}{\partial x}\big[\zeta + g(\zeta)\,t - x\big] = \zeta_x + \zeta_x\, g'(\zeta)\,t - 1 \ , \tag{11.18}$$

from which we conclude

$$\rho_t = -\frac{f'(\zeta)\,g(\zeta)}{1+g'(\zeta)\,t} \tag{11.19}$$

$$\rho_x = \frac{f'(\zeta)}{1+g'(\zeta)\,t} \ . \tag{11.20}$$

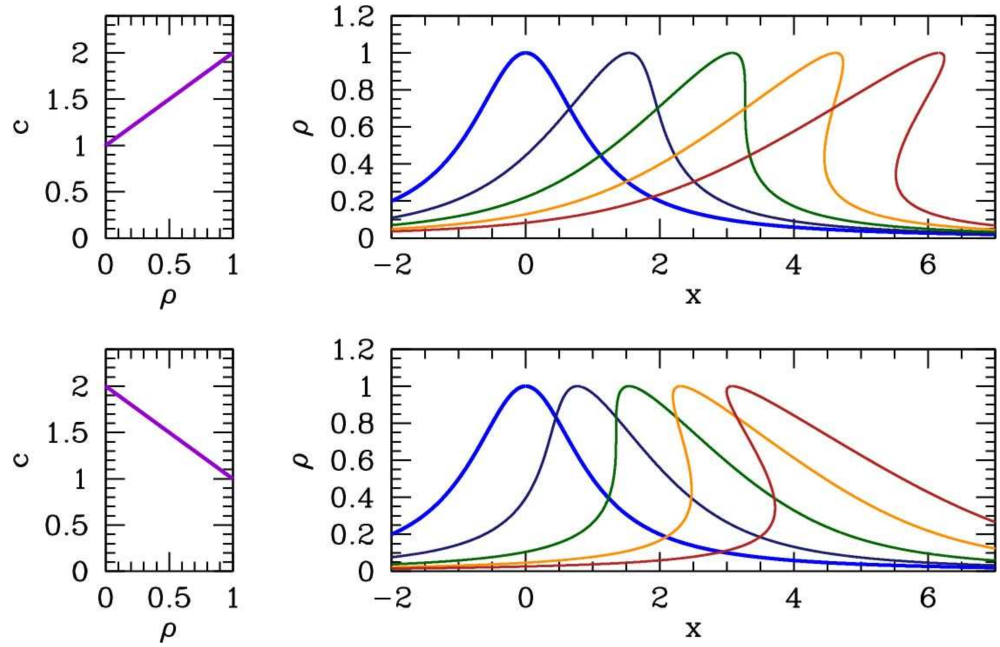

Figure 11.1: Forward and backward breaking waves for the nonlinear continuity equation $\rho_t + c(\rho)\,\rho_x = 0$, with $c(\rho) = 1 + \rho$ (top panels) and $c(\rho) = 2 - \rho$ (bottom panels). The initial conditions are $\rho(x, t = 0) = 1/(1 + x^2)$, corresponding to a break time of $t_{\rm B} = \frac{8}{3\sqrt{3}}$. Successive $\rho(x, t)$ curves are plotted for $t = 0$ (thick blue), $t = \frac{1}{2}t_{\rm B}$ (dark blue), $t = t_{\rm B}$ (dark green), $t = \frac{3}{2}t_{\rm B}$ (orange), and $t = 2t_{\rm B}$ (dark red).

Thus, $\rho_t + c(\rho)\,\rho_x = 0$, since $c(\rho) = g(\zeta)$.

As any wave disturbance propagates, different values of ρ propagate with their own velocities. Thus, the solution $\rho(x, t)$ can be constructed by splitting the curve $\rho(x, t = 0)$ into level sets of constant ρ, and then shifting each such set by a distance $c(\rho)\,t$. For $c(\rho) = c_0$, the entire curve is shifted uniformly. When $c(\rho)$ varies, different level sets are shifted by different amounts.

We see that ρ_x diverges when $1 + g'(\zeta)\,t = 0$. At this time, the wave is said to *break*. The break time $t_{\rm B}$ is defined to be the smallest value of t for which $\rho_x = \infty$ anywhere. Thus,

$$t_{\rm B} = \min_{\substack{\zeta \\ g'(\zeta)<0}} \left(-\frac{1}{g'(\zeta)} \right) \equiv -\frac{1}{g'(\zeta_{\rm B})} \ . \tag{11.21}$$

Breaking can only occur when $g'(\zeta) < 0$, and differentiating $g(\zeta) = c\big(f(\zeta)\big)$, we have that $g'(\zeta) = c'(f)\,f'(\zeta)$. We then conclude

$$\begin{aligned} c' < 0 \quad &\Longrightarrow \quad \text{need } f' > 0 \text{ to break} \\ c' > 0 \quad &\Longrightarrow \quad \text{need } f' < 0 \text{ to break} \ . \end{aligned}$$

Thus, if $\rho(x = \zeta, t = 0) = f(\zeta)$ has a hump profile, then the wave breaks forward (*i.e.* in the direction of its motion) if $c' > 0$ and backward (*i.e.* opposite to the direction of its motion)

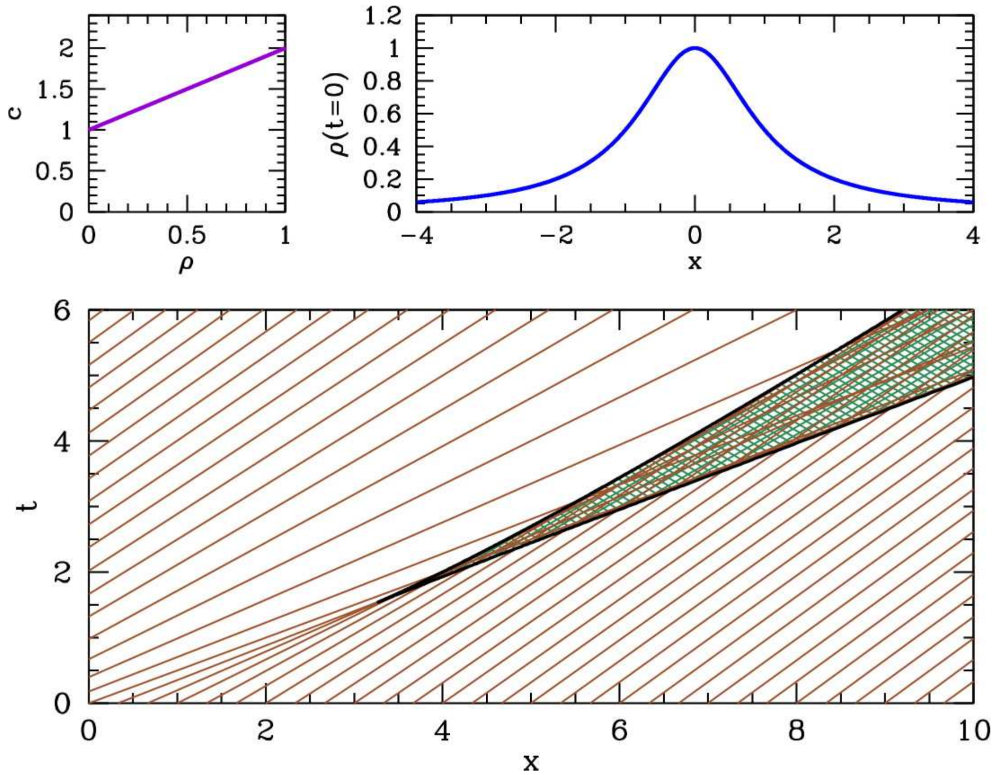

Figure 11.2: Crossing of characteristics of the nonlinear continuity equation $\rho_t + c(\rho)\,\rho_x = 0$, with $c(\rho) = 1 + \rho$ and $\rho(x, t = 0) = 1/(1 + x^2)$. Within the green hatched region of the (x, t) plane, the characteristics cross, and the function $\rho(x, t)$ is apparently multivalued.

if $c' < 0$. In fig. 11.1 we sketch the breaking of a wave with $\rho(x, t = 0) = 1/(1 + x^2)$ for the cases $c = 1 + \rho$ and $c = 2 - \rho$. Note that it is possible for different regions of a wave to break at different times, if, say, it has multiple humps.

Wave breaking occurs when neighboring characteristic cross. We can see this by comparing two neighboring characteristics,

$$x_\zeta(t) = \zeta + g(\zeta)\,t \tag{11.22}$$

$$\begin{aligned} x_{\zeta+\delta\zeta}(t) &= \zeta + \delta\zeta + g(\zeta + \delta\zeta)\,t \\ &= \zeta + g(\zeta)\,t + \big(1 + g'(\zeta)\,t\big)\,\delta\zeta + \ldots \ . \end{aligned} \tag{11.23}$$

For these characteristics to cross, we demand

$$x_\zeta(t) = x_{\zeta+\delta\zeta}(t) \quad \Longrightarrow \quad t = -\frac{1}{g'(\zeta)} \ . \tag{11.24}$$

Usually, in most physical settings, the function $\rho(x, t)$ is single-valued. In such cases, when

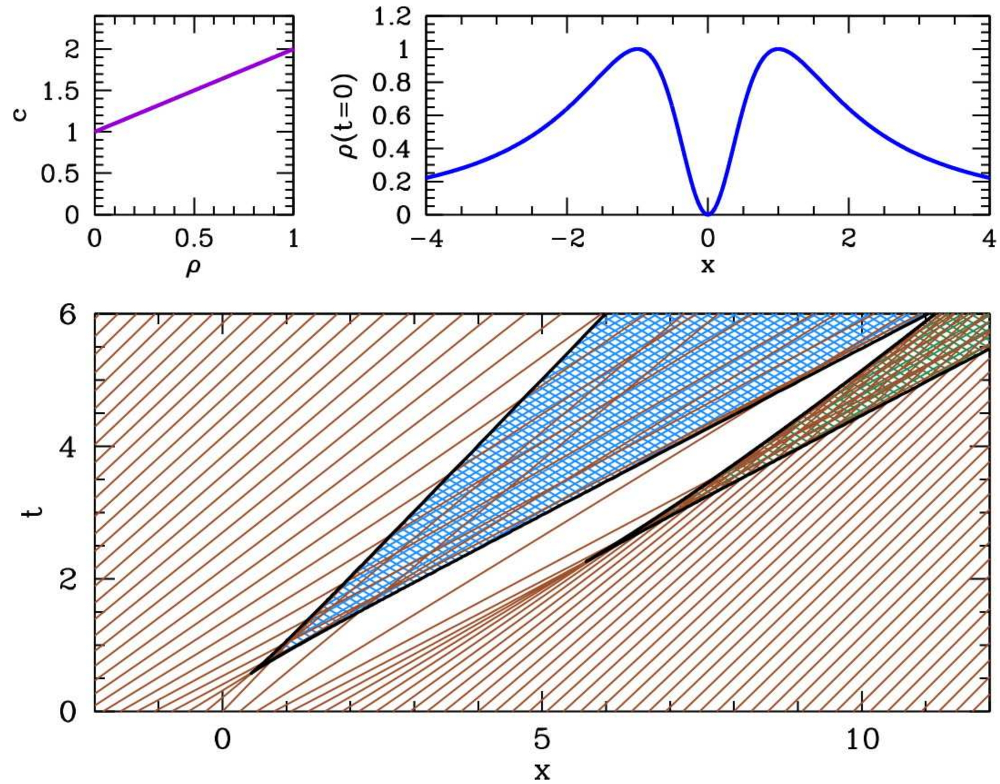

Figure 11.3: Crossing of characteristics of the nonlinear continuity equation $\rho_t + c(\rho)\,\rho_x = 0$, with $c(\rho) = 1 + \rho$ and $\rho(x, t = 0) = \big[x/(1 + x^2)\big]^2$. The wave now breaks in two places and is multivalued in both hatched regions. The left hump is the first to break.

the wave breaks, the multivalued solution ceases to be applicable[2]. Generally speaking, this means that some important physics has been left out. For example, if we neglect viscosity η and thermal conductivity κ, then the equations of gas dynamics have breaking wave solutions similar to those just discussed. When the gradients are steep – just before breaking – the effects of η and κ are no longer negligible, even if these parameters are small. This is because these parameters enter into the coefficients of higher derivative terms in the governing PDEs, and even if they are small their effect is magnified in the presence of steep gradients. In mathematical parlance, they constitute *singular perturbations*. The shock wave is then a thin region in which η and κ are crucially important, and the flow changes rapidly throughout this region. If one is not interested in this small scale physics, the shock region can be approximated as being infinitely thin, *i.e.* as a discontinuity in the inviscid limit of the theory. What remains is a set of *shock conditions* which govern the discontinuities of various quantities across the shocks.

[2]This is even true for water waves, where one might think that a multivalued height function $h(x, t)$ is physically possible.

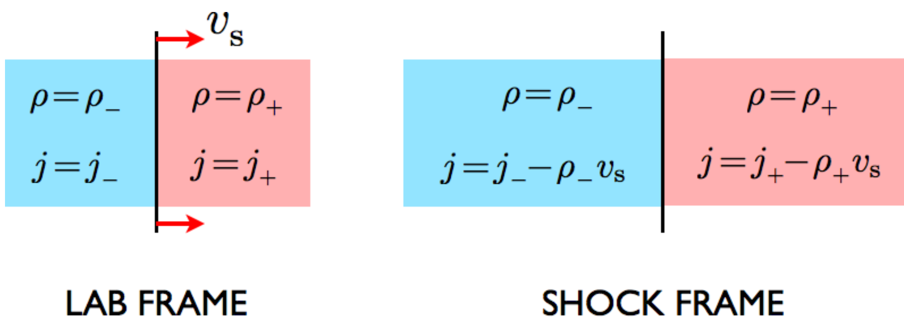

Figure 11.4: Current conservation in the shock frame yields the shock velocity, $v_s = \Delta j/\Delta\rho$.

11.2 Shocks

We now show that a solution to eqn. 11.3 exists which is single valued for almost all (x, t), *i.e.* everywhere with the exception of a set of zero measure, but which has a discontinuity along a curve $x = x_s(t)$. This discontinuity is the shock wave.

The velocity of the shock is determined by mass conservation, and is most easily obtained in the frame of the shock. The situation is as depicted in fig. 11.4. If the density and current are $(\rho_-\,, j_-)$ to the left of the shock and $(\rho_+\,, j_+)$ to the right of the shock, and if the shock moves with velocity v_s, then making a Galilean transformation to the frame of the shock, the densities do not change but the currents transform as $j \to j' = j - \rho v$. Thus, in the frame where the shock is stationary, the current on the left and right are $j_\pm = j_\pm - \rho_\pm v_s$. Current conservation then requires

$$v_s = \frac{j_+ - j_-}{\rho_+ - \rho_-} = \frac{\Delta j}{\Delta\rho} \ . \tag{11.25}$$

The special case of quadratic $j(\rho)$ bears mention. Suppose

$$j(\rho) = \alpha\rho^2 + \beta\rho + \gamma \ . \tag{11.26}$$

Then $c = 2\alpha\rho + \beta$ and

$$\begin{aligned} v_s &= \alpha(\rho_+ + \rho_-) + \beta \\ &= \tfrac{1}{2}(c_+ + c_-) \ . \end{aligned} \tag{11.27}$$

So for quadratic $j(\rho)$, the shock velocity is simply the average of the flow velocity on either side of the shock.

Consider, for example, a model with $j(\rho) = 2\rho(1-\rho)$, for which $c(\rho) = 2 - 4\rho$. Consider an initial condition $\rho(x = \zeta, t = 0) = f(\zeta) = \frac{3}{16} + \frac{1}{8}\Theta(\zeta)$, so initially $\rho = \rho_1 = \frac{3}{16}$ for $x < 0$ and $\rho = \rho_2 = \frac{5}{16}$ for $x > 0$. The lower density part moves faster, so in order to avoid multiple-valuedness, a shock must propagate. We find $c_- = \frac{5}{4}$ and $c_+ = \frac{3}{4}$. The shock velocity is then $v_s = 1$. Ths situation is depicted in fig. 11.5.

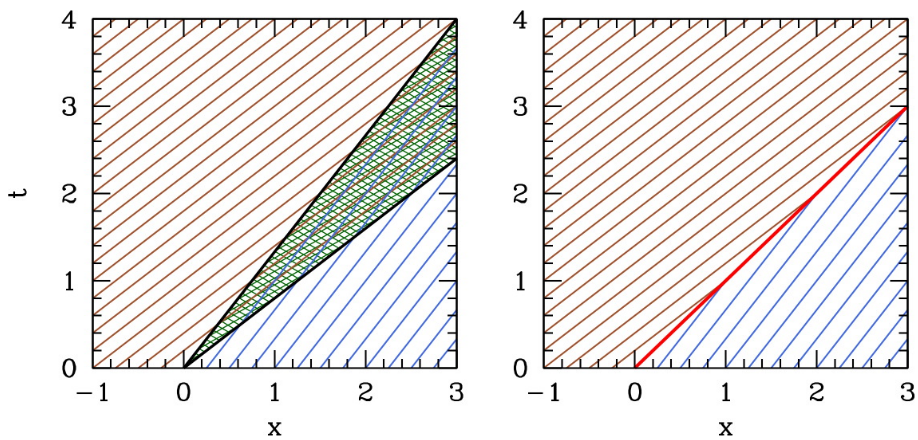

Figure 11.5: A resulting shock wave arising from $c_- = \frac{5}{4}$ and $c_+ = \frac{3}{4}$. With no shock fitting, there is a region of (x, t) where the characteristics cross, shown as the hatched region on the left. With the shock, the solution remains single valued. A quadratic behavior of $j(\rho)$ is assumed, leading to $v_{\rm s} = \frac{1}{2}(c_+ + c_-) = 1$.

11.3 Internal Shock Structure

At this point, our model of a shock is a discontinuity which propagates with a finite velocity. This may be less problematic than a multivalued solution, but it is nevertheless unphysical. We should at least understand how the discontinuity is resolved in a more complete model. To this end, consider a model where

$$j = J(\rho, \rho_x) = J(\rho) - \nu \rho_x \ . \tag{11.28}$$

The $J(\rho)$ term contains a nonlinearity which leads to steepening and broadening of regions where $\frac{dc}{dx} > 0$ and $\frac{dc}{dx} < 0$, respectively. The second term, $-\nu\rho_x$, is due to diffusion, and recapitulates *Fick's law*, which says that a diffusion current flows in such a way as to reduce gradients. The continuity equation then reads

$$\rho_t + c(\rho)\, \rho_x = \nu \rho_{xx} \ , \tag{11.29}$$

with $c(\rho) = J'(\rho)$. Even if ν is small, its importance is enhanced in regions where $|\rho_x|$ is large, and indeed $-\nu\rho_x$ dominates over $J(\rho)$ in such regions. Elsewhere, if ν is small, it may be neglected, or treated perturbatively.

As we did in our study of front propagation, we seek a solution of the form

$$\rho(x, t) = \rho(\xi) \equiv \rho(x - v_{\rm s} t) \qquad ; \qquad \xi = x - v_{\rm s} t \ . \tag{11.30}$$

Thus, $\rho_t = -v_{\rm s}\, \rho_x$ and $\rho_x = \rho_\xi$, leading to

$$-v_{\rm s}\, \rho_\xi + c(\rho)\, \rho_\xi = \nu \rho_{\xi\xi} \ . \tag{11.31}$$

Integrating once, we have

$$J(\rho) - v_{\rm s}\, \rho + A = \nu\, \rho_\xi \ , \tag{11.32}$$

where A is a constant. Integrating a second time, we have

$$\xi - \xi_0 = \nu \int\limits_{\rho_0}^{\rho} \frac{d\rho'}{J(\rho') - v_{\rm s}\,\rho' + A} \ . \tag{11.33}$$

Suppose ρ interpolates between the values ρ_1 and ρ_2. Then we must have

$$J(\rho_1) - v_{\rm s}\,\rho_1 + A = 0 \tag{11.34}$$

$$J(\rho_2) - v_{\rm s}\,\rho_2 + A = 0 \ , \tag{11.35}$$

which in turn requires

$$v_{\rm s} = \frac{J_2 - J_1}{\rho_2 - \rho_1} \ , \tag{11.36}$$

where $J_{1,2} = J(\rho_{1,2})$, exactly as before! We also conclude that the constant A must be

$$A = \frac{\rho_1 J_2 - \rho_2 J_1}{\rho_2 - \rho_1} \ . \tag{11.37}$$

11.3.1 Quadratic $J(\rho)$

For the special case where $J(\rho)$ is quadratic, with $J(\rho) = \alpha\rho^2 + \beta\rho + \gamma$, we may write

$$J(\rho) - v_{\rm s}\,\rho + A = \alpha(\rho - \rho_2)(\rho - \rho_1) \ . \tag{11.38}$$

We then have $v_{\rm s} = \alpha(\rho_1 + \rho_2) + \beta$, as well as $A = \alpha\rho_1\rho_2 - \gamma$. The moving front solution then obeys

$$d\xi = \frac{\nu\, d\rho}{\alpha(\rho - \rho_2)(\rho - \rho_1)} = \frac{\nu}{\alpha(\rho_2 - \rho_1)}\, d\ln\!\left(\frac{\rho_2 - \rho}{\rho - \rho_1}\right) \ , \tag{11.39}$$

which is integrated to yield

$$\rho(x,t) = \frac{\rho_2 + \rho_1 \exp\!\Big[\alpha(\rho_2 - \rho_1)\big(x - v_{\rm s}t\big)/\nu\Big]}{1 + \exp\!\Big[\alpha(\rho_2 - \rho_1)\big(x - v_{\rm s}t\big)/\nu\Big]} \ . \tag{11.40}$$

We consider the case $\alpha > 0$ and $\rho_1 < \rho_2$. Then $\rho(\pm\infty, t) = \rho_{1,2}$. Note that

$$\rho(x,t) = \begin{cases} \rho_1 & \text{if } x - v_{\rm s}t \gg \delta \\ \rho_2 & \text{if } x - v_{\rm s}t \ll -\delta \ , \end{cases} \tag{11.41}$$

where

$$\delta = \frac{\nu}{\alpha\,(\rho_2 - \rho_1)} \tag{11.42}$$

is the thickness of the shock region. In the limit $\nu \to 0$, the shock is discontinuous. All that remains is the *shock condition*,

$$v_{\rm s} = \alpha(\rho_1 + \rho_2) + \beta = \tfrac{1}{2}\big(c_1 + c_2\big) \ . \tag{11.43}$$

We stress that we have limited our attention here to the case where $J(\rho)$ is quadratic. It is worth remarking that for *weak shocks* where $\Delta\rho = \rho_+ - \rho_-$ is small, we can expand $J(\rho)$ about the average $\frac{1}{2}(\rho_+ + \rho_-)$, in which case we find $v_{\rm s} = \frac{1}{2}(c_+ + c_-) + \mathcal{O}\big((\Delta\rho)^2\big)$.

11.4 Shock Fitting

When we neglect diffusion currents, we have $j = J$. We now consider how to fit discontinuous shocks satisfying

$$v_s = \frac{J_+ - J_-}{\rho_+ - \rho_-} \tag{11.44}$$

into the continuous solution of eqn. 11.3, which are described by

$$x = \zeta + g(\zeta)\,t \tag{11.45}$$

$$\rho = f(\zeta) \ , \tag{11.46}$$

with $g(\zeta) = c\big(f(\zeta)\big)$, such that the multivalued parts of the continuous solution are eliminated and replaced with the shock discontinuity. The guiding principle here is number conservation:

$$\frac{d}{dt}\int\limits_{-\infty}^{\infty} dx\,\rho(x,t) = 0 \ . \tag{11.47}$$

We'll first learn how do fit shocks when $J(\rho)$ is quadratic, with $J(\rho) = \alpha\rho^2 + \beta\rho + \gamma$. We'll assume $\alpha > 0$ for the sake of definiteness.

11.4.1 An Important Caveat

Let's multiply the continuity equation $\rho_t + c(\rho)\,\rho_x = 0$ by $c'(\rho)$. Thus results in

$$c_t + c\,c_x = 0 \ . \tag{11.48}$$

If we define $q = \frac{1}{2}c^2$, then this takes the form of a continuity equation:

$$c_t + q_x = 0 \ . \tag{11.49}$$

Now consider a shock wave. Invoking eqn. 11.25, we would find, *mutatis mutandis*, a shock velocity

$$u_s = \frac{q_+ - q_-}{c_+ - c_-} = \tfrac{1}{2}(c_+ + c_-) \ . \tag{11.50}$$

This agrees with the velocity $v_s = \Delta j/\Delta\rho$ only when $j(\rho)$ is quadratic. Something is wrong – there cannot be two velocities for the same shock.

The problem is that eqn. 11.48 is not valid across the shock and cannot be used to determine the shock velocity. There is no conservation law for c as there is for ρ. One way we can appreciate the difference is to add diffusion into the mix. Multiplying eqn. 11.29 by $c'(\rho)$, and invoking $c_{xx} = c'(\rho)\,\rho_{xx} + c''(\rho)\,\rho_x^2$, we obtain

$$c_t + c\,c_x = \nu c_{xx} - \nu c''(\rho)\,\rho_x^2 \ . \tag{11.51}$$

We now see explicitly how nonzero $c''(\rho)$ leads to a different term on the RHS. When $c''(\rho) = 0$, the above equation is universal, independent of the coefficients in the quadratic $J(\rho)$, and is known as *Burgers' equation*,

$$c_t + c\, c_x = \nu c_{xx} \ . \tag{11.52}$$

Later on we shall see how this nonlinear PDE may be linearized, and how we can explicitly solve for shock behavior, including the merging of shocks.

11.4.2 Recipe for shock fitting ($J'''(\rho) = 0$)

Number conservation means that when we replace the multivalued solution by the discontinuous one, the area under the curve must remain the same. If $J(\rho)$ is quadratic, then we can base our analysis on the equation $c_t + c\, c_x = 0$, since it gives the correct shock velocity $v_{\rm s} = \frac{1}{2}(c_+ + c_-)$. We then may then follow the following rules:

(i) Sketch $g(\zeta) = c\big(f(\zeta)\big)$.

(ii) Draw a straight line connecting two points on this curve at ζ_- and ζ_+ which obeys the equal area law, *i.e.*

$$\tfrac{1}{2}(\zeta_+ - \zeta_-)\Big(g(\zeta_+) + g(\zeta_-)\Big) = \int\limits_{\zeta_-}^{\zeta_+} \!d\zeta\; g(\zeta) \ . \tag{11.53}$$

(iii) This line evolves into the shock front after a time t such that

$$x_{\rm s}(t) = \zeta_- + g(\zeta_-)\, t = \zeta_+ + g(\zeta_+)\, t \ . \tag{11.54}$$

Thus,

$$t = -\frac{\zeta_+ - \zeta_-}{g(\zeta_+) - g(\zeta_-)} \ . \tag{11.55}$$

Alternatively, we can fix t and solve for $\zeta_\pm$. See fig. 11.6 for a graphical description.

(iv) The position of the shock at this time is $x = x_{\rm s}(t)$. The strength of the shock is $\Delta c = g(\zeta_-) - g(\zeta_+)$. Since $J(\rho) = \alpha\rho^2 + \beta\rho + \gamma$, we have $c(\rho) = 2\alpha\rho + \beta$ and hence the density discontinuity at the shock is $\Delta\rho = \Delta c/2\alpha$.

(v) The break time, when the shock first forms, is given by finding the steepest chord satisfying the equal area law. Such a chord is tangent to $g(\zeta)$ and hence corresponds to zero net area. The break time is

$$t_{\rm B} = \min_{\substack{\zeta \\ g'(\zeta)>0}} \bigg(-\frac{1}{g'(\zeta)}\bigg) \equiv -\frac{1}{g(\zeta_{\rm B})} \ . \tag{11.56}$$

(vi) If $g(\infty) = g(-\infty)$, the shock strength vanishes as $t \to \infty$. If $g(-\infty) > g(+\infty)$ then asymptotically the shock strength approaches $\Delta g = g(-\infty) - g(+\infty)$.

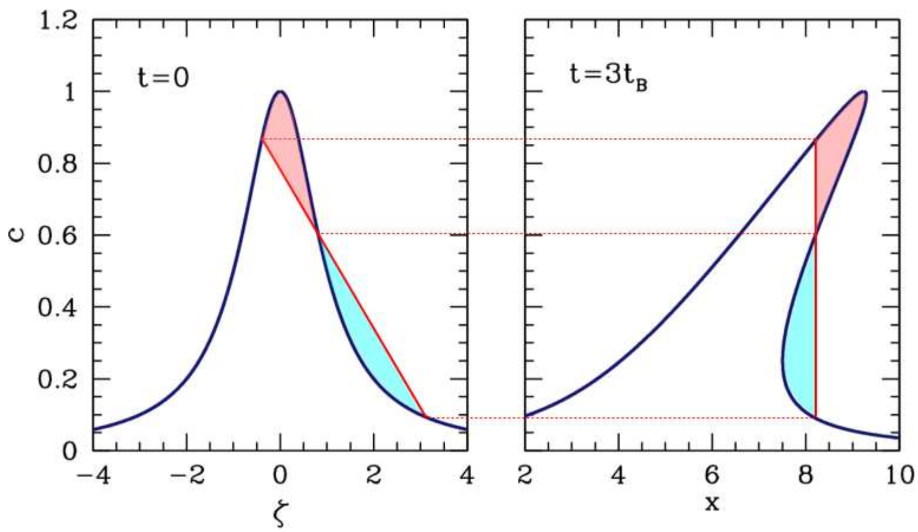

Figure 11.6: Shock fitting for quadratic $J(\rho)$.

11.4.3 Example problem

Suppose the $c(\rho)$ and $\rho(x, t = 0)$ are such that the initial profile for $c(x, t = 0)$ is

$$c(x,0) = c_0 \cos\left(\frac{\pi x}{2\ell}\right) \Theta\big(\ell - |x|\big) \ , \tag{11.57}$$

where $\Theta(s)$ is the step function, which vanishes identically for negative values of its argument. Thus, $c(x, 0) = 0$ for $|x| \geq \ell$.

(a) Find the time $t_{\rm B}$ at which the wave breaks and a shock front develops. Find the position of the shock $x_{\rm s}(t_{\rm B})$ at the moment it forms.

Solution : Breaking first occurs at time

$$t_{\rm B} = \min_x \frac{-1}{c'(x,0)} \ . \tag{11.58}$$

Thus, we look for the maximum negative slope in $g(x) \equiv c(x, 0)$, which occurs at $x = \ell$, where $c'(\ell, 0) = -\pi c_0/2\ell$. Therefore,

$$t_{\rm B} = \frac{2\ell}{\pi c_0} \quad , \quad x_{\rm B} = \ell \ . \tag{11.59}$$

(b) Use the shock-fitting equations to derive $\zeta_\pm(t)$.

Solution : The shock fitting equations are

$$\tfrac{1}{2}\,(\zeta_+ - \zeta_-)\,\Big(g(\zeta_+) + g(\zeta_-)\Big) = \int\limits_{\zeta_-}^{\zeta_+} \! d\zeta\; g(\zeta) \tag{11.60}$$

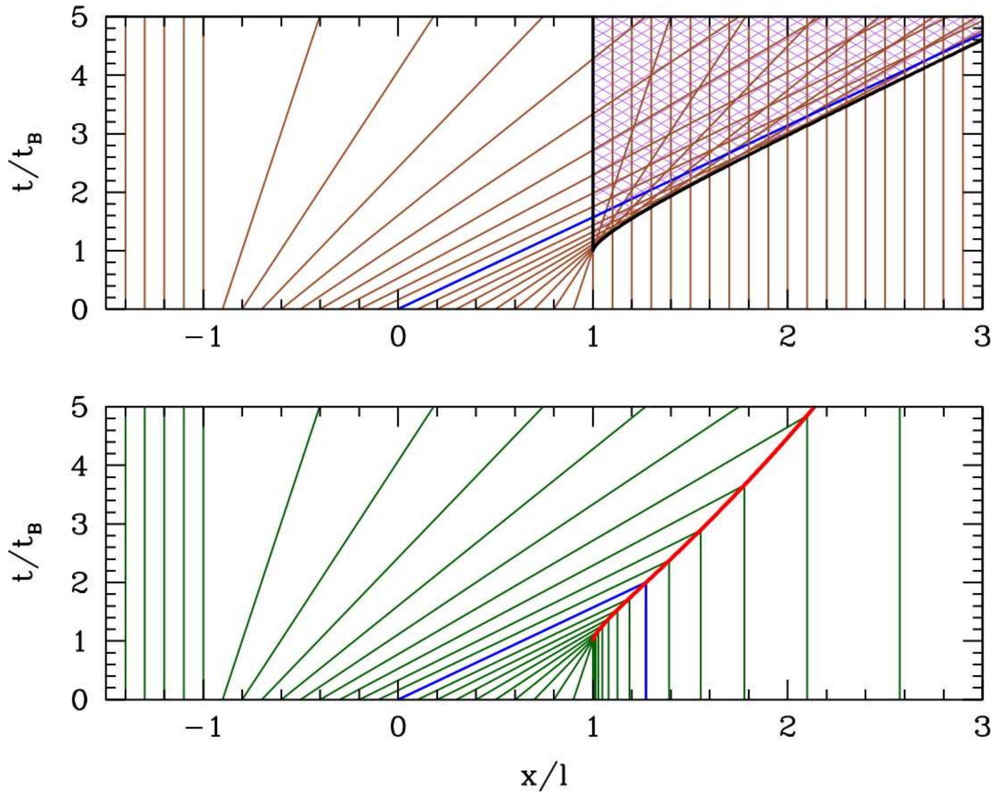

Figure 11.7: Top : crossing characteristics (purple hatched region) in the absence of shock fitting. Bottom : characteristics in the presence of the shock.

and

$$t = \frac{\zeta_+ - \zeta_-}{g(\zeta_-) - g(\zeta_+)} \ . \tag{11.61}$$

Clearly $\zeta_+ > \ell$, hence $g(\zeta_+) = 0$ and

$$\int\limits_{\zeta_-}^{\zeta_+} d\zeta \, g(\zeta) = c_0 \cdot \frac{2\ell}{\pi} \int\limits_{\pi\zeta_-/2\ell}^{\pi/2} dz \, \cos z = \frac{2\ell \, c_0}{\pi} \left\{ 1 - \sin\!\left(\frac{\pi\zeta_-}{2\ell}\right) \right\} . \tag{11.62}$$

Thus, the first shock fitting equation yields

$$\tfrac{1}{2} \, (\zeta_+ - \zeta_-) \, c_0 \cos\!\left(\frac{\pi\zeta_-}{2\ell}\right) = \frac{2\ell \, c_0}{\pi} \left\{ 1 - \sin\!\left(\frac{\pi\zeta_-}{2\ell}\right) \right\} . \tag{11.63}$$

The second shock fitting equation gives

$$t = \frac{\zeta_+ - \zeta_-}{c_0 \cos\left(\frac{\pi\zeta_-}{2\ell}\right)} \ . \tag{11.64}$$

Eliminating $\zeta_+ - \zeta_-$, we obtain the relation

$$\sin\!\left(\frac{\pi\zeta_-}{2\ell}\right) = \frac{4\ell}{\pi c_0 t} - 1 \ . \tag{11.65}$$

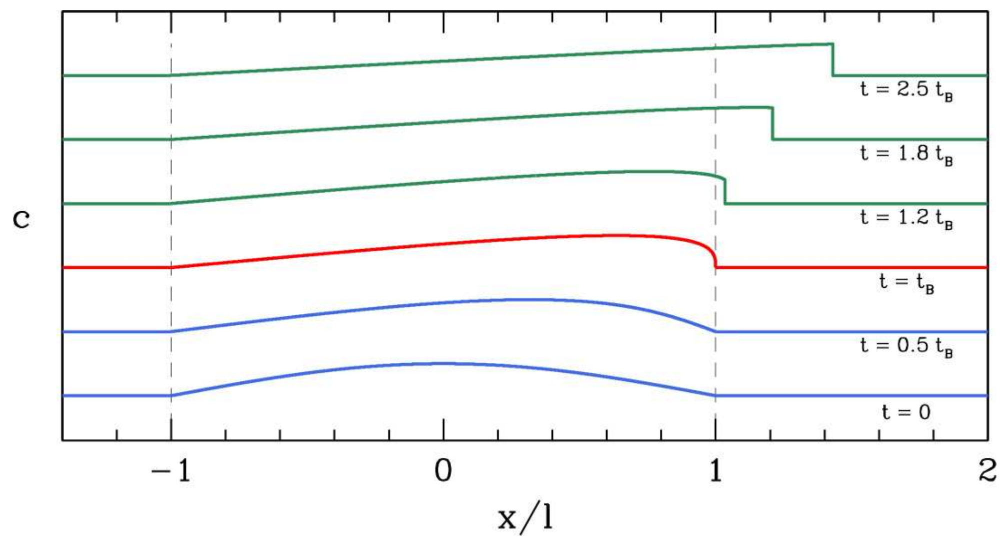

Figure 11.8: Evolution of $c(x,t)$ for a series of time values.

Thus,

$$\zeta_-(t) = \frac{2\ell}{\pi}\,\sin^{-1}\!\left(\frac{4\ell}{\pi c_0 t} - 1\right) \tag{11.66}$$

$$\begin{aligned}\zeta_+(t) &= \zeta_- + \frac{4\ell}{\pi}\cdot\frac{1-\sin(\pi\zeta_-/2\ell)}{\cos(\pi\zeta_-/2\ell)}\\ &= \frac{2\ell}{\pi}\left\{\sin^{-1}\!\left(\frac{4\ell}{\pi c_0 t} - 1\right) + 2\sqrt{\frac{\pi c_0 t}{2\ell} - 1}\,\right\} ,\end{aligned} \tag{11.67}$$

where $t \ge t_{\rm B} = 2\ell/\pi c_0$.

(c) Find the shock motion $x_s(t)$.

Solution : The shock position is

$$\begin{aligned}x_{\rm s}(t) &= \zeta_- + g(\zeta_-)\,t\\ &= \frac{2\ell}{\pi}\sin^{-1}\!\left(\frac{2}{\tau} - 1\right) + \frac{4\ell}{\pi}\sqrt{\tau - 1}\ ,\end{aligned} \tag{11.68}$$

where $\tau = t/t_{\rm B} = \pi c_0 t/2\ell$, and $\tau \ge 1$.

(d) Sketch the characteristics for the multivalued solution with no shock fitting, identifying the region in (x,t) where characteristics cross. Then sketch the characteristics for the discontinuous shock solution.

Solution : See fig. 11.7.

(e) Find the shock discontinuity $\Delta c(t)$.

Solution : The shock discontinuity is

$$\Delta c(t) = g\big(\zeta_-\big) - g\big(\zeta_+\big) = c_0 \cos\!\left(\frac{\pi\zeta_-}{2\ell}\right)$$
$$= \sqrt{\frac{8\ell\, c_0}{\pi t}\left(1 - \frac{2\ell}{\pi c_0 t}\right)} = 2c_0\,\frac{\sqrt{\tau-1}}{\tau}\ . \tag{11.69}$$

(f) Find the shock velocity $v_\mathrm{s}(t)$.

Solution : The shock wave velocity is

$$c_\mathrm{s}(t) = \tfrac{1}{2}\Big[\,g\big(\zeta_-\big) + g\big(\zeta_+\big)\Big] = \tfrac{1}{2}\,\Delta c(t)$$
$$= \sqrt{\frac{2\ell\, c_0}{\pi t}\left(1 - \frac{2\ell}{\pi c_0 t}\right)}\ . \tag{11.70}$$

(g) Sketch the evolution of the wave, showing the breaking of the wave at $t = t_\mathrm{B}$ and the subsequent evolution of the shock front.

Solution : A sketch is provided in Fig. 11.8.

11.5 Long-time Behavior of Shocks

Starting with an initial profile $\rho(x,t)$, almost all the original details are lost in the $t \to \infty$ limit. What remains is a set of propagating triangular waves, where only certain gross features of the original shape, such as its area, are preserved.

11.5.1 Fate of a hump

The late time profile of $c(x,t)$ in fig. 11.8 is that of a triangular wave. This is a general result. Following Whitham, we consider the late time evolution of a hump profile $g(\zeta)$. We assume $g(\zeta) = c_0$ for $|\zeta| > L$. Shock fitting requires

$$\tfrac{1}{2}\Big[g(\zeta_+) + g(\zeta_-) - 2c_0\Big](\zeta_+ - \zeta_-) = \int\limits_{\zeta_-}^{\zeta_+}\! d\zeta\,\big(g(\zeta) - c_0\big)\ . \tag{11.71}$$

Eventually the point ζ_+ must pass $x = L$, in which case $g(\zeta_+) = c_0$. Then

$$\tfrac{1}{2}\Big[g(\zeta_+) - c_0\Big](\zeta_+ - \zeta_-) = \int\limits_{\zeta_-}^{L}\! d\zeta\,\big(g(\zeta) - c_0\big) \tag{11.72}$$

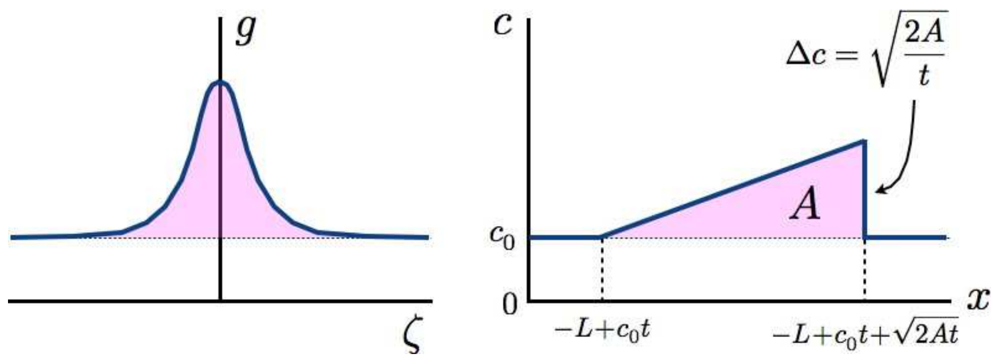

Figure 11.9: Initial and late time configurations for a hump profile. For late times, the profile is triangular, and all the details of the initial shape are lost, save for the area A.

and therefore

$$t = \frac{\zeta_+ - \zeta_-}{g(\zeta_-) - c_0} \ . \tag{11.73}$$

Using this equation to eliminate ζ_+, we have

$$\tfrac{1}{2}\big(g(\zeta_-) - c_0\big)^2 \, t = \int\limits_{\zeta_-}^{L} d\zeta \, \big(g(\zeta) - c_0\big) \ . \tag{11.74}$$

As $t \to \infty$ we must have $\zeta_- \to -L$, hence

$$\tfrac{1}{2}\big(g(\zeta_-) - c_0\big)^2 \, t \approx \int\limits_{-L}^{L} d\zeta \, \big(g(\zeta) - c_0\big) \equiv A \ , \tag{11.75}$$

where A is the area under the hump to the line $c = c_0$. Thus,

$$g(\zeta_-) - c_0 \approx \sqrt{\frac{2A}{t}} \ , \tag{11.76}$$

and the late time motion of the shock is given by

$$x_{\rm s}(t) = -L + c_0 t + \sqrt{2At} \tag{11.77}$$

$$v_{\rm s}(t) = c_0 + \sqrt{\frac{A}{2t}} \ . \tag{11.78}$$

The shock strength is $\Delta c = g(\zeta_-) - c_0 = \sqrt{2A/t}$. Behind the shock, we have $c = g(\zeta)$ and $x = \zeta + g(\zeta)\, t$, hence

$$c = \frac{x+L}{t} \qquad \text{for} \quad -L + c_0 t < x < -L + c_0 t + \sqrt{2At} \ . \tag{11.79}$$

As $t \to \infty$, the details of the original profile $c(x,0)$ are lost, and all that remains conserved is the area A. Both shock velocity and the shock strength decrease as $t^{-1/2}$ at long times, with $v_{\rm s}(t) \to c_0$ and $\Delta c(t) \to 0$.

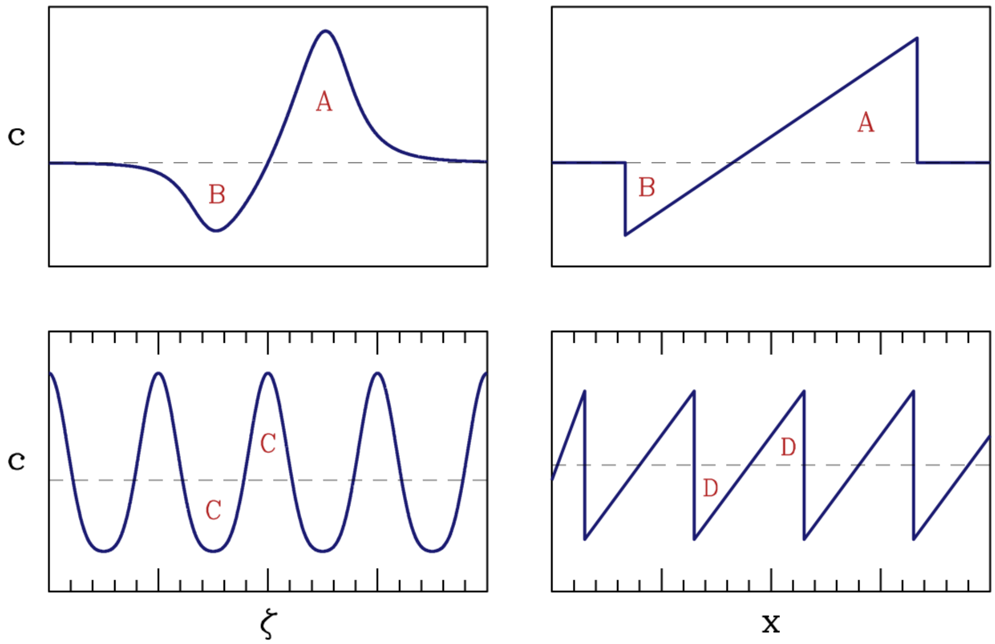

Figure 11.10: Top panels : An N-wave, showing initial (left) and late time (right) profiles. As the N-wave propagates, the areas A and B are preserved. Bottom panels : A P-wave. The area D eventually decreases to zero as the shock amplitude dissipates.

11.5.2 N-wave and P-wave

Consider the initial profile in the top left panel of fig. 11.10. Now there are two propagating shocks, since there are two compression regions where $g'(\zeta) < 0$. As $t \to \infty$, we have $(\zeta_-\,,\,\zeta_+)_{\rm A} \to (0\,,\,\infty)$ for the A shock, and $(\zeta_-\,,\,\zeta_+)_{\rm B} \to (-\infty\,,\,0)$ for the B shock. Asymptotically, the shock strength

$$\Delta c(t) \equiv c\big(x_{\rm s}^-(t),t\big) - c\big(x_{\rm s}^+(t),t\big) \tag{11.80}$$

for the two shocks is given by

$$x_{\rm s}^{\rm A}(t) \approx c_0 t + \sqrt{2At} \quad , \quad \Delta c_{\rm A} \approx +\sqrt{\frac{2A}{t}} \tag{11.81}$$

$$x_{\rm s}^{\rm B}(t) \approx c_0 t - \sqrt{2Bt} \quad , \quad \Delta c_{\rm B} \approx -\sqrt{\frac{2B}{t}}\ , \tag{11.82}$$

where A and B are the areas associated with the two features This feature is called an N-wave, for its N (or inverted N) shape.

The initial and late stages of a periodic wave, where $g(\zeta+\lambda) = g(\zeta)$, are shown in the right panels of fig. 11.10. In the $t \to \infty$ limit, we evidently have $\zeta_+ - \zeta_- = \lambda$, the wavelength. Asymptotically the shock strength is given by

$$\Delta c(t) \equiv g(\zeta_-) - g(\zeta_+) = \frac{\zeta_+ - \zeta_-}{t} = \frac{\lambda}{t}\ , \tag{11.83}$$

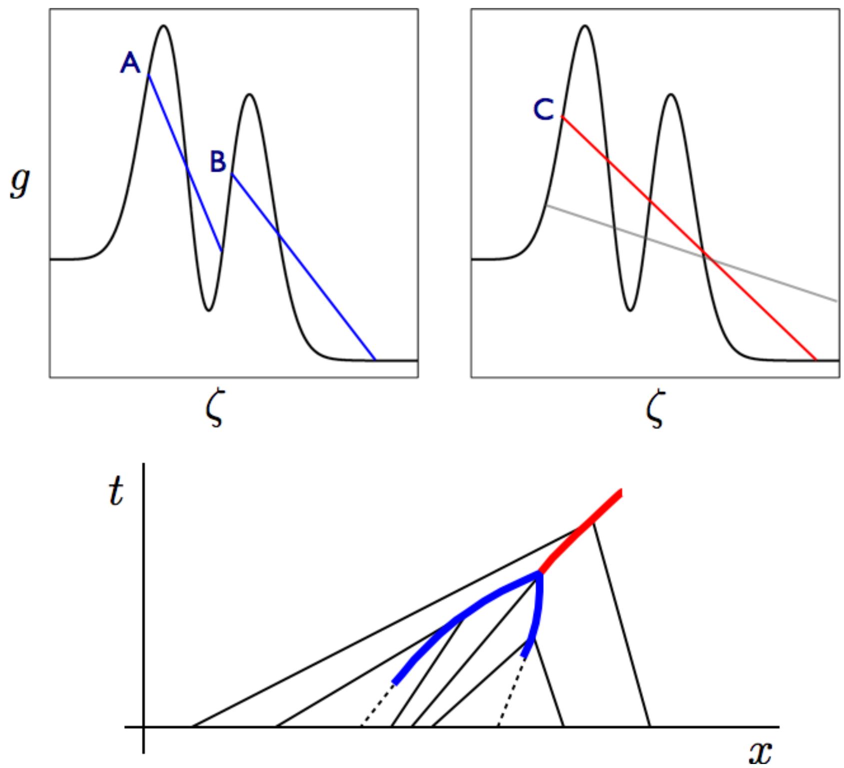

Figure 11.11: Merging of two shocks. The shocks initially propagate independently (upper left), and then merge and propagate as a single shock (upper right). Bottom : characteristics for the merging shocks.

where we have invoked eqn. 11.55. In this limit, the shock train travels with constant velocity c_0, which is the spatial average of $c(x, 0)$ over one wavelength:

$$c_0 = \frac{1}{\lambda} \int_0^{\lambda} d\zeta \; g(\zeta) \; . \tag{11.84}$$

11.6 Shock Merging

It is possible for several shock waves to develop, and in general these shocks form at different times, have different strengths, and propagate with different velocities. Under such circumstances, it is quite possible that one shock overtakes another. These two shocks then merge and propagate on as a single shock. The situation is depicted in fig. 11.11. We label the shocks by A and B when they are distinct, and the late time single shock by C. We must have

$$v_{\rm s}^{\rm A} = \tfrac{1}{2}\, g\big(\zeta_+^{\rm A}\big) + \tfrac{1}{2}\, g\big(\zeta_-^{\rm A}\big) \tag{11.85}$$

$$v_{\rm s}^{\rm B} = \tfrac{1}{2}\, g\big(\zeta_+^{\rm B}\big) + \tfrac{1}{2}\, g\big(\zeta_-^{\rm B}\big) \; . \tag{11.86}$$

The merging condition requires

$$\zeta_+^{\rm A} = \zeta_-^{\rm B} \equiv \xi \tag{11.87}$$

as well as

$$\zeta_+^{\rm C} = \zeta_+^{\rm B} \qquad , \qquad \zeta_-^{\rm C} = \zeta_-^{\rm A} \ . \tag{11.88}$$

The merge occurs at time t, where

$$t = \frac{\zeta_+ - \xi}{g(\xi) - g(\zeta_+)} = \frac{\xi - \zeta_-}{g(\zeta_-) - g(\xi)} \ . \tag{11.89}$$

Thus, the slopes of the A and B shock construction lines are equal when they merge.

11.7 Shock Fitting for General $J(\rho)$

When $J(\rho)$ is quadratic, we may analyze the equation $c_t + c\, c_x$, as it is valid across any shocks in that it yields the correct shock velocity. If $J'''(\rho) \neq 0$, this is no longer the case, and we must base our analysis on the original equation $\rho_t + c(\rho)\, \rho_x = 0$.

The coordinate transformation

$$(x, c) \longrightarrow (x + ct \, , \, c) \tag{11.90}$$

preserves areas in the (x, c) plane and also maps lines to lines. However, while

$$(x, \rho) \longrightarrow (x + c(\rho)\, t \, , \, \rho) \tag{11.91}$$

does preserve areas in the (x, ρ) plane, it does not map lines to lines. Thus, the 'pre-image' of the shock front in the (x, ρ) plane is not a simple straight line, and our equal area construction fails. Still, we can make progress. We once again follow Whitham, §2.9.

Let $x(\rho, t)$ be the inverse of $\rho(x, t)$, with $\zeta(\rho) \equiv x(\rho, t = 0)$. Then

$$x(\rho, t) = \zeta(\rho) + c(\rho)\, t \ . \tag{11.92}$$

Note that $\rho(x, t)$ is in general multi-valued. We still have that the shock solution covers the same area as the multivalued solution $\rho(x, t)$. Let $\rho_\pm$ denote the value of ρ just to the right $(+)$ or left $(-)$ of the shock. For purposes of illustration, we assume $c'(\rho) > 0$, which means that $\rho_x < 0$ is required for breaking, although the method works equally well for $c'(\rho) < 0$. Assuming a hump-like profile, we then have $\rho_- > \rho_+$, with the shock breaking to the right. Area conservation requires

$$\int\limits_{\rho_+}^{\rho_-} \! d\rho \; x(\rho, t) = \int\limits_{\rho_+}^{\rho_-} \! d\rho \, \big[\zeta(\rho) + c(\rho)\, t \big] = (\rho_- - \rho_+)\, x_{\rm s}(t) \ . \tag{11.93}$$

Since $c(\rho) = J'(\rho)$, the above equation may be written as

$$\begin{aligned}
(J_+ - J_-)\,t - (\rho_+ - \rho_-) &= \int\limits_{\rho_+}^{\rho_-} \! d\rho \; \zeta(\rho) \\
&= \rho_-\,\zeta_- - \rho_+\,\zeta_+ - \int\limits_{\zeta_+}^{\zeta_-} \! d\zeta \; \rho(\zeta) \ . \qquad (11.94)
\end{aligned}$$

Now the shock position $x_s(t)$ is given by

$$x_s = \zeta_- + c_-\,t = \zeta_+ + c_+ t \ , \qquad (11.95)$$

hence

$$\Big[(J_+ - \rho_+ c_+) - (J_- - \rho_- c_-)\Big] = \frac{c_+ - c_-}{\zeta_+ - \zeta_-} \int\limits_{\zeta_-}^{\zeta_+} \! d\zeta \; \rho(\zeta) \ . \qquad (11.96)$$

This is a useful result because $J_\pm$, $\rho_\pm$, and $c_\pm$ are all functions of $\zeta_\pm$, hence what we have here is a relation between ζ_+ and ζ_-. When $J(\rho)$ is quadratic, this reduces to our earlier result in eqn. 11.53. For a hump, we still have $x_s \approx c_0 t + \sqrt{2At}$ and $c - c_0 \approx \sqrt{2A/t}$ as before, with

$$A = c'(\rho_0) \int\limits_{-\infty}^{\infty} \! d\zeta \, \big[\rho(\zeta) - \rho_0\big] \ . \qquad (11.97)$$

11.8 Sources

Consider the continuity equation in the presence of a source term,

$$\rho_t + c\,\rho_x = \sigma \ , \qquad (11.98)$$

where $c = c(x,t,\rho)$ and $\sigma = \sigma(x,t,\rho)$. Note that we are allowing for more than just $c = c(\rho)$ here. According to the discussion in the Appendix, the characteristic obey the coupled ODEs[3],

$$\frac{d\rho}{dt} = \sigma(x,t,\rho) \qquad (11.99)$$

$$\frac{d\sigma}{dt} = c(x,t,\rho) \ . \qquad (11.100)$$

In general, the characteristics no longer are straight lines.

[3]We skip the step where we write $dt/ds = 1$ since this is immediately integrated to yield $s = t$.

11.8.1 Examples

Whitham analyzes the equation

$$c_t + c\,c_x = -\alpha\,c\ , \tag{11.101}$$

so that the characteristics obey

$$\frac{dc}{dt} = -\alpha\,c \qquad , \qquad \frac{dx}{dt} = c\ . \tag{11.102}$$

The solution is

$$c_\zeta(t) = e^{-\alpha t}\,g(\zeta) \tag{11.103}$$

$$x_\zeta(t) = \zeta + \frac{1}{\alpha}\left(1 - e^{-\alpha t}\right) g(\zeta)\ , \tag{11.104}$$

where $\zeta = x_\zeta(0)$ labels the characteristics. Clearly $x_\zeta(t)$ is not a straight line. Neighboring characteristics will cross at time t if

$$\frac{\partial x_\zeta(t)}{\partial \zeta} = 1 + \frac{1}{\alpha}\left(1 - e^{-\alpha t}\right) g'(\zeta) = 0\ . \tag{11.105}$$

Thus, the break time is

$$t_{\rm B} = \min_{\substack{\zeta \\ t_{\rm B} > 0}} \left[-\frac{1}{\alpha}\,\ln\left(1 + \frac{\alpha}{g'(\zeta)}\right)\right] . \tag{11.106}$$

This requires $g'(\zeta) < -\alpha$ in order for wave breaking to occur.

For another example, consider

$$c_t + c\,c_x = -\alpha\,c^2\ , \tag{11.107}$$

so that the characteristics obey

$$\frac{dc}{dt} = -\alpha\,c^2 \qquad , \qquad \frac{dx}{dt} = c\ . \tag{11.108}$$

The solution is now

$$c_\zeta(t) = \frac{g(\zeta)}{1 + \alpha\,g(\zeta)\,t} \tag{11.109}$$

$$x_\zeta(t) = \zeta + \frac{1}{\alpha}\,\ln\big(1 + \alpha\,g(\zeta)\,t\big)\ . \tag{11.110}$$

11.8.2 Moving sources

Consider a source moving with velocity u. We then have

$$c_t + c\,c_x = \sigma(x - ut)\ , \tag{11.111}$$

where u is a constant. We seek a moving wave solution $c = c(\xi) = c(x - ut)$. This leads immediately to the ODE

$$(c - u)\, c_\xi = \sigma(\xi) \ . \tag{11.112}$$

This may be integrated to yield

$$\tfrac{1}{2}(u - c_\infty)^2 - \tfrac{1}{2}(u - c)^2 = \int\limits_\xi^\infty d\xi'\, \sigma(\xi') \ . \tag{11.113}$$

Consider the supersonic case where $u > c$. Then we have a smooth solution,

$$c(\xi) = u - \left[(u - c_\infty)^2 - 2\int\limits_\xi^\infty d\xi'\, \sigma(\xi')\right]^{1/2} , \tag{11.114}$$

provided that the term inside the large rectangular brackets is positive. This is always the case for $\sigma < 0$. For $\sigma > 0$ we must require

$$u - c_\infty > \sqrt{2\int\limits_\xi^\infty d\xi'\, \sigma(\xi')} \tag{11.115}$$

for all ξ. If $\sigma(\xi)$ is monotonic, the lower limit on the above integral may be extended to $-\infty$. Thus, if the source strength is sufficiently small, no shocks are generated. When the above equation is satisfied as an equality, a shock develops, and transients from the initial conditions overtake the wave. A complete solution of the problem then requires a detailed analysis of the transients. What is surprising here is that a supersonic source need not produce a shock wave, if the source itself is sufficiently weak.

11.9 Burgers' Equation

The simplest equation describing both nonlinear wave propagation and diffusion equation is the one-dimensional *Burgers' equation*,

$$c_t + c\, c_x = \nu\, c_{xx} \ . \tag{11.116}$$

As we've seen, this follows from the continuity equation $\rho_t + j_x$ when $j = J(\rho) - \nu\rho_x$, with $c = J'(\rho)$ and $c''(\rho) = 0$.

We have already obtained, in §11.3.1, a solution to Burgers' equation in the form of a propagating front. However, we can do much better than this; we can find *all* the solutions to the one-dimensional Burgers' equation. The trick is to employ a nonlinear transformation of the field $c(x, t)$, known as the *Cole-Hopf transformation*, which linearizes the PDE. Once again, we follow the exceptionally clear discussion in the book by Whitham (ch. 4).

The Cole-Hopf transformation is defined as follows:

$$c \equiv -2\nu\,\frac{\varphi_x}{\varphi} = \frac{\partial}{\partial x}\big(-2\nu\ln\varphi\big)\ . \tag{11.117}$$

Plugging into Burgers' equation, one finds that $\varphi(x,t)$ satisfies the *linear* diffusion equation,

$$\varphi_t = \nu\,\varphi_{xx}\ . \tag{11.118}$$

Isn't that just about the coolest thing you've ever heard?

Suppose the initial conditions on $\varphi(x,t)$ are

$$\varphi(x,0) = \Phi(x)\ . \tag{11.119}$$

We can then solve the diffusion equation 11.118 by Laplace transform. The result is

$$\varphi(x,t) = \frac{1}{\sqrt{4\pi\nu t}}\int\limits_{-\infty}^{\infty}\!dx'\;e^{-(x-x')^2/4\nu t}\;\Phi(x')\ . \tag{11.120}$$

Thus, if $c(x,t=0)=g(x)$, then the solution for subsequent times is

$$c(x,t) = \frac{\int_{-\infty}^{\infty} dx'\,(x-x')\,e^{-H(x,x',t)/2\nu}}{t\int_{-\infty}^{\infty} dx'\,e^{-H(x,x',t)/2\nu}}\ , \tag{11.121}$$

where

$$H(x,x',t) = \int\limits_0^{x'}\!dx''\;g(x'') + \frac{(x-x')^2}{2t}\ . \tag{11.122}$$

11.9.1 The limit $\nu\to 0$

In the limit $\nu\to 0$, the integrals in the numerator and denominator of eqn. 11.121 may be computed via the method of steepest descents. This means that extremize $H(x,x',t)$ with respect to x', which entails solving

$$\frac{\partial H}{\partial x'} = g(x') - \frac{x-x'}{t}\ . \tag{11.123}$$

Let $\zeta=\zeta(x,t)$ be a solution to this equation for x', so that

$$x = \zeta + g(\zeta)\,t\ . \tag{11.124}$$

We now expand about $x'=\zeta$, writing $x'=\zeta+s$, in which case

$$H(x') = H(\zeta) + \tfrac{1}{2}H''(\zeta)\,s^2 + \mathcal{O}(s^3)\ , \tag{11.125}$$

where the x and t dependence is here implicit. If $F(x')$ is an arbitrary function which is slowly varying on distance scales on the order of $\nu^{1/2}$, then we have

$$\int_{-\infty}^{\infty} dx'\, F(x')\, e^{-H(x')/2\nu} \approx \sqrt{\frac{4\pi\nu}{H''(\zeta)}}\; e^{-H(\zeta)/2\nu}\, F(\zeta)\ . \tag{11.126}$$

Applying this result to eqn. 11.121, we find

$$c \approx \frac{x-\zeta}{t}\ , \tag{11.127}$$

which is to say

$$c = g(\zeta) \tag{11.128}$$

$$x = \zeta + g(\zeta)\, t\ . \tag{11.129}$$

This is precisely what we found for the characteristics of $c_t + c\, c_x = 0$.

What about multivaluedness? This is obviated by the presence of an additional saddle point solution. *I.e.* beyond some critical time, we have a discontinuous change of saddles as a function of x:

$$x = \zeta_\pm + g(\zeta_\pm)\, t \quad \longrightarrow \quad \zeta_\pm = \zeta_\pm(x,t)\ . \tag{11.130}$$

Then

$$c \sim \frac{1}{t} \cdot \frac{\frac{x-\zeta_-}{\sqrt{H''(\zeta_-)}}\, e^{-H(\zeta_-)/2\nu} + \frac{x-\zeta_+}{\sqrt{H''(\zeta_+)}}\, e^{-H(\zeta_+)/2\nu}}{\frac{1}{\sqrt{H''(\zeta_-)}}\, e^{-H(\zeta_-)/2\nu} + \frac{1}{\sqrt{H''(\zeta_+)}}\, e^{-H(\zeta_+)/2\nu}}\ . \tag{11.131}$$

Thus,

$$H(\zeta_+) > H(\zeta_-) \qquad \Rightarrow \qquad c \approx \frac{x-\zeta_-}{t} \tag{11.132}$$

$$H(\zeta_+) < H(\zeta_-) \qquad \Rightarrow \qquad c \approx \frac{x-\zeta_+}{t}\ . \tag{11.133}$$

At the shock, these solutions are degenerate:

$$H(\zeta_+) = H(\zeta_-) \qquad \Rightarrow \qquad \tfrac{1}{2}(\zeta_+ - \zeta_-)\big(g(\zeta_+) + g(\zeta_-)\big) = \int_{\zeta_-}^{\zeta_+} d\zeta\, g(\zeta)\ , \tag{11.134}$$

which is again exactly as before. We stress that for ν small but finite the shock fronts are smoothed out on a distance scale proportional to ν.

What does it mean for ν to be small? The dimensions of ν are $[\nu] = L^2/T$, so we must find some other quantity in the problem with these dimensions. The desired quantity is the area,

$$A = \int_{-\infty}^{\infty} dx\, \big[g(x) - c_0\big]\ , \tag{11.135}$$

where $c_0 = c(x = \pm\infty)$. We can now define the dimensionless ratio,

$$\mathsf{R} \equiv \frac{A}{2\nu} \ , \tag{11.136}$$

which is analogous to the Reynolds number in viscous fluid flow. R is proportional to the ratio of the nonlinear term $(c - c_0)\, c_x$ to the diffusion term νc_{xx}.

11.9.2 Examples

Whitham discusses three examples: diffusion of an initial step, a hump, and an N-wave. Here we simply reproduce the functional forms of these solutions. For details, see chapter 4 of Whitham's book.

For an initial step configuration,

$$c(x, t = 0) = \begin{cases} c_1 & \text{if } x < 0 \\ c_2 & \text{if } x > 0 \ . \end{cases} \tag{11.137}$$

We are interested in the case $c_1 > c_2$. Using the Cole-Hopf transformation and applying the appropriate initial conditions to the resulting linear diffusion equation, one obtains the complete solution,

$$c(x,t) = c_2 + \frac{c_1 - c_2}{1 + h(x,t)\, \exp\big[(c_1 - c_2)(x - v_{\rm s} t)/2\nu\big]} \ , \tag{11.138}$$

where

$$v_{\rm s} = \tfrac{1}{2}(c_1 + c_2) \tag{11.139}$$

and

$$h(x,t) = \frac{\text{erfc}\Big(-\frac{x - c_2 t}{\sqrt{4\nu t}}\Big)}{\text{erfc}\Big(+\frac{x - c_1 t}{\sqrt{4\nu t}}\Big)} \ . \tag{11.140}$$

Recall that $\text{erfc}(z)$ is the complimentary error function:

$$\text{erf}(z) = \frac{2}{\sqrt{\pi}} \int\limits_0^z \! du\, e^{-u^2} \tag{11.141}$$

$$\text{erfc}(z) = \frac{2}{\sqrt{\pi}} \int\limits_z^\infty \! du\, e^{-u^2} = 1 - \text{erf}(z) \ . \tag{11.142}$$

Note the limiting values $\text{erfc}(-\infty) = 2$, $\text{erfc}(0) = 1$ and $\text{erfc}(\infty) = 0$. If $c_2 < x/t < c_1$, then $h(x,t) \to 1$ as $t \to \infty$, in which case the solution resembles a propagating front. It is convenient to adimensionalize $(x,t) \to (y,\tau)$ by writing

$$x = \frac{\nu\, y}{\sqrt{c_1 c_2}} \qquad , \qquad t = \frac{\nu\, \tau}{c_1 c_2} \qquad , \qquad r \equiv \sqrt{\frac{c_1}{c_2}} \ . \tag{11.143}$$

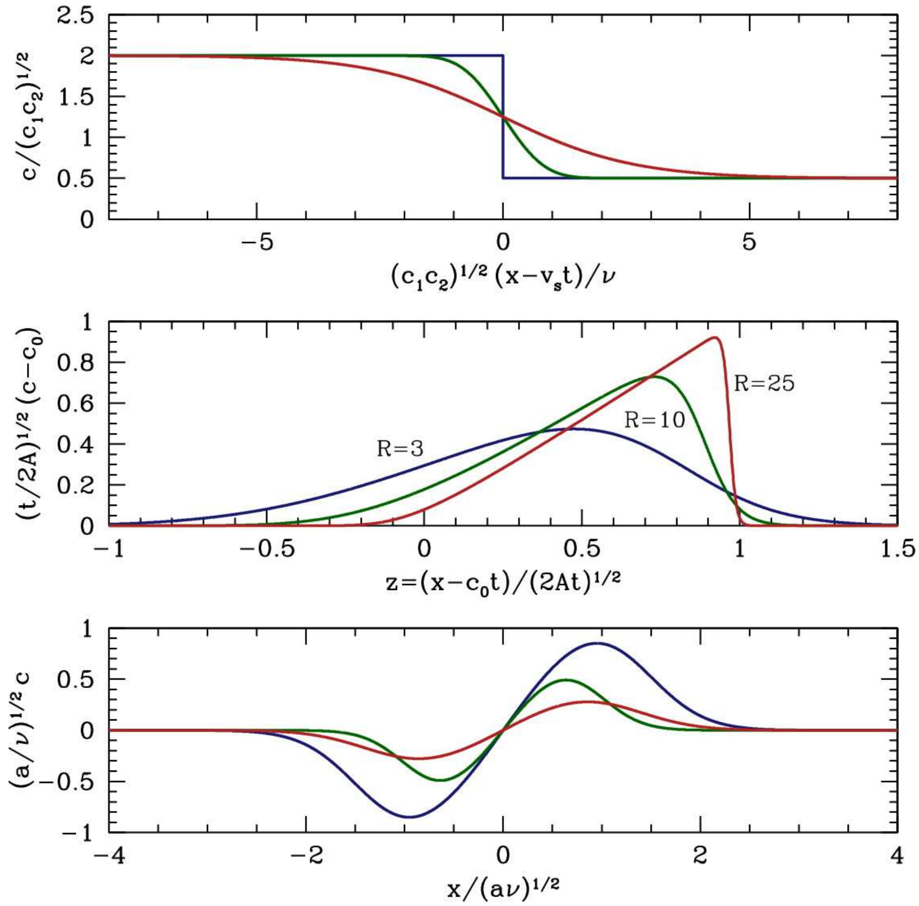

Figure 11.12: Evolution of profiles for Burgers' equation. Top : a step discontinuity evolving into a front at times $\tau = 0$ (blue), $\tau = \frac{1}{5}$ (green), and $\tau = 5$ (red).. Middle : a narrow hump $c_0 + A\delta(x)$ evolves into a triangular wave. Bottom : dissipation of an N-wave at times $\tau = \frac{1}{4}$ (blue), $\tau = \frac{1}{2}$ (green), and $\tau = 1$ (red).

We then have

$$\frac{c(z,\tau)}{\sqrt{c_1 c_2}} = r^{-1} + \frac{2\alpha}{1 + h(z,\tau)\,\exp(\alpha z)} \ , \tag{11.144}$$

where

$$h(z,\tau) = \text{erfc}\bigg(-\,\frac{z+\alpha\tau}{2\sqrt{\tau}}\bigg) \bigg/ \text{erfc}\bigg(+\,\frac{z-\alpha\tau}{2\sqrt{\tau}}\bigg) \tag{11.145}$$

and

$$\alpha \equiv \tfrac{1}{2}\big(r - r^{-1}\big) \qquad , \qquad z \equiv y - \tfrac{1}{2}\big(r + r^{-1}\big)\,\tau \ . \tag{11.146}$$

The second example involves the evolution of an infinitely thin hump, where

$$c(x, t=0) = c_0 + A\,\delta(x) \ . \tag{11.147}$$

The solution for subsequent times is

$$c(x,t) = c_0 + \sqrt{\frac{\nu}{\pi t}} \cdot \frac{(e^{\mathsf{R}}-1)\,\exp\left(-\frac{x-c_0 t}{4\nu t}\right)}{1+\frac{1}{2}(e^{\mathsf{R}}-1)\,\mathrm{erfc}\left(\frac{x-c_0 t}{\sqrt{4\nu t}}\right)} \ , \tag{11.148}$$

where $\mathsf{R} = A/2\nu$. Defining

$$z \equiv \frac{x - c_0 t}{\sqrt{2At}} \ , \tag{11.149}$$

we have the solution

$$c = c_0 + \left(\frac{2A}{t}\right)^{1/2} \frac{1}{\sqrt{4\pi\mathsf{R}}} \cdot \frac{(e^{\mathsf{R}}-1)\,e^{-\mathsf{R}z^2}}{1+\frac{1}{2}(e^{\mathsf{R}}-1)\,\mathrm{erfc}(\sqrt{\mathsf{R}}\,z)} \ . \tag{11.150}$$

Asymptotically, for $t \to \infty$ with x/t fixed, we have

$$c(x,t) = \begin{cases} x/t & \text{if } 0 < x < \sqrt{2At} \\ 0 & \text{otherwise} \ . \end{cases} \tag{11.151}$$

This recapitulates the triangular wave solution with the two counterpropagating shock fronts and dissipating shock strengths.

Finally, there is the N-wave. If we take the following solution to the linear diffusion equation,

$$\varphi(x,t) = 1 + \sqrt{\frac{a}{t}}\, e^{-x^2/4\nu t} \ , \tag{11.152}$$

then we obtain

$$c(x,t) = \frac{x}{t} \cdot \frac{e^{-x^2/4\nu t}}{\sqrt{\frac{t}{a}} + e^{-x^2/4\nu t}} \ . \tag{11.153}$$

In terms of dimensionless variables (y, τ), where

$$x = \sqrt{a\nu}\; y \qquad , \qquad t = a\tau \ , \tag{11.154}$$

we have

$$c = \sqrt{\frac{\nu}{a}}\, \frac{y}{\tau} \cdot \frac{e^{-y^2/4\tau}}{\sqrt{\tau} + e^{-y^2/4\tau}} \ . \tag{11.155}$$

The evolving profiles for these three cases are plotted in fig. 11.12.

11.9.3 Confluence of shocks

The fact that the diffusion equation 11.118 is linear means that we can superpose solutions:

$$\varphi(x,t) = \varphi_1(x,t) + \varphi_2(x,t) + \ldots + \varphi_N(x,t) \ , \tag{11.156}$$

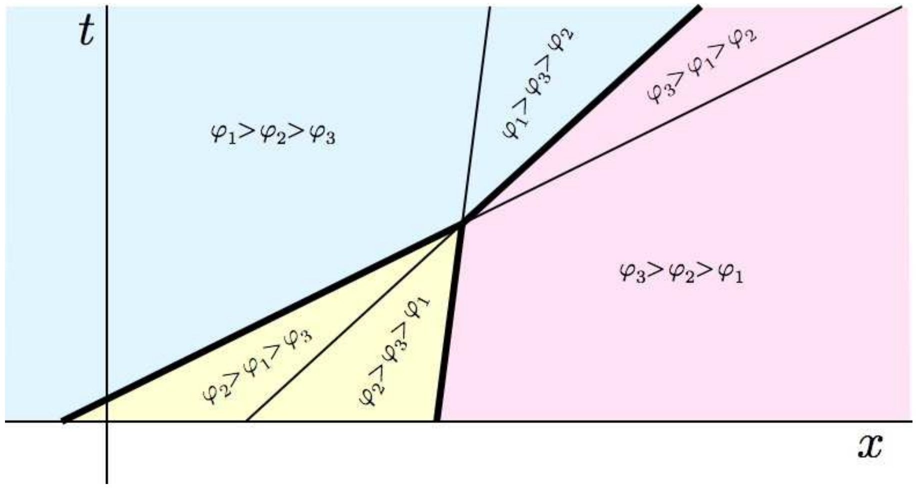

Figure 11.13: Merging of two shocks for piecewise constant initial data. The (x,t) plane is broken up into regions labeled by the local value of $c(x,t)$. For the shocks to form, we require $c_1 > c_2 > c_3$. When the function $\varphi_j(x,t)$ dominates over the others, then $c(x,t) \approx c_j$.

where

$$\varphi_j(x,t) = e^{-c_j(x-b_j)/2\nu} \, e^{+c_j^2 t/4\nu} \ . \tag{11.157}$$

We then have

$$c(x,t) = -\frac{2\nu\varphi_x}{\varphi} = \frac{\sum_i c_i \, \varphi_i(x,t)}{\sum_i \varphi_i(x,t)} \ . \tag{11.158}$$

Consider the case $N=2$, which describes a single shock. If $c_1 > c_2$, then at a fixed time t we have that φ_1 dominates as $x \to -\infty$ and φ_2 as $x \to +\infty$. Therefore $c(-\infty,t) = c_1$ and $c(+\infty) = c_2$. The shock center is defined by $\varphi_1 = \varphi_2$, where $x = \frac{1}{2}(c_1 + c_2)\, t$.

Next consider $N = 3$, where there are two shocks. We assume $c_1 > c_2 > c_3$. We identify regions in the (x,t) plane where φ_1, φ_2, and φ_3 are dominant. One finds

$$\varphi_1 > \varphi_2 \quad : \quad x < \tfrac{1}{2}(c_1 + c_2)\, t + \frac{b_1 c_1 - b_2 c_2}{c_1 - c_2} \tag{11.159}$$

$$\varphi_1 > \varphi_3 \quad : \quad x < \tfrac{1}{2}(c_1 + c_3)\, t + \frac{b_1 c_1 - b_3 c_3}{c_1 - c_3} \tag{11.160}$$

$$\varphi_2 > \varphi_3 \quad : \quad x < \tfrac{1}{2}(c_2 + c_3)\, t + \frac{b_2 c_2 - b_3 c_3}{c_2 - c_3} \ . \tag{11.161}$$

These curves all meet in a single point at $(x_{\rm m}, t_{\rm m})$, as shown in fig. 11.13. The shocks are the locus of points along which two of the φ_j are equally dominant. We assume that the intercepts of these lines with the x-axis are ordered as in the figure, with $x^*_{12} < x^*_{13} < x^*_{23}$, where

$$x^*_{ij} \equiv \frac{b_i c_i - b_j c_j}{c_i - c_j} \ . \tag{11.162}$$

When a given $\varphi_i(x,t)$ dominates over the others, we have from eqn. 11.158 that $c \approx c_i$. We see that for $t < t^*$ one has that φ_1 is dominant for $x < x^*_{12}$, and φ_3 is dominant for $x > x^*_{23}$, while φ_2 dominates in the intermediate regime $x^*_{12} < x < x^*_{23}$. The boundaries between these different regions are the two propagating shocks. After the merge, for $t > t_{\rm m}$, however, φ_2 *never dominates*, and hence there is only one shock.

11.10 Appendix I : The Method of Characteristics

Consider the quasilinear PDE

$$a_1(\boldsymbol{x},\phi)\,\frac{\partial\phi}{\partial x_1} + a_2(\boldsymbol{x},\phi)\,\frac{\partial\phi}{\partial x_2} + \ldots + a_N(\boldsymbol{x},\phi)\,\frac{\partial\phi}{\partial x_N} = b(\boldsymbol{x},\phi)\ . \tag{11.163}$$

This PDE is called 'quasilinear' because it is linear in the derivatives $\partial\phi/\partial x_j$. The N independent variables are the elements of the vector $\boldsymbol{x} = (x_1,\ldots,x_N)$. A solution is a function $\phi(\boldsymbol{x})$ which satisfies the PDE.

Now consider a curve $\boldsymbol{x}(s)$ parameterized by a single real variable s satisfying

$$\frac{dx_j}{ds} = a_j\big(\boldsymbol{x},\phi(\boldsymbol{x})\big)\ , \tag{11.164}$$

where $\phi(\boldsymbol{x})$ is a solution of eqn. 11.163. Along such a curve, which is called a *characteristic*, the variation of ϕ is

$$\frac{d\phi}{ds} = \sum_{j=1}^N \frac{\partial\phi}{\partial x_j}\,\frac{dz_j}{ds} = b\big(\boldsymbol{x}(s),\phi\big)\ . \tag{11.165}$$

Thus, we have converted our PDE into a set of $(N+1)$ ODEs. To integrate, we must supply some initial conditions of the form

$$g\big(\boldsymbol{x},\phi\big)\Big|_{s=0} = 0\ . \tag{11.166}$$

This defines an $(N-1)$-dimensional hypersurface, parameterized by $\{\zeta_1,\ldots,\zeta_{N-1}\}$:

$$x_j(s=0) = h_j(\zeta_1,\ldots,\zeta_{N-1}) \qquad , \qquad j = 1,\ldots,N \tag{11.167}$$

$$\phi(s=0) = f(\zeta_1,\ldots,\zeta_{N-1})\ . \tag{11.168}$$

If we can solve for all the characteristic curves, then the solution of the PDE follows. For every $\boldsymbol{x}$, we identify the characteristic curve upon which $\boldsymbol{x}$ lies. The characteristics are identified by their parameters $(\zeta_1,\ldots,\zeta_{N-1})$. The value of $\phi(\boldsymbol{x})$ is then $\phi(\boldsymbol{x}) = f(\zeta_1,\ldots,\zeta_{N-1})$. If two or more characteristics cross, the solution is multi-valued, or a shock has occurred.

11.10.1 Example

Consider the PDE

$$\phi_t + t^2\,\phi_x = -x\,\phi\ . \tag{11.169}$$

We identify $a_1(t,x,\phi) = 1$ and $a_2(t,x,\phi) = t^2$, as well as $b(t,x,\phi) = -x\,\phi$. The characteristics are curves $\big(t(s), x(s)\big)$ satisfing

$$\frac{dt}{ds} = 1 \qquad , \qquad \frac{dx}{ds} = t^2 \ . \tag{11.170}$$

The variation of ϕ along each characteristics is given by

$$\frac{d\phi}{ds} = -x\,\phi \ . \tag{11.171}$$

The initial data are expressed parametrically as

$$t(s=0) = 0 \tag{11.172}$$
$$x(s=0) = \zeta \tag{11.173}$$
$$\phi(s=0) = f(\zeta) \ . \tag{11.174}$$

We now solve for the characteristics. We have

$$\frac{dt}{ds} = 1 \quad \Rightarrow \quad t(s,\zeta) = s \ . \tag{11.175}$$

It then follows that

$$\frac{dx}{ds} = t^2 = s^2 \quad \Rightarrow \quad x(s,\zeta) = \zeta + \tfrac{1}{3}s^3 \ . \tag{11.176}$$

Finally, we have

$$\frac{d\phi}{ds} = -x\,\phi = -\big(\zeta + \tfrac{1}{3}s^3\big)\,\phi \quad \Rightarrow \quad \phi(s,\zeta) = f(\zeta)\,\exp\big(-\tfrac{1}{12}s^4 - s\zeta\big) \ . \tag{11.177}$$

We may now eliminate (ζ, s) in favor of (x,t), writing $s = t$ and $\zeta = x - \frac{1}{3}t^3$, yielding the solution

$$\phi(x,t) = f\big(x - \tfrac{1}{3}t^3\big)\,\exp\big(\tfrac{1}{4}t^4 - xt\big) \ . \tag{11.178}$$

11.11 Appendix II : Shock Fitting an Inverted Parabola

Consider the shock fitting problem for the initial condition

$$c(x,t=0) = c_0\bigg(1 - \frac{x^2}{a^2}\bigg)\,\Theta(a^2 - x^2) \ , \tag{11.179}$$

which is to say a truncated inverted parabola. We assume $j'''(\rho) = 0$. Clearly $-c_x(x,0)$ is maximized at $x = a$, where $-c_x(a,0) = 2c_0/a$, hence breaking first occurs at

$$\big(x_{\rm B}\,,\,t_{\rm B}\big) = \bigg(a\,,\,\frac{a}{2c_0}\bigg) \ . \tag{11.180}$$

Clearly $\zeta_+ > a$, hence $c_+ = 0$. Shock fitting then requires

$$\tfrac{1}{2}(\zeta_+ - \zeta_-)(c_+ + c_-) = \int\limits_{\zeta_-}^{\zeta_+} d\zeta \, c(\zeta) \tag{11.181}$$

$$= \frac{c_0}{3a^2}\,(2a + \zeta_-)(a - \zeta_-)^2 \ . \tag{11.182}$$

Since

$$c_+ + c_- = \frac{c_0}{a^2}\,(a^2 - \zeta_-^2) \ , \tag{11.183}$$

we have

$$\zeta_+ - \zeta_- = \tfrac{2}{3}\,(2a + \zeta_-)\bigg(\frac{a - \zeta_-}{a + \zeta_-}\bigg) \ . \tag{11.184}$$

The second shock-fitting equation is

$$\zeta_+ - \zeta_- = (c_- - c_+)\,t \ . \tag{11.185}$$

Eliminating ζ_+ from the two shock-fitting equations, we have

$$t = \frac{2a^2}{3c_0} \cdot \frac{2a + \zeta_-}{(a + \zeta_-)^2} \ . \tag{11.186}$$

Inverting to find $\zeta_-(t)$, we obtain

$$\frac{\zeta_-(t)}{a} = \frac{a}{3c_0 t} - 1 + \frac{a}{3c_0 t}\,\sqrt{1 + \frac{6c_0 t}{a}} \ . \tag{11.187}$$

The shock position is then $x_s(t) = \zeta_-(t) + c_-\big(\zeta_-(t)\big)\,t$.

It is convenient to rescale lengths by a and times by $t_B = a/2c_0$, defining q and τ from $x \equiv aq$ and $t \equiv a\tau/2c_0$. Then

$$q_-(\tau) = \frac{\zeta_-}{a} = \frac{2}{3\tau} - 1 + \frac{2}{3\tau}\,\sqrt{1 + 3\tau} \ . \tag{11.188}$$

and

$$q_s(\tau) = \frac{x_s}{a} = -1 + \frac{2}{9\tau}\,\Big[(1 + 3\tau)^{3/2} + 1\Big] \ . \tag{11.189}$$

The shock velocity is

$$\dot{q}_s = -\frac{2}{9\tau^2}\,\Big[1 + (1 + 3\tau)^{3/2}\Big] + \frac{1}{\tau}\,(1 + 3\tau)^{1/2} \tag{11.190}$$

$$= \tfrac{3}{4}\,(\tau - 1) + \tfrac{81}{64}\,(\tau - 1)^2 + \ldots \ ,$$

with $v_s = 2c_0\,\dot{q}_s = \frac{1}{2}c_-$ if we restore units. Note that $\dot{q}_s(\tau = 1) = 0$, so the shock curve initially rises vertically in the (x, t) plane. Interestingly, $v_s \propto (\tau - 1)$ here, while for the example in §11.4.3, where $c(x, 0)$ had a similar profile, we found $v_s \propto (\tau - 1)^{1/2}$ in eqn. 11.69.